The Synthesis and Biological Evaluation of Anti-Adhesion Glycoconjugates Against Opportunistic Pathogenic *Candida albicans*

A thesis submitted to Maynooth University in fulfilment of the requirements for the degree of

Doctor of Philosophy

by

Harlei Martin, B.Sc.

Department of Chemistry,

Maynooth University,

Maynooth,

Co. Kildare, Ireland.

October 2019

Research Supervisor: Dr Trinidad Velasco-Torrijos

Head of Department: Dr Jennifer McManus

To my family and John.

Thank you for everything.

Table of Contents

Acknowledgements

The completion of this thesis would not have been possible without the help of several people that deserve a special mention. First and foremost, my supervisor Dr Trinidad Velasco Torrijos for her constant support, encouragement, enthusiasm and generosity of her time. I could not have asked for better supervisor, mentor and friend. It has been an honour to work with you over the last few years.

I would like to thank Maynooth University for awarding me the John and Pat Hume Scholarship which allowed me to complete my PhD and to the Heads of Department, Dr John Stephens and Dr Jennifer McManus, for allowing me to complete my research at Maynooth University. Thank you to all the academic staff in the Chemistry Department for being there to help me throughout my PhD. Especially to Dr Denise Rooney who provided me with constant reassurance and encouragement. Thank you to Prof Kevin Kavanagh in the Biology Department for carrying out the biological assays and for teaching me the techniques to carry out the assays myself. A special thanks to all the technical and administrative staff in the department. To Ria, Noel, Barbara, Orla, Anne, Carmel, Ollie, Walter, Eliza, Ken, Donna and Carol – thank you for all the help and assistance.

Thank you to the IRC for awarding me with the Ulysses grant which allowed me to carry out research in Grenoble, France. Thank you to Prof Olivier Renaudet in the Univeristé Grenoble Alpes for allowing me to work in his laboratory and to Dr David Goyard for sharing his expertise with me, helping me during my time in France and for providing an expensive courier service to personally collect my compound to continue the synthesis in Grenoble.

Thank you to the postgrads, past and present, for making the department the weird and wonderful place that it is. For all the tearoom chats, drunken Roost nights out and for reminding each other constantly that we are not alone on this crazy journey! A special shout out to Stephen for our Chinese adventure (nothing is as it seems in China!!), our countless coffees, conversations and Tuesday evening pints (and tequilas), to Amanda for always being my voice of reason, my agony aunt and my go-to-person for an evening cup of tea, to Luke for providing me with unlimited ‘treats’

and laughs that always cheered me up on down days, to Matt-chew for starting and (more importantly) finishing this adventure together, and to Jason & Michelle for all the chats away from the synthetic lab. A huge thank you to previous members of the TVT group, Jessica and Andrew, for showing me the ropes when I first started in the lab, and to the new group members, Kyle, Eoin and Marwa. I hope you all enjoy your time here as much as me. Thanks to Drs Muhib, Mark and Caroline, and to all the other postgrads, Aoife (the perfect roommate on our trip to Barcelona), Mark G (we've finally made it!), Grace (no more 'playing around' with page numbers!), Michelle K, Alessandro, Mi, Paddy (I will never forget the yogurt and olive oil), Kenneth, Kobi, Caytlin, Conor G, Conor W, Ales, Hua, Clara and anyone else I didn't mention. Thank you for the friendship. Best of luck with your research! A special mention for my 'mushy' friend Eoin in the Biology Department who always provided a distraction when needed. Congratulations Dr O'Connor - Roll on graduation!

A huge thanks to my family for their continued love and support, to my sister, Maxine, my Dad, and especially my Mam whose non-stop encouragement and guidance has helped me through my whole life. For always inspiring me to do my best and reach for the stars. Thank you to all my cousins (especially Lacey – a night out is desperately needed!) and to my aunts and uncles who have been there to support me when I needed it most.

Last but by no means least, I would like to thank John for the never-ending encouragement, love and support over the last few years. We started this journey as great friends and housemates and it has grown into so much more. I cannot put into words how much I love, respect and appreciate you. You have always been there for me when I needed it most and have been a constant source of happiness in my life. I could not have got this far without you. You are the best!

Declaration

I declare that the work presentated in this thesis was carried out in accordance with the regulations of Maynooth Univeristy. The work is original, except where indicated by reference, and has not been submitted before, in whole or in part, to this or any other university for any other degree.

Signed: _____ Date: _____

Harlei Martin, B.Sc. (Hons)

Abstract

Anti-adhesion therapy can be used to prevent infectious diseases caused by fungi and bacteria. Anti-adhesion ligands interfere with the ability of the fungi or bacteria to adhere to cells in the host organism. New forms of therapy are needed since the inappropriate use of antifungal agents and antibiotics has led to an increase in fungal and bacterial strains resistant to conventional forms of treatment.

In this thesis, anti-adhesion compounds of *Candida albicans* to buccal epithelial cells (BEC) are considered. It was found that glycomimetics built around aromatic scaffolds could be potential anti-adhesion ligands. Using synthetic carbohydrate chemistry and Copper-Catalyzed Azide-Alkyne Cycloaddtion (CuAAC) chemistry, a first generation of monovalent, divalent and trivalent anti-adhesion ligands were synthesised. After this initial SAR (Structure Activity Relationship) study a divalent galactoside was identified as the lead compound, capable of displacing 50 % of yeast cells already attached to the BECs. Fluorescence studies suggest that this compound may bind to structural components of the fungal cell wall.

In the pursuit of increasing the potency of this lead compound, anti-adhesion ligands with alternative scaffolds were synthesised and evaluated in biological assays. It was found that the squaramide derivatives did not improve the anti-adhesive properties of the original compounds. However, a norbornene derivative showed better results than the lead compound in two of the assays and had the ability to displace 45 % of yeast already attached to the BECs.

To exploit the 'Multivalent/Chelate Effect' and increase the potency of the divalent galactoside, multivalent displays of the lead compound were then synthesised. The lead compound was attached to different scaffolds using a triethyl glycol linker and CuAAC chemistry. This resulted in glycoclusters and glycodendrimers having different valencies (three to sixteen copies of the lead compound), flexibilities and carbohydrate presentation.

The ultimate aim of this research is to identify the *Candida* cell wall component responsible for the adhesion process with which the lead compound is interacting. Photoaffinity labelling (PAL) may be used to identify target proteins. PAL probes

containing two different phototags, a benzophenone and a diazirine derivative, were synthesised. The phototags were covalently linked to the lead compound using coupling chemistry and aza-Micheal addition reactions.

Abbreviations

[α] = Specific rotation [expressed without units, the units are (deg.mL)/(g.dm)]

Ac = Acetyl

Ac_2O = Acetic anhydride

Aq = Aqueous

Ar = Aromatic

Atm = Atmospheric pressure

ATR = Attenuated Total Reflection

Boc = *t*-butyloxycarbonyl

°C = Degrees Celsius

$CDCl_3$ = Deuterated chloroform

CDMT = 2-Chloro-4,6-dimethoxy-1,3,5-triazine

COSY = Correlation Spectroscopy

CuAAC = Copper(I) catalysed azide-alkyne cycloaddition

d_5-Pyridine = Deuterated pyridine

DCM = Dichloromethane

DEPT = Distortionless enhancement by polarization transfer

DIPEA = Diisopropylethylamine

DMF = Dimethylformamide

DMSO = Dimethylsulfoxide

DMTMM = 4-(4,6-Dimethoxy-1,3,5-triazin-2-yl)-4-methylmorpholin-4-ium chloride

e.g. = *Exempli gratia* (Latin for 'for example')

Equiv = Equivalents

ESI = Electrospray ionisation

Et_2O = Diethyl ether

EtOAc = Ethyl acetate

EtOH = Ethanol

Fuc = Fucose

Gal = Galactose

GalNAc = *N*-Acetylgalactosamine

Glc = Glucose

GlcNAc = *N*-Acetylglucosamine

h = Hours

HCl = Hydrochloric acid

HMBC = Heteronuclear Multiple Bond Correlation

HPLC = High Performance Liquid Chromatography

HR-MS = High Resolution Mass Spectrometry

HSQC = Heteronuclear Single Quantum Coherence

I = Isoleucine

i.e. = *Id est* (Latin for 'that is')

IR = Infrared spectroscopy

L = Leucine

Lac = lactose

K = Kelvin

K = Lysine

Man = mannose

MeCN = Acetonitrile

MeOD = Deuterated methanol

MeOH = Methanol

mg = Milligram

MIC = Minimal Inhibitory Concentration

min = Minutes

mL = Millilitre

mm = Millimetre

µm = Micrometre

NEt_3 = Triethylamine

nm = Nanometre

NMM = *N*-methylmorpholine

NMR = Nuclear Magnetic Resonance

OAc = Acetoxy group

OH = Hydroxy group

Pd/C = Palladium on activated carbon

Pet Ether = Petroleum ether

R + Arginine

R_f = Retention Factor

rt = Room temperature

SAR = Structure Activity Relationship

sat. = Saturated

sec = Seconds

TBTU = *O*-(Benzotriazol-1-yl)-*N,N,N',N'*-tetramethyluronium tetrafluoroborate

TFA = Trifluoroacetic acid

THF = Tetrahydrofuran

TLC = Thin Layer Chromatography

TOF = Time of Flight

UPLC = Ultra Performance Liquid Chromatography

V = Valine

Chapter 1

Introduction

1.1 Fungal Infections

Fungal infections affect over a billion people globally. 1.5 billion people worldwide are estimated to have superficial fungal infections of the skin, nails and hair,[1] tens of millions of people suffer from mucosal candidiasis and more than 150 million people have serious fungal diseases. These infections can have a huge impact on people's lives and can also be fatal. The severity of fungal infections can range from asymptomatic-mild mucocutaneous infections to potentially lethal systemic infections. The mortality associated with fungal disease is greater than 1.6 million,[2] which is similar to that of tuberculosis,[3] and 3-fold greater than malaria.[4] The HIV/AIDS pandemic, tuberculosis, chronic obstructive pulmonary disease (COPD), asthma and the increasing incidence of cancers are the major drivers of fungal infections both in developed and developing countries. Recent global estimates found 3 million cases of chronic pulmonary aspergillosis, 700,000 cases of invasive candidiasis, 500,000 cases of *Pneumocystis jirovecii* pneumonia, and over 200,000 cases of cryptococcal meningitis complicating HIV/AIDs.[5] The epidemiology of fungal diseases has changed significantly over the past decades. Nonetheless, *Aspergillus*, *Candida*, *Cryptococcus* species, *Pneumocystis jirovecii* and endemic dimorphic fungi such as *Histoplasma capsulatum* remain the main fungal pathogens responsible for the majority of cases of serious fungal diseases.[5]

1.1.1 Candida albicans

The genus *Candida* includes about 200 different species, with only a few species being human opportunistic pathogens that cause infections mainly in immunocompromised hosts. *Candida albicans* is the most common fungal opportunistic pathogen. The fungus is dimorphic since it grows as both yeast and filamentous cells. It is a commensal colonizer in humans and exists in the gastrointestinal and genitourinary tracts, as part of the oral and conjunctival flora.[6] However, it is known to cause infections when the host becomes immunocompromised. These infections can be superficial and affect the skin (cutaneous candidosis), the mucous membrane of the oral and vulvovaginal cavities, and the fingernails (paronychial and onychial candidosis).[7] *Candida* infections can

also be invasive and enter the bloodstream and disseminate to internal organs. Factors that contribute to fungal invasion include: surgery (especially abdominal), burns, long-term stay in intensive care unit, previous administration of broad-spectrum antibiotics and immunosuppressive agents, anti-neoplastic chemotherapy, organ transplantation, hemodialysis and central venous catheters.[8]

There are three main factors that contribute to the high mortality of invasive fungal infections. Firstly, since conventional microbiological approaches are insensitive, non-specific and laborious, a trustworthy, timely diagnosis is challenging. Secondly, the clinical signs and symptoms of an invasive fungal infection may not be present until the infection is at an advanced stage.[9] Thirdly, and most significantly, current antifungal therapies are inadequate, and the overuse of these drugs have led to the development of antifungal resistance.[10]

1.1.2 Antifungal Resistance

Antifungal resistance can develop in different ways, depending on the mode of action of the antifungal drug. Resistance mechanisms include reduction in the intracellular accumulation of the drug, decrease in the affinity for the target, and counteraction of the drug effect.[11]

The largest family of antifungal drugs is the azole family. Azoles inhibit the activity of the enzyme Erg11p, a lanosterol 14-α-demethylase,[12] which is involved in the biosynthesis of ergosterol. Depletion of ergosterol leads to structural damage of the cell membrane resulting in cell death. Ergosterol, analogous to cholesterol in animals, is the largest sterol component of the fungal cell membrane. Ergosterol and cholesterol have sufficient structural differences, therefore most antifungal agents which target ergosterol binding or biosynthesis do not also interact with the cholesterol of host cells. The azole family of antifungal drugs includes the imidazoles (micoazole, econazole, clotrimazole and ketoconazole) and the triazoles (fluconazole, itraconazole). Many antifungal azoles can be administered topically to treat superficial fungal infections, as well as intravenously for the treatment and prevention of invasive fungal infections.[13]

In recent years, fluconazole and intraconazole have been widely used for the prevention and treatment of systemic fungal infections because of their bioavailability and safety profiles.[14] As a result, fluconazole resistance has been described in a high percentage of patients. In particular, azole-resistant *C. albicans* is frequent in HIV-infected patients with oropharyngeal candidiasis (also known as oral thrush). The three main mechanisms leading to azole resistance in *C. albicans* are the following (with others shown in Figure 1.1):

- Point mutations of *ERG11*, the gene encoding the target protein (Erg11p) of the azole, that reduces the binding affinity of the protein to the azole antifungals;
- Overexpression of *ERG11*, leading to an increase in the intracellular concentration of the target protein (Erg11p);
- Overexpression of efflux membrane transporters, which decreases the intracellular concentration of the antifungal drug.[15]

Since *Candida* have also developed resistance to other antifungal drugs such as the echinocandins[16] and polyenes[17], there is an urgent need for the development of new drugs to fight these fungal infections. One way to tackle this problem is to use the anti-adhesion approach, which blocks the adhesion of the pathogen to the host cell, the first step in the pathogenesis of microbial infections.

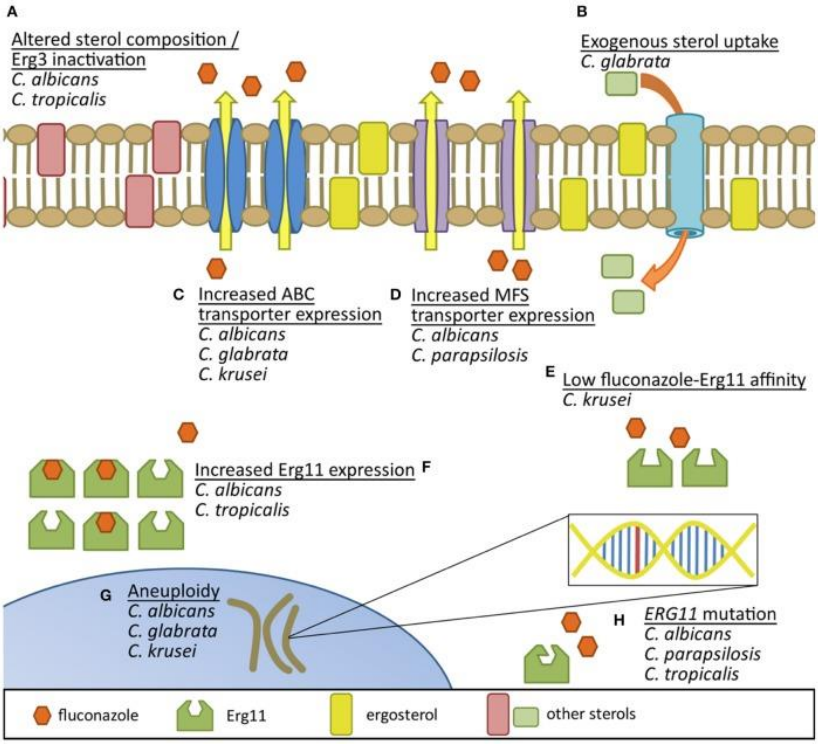

Figure 1.1: Comparison of documented fluconazole resistance mechanisms in *Candida* species reprinted from Whaley *et al*.[18] A) Erg3 inactivation leads to the utilization of alternative sterols in the yeast membrane; B) Uptake of exogenous sterols helps circumvent endogenous sterol production by fluconazole; C) Increased expression of ATP-binding cassette efflux pumps and (D) major facilitator superfamily transporters reduce accumulation of azoles; E) Inherently low affinity of fluconazole binding to species-specific Erg11 may decrease fluconazole's potential to inhibit the protein; F) Increased expression of Erg11 protein can help overcome azole activity; G) Aneuploidy (presence of an abnormal number of chromosomes) may promote genetic adaption to azole exposure; and H) Mutations in *ERG11* can also result in proteins with reduced affinity for fluconazole binding. Reprinted with permission from Frontiers.

1.2 Mechanisms of Adhesion in Fungi

As mentioned above, there has been a huge increase in the incidence of fungal infections in the past few decades. Hence, a vast amount of research has been put into elucidating host-pathogen relationships. In particular, the initial interactions of the fungi to the host cells are essential to the colonization of the host and initiation of disease.[19-21] Adhesins are cell-surface biomolecules, usually proteins, that mediate the adhesion of the microbe to other cells or to surfaces. Fungal pathogens display a

large variety of adhesins on their surface, and are therefore able to adhere to a variety of cell types within the host. They can also interact with numerous ligands present in various host sites, such as biological fluids, extracellular membrane and basement membranes.[22]

1.2.1 Adhesins Present in Different Phyla of Fungi

The phyla Ascomycota is one of the seven phyla in the Fungi Kingdom (Figure 1.2).[23] Within this phylum there are three subphyla which contain well-known human and plant pathogens. Taphriomycotina contains *Schizosaccharomyces* and *Pneumocystis* genera, Saccharomycotina contains *Saccharomyces* and *Candida* genera, while Pezizomycotina contains *Aspergillus* and *Blastomyces* and many other genera.[24]

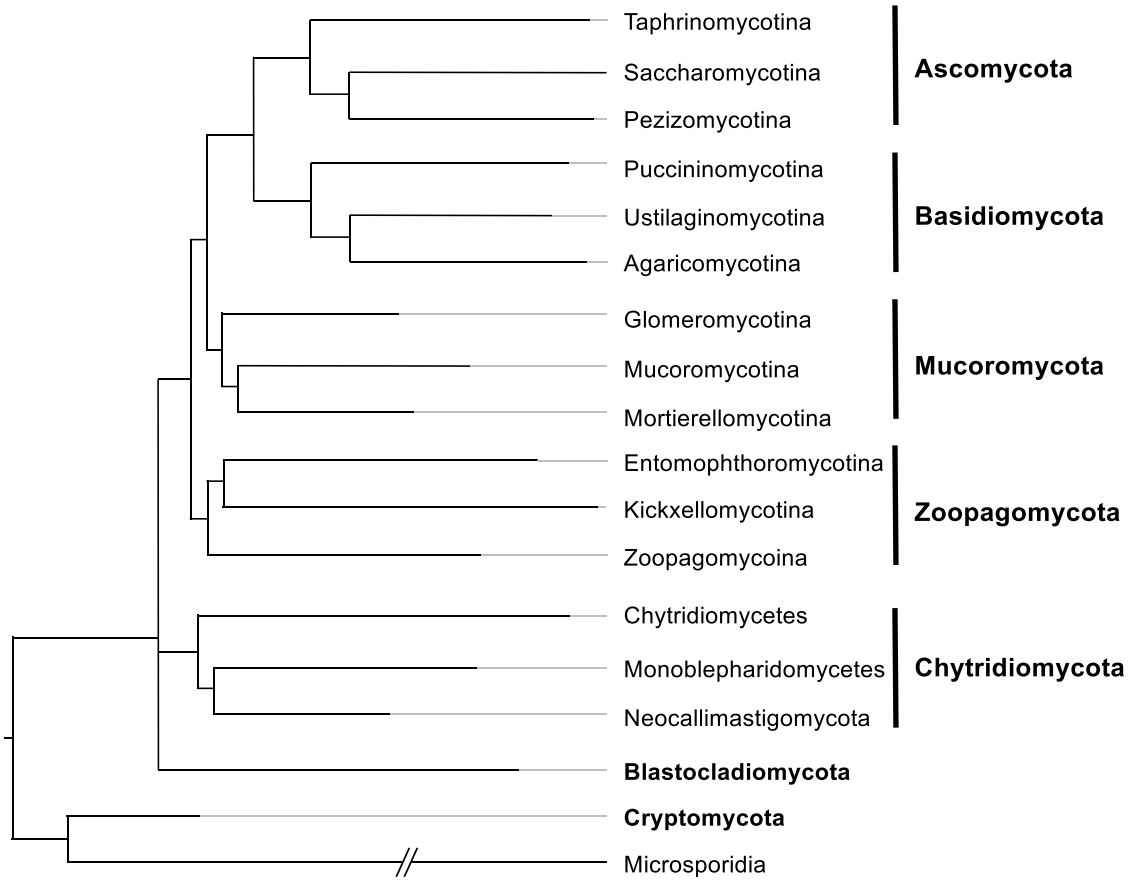

Figure 1.2: Phylogenetic relationship of the fungal phyla (in bold) and subphyla.[23]

1.2.1.1 Adhesins of Ascomycota

Most of the well-characterised fungal adhesins are found in *Saccharomyces* and *Candida*, two genera of the subphylum Saccharomycotina. These adhesins are

generally 600-2500 residue mannoproteins, which are covalently bound to the glucan in the cell wall through modified GPI (glycosyl-phosphatidyl-inositol) anchors. GPI anchors are glycolipid anchors for many cell surface glycoproteins. Many have discrete binding domains (Figure 1.3 A1 and A3), but others do not (Figure 1.3 A2). They can interact with adhesins on fungi, bacteria and mammalian cells or abiotic surfaces. The binding mechanisms include ligand binding, hydrophobic effect, and amyloid-like protein-protein aggregation.[22, 25]

Pezizomycotina includes *Aspergillus* and most of the top ten plant pathogens, including *Magnaporthe* and *Botrytis* genera. Adhesins in this subphylum comprise of fungal hydrophobins that mediate their binding to hydrophobic surfaces, including plant hosts. These are small cysteine-rich proteins that self-assemble through amyloid-like interactions and are known for their ability to coat the conidial surface in *Aspergillus* and other filamentous Ascomycota, in addition to abiotic surfaces.[26-28]

Taphrinomycotina are the third branch of the Ascomycota tree and adhesins have been characterized in the fission yeast *Schizosaccharomyces* and the AIDS-related opportunisitic pathogen *Pneumocystis*. In *Schizosaccharomyces pombe* Gsf2 is a galactose-specific lectin with a secretion signal and a GPI addition signal. In *S. pombe* and *Schizosaccharomyces japonica*, Linder and Gustafson[29] identified a family of proteins, including the adhesin Map4, with Ser/Thr-rich repeats and secretion signals, but none have GPI addition signals. Instead there are often recognizable lectin-like domains and a *Schizosaccharomyces*-specific domain (Figure 1.3 E). *Pneumocystis* adhesins include *Pneumocystis jirocvecii* Int1, an RGD-containing protein without a signal sequence, and a C-terminus region similar to the Bud4 GTP-binding protein. Int1 appears to be expressed on the surface of cells, even when exogenously expressed in *S. cerevisiae*. Int1 expression in *P. jirocvecii* and *S. cerevisiae* mediates Ca^{2+} dependent binding to fibronectin.[30]

1.2.1.2 Adhesins of Basidomycota

Relatively few adhesins are known from Basidomycota. The best studied are those of the encapsulated yeast *Cryptococcus neoformans*. Glucuronoxylomannan, the main constituent of the *C. neoformans* capsule, has been reported to have adhesive and

anti-adhesive properties. Mannoprotein MP84 is an adhesin with secretion and GPI addition signals, as well as *N*- and *O*-glycosidation sequences (Figure 1.3 F). It was reported that MP84 binds to lung epithelial cells and inhibits the binding of *C. neoformans* to lung epithelial cells.[31]

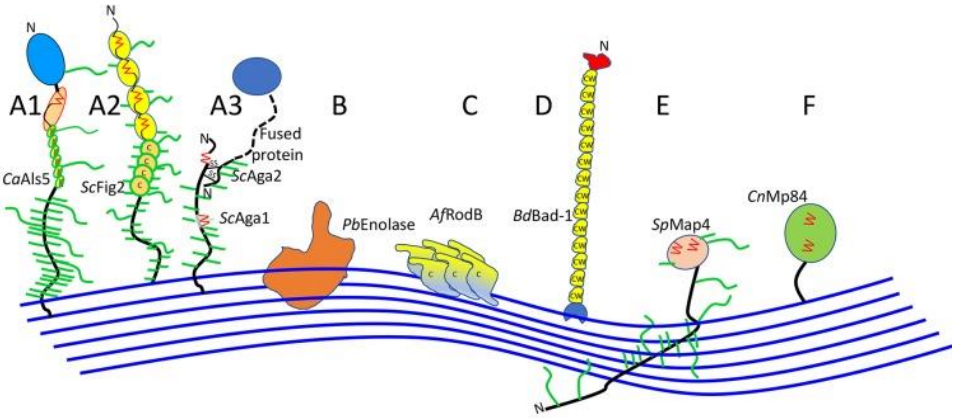

Figure 1.3: Diagram of fungal adhesins, showing different domain arrangements and cell wall associations reprinted from Lipke *et al.*[24]. The cell wall is shown as blue lines, representing glucan polymers. Abbreviations for the genus and species are in italics: *Ca, C. albicans; Sc, S. cerevisiae; Pb, Paracoccidioides braziliensis; Af, A. fumigatus; Bd, Blastomyces dermatitidis; Sp, S. pombe; Cn, C. neoformans,* with the adhesin name beside. Hydrophobic domains are shown in yellow. Potential amyloid-forming β-aggregation core sequences are shown as red zigzags; *O*-linked glycosidations are short green lines, *N*-glycans are longer green lines. C represents Cys-rich sequences in *Sc*Fig2 (A2) and *Af*RodB (C), and CW the Cys/Trp-rich domains in Bad-1 (D). Adhesins labelled (A) are covalently attached to the wall through modified GPI anchors, and (F) may be as well. The other sub-figure indices (B through E) show other cell wall attachment modes.[24] Reprinted with permission from MDPI.

1.2.2 Mechanisms of Adherence of the Candida Species

Interactions of *Candida* yeasts and hyphae with the host cells are crucial for the initial colonization of the host. Adherence of *C. albicans* to inert surfaces and biological substrates is considered a major attribute to its virulence. *C. albicans* displays a large repertoire of adhesins and has a highly complex cell wall.[32] The fungal cell wall plays a vital role in these interactions as it acts as an interface between the pathogen and its host. Fungal cell walls are structurally unique, with each species having distinctive

glycan polymers and proteins cross-linked together to form a complex network, which forms the structural basis of the cell wall.[33] Most cell wall proteins are glycoproteins, which are highly glycosylated and contain negatively charged phosphate groups in their carbohydrate side chains, which affect the electrostatic charge of the membrane. Cell wall proteins also contribute to the cell surface hydrophobicity, which is important for adherence to biomaterials, such as catheters, prostheses or medical implants.[22]

1.2.2.1 Cell Wall of *C. albicans*

The cell wall of *C. albicans* is a highly dynamic structure, organised into several layers which are mainly composed of polysaccharides (Figure 1.4). These polysaccharides are made up of D-glucose, *N*-acetyl-D-glucosamine and D-mannose monosaccharides, with some reports suggesting the presence of sialic acid in the *Candida* cell wall. Glucans and chitin form the rigid framework of the cell wall. Glucans are composed of highly branched glucose homopolymers with β-1,3 and β-1,6 linkages. Chitin is a linear polymer of β-1,4-D-GlcNAc, which provides cross-linking and strength to the glucan scaffold. Another polymer, mannan, which is a polysaccharide consisting of mannose residues with α-1,2 or α-1,3 linkages, is also part of the *Candida* cell wall. These polymers are only found in covalent association with proteins (mannoproteins) and never as unconjugated oligosaccharides. Mannan can also be found as linear chains of α-1,6 linked mannose with branched side chains consisting of mannose with α-1,2 or α-1,3 linkages. β-1,2-oligiomannosides are present in the cell wall and are linked by phosphodiester bonds to the other carbohydrate chains. Sialic acids are the terminal residues of the carbohydrate side chains of mannoproteins.[34]

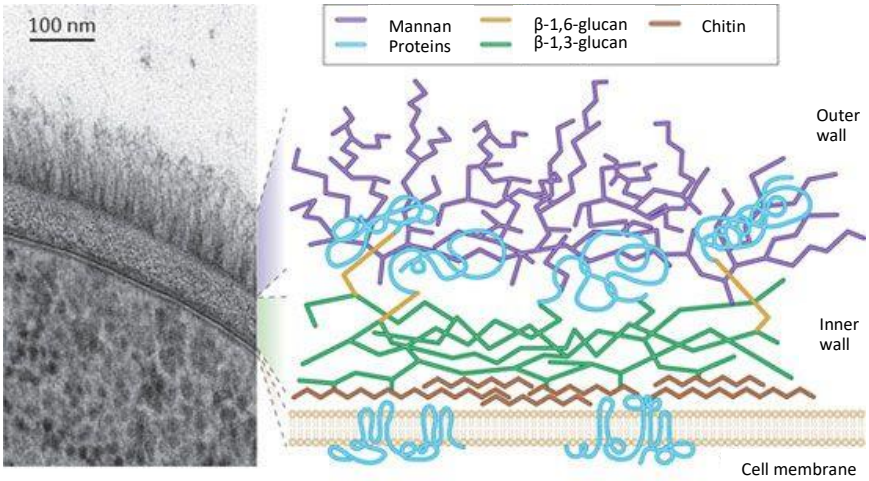

Figure 1.4: Structure of *C. albicans* cell wall adapted from Gow *et al.*[35]. Reprinted with permission from Springer Nature.

Mannoproteins are the major component of the outer layer of the cell wall forming fimbriae, where they appear as a network of fibrils arranged perpendicularly to the cell surface. There are two main classes of mannoproteins present in the cell wall: GPI-proteins and Pir proteins. GPI-proteins have a GPI-anchor to the carbohydrates in the cell walls and include the adhesins Als1p and Als3p. These proteins are localized in the outer cell wall and are linked mainly to β-glucans by their GPI-anchor. Pir proteins are proteins encoded by members of the *PIR* (proteins with internal repeats) gene family. They are localized in the inner layer of the cell wall and are covalently linked to the β-1,3-glucans. These proteins contain an N-terminal signal peptide, and internal repeat region, and a highly conserved C-terminal region.[22]

1.2.2.2 Adhesins in *C. albicans*

1.2.2.2.1 Glycans

Glycans in the cell wall of *C. albicans* have been found to influence the adherence of the yeast cells. As stated above, the cell wall is rich in glycosylated mannoproteins, and it is reported that the carbohydrate part of these biomolecules may contribute to the adhesion of the yeast to host cells. Kanbe *et al*.[36] reported that the mannan portion of a mannoprotein, obtained from an extraction of the fungal cells, is responsible for the adherence of the *C. albicans* to spleen and lymph tissue. Further research explored the adhesive characteristics of the acid stable moiety of the *C.*

albicans phosphomannoprotein complex (PMPC). Complete digestion of the acid-stable moiety with an α-mannosidase or hydrolysis with 0.6 N sulphuric acid destroyed the adhesion activity of the yeast to the spleen cells. It was found that both the mannan core and the oligomannosyl side chains are responsible for the adhesion activity of the acid-stable part of the PMPC.[37] In an adherence model using Caco-2 (human colon carcinoma epithelial) cells, Dalle *et al*.[38] reported that α-1,2 and β-1,2 oligomannosides are involved in the adhesion of *C. albicans* to epithelial cells. In this study, preincubation of the yeast with monoclonal antibodies (MAbs) specific for α-1,2 and β-1,2 mannan resulted in a dose-dependent decrease in adhesion. Also, in competitive assays β-1,2 and α-1,2 tetramannosides were the most potent carbohydrate inhibitors, with IC_{50} values of 2.58 and 6.99 mM, respectively. Dromer *et al*.[39] also found that administration of β-1,2 tetramannosides in a mouse model prior to inoculation with *C. albicans* prevented colonization of the yeast. The α-1,2 tetramannosides, in this study, had no effect on the yeast.

The glycosylation of mannoproteins is highly complex and involves several protein mannosyltransferases (Pmt) and mannosyltransferases (Mnt). Pmts mediates the first mannosylation step in *O*-glycosylation which occurs in the endoplasmic reiticulum.[40] The addition of further mannose residues to the first *O*-linked mannose occurs in the Golgi and involves many Mnts.[41] Cells lacking Pmt activity show reduced adherence to endothelial cells[40] and reduced colonization of organs in a mouse model.[42] A similar trend is seen when cells with a lack of Mnts are tested for their adherence properties. Deletion of the genes that code these proteins, resulted in a significant reduction of adherence to human buccal epithelial cells (BECs).[41]

Other cell wall carbohydrates are also involved in adherence. *C. albicans* synthesises sialic acids and express them on the cell surface. These sialic acids contribute to the negatively charged character of the yeast cell, which is an important factor involved in fungal interactions with host cells. Adhesion of the yeast cells to a cationic solid phase substrate (poly-L-lysine) was partly mediated by the sialic acids, since the number of adherent cells was significantly reduced after treatment with sialidase (an enzyme that hydrolyses the terminal sialic acid residues in oligosaccharides, glycoproteins, glycolipids etc.).[32]

1.2.2.2.2 Agglutinin-like Sequence Proteins

Agglutinin-like sequence (Als) proteins are the most widely expressed adhesins in *C. albicans*.[43] The ALS gene family encodes a group of GPI-anchored proteins that function as adhesins. There are at least eight distinct *ALS* genes in the *C. albicans* genome.[44] Mature Als proteins are highly homologous to each other. They consist of a 300-residue N-terminal region predicted to have an immunoglobulin-like fold (Ig), a 104-residue conserved threonine-rich region (T), a central domain compromising a variable number of tandem repeats (TR) of a threonine-rich sequence, and a heavily glycosylated C-terminal serine/threonine stalk region, also varible in length.[22, 45] The N-terminal domain in Als proteins mediate substrate-specific adherence. Comparative energy-based models suggest differences in key physiochemical properties of the N-terminal domains of different Als proteins. These differences include surface area, hydrophobicity and electrostatic charge and govern their distinct adherence and invasive biological functions.[46]

Of the Als proteins, Als1p, Als3p and Als5p have been extensively characterized and research suggests that they play an important role in the adherence of *C. albicans* to host cells. Als1p[45, 47] and Als3p[48] were reported to bind to human endothelial and epithelial cells, with Als5p also reported to bind to extracellular matrix (ECM) proteins.[45]

ALS1 encodes for the cell surface protein Als1p that mediates adherence of *C. albicans* to endothelial cells. Als1p has an N-terminal domain, which contains a signal peptide; a middle region, which has twenty 36-amino acid tandem repeats; and a C-terminal domain, which contains a GPI-anchor sequence. Site-directed mutagenesis was used to outline the regions in Als1p required for endothelial cell adherence and cell surface expression of the protein. The mutant alleles of *ALS1* containing either deletions or insertions were expressed in the normally non-adherent *S. cerevisiae*. Results found that in this model of Als1p, the endothelial cell binding region is localized in the N-terminus, the tandem repeats are essential for the proper presentation of the binding site, and the C-terminus is required for localizing Als1p to the cell surface.[47] It has also been found that Als1p is important for the adherence to the oral mucosa during the early stage of an infection.[49]

Zhao *et al.*[48] carried out a study with mutant strains of Als1p and Als3p. The results from this study demonstrated functional similarities and differences between these proteins and suggest that loss of Als3p affects *C. albicans* adhesion more than loss of Als1p.

Als5p is another *C. albicans* adhesin which is highly homologous to Als1p.[45, 50] The adherence of *C. albicans* and *S. cerevisiae* yeast cells expressing either of the Als proteins to specific peptides was studied using a random, polyethylene glycol (PEG)-bead based peptide library. The results show that the two adhesins recognize a broad array of target ligands, in particular those containing the sequence motif "τϕ+" where "τ" represents a residue with high turn propensity, "ϕ" represents a bulky hydrophobic residue and "+" represents R or K. This shows the adherence recognition systems of these adhesins is degenerate, as they are neither highly specific nor highly organized as to their protein or peptide targets. This recognition system allows the microorganism to adhere to a large repertoire of targets.[51]

1.2.2.2.3 Hyphal Cell Wall Adhesins

Hwp1p (hyphal wall protein 1) is found exclusively at the germ tube surface. It is another adhesin of *C. albicans* that mediates binding to BEC. Hwp1 is the first *C. albicans* cell surface protein that was found to be required for biofilm formation *in vivo*. In an *in vivo* model using venous catheters, the *HWP1* null mutant was defective in biofilm formation, producing only yeast microcolonies in the catheter lumen.[52] Hwp1p is a substrate for mammalian transglutaminase. It mediates the attachment of germ tubes to transglutaminase-expressing epithelial cells.[53]

1.2.2.2.4 Integrins

Integrins are transmembrane receptors that facilitate cell-extracellular matrix adhesion. Since, *C. albicans* bind and adhere to numerous ECM proteins, it has been hypothesised that there are integrin-like receptors at the yeast cell surface. In mammalian cells, integrins are heterodimeric or heterotrimeric transmembrane proteins which recognise various ECM proteins by their peptide sequence, usually the tripeptide RGD (arginylglycylaspartic acid). They are therefore involved in various physiochemical or pathological processes such as diapedesis (passage of cells

through the intact vessel wall), cohesion inside tissues, and tumour metastasis. α5β1 is an integrin that binds to matrix macromolecules, in particular fibronectin, where it recognizes the RGD sequence in the central region of the molecule. Numerous antibodies to human integrins, recognising α5 and β1 subunits, bound to *Candida* cells, and RGD peptides inhibited adherence of *Candida* cells to various ligands. This suggests that there is an important role for an α5β1-like integrin receptor as a mediator of *Candida*-host cell interaction.[54]

Research for integrin-like proteins led to the isolation of *INT1* gene in *C. albicans*. *INT1* expression in *S. cerevisiae* allowed this normally non-adherent yeast to adhere to human epithelial cells. Disruption of *INT1* in *C. albicans* suppressed adherence to epithelial cells and virulence in mice.[55] Other integrin-like proteins have been suggested in *C. albicans* such as a protein with a high sequence homology to alcohol dehydrogenase (ADH), although its function as an adhesin is unknown.[56]

1.2.2.2.5 Lectin-like proteins

Lectins are defined as carbohydrate binding proteins other than enzymes or antibodies and exist in most living organisms. They are involved in diverse biological processes and mediate the interaction and communication between cells. A lectin usually contains two or more binding sites for carbohydrate units and interact with them non-covalently in a manner that is usually reversible and highly specific. Binding results from numerous weak interactions, with dissociation constants in the millimolar range for monosaccharides, which combine to form a stronger attraction.[57]

In *Candida glabrata*, the *EPA* (epithelial adhesion) gene family encode a major group of adhesins.[58] The general structure of Epa proteins is similar to that of the Als proteins of *C. albicans*. Epa1p is a Ca^{2+}-dependent lectin that binds to lactose and *N*-acetyllactosamine-containing glycoconjugates. Lactose and *N*-acetyllactosamine inhibited 50 % of *C. glabrata* binding to epithelial cells at a concentration of 1.25 to 1.5 mM.[59]

Lectin-like proteins have also been investigated as adhesins in *C. albicans*. Early studies have shown that simple sugars (such as fucose, glucosamine and *N*-

acetylglucosamine)[60-62] can inhibit adherence of the yeast to human BEC, which will be discussed later in Section 2.1.5.

Adherence of *C. albicans* to basement membrane proteins, such as type IV collagen, is a crucial step in the development of candidiasis. Alonso *et al*.[63] studied the interaction of *C. albicans* yeast cells with the three main domains of type IV collagen. It was found that several sugars known to be part of the *N*-linked oligosaccharide chains of collagen IV inhibited the adhesion to immobilized 7S, the N-terminal cross-linking domain of collagen IV. *N*-acetylglucosamine, L-fucose and methylmannoside caused similar inhibition, whereas *N*-acetyllacosamine was a more effective inhibitor. Glucose, galactose, lactose and heparin sulfate did not affect the binding of the yeast. Combinations of the inhibitory sugars at suboptimal inhibition concentrations did not reduce *C. albicans* adhesion more than the individual sugars, suggesting that a single lectin is responsible for the interaction.

1.3 Anti-Adhesion Strategies with Small Molecules

Upon encountering the host cell, microorganisms must first attach via weak, non-specific interactions with the host cell surface. This is mediated by physiochemical properties of the microorganism and host cell surfaces, such as charge and hydrophobicity. This process is known to be a reversible adsorption step, which is followed by initial adhesion. This is mediated by specific interactions, where the binding moieties vary depending on both the microorganism and host cell. Generally, this process involves adhesins (proteins) on the microorganism interacting with carbohydrates or other recognition epitopes on the host cell surface.

All steps of this multi-stage process can be targeted in the anti-adhesion strategy. The surface properties of either the microorganism or the host cell can be changed to prevent non-specific interactions. The biogenesis of microbial adhesins or host cell receptors can be inhibited, either by interfering with the biosynthesis of subunits or blocking translocation and surface assembly. The specific interactions between microbial adhesins and host cell receptors can be targeted in several ways. Anti-adhesion compounds can competitively inhibit attachment by mimicking microbial or host cell binding partners. Alternatively, antibodies recognizing microbial surface

epitopes can be used to either actively or passively immunize the host.[64] These different strategies are shown in Figure 1.5. In the following sections the anti-adherence strategies used to combat bacterial infections are first discussed. Due to the vast amount of knowledge of bacterial adhesins, many anti-adhesion ligands have been designed to target specific steps in the adherence process. Following this the anti-adherence strategy of fungi, in particular *Candida*, are discussed. In this case, there is a lack of structural knowledge of the adhesins mediating this process and hence, this hampers a focused design approach in many incidences.

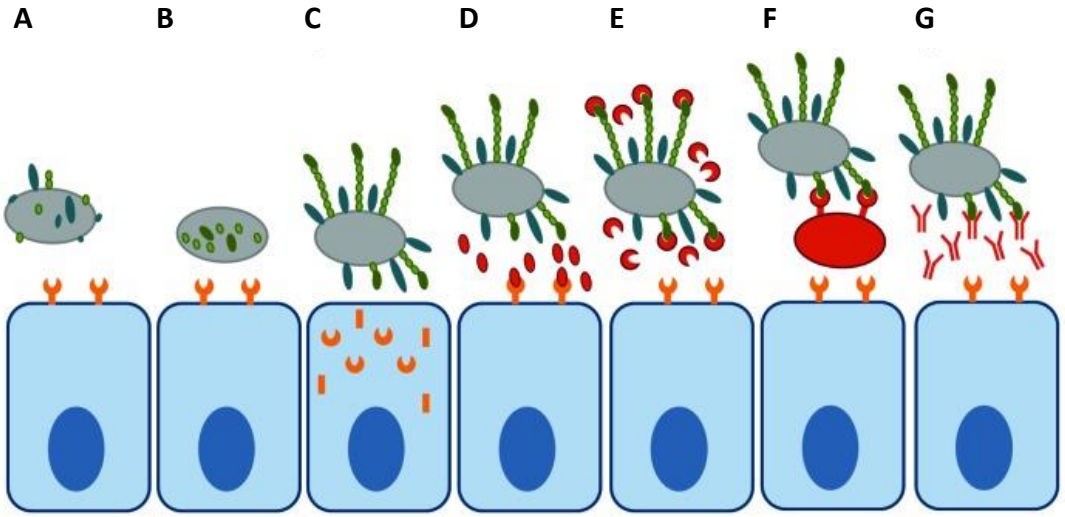

Figure 1.5: Strategies for anti-adhesion therapy reprinted from Krachler *et al.*[64]. Microbial attachment can be inhibited by interfering with adhesin biosynthesis (A), adhesin assembly (B), or host receptor assembly (C). Binding can be inhibited by competitive replacement of the adhesin from the host (D) or of the host receptor from the adhesin (E) using soluble molecules, or by using designer microbes (F). Antibodies against microbial adhesins can block surface epitopes required for binding (G).[64] Reprinted with permission from Taylor & Francis Online.

1.3.1 Anti-Adhesion Strategy in Bacteria

Anti-adhesion therapy has become an important discovery pathway to prevent and treat bacterial infections due to the numerous emerging strains of bacteria which have become resistant to conventional antibiotics. Bacteria resistant to anti-adhesion agents may also be expected eventually, but because these agents do not act by killing or arresting growth of the pathogen, as antibiotics do, it is reasonable to assume that strains resistant to anti-adhesion agents will be diluted with the

sensitive bacteria whose adhesion is inhibited and shed out of the host. The spread of bacteria resistant to anti-adhesion agents is expected to occur at significantly lower frequencies than that of bacteria resistant to antibiotics.[65]

Extensive research has been carried out on the process of bacterial adhesion. Many adhesins in bacterial species have been characterized and their modes of action have been reported. With this knowledge, numerous strategies have been developed to prevent bacterial adhesion and hence the development of infections.

1.3.1.1 Disrupting Surface Receptor Biogenesis

1.3.1.1.1 Pathogen Receptors:

Several studies have described that sub-inhibitory concentrations of certain antibiotics, in particular, the fluoroquinolone ciprofloxacine **1.1** and the aminoglycoside amikacin **1.2** (Figure 1.6), can lead to altered physicochemical properties of the bacterial surface and decreased bacterial adhesion to host cells in uropathogenic *Escherichi coli*. This is thought to be caused by abnormal protein synthesis, which leads to the production of partially or incorrectly folded proteins. This results in the impaired surface display of outer membrane proteins and the assembly of fimbrial adhesins. The resulting change in surface charge as well as inhibition of specific interactions with host receptors act synergistically in preventing adhesion.[66-68]

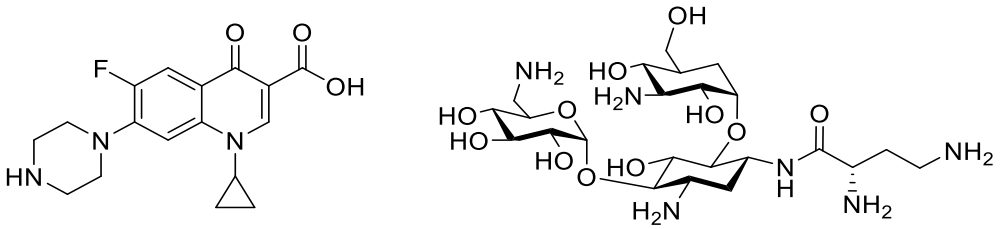

1.1 **1.2**

Figure 1.6: Structure of fluoroquinolone ciprofloxacine **1.1** and the aminoglycoside amikacin **1.2**.

Chaperone–usher (C/U) pili are large, multi-subunit organelles mediating host cell adhesion and are important virulence factors in a range of bacterial pathogens, including *E. coli* and species of *Salmonella*, *Yersinia*, *Pseudomonas*, *Klebsiella,* and *Haemophilus*. C/U pilus biogenesis is accomplished by translocation of pilin subunits

and subsequent association with a periplasmic chaperone, which delivers them to an outer membrane usher complex. The structure of the complex between the P pilus chaperone PapD and a synthetic peptide mimicking the C-terminus of the pilus protein PapG was solved and used as a basis to rationally design small molecule inhibitors to prevent pilus assembly (pilicides) by disrupting the chaperon–pilin complex. Two families of pilicides, amino acid derivatives and pyridinone derivatives, were designed to target the active site of the periplasmic chaperones[69] or to interfere with association of the chaperone-pilin-usher complex.[70, 71] An example of one pilicide, compound **1.3**, is shown in Figure 1.7 a. These compounds target the specific interaction between the chaperone-subunit complexes and the N-terminal domain of the usher, a unique protein-protein interaction site essential to the biogenesis of pili (Figure 1.7 b-d). The pilicide occupies the usher N-terminal binding site on the chaperone-subunit complex and thus pauses pilus assembly. This resulted in an inhibition of bacterial adherence and biofilm formation in uropathogenic bacteria.

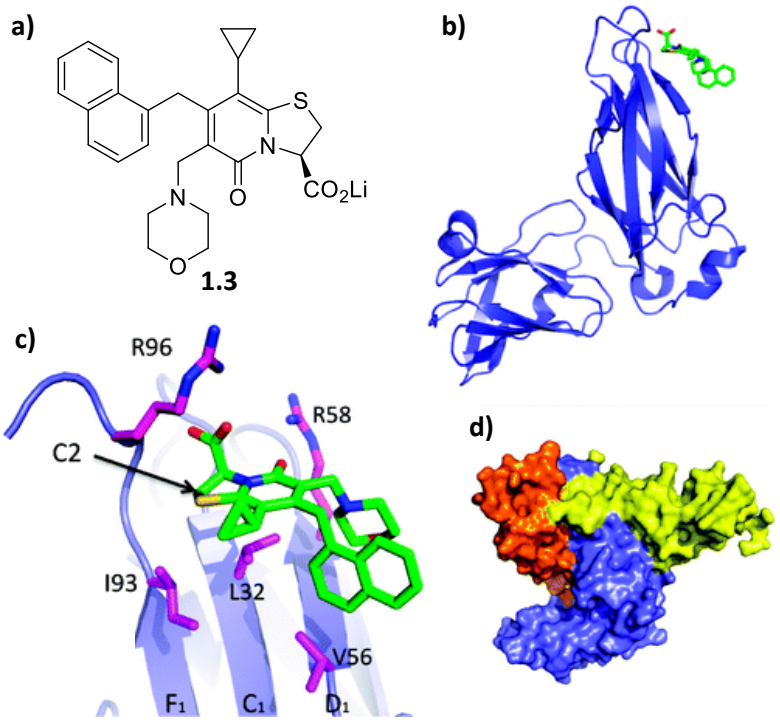

Figure 1.7: a) Structure of pilicide **1.3**; b) The pilicide **1.3** (green) binds to the N-terminal domain of the chaperone PapD (blue); c) The pilicide **1.3** (green) occupies a hydrophobic patch formed by I93, L32 and V56 amino acids (purple); d) Structure of the chaperone-subunit complex, where the chaperone is shown in blue, the subunit in orange and the usher N-terminal domain in yellow.[71]

1.3.1.1.2 Host Cell Receptor

Many bacterial adhesins rely on host glycosphingolipids (GSLs) for host cell binding and membrane translocation.[72] Depletion of GSLs from the host cell membrane has been proposed as an efficient strategy to prevent or treat infections.[73] Administering inhibitors specific for enzymes in the GSL biosynthetic pathway can deplete the amount of GSL of the host cell membrane. Ceramide glucosyltransferase catalyses the initial step in the glucosylceramide-based GSL synthetic pathway, where glucose is transferred from UDP-glucose to ceramide to produce glucosylceramide, which is the core component of GSLs. Inhibiting ceramide glucosyltransferase was shown to successfully reduce bacterial colonisation of cultivated human uroepithelial cells and in a murine model of urinary tract infection (UTI). Here, the iminosugar, *N*-butyldeoxynojirimycin, blocked the ceramide-specific glucosyltransferase and decreased the GSL content in a dose-dependent manner. This depletion significantly inhibited P-fimbriated bacterial attachment *in vitro*. In the murine model, depletion of GSLs *in vivo*, reduced susceptibility to experimental UTI with P-fimbriated *E. coli*.[74]

1.3.1.2 Competition-Based Strategies

1.3.1.2.1 Sugar-Based Inhibitors

Specific bacterial host interactions are frequently mediated by carbohydrates, which are present in large numbers both on the bacterial surface (in the form of capsules, lipopolysaccharides, and glycoproteins) and the host surface (as glycoproteins and glycosphingolipids). Therefore, a large body of research has focused on the use of glycomimetics and synthetic glycosides as anti-adhesive agents by competitively inhibiting pathogen binding.

In Gram-negative bacteria, lectins usually exist in the form of polymorphic fimbriae or pili. They are often made up of hundreds of protein subunits that bind host oligosaccharides.[75] Lectins in Gram-positive bacteria are generally within the peptidoglycan layer or anchored to the cytoplasmic membrane that cross the peptidoglycan layer and extend beyond the cell wall.[76] There has been substantial interest in determining the specificity of bacterial lectins to their associated oligosaccharides, but there has been experimental challenges associated with this.

Numerous techniques have been used to extend the knowledge in this area, including: direct-binding assays, measurement of *in vitro* cell adherence to tissue culture cells in the presence of oligosaccharides, and determining virulence *in vivo* when exogenous oligosaccharide receptors are present. Table 1.1 lists some of the oligosaccharide structures found on host cell surfaces that are recognised by pathogen lectins.

Table 1.1: Examples of pathogen oligosaccharide adherence sites on host mucosal surfaces recognised by pathogen lectins.[77] Reprinted from Advances in Food and Nutrition Research, Vol. 55, Shoaf-Sweeney, K. D., Hutkins, R. W., Chapter 2: Adherence, Anti-Adherence, and Oligosaccharides: Preventing Pathogens from Sticking to the Host, page 110, Copyright (2008), with permission from Elsevier.

Organism	Target Molecule	Target Tissue
Escherichia coli		
Type 1 pili	Man(α1-3)[Man(α1-6)]Man	Urinary
P-fimbriae	Gal(α1-4)Gal	Urinary
S-fimbriae	NeuAc(α2-3)Gal(β1-3)GalNAc	Neural
CFA/1	NeuAc(α2-8)-	Intestinal
K1	GlcNAc(β1-4)GlcNAc	Endothelial
F5 (K99)	NeuGc(α2-3)Gal(β1-4)Glc	Intestinal
Bordetella pertussis	Gal(β1-3)GalNAc(β1-4)Gal(β1-4)Glc	Respiratory
Haemophilus influenza	$[NeuAc(\alpha2\text{-}3)]_{0,1}$Gal(β1-4)GlcNAc-(β1-3)Gal(β1-4)GlcNAc	Respiratory
Helicobacter pylori	NeuGc(α2-3)Gal(β1-4)GlcNAc	Stomach
	Fuc(α1-2)Gal(β1-3)[Fuc(α1-4)]Gal	Stomach
Klebsiella pneumonia	Man	Respiratory
Mycococcus pneumonia	NeuGc(α2-3)Gal(β1-4)GlcNAc	Respiratory
Neisseria gonorrhoea	Gal(β1-4)GlcNAc	Genital
Pseudomonas aeruginosa	Gal(β1-3)GlcNAc(β1-3)Gal(β1-4)Glc	Respiratory
Salmonella typhimurium	Man	Intestinal
	Gal(β1-4)GalNAc	Intestinal
Streptococcus pneumonia	$[NeuAc(\alpha2\text{-}3)]_{0,1}$Gal(β1-4)GlcNAc-(β1-3)Gal(β1-4)GlcNAc	Respiratory
Streptococcus suis	Gal(α1-4)Gal(β1-4)Glc	Respiratory

The lectin-mediated adhesion can be inhibited both *in vitro* and *in vivo* by either simple or complex carbohydrates that compete with the binding of the lectins to host-cell glycoproteins or glycolipids.[78] The affinity of simple sugars (mono- or disaccharides) to lectins is usually low, in the millimolar range. An increase in several

orders of magnitude in the affinity can be achieved by suitable chemical derivatization. These modifications can be efficiently designed if the structure of the lectin is available, such as FimH in *E. coli* (discussed further in Section 2.1.4.1) and LecA and LecB in *P. aeruginosa* (dicussed further in Section 2.1.4.2). FimH is one of the most extensively studied lectins as a target for design of anti-adhesion glycomimetics. There are many examples of α-mannosides reported as inhibitors of *E. coli* adhesion which act by blocking the binding of FimH to epithelial cells. For example, hydrophobic α-mannosides, such as 4-methylumbelliferyl α-mannoside and *p*-nitro-*o*-chlorophenyl α-mannoside, were 500-1000 times more effective at inhibiting the adhesion of type 1 fimbriated *E. coli* to yeasts or ileal epithelial cells than methyl α-mannoside.[79] Using multivalent ligands also increased the affinity of the inhibitors to the bacterial lectins.[80] When 3'-sialyllactose (NeuAc(α2-3)Gal(β1-4)Glc) were covalently attached to human serum albumin (20 moles of sugar per mole of protein), the inhibition of adhesion of the bacteria to epithelial cells was two orders of magnitude better than the oligosaccharide by itself.[81] The multivalent effect will be discussed in more detail in Chapter 4.

Streptococcus suis is a Gram-positive bacterium, which causes sepsis and meningitis in pigs and humans. Carbohydrate-binding specificities of *S. suis* have been identified, and these studies have shown that many strains recognize Gal(α1-4)Gal (galabiose) containing oligosaccharides present in host glycolipids. Oligosaccharides containing the Gal(α1-4)Gal structure inhibited adhesion of *S. suis* at micromolar concentrations, whereas oligosaccharides containing Gal(α1-3)Gal or Gal(α1-6)Gal structures only inhibited the adhesion at millimolar concentrations.[82] The *S. suis* adhesin binding to Gal(α1-4)Gal-oligosaccharides, Streptococcal adhesin P (SadP), was recently identified.[83] It has a Gal(α1-4)Gal-binding N-terminal domain and a C-terminal LPNTG-motif for cell wall anchoring.

Screening of a library of chemically modified Gal(α1-4)Gal derivatives has identified compounds that inhibit *S. suis* adhesion with unusually high affinity (nanomolar range). In this study, it was found that phenylurea derivatisation at C3' and methoxymethylation at O2' of galabiose provided inhibitors of *S. suis* adhesion.[84] Also, the design of multivalent Gal(α1-4)Gal-containing dendrimers has resulted in a

significant increase of the inhibitory potency of the disaccharide.[85] Once the structures of the receptors are known, more potent high-affinity receptor analogs can be designed. SadP adhesin represents a promising target for the design of anti-adhesion ligands for the prevention and treatment of *S. suis* infections.

1.3.2 Anti-Adhesion Strategy in Fungi

The degree of knowledge regarding fungal adhesins is more limited than those in bacteria, since fungi are complex, eukaryotic cells that have cell walls which are structurally unique, with each species displaying distinctive glycan polymers and proteins. Hence, the majority of studies of fungal adhesion involve testing a compound's ability to inhibit adhesion, and then trying to determine the adhesin responsible. Therefore, this lack of structural knowledge hampers a focused design approach for the development of anti-adhesion agents for fungal pathogens. High affinity ligands can only be developed if the structure of the adhesin is known. With that being said, recently, there have been some breakthroughs in this area where some fungal adhesins e.g. FleA in *A. fumigatus* (discussed in Section 2.1.4.3), has been identified, fully characterized and crystal structures have been solved. Hence, the development of high-affinity anti-adhesion ligands is now becoming possible for fungal pathogens.

The majority of research on anti-adhesion ligands based on small molecules used to inhibit adhesion of fungi has focused on *C. albicans*. Small molecules display different modes of action to inhibit the process of adhesion of fungi to host cells although in most cases their mode of action is unknown. The biosynthesis of cell wall components, the localization of GPI-anchored proteins, down-regulation of genes that encode for adhesins, the disruption of the cell membrane and the use of small molecules that competitively inhibit the interaction between the fungal adhesin and the host cell receptors have been targeted. Small molecules, both synthetic and natural, have been tested for their anti-adhesive properties towards *C. albicans*.

1.3.2.1 Disruption of biosynthesis of cell wall components

As mentioned earlier, β-1,6-glucan is a fungus specific cell wall component that is essential for the retention of many cell wall proteins. Kitamura *et al.*[86] reported the

discovery of a small molecule inhibitor **1.4** of β-1,6-glucan biosynthesis in yeast. This leads to the release of cell wall proteins, which play a critical role in virulence, from the cell (shown in Figure 1.8). The adhesion of *C. albicans* cells to mammalian cells and their hyphal elongation were strongly reduced by the drug treatment.

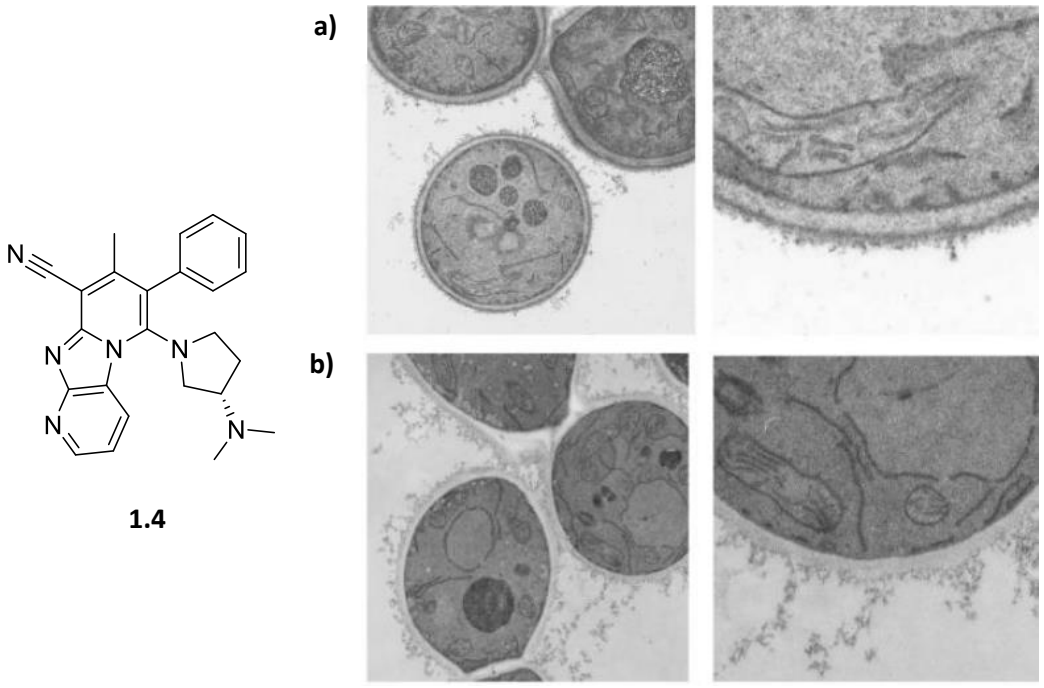

1.4

Figure 1.8: Shows the structure of the small molecule inhibitor **1.4** of β-1,6-glucan biosynthesis; a) microscopic images of untreated *C. albicans* cells; b) microscopic images of *C. albicans* cells treated with compound **1.4**.[86] Adapted with permission from American Society for Microbiology.

Anti-adhesion tests of fluconazole **1.5**, a well-known, bis-triazole antifungal drug, began in the early 1990s. Darwazeh *et al.*[87] explored the effect of systemic fluconazole intake on *Candida* adhesion to BEC obtained from healthy volunteers on systemic fluconazole therapy. It was found that the fluconazole significantly reduced the number of BEC with adherent yeast. There was a 48.7 % reduction in adhesion during the therapy compared to before the fluconazole therapy. Several other studies have also shown significant reduction of adherence of *C. albicans* isolates to denture acrylic and BEC after treatment with fluconazole.[88-90] It is known that fluconazole inhibits the production of lanosterol 14-α-demethylase (discussed in Section 1.1.1). This affects the cell wall composition of the *C. albicans* and hence the ability to adhere to BEC.

Several tetrazole compounds were reported to have anti-adherent properties against *C. albicans*. Compound **1.6** was found to be the most active of a series of 2,5-disubstituted tetrazoles that were tested as inhibitors of *C. albicans* adhesion. This compound efficiently reduced the adherence of *C. albicans* to Caco-2 cells by 86 %, at 16 µg/mL.[91] More 2,5-disubstituted tetrazoles were tested by Staniszewska *et al.*.[92] Compound **1.7** reduced the adhesion of *C. albicans* to Caco-2 cells by >50 % at 0.0313 mg/mL.[92] Tetrazole derivatives with pyrrolidine scaffolds were also tested for anti-adherent properties. Compound **1.8** and other derivatives were tested for their ability to prevent *C. albicans* adhesion to TR-146 cell-line. Compound **1.8** reduced the adherence of the yeast most efficiently (over 98 % reduction at 46.05 mM).[93] These new antifungal drugs (structures in Figure 1.9) cause yeast cell death, but also inhibit adhesion. It is suggested that adhesion is inhibited by disrupting cell wall biogenesis, the process that results in the biosynthesis of macromolecules, assembly and arrangement of these components to form the cell wall.

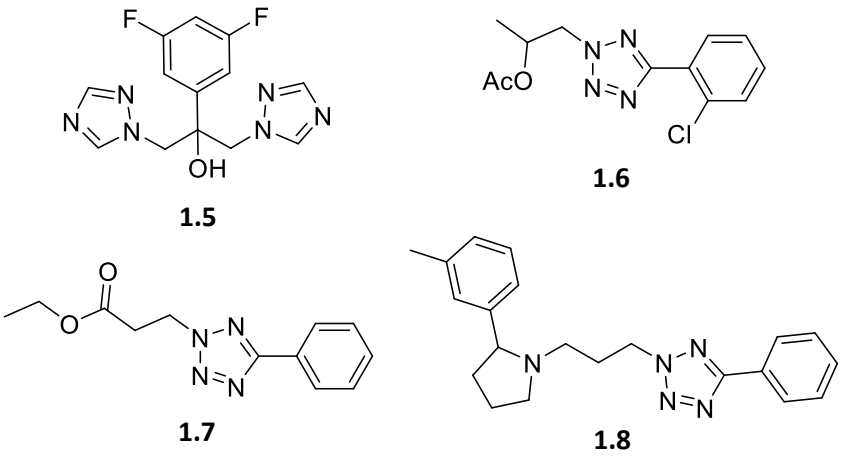

1.5 **1.6** **1.7** **1.8**

Figure 1.9: Structures of triazole and tetrazole compounds that show anti-adhesive properties towards *C. albicans* by disrupting cell wall biogenesis.

1.3.2.2 Disruption of localization of GPI-anchor Proteins

GPI-anchored cell wall mannoproteins are required for the adhesion of pathogenic fungi, such as *C. albicans*, to human epithelium. Tsukahara *et al.*[94] discovered an isoquinoline derivative, compound **1.9**, that inhibits cell wall localization of GPI-anchored mannoproteins in *S. cerevisiae* and *C. albicans*. This compound inhibits the adhesion of *C. albicans* cells to a mammalian epithelial cell monolayer (Figure 1.10). The molecular target of this compound was found to be the protein product of a

novel gene, *GWT1*. They suggest that the function of this Gwt1 protein may be in GPI synthesis, intracellular transport of GPI-anchored protein, and transfer of the GPI-anchored protein to the cell wall.

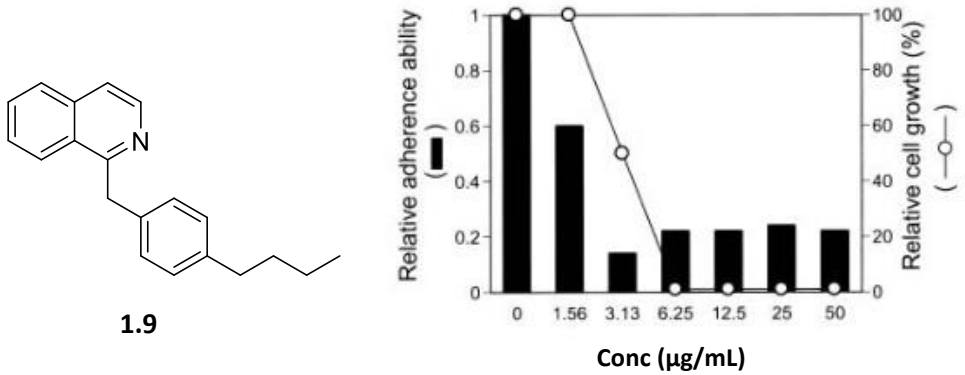

Figure 1.10: Structure of isoquinoline derivative **1.9**; Graph showing the effect of compound **1.9** on the adherence ability of *C. albicans*.[94]

1.3.2.3 Inhibition of degradative enzyme production

Extensive research on the anti-adhesive properties of sulfone derivatives has been conducted in Staniszewska's laboratory.[95-97] Compounds **1.10** and **1.11** (Figure 1.11) were evaluated against the adhesion of a wild-type *C. albicans* strain and 3 mutant strains to Caco-2 cell line. First, the fungi were pre-treated with the sulfone derivatives. The first compound **1.10** significantly altered the adherence properties in a concentration-dependent manner. Adhesion of the wild type *C. albicans* was 10.8 fold lower than the non-treated controls at a concentration of 8 μg/mL, and was 5.2 fold lower at a concentration of 16 μg/mL. The mutant strains displayed a larger inhibition of adhesion. When the fungi were post-treated with the sulfone derivatives at 16 μg/mL, there was a very significant reduction of adhesion, ranging from 44.0 fold to 112.1 fold.[95] Compound **1.11** also exhibited reduced adhesion, but to a lesser degree than compound **1.10**.

In another study, structurally similar sulfones were tested against *C. albicans.* Compound **1.12** and the previously tested sulfone derivatives **1.10** and **1.11** (Figure 1.11) were also tested for the ability to inhibit the adhesion to epithelial cells. Pre-treating the cells with sulfone **1.12** and **1.10** (8–16 μg/mL) did not significantly affect adhesion of all the *Candida* strains tested compared to their non-treated

counterparts. Compound **1.11** altered adhesion of the strains significantly at all the concentrations tested. In 62 % of all the strains tested the concentration of 16 µg/mL inhibited attachment of cells to Caco-2.[96]

In 2018, more tests were carried out on compound **1.10** and a new β-ketosulfone compound **1.13** (Figure 1.11). Pre-treatment of yeast cells with the β-ketosulfone at 16 µg/mL significantly affected the yeast adhesion to the Caco-2 cell line. Adhesion of *C. albicans* was reduced by 49.46 % (1.97-fold compared to the untreated control).[97]

These sulfone derivatives successfully inhibit degradative enzyme production, for example Saps (Secreted aspartyl proteases). *SAP2* is downregulated in the presence of these sulfone derivatives. This enzyme degrades extracellular matrix and host surface proteins, such as keratin, collagen, vimentin, and mucin, but also several host defense proteins such as secretory IgA and salivary lactoferrin. The ability of these compounds to inhibit enzyme production may influence the adhesion of *C. albicans* to host cells.

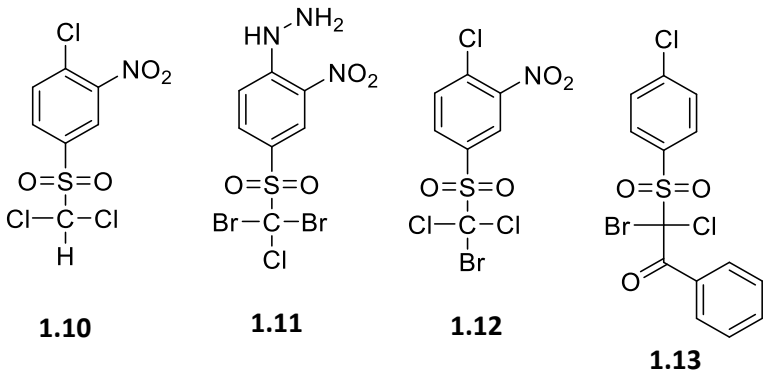

1.10 **1.11** **1.12** **1.13**

Figure 1.11: Structure of sulfone-derivatives that have anti-adhesive properties towards *C. albicans.*

1.3.2.4 Down-regulation of Genes that Encode Adhesins

Numerous natural products have been tested for their anti-adhesive properties towards *C. albicans* adhesion. These include polyphenols such as curcumin, pyrogallol, magnolol and honokiol, and anthraquinone derivatives such as purpurin, alizarin, chrysazin and emodin. These compound's mechanism of action involves the

down-regulation of genes that encode adhesins that mediates the adhesion of *C. albicans*.

1.3.2.4.1 Polyphenols

Curcumin **1.14** (Figure 1.12) is a yellow–orange polyphenol compound produced by the rhizome of *Curcuma longa* plants, which is widely used as a spice in Asian cooking. This compound has been shown to possess a wide range of pharmacological activities. Antifungal activity was assessed by experiments done with crude extracts of *C. longa*. This work focused on the evaluation of curcumin antifungal activity against 23 fungi strains of clinical interest as well as its ability to inhibit the adhesion of *Candida* spp. to human BEC. Curcumin extracts were able to inhibit the adhesion to BEC of all the *Candida* species. Curcumin was 2.5 fold more potent than fluconazole at inhibiting the adhesion of *C. albicans*, showing >50 % inhibition of adhesion to BEC.[98]

In another study, 14 polyphenols were tested for their anti-fungal properties. From these compounds curcumin **1.14** and pyrogallol **1.15** (Figure 1.12) showed the best anti-fungal properties. These compounds were also evaluated using phenotypic assays, where it was demonstrated that pre-coating coverslips with **1.14** significantly reduced *C. albicans* adhesion by 55.3 %, whereas **1.15** coating only led to a slight reduction in adhesion of 15.63 %.[99] Expression of the adhesins Als3 and Hwp1 was shown to be significantly downregulated by **1.14**, whereas **1.15** showed no significant downregulation of the adhesins following treatment.

Magnolol **1.16** and honokiol **1.17** (Figure 1.12) are lignans found in the bark of species of magnolia. The effects of these compounds on *C. albicans* adherence to the surface of mammalian cells was investigated. Magnolol **1.16** and honokiol **1.17** at concentrations of 4–32 μg/mL significantly inhibited the adhesion of *C. albicans* cells to the surface of HSC-T6 cells (immortalized rat hepatic stellate cell line).[100] Treatment with magnolol and honokiol, resulted in three adhesion-related genes *HWP1*, *ALS3*, and *ECE1* being significantly down-regulated.

1.3.2.4.2 Anthraquinone Derivatives

Purpurin **1.18** (Figure 1.12), is a naturally occurring red/yellow dye from the roots of the madder plant (*Rubia tincorum*). The anti-adhesion properties of purpurin were evaluated at a range of concentrations. It was found that purpurin **1.18** has an effect on adhesion of *C. albicans* in a dose-dependent manner. Also, expressions of adhesion-related genes, namely *ALS1*, *EFG1* and *HWP1* were decreased in comparison to the control.[101]

Alizarin **1.19** (Figure 1.12) is a red dye derived from the roots of plants of the madder genus. Chrysazin **1.20** (Figure 1.12) is a synthetic derivative of alizarin. Alizarin **1.19** and chrysazin **1.20** appear to inhibit cell adhesion, biofilm formation, and hyphal development in *C. albicans* by regulating the hypha-specific genes.[102] Alizarin also downregulated the expression of several hypha-specific and biofilm related genes (*ALS3, ECE1, ECE2*, and *RBT1*), which affect the adhesive properties of the yeast.

Emodin **1.21** (Figure 1.12) is a natural secondary plant product, originally isolated from the rhizomes of *Rheum palmatum*. The studies were performed on 50 strains of *C. albicans* with a proven ability to form biofilm, which were isolated from the vaginas of women from different age groups. Emodin **1.21** suppressed adhesion in the case of 30 of the 50 tested clinical strains, whereas only 15 of the 50 strains were susceptible to emodin **1.21** action when the biofilm was fully established.[103] Due to the structural similarities of purpurin and alizarin, it is assumed that this compound may also cause downregulation of genes relating to adhesion. Interestingly, emodin added to *Candida* culture also inhibited the phosphorylation of many cellular proteins, leading to the inhibition of protein kinase CK2, which governs the interactions of *C. albicans* with endothelial and oral epithelial *cells in vitro* and virulence during oropharyngeal candidiasis.

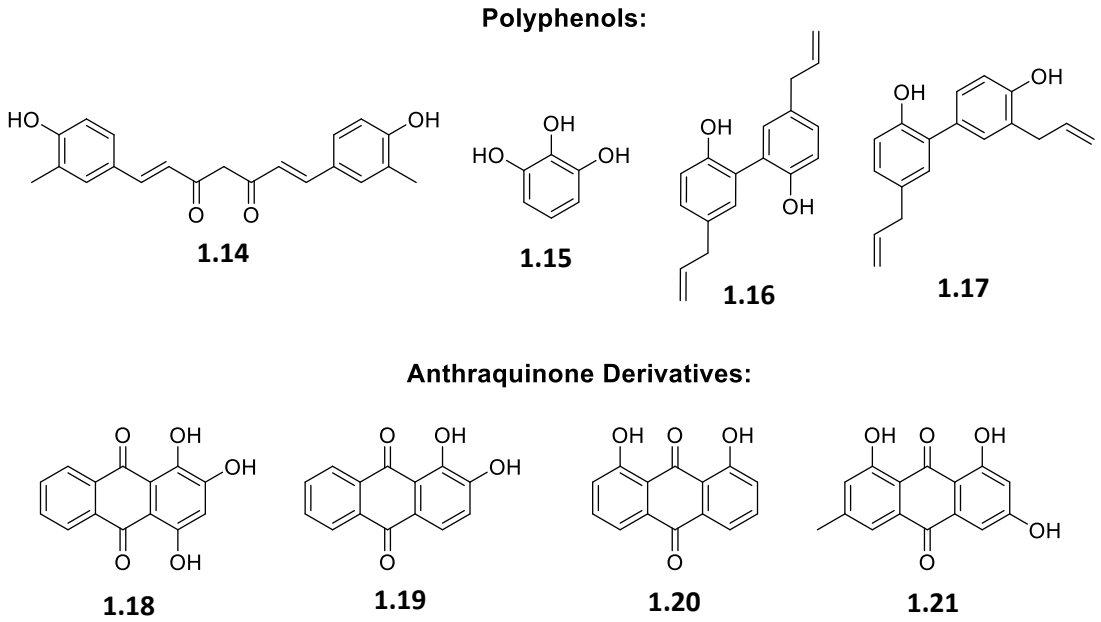

Figure 1.12: Structure of polyphenols and anthraquinone derivatives that have been shown to inhibit the adhesion of *C. albicans* by down-regulation of genes that encode adhesins.

1.3.2.5 Membrane Distortions

1.3.2.5.1 Quaternary Ammonia Compounds

Many quaternary ammonium compounds have been found to have anti-adhesive properties against *C. albicans* and some of their structures are shown in Figure 1.13. Non-antibiotic, antimicrobial agents (cetrimonium bromide **1.22**, cetylpyridinium chloride **1.23** and dequalinium chloride **1.24**) were shown to reduce the adherence of *C. albicans* to human BEC *in vitro*, during research first carried out in 1992.[104]

Research has also been carried out on surfactants **1.25**-**1.28** to test their anti-adhesive properties against *C. albicans*: cetyltrimethylammonium chloride (CTAC) **1.25**, sodium dodecyl sulfate (SDS) **1.26**, *N*-hexadecyl-*N*–*N*'-dimethyl-3-ammonio-1-propane-sulfonate (HPS) **1.27** and octylphenoxypolyethoxyethanol (Triton X-100) **1.28**. All the surfactants tested displayed a decrease in the number of yeasts adhered to BECs; however, a significant reduction was obtained by CTAC **1.25** and HPS **1.27** in all concentrations tested (0.3-3 μg/ml) and for SDS **1.26** and Triton X-100 **1.28** at the concentrations of 3 μg/ml and 1.5 μg/ml.[105]

The cationic charge leads to denaturation of adhesins on the *C. albicans* cells by these surfactants. The principal factor which inhibits adherence is the disruption of the fungal membrane and a steric interference of the approach of the microbial cell to the epithelial cell (long hydrophobic chains decrease contact between microbial cell and the substrate). Also, alternation of cell surface hydrophobicity and cell zeta potential is also suggested to contribute.[105]

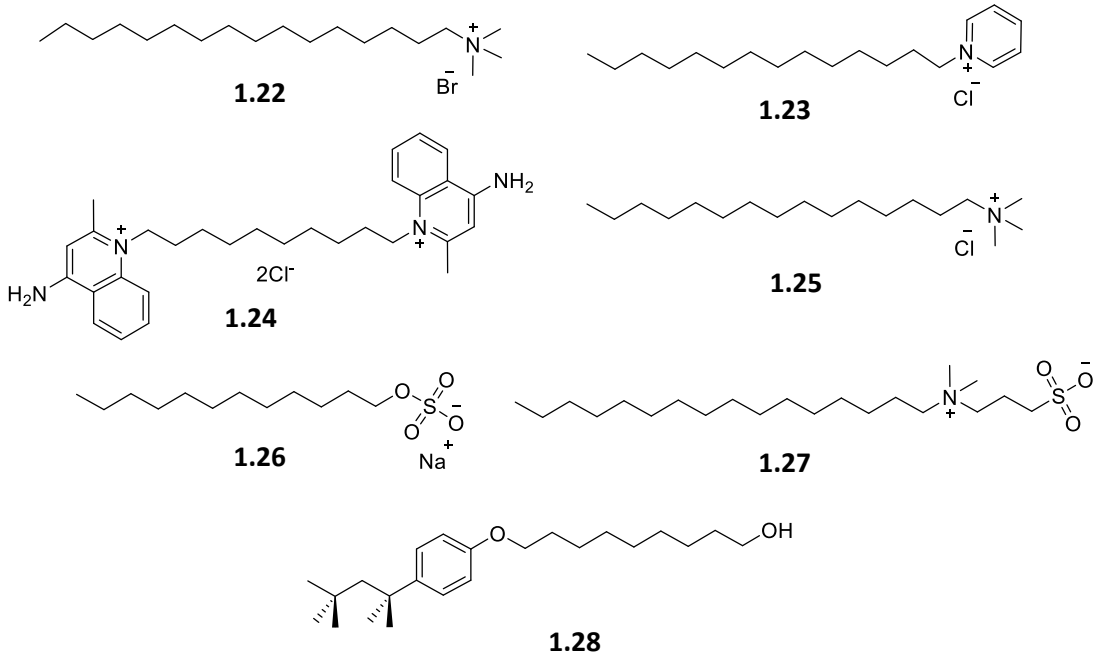

Figure 1.13: Structure of compounds **1.22**-**1.28** that have the ability of reducing the adhesion of *C. albicans* by disruption of the fungal membrane.

A group of biodegradable alanine-derived gemini quaternary ammonium salts (gemini-QAS) with various alkyl chains and spacer lengths was tested for anti-adhesive and anti-biofilm activity (structures of two examples are shown in Figure 1.14, compounds **1.29** and **1.30**). Gemini quaternary ammonium salts effectively inhibited fungal cell adhesion to polystyrene and silicone surfaces. The deposition of gemini-QAS on the polystyrene plate inhibited the adhesion of *C. albicans* cells. Similarly, compounds **1.29** and **1.30** (Figure 1.14 a) were tested for their influence on *C. albicans* adhesion to silicone catheter. Both of them exhibited anti-adhesive properties, with compound **1.29** showing slightly better activity.[106]

Medium alkyl chain cationic lipo-oxazoles comprising six to thirteen carbon twin chains and a quaternary ammonium unit were synthesized and evaluated for their *in*

vitro anti-*Candida* and biofilm inhibition activity. Heptyl and octyl chain analogues showed promising anti-fungal activity. Cationic lipo-oxazole compound **1.31** (structure shown in Figure 1.14 b) was evaluated for its ability to inhibit *Candida* cell adhesion to polystyrene surfaces. Compound **1.31** demonstrated about 60 % reduction in adhesion at the concentration range of 12.5 µg/ml compared to growth control in which no drug was added.[107] This cationic agent reportedly reacts with the phospholipid component in the cell membrane, thereby producing membrane distortions often leading to a complete loss of structural organization of the cells.

The same research group then evaluated lipo-benzamide compounds fused with varying lengths of hydrocarbon chains (C_2-C_{18}) for antifungal activity against *C. albicans*. Quaternary ammonium group containing C_9 hydrocarbon chain derivative **1.32** (Figure 1.14 b) was able to inhibit *Candida* cell adhesion to the polystyrene surface in a concentration dependent manner. This compound inhibits 90 % *Candida* cell adhesion on polystyrene surface at 12.5 µg/ml concentration compared to growth control in which no drug was added.[108]

Double-headed cationic surfactants with varying hydrocarbon chain length (n-$C_{13}H_{27}$ and $C_{15}H_{31}$) were synthesised and their anti-fungal properties were investigated. The ability of these surfactant coatings to inhibit fungal adhesion was tested using different surfaces: polystyrene, silicone, glass and stainless steel. The adhesion studies were focused on C14(DAPACl)$_2$ **1.33**, C16(DAPACl)$_2$ **1.34**, C14(TAPABr)$_2$ **1.35** and C16(TAPABr)$_2$ **1.36** (Figure 1.14 c). The adhesion of *C. albicans* to polystyrene was not greatly affected by the tested compounds, with the chlorides showing slightly better results. *C. albicans* adhesion to silicone catheters was reduced by C16 dicephalic surfactants **1.34** and **1.36**. Significant reduction (approx. 50 %) was observed for C16(TAPABr)$_2$ **1.36** at 100 µM. Interestingly, C14 compounds (**1.33** and **1.35**) caused the stimulation of *C. albicans* adhesion. The amount of adherent cells on the stainless steel surface was strongly reduced by both chlorides **1.33** and **1.34** at the concentration of 100 µM. The anti-adhesive activity of dicephalic surfactants to the glass surface was independent of the compound structure and for most cases, significant reduction in the amount of adherent cells was only achieved at concentrations at high as 400 µM.[109] Interestingly, these compounds did not cause

DNA leakage from the *C. albicans* cells, with the exception of C14(DAPACl)$_2$ **1.34**. Therefore, the mode of action of dicephalic surfactants does not concerns cell lysis. Further studies showed that the dicephalic surfactants impacted ROS production and accumulation of lipid droplets.

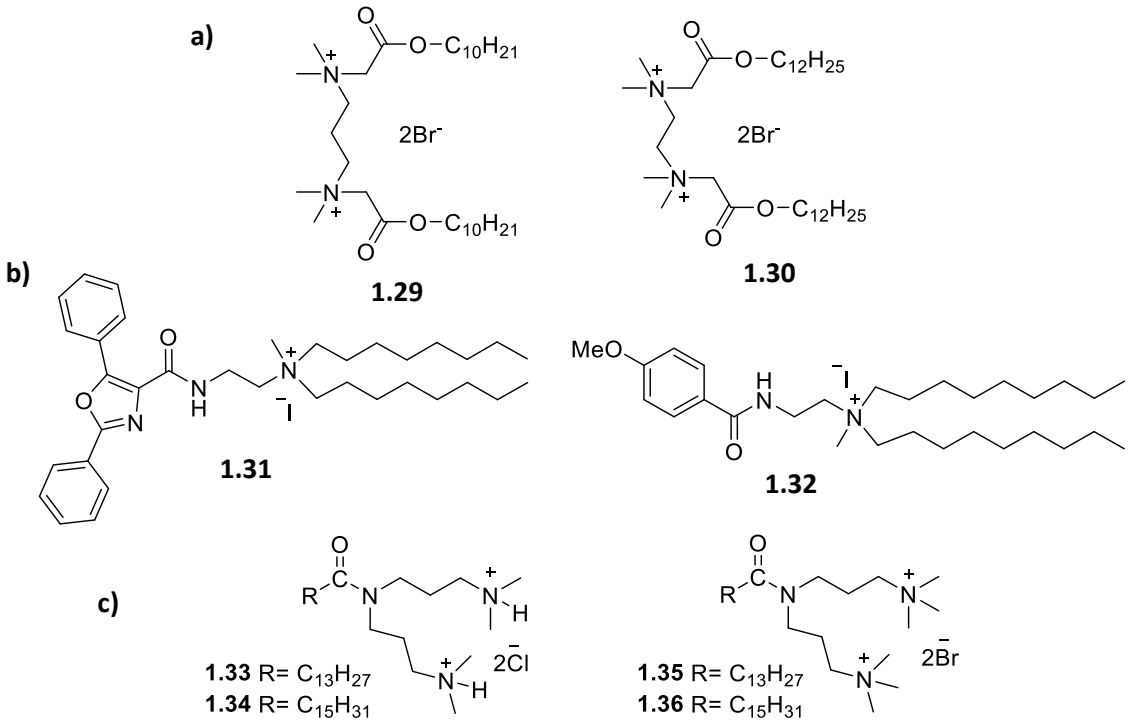

Figure 1.14: Structures of quaternary ammonium compounds that inhibit the adhesion of *C. albicans.* a) Structures of biodegradable alanine-derived gemini quaternary ammonium salts; b) structures of medium alkyl chain cationic lipo-oxazole and lipo-benzamide compounds; c) structure of double-headed cationic surfactants.

1.3.2.5.2 Non-Antibiotic Antimicrobial Agents

Non-antibiotic antimicrobial agents have a similar effect as the quaternary ammonia compounds on the adhesion of *C. albicans*. Several studies have shown that chlorhexidine gluconate **1.37** is able to reduce the adhesion of *C. albicans* cells to BECs at very low concentrations (as low as 0.00005 % v/v).[104, 110-112] In recent years, in fact, chlorhexidine is often used as a positive control when testing the adhesive properties of other compounds.[113-116] This antifungal impairs the integrity of the cell wall and the plasma membrane entering the cytoplasm resulting in leakage of cell contents and leading to cell death.

Another known antimicrobial agent, taurolidine **1.38** (Figure 1.15) was analysed for its anti-adhesive properties, first in 1987. Taurolidine **1.38**, generally recommended for use at a 2.0 % concentration, was shown to significantly reduce the adherence of both exponential and stationary phase *C. albicans* (vaginal isolate) to epithelial cells at concentrations greater than 0.1 %.[117] It reacts with the fungal cell wall and taurolidine causes a loss of microbial fimbriae and flagellae which effects the adhesion of the yeast.

Brolene is a non-antibiotic, antimicrobial preparation, which contains propamidine isethionate **1.39** as the antimicrobially active agent and contains benzalkonium chloride **1.40** (Figure 1.15) as a preservative, both of which are cationic agents. Two strains of *C. albicans*, including one clinical isolate from a diagnosed oral infection, were employed in this study. At both concentrations examined (10 and 100 % w/v), Brolene significantly reduced the adherence of *C. albicans* to BEC. These effects were observed for both strains, when either the BEC or yeast were treated. Reductions in adherence ranged from 25.91 - 76.02 %. [118]

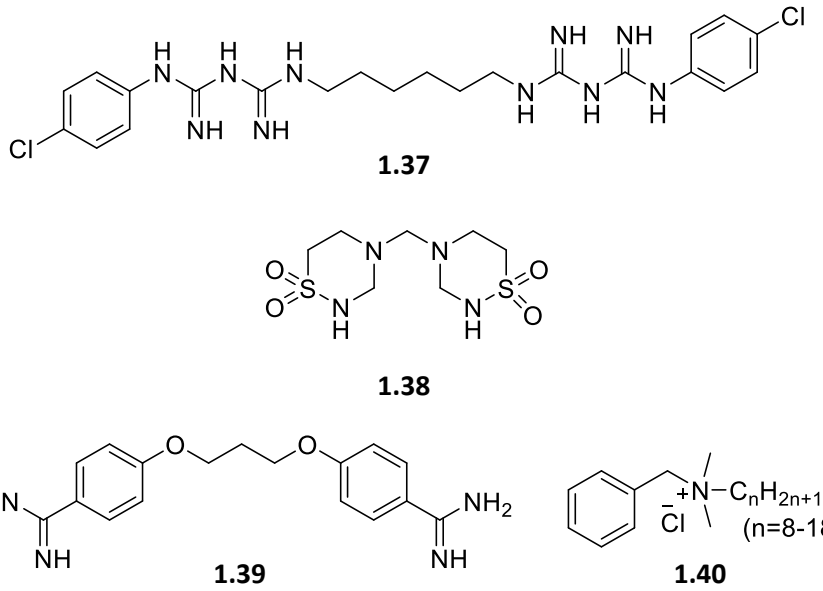

Figure 1.15: Structure of non-antibiotic antimicrobial agents that have been shown to inhibit the adhesion of *C. albicans.*

1.3.2.5.3 Terpenes and Terpenoids

Terpenes are a large and diverse class of natural, organic compounds, produced by a variety of plants, particularly conifers, and by some insects. The amyrins are three closely related natural chemical compounds of the triterpene class: α-amyrin (ursane skeleton), β-amyrin (oleanane skeleton) and δ-amyrin. They are widely distributed in nature and have been isolated from a variety of plant sources such as epicuticular wax. The antifungal activity of amyrin pentacyclic triterpene and 15 synthetic derivatives was evaluated against *Candida* species. Among the 15 derivatives, α- and β-amyrin formiate **1.41** and **1.42** (Figure 1.16) and α- and β-amyrin acetate were the most active, inhibiting growth of all the *Candida* species tested in concentrations that ranged from 30 to 250 μg/mL. α- and β-amyrin formiate **1.41** and **1.42** also inhibited the adhesion ability of *C. albicans* to BEC by 65.3 %.[119]

Terpenoids**,** are a large and diverse class of naturally occurring organic chemicals derived from terpenes. Most are multicyclic structures with oxygen containing functional groups. About 60 % of known natural products are terpenoids. Two abietane diterpenoids isolated from *Salvia austriaca*, taxodone **1.43** and 15-deoxy-fuerstione **1.44** (Figure 1.16) were tested in *C. albicans*. Taxodone **1.43** was found to significantly limit the degree of *Candida* adhesion by about 41 % depending on the concentration. The inhibition of biofilm formation by *C. albicans* was independent of the taxodone **1.43** concentration used, ranging from 76.4 % at 1/2 MIC to 75.5 % at 1/4 MIC. 15-Deoxy-fuerstione **1.44** was not as effective in the inhibition of *C. albicans* adherence as taxodone, and reached 38.3 % at 1/4 MIC.[120]

It has been suggested that the application of abietane diterpene may lead to the formation of hydroxyl radicals, which are then involved in the disruption of microbial cell membrane and leakage of intracellular materials. The mechanism of action of the terpenoides has not been explained completely, but it is speculated that it involves the rupture of the membrane by the lipophylic compounds and their functional groups interfere with the structure of the enzymatic proteins. Additionally, it could be involved in the inhibition of the synthesis of 1,3-β-D-glucan which participates in the synthesis of the cellular wall of the fungi.[119, 120] All of these processes impact the adhesion of *C. albicans*.

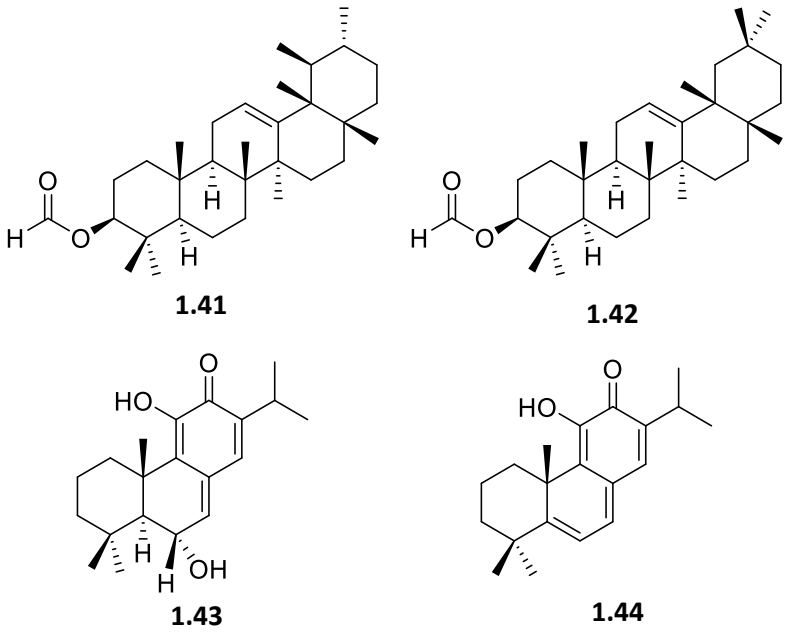

Figure 1.16: Structure of two terepenes (**1.41** and **1.42**) and two terpenoids (**1.43** and **1.44**) that inhibited the adhesion of *C. albicans*.

1.3.2.6 Blocking the Interaction of Fungal Adhesins and Host Cell Receptors

The inhibition of the interaction between the fungal adhesin and the host cell receptor can be attempted through several approaches, including: 1. Competitive binding with analogues of host cell receptors; 2. Binding to specific lectins; 3. Use of anti-adhesion antibodies; 4. Modulations induced by drugs, enzymes or other substance; 5. Use of inhibitors of enzymes involved in biosynthesis of the cell wall components.[121]

High affinity binding to FleA, an adhesin in *A. fumigatus*, has been successfully achieved by glycoconjugates that interact with this adhesin. The glycoconjugates prevents the adhesin in the fungi interacting with host cells and hence inhibits infection (discussed in Section 2.1.4.3). High affinity ligands can be designed when the structure of the adhesin is known.

The nitro-benzene compound **1.45** (Figure 1.17) was identified in 2018 by Marc *et al*.,[122] which possesses various structural moieties present in known anti-biofilm agents. Compounds containing an *N*-(oxazolylmethyl)-thiazolidinedione scaffold were found to be selective inhibitors of *C. albicans* biofilm formation. *In silico* screening suggested that the compounds could act by binding to the *C. albicans* Als

surface proteins, especially Als1, Als3, Als5 and Als6, which are well-known adhesin proteins. The binding pocket of these proteins have a large percentage of polar amino acids, which could account for their ability for polar interactions with various ligands, including the *N*-(oxazolylmethyl)-thiazolidinediones present in compound **1.45**.[122]

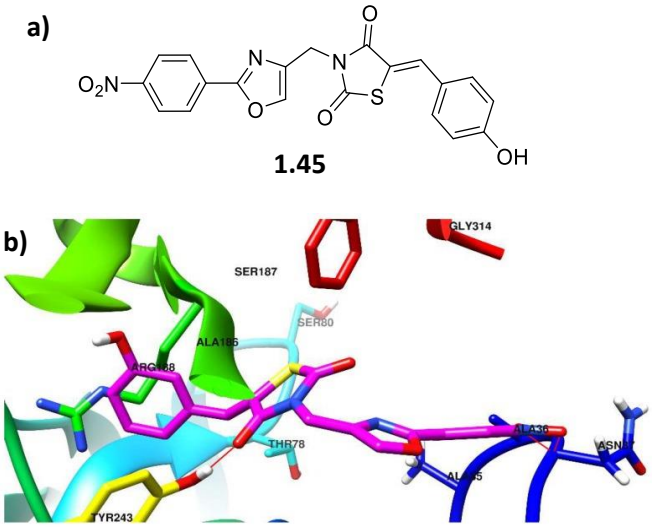

Figure 1.17: a) Structure of N-(oxazolylmethyl)-thiazolidinedione compound **1.45**; b) Compound **1.45** docked in the binding site of the *C. albicans* Als1 surface protein.[122] Reprinted with permission from MDPI.

1.3.2.7 Unknown/Other Mode of Action

Thiazole **1.46** and diazanaphthalene **1.47** functionalities are also present in compounds that exhibit anti-adhesion activity and their structures are shown in Figure 1.18. Compound **1.46** inhibited adhesion of *C. albicans* to human BEC by 75 % at MIC values (1-4 mg/L for most strains).[123] This antifungal, which was also tested on *Cryptococcus* strains, mode of action is related to the interference with the antioxidant system and accumulation of superoxide radicals. This compound initiates some accumulation of harmful events on the fungal cell that causes a failure in protecting the fungi from executing the virulence factors, such as *C. albicans* adhesion. Silmitasertib (CX-4945) **1.47**, an anti-tumour drug which is a selective inhibitor of protein kinase CK2, has been found to have anti-fungal properties. It effectively inhibited the adhesion phase of the biofilm formation process of *C. albicans* by 42 % at the concentration of 62.5 µg/mL (1/4 MIC).[124] The

mode of action of this compound is unknown, but could prevent possible cancer-associated candidiasis.

Chemical screening of 30,000 compounds by Fazyl *et al*.[125], identified filastatin **1.48** (Figure 1.18) as a small molecule inhibitor of *C. albicans* adhesion, morphogenesis and pathogenesis. Preliminary tests showed that filastatin **1.48** significantly reduced the adhesion of *C. albicans* to polystyrene at a concentration of 25 μM. Interestingly, this compound could also affect adhesion after the *C. albicans* cells had already bound to the polystryene. Filastatin reduced the amount of bound cells when added after adhesion, although not as efficiently as when the compound and cells are co-incubated at the beginning of the experiment. The ability of filastatin **1.48** to inhibit adhesion to epithelial cells was also determined, at the same concentration as the previous test (25 μM). Filstatin **1.48** significantly inhibited the adherence of GFP-encoding (Green Fluroescent Protein) *C. albicans* to monolayers of human lung epithelial cells as determined by fluorescence quantitation and microscopy.[125] The mode of action is unknown, but due to the multiple activites of filastatin, it is possibile that multiple targets exist.

Previous studies showed that cyclooxygenase inhibitors, such as aspirin, caused a significant reduction in fungal adhesion of fluconazole resistant *C. albicans* at concentrations between 1-10 mM.[126] Nitric oxide (NO) has also been shown to affect adhesion of fungi. (NO)-releasing xerogel surfaces are effective inhibitors of *C. albicans* adhesion with an NO flux as low as 2 pmol cm^{-2} s^{-1} significantly reducing adhesion.[127] Madariaga-Venegas *et al*.[128] combined these concepts and evaluated the antifungal/antibiofilm effect of a nitric-oxide releasing aspirin (NO-ASA) **1.49** (Figure 1.18) on *C. albicans* isolates from denture stomatitis patients *in vitro*. The ability of *C. albicans* to adhere to polystyrene microtiter plates was evaluated. It was found that 125 μM NO-ASA **1.49** inhibited adhesion in all tested strains, with reductions in adhesion ranging from 20-77 % depending on the strain. This effect was dose-dependent, as 500 μM NO-ASA **1.49** resulted in a stronger inhibition, with reductions ranging from 45-97 %. Interestingly, it was found that 500 μM of aspirin actually increased adhesion of the fungi to the polystyrene plate. NO-ASA causes no

antifungal effect, possibly the effect of NO-ASA could be mediated at least in part by inhibition of PGE_2 synthesis.

In an *in vitro* model of denture stomatitis, compound **1.50** (Figure 1.18), a novel antifungal molecule, effectively prevented candidal adhesion and biofilm development on denture acrylic surfaces. In this model, biofilm viability was reduced by 85 %, 66 % and 97 %, when compound **1.50** was added before, after, or both before and after the 1.5 h adhesion phase respectively.[129] This antifungal is toxic to fungi and not to human cell lines or bacteria and may cause cell membrane damage.

The effect of sub inhibitory concentrations of gentian violet **1.51** (Figure 1.18) on the germ tube formation by *C. albicans* and its adherence ability to oral epithelial cells was investigated. The effect of sub inhibitory concentrations of gentian violet **1.51** on the adherence ability (2.4 μg/mL) was determined. Sub inhibitory concentrations of gentian violet **1.51** significantly reduced the adherence ability of *C. albicans* by 57 %, with similar results seen for all strains tested.[114] At high concentrations, gentian violet **1.51** killed *C. albicans*, whereas at subinhibitory concentrations it reduced its virulence by preventing the adherence ability and germ tube formation. Gentian violet **1.51** may have interfered with the production of adhesins or may have caused a mechanical disruption of the adhesins already present in the outer envelopes.

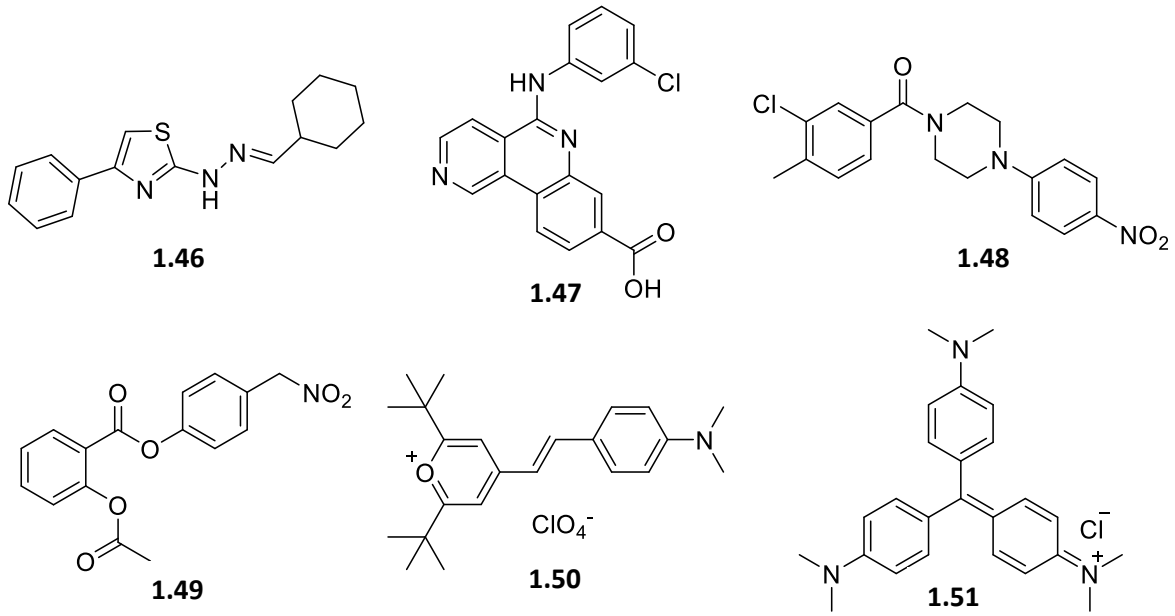

Figure 1.18: Structures of compounds with an unknown mechanism of action that cause inhibition of adherence in *C. albicans*.

Many essential oils and extracts from plants have also been found to inhibit adhesion of *C. albicans*, but their active compound is generally unknown, as they are composed of complex mixtures of both polar and non-polar natural compounds.[130-133]

1.4 Aims

The need for the development of new methods to fight fungal infections is of huge importance to global public health in the rise of resistance to conventional antifungal therapies. The aim of the research described in this thesis is to develop novel compounds to tackle fungal infection, in particular in the treatment of *C. albicans* infection. As discussed earlier, several strategies have targeted the adhesion of fungi to host cells as a key step in the infection process. As such, a diverse range of compounds have been evaluated as inhibitors of *C. albicans* adhesion. Most of the compounds described previously in Section 1.4 are antifungal agents which also possess anti-adhesion properties. Hence, *C. albicans* could become resistant to these types of drugs. The need for non-antifungal, anti-adhesive agents is very important. It is well documented that carbohydrate interactions are hugely important in the adhesion process, and this has been successfully investigated with bacterial pathogens. However, there are very few examples of carbohydrate based inhibitors of fungal adhesion.

The first objective was to carry out an SAR study to screen a small library of aromatic glycoconjugates to determine the structural features required for anti-adhesive properties (Chapter 2). Once a lead compound was identified, we wanted to develop more potent anti-adhesion ligands. To achieve this, we altered the core scaffold of the aromatic ligands (Chapter 3) and created multivalent displays of the lead compound (Chapter 4).

The ultimate aim of this research is to determine the adhesins in the *C. albicans* with which the glycoconjugates are interacting. First, the lead compound was fluorescently labelled to determine the site of action of these anti-adhesion glycoconjugates (Chapter 2). The photo-affinity labelling approach was then considered and preliminary synthesis towards a photoaffinity tagged derivative of

the lead compound was investigated (Chapter 5). This technique may be used to identify the adhesin in the *C. albicans*. Finding the target of the glycoconjugates will allow for the development of high-affinity ligands to tackle the emerging problem of resistant candidal strains and a method of treating *Candida* infections.

Chapter 2

First Generation Aromatic Glycoconjugates as Inhibitors of Fungal Adhesion

2.1 Introduction

2.1.1 Aromatic Scaffolds:

Aromatic scaffolds have been used extensively in the synthesis of glycoconjuagtes for many years for several reasons. They have varied chemical reactivities, can be functionalized in many ways using well known reactions such as electrophilic and nucleophilic aromatic substitution (S_EAr and S_NAr), they provide a rigid framework and may have specific spectroscopic properties. They can also be characterized in a straightforward manner compared to more complex structures such as polymers and nanoparticles. Importantly, they provide a versatile and polyvalent framework where simple sugars or complex oligosaccharides can be displayed for a variety of biological applications.[134] Also, the water-solubility is generally good in these compounds due to the hydrophobicity of the aromatic core being overcome by the polar sugar residues. Glycoconjugates with an aromatic core were first reported in the literature in the early 1960s by Yariv *et al*.[135] These 1,3,5-tris-(*p*-glycosyloxyphenylazo)-2,4,6-trihydroxybenzenes compounds were used as artificial antigens.

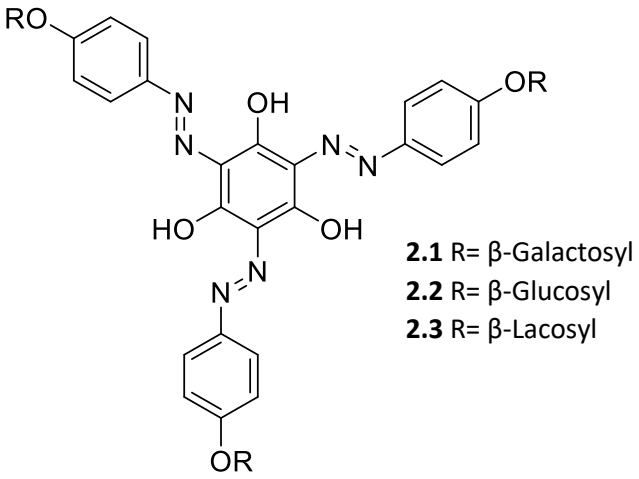

2.1 R= β-Galactosyl
2.2 R= β-Glucosyl
2.3 R= β-Lacosyl

Figure 2.1: Structure of 1,3,5-tris-(*p*-glycosyloxyphenlazo)-2,4,6-trihydroxybenzenes.[135]

Since these first aromatic glycoconjugates, numerous different aromatic centred scaffolds have been employed in the synthesis of di- and tri-substituted benzene containing glycoconjugates, glycoclusters, glycodendrimers, glycoconjugates from self-assembled aromatic systems and glycofullerenes.[134] Di- and tri-substituted benzene glycoconjugates have been built using a variety of different synthetic

strategies, including Lewis acid promoted glycosidations,[136] pre-activation strategies,[137, 138] CuAAC reactions[139, 140] and, Pd-catalysed Heck couplings and Songashira couplings.[141, 142]

2.1.2 Divalent Aromatic-Centred Glycoconjugates

Lewis acid promoted glycosidation reactions between peracetylated sugars and various di- and tri-hydroxylated benzenes have been performed using boron trifluoride etherate[143] or zinc chloride[136] as the catalyst. These reactions resulted in aryl centred divalent mannosides and glucosides in moderate yields. In an effort to improve the efficiency and stereoselectively of glycosidation reactions, Roy *et al*. used activated precursors to synthesise dendronized divalent α-D-mannopyranylated conjugates. In these glycoconjugates, the glycosides and the aromatic core were pre-activated with amino and isothiocyanato functional groups which could then be linked using thiourea coupling chemistry. For example, in the formation of the divalent α-D-mannopyranoside **2.4** shown in Figure 2.2, the primary amine of 3-(2-aminoethylthio)propyl mannopyranoside was coupled to an aromatic core containing two isothiocyanato functional groups. This formed a thiourea linkage between the aminated heteroaliphatic glycoside to the aromatic scaffold. Interestingly, this divalent cluster exhibited greatly improved affinities for multivalent plant lectins compared to the monosaccharide standards, showing the effectiveness of divalent glycoconjugates in comparison to the monovalent derivatives.[137]

Copper catalysed azide-alkyne cycloaddition (CuAAc) was later used to assemble dimeric molecules. This method is reliable, efficient, robust, chemoselective and it is tolerant to a wide variety of reaction conditions. It has been used to synthesis complex glycodendrimers, but has also been used to prepare simple divalent glycomimetics from aromatic scaffolds such as **2.5** in Figure 2.2.[139, 144] Various organometallic catalysts have also been used in glycoconjugation chemistry. Olefin metathesis of *O*-linked allylbenzene or stryl derivatives catalysed by ruthenium carbenoids was used to synthesise homodimers. In particular, stable Grubb's ruthenium catalysts were used because of their functional group tolerance and chemo- and stereoselective transformations. Roy *et al*. used these catalysts for olefin

metathesis of ω-alkenyl glycosides leading to compound **2.6**.[145] The use of Pd-catalysed Sonogashira-Heck-Cassar (SHC) cross-coupling reactions also allowed efficient fixation of many carbohydrate derivatives onto divalent aromatic platforms through alkyne-alkyne (Glaser) or alkyne-haloaryl reactions. Roy *et al*. utilized a Pd-catalysed Sonogashira reaction using two equivalents of prop-2-ynyl α-D-mannopyranoside with 1,4-diiodobenzene to form the corresponding bisethynylene homodimer **2.7**.[141]

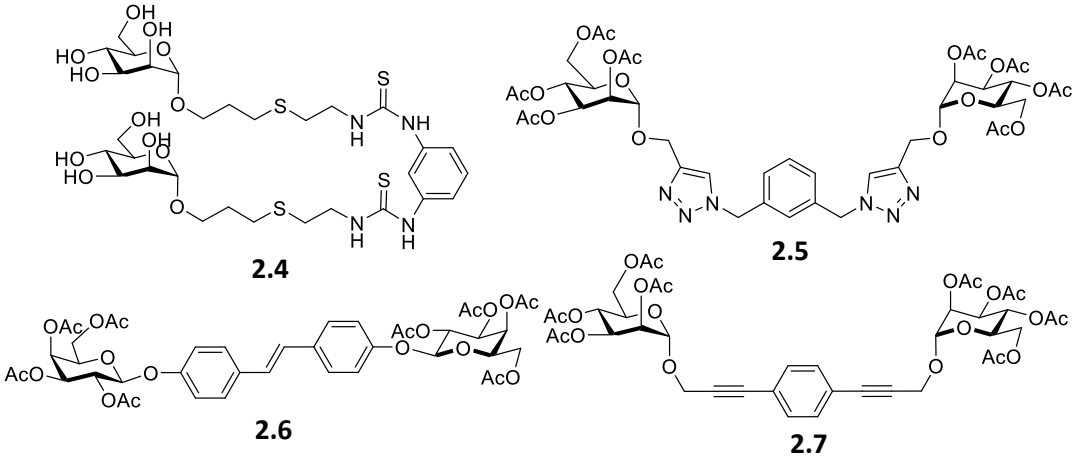

Figure 2.2: Structures of divalent aromatic centred glycoconjugates using different synthetic strategies; activated precursors **2.4**,[137] CuAAc chemistry **2.5**,[139] olefin self-metathesis **2.6**,[145] and Pd-catalysed Sonogashira chemistry **2.7**.[141]

2.1.3 Trivalent Aromatic-Centred Glycoconjugates

Trisubstituted benzene glycoconjugates have been built with equivalent efficiency using comparable synthetic strategies as those used for the divalent derivatives. Interestingly, subsequent enhancements in their biological activities were recorded in some cases. Lewis acid-promoted glycosidations have been directly performed from 1,3,5-benzenetrimethanol and an excess of an adequately protected galactosyl epoxide using $ZnCl_2$ as a catalyst. These reactions resulted in tris β-galactosides **2.8**.[136] The preactivation strategy was also employed to form trivalent glycoconjugates. Again, the glycosides and the aromatic core were pre-activated with amino and isothiocyanato functional groups which could then be linked using thiourea coupling chemistry. Commerically available 3,5-dinitroaniline was reduced and treated with thiophosgene to provide 1,3,5-triisothiocyanatobenzene, which was coupled with mannosides via thiourea linkages under mild conditions to give

trivalent compound **2.9**.[138] Phloroglucinol has been used as the initial building block to synthesis trivalent glycoconjugates using CuAAC chemistry. It has been functionalized with an azidoethoxy linker which was then reacted with prop-2-ynyl α-D-mannopyranoside.[144] An inverted synthetic strategy has also been recently adapted. In this case, 1,3,5-tris(alkynyloxy)benzene, prepared from phloroglucinol and propargyl bromide, and peracetylated lactosyl azide were reacted under CuAAc conditions to form trivalent glycoconjugates **2.10**. These compounds, along with tetravalent derivatives, were tested against two plant agglutinins and adhesion/growth-regulatory lectins (galectins).[140] SHC cross-couplings have also been advantageously adapted for trivalent epitopes' presentation. Sengupta and Sadhukhan[142] used a one-step Pd-catalysed methodology in order to generate multiantennary glycoclusters. A threefold Sonogashira cross-coupling reaction of propargyl β-D-glucoside with 1,3,5-tribromobenzene in the presence of $Pd(dba)_2$ gave rise to the centrally planar triantennary glycocluster **2.11**.

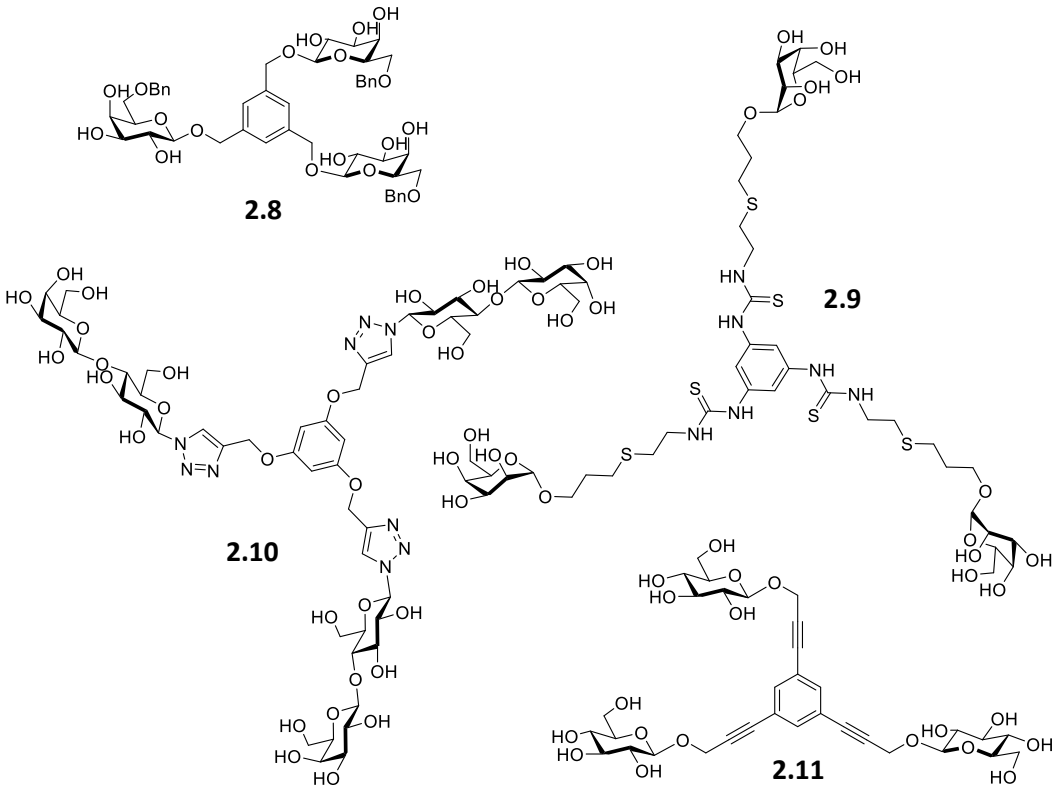

Figure 2.3: Structures of trivalent aromatic centred glycoconjugates using different synthetic strategies; Lewis acid promoted glycosidation **2.8**,[136] activated precursors **2.9**,[138] CuAAc chemistry **2.10**,[140] and Pd- catalysed Sonogashira chemistry **2.11**.[142]

2.1.4 Glycoconjugates as Anti-Adhesion Ligands

Aromatic glycoconjugates such as those described earlier have been tested for interactions with lectins e.g. galectin. This section will briefly review aromatic glycoconjugates that have been used as anti-adhesion ligands that can block attachment of pathogens. In the field of anti-adhesion glycoconjugates, high affinity ligands can be designed when detailed structural knowledge of the pathogen lectins involved in adhesion are available. As discussed in Chapter 1, many lectins and other adhesins are known and characterised in numerous species of bacteria. On the other hand, little is known about the adhesins that mediate the interaction of fungi with host cells.

2.1.4.1 FimH in *Escherichia coli*

FimH is the adhesive component of the type 1 pilus, which are essential virulence factors for the establishment of the bacterial *Escherichia coli* urinary tract infections.[146] Blocking FimH binding to mannosylated proteins with FimH antibodies or small molecules is sufficient to prevent bacterial entry and infection. It was found that α-D-mannosides and mannosylated glycoconjugate dendrimers bind with high affinity to the bacterial lectin FimH. This was confirmed with X-ray crystal structure studies, where the structure of FimH in complex with mannose involves an intense hydrogen bonding network.[147] The measured affinity of mannose for FimH found that the lectin binds the monosaccharide exceptionally well (K_d = 2.3 μM).[148]

Long chain alkyl- and arylmannosides display very high affinity for FimH even as monovalent ligands. This is likely due to increased hydrophobic interactions with Ile-52 and two tyrosine residues, Tyr-48 and Tyr-137, lining the hydrophobic rim of the binding pocket. Figure 2.4 b shows the hydrophobic contact between the FimH binding pockets and butyl α-D-mannoside. A separate crystal structure of the FimH binding domain bound to oligomannose-3 (structure shown in Figure 2.4 c) was recently solved[149] that reveals an “open gate” between Tyr-48 and Tyr-137 into which oligomannose-3 inserts, adopting a conformation in which the second mannose residue interacts with Tyr-48 (Figure 2.4 d). Interestingly, the latter conformation is different from that seen in monomannose-bound forms of FimH. This conformational

flexibility of the tyrosine residues seen in these X-ray structures provides a rationale for designing arylmannosides with increased binding affinity relative to alkylmannosides by introducing additional hydrophobic and ring stacking interactions with Tyr-48 or Tyr-137.

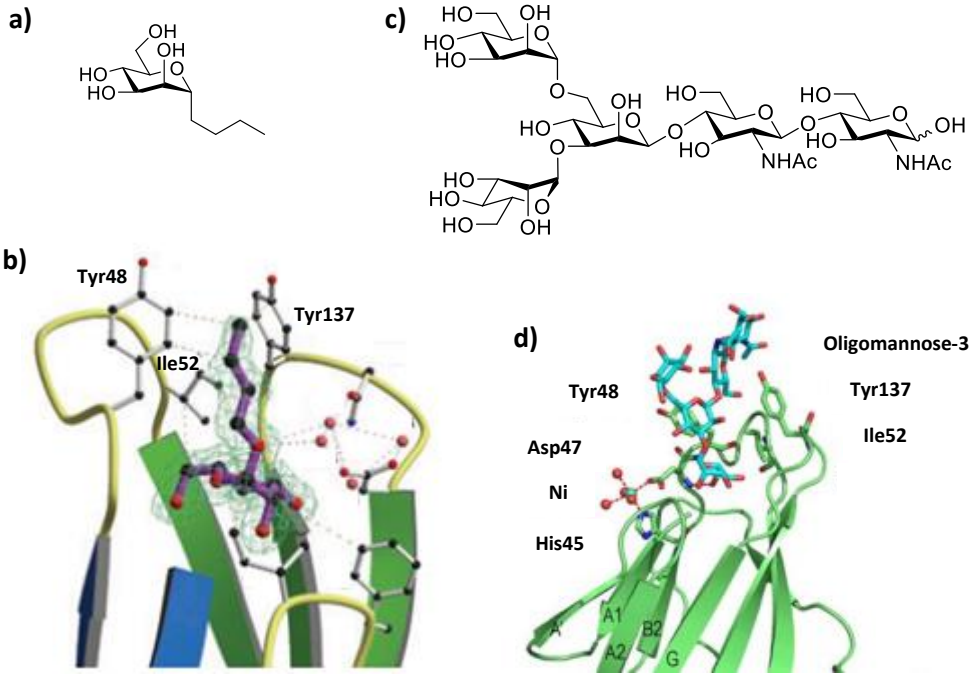

Figure 2.4: a) Structure of butyl α-D-mannoside; b) Shows the mannose-binding domain of FimH indicating the hydrophobic contact between the amino acids, Ile-52, Tyr-48 and Tyr-137, and butyl α-D-mannoside;[148] Reprinted with permission from John Wiley and Sons. c) Structure of oligomannose-3; d) Crystal structure of the FimH binding domain bound to oligomannose-3 that reveals an "open gate" between Tyr-48 and Tyr-137.[149] Reprinted with permission from PLOS One.

Using this information, Janetka *et al*.[150] designed a series of potent small molecule FimH antagonists using the weak inhibitor α-D-phenylmannoside as an initial starting point for X-ray structure-guided optimization. Addition of substituents with increased hydrophobicity resulted in potency enhancement, in particular when using aromatic groups. After a Structure Activity Relationship (SAR) study, it was found that 4'-biaryl groups substituted on the meta position with H-bond acceptors such as amides **2.12** or esters **2.13** are the most potent analogues, two of which are shown in Figure 2.5. This is due to an optimal π-stacking arrangement of the biaryl moieties with Tyr-48 and a H-bonding interaction with Arg-98. Dimers derived from these

mannosides **2.14** were also designed, which showed a 4-fold increase in cellular potency relative to that expected from two monomeric units, due to the 'multivalent effect' (This will be discussed in detail in Chapter 4).

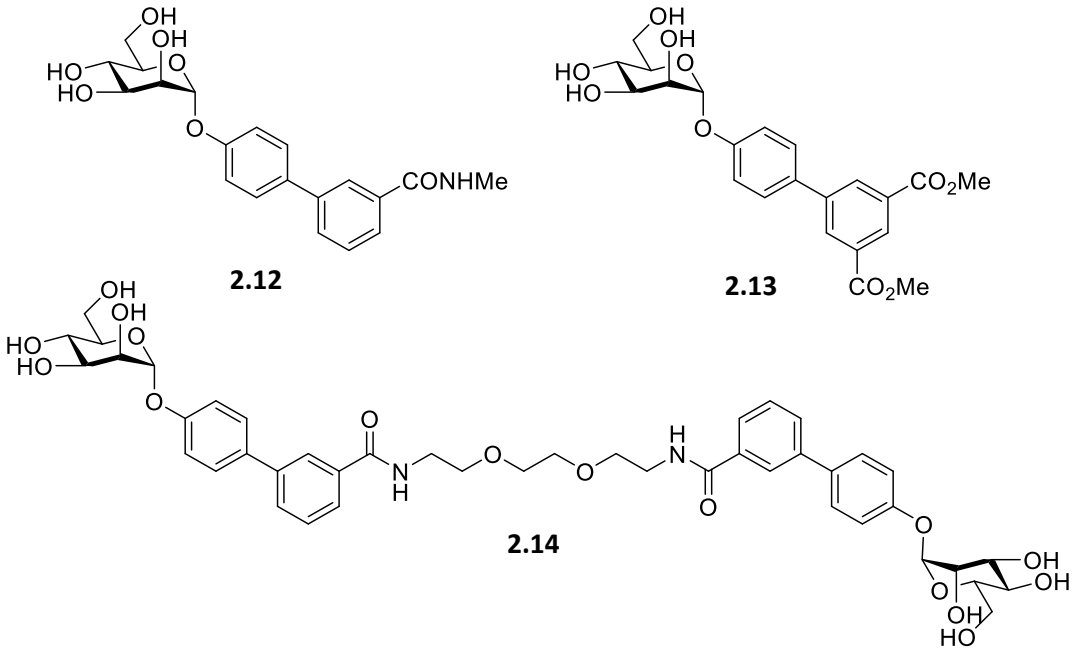

Figure 2.5: Shows the structure of the monomeric (**2.12** and **2.13**) and dimeric (**2.14**) mannosides used as FimH anagonists.

2.1.4.2 LecA and LecB in *Pseudomonas aeruginosa*

Pseudomonas aeruginosa in an opportunistic pathogen which causes fatal lung infections in immunocompromised patients, in particular in cystic fibrosis and hospitalised patients. The treatment of these infections is difficult due to the emergence of antimicrobial multiresistance. To establish itself in the host, *P. aeruginosa* uses host carbohydrate recognition for anchoring to mucosa through carbohydrate binding proteins including soluble lectins or adhesins exposed on pili, flagella, or fimbriae.[151] Two soluble lectins have been identified in *P. aeruginosa*, LecA (PA-IL) and LecB (PA-IIL).[152] The structure of both lectins have been solved using X-ray crystallography, showing a tetrameric arrangement of β-sandwich-folded monomers with a calcium ion in the carbohydrate binding domain (shown in Figure 2.6).[153] LecA binds to α-galactosyl residues present on glycosphingolipids in lung epithelial cell membranes,[154, 155] while LecB binds to several fucosylated or mannosylated epitopes.[156, 157]

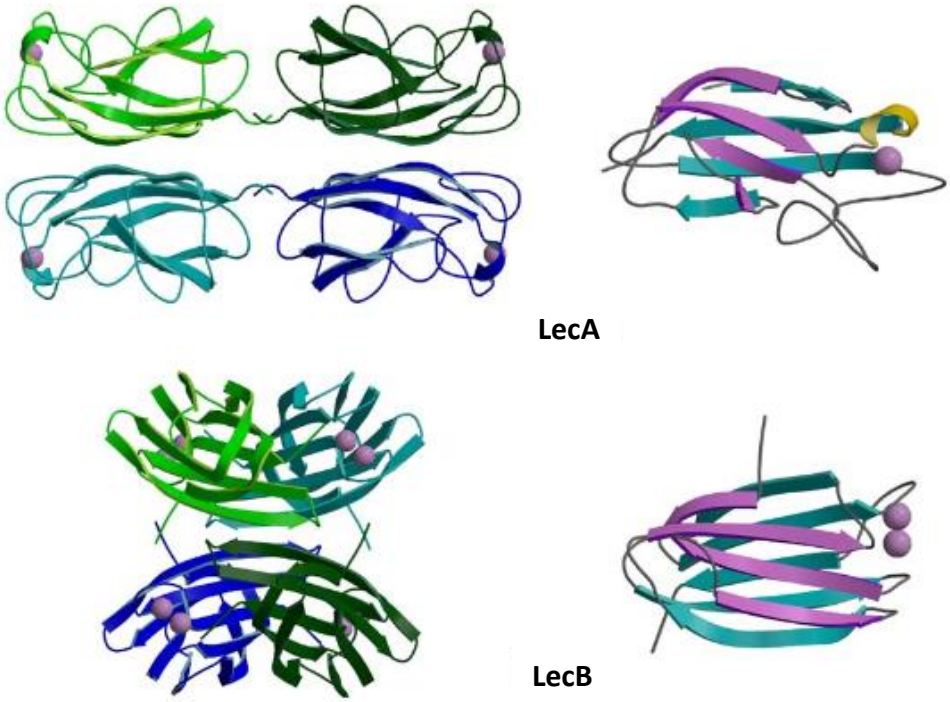

Figure 2.6: Crystal structure of the LecA and LecB, showing the tetrameric and monomeric structures. The associated calcium ions are shown.[153] Reprinted from Microbes and Infection, vol. 6, Imberty, A., Wimmerová, M., Mitchell, E. P., Gilboa-Garber, N., Structures of the lectins from Pseudomonas aeruginosa: insights into the molecular basis for host glycan recognition, 837-853, Copyright (2004), with permission from Elsevier.

Studies have shown that simple sugars can limit the infection of *P. aeruginosa.* For example, α-methyl-galactoside and α-methyl-fucoside were shown to limit the spread of infection in a murine pneumonia model, acting as LecA- and LecB-specific inhibitors. These two carbohydrates were found to be most active at a concentration of 50 mM.[158] The adhesion of *P. aeruginosa* to human respiratory epithelial cells was significantly inhibited using human milk oligosaccharides. 2'-Fucosyllactose and 3-fucosyllactose (structure shown in Figure 2.7) significantly inhibited the adhesion of *P. aeruginosa* to respiratory epithelial cells and to intestinal epithelial cells to a lesser extent.[159] Using this information, many groups have synthesised a large number of glycoclusters to inhibit the carbohydrate-lectin interactions during the infection process. Recent studies have identified a novel divalent ligand **2.15** from a focused galactoside-conjugate array which binds LecA with very high affinity (K_d = 82 nM). Crystal structures of this ligand complexed to LecA confirmed its ability to chelate

two binding sites of LecA. This compound has been shown to lower the cellular invasiveness of *P. aeruginosa* by up to 90 % at concentrations of 0.05-5 µM.[160]

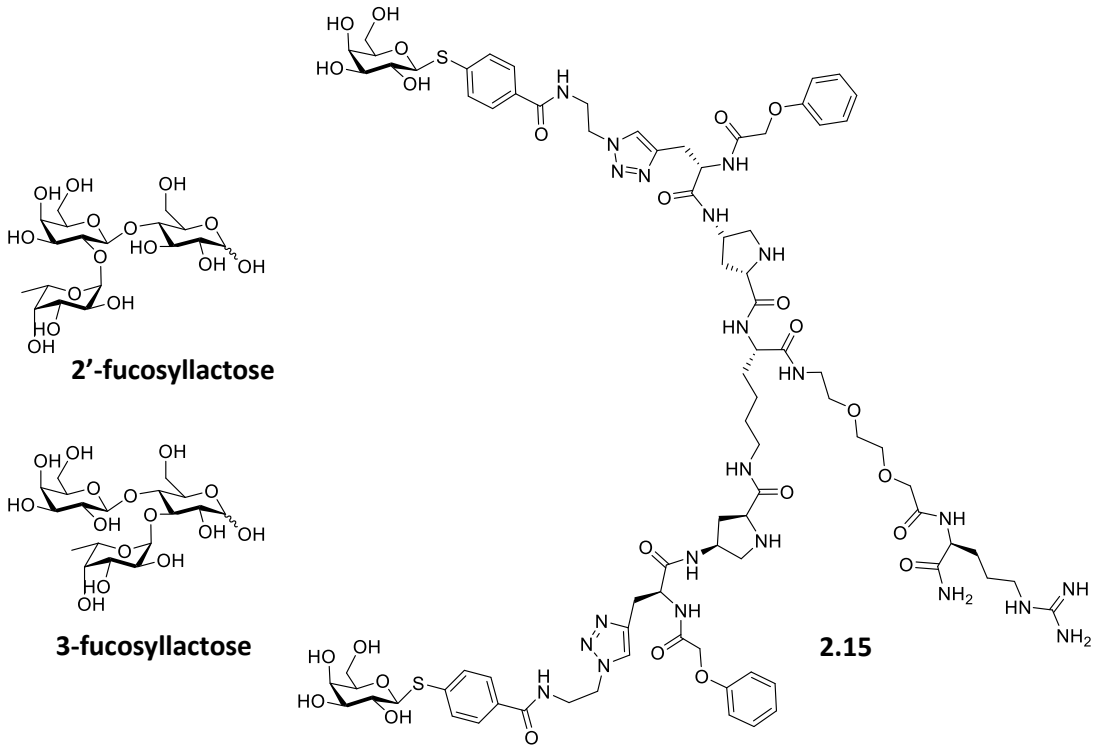

Figure 2.7: Shows the structure of 2'-fucosyllactose, 3-fucosyllactose and the divalent galactoside **2.15** known to inhibit the adhesion of *P. aeruginosa*.

Using these previous studies, Vidal and coworkers[161] designed calix[4]arene-based glycoclusters functionalized with galactosides and fucosides. These glycoclusters consisted of propargylated calix[4]arenes, which were reacted with the carbohydrate moiety using CuAAC chemistry. Triethylene glycol spacers were used between the scaffold and the carbohydrates. These multivalent glycoclusters were found to have anti-biofilm formation properties, as well as anti-adhesive properties. A dose-dependent inhibition of adhesion was observed at concentrations of 25-2500 µM. Inhibition of adhesion reached 70 % and 90 % with the galactosylated glycoclusters **2.16** and fucosylated glycoclusters **2.17**, while inhibition only reached 30 % and 65 % with the monovalent α-methyl-galactoside and α-methyl-fucoside. The fucosylated ligands had greater inhibition since fucose has higher affinity for LecB (µM) than galactose has for LecA (mM). An *in vivo* mouse model of the lung infection treated with these glycoclusters showed almost complete protection against *P. aeruginosa* at higher concentrations (mM). These higher concentrations are required in *in vivo*

assays since pharmacokinetic processes come into consideration. In these tests there are issues around the availability and accessibility of the soluble lectins. These synthetic glycoclusters must also compete with high affinity natural ligands, as well as the presence of competing unidentified adhesins or other lectins.[161]

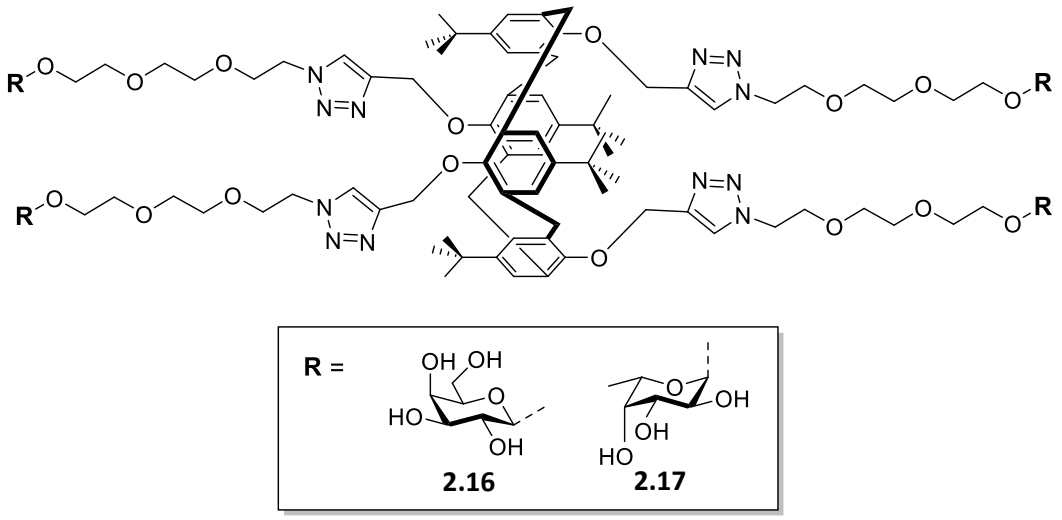

Figure 2.8: Structure of multivalent glycoclusters **2.16** and **2.17** used as anti-adhesive agents against *P. aeruginosa* lung infection.[161]

2.1.4.3 FleA in *Aspergillus fumigatus*

FleA, a fucose binding lectin, was recently identified in the opportunistic mold, *Aspergillus fumigatus*.[162, 163] This fungus causes fatal lung infections in immunocompromised patients. The critical initial stage of adhesion to pneumocytes (surface epithelial cells of the alveoli) is partly mediated by the fucose-binding lectin FleA.[162, 163] The 3D structure of this lectin is known and was solved by X-ray crystallography.[164] FleA forms homodimers and adopts a six-bladed β-propellor fold. It has six functional fucose binding sites per protomer, located at each interface between adjacent blades and two opposite binding surfaces on the dimer (Figure 2.9). Fucose recognition requires three amino acids: Arg, Glu/Gln and Tyr/Trp. Minor variations in this amino acid composition results in six non-equivalent binding sites and therefore exhibit different oligosaccharide preferences.[164] Glycan array studies confirmed that shorter fucosylated oligosaccharides are preferred over large branched structures, and non-fucosylated epitopes are not recognized by FleA.[163] 2*E*-hexenyl-α-L-fucopyranoside was found to be a potent FleA antagonist with

nanomolar efficacy and inhibits the binding and phagocytosis of *A. fumigatus* conidia by lung macrophages.[165]

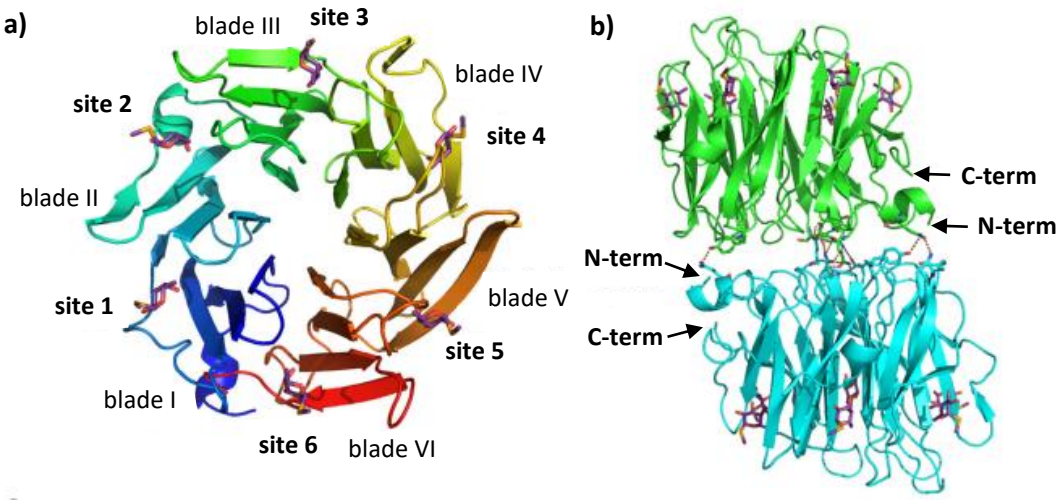

Figure 2.9: a) Structure of FleA monomer with individual blades and binding sites labelled in complex with α-methyl-seleno-fucoside; b) and side-view of FleA dimer with intermonomer contacts shown.[163] Reprinted with permission from PLOS One.

Using this information, Varrot, Goudin and co-workers[166] designed mono-, di-, hexa- and octavalent fucosides with different sized oligo ethylene glycol spacers. They wanted to determine the structural features of these glycoconjugates that were necessary to tightly interact with the lectin FleA. It was found that multivalency greatly increased the affinity of the fucosides for FleA. For example, the monovalent fucoside **2.18** had low affinity for the lectin (K_d = 140 µM), whereas the octavalent fucoside **2.19** was highly potent (K_d = 0.04 µM). The ethylene glycol linker length also effected the affinity of the fucosides for FleA. Comparing divalent fucosides with varying linker lengths, found that fucoside **2.21** (K_d = 0.94 µM) was significantly more potent than fucoside **2.20** (K_d = 3.8 µM) which had a shorter linker, and fucoside **2.22** (K_d = 52 µM) which had a longer linker. Adhesion assays were carried out using these fucosides, where the adhesion between the alveolar pneumocytes and *A. fumigatus* conidia in the presence of the fucosides were measured. No inhibition was observed for the monovalent compound **2.18** and the divalent compound **2.20** at 10 mM (concentration expressed in mol of fucose units). At 100 µM, compound **2.20** reduced adherence (63 % compared to the untreated control of 100 %). However, when the linker length was increased (compound **2.21**), 76 % inhibition was observed at a

concentration of 10 µM and 70 % at 100 µM. Two hexavalent ligands (structures not shown) were significantly more powerful antiadhesives compared to the divalent fucosides. Both these compounds reached about 50 % adhesion inhibition at a fucoside concentration of 10 µM.[166]

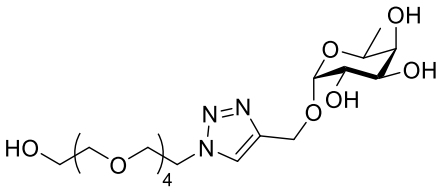

2.18

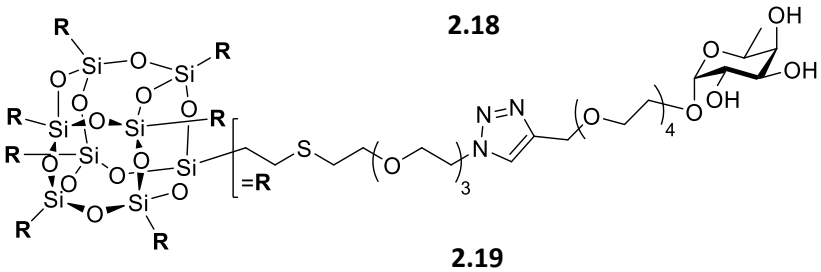

2.19

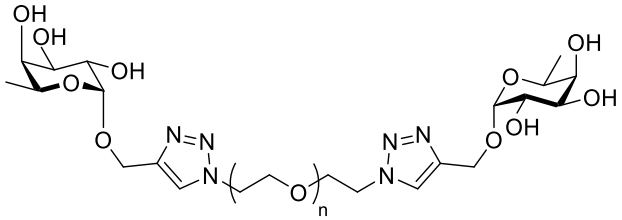

2.20: n = 2
2.21: n = 11
2.22: n = 27

Figure 2.10: Structures of the monovalent fucoside **2.18**, octavalent fucoside **2.19**, and divalent fucosides **2.20**-**2.22** designed to interact with the lectin FleA.[166]

2.1.4.4 Inhibition of Adhesion in *Burkholderia multivorans*

Another example of aromatic glycoconjugates used to inhibit adhesion are the bivalent lactosides which were tested as potential inhibitors of *Burkholderia multivorans* by Murphy, McClean and coworkers.[167] In this case the structure of the target lectin or adhesin are unknown. *B. multivorans* is a species of the *Burkholderia cepacia* complex (Bcc), which is an opportunistic human pathogen that most often causes pneumonia in immunocompromised individuals with underlying lung disease (e.g. cystic fibrosis). *B. cepacia* bind to glycolipid receptors, including asialo GM1 and asialo GM2 on epithelial cells in the lungs.[168] However, the identity of these receptors is not known. McClean and co-workers[169] have developed a rapid, reliable

quantitative PCR (polymerase chain reaction) technique for the identification of Bcc adhering to lung epithelial cells *in vitro*. Using this approach, it was found that millimolar concentrations of lactose could decrease bacterial attachment to lung epithelial cells by over 50 %. The preparation of bivalent lactosides based on terephthalamides have been previously shown to inhibit galectins (proteins that bind β-galactosides). McClean and coworkers then examined whether these galectin inhibitors could also inhibit attachment of *B. multivorans* to lung epithelial cells. Results showed that lactoside **2.23** strongly inhibited the binding of *B. multivorans* to lung epithelial cells at a range of concentrations (9-90 μM). In comparison, the more rigid derivative **2.24** was unable to inhibit adhesion. In fact, at certain concentrations it led to an increase in bacterial adhesion to the epithelial cells. Finally, the tertiary amide derivative **2.25** decreased attachment at low concentrations, but at higher concentrations, it led to an increase in bacterial attachment.

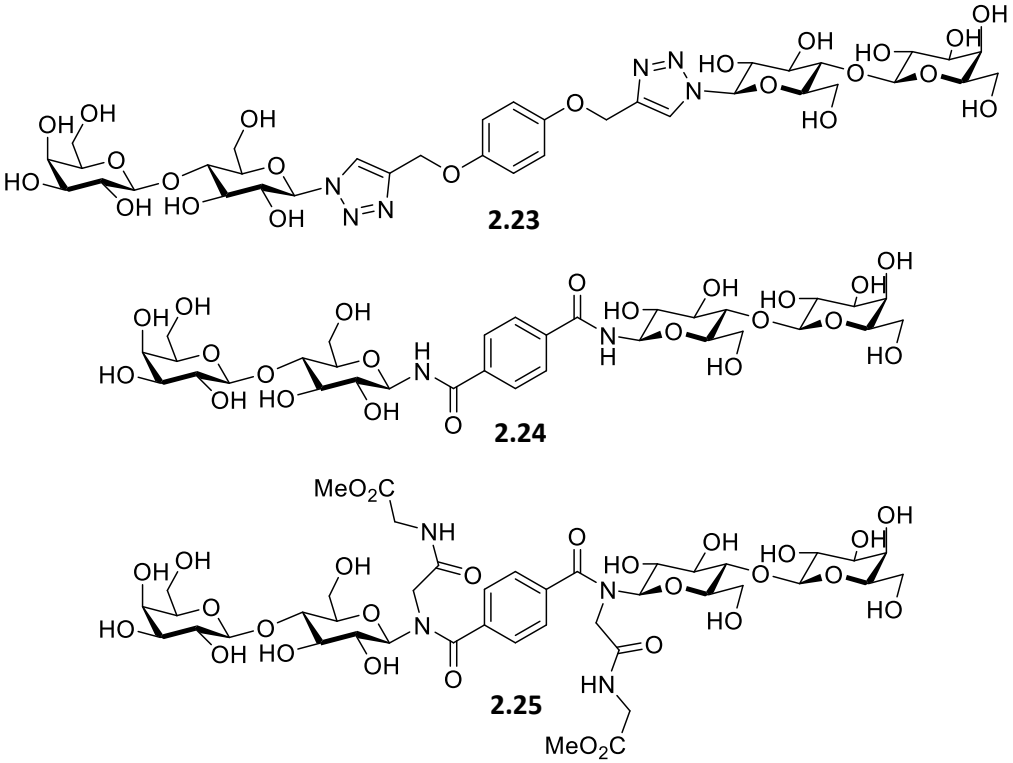

Figure 2.11: Structure of bivalent lactosides used to inhibit the adhesion of *B. multivorans* to lung epithelial cells.

2.1.5 Inhibition of Adhesion in Candida albicans:

Early reports indicate that some *C. albicans* adhesins recognise and bind to a broad range of cell surface glycans and carbohydrates.[60-62] In these studies it was found that simple sugars can affect the adhesion process of *C. albicans* to human buccal epithelial cells (BECs). Sandin *et al.*[60] showed evidence for mannose-mediated adhesion to BECs. Concanavalin A (ConA), a lectin that recognises mannose and glucose, inhibited the adherence of pretreated yeasts to BECs. This suggests that ConA is binding to and blocking the mannose containing receptors on the yeast surface or mannose moieties of the indigenous lectin associated with the yeast cell surface. ConA also inhibited the adhesion of pretreated BECs with non-treated yeasts. This result indicates that mannose containing moieties on the buccal cell surface could be acting as receptors for the *C. albicans.* Also, the presence of α-D-methyl mannoside in the incubation medium during the assay inhibited adhesion of the *C. albicans* to the BECs. Critchley and Douglas[61] investigated the effect of several lectins and sugars on the adhesion of *C. albicans* to buccal and vaginal epithelial cells. The adherence of most *Candida* strains were inhibited by L-fucose and winged-pea lectin (specific for L-fucose), suggesting that a glycoside containing α-L-fucosyl residues might function as a receptor for these strains of *Candida*. Other lectins, such as wheat-germ agglutinin (specific for *N*-acetyl-β-D-glucosaminyl residues) or peanut lectin (specific for D-galactosyl residues) had little effect on the adherence of these strains. In contrast, the adherence of one *Candida* strain was efficiently inhibited by *N*-acetyl-D-glucosamine and wheat-germ agglutinin and was unaffected by winged-pea lectin and peanut lectin. The adhesion of all *Candida* strains were significantly enhanced by ConA lectin. This lectin is known to have multiple binding sites and can therefore promote adhesion by acting as bridges between α-D-mannosyl residues on the yeast and epithelial surfaces.

Cell surface glycoconjugates as possible adhesion receptors for *C. albicans* on human BEC have also been investigated. Brassart *et al.*[62] conducted a study to investigate the ability of soluble glycopeptides and oligosaccharides at inhibiting the adhesion of yeast to exfoliated cells. Prelimary studies showed that fucose played a role in inhibiting the adhesion process. Then using human milk oligosaccharides as probes,

the minimal requirement for activity was found to be the Fucα(1-2)Galβ determinant. This study concluded that this disaccharide, part of the cell surface glycoconjugates, may act as a part of a complex adhesion mechanism, which possibily requires multireceptor specificities.

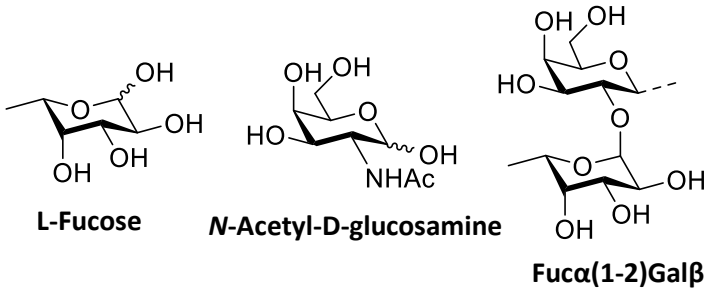

Figure 2.12: The structure of two monosaccharides, L-fucose and N-acetyl-D-glucosamine found to inhibit the adhesion of *C. albicans*, and the structure of the minimal requirement from human milk oligosaccharides: Fucα(1-2)Galβ.

More complex carbohydrate-based compounds have been found to participate in the adhesion process of *C. albicans*. Glycosphingolipids in particular can act as adhesion receptors for yeasts. *C. albicans* bound specifically to lactosylceramide (Galβ(1-4)Glcβ(1-1)Cer, structure shown in Figure 2.13), and required the terminal galactosyl residue for binding.[170] It has also been reported that *C. albicans* yeast form expresses a fimbrial adhesin that binds to asialo-GM_1 (Gangliotetraosylceramide: βGal(1-3)βGalNAc(1-4) βGal(1-4)βGlc(1-1)Cer), a glycosphingolipid displayed on the surface of human BEC (structure shown in Figure 2.13). It was found that the minimal carbohydrate sequence required for binding is βGalNAc(1-4)βGal.[171] This and other disaccharides and some of its synthetic derivatives have been shown to inhibit purified fimbrial or pathogen binding *in vitro*. The *in vivo* efficacy of the propyl derivatives of this disaccharide were evaluated, in particular, Fimbrigal-P, octyl *O*-(2-acetamido-2-deoxy-β-D-galactopyranosyl)-(1-4)-2-*O*-propyl-β-D-galactopysanoside (structure shown in Figure 2.13). Fimbrigal-P was shown to reduce the oral fungal burden in a rat oral candidiasis model, indicating that it makes a promising candidate for the prevention and treatment of microbial infections in which the pathogen relies on the βGalNAc(1-4)βGal disaccharide to establish adherence.[172]

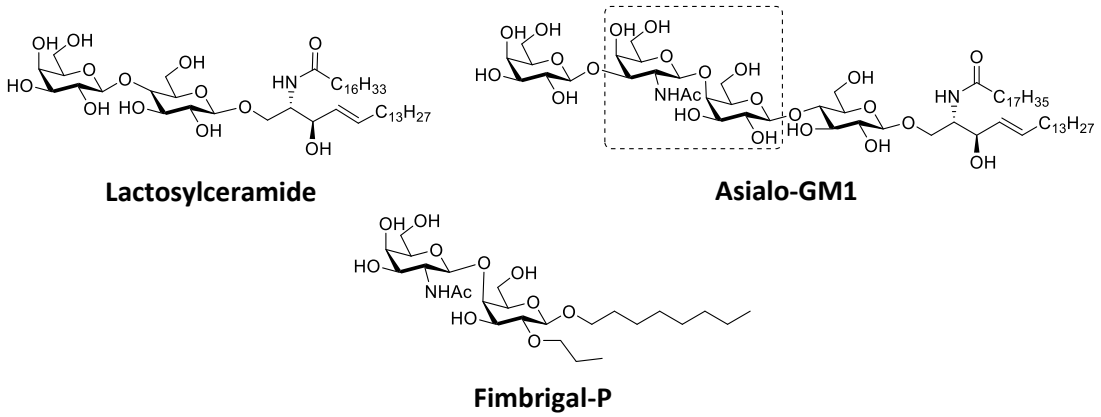

Figure 2.13: Structure of lactosylceramide, asialo-GM_1 highlighting the minimal binding sequence, and Fimbrigal-P.

2.2 Chapter Objective

This chapter deals with the synthesis of aromatic centred glycoconjugates as potential anti-adhesion ligands against *C. albicans*. As discussed earlier, cell surface glycans are important receptors for *C. albicans* adhesion and warrant the development of anti-adherence ligands that can mimic them. These glycocomimetics can thus disrupt *C. albicans* – epithelial cell interactions, preventing adherence of the yeast to the epithelial cells, and hence prevent infection. These compounds could represent a promising strategy to overcome fungal infections. However, lack of structural knowledge of the fungal adhesins that recognise these carbohydrates hampers a focused design approach. In this study, we opted instead to screen a small library of synthetic glycomimetics with a diverse presentation of carbohydrate binding epitopes in order to identify structural features that can lead to effective inhibition of fungal adherence. This chapter describes the synthesis of an aromatic-core glycoconjugate (AGC) library and their subsequent evaluation as inhibitors of the adherence of *C. albicans* to BECs.

The popularity of AGCs is partly due to the versatility in functionality and the substitution patterns that can be achieved from readily available starting materials as discussed in previous sections. Thus, 1,3- and 1,3,5-functionalized aromatic derivatives were explored as the starting point in the design of the anti-adherence AGCs library (Figure 2.14).

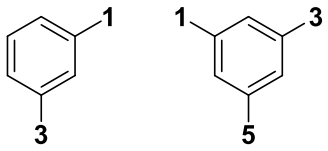

Figure 2.14: 1,3 and 1,3,5-functionalized aromatic derivatives were chosen as the starting point in the design of the anti-adherence AGCs library.

It is well known that multivalency, i.e. the number of carbohydrates presented in a ligand, can be an important factor that modulates carbohydrate protein interactions. Hence, mono-, di- and trivalent analogues were investigated. Carbohydrate moieties present in the epithelial cell surface and reported to bind *C. albicans* were selected to be grafted onto the aromatic scaffold. These included galactose, fucose, mannose, *N*-acetyl glucosamine, *N*-acetyl galactosamine and lactose derivatives. Triazolyl-containing spacer groups of different lengths, generated by means of Copper-Catalyzed Azide-Alkyne Cycloaddition (CuAAC) reactions, were used to connect the glycosides to the central aromatic core. With this modular approach, a small collection of glycoconjugates was readily assembled, in which (i) the carbohydrate moiety, (ii) the valency and (iii) the distance between the binding epitopes were varied (Figure 2.15). This provided sufficient structural diversity for an initial screening of the requirements for fungal anti-adherence activity.

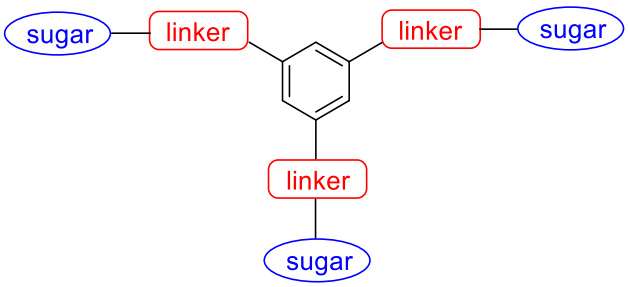

Figure 2.15: Core scaffold utilised for the synthesis of the aromatic glycoconjugates.

2.3 The Synthesis of AGCs (Aromatic-Core Glycoconjugates)

2.3.1 Triazole Containing Glycoconjugates

The triazole linkage used to connect the glycoside to the aromatic core is an important feature of these ligands. It provides a reliable, straightforward synthetic route to numerous different analogues by changing the *O*-acetyl sugar azide (which

are also easy to prepare). 1,4-Disubstituted 1,2,3-triazoles are of great biological interest as they possess high chemical stability, display aromatic character and can act as hydrogen bond acceptors.[173] They can therefore mimic the electronic properties and atom arrangement of peptide bonds, without being susceptible to hydrolytic cleavage.[174] Copper (I) catalysed azide-alkyne cycloaddition (CuAAC) has been employed to incorporate triazoles in a vast array of medicinal chemistry and chemical biology projects. Recent literature has shown the use of this reaction to construct functionally diverse carbohydrate derivatives.[175]

The regioselective synthesis of 1,4-disubstituted 1,2,3-triazoles occurs via a CuAAC reaction reported independently by the Tornøe and Meldal groups in Denmark,[176] and the Sharpless and Folkin laboratories in the U.S.[177] Prior to these reports, the uncatalysed 1,3-dipolar cycloaddition was utilised in the synthesis of substituted triazoles. However, this method had numerous disadvantages, including the need for high temperatures, long reaction times and a mixture of products, the 1,4- and 1,5-triazole regioisomers **2.28** and **2.29**. In contrast, the copper catalysed reaction transforms organic azides **2.27** and terminal alkynes **2.26** into the 1,4-disubstituted 1,2,3-triazoles **2.28** exclusively, without the need for elevated temperatures (Scheme 2.1).[173]

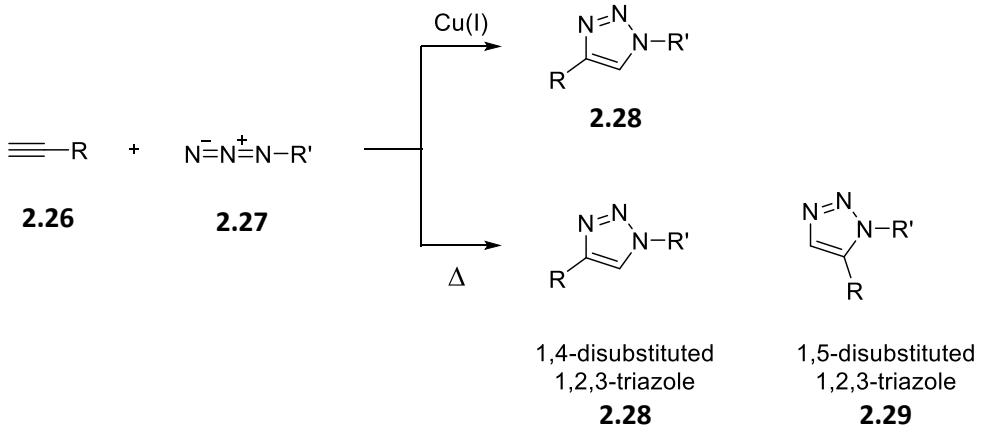

Scheme 2.1: Huisgen 1,3-dipolar cycloaddition of azides and alkynes requires heating and results in mixtures of both 1,4- and 1,5-regioisomers (bottom), whereas CuAAC produces only 1,4-disubstituted 1,2,3-triazoles at rt.

Scheme 2.2 shows the current proposal of the CuAAC reaction mechanism. The formation of the σ, π-di(copper) acetylide **2.30** initiates the reaction. The acetylide

engages in both σ and π bonding with the copper(I). This complex binds to the azide **2.27** (step i) to form the azide/alkyne/copper(I) ternary complex **2.31**. Metallacycle **2.32** formation (step ii) occurs where one copper(I) is oxidized to copper(III). Reductive ring contraction (step iii) follows to afford the copper (I) triazolide **2.33**, which deprotonates an alkyne **2.26** to complete the catalytic cycle (step iv). Amoung the four structures depicted in the catalytic cycle, both σ, π-di(copper) acetylide **2.30**[178] and the copper(I) triazolide **2.33**[179] have been fully characterized and verified as viable intermediates in the reaction. The scarcity of evidence for the structures **2.31** and **2.32** emphasizes that steps ii and iii are fast in the catalytic cycle. Intermediate **2.31** has only been detected once using an ion-tagged electron spray ionization mass spectrometric method.[180] Folkin and co-workers, using a copper isotope labelling experiment, found that the dicopper metallacycle **2.32** was involved in a rapid internal rearrangement equilibrium to scramble the two copper centres.[181]

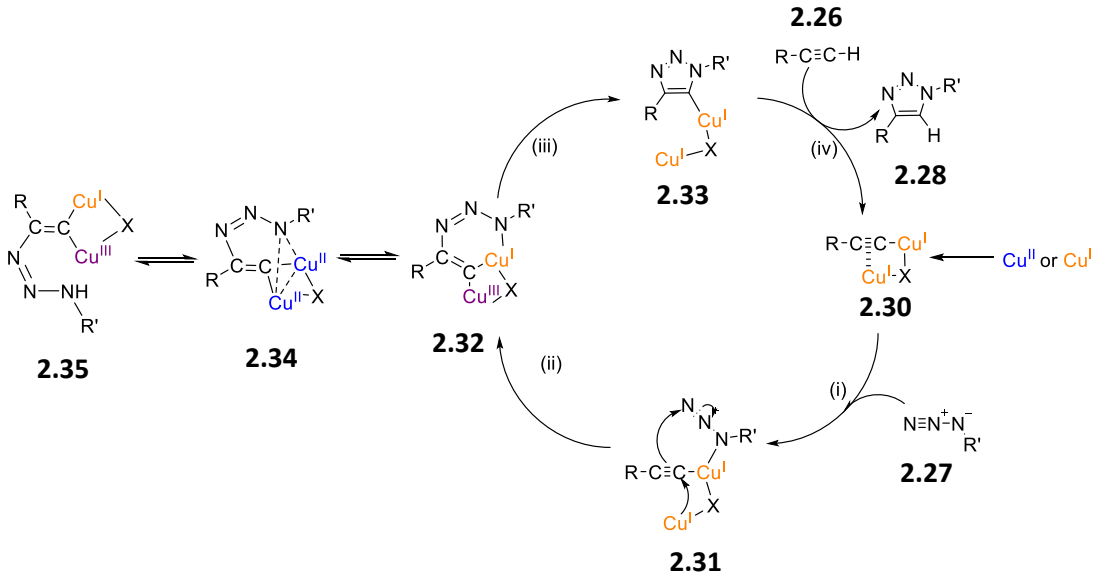

Scheme 2.2: Outline of the plausible mechanism for the Cu(I) catalysed reaction between organic azides and terminal alkynes.[182]

2.3.2 Synthesis of Sugar Azides

All the *O*-acetyl sugar azides discussed in this chapter were synthesised from well-known synthetic routes. The galactose **2.40**,[183] glucose **2.41**,[183] lactose **2.43**[184], mannose **2.42**,[185] and fucose **2.45**[183] derivatives were made from the corresponding peracetylated precursors. The azide was introduced at the anomeric centre using

$TMSN_3$ and $SnCl_4$. $SnCl_4$ is used to activate the anomeric acetyl and due to neighbouring group precipitation, exclusively β-anomers were obtained for the peractylated galactose, glucose, fucose and lactose and the α-anomer for mannose. Scheme 2.3 shows the synthesis the D-sugar azides, while Scheme 2.4 shows the synthesis of L-fucose azide.

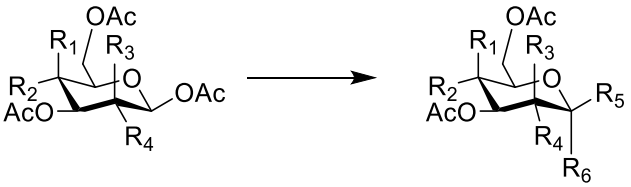

2.36 Gal
2.37 Glc
2.38 Man
2.39 Lac

2.40 Gal
2.41 Glc
2.42 Man
2.43 Lac

Gal: R_1=OAc, R_2=H, R_3=H, R_4=OAc, R_5=N_3, R_6=H
Glc: R_1=H, R_2=OAc, R_3=H, R_4=OAc, R_5=N_3, R_6=H
Man: R_1=H, R_2=OAc, R_3=OAc, R_4=H, R_5=H, R_6=N_3

Lac: R_1=H, R_2= 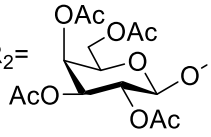 , R_3=H, R_4=OAc, R_5=N_3, R_6=H

Scheme 2.3: Synthesis of D-sugar azides. *Reagents and Conditions*: $TMSN_3$, $SnCl_4$, anhydrous DCM, N_2, 16 h, 79-97 %.

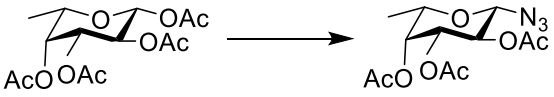

2.44 **2.45**

Scheme 2.4: Synthesis of L-fucose azide. *Reagents and Conditions*: $TMSN_3$, $SnCl_4$, anhydrous DCM, N_2, 16 h, 84 %.

To prepare the 1-azidoethoxy-2,3,4,6-tetra-*O*-acetyl-β-D-galactopyranoside **2.47**, the peractylated galactose **2.36** was first reacted with 2-chloroethanol using boron trifluoride etherate as an activating agent to form compound **2.46**, which was then reacted with NaN_3 to form the desired azide **2.47**.[186]

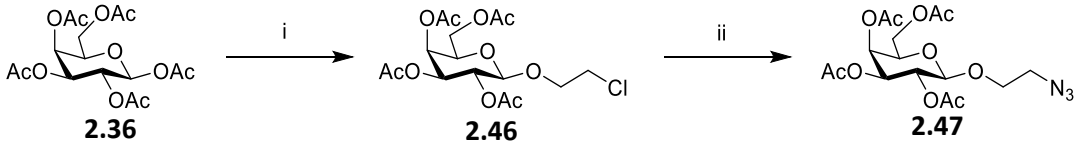

2.36 **2.46** **2.47**

Scheme 2.4: Synthesis of 1-azidoethoxy-2,3,4,6-tetra-*O*-acetyl-β-D-galactopyranoside **2.47**. *Reagents and Conditions*: i) $BF_3.OEt_2$, 2-chloroethanol, DCM, rt, 16 h, 75 %; ii) NaN_3, DMF, 80 ˚C, 16 h, 80 %.

The β-azido *N*-acetyl-D-galactosamine **2.52** and β-azido *N*-acetyl-D-glucosamine **2.53** were prepared following a different route (Scheme 2.5). Here the *N*-acetyl-D-glycosamine **2.48** and **2.49** were reacted with NaN_3 in the presence of 2-chloro-1,3-dimethylimidazolinium chloride (DMC) and a base, 2,6-lutidine, in D_2O for 66 hours at 6°C.[187] DMC is an excellent agent for selective activation of the anomeric hydroxyl groups. The reaction proceeds through a reactive intermediate formed as a result of the preferential attack of the anomeric hydroxyl group towards DMC. This occurs since the pK_a values of the hemiacetal anomeric hydroxyl groups are much lower than those of the other hydroxyl groups and water. The resulting azides **2.50** and **2.51** were then acetylated using acetic anhydride/pyridine reaction conditions to form the desired products **2.52** and **2.53**.

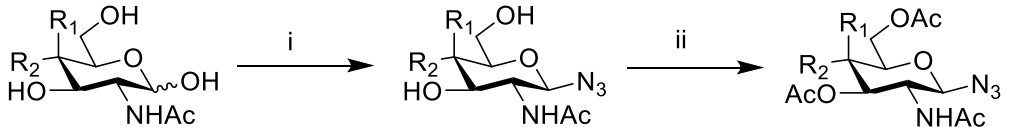

2.48 GalNAc
2.49 GlcNAc

2.50 GalNAc
2.51 GlcNAc

2.52 GalNAc
2.53 GlcNAc

GalNAc: R_1=OH, R_2=H
GlcNAc: R_1=H, R_2=OH

GalNAc: R_1=OAc, R_2=H
GlcNAc: R_1=H, R_2=OAc

Scheme 2.5: Synthesis of β-azido *N*-acetyl-D-galactosamine **2.52** and β-azido *N*-acetyl-D-glucosamine **2.53**. *Reagents and Conditions*: i) NaN_3, DMC, 2,6-lutidine, D_2O, 6 ˚C, 66 h, 75-78 %; ii) Ac_2O, pyridine, rt, h, 85-90 %.

2.3.3 Synthesis of Monovalent AGCs

Three monovalent ligands were synthesised according to the route shown in Scheme 2.6 and their structures are shown in Figure 2.16. The synthesis of the monovalent ligands utilized the 1,3 aromatic core **2.56**. AGCs **2.60** and **2.61** have a sugar moiety (galactose and fucose, respectively) bonded directly through the anomeric position

to triazolyl linkages to the aromatic core. AGC **2.62** is similar to compound **2.60**, but there are *O*-ethylene spacers in addition to the triazolyl linkages between the galactose and the aromatic core.

The synthesis of the monovalent AGCs are shown in Scheme 2.6. 3-aminobenzoic acid **2.54** was reacted with propionyl chloride. The resulting carboxylic acid **2.55** was reacted with propargylamine using TBTU (mechanism shown in Section 2.3.3.1) to give the amide **2.56** in 98 % yield. The attachment of the carbohydrate moiety to the aromatic scaffold was effected by means of the CuAAc reaction. The corresponding *O*-acetyl-1-β-azido-glycoside **2.40**, **2.45**, or **2.47** was reacted with the monovalent scaffold **2.59** using copper sulphate and sodium ascorbate as the catalytic system giving glycoconjugates **2.57**-**2.59** in 76-88 % yield. The deacetylation of these compounds were accomplished under mild basic conditions to give the monovalent glycosyl AGCs **2.60**-**2.62** in 87-94 % yield. The ^{1}H NMR for AGC **2.61**, a representative example of the monovalent series, is shown in Figure 2.17. The characteristic signals of the monovalent fucose ligand are shown. The integration proves that it is a monovalent ligand, since the triazolyl-H and the H-1 of the fucose both integrate for one each, while each of the aromatic protons also integrate for one each.

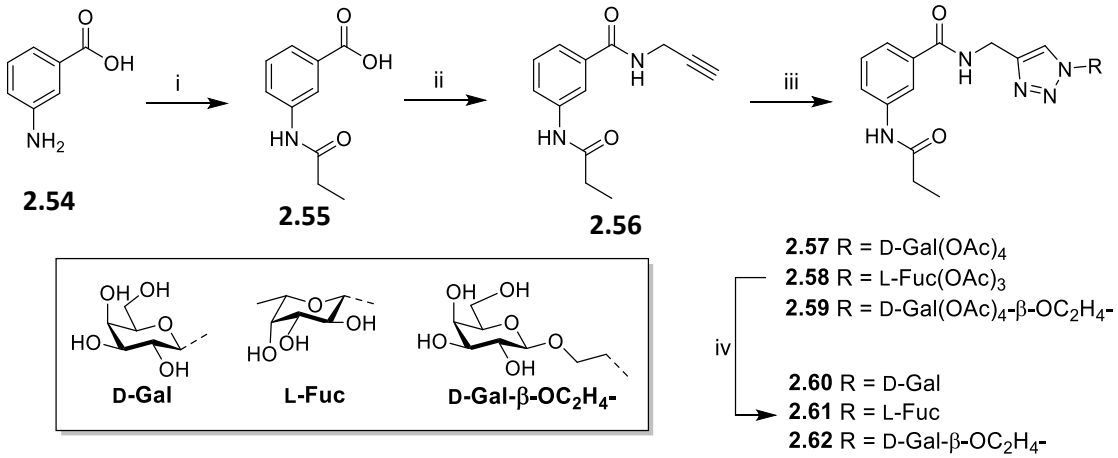

Scheme 2.6: Synthesis of monovalent ACG **2.60-2.62**. *Reagents and conditions*: i) C_2H_5COCl, NEt_3, THF, N_2, rt, 16 h, 23%; ii) TBTU, NEt_3, propargylamine, DMF, 16 h, 98%; iii) *O*-Acetyl sugar azide **2.40**, **2.45** or **2.47**, $CuSO_4.5H_2O$/Na Asc, CH_3COCH_3/H_2O, 16-24 h, 76-88 %; iv) MeOH, NEt_3, H_2O, 45°C, 87-94 %.

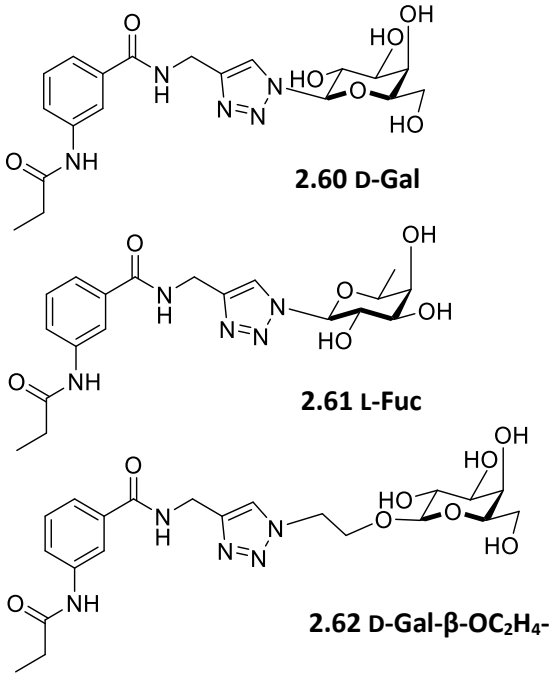

Figure 2.16: Structure of monovalent AGCs.

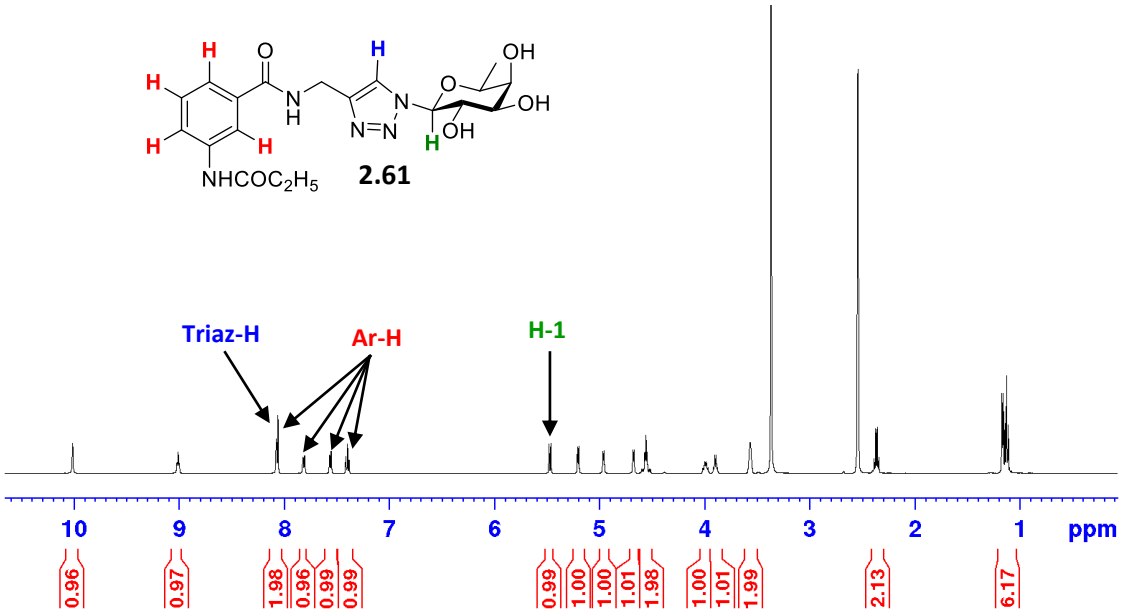

Figure 2.17: ^{1}H NMR spectrum of the monovalent fucose derivative **2.61** in DMSO-d_6. Characteristic signals highlighted.

2.3.3.1 TBTU as a Coupling Reagent

TBTU (2-(1H-benzotriazole-1-yl)-1,1,3,3-tetrametylaminium tetraflouroborate) was first used as a coupling reagent in 1989[188], where it was considered ideally suited for solid-phase peptide synthesis. It was originally believed to have an uronium structure but crystallography data and solution studies revealed it actually has an aminium structure, in particular TBTU is a guanidinium *N*-oxide salt.[189] Nevertheless, by custom, TBTU along with similar reagents are still considered to be uronium coupling reagents. HOBt is often used in conjunction with TBTU to reduce racemisation occurring during the peptide bond formation.[188]

TBTU was used as the coupling reagent to form the monovalent scaffold **2.56** and the mechanism is shown in Scheme 2.7. First, the carboxylic acid **2.55** is deprotonated under mild basic conditions. The carboxylate anion **2.63** then attacks the aminium carbocation of the TBTU to form the activated ester **2.64**. This also results in the formation of OBt^- (an anionic benzotiazole *N*-oxide), which then attacks the electrophilic carbon of the active ester, to give a second active ester intermediate **2.65** and *N*,*N*'-dimethylurea bi-product **2.66**. The propargylamine then attacks the electrophilic carbon of the activated ester to form the desired amide product **2.56** and a molecule of HOBt. However, it is important to highlight, that this is not the only pathway possible and the amide product can be formed via a number of routes. The amine could also attack the first active ester **2.64** generating the amide product. Also, the carboxylate ion can attack the active ester to form an anhydride, which could then react with the amine to form the amide product.

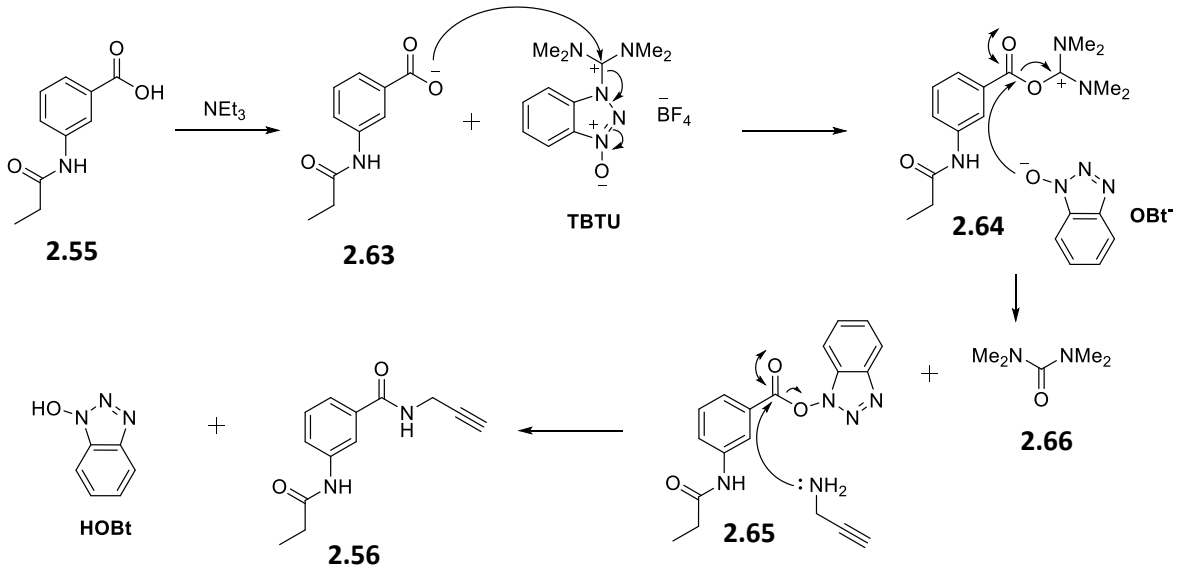

Scheme 2.7: Mechanism of TBTU mediated amide bond formation in **2.56** from the carboxylic acid **2.55**.

2.3.4 Synthesis of Divalent AGCs

Firstly, eight aromatic divalent ligands **2.78**-**2.85** were synthesised and are shown in Figure 2.18. All of these compounds utilise the 1,3,5-aromatic core with triazolyl linkages to the carbohydrate moieties. AGCs **2.78**, **2.69** and **2.81**-**2.83** have the sugar moiety (galactose, fucose, mannose, lactose and glucose derivatives, respectively) bonded directly through the anomeric position to a triazolyl linkage. However, compound **2.80** is similar to AGC **2.78** except it has an *O*-ethylene spacer in addition to the triazole linkage between the galactose and the core. AGCs **2.84** and **2.85** contain *N*-acetylated glycosamine moieties. Compound **2.84** contains two galactosamine derivatives, while compound **2.85** contains glucosamine analogues.

The synthesis of the divalent glycosides **2.78**-**2.85**, is depicted in Scheme 2.8. 5-Aminoisophthalic acid **2.67** was reacted with propionyl chloride. The resulting dicarboxylic acid **2.68** was reacted with propargylamine using freshly prepared 4-(4,6-dimethoxy-1,3,5-triazin-2-yl)-4-methylmorpholinium chloride (DMTMM) to give the diamide **2.69** in 78 % yield. This diamide was used as the divalent scaffold in the synthesis of all the divalent anti-adhesion compounds. TBTU was initially used for this reaction but the yield was poor (around 40 %). It was found that DMTMM was the

coupling reagent that performed best (around 80 %) to give the diamide **2.69** (mechanism shown in Scheme 2.10). The attachment of the carbohydrate moiety to the aromatic scaffold was effected by means for the CuAAc reaction. *O*-Acetyl-1-β-azido-glycosides **2.40**-**2.43**, **2.45**, **2.47**, **2.52** and **2.53** were reacted with the divalent scaffold **2.77** using copper sulphate and sodium ascorbate as the catalytic system. If the cycloaddition was carried out using conventional heating, the reaction times were long (up to four days) and the yields were moderate. However, it was found that if the reaction was carried out using microwave irradiation, it proceeded with yields typically up to 85 % for the protected glycoconjugate and with a drastic reduction in reaction times (10-30 mins). The deactylation was accomplished under mild basic conditions to give the divalent AGCs **2.78**-**2.85** in excellent yields.

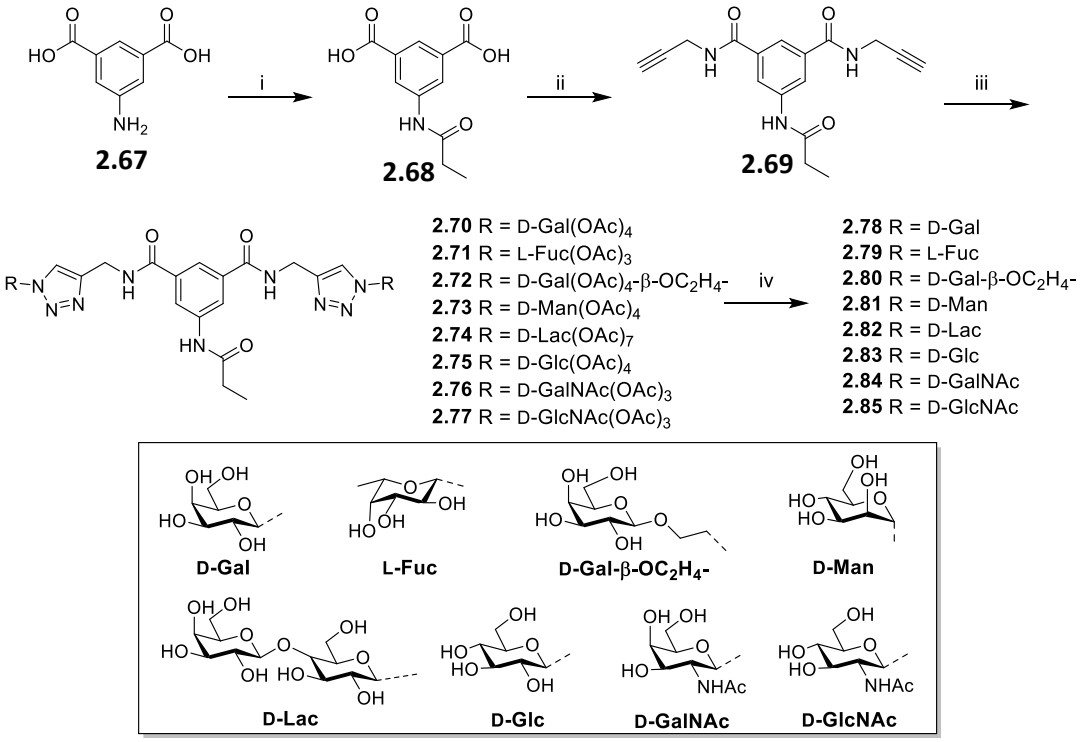

Scheme 2.8: Synthesis of divalent ACG **2.78**-**2.85**. *Reagents and conditions*: i) C_2H_5COCl, NEt_3, THF, N_2, rt, 22 h, 77 %; ii) DMTMM, propargylamine, DMF, N_2, rt, 16 h, 78 %; iii) corresponding *O*-Acetyl sugar azide **2.40**-**2.43**, **2.45**, **2.47**, **2.52** or **2.53**, $CuSO_4.5H_2O$/Na Asc, CH_3CN/H_2O, 42-84 %; iv) MeOH, NEt_3, H_2O, 45°C, 88-94 %.

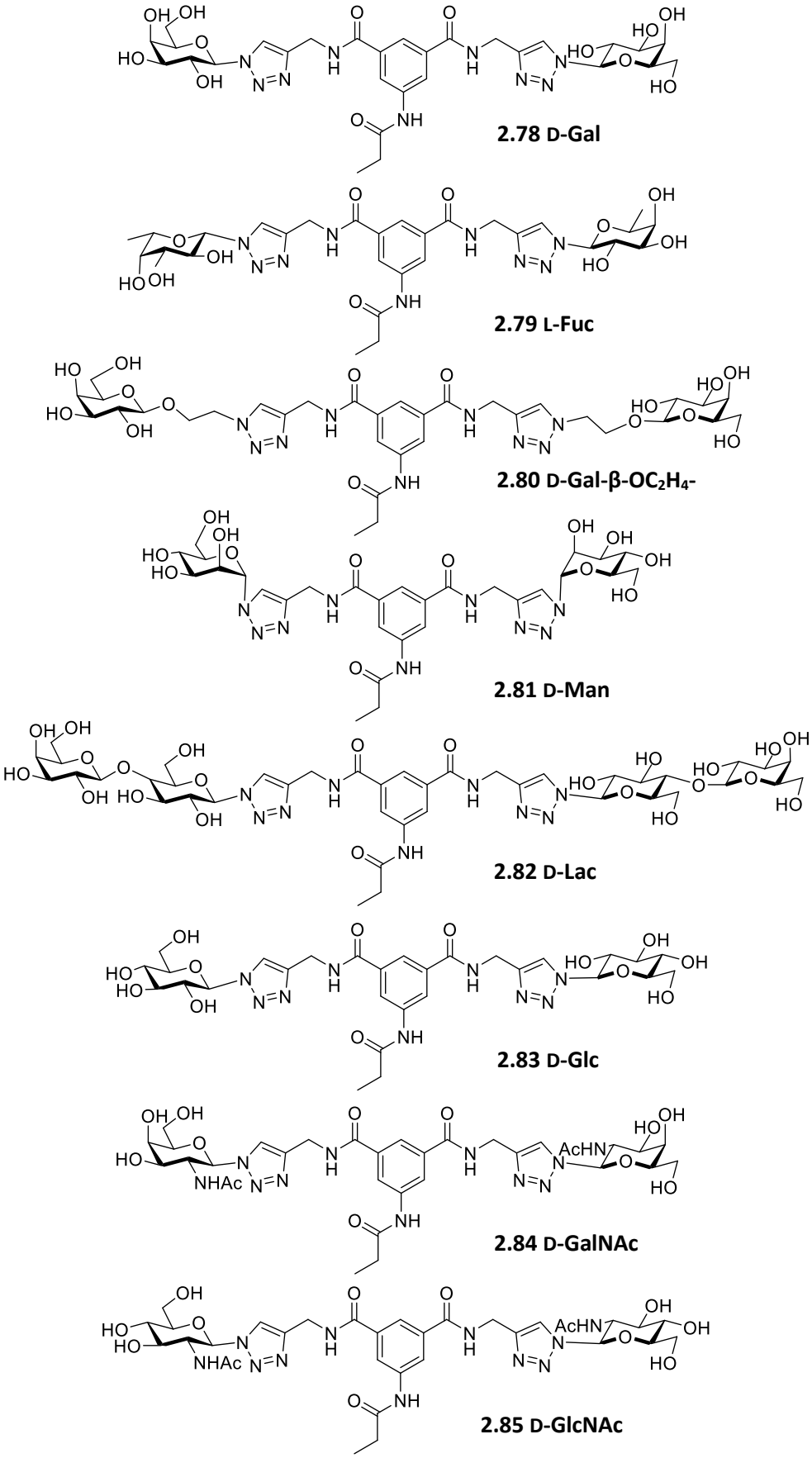

Figure 2.18: Structure of Divalent AGCs.

2.3.4.1 DMTMM as a Coupling Reagent

DMTMM has been highlighted as an effective activating agent for amide bond formation and peptide synthesis.[190] Although initially reported by Kaminski *et al*. in 1998,[191] it was not until Kunishima and co-workers[192, 193] optimised its usage that it began receiving interest as an alternative reagent for amide bond formations. DMTMM **2.88**, which is a white solid, is synthesised by the reaction of 2-chloro-4,6-dimethoxy-1,3,5-triazine (CDMT) **2.86** with N-methylmorpholine (NMM) **2.87** in THF at rt (Scheme 2.9). It is extremely easy to purify as the solid precipitates readily. However, it can be unstable and can only be used for one month after synthesis. As shown in Scheme 2.9, DMTMM **2.88** can undergo demethylation at the morpholinium nitrogen when suspended in DCM, while in THF it was found to be more stable with only 13% DMTM **2.89** detected after 13 hours.

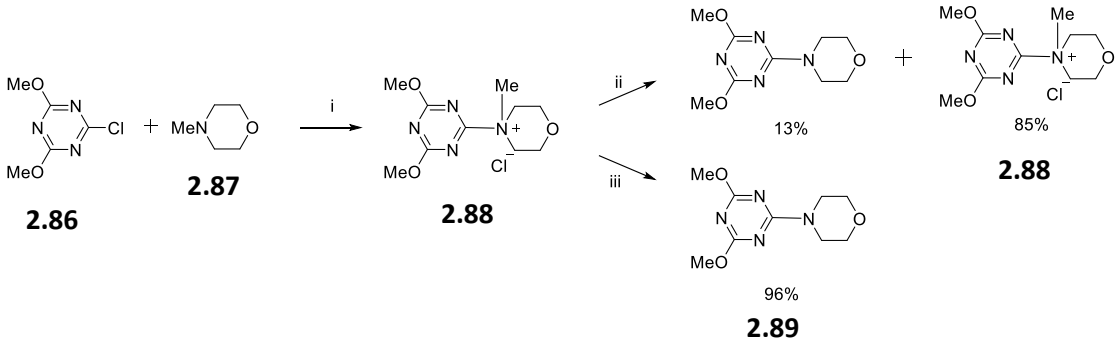

Scheme 2.9: *Reagents and conditions*: i) THF, rt, 30 min, 100 %; ii) THF, rt, 13 h; iii) DCM, rt, 3 h.

DMTMM was used as the coupling reagent to form the divalent scaffold **2.69** as shown in Scheme 2.10. In this reaction, the dicarboxylic acid **2.68** is deprotonated using a mild base to give the carboxylate ion **2.90**, which reacts with the DMTMM **2.88** in a S_NAr transformation. After an electron rearrangement, the activated ester **2.92** is formed, releasing a molecule of *N*-methylmorpholine. The resulting ester is highly reactive and can undergo nucleophilic attack. The propargylamine hence reacts with the activated ester **2.92** to form the amide, along with the triazinone by-product **2.95**. This mechanism occurs simultaneously with the other carboxylic to yield the diamide **2.69**.

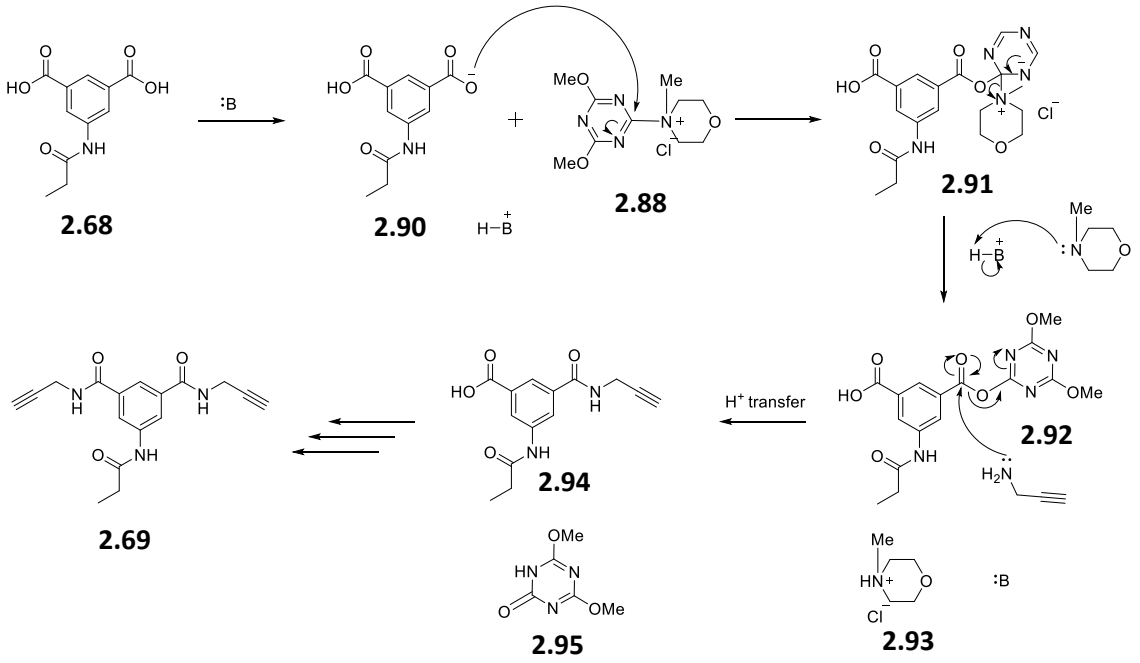

Scheme 2.10: Mechanism of DMTMM mediated amide bond formation in **2.69** from the dicarboxylic acid **2.68**.

2.3.4.2 Synthesis of AGC 2.98

To determine the importance of the linkage of the carbohydrate to the aromatic centre for the anti-adherence effect, a rigid divalent analogue without the triazole linker **2.98** was synthesised. Here, the 2,3,4,6-tetra-*O*-acetyl-1-β-azido-galactoside **2.40** was reduced to 2,3,4,6-tetra-*O*-acetyl-β-galactopyranosylamine **2.96**[194] using H_2/Pd (C), which was coupled directly to the dicarboxylic acid scaffold **2.68** using TBTU as the coupling reagent (mechanism outlined in Section 2.3.3.1). The peractylated compound **2.97** was formed in 68 % yield and was then deprotected under mild basic conditions to give the desired rigid, divalent AGC **2.98** in 96 % yield.

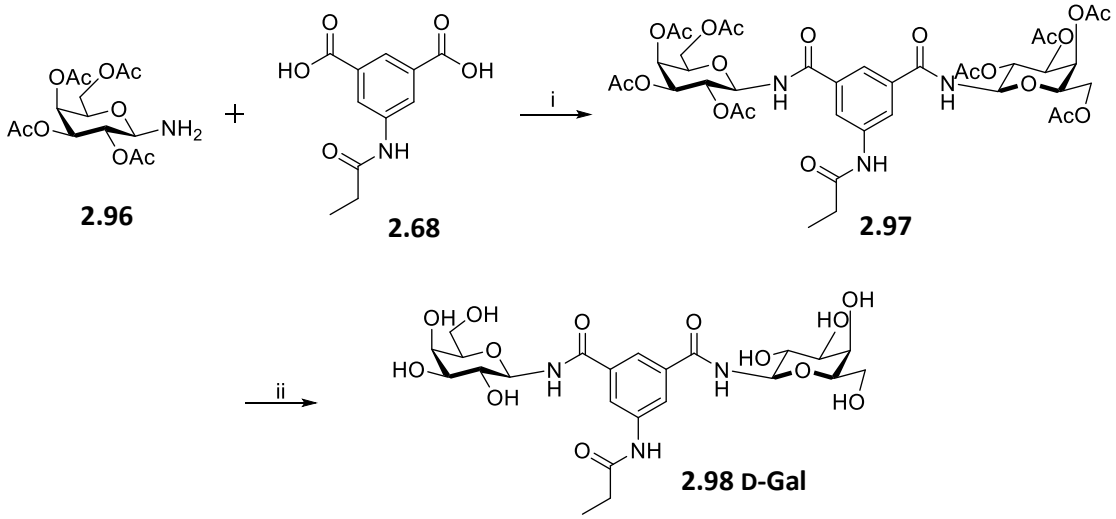

Scheme 2.14: Synthesis of directly linked galactosyl group **2.98**. *Reagents and conditions*: i) TBTU, NEt_3, DMF, N_2, 16 h, 68 %; ii) MeOH, NEt_3, H_2O, 45˚C, 96 %.

2.3.4.3 Synthesis of Heterodivalent AGC 2.101

A heterodivalent ligand **2.101** was also synthesised, which contained both galactosyl and mannosyl moieties. To synthesise this ligand, the 2,3,4,6-tetra-*O*-acetyl-α-azido-mannoside **2.42** was reacted with the divalent scaffold **2.69**, first under CuAAC conditions. This was achieved by having the scaffold in excess, i.e. using 4 equivalents of the scaffold **2.69** and one equivalent of mannosyl azide **2.42**. This crude mixture was purified by column chromatography. After chromatography, ^{1}H NMR showed that there was 1 equivalent of product **2.99** along with 1 equivalent of the scaffold **2.69** appearing as one spot on the TLC. Trituration with hot water removed the scaffold, leaving the desired product **2.99**.

In the reaction of galactosyl azide **2.40** with the divalent scaffold **2.69**, the purification of the monovalent intermediate was not possible, even after trituration with hot water. It was postulated that the corresponding intermediate interacted strongly with the divalent scaffold **2.69** and they were therefore not separable.

Following the attachment of the mannose azide, the galactose azide **2.40** was then reacted with compound **2.99** under CuAAC conditions, affording the peractylated derivative of the heterodivalent ligand **2.100**. This was then deprotected using standard conditions, i.e. methanol, NEt_3 and water, to give the final product **2.101** (Scheme 2.15).

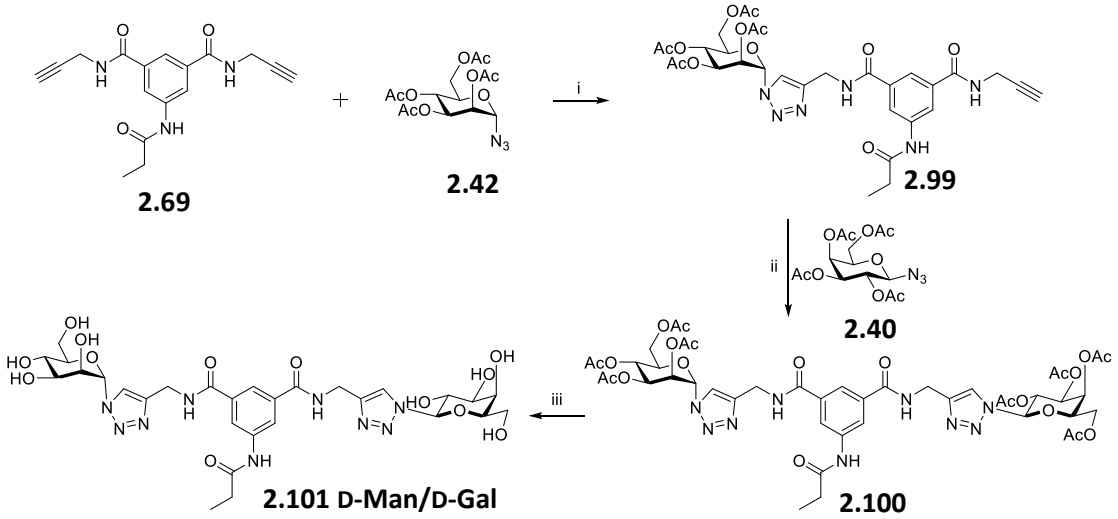

Scheme 2.15: Synthesis of the divalent asymmetric AGC. *Reagents and conditions*: i) $CuSO_4.5H_2O$/Na Asc, CH_3CN/H_2O, MW at 100 ˚C, 10 mins, 34 %; ii) 2,3,4,6-tetra-*O*-acetyl-1-β-azido-galactoside **2.40**, $CuSO_4.5H_2O$/Na Asc, CH_3COCH_3/H_2O, rt, 16 h, 84 %; iii) MeOH, NEt_3, H_2O, 45˚C, 6 h, 89 %.

2.3.5 Synthesis of Trivalent AGCs

Three trivalent AGCs were also synthesised **2.107**-**2.109** and their structures are shown in Scheme 2.11 and Figure 2.19. All these compounds also utilise the 1,3,5 aromatic core **2.103**. AGCs **2.107** and **2.108** have the three sugar moieties (galactose and fucose, respectively) bonded directly through the anomeric position to triazolyl linkages to the aromatic core. AGC **2.109** is similar to compound **2.107**, but there are *O*-ethylene spacers in addition to the triazolyl linkages between the galactoses and the aromatic core.

The synthesis of the trivalent AGCs, **2.107**-**2.109**, are shown in Scheme 2.11. 1,3,5-Trimesoyl chloride **2.102** was reacted with propargylamine in the presence of NEt_3 to give the triamide **2.103** in 44 % yield. A coupling reagent was not needed in this case, since 1,3,5-trimesoyl chloride is very reactive due to the excellent leaving ability of the chloride ion. Hence the propargylamine undergoes nucleophilic attack directly with the carbonyl carbon of the acyl chloride forming the amide bond. The attachment of the carbohydrate moiety to the aromatic scaffold was effected by means of the CuAAc reaction as outlined previously. The corresponding *O*-acetyl-1-β-azido-glycoside **2.40**, **2.45** or **2.47** were reacted with the trivalent scaffold **2.103**

using copper sulphate and sodium ascorbate as the catalytic system. The deacetylation of the peracetylated trivalent ligands **2.104**-**2.106** was accomplished under mild basic conditions to give the trivalent AGCs **2.107**-**2.109** in excellent yield.

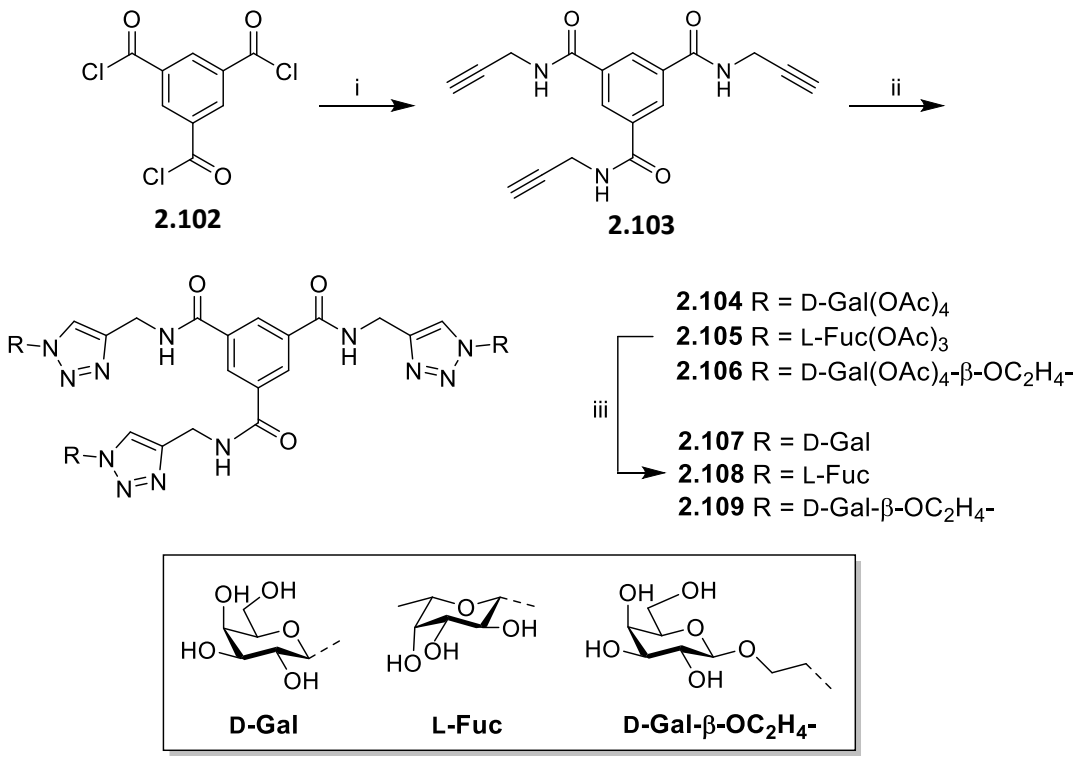

Scheme 2.11: Synthesis of trivalent ACG **2.107**-**2.109**. *Reagents and conditions*: i) propargylamine, NEt_3, DCM, 0 °C 3h, 44 %; ii) *O*-Acetyl sugar azide **2.40**, **2.45** or **2.47**, $CuSO_4.5H_2O$/Na Asc, CH_3COCH_3/H_2O, 16-24 h, 50-72 %; iii) MeOH, NEt_3, H_2O, 45 °C, 83-89 %.

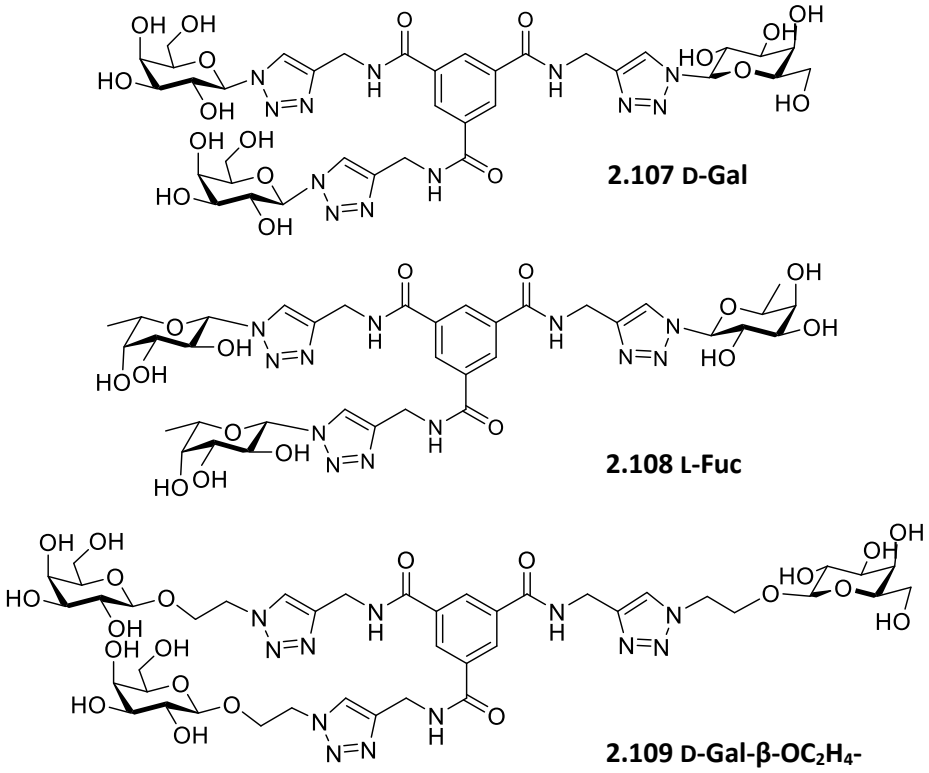

Figure 2.19: Structure of trivalent AGCs.

2.4 Biological Evaluation

The biological evaluation of compounds **2.60**-**2.62**, **2.78**-**2.85**, **2.98**, **2.101** and **2.107**-**2.109** was carried out in collaboration with Prof. Kevin Kavanagh in the Medical Mycology laboratory in the Biology Department of Maynooth University. I carried out the biological assays in this section, along with 4th Year research project students: Mairead McGovern, Aisling Gilroy, Stephenie Mullins and Sarah Howell. The experimental details of these assays are shown in Section 7.3.

2.4.1 Toxicity Assays

The toxicity of the compounds against *C. albicans* was firstly evaluated. Their toxicity was compared to the toxicity of a known anti-fungal drug, caspofungin,[195] which decreased the growth of the *C. albicans* dramatically. None of the compounds showed significant ability to inhibit the growth of yeast cells at the range of concentrations used in the subsequent adherence assays. This implies that any reduction of adherence observed is not due to toxic effects (Figure 2.20).

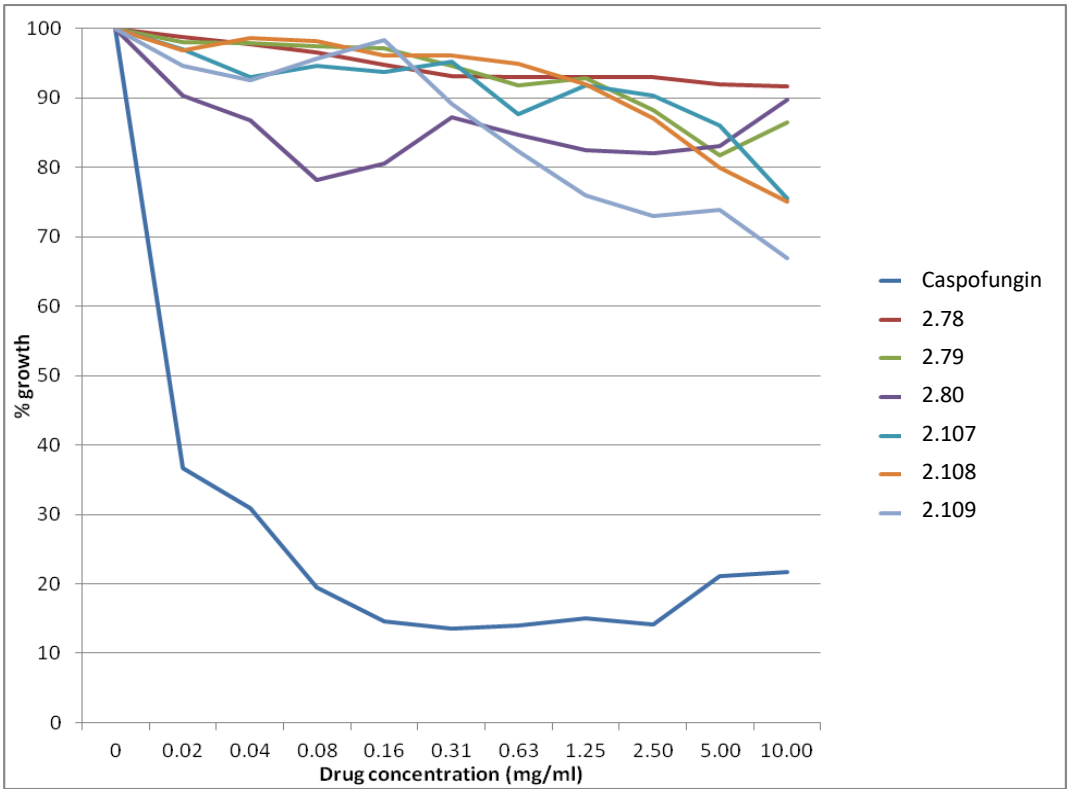

Figure 2.20: Toxicity assay of several AGCs against *C. albicans*.

2.4.2 Adherence Assays

The ability of the glycoconjugates to inhibit adherence of *C. albicans* was evaluated in different assays: exclusion, competitive and displacement assays.

2.4.2.1 Exclusion Assay

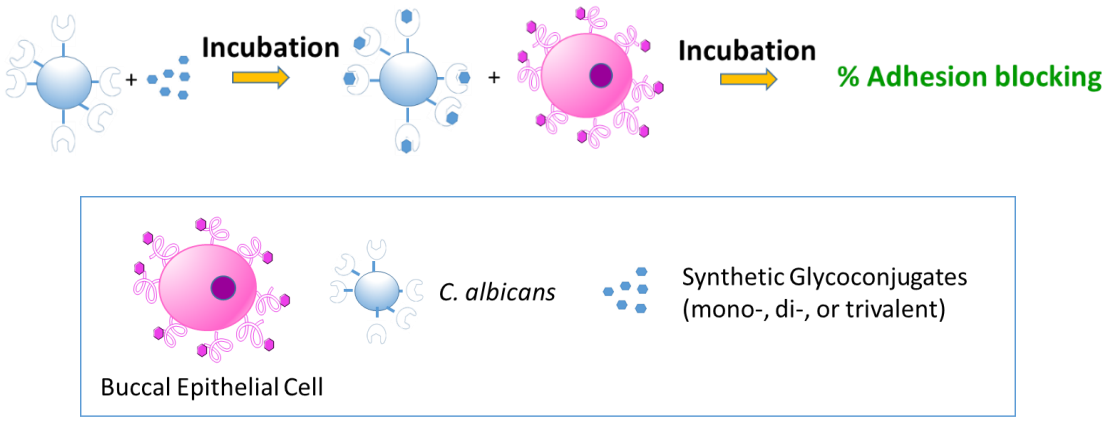

Figure 2.21: Diagram showing the exclusion assay carried out on AGCs.

This is the initial adherence assay that was performed to evaluate anti-adhesion activity of the AGCs. *C. albicans* cells were treated with the glycoconjugates, allowing

for an incubation period, then the treated yeast cells were exposed to the exfoliated BECs. The percentage increase or decrease of the number of *C. albicans* cells adhering to the BECs after treatment with the AGCs compared to the adherence of the untreated yeast in represented is Table 2.1. To calculate the change in adhesion the average number of yeast attached to each BEC in the control are counted and compared to the average number of yeast attached to the BEC in the presence of the AGCs.

Table 2.1: Effect of AGCs on adherence of *C. albicans* to BECs (estimated according to exclusion assays, at AGCs concentration = 13.8 µM. Standard error (SE) in all cases was less than 10% of mean change in adherence). *Calculated at 1.38 µM. **Calculated from competitive assay at 1.38 µM

AGCs	Valency	% Increase/Decrease of Adherence
2.60 D-Gal	1	-14.5
2.61 L-Fuc	1	-2
2.62 D-Gal-β-OC_2H_4	1	-7.5
2.78 D-Gal	2	-80
2.79 L-Fuc	2	-8
2.80 D-Gal-β-OC_2H_4	2	-35
2.81 D-Man	2	+3
2.82 D-Lac	2	+6.5
2.83 D-Glc	2	-33*
2.84 D-GalNAc	2	-59**
2.85 D-GlcNAc	2	-45
2.98 D-Gal	2	-26
2.101 D-Gal/D-Man	2	-24
2.107 D-Gal	3	-45
2.108 L-Fuc	3	-30
2.109 D-Gal-β-OC_2H_4	3	-42

2.4.2.1.1 Effect of Valency

To test the effect of valency, monovalent, divalent and trivalent derivatives of the anti-adhesion ligands were synthesised. The results presented in Table 2.1 show the impact of the valency effect in the anti-adherence ability of the AGCs: monovalent compounds, in which only one carbohydrate moiety is present, are considerably less active than their di- and trivalent counterparts.

Comparing the results of the galactosyl anti-adhesion ligands after the exclusion assay, it is clear that the divalent AGC **2.78** worked best (Figure 2.22 a). AGC **2.78** decreased the adherence by 80 %, while the trivalent AGC **2.107** reduced the adhesion by 45 % and the monovalent AGC **2.60** by 14.5 %. This highlights the importance of having a divalent galactosyl ligand to inhibit the adhesion of *C. albicans* to BEC. In the case of the fucosyl AGCs, it was found that the anti-adhesive properties of the ligands increased with increasing valency, where the monovalent derivative **2.61** was least effective with a decrease of 2 % and the trivalent ligand **2.108** was most effective with a decrease of 30 % (Figure 2.22 b). Since the divalent galactose compound showed considerably better results than any of the fucosyl compounds, these compounds were not focused on throughout the rest of the assays.

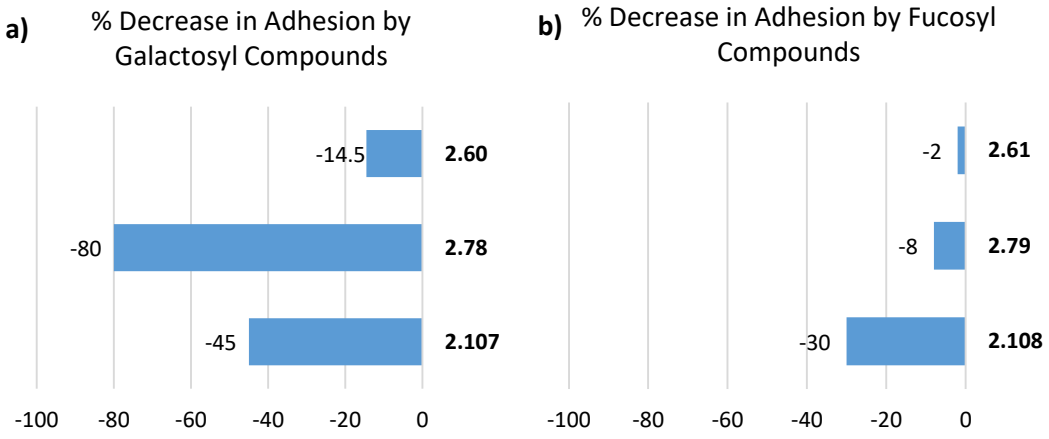

Figure 2.22: Graphs showing the percentage decrease in adhesion of *C. albicans* to BECs after an exclusion assay after exposure to: a) galactosyl compounds **2.60** (monovalent), **2.78** (divalent) and **2.107** (trivalent); b) fucosyl compounds **2.61** (monovalent), **2.79** (divalent) and **2.108** (trivalent).

2.4.2.1.2 Effect of Different Sugars

To test the effect of different sugars on the anti-adherence effect of the AGCs, different derivatives of the monovalent, divalent and trivalent AGCs were synthesised and evaluated in the exclusion assay. Focusing on the divalent AGCs, there are a wide variety of results from the exclusion assay, as seen in Figure 2.23.

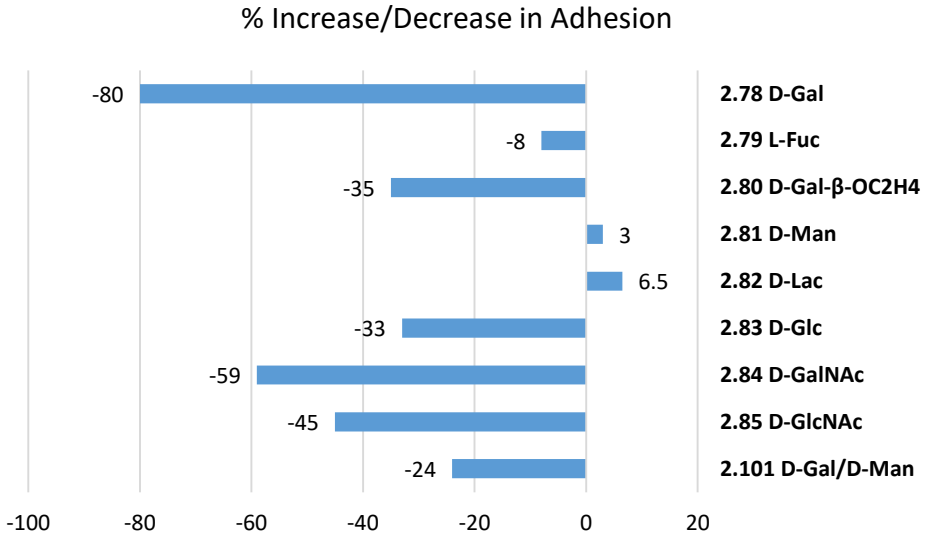

Figure 2.23: Graph showing the percentage increase/decrease in adhesion of *C. albicans* to BECs after an exclusion assay after exposure to divalent AGCs at 13.8 µM, except divalent AGC **2.83** at 1.38 µM and **2.84** at 1.38 µM in competitive assay.

It can be clearly seen that divalent galactoside **2.78** was identified as the most active compound of the AGCs library screened, showing a remarkable 80 % decrease in adherence of the yeast to the BECs after treatment. This was followed by the *N*-acetyl glucosamine derivative **2.85**, which decreased adhesion by 45 %. Remarkably, changing from the glucosamine to the glucose derivative had an effect on the anti-adherence properties of the divalent AGCs, since the divalent glucosyl AGC **2.83** only inhibited adhesion by 33 %. Interestingly, compound **2.101**, a structural analogue of **2.78** in which one of the galactosyl moieties has been replaced by mannose, is only capable of producing a 24 % reduction in yeast adherence. This highlights the importance of a divalent galactosyl pattern as a recognition motif. In Figure 2.23, it can also be seen that the mannosyl and lactosyl divalent AGCs actually promoted adhesion by 3 % and 6.5 %, respectively.

The divalent galactoside **2.78** was then evaluated at lower concentrations. Significantly, the anti-adherence ability of this compound was maintained at a 100-fold dilution in concentration (0.1 mg/mL, 0.14 µM) as shown in Figure 2.24.

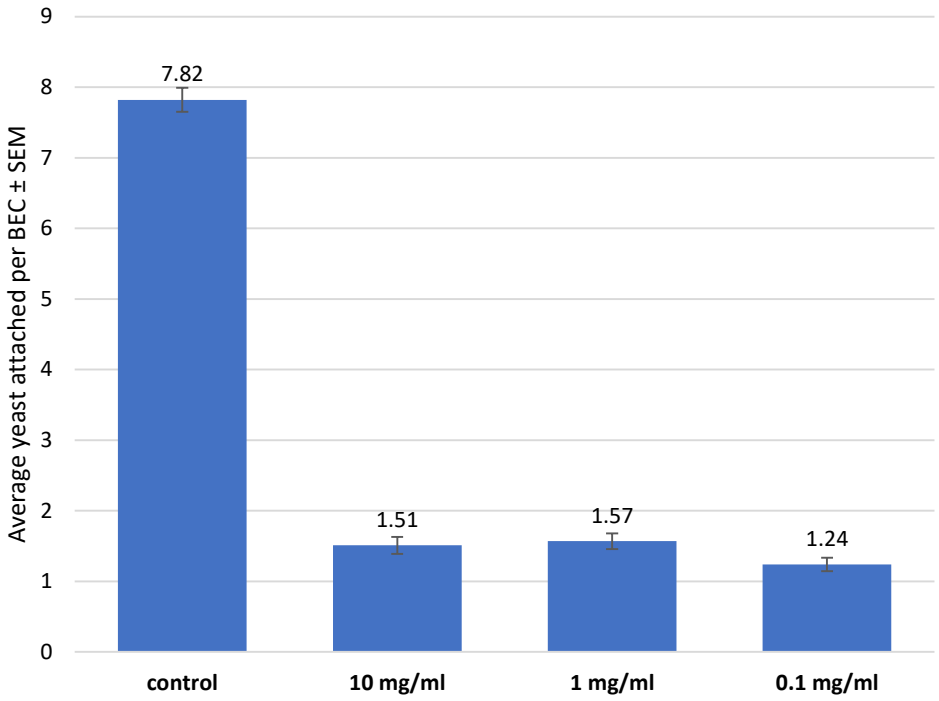

Figure 2.24: Shows the effect of divalent **2.78** (concentrations 10, 1, 0.1 mg/mL) on the adherence of *C. albicans* to BECs after the Exclusion assay where the *C. albicans* was pre-incubated. The data displays average yeast adherence per BEC.

2.4.2.1.3 Effect of Linker

From Table 2.1 it is clear that the linker connecting the galactosyl moieties to the aromatic scaffold appears to also influence the anti-adherence ability of the glycoconjugates. The more flexible *O*-galactosides **2.62**, **2.80**, **2.109** inhibited yeast adherence less effectively than their respective analogues **2.60**, **2.78**, **2.107**, in which the triazolyl spacer group is directly attached to the anomeric galactosyl carbon.

After the initial screening of the anti-adhesion ligands, the divalent galactosyl compound **2.78** was deemed the lead compound. Studies were then carried out to determine if the distance between the galactose moieties was important to cause an anti-adhesive effect. Hence, the anti-adhesive nature of compounds **2.80** and **2.98** were compared to the lead compound **2.78**. In the exclusion assay, the smaller, more

rigid galactosyl derivative **2.98** decreased the adhesion of the yeast to the BEC by only 26 %. The more flexible derivative, with the extra ethyl linker, compound **2.80** decreased the adhesion by 35 % (Figure 2.25). Hence, from this comparison it is clear that having the galactose moieties too close and locked in a rigid structure, as in compound **2.98**, does not result in a good anti-adhesive ligand. Having a more flexible structure, as in compound **2.80** is also not the optimum structure to decrease the adhesion of the yeast to the BEC.

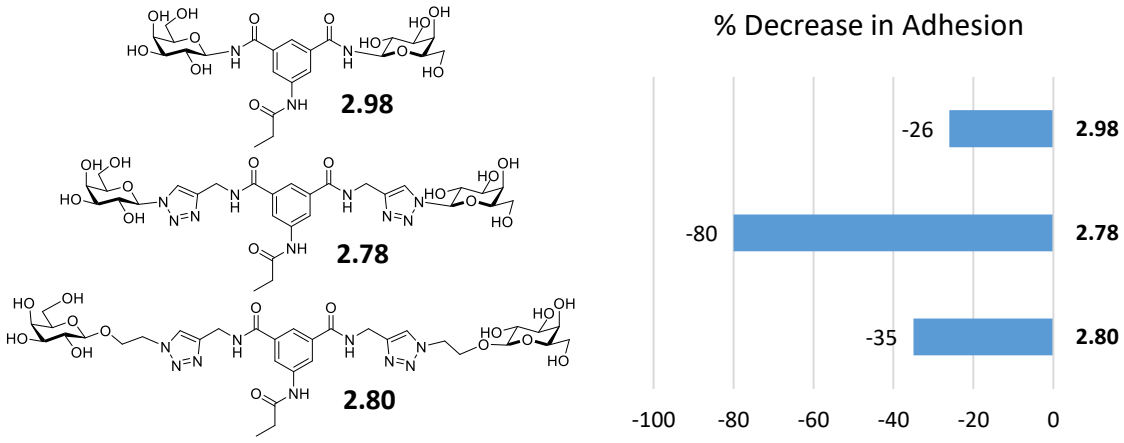

Figure 2.25: Structure of AGCs **2.98**, **2.78** and **2.80**. Graph showing the percentage decrease in adhesion of *C. albicans* to BECs after an exclusion assay after exposure to galactosyl compounds **2.98**, **2.78** and **2.80**.

2.4.2.2 Competitive Assay

Figure 2.26: Diagram showing the competition assay carried out on AGCs.

The best preforming compounds were then evaluated in a competition assay, in which their anti-adherence ability was tested in the presence of both *C. albicans* and BECs (Figure 2.26). Co-incubation with compound **2.78** resulted in a reduction in adherence of yeast cells to BECs of 60 %, even at the lowest concentration (Figure 2.27). Whereas, co-incubation with compound **2.80** resulted in only 45 % decrease in adhesion. Again, emphasising the requirement of having the galactosyl moieties at the correct distance and orientation for having good anti-adhesive properties. The

anti-adhesion properties of AGC **2.78** in the competition assay was then evaluated at lower concentrations. Again, the anti-adherence ability of this compound was maintained at 100-fold dilution (Figure 2.28).

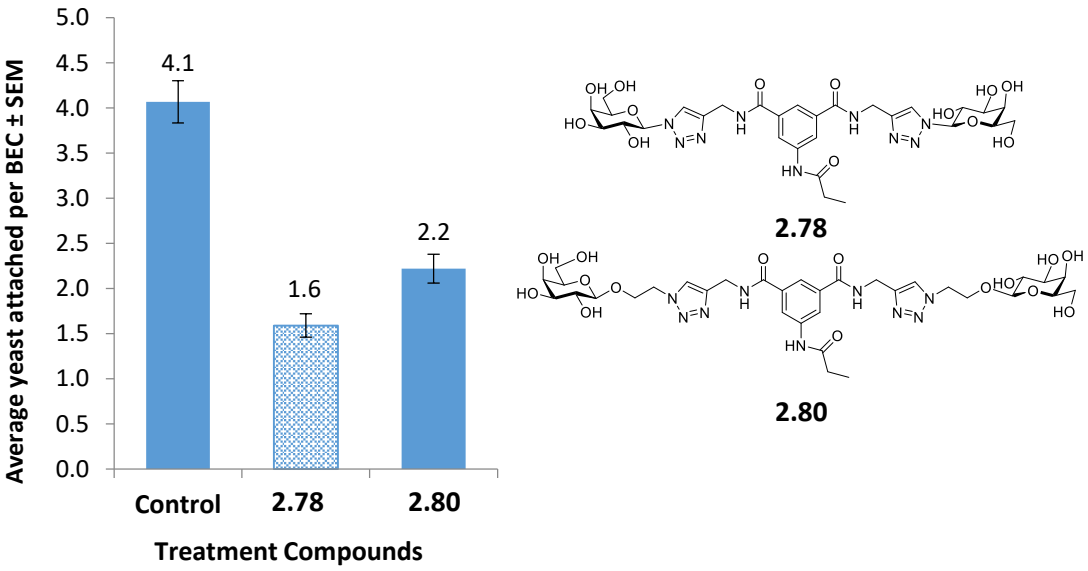

Figure 2.27: Shows the structure of galactosyl anti-adhesion ligands **2.78** and **2.80**, and the results from the competitive assay after each compound was co-incubated with the *C. albicans* and the BECs.

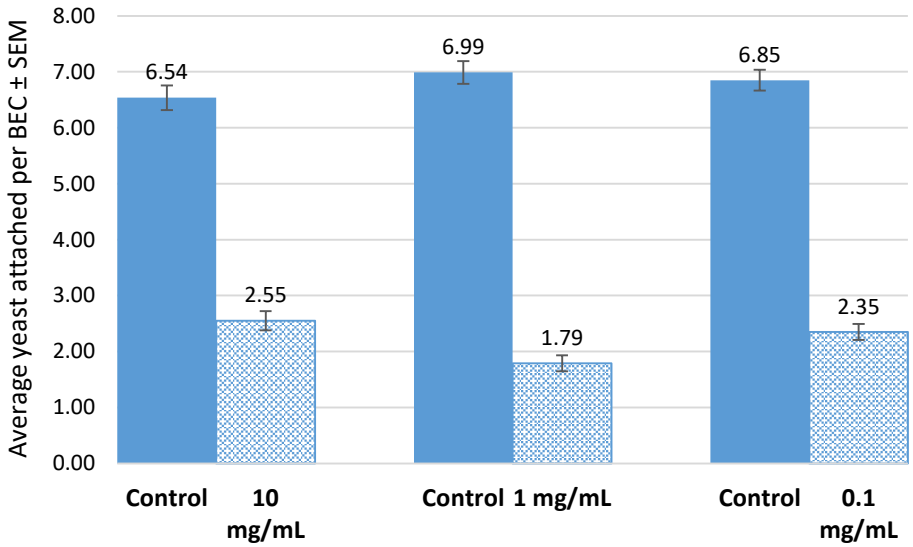

Figure 2.28: Shows the effect of divalent **2.78** (concentrations 10, 1, 0.1 mg/mL) on the adherence of *C. albicans* to BECs after the Competition assay. The data displays average yeast adherence per BEC.

2.4.2.3 Displacement Assay

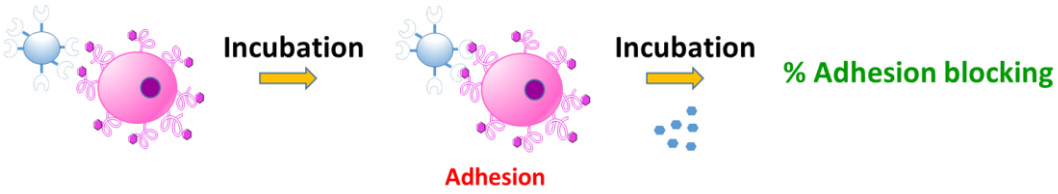

Figure 2.29: Diagram showing the displacement assay carried out on AGCs.

The displacement assay was then carried out on the best preforming AGCs. Here, the *C. albicans* and the BECs are co-incubated and adhesion is allowed to occur. The synthetic AGCs are then introduced and the percentage of adhesion blocking is determined (Figure 2.29). This assay was performed using glycoconjugates **2.78** (0.1 mg/mL, 0.138 µM) and **2.80** (0.11 mg/mL, 0.138 µM), which were added to a mixture of *C. albicans* and BECs, which had been previously incubated together. The ability of the compounds to reverse the adherence of the yeast to the BECs was then examined. Two controls were used in this assay: control 1 involved the assessment of the binding of *C. albicans* to BECs prior to compound exposure; control 2 involved BECs and adherent yeast cells being re-incubated in PBS for 90 minutes prior to a second filtration step. It was found that **2.78** imparted a reduction in adherence of 56% (compared to control 1) and 31 % (compared to control 2) as shown in Figure 2.30 a. These results suggest that divalent galactoside **2.78** binds with higher affinity to the *C. albicans* preventing its interaction with BECs. After the addition of compound **2.80**, only 12 % of BEC had no yeast attached (Figure 2.30 c). Here, the larger percentage of BEC with no yeast attached indicates a better anti-adhesion ligand. From these two assays it is apparent that compound **2.78** has the most favourable structure to reduce the adherence of *C. albicans* to the BEC, indicating that the flexibility in compound **2.80** is a hindrance.

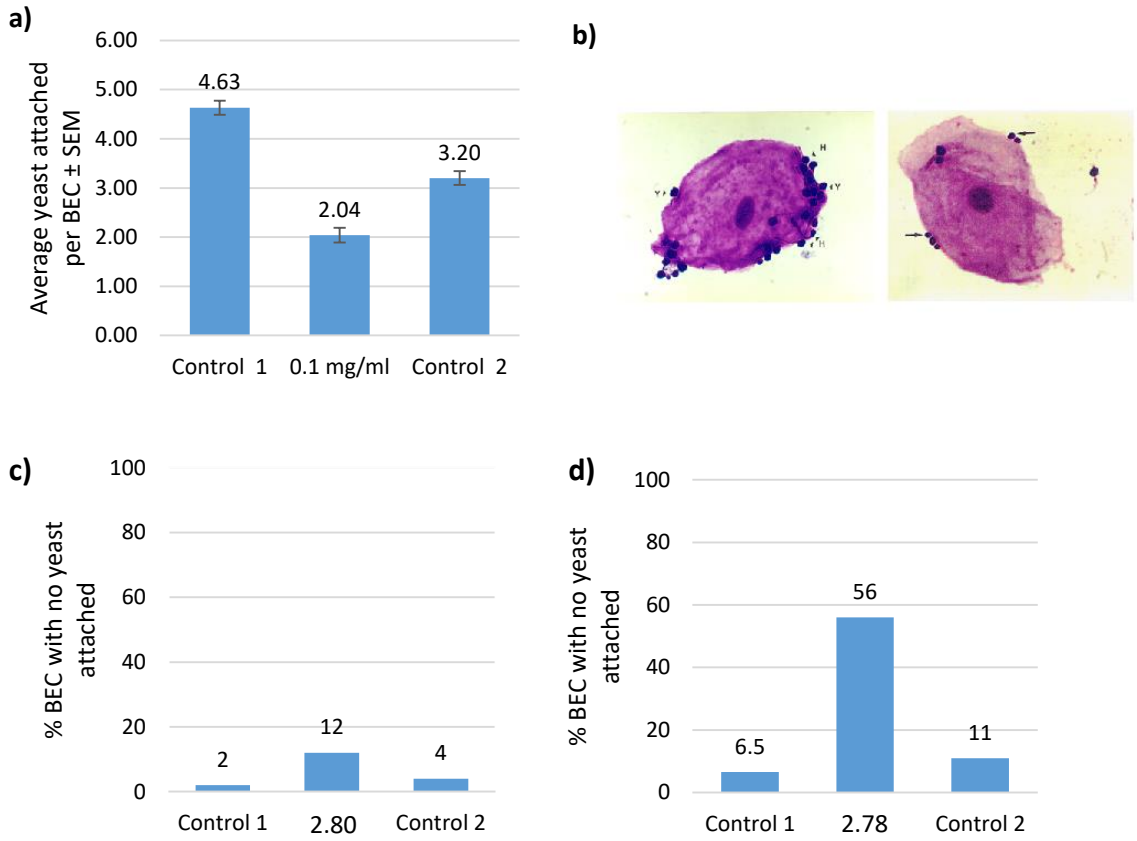

Figure 2.30: a) Shows the results from the Displacement Assay, where *C. albicans* and BECs were co-incubated and compound **2.78** (concentration 0.1 mg/mL) was subsequently added; control 1 involved the assessment of the binding of *C. albicans* to BECs prior to exposure; control 2 involved BECs and adherent yeast cells being re-incubated in PBS for 90 minutes prior to a second filtration step; b) Optical microscopy image of *C. albicans* attached to BEC before *(left)* and after *(right)* treatment with **2.78**; c) Graph showing the results from the Displacement Assay, where *C. albicans* and BECs were co-incubated and compound **2.80** (concentration 0.1 mg/mL) was subsequently added; d) Graph showing the results from the Displacement Assay, where *C. albicans* and BECs were co-incubated and compound **2.78** (concentration 0.1 mg/mL) was subsequently added.

2.5 Fluorescence Imaging

A fluorescently labelled analogue of galactosylated AGC **2.78**, compound **2.115**, was synthesized to investigate possible sites of interaction of anti-adherence AGCs with *C. albicans* (Scheme 2.12). 5-Aminoisophthalic acid **2.67** was reacted with di-*tert*-butyl dicarbonate to protect the amine group resulting in compound **2.110**. DMTMM **2.88** was then used to couple propargylamine to the resulting dicarboxylic acid to give the diamide **2.111** in 95 % yield. Galactosyl azide **2.40** was then attached to the

N-Boc-protected divalent scaffold **2.111** using the CuAAc methodology outlined previously. The 2,3,4,6-tetra-*O*-acetyl-β-azido-galactoside **2.40** was reacted with **2.111** using copper sulphate and sodium ascorbate at room temperature for 16 hours. Column chromatography was used to isolate the pure peractylated compound **2.112** in 71 % yield. The *tert*-butyloxycarbonyl group was then removed using TFA/DCM in 99 % yield to reveal the free amine group in compound **2.113**, which was reacted directly with fluorescein isothiocyanate (FITC). This reaction was carried out in the dark at room temperature overnight, followed by one hour in the MW at 50˚C to produce the crude product **2.114**. Without further purification, the crude product was deactylated using mild basic conditions to give the FITC-labelled galactosyl AGC **2.115**, which was triturated with DCM to remove excess FITC. NMR analysis showed that ~40 % of the product was fluorescently labelled. The signal for the anomeric proton of the galactose moieties consists of two overlapping doublets. The doublet with the higher integration (0.6) represents the non-FITC labelled compound, while the doublet with the integration of 0.4 represents the anomeric proton of the galactose sugar of compound **2.115**, the FITC labelled compound. NMR analysis is often used to determine the amount of fluorescently labelled compound present in a sample.[196, 197]

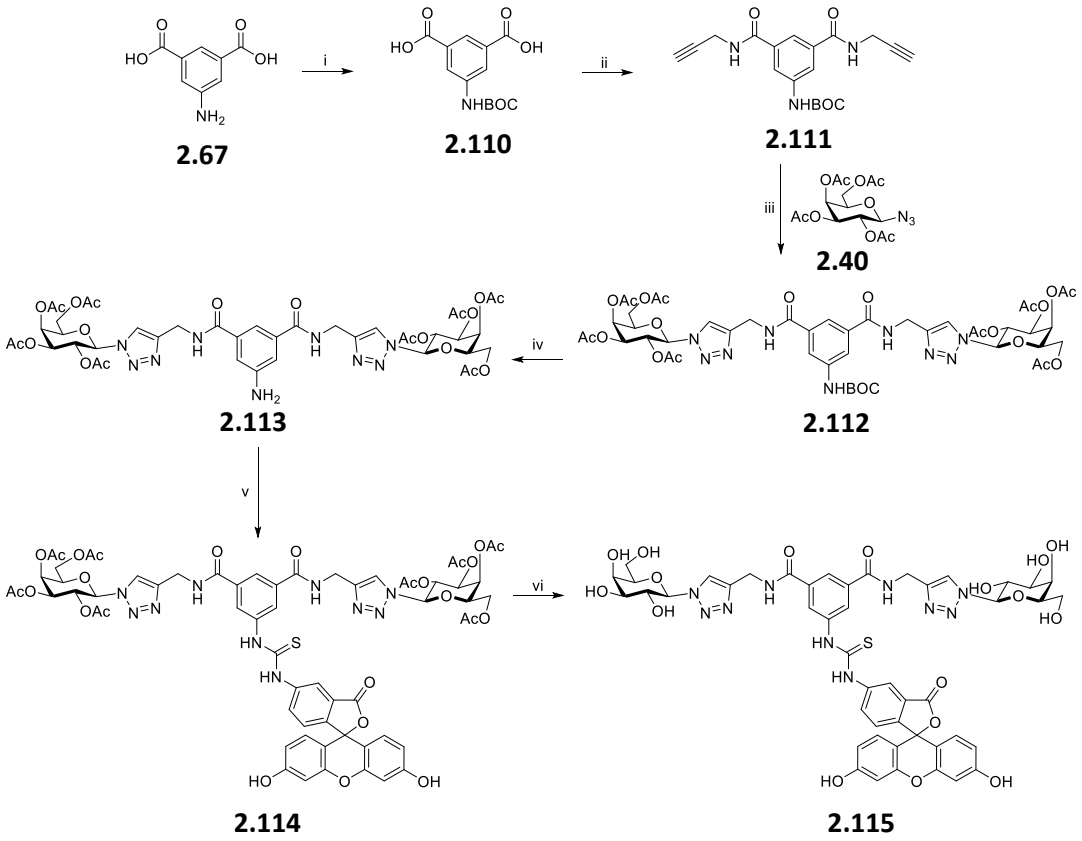

Scheme 2.12: Synthesis of fluorescently labelled galactoside ligand **2.115**. *Reagents and conditions*: i) Di-*tert*-butyl dicarbonate, NaOH, 1,4-dioxane, 0 ˚C to rt, 3 h, 86 %; ii) DMTMM, propargylamine, THF, 48 h, 95 %; iii) 2,3,4,6-tetra-*O*-acetyl-1-β-azido-galactoside **2.40**, $CuSO_4.5H_2O$/Na Asc, CH_3COCH_3/H_2O, rt, 16 h, 71 %; iv) TFA, DCM, 2 h, rt, 99 %; v) FITC, acetone, 50 ˚C, MW, 1 h, then in the dark, rt, 16 h, 40 %; vi) MeOH, NEt_3, H_2O, 45 ˚C, 6 h.

As controls, *C. albicans* with no treatment were imaged under an Olympus Fluoview 1000 confocal microscope to discard yeast autofluorescence (Figure 2.31 a). In addition, *C. albicans* cells were incubated with fluorescin isothiocyanate (FITC) and imaged (Figure 2.31 b). FITC-labelled galactoside **2.115** was then co-incubated with *C. albicans* cells and the cells were imaged. In this case, strong localized fluorescence at the surface of the yeast cells can be clearly observed. These images suggest that compound **2.115** is interacting with some structural components of the cell wall of the yeast cells (Figure 2.31 c). From the biological assays it is clear that the components in the yeast cell wall have high selectivity for the galactosyl AGCs that preformed best in the biological assays (Section 2.4). This suggests that the AGCs are

interacting with a lectin in the cell surface of the *C. albicans*, since lectins are proteins that bind specific carbohydrates.

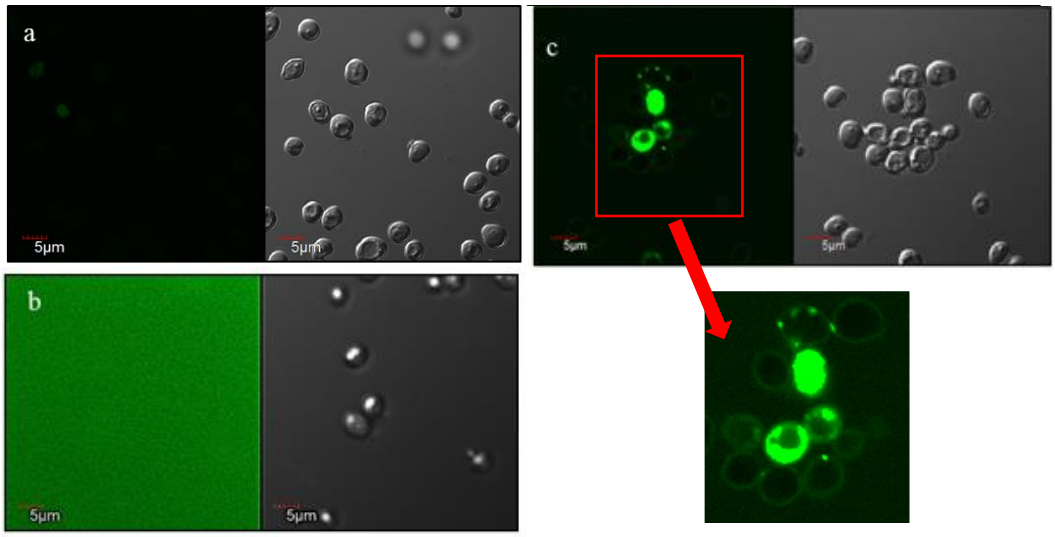

Figure 2.31: Confocal microscope images of *C. albicans* cells: a) without treatment; b) co-incubated with FITC; c) co-incubated with fluorescently labelled galactosyl AGC **2.115**, with zoomed in image of the localised fluorescence around the surface of the yeast cells. A wavelength of 488 nm laser was used for excitation and emission at 500-600 nm.

2.6 Conclusion

In conclusion, a small library of AGCs were designed to conduct a preliminary SAR study on their ability to inhibit the adherence of the pathogenic yeast *C. albicans*. Mono- (**2.60**-**2.62**), di- (**2.78**-**2.85**, **2.98** and **2.101**) and trivalent (**2.107**-**2.109**) AGCs were synthesised which included derivatives having different sugar moieties and different linkers from the sugar to the aromatic core. These AGCs were designed with sugar moieties that mimicked the cell surface glycans of the host cell to ensure the yeast would recognise them. Different linkers were used to determine if the distance between the sugars and the core would have an effect on the anti-adhesive properties of the AGCs. All these compounds were designed around a 1,3- or 1,3,5-aromatic core, which allowed for a convergent synthetic route using accessible building blocks. *O*-acetyl sugar azides were synthesised from well-known synthetic routes and were bonded to the aromatic core using CuAAC reaction conditions. The resulting peracetylated compounds were then deprotected to give the desired AGCs.

The anti-adherence properties of the AGCs were then tested using three adherence assays: exclusion, competition and displacement. The anti-adherence assays allowed for the identification of divalent galactosyl derivative **2.78** as an efficient inhibitor of *C. albicans* adherence, being able to displace over 50 % of yeast cells already attached to BECs. The precise three-dimensional presentation of the galactosyl moieties in **2.78** appears to be a requirement for efficient adherence inhibition, since the other divalent galactosyl analogues **2.80** and **2.98** have significantly lower abilities at decreasing adherence. Also, the heterodivalent analogue **2.101** did not inhibit the adhesion of the yeast to the BEC significantly. This suggests that AGC **2.78** is interfering with a specific recognition process that is a part of the complex *C. albicans* adherence mechanisms. There is a requirement for a divalent galactosyl ligand, where the sugar moieties are at the optimum distance and orientation for interacting with the yeast. Fluorescence studies suggest that a potential target for **2.78** could be a fungal cell wall lectin, since it has high specificity to the type of sugar in the AGC. For example, the divalent mannosyl and lactosyl AGCs actually promoted adhesion, instead of the desired effect to inhibit the adhesion process.

The synthetic accessibility and high efficacy shown by **2.78** in the biological assays make this compound a promising lead for development of new fungal anti-adherence agents, less prone to the development of resistance mechanisms than conventional fungicidal treatments.

Chapter 3

Second Generation of Glycoconjugates as Inhibitors of Fungal Adhesion: Alternative Scaffolds

3.1 Introduction

Synthetic glycoconjugates can be built around many scaffolds, not only aromatic frameworks. They can also be assembled around aliphatic, carbohydrate and peptide scaffolds, along with more unusual scaffolds such as cyclophosphazene cores, azamacrocycle cyclams, linear pentaerythrityl phosphodiester oligomers and polyhedral oligosilsesquioxanes (Figure 3.1).[198] The use of different scaffolds results in a diverse display of the carbohydrate moieties which may affect the biological activity of the glycoconjugates.

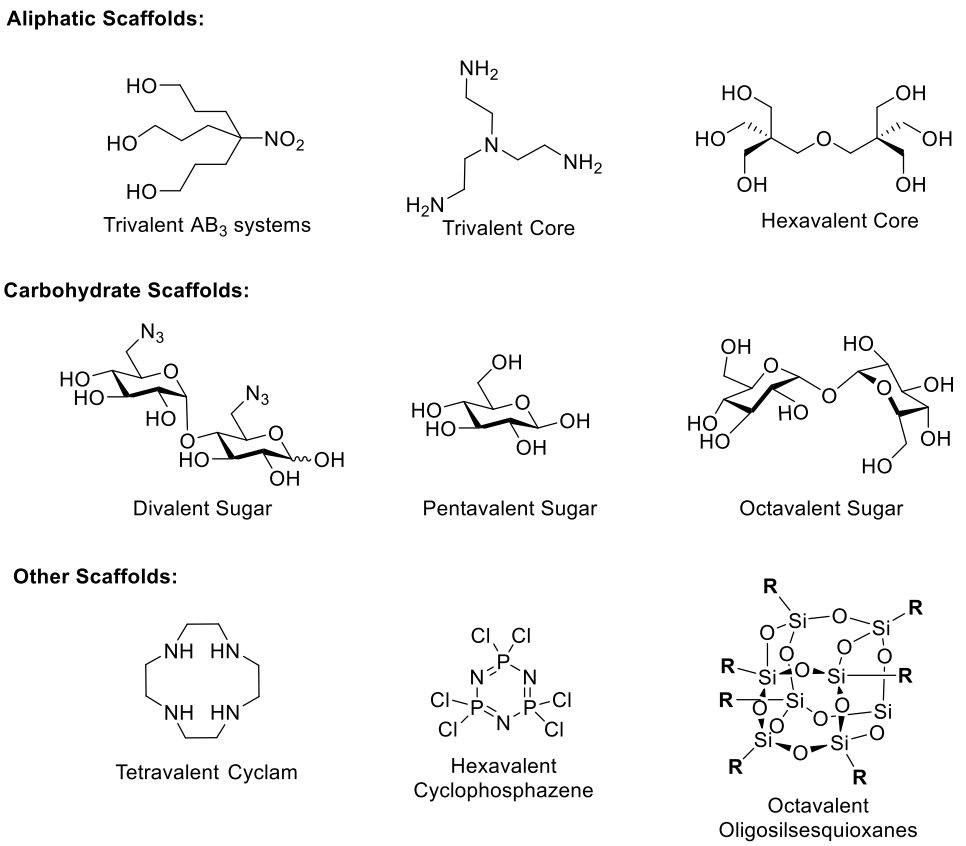

Figure 3.1: Common scaffolds used in the design of glycoclusters and glycodendrimers.[198]

Generally, it is assumed that the inner scaffolds play a passive role by only providing physical support to the attached carbohydrates. However, recent studies show that scaffolds actively influence recognition and can potentially modulate lectin-mediated signalling properties of glycoconjugates. It was found that scaffolds of glycoconjugates help the covalently attached carbohydrates to become more

spontaneous in lectin binding and they help diversify the lattice forming or cross-linking properties of glycoconjugates.[199]

With this in mind, we wanted to explore the effect of molecular scaffolds in a second generation of analogues of the lead compound **2.78** identified in earlier work (discussed in Chapter 2). We chose to investigate squaramide and norbornene core frameworks, both of which are not commonly used in the synthesis of glycoconjugates, but still would allow for the introduction of the two triazolyl galactoside moieties required for anti-adhesion activity in the first generation of compounds.

3.1.1 Squaramides

Squaramides have been extensively investigated across diverse areas of the chemical and biological sciences. Squaramides are a family of conformationally rigid cyclobutene ring derivatives, which are derived from squaric acid (3,4-dihydroxycyclobut-3-ene-1,2-dione). Squaramides are able to form up to four hydrogen bonds; two carbonyl hydrogen-bond acceptors and two NH hydrogen bond donors. Interestingly, squaramides are considered to be aromatic compounds. The lone pair on the nitrogen atoms can delocalize into the cyclo-butenedione ring system resulting in the four-membered ring with aromatic character (Hückel's rule: [4n + 2] π electrons, n = 0). In addition, an enhancement in the squaramides aromaticity is observed when they participate in hydrogen bonding.[200] These properties have led to squaramides being used in areas of self-assembly and molecular recognition processes since they can benefit from favourable thermodynamic stability brought about by aromatic gain.

It is possible to readily synthesise monoamide derivatives, as well as, symmetrical and unsymmetrical diamide derivatives from diester squarates. The selective formation of the monoamide is explained by the much faster amidation of the diester compared to the resulting ester amide. This allows the selective and sequential amidation if an additional base is added (usually triethylamine, or a basic aqueous buffer solution) to the ester amide in the presence of a second amine (Scheme 3.1). This concept was first reported by Rajewsky and coworkers.[201]

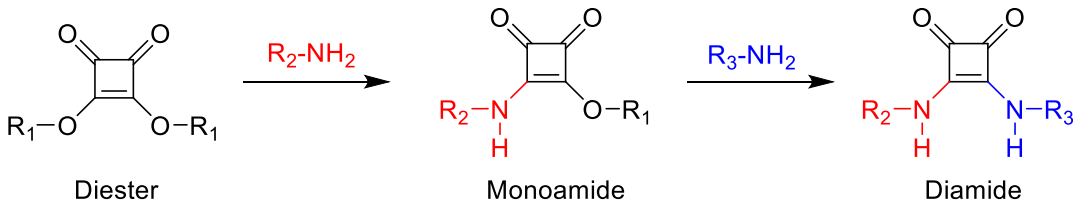

Scheme 3.1: General scheme for the sequential amidation of squarates resulting in symmetrical (if $R_2 = R_3$) and unsymmetrical (if $R_2 \neq R_3$) diamides of squaric acid, where R_1-R_3 can be any alkyl or aryl substituent.[202]

Squaramides have found uses in areas of materials science and biology. In particular in self-assembly, organocatalysis, molecular recognition, medicinal chemistry and bioconjugation.[203]

Due to their selectivity in relation with amino functional groups, squaric acid esters are widely applied in carbohydrate chemistry as linker molecules between amino-saccharides and proteins.[202] Carbohydrate conjugations mediated by squaramide tethers are often used for the grafting of carbohydrate epitopes onto peptides and proteins. For example, squaramides have been used to link mannosides to BSA (bovine serum albumin) which acts as a carrier protein for immunological investigations. Nifantiev *et al.*[204] synthesised 3-aminopropyl glycosides of a heptasaccharide fragment of the cell wall mannan from *Candida*, which corresponds to the antigenic Factor 9. The aminopropyl glycoside of the heptamannoside **3.1** was reacted with diethyl squarate **3.2** to give the monoamide **3.3**, which was then coupled to BSA (bovine serum albumin) to produce the target neoglycoconjugate **3.4** (Scheme 3.2). This compound was analysed for the capacity to induce protective humoral immunity and appropriate cellular immunity.[205] This research provides some insights on the immunomodulatory properties of oligomannosides and contributed to the development of synthetic oligosaccharide vaccines against fungal diseases.

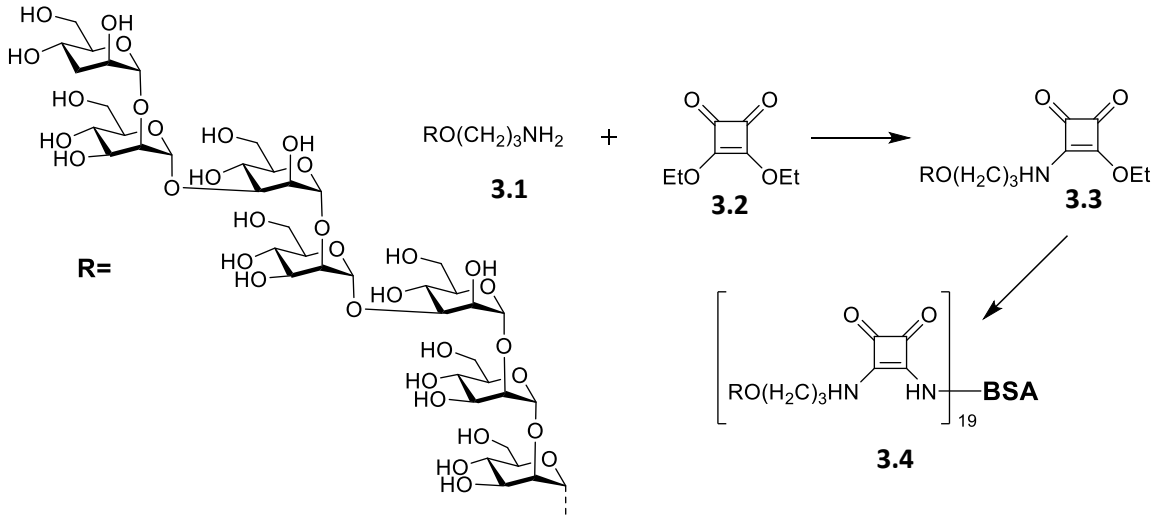

Scheme 3.2: Structure and synthesis of BSA-based glycoconjugates.[204]

Squaramides have also been used to link two saccharides together. For example, a bivalent glycopeptide ligand with the capacity to bridge two putative carbohydrate binding sites on FimH was designed and synthesized. The well-known squaric acid diester linkage strategy was applied to connect the monosaccharide and the trisaccharide part of the bivalent glycopeptide target structure **3.5**. The synthetic assembly relies on peptide coupling chemistry and the squaric acid diester to link two different amines in two subsequent steps.[206]

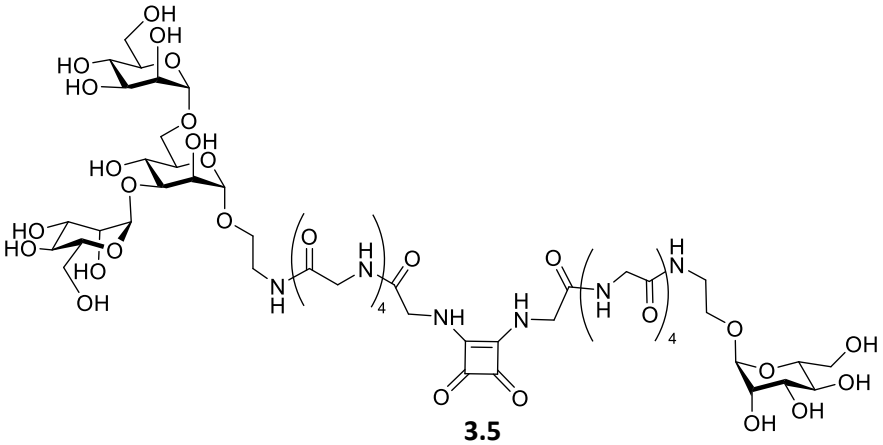

Figure 3.2: Structure of bivalent glycopeptide ligand **3.5**.

Lindhorst and coworkers have synthesised a series of α-D-mannosidic squaric acid monoamides, which were used to study the carbohydrate binding of type 1-fimbriated *E. coli*.[207] In this study it was shown that the squaric acid monoamide **3.6**, shown in Figure 3.3, exceeds *p*-nitrophenyl α-D-mannoside in potency as an inhibitor

of type 1 fimbriae-mediated bacterial adhesion, according to an ELISA (enzyme-linked immunosorbent assay). It was assumed that this result was due to additional interactions of the extended aglycon moiety in compound **3.6**, relative to *p*-nitrophenyl α-D-mannoside, at the entrance of the FimH carbohydrate recognition domain (CRD). More recently, Lindhorst and coworkers[208] further investigated the mechanism of the bacterial adhesion on mannosidic squaric acid monoamides. In this study it was considered whether the high inhibitory potency of the squaric acid derivative **3.6**, is not due to additional interactions with the CRD, but to the formation of a covalent bond within the FimH CRD. This hypothesis is justified by the special reactivity of squaric acid monoesters, which are frequently used for bioconjugation (as discussed previously). However, when compound **3.7**, which is a diamide lacking the potential for covalent crosslinking within the FimH CRD was tested, it was found that it exceeded the adhesion inhibition ability of the monoamide **3.6**. A covalently crosslinked ligand-inhibitor complex after incubation with **3.6** is hence very unlikely. Therefore, mannosides such as **3.6** and **3.7** and similar derivatives constitute promising candidates for a new class of low-molecular-weight anti-adhesives for type 1-fimbriated bacteria, exceeding the inhibitory potencies of many other mannosides.

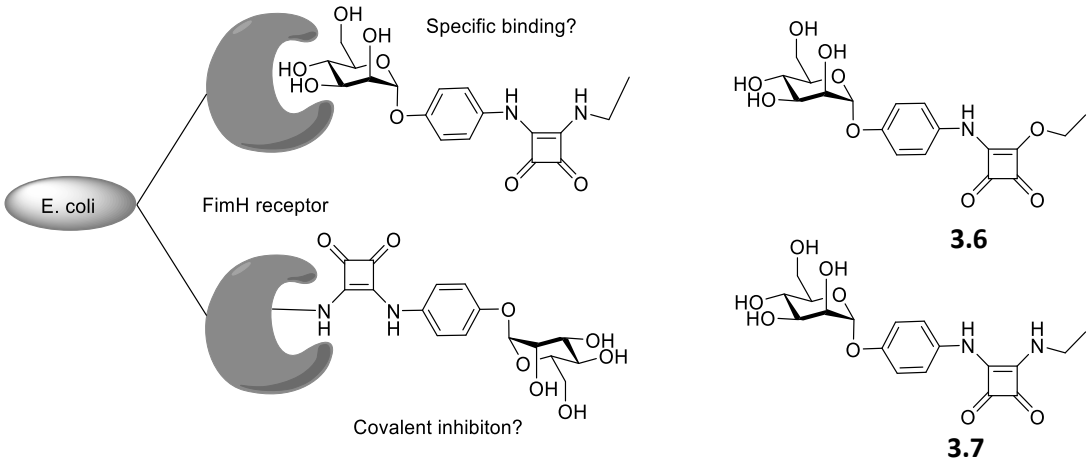

Figure 3.3: Inhibition of *E. coli* binding to squaric acid derivatives of mannose showing specific binding (via mannose) and unspecific covalent binding (via amidation of the squaric acid ester amide). The structures of the two investigated mannoside derivatives are also shown, with **3.6** being able to form a covalent bond to the protein and **3.7** exhibiting only a specific binding motif.[208]

There are very limited examples in which squaramides have been used as scaffolds to display carbohydrates in a multivalent fashion. However, due to their success in the formation of anti-adhesion ligands for FimH receptor in *E. coli*, they could prove to be successful scaffolds for a second generation of fungal anti-adhesion compounds.

3.1.2 Norbornenes

Norbornene, or bicyclo[2.2.1]hept-2-ene, is a cyclic alkene with a dense three-dimensional structure consisting of a cyclohexene ring with a bridging methylene in the *para*-position. The molecule carries a double bond which induces significant ring strain and reactivity. Norbornene is prepared by a Diels-Alder reaction of cyclopentadiene and ethylene. Many substituted norbornenes can be prepared in a similar manner. The most common use of norbornenes is in the formation of polymers. Norbornene and its derivatives can be polymerized in three different ways and are shown in Figure 3.4.[209] The best known polymerization of norborene is the ring-opening metathesis polymerization (ROMP), where the cyclohexene ring opens at the double bond, leaving a pentane ring co-planar with the polymer chain. Little is known about the cationic (or radical) polymerization of norbornene, where a low molar mass oligomeric material with 2,7-connectivity is formed. Vinyl-type polymerization leaves the bicyclic structural unit intact and opens only the double bond of the π-component.

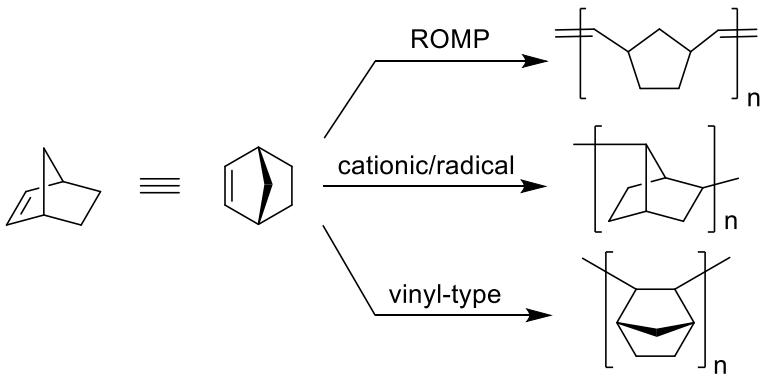

Figure 3.4: Schematic representation of the three different types of polymerization for norbornene.[209]

In the field of glycochemistry, norbornenes have mostly been used to form polyvalent carbohydrate ligands. In one study, saccharide-substituted polymers, prepared by ring-opening metathesis of oxanorbornene monomer **3.8**, act as polyvalent ligands for the mannose/glucose-binding protein Concanavalin A. The inhibitory properties of the polyvalent ligands were compared with those of the corresponding monosaccharides. It was found that the polyvalent ligands display significant increase in functional affinity in all cases. For the mannose-containing polymer **3.9**, shown in Figure 3.5, there is a 50,000-fold enhancement in inhibitory activity to the monovalent derivative.[210]

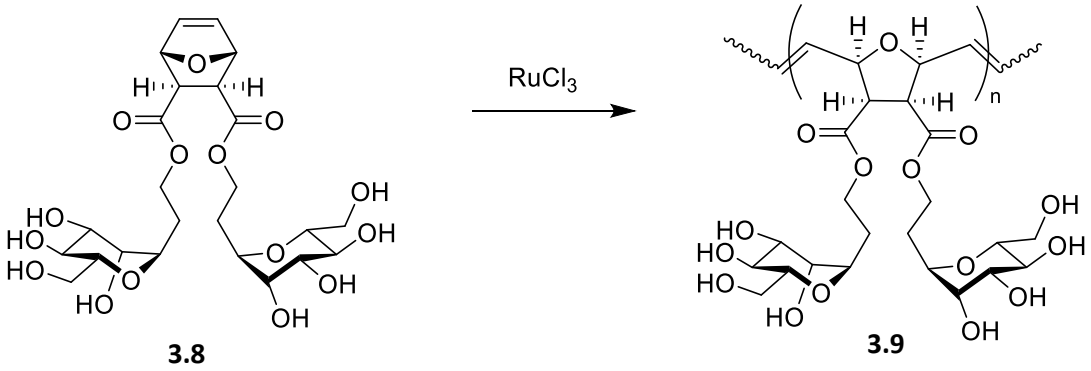

Figure 3.5: Polymerization reaction from mannose-substituted oxanorbornene **3.8** to form mannose neoglycopolymer **3.9**.[210]

Another use of norbornenes is in the site-specific post-synthetic coupling of complex molecules under mild conditions. Inverse electron-demand Diels-Alder (DAinv) cycloaddition reactions can be used as a biorthogonal reaction for the selective and efficient modification of biomolecules. Here, the norbornene moieties are used as the dienophiles which are rapidly conjugated to tetrazine dienes to site-specifically label proteins.[211]

This technique has been utilized in metabolic glycoengineering (MGE), since it allows the introduction of unnaturally modified carbohydrates into cellular glycans and their visualization through biorthogonal ligation. Two norbornene-modified mannosamine derivatives (*exo* **3.10**/*endo* **3.11**) were synthesised. A human cell line was grown in the presence of **3.10** or **3.11** (Figure 3.6). Cells were then treated with Tz-biotin (tetrazine containing compound linked to a biotin moiety with a PEG chain) and subsequently treated with streptavidin-Alexa Fluor-55 to allow their visualization.

The results show that labelling with both mannosamine derivatives leads to staining. This implies that both derivatives were incorporated into cell-surface glycoconjugates and could be visualized with the aid of the DAinv reaction.[212]

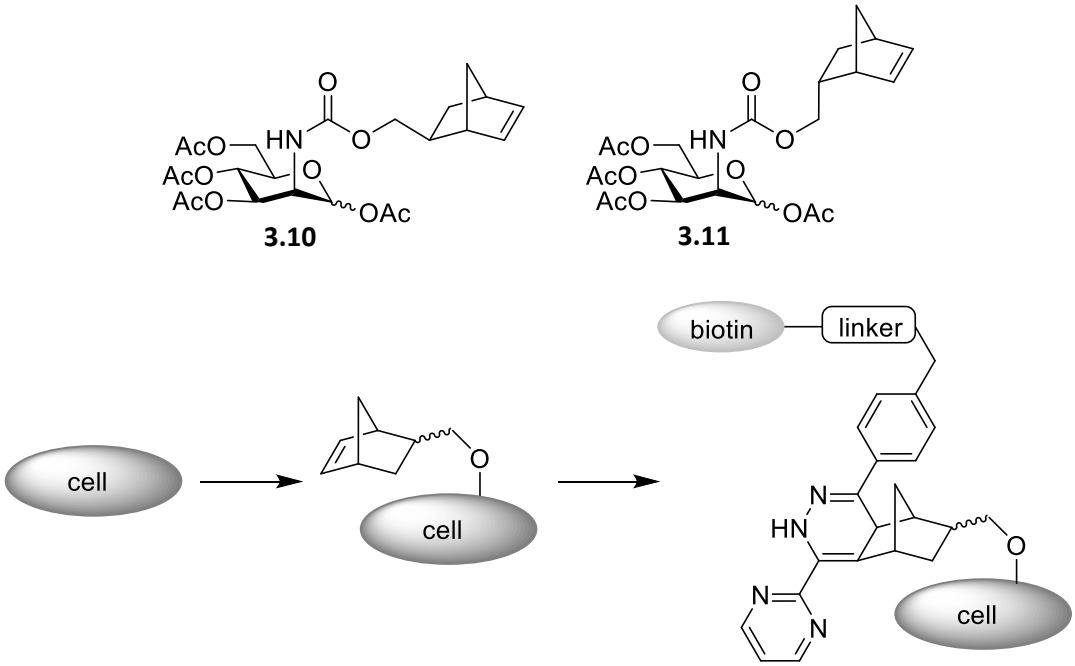

Figure 3.6: a) Structure of mannosamine derivatives **3.10** and **3.11** with norbornene units attached through carbamate linkages; b) Strategy for MGE experiments. Cells were fed with sugars **3.10** and **3.11** and then treated with Tz-biotin, where Tz-biotin = tetrazine containing compound linked to a biotin moiety with a PEG chain.[212]

3.2 Chapter Objective

As discussed in the previous chapter, a small library of multivalent aromatic glycoconjugates were synthesised. A divalent galactoside **2.78** with a 1,3,5-functionalized aromatic core could inhibit the adherence of *C. albicans* to BECs. It was found that the precise three-dimensional presentation of the galactosyl moieties in compound **2.78** appeared to be a requirement for the efficient adherence inhibition. Since the presence of the terminal galactosides seemed to be an important structural factor in determining anti-adhesion activity against *C. albicans*, we decided to explore alternative molecular frameworks to generate analogues of compound **2.78**, which display both galactosyl moieties for an improved presentation to the receptor mediating the adhesion of *C. albicans* to BECs.

The first generation aromatic core glycoconjugates (AGCs) were built around scaffolds with a 1,3 or 1,3,5 substitution pattern. We decided to first explore a 1,4 substituted analogue of compound **2.78**. Given the planar, aromatic character of squaramide derivatives, we decided to synthesise a series of analogues of lead compound **2.78** with a squaramide core as a relevant comparison to the benzene core glycoconjugates described in Chapter 2.

While the 1,4-disubtitutes and *N,N*-dipropargyl squaramide scaffolds can be readily prepared, no further functionalization is possible once the grafting of the carbohydrate moieties through CuAAC takes place. To overcome this drawback, we sought for a suitable molecular scaffold which would still afford the formation of the *N,N*-dipropargyl amides required for CuAAC reaction with sugar azides, while allowing for the introduction of reporter tags, such as fluorescent labels, or other chemically reactive groups to continue derivatization of the analogues. Hence, we decided to investigate 5-norbornene dicarboxylic acids as starting material to synthesis the next family of analogues of lead compound **2.78**. In addition, the use of the 2-*endo*, 3-*exo*-dicarboxylic acid (*trans*) or the *endo*-2,3-dicarboxylic acid (*cis*) may allow for a different spatial presentation of the galactosyl moieties.

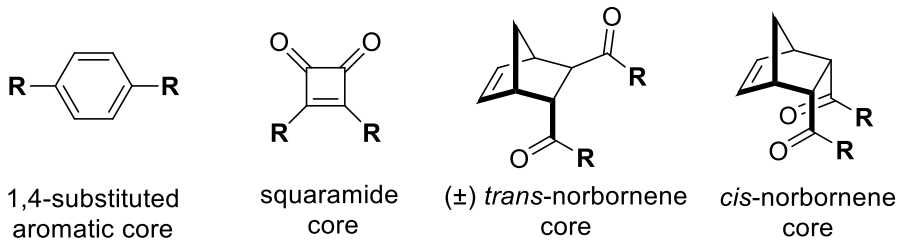

Figure 3.7: Structures of the alternative core scaffolds used in the synthesis of the next generation of anti-adhesion ligands.

3.3 Synthesis of Alternative Scaffold Glycoconjugates

3.3.1 1,4-Substituted Glycoconjugate

A 1,4-substitued analogue **3.15** of the lead compound **2.78** was synthesised (Scheme 3.3), where the divalent galactosyl moieties were linked to the aromatic core through a triazolyl linkage. Here, terephthalic acid **3.12** was reacted with propargyl amine using freshly prepared DMTMM to give the diamide **3.13** in 81 % yield. The resulting

divalent scaffold was reacted with galactosyl azide **2.40** using CuAAC methodology under microwave irradiation, resulting in a 73 % yield of the protected glycoconjugate **3.14**. The deacetylation of this compound was accomplished under mild basic conditions to give compound **3.15** in excellent yield.

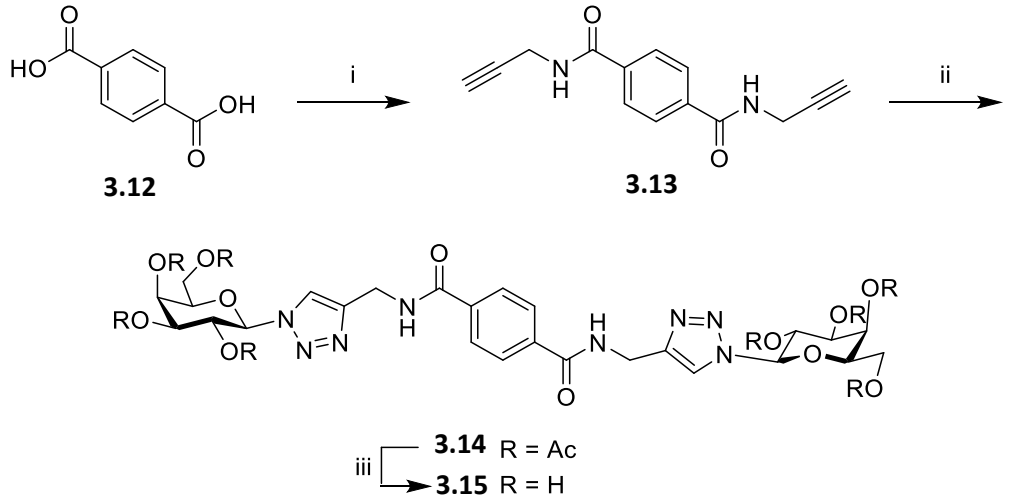

Scheme 3.3: Synthesis of 1,4-benzene core divalent galactosyl **3.15**. *Reagents and conditions:* i) DMTMM, propargylamine, DMF, N_2, 16 h, 81 %; ii) galactosyl azide **2.40**, $CuSO_4.H_2O$/Na Asc, CH_3CN/H_2O, 100 °C in MW, 10 min, 73 %; iii) methanol, NEt_3, H_2O, 45 °C, 6 h, 94 %.

3.3.2 Squaramide Glycoconjugates

A series of analogues of lead compound **2.78** (compounds **3.20**-**3.22**) featuring a squaramide as the core scaffold were synthesised (Scheme 3.4). These analogues are a relevant comparison to the benzene core glycoconjugates described in Chapter 2. In this series of analogues, all three compounds are divalent with terminal galactosides. **3.20** has the galastosyl moieties bonded through the anomeric position to a triazolyl linkage to the squaramide core. **3.21** has an *O*-ethylene spacer in addition to the triazole linkage between the galactosyl moieties and the core. **3.22** has lactosyl moieties bonded through the anomeric position to a triazolyl linkage to the squaramide core.

The syntheses of these squaramide analogues are shown in Scheme 3.4. Diethyl squarate **3.2** was reacted with propargylamine to give *N,N*-dipropargyl squaramide **3.16** in 81 % yield. The mechanism of this reaction is shown in Scheme 3.5. Here, the

propargylamine attacks an α-carbon of the diethyl squarate **3.2**, forming an enolate intermediate. The ketone group then reforms and the ethoxy leaving group departs, which is protonated to give EtOH as a by-product. The reaction is repeated on the other α-carbon to give the desired product **3.16**. CuAAC reaction of compound **3.16** with tetra-*O*-acetyl-1-β-azido-galactoside **2.40**, tetra-*O*-acetyl-1-β-*O*-2-azidoethyl-galactoside **2.47** and hepta-*O*-acetyl-1-β-azido-lactoside **2.43** produced divalent compounds **3.17**, **3.18** and **3.19**, respectively. The acetyl protecting groups were removed under mild basic conditions to give the corresponding deprotected compounds **3.20**, **3.21** and **3.22**. All these derivatives display terminal galactosides.

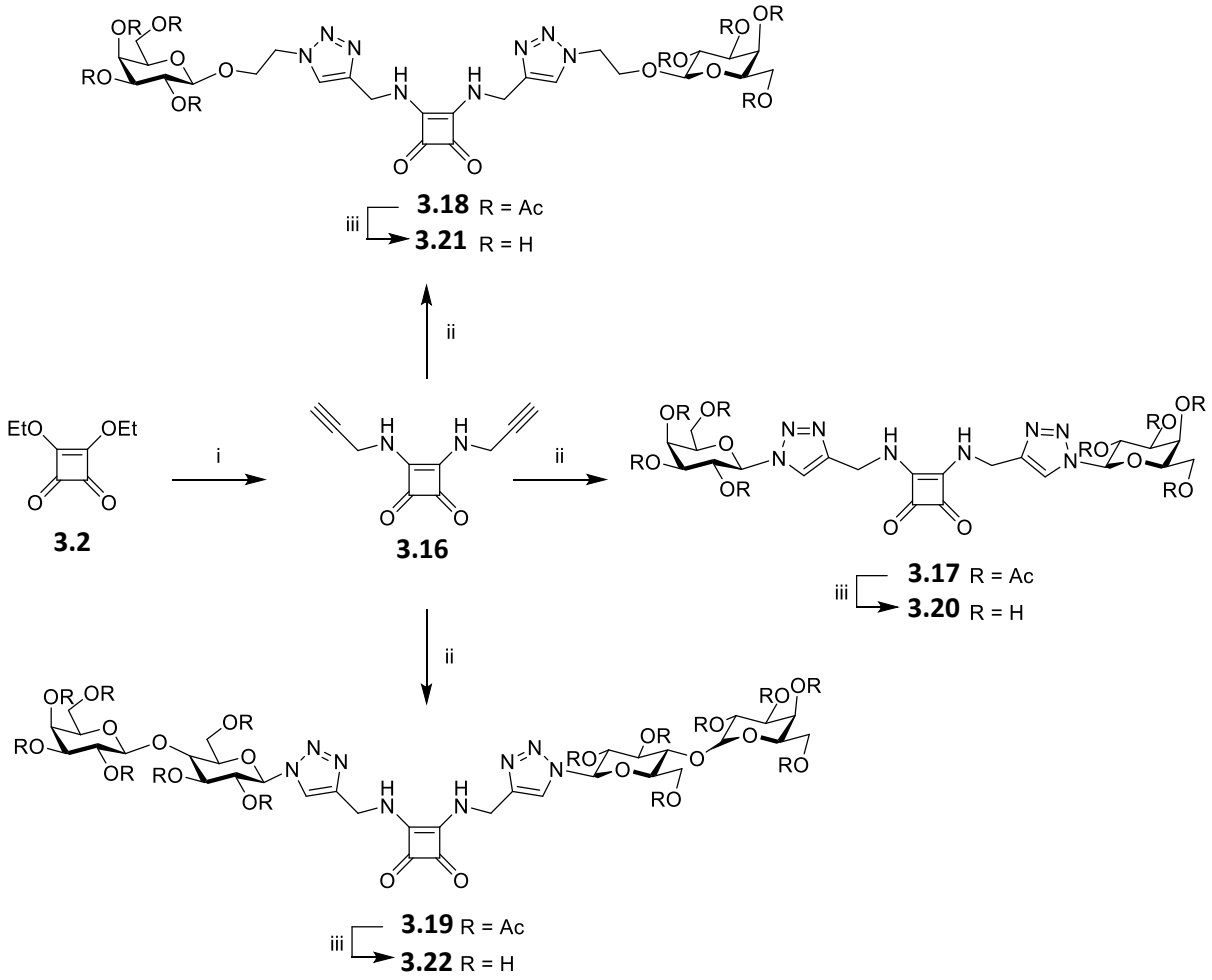

Scheme 3.4: Synthesis of divalent galactosyl squaramides **3.20**, **3.21** and **3.22**. *Reagents and conditions*: i) propargylamine, NEt_3, EtOH, 16 h, 81 %; ii) $CuSO_4.5H_2O$/Na Asc, CH_3CN/H_2O, 100 °C in MW, 10 min, and (a) 2,3,4,6-tetra-*O*-acetyl-1-β-azido-galactoside **2.40**, 81 % for **3.17**; (b) tetra-*O*-acetyl-1-β-*O*-2-azidoethyl-galactoside **2.47**, 80 % for **3.18**; (c) hepta-*O*-acetyl-1-β-azido-lactoside **2.43**, 75 % for **3.19**; iii) methanol, NEt_3, H_2O, 45 °C, 6 h, 77-99 %.

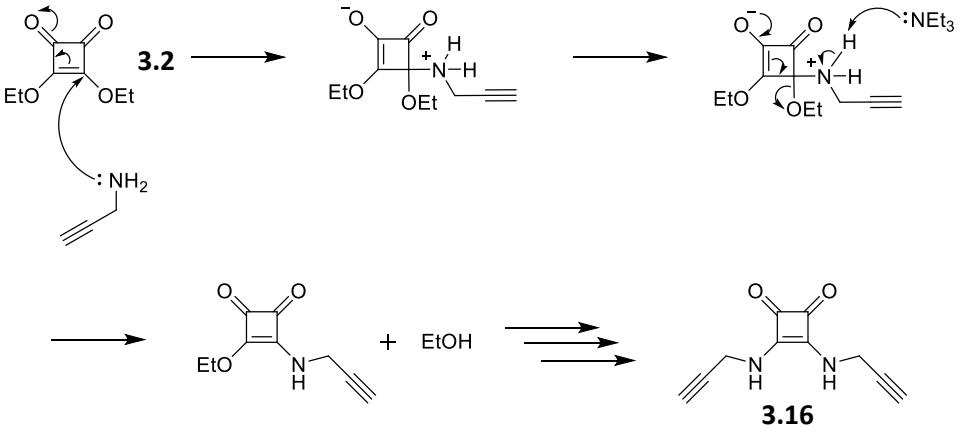

Scheme 3.5: Reaction mechanism of commercially available diethyl squarte and propargylamine to give the diamide **3.16**.

3.3.2.1 Gelation Ability

Previous research in the group of Dr. Trinidad Velasco-Torrijos has shown the ability of *O*-glycolipid squaramide compounds of forming low molecular weight gelators (LMWGs). These compounds (**JRO-SQ-1** and **JRO-SQ-2**, Figure 3.8) had a squaramide core, with a galactose moiety on one side and a lipid chain (C_{16}) on the other side. It was found that the acetylated derivative **JRO-SQ-1** showed a preference to form opaque gels with relatively high polarity solvents such at EtOAc, MeCN, EtOH and a solvent mixture of EtOH:H_2O (1:1) with critical gelation concentrations (CGCs) ranging from 0.7 to 1.7 w/v %. On the other hand, the deacetylated derivative **JRO-SQ-2**, which features free hydroxyl groups, was able to form a transparent gel in EtOH:H_2O (1:1) with 0.1 w/v % and excellent rheological properties.[213]

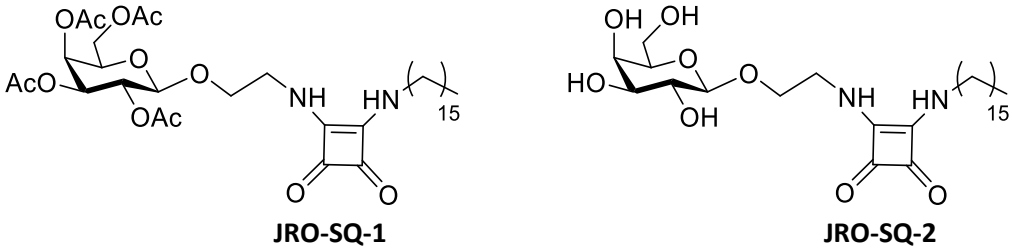

Figure 3.8: Structure of *O*-glycolipid squaramide LMWGs **JRO-SQ-1** and **JRO-SQ-2**.[213]

The gelation ability of the acetylated compounds **3.17** and **3.18**, and the deacetylated compounds **3.20** and **3.21** were then tested. Compound **3.17** formed a partial gel in EtOH after heating to 50 °C and sonication at a concentration of 20 mg/mL.

Compound **3.17** also formed sprinkle-shaped aggregates in EtOAc when heated to 50 °C and allowed to cool. The other compounds **3.18**, **3.20** and **3.21** did not show any significant results when testing their gelation ability. This confirms the requirement of having a lipid chain in the formation of LMWGs.

3.3.3 Norbornene Glycoconjugates

A series of analogues of lead compound **2.78** with a norbornene core were also synthesised (Scheme 3.6). For this family of compounds, 5-norbornene dicarboxylic acids **3.23** and **3.24** were used as starting materials. Using different isomers of the starting material resulted in two divalent galactosyl compounds with a different spatial presentation of the galactosyl moieties. One of the derivatives **3.29** has a *trans* orientation of the diamides, while the other derivative **3.30** has a *cis* orientation of the amides. Inadvertently, a monovalent galactosyl derivative **3.31** was also synthesised.

The synthesis of the norbornene core glycoconjugates are shown in Scheme 3.6. 5-Norbornene-2-*endo*,3-*exo*-dicarboxylic acid (*trans*) **3.23** and the *cis*-5-norbornene-*endo*-2,3-dicarboxylic acid **3.24** were reacted with propargylamine with TBTU used as the coupling reagent to give the diamides **3.25** and **3.26**. CuAAC reaction of **3.25** and **3.26** with tetra-*O*-acetyl-1-β-azido-galactoside **2.40** produced the peracetylated divalent compounds **3.27** and **3.28**, repectively. Interestingly, neither the *trans*-product **3.27** or the *cis*-product **3.28** showed symmetry. This can be seen in the ^{1}H NMR spectra shown in Figure 3.9. It can be clearly seen for both compounds that the triazolyl hydrogen is not represented by one peak (at 7.8 ppm), indicating that the triazolyl protons are not in equivalent magnetic environments. In the *trans*-product **3.27** the anomeric proton (H-1) of the galactosyl moieties appears as a doublet, while in the *cis*-product **3.28** the anomeric proton (H-1) appears as a multiplet. This suggests that in the *trans*-product **3.27** the two galactosyl moieties are in the same magnetic environment, while in the *cis*-product **3.28** the two galactosyl moieties are in different environments. In the *cis*-product **3.28** the sugars are in closer proximity to one another and have an influence on the environment of the other galactosyl moiety.

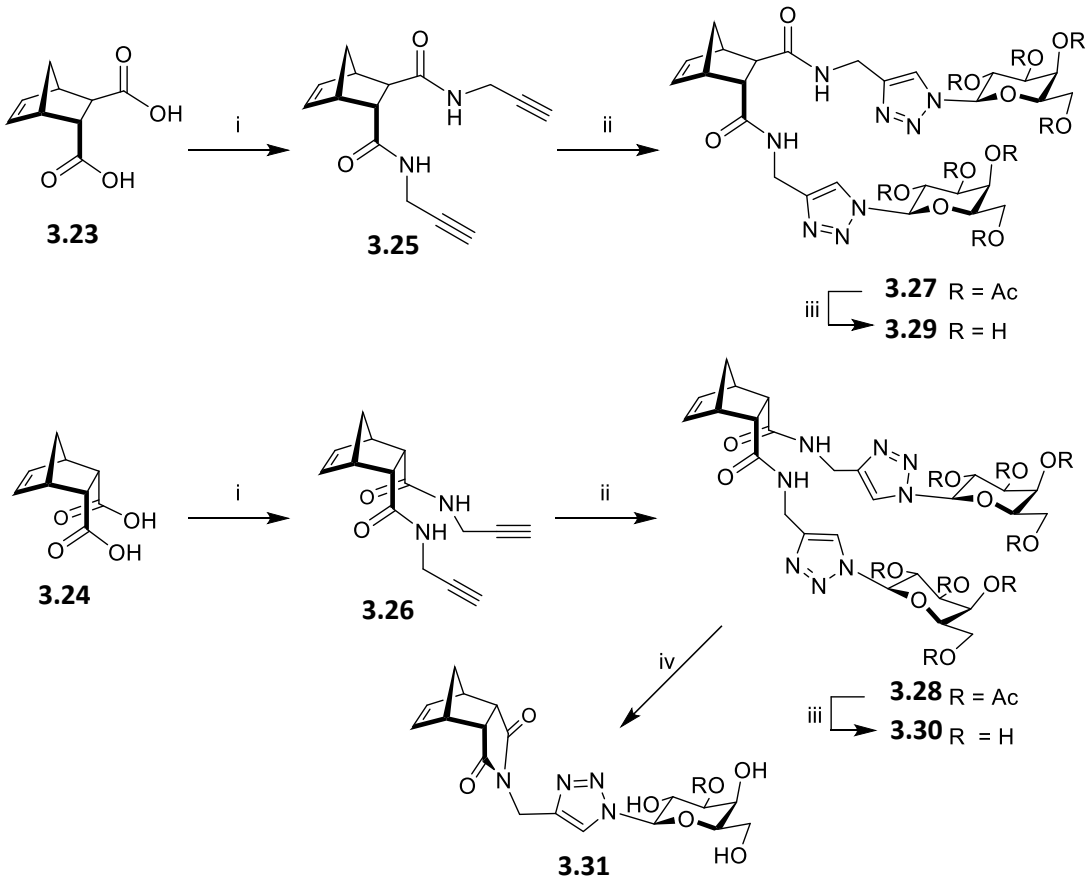

Scheme 3.6: Synthesis of divalent and monovalent galactosyl norbornenes **3.29**, **3.30** and **3.31**. *Reagents and conditions*: i) propargylamine, TBTU, NEt_3, DMF, N_2, 48 h, 79-93 %; ii) 2,3,4,6-tetra-*O*-acetyl-1-β-azido-galactoside **2.40**, $CuSO_4.5H_2O$/Na Asc, CH_3CN/H_2O, 100 °C in MW, 20 min, 54-74 %; iii) methanol, NEt_3, H_2O, 45 °C, 6 h; iv) Amberlite H^+ resin, 30 min, quantitative yield.

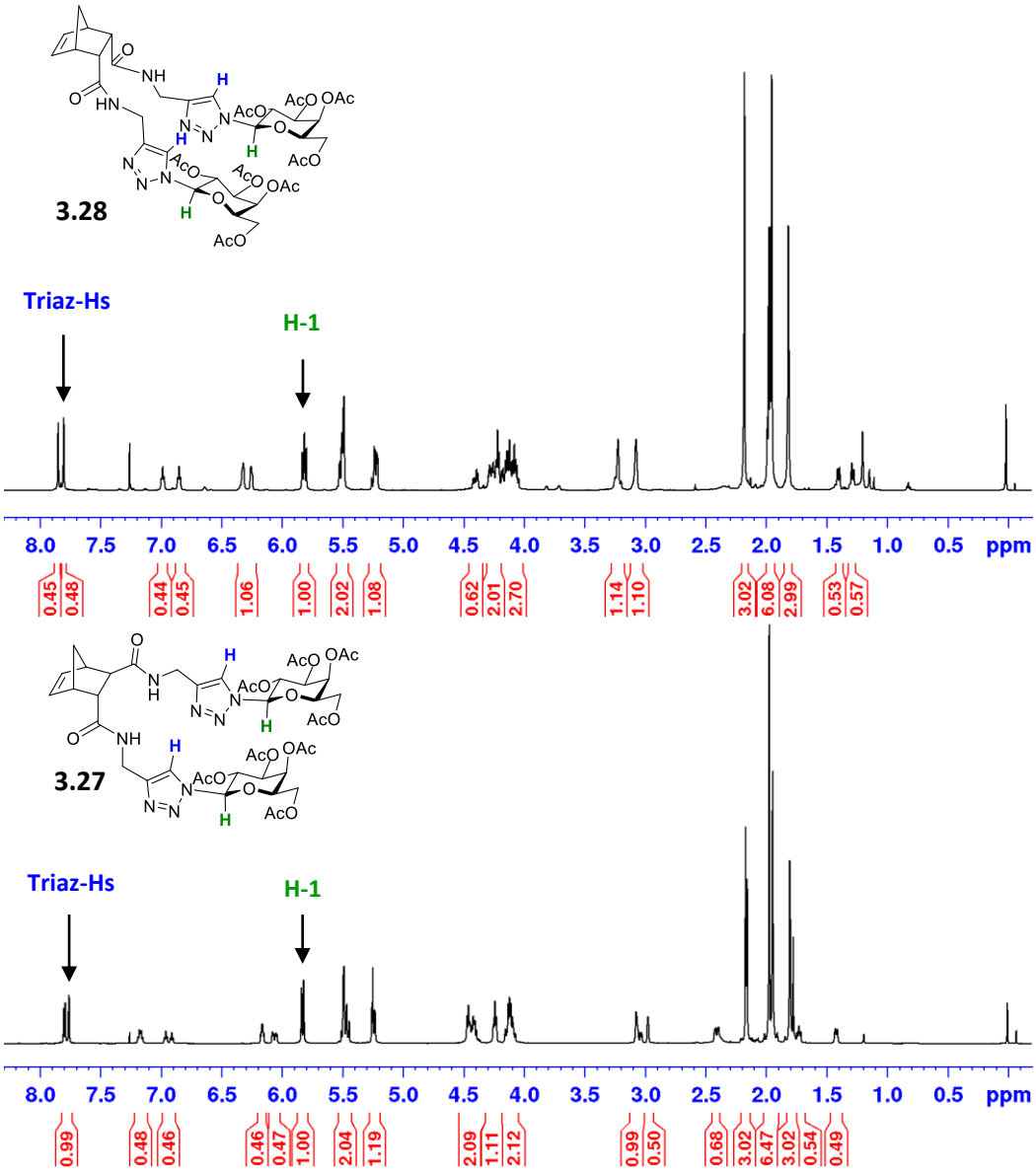

Figure 3.9: ^{1}H NMR spectra of compounds **3.27** and **3.28** in $CDCl_3$.

The acetyl protecting groups were removed under mild basic conditions to give the corresponding deprotected compounds **3.29** and **3.30**. To purify the deprotected glycoconjugates, the reaction mixtures are generally treated with Amberlite H^+ resin. Interestingly, treatment of the acetylated *cis*-norbornene compound **3.28** with Amberlite H^+ resulted in the departure of one of the galactosyl-triazolyl moieties and formation of the monovalent glycoconjugate **3.31**. To further analyse this occurrence, two divalent, non-glycosylated *cis*-compounds **3.32** and **3.33** were synthesised (Scheme 3.7). Both these compounds were treated with Amberlite H^+, 1 M HCl and then 5 M HCl. It was found that both compounds **3.32** and **3.33** stayed

intact and the monovalent derivatives were not formed. This indicates the need for the presence of triazolyl-sugar moieties for this intramolecular elimination to take place. We assume this did not occur in the case of the *trans*-compound **3.27**, since the triazolyl-galactosyl groups are not in close proximity as in the *cis*-compound **3.28**.

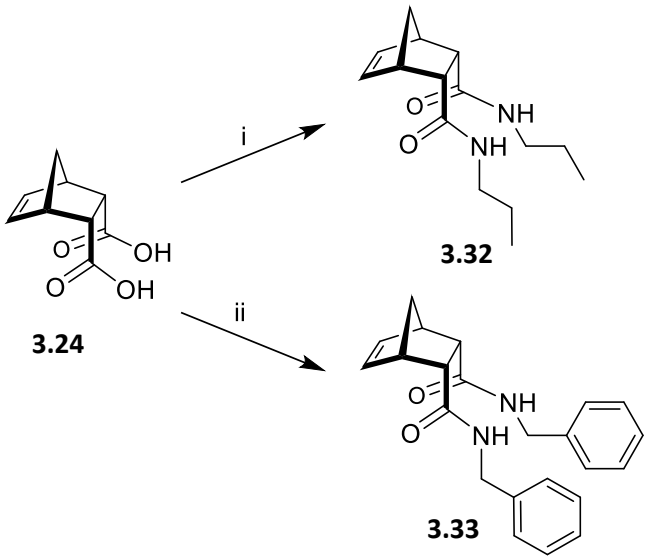

Scheme 3.7: Synthesis of divalent non-glycosylated *cis*-compounds **3.32** and **3.33**. *Reagents and conditions*: i) propylamine, TBTU, NEt_3, DMF, N_2, 16 h, 82 %; ii) benzylamine, TBTU, NEt_3, DMF, N_2, 16 h, 97 %.

3.4 Biological Evaluation

The biological evaluation of compounds **3.15**, **3.20**-**3.22** and **3.29**-**3.31** was again carried out in collaboration with Prof. Kevin Kavanagh in the Medical Mycology laboratory in the Biology Department of Maynooth University. The work in this section was carried out by me and 4th Year research project student Matthew Dwyer. A similar range of adherence assays, as discussed in Chapter 2, were carried out at different concentrations of the alternative scaffold glycoconjugates. All assays were compared to the initial lead compound **2.78**. Exclusion, competition and displacement assays, which were described in Section 2.4, were carried out using all of the second generation glycoconjugates. Toxicity assays confirmed that all compounds tested are non-toxic to the *C. albicans* at the concentrations used in the adherence assays.

3.4.1 1,4-Aromatic Scaffolds

First the exclusion assay, where the yeast were pre-treated with the glycoconjugates **2.78** and **3.15**, was carried out. At 13.8 µM, compound **2.78** (at 10 mg/mL) caused 42 % reduction in adherence, while compound **3.15** (at 9 mg/mL) showed 33.5 % reduction in adherence (Figure 3.10 a). This assay was then repeated at lower concentrations of compound **3.15**, 1.38 µM and 0.138 µM. It was found that at both the lower concentrations of compound **3.15** there was a 61 % reduction in adherence (Figure 3.10 b). The exclusion assay, where the BEC were pre-treated with the glycoconjugates, showed that compound **2.78** reduced the adherence by 41.5 %, while compound **3.15** reduced adherence by 25 %.

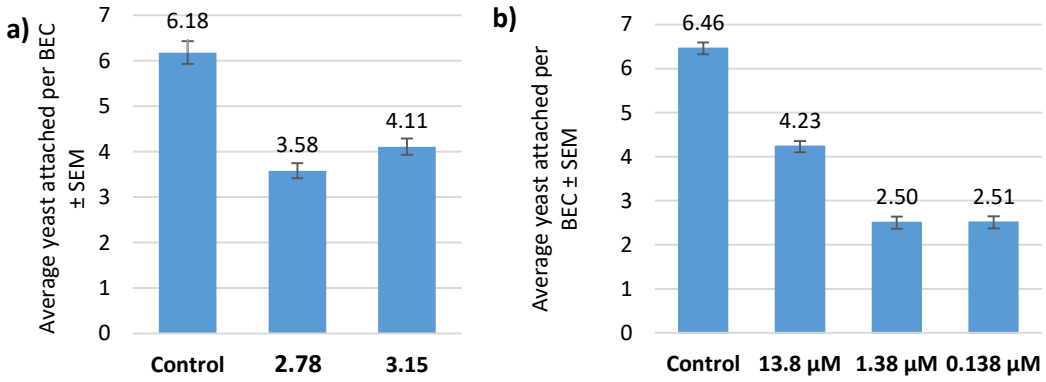

Figure 3.10: Results from the exclusion assay where the yeast were pre-treated: a) Shows the average number of yeast attached per BEC for compound **2.78** and **3.15** at 13.8 µM; b) Shows the average number of yeast attached per BEC for compound **3.15** at varying concentration (13.8 µM, 1.38 µM and 0.138 µM).

The competition assay, where all three components (the yeast, BEC and glycoconjugates) are co-incubated showed a similar trend as the previous assay: compound **3.15** did not reduce the adherence as well as compound **2.78**. The competition assay was carried at 13.8 µM, 1.38 µM and 0.138 µM of the synthetic glycoconjugates. The average percentage decrease in adhesion is shown in Figure 3.11 a. Interestingly, both compounds show greatest anti-adhesive properties at 1.38 µM.

The displacement assay showed a better response for compound **3.15**. In this assay the yeast and BECs were co-incubated first and the glycoconjugates were

subsequently added. The first control shown in Figure 3.11 (b) involved the assessment of the binding of *C. albicans* to BECs prior to exposure to the glycoconjugates (and DMSO in the control). Control 2 shows the average number of yeast attached per BEC after the second filtration. The results show a 56 % reduction in adherence for **2.78** at 0.138 µM compared to control 1 and a 36 % reduction compared to control 2, and a 63 % reduction of **3.15** compared to control 1 and a 48 % reduction compared to control 2 (Figure 3.10 b).

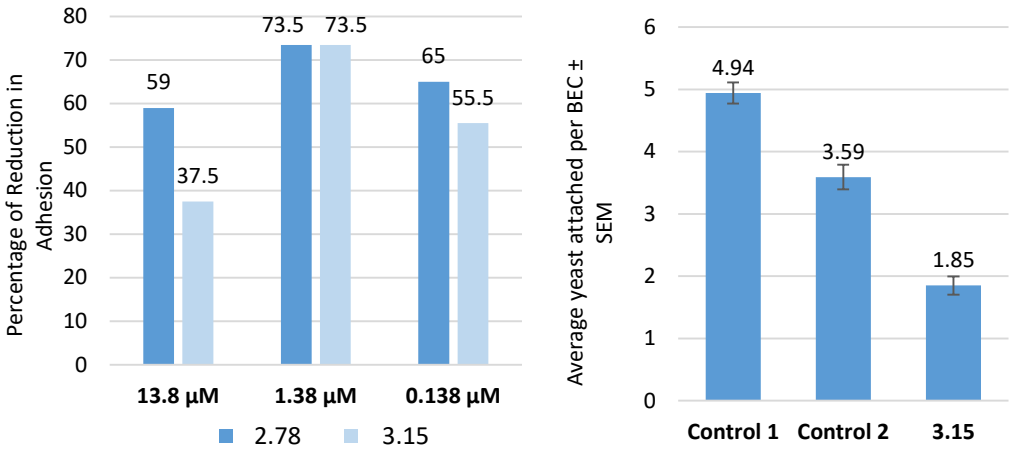

Figure 3.11: a) Results from competition assay showing the percentage decrease in adhesion of compound **2.78** and **3.15**; **b)** Results from displacement assay showing the average number of yeast attached per BEC for compound **3.15** at 0.138 µM.

3.4.2 Squaramides

The exclusion assay where the yeast were pre-treated (Figure 3.12 a) showed that compound **2.78** has the best anti-adhesive properties, reducing adherence by 45 %. Compound **3.21** and **3.22** show similar results, reducing adherence by 33-34 %. Compound **3.20** does not perform as well as the other squaramides, showing a 27 % reduction in adhesion. When the BEC are pre-treated with the glycoconjugates, the percentage reduction is smaller for all compounds tested (Figure 3.12 b). This indicates that the glycoconjugates are interacting with the *C. albicans* more efficiently than with the BECs.

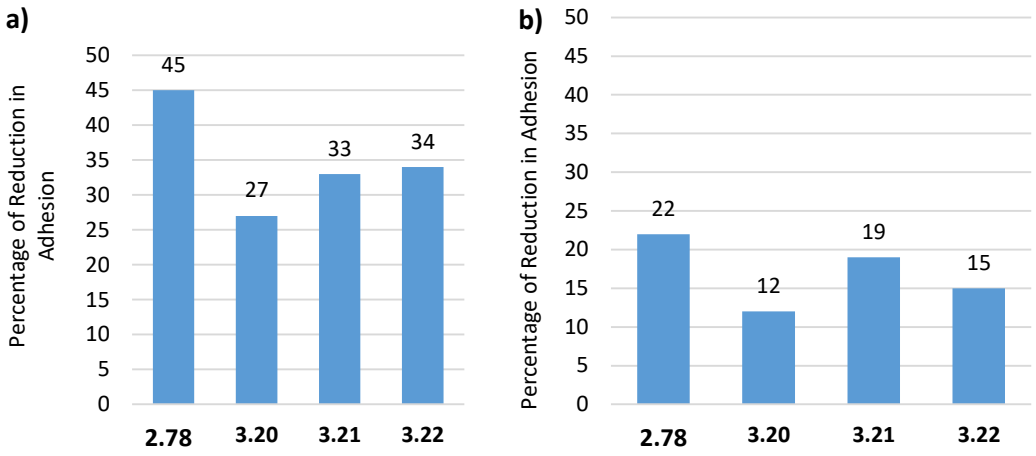

Figure 3.12: Results from exclusion assay where a) the yeast are pre-treated and b) the BEC are pre-treated. All compounds were tested at 13.8 µM.

In the competitive assay, compound **2.78** showed the best results, inhibiting adhesion by 36 %. Compounds **3.21** and **3.22** showed similar results again, inhibiting adhesion by 29-30 %. Consistently, compound **3.20** showed the lowest decrease in adhesion (11 %).

The displacement assay was carried out on the two best-performing squaramide compounds, **3.21** and **3.22**, and the results are shown in Figure 3.13. As a result of this second filtration, 14 % of yeast were blocked from adhering. Compounds **3.21** and **3.22** recorded a reduction of 35 % and 39 %, respectively. Taking into account the results from the control after the second filtration, compound **3.21** showed a 21 % reduction and compound **3.22** showed a 25 % reduction. The results from the displacement assay of compound **2.78** (Section 2.4.2.3) show that this compound displaced yeast cells from BECs more efficiently than compounds **3.21** and **3.22**.

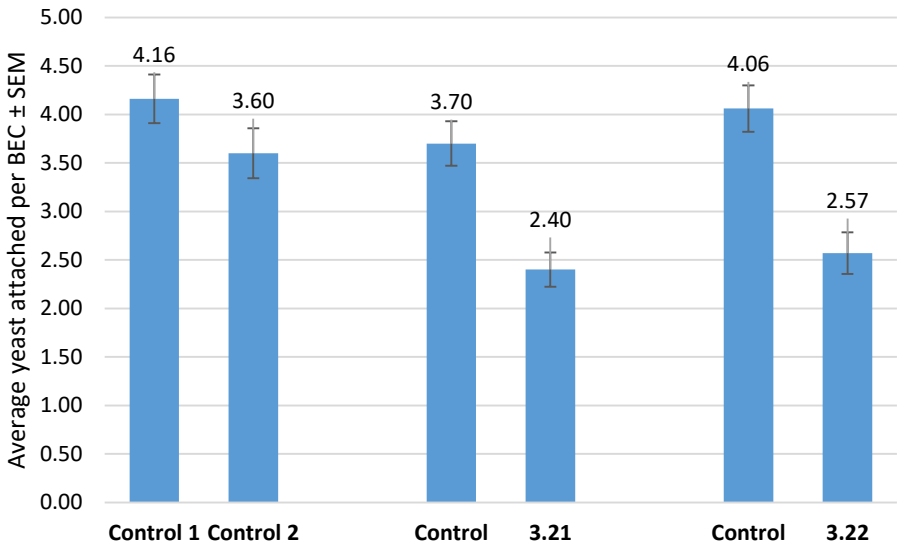

Figure 3.13: Shows the results from the displacement assay, where *C. albicans* and BECs were co-incubated and compounds **3.21** and **3.22** (concentration 13.8 µM) were subsequently added; control 1 involved the assessment of the binding of *C. albicans* to BECs prior to exposure; control 2 shows the average number of yeast attached per BEC after the second filtration.

3.4.3 Norborenes

The exclusion assay where the yeast were pre-treated showed good results for the norbornene analogues **3.29**-**3.31** (Figure 3.14 a). The norbornenes were compared to the initial lead compound **2.78** which reduced adherence by 51 % in this particular assay. The *trans*-norbornene compound **3.29** and the monovalent derivative **3.31** showed similar results, where they reduced the adherence by 46 % and 43 %, respectively. The *cis*-norbornene compound **3.30** showed very promising results in this assay, as it caused an inhibition of adherence greater than the lead compound **2.78**. Compound **3.30** reduced the adherence by 65 %.

In the competition assay (Figure 3.14 b), the two divalent norbornenes **3.29** and **3.30** showed similar results, causing an inhibition of adhesion of the yeast to the BECs greater than the lead compound **2.78**. The monovalent derivative **3.31** did not significantly inhibit the adhesion (17 % inhibition).

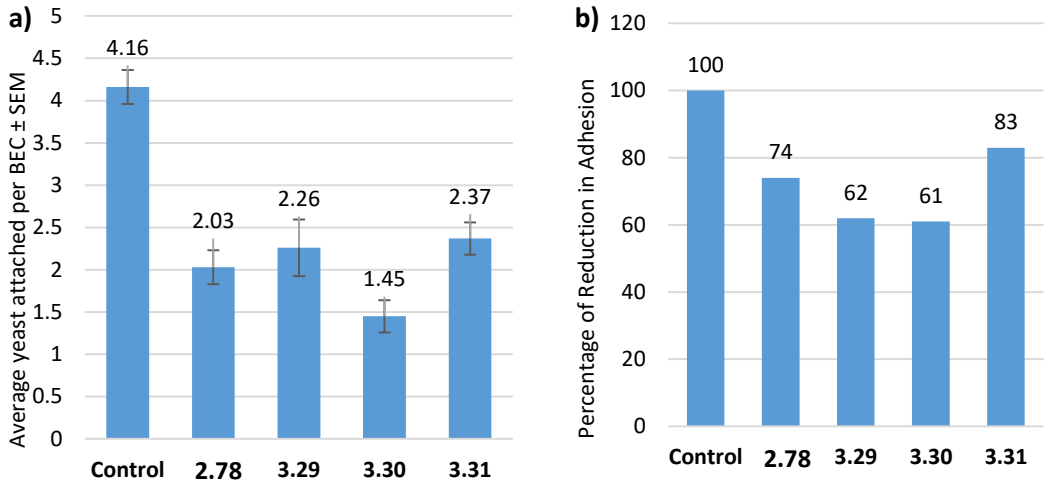

Figure 3.14: a) Results from exclusion assay where the norbornene analogues **3.29**-**3.31** are compared to the lead compound **2.78** at 13.8 µM; b) Results from competition assay showing the percentage decrease in adhesion of *C. albicans* to BEC compared to the control.

Finally, the norbornene analogues were tested using the displacement assay (Figure 3.15). Similarly to previous displacement assays there are two controls. The first control is involved in the assessment of the binding of *C. albicans* to BECs prior to exposure to the glycoconjugates (and DMSO in the control). Control 2 shows the average number of yeast attached per BEC after the second filtration. Comparing the average number of yeast attached per BEC for the norbornene analogues to the those in the control, we obtained the following results. The divalent *trans*-norbornene **3.29** and the monovalent norbornene compound **3.31** show very similar results. Compounds **3.29** and **3.31** showed a 23 % reduction in adherence compared to control 1, and only 7-8 % reduction compared to control 2. The divalent *cis*-norbornene compound **3.30** showed the best results with 45 % reduction in adherence compared to control 1, and 34 % reduction compared to control 2.

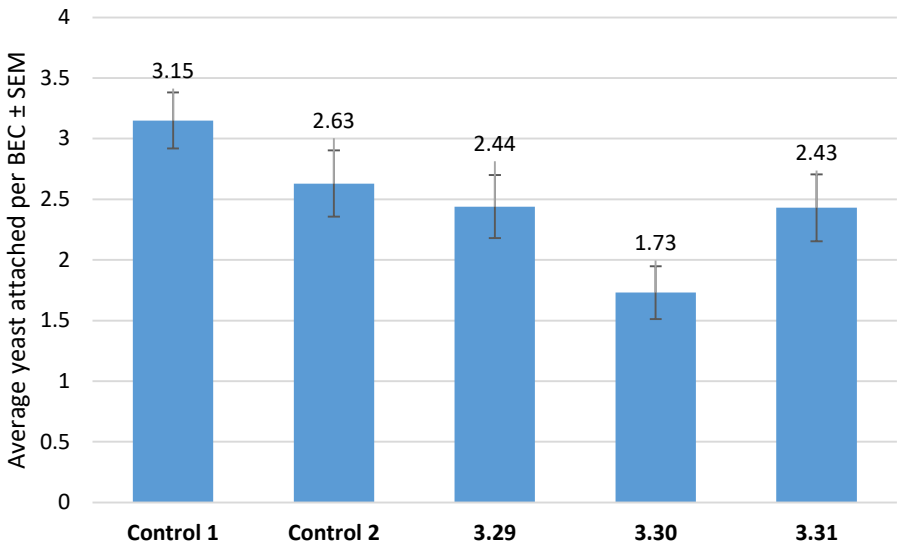

Figure 3.15: Shows the results from the displacement assay, where *C. albicans* and BECs were co-incubated and compounds **3.29**-**3.31** (concentration 13.8 µM) were subsequently added; control 1 involved the assessment of the binding of *C. albicans* to BECs prior to exposure; control 2 shows the average number of yeast attached per BEC after the second filtration.

3.5 Conclusion

The effect of molecular scaffolds in the anti-adhesion activity against *C. albicans* of divalent triazolyl-galactosides was investigated. A range of analogues of the lead compound from Chapter 2, compound **2.78**, were synthesised and tested for their anti-adhesive properties. The 1,4-disubstitued aromatic glycoconjugate **3.15** was readily synthesised using similar methodology as the original lead compound. This compound performed moderately well in the adherence assays, exhibiting marginally lower anti-adhesive properties than compound **2.78** in the exclusion and competition assays. In the displacement assay, compound **3.15** displaced a larger percentage of yeast from the BEC than **2.78**. However, since this compound cannot be further derivatized, no further studies were carried out.

A series of divalent squaramide analogues were also synthesised. Diethyl squarate was used as the starting material, which was reacted with properglyamine to give the divalent squaramide scaffold **3.16**. CuAAC methodology was used to conjugate the sugars to the scaffold, and deacetylation gave the desired glycoconjugates **3.20**-**3.22**.

The more rigid galactosyl compound **3.20** proved to be least active in the adherence assays, while the more flexible galactosyl compound **3.21** and the lactosyl compound **3.22** both displayed better results in the assays. Since these two compounds have similar anti-adherence properties, this suggests that they display the terminal galactosyl moieties in a similar orientation. Compounds **3.21** and **3.22** did not perform as well as **2.67** in the adherence assays. This could indicate that the three-dimensional presentation of the galactosyl moieties in compound **2.78** is better at interacting with the receptor, that mediates adhesion between the *C. albicans* and the BEC, than the presentation of the terminal galactosyl moieties in the squaramide derivatives **3.20**-**3.22**.

The synthesis of the norbornene core glycoconjugates began with 5-norbornene-2-*endo*, 3-*exo*-dicarboxylic acid (*trans*) or *cis*-5-norbornene-*endo*-2,3-dicarboxylic acid, which were reacted with propargylamine to give the two divalent norbornene scaffolds **3.25** and **3.26**. CuAAC methodology was used to join the sugars to the scaffold to give the peracetylated divalent compounds **3.27** and **3.28**. The deacetylation of the glycoconjugates gave the desired compounds **3.29** and **3.30**. During the purification of the *cis*-compound **3.30**, the monovalent norbornene compound **3.31** was formed. The anti-adherence properties of the three norbornene compounds were then tested using the same adherence assays. The *cis*-compound **3.30** consistently showed the best results in all three adherence assays, having the ability to displace up to 45 % of yeast already attached to the BECs. This compound also showed better results than the initial lead compound **2.78** in the exclusion and competition assays.

In conclusion, in an effort to find a glycoconjugate with better anti-adhesive properties than our initial divalent AGC **2.78**, we found a potential candidate in the divalent *cis*-norbornene compound **3.30**. These results show a promising new scaffold (norbornene) that can be considered in the development of new anti-adhesion ligands, which has the potential to be further derivatized with fluorescent labels and other chemically reactive groups. There is also the possibility to form polymers with this compound using the ROMP technique outlined in Section 3.1.2 to create polyvalent anti-adhesion ligands.

Chapter 4

Enhancing Affinity Through Multivalency

4.1 Introduction

4.1.1 Multivalent Effect

The initiation of a multitude of human diseases are mediated by protein-carbohydrate recognition. In particular, as discussed previously, for a microbe to infect its host, it first adheres to the host cell using proteins that interact with carbohydrate epitopes displayed on the host cell surface. The development of small-molecule inhibitors of the adhesion process has been extensively studied for a number of years and reviewed in earlier chapters. The use of glycoconjugates as anti-adhesion ligands is desirable since they are intended to be non-cytotoxic and could be applied to a wide variety of human diseases. However, as mentioned before, carbohydrates interact with their protein receptors with very low affinity, with millimolar to micromolar dissociation constants. Consequently, one of the major focuses of current carbohydrate research includes the development of strategies for increasing the lectin-ligand binding affinities to levels required for therapeutic use.[214] In nature, carbohydrate ligands are expressed multiple times on the cell surface to counteract this problem, leading to stronger interactions. This phenomenon has become known as the 'multivalent effect' or 'cluster glycoside effect' (depicted in Figure 4.1), which was first reported by Lee and co-workers in 1995.[215] A large variety of multivalent carbohydrate ligands have been designed, synthesised and tested to determine the efficacy of the multivalent effect. A strong cluster glycoside effect requires two components: a lectin with clustered sugar binding sites and a multivalent ligand that can present sugars with proper orientation and spacing.[215] There are numerous examples of this in the literature, some of which will be discussed in the following sections.

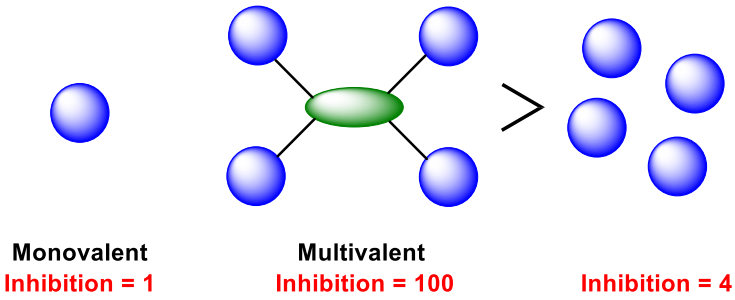

Figure 4.1: The Multivalent Effect can be described as the increase of the biological response observed for compounds possessing more than one bioactive units connected to a common scaffold compared to the sum of the contributions given by the individual bioactive molecules.[216]

It is known that multivalent carbohydrate ligands have higher affinity for lectins than their monovalent counterparts. The method by which this is achieved is not well understood. However, there are four main mechanisms thought to be involved in this process:

1. Simple multivalent enhancement effects can be described by a statistical or proximity effect arising from when multiple ligands are closely clustered around a receptor.
2. The intramolecular, or chelate, binding effect, where a bivalent ligand will interact with a bivalent receptor with higher affinity than the monovalent equivalent. This is well excepted in chemistry, particularly in inorganic chemistry where countless natural and synthetic metal complexes with multidentate ligands are known. This effect can also be applied to protein-carbohydrate interactions, where there is an entropic and enthalpic advantage when using multivalent ligands. When a multivalent ligand is binding, the entropic barrier is overcome by the first binding event, and all subsequent binding interactions can proceed with smaller entropic penalties. This results in stronger binding due to lower entropic penalties.
3. Multivalent ligands can also bind multivalent receptors intermolecularly, which may lead to the formation of aggregates that precipitate from solution. These aggregates can be stabilized by different forces, including protein-

protein interactions. This irreversible precipitation is kinetically very favourable.

4. Steric stabilization involves the binding of a large species near the surface of a carbohydrate binding protein, which may prevent the approach of other macromolecules. This effect would be most significant for polymeric ligands and ligands that offer substantial steric bulk, and is also more significant in aggregation assays where the approach of multiple macromolecules form the basis of the assay.[217]

The strength of the protein-carbohydrate interaction may be difficult to determine. However, a wide variety of assays have been developed for the measurement of these binding constants.[217] The most common techniques include:

- The inhibition of hemagglutination assay: The multivalent nature of the carbohydrate-lectin interaction often leads to crosslinking and aggregate formation. Agglutination of red blood cells is caused by lectin-red blood cell crosslinking and is the basis of the hemagglutination inhibition assay.[218]
- The enzyme-linked lectin assay (ELLA): This assay is performed on microtiter plates in a manner analogous to the common ELISA (enzyme-linked immunosorbent assay) technique in which enzyme-linked reagents are used to detect specific carbohydrate moieties on the surface of viable cells in suspension using soluble substrates. The amount of lectin binding may be determined quantitatively using automated ELISA plate readers.[219]
- Isothermal titration microcalorimetry (ITC): This technique provides insights into the thermodynamic basis for the enhanced affinities of multivalent glycosides binding to lectins. ITC measurements provides values for the binding enthalpy, ΔH, the association constant, K_a, and the number of binding sites on the protein. From the measurements of K_a, the free energy of binding, ΔG, can be calculated. The entropy of binding, ΔS, can then be obtained from ΔH and ΔG. Thus, ITC measurements can determine the complete thermodynamics of binding of a carbohydrate to a lectin.[220]
- Surface-plasmon resonance (SPR) imaging: This is an optical technique that is used to spatially monitor localized differences in the reflectivity of incident

light from a prism-gold film interface that result from molecules adsorbing to or desorbing from the gold film. SPR imaging can be used to study the interactions of carbohydrate arrays with proteins adsorbing from solution without the use of reporter groups (such as fluorescent, radioactive or enzymatic groups).[221]

4.1.2 Design of Multivalent Inhibitors of Adhesion

Multivalent glycoconjugates with various valencies and spatial arrangement of ligands have been developed to increase the affinity of the carbohydrate-protein interactions. The multivalent glycoconjugates can have defined molecular structures built around scaffolds such as calixarenes, dendrimers, cyclodextrins, cyclopeptides and fullerenes, or have higher valencies such as polymers, nanoparticles and quantum dots. A wide variety of scaffolds are required since the biological activity of these multivalent glycoconjugates is unpredictable.

We know the scaffold plays an important role in the biological activity of multivalent glycoconjugates, but the linker between the glycoconjugates to the scaffold is also important.[222] Oligo(ethyleneglycol)s have commonly been utilised as linkers in the design of multivalent glycoconjugates. These are used due to their water solubility, the availability of various lengths, and due to the presence of the alcohol functional groups they can be easily derivatized to alternative functional groups or can be used directly in the formation of glycosidic bonds. They also provide some flexibility to multivalent ligands due to the sp^3 hybridized orbitals of the carbon and oxygen atoms. Triethylene glycol is the one of the most commonly used oligo(ethyleneglycol)s used as a linker in multivalent glycoconjugates.

There are numerous examples in the literature of the increased affinity of multivalent ligands for lectins, in comparison to their monovalent counterparts. Most studies involve isolated plant and bacterial lectins, where the techniques to measure the affinity, mentioned above, can be performed. The following are some examples of the development of multivalent ligands that have higher affinity for their targets than monovalent derivatives.

4.1.2.1 Plant Lectin: ConA inhibitors

Most plant lectins are simple lectins composed of small number of subunits and are of moderate size. Many of these are well-studied since they are readily available in large quantities. They show a wide range of specificities and have been used as model systems for the study of protein-carbohydrate interactions. Concanavalin A (ConA) is a lectin extracted from the jack-bean that binds specifically to terminal α-D-mannosyl and α-D-glucosyl residues. It consists of four subunits in a tetrahedral orientation, where the binding sites are 72 Å apart (shown in Figure 4.2).

The study of the effect of multivalent ligands on ConA began by Roy *et al*.[137] when divalent mannosides such as that previously shown in Figure 2.2 and now in Figure 4.2 (compound **2.4**) was found to be 19 times more potent per sugar in an enzyme-linked lectin assay (ELLA) than the monovalent reference compound allyl α-D-mannoside. The potency of multivalent glycoconjugates must be compared to the potency of the relative monosaccharide, since an increase in affinity is real only if the increase is sustained when it is expressed as a relative potency per sugar ligand. Hexavalent ruthenium complexes **4.1** were then developed where the relative potency per sugar was increased further to 37 times more potent.[223] Kiessling and coworkers[224] prepared polyvalent systems consisting of mannosylated polymers **4.2**. These polymers were synthesised by ring opening metathesis polymerization (ROMP), which was discussed in Section 3.1.2, where a mannosylated norbornene-imide derivative was the monomer. Polymers of varying length were synthesised and evaluated using the hemagglutination inhibition assay for their affinity to ConA. An increase in potency was observed in relation to the length of the polymer chain. The decamer showed a 200-fold enhancement, while the 143-mer had a maximum potency increase of 2000 relative to the monomer. This increase in potency was expected to be due to the chelation effect, which is possible for the longer polymers which can reach multiple binding sights simultaneously, and also to statistical effects, due to the presence of multiple mannose residues in close proximity.

Large dendrimers have also been tested for their binding to ConA. PAMAM (polyamidoamine) dendrimers with terminal mannose residues **4.3** yielded enhancements of up to 600-fold per sugar in a hemagglutination inhibition assay.

This effect is due to chelation and statistical effects, along with aggregation. Nanoparticles with mannose and glucose linked residues were also prepared and evaluated as multivalent ConA ligands.[225] The most potent particle **4.4** contained 680 mannose moieties on the surface. The relative increase in affinity of each sugar was more than 100-fold stronger as an inhibitor than monovalent methyl α-D-mannoside. More effective particles for ConA interaction were found to be based on the self-assembly of rod-shaped tetra(*p*-phenylene)-based vesicles and micelles.[226] Micelles derived from compound **4.5** were 1800-fold more potent per sugar than α-D-mannoside. The mode of action of these particles was observed by TEM, where sizeable spherical aggregates of ConA molecules attached to the micelles were detected.

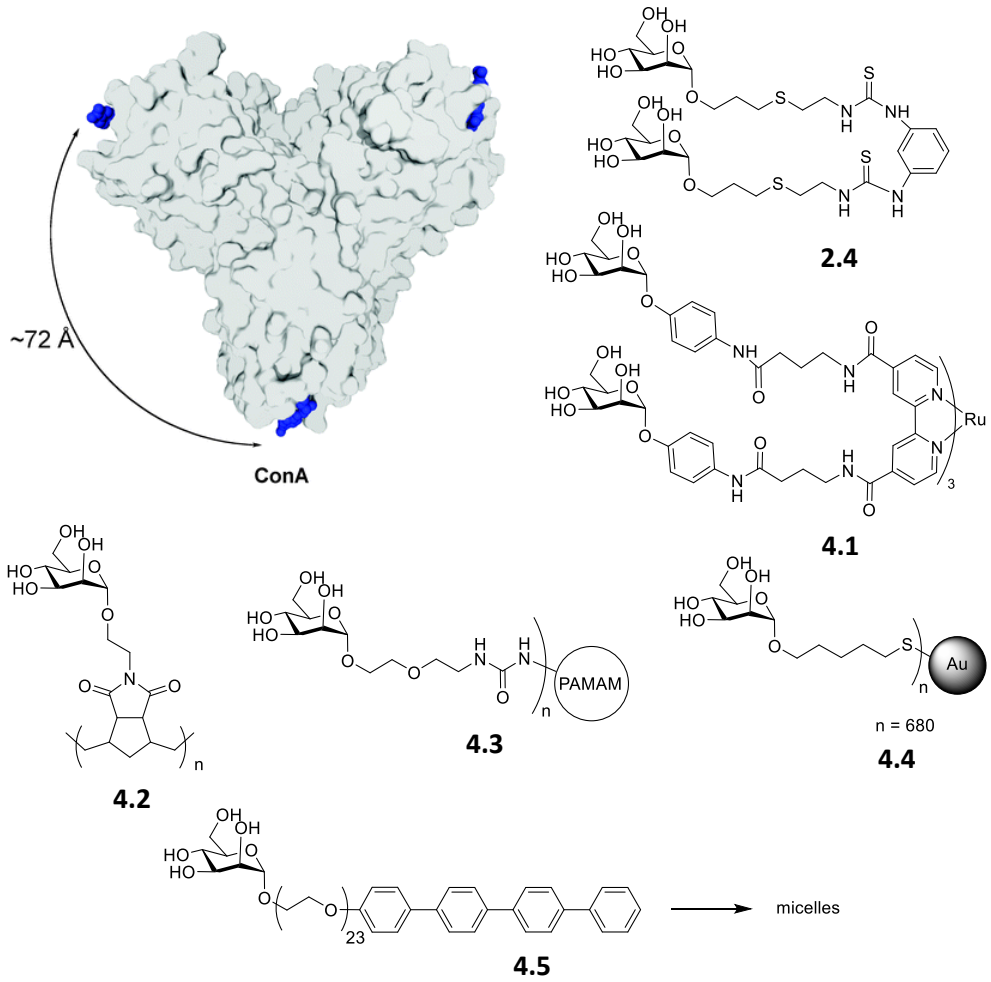

Figure 4.2 : Structure of ConA with bound mannose derivatives and the structures of selected ConA ligands/inhibitors.[227] Adapted with permission from The Royal Society of Chemistry.

4.1.2.2 Bacterial Adhesin: BC2L-A from *Burkholderia cenocepacia*

The *B. cenocepacia* bacterium contains three soluble carbohydrate-binding proteins, including *B. cenocepacia* lectin A (BC2L-A). This lectin binds to oligomannose-type *N*-glycan structures to adhere to host cells. Renaudet and co-workers[228] designed several mannosylated glycoclusters and glycodendrimers with varying valencies and core scaffolds and their structures are shown in Figure 4.3. Highly efficient CuAAC protocols were used to attach mannosyl moieties to tetra- and hexavalent 'regioselectively addressable functionalized template' (RAFT) cyclopeptides **R_4** and **R_6** respectively, tetravalent lysine-based dendrons **D_4**, and to hexavalent cyclotriphosphazene-based cores **P_6**. These were then used to create tetracosavalent (24-valent) glycodendrimers. The hexavalent cyclopeptide **R_6** was functionalized with the tetravalent cyclopeptide to give **RR_{24}**, and with the lysine-based dendron **D_4** to give **RD_4**. The phosphazene core **P_6** was conjugated to both the tetravalent cyclopeptide **R_4** to give **PR_{24}** and to the lysine-based dendron **D_4** to give **PD_{24}**. The interactions of these glycoclusters and glycodendrimers with BC2L-A were determined using isothermal titration calorimetry.

The tetra- and hexavalent compounds formed complexes with the lectin, where all of the mannose residues were involved in the binding. However, there was not a huge increase in affinity observed compared to the monovalent interaction. Of these glycoclusters, it was found that the hexavalent cyclopeptide (**R_6**) compound showed the best binding properties (K_d = 199 nM), where each sugar residue was three times more potent than methyl α-D-mannoside.

The tetracosavalent compounds (**RR_{24}** and **PD_{24}**) were then tested. It was found that the core scaffold did not affect the binding affinity. However, the scaffold used to present the sugars at the periphery had a significant effect. In the compounds where the mannose residues are connected to the more flexible lysine-based dendron there is stronger binding. Compound **PD_{24}** was found to have the lowest binding constant of this study (K_d = 51 nM), which is the highest affinity currently known for a fully synthetic multivalent glycodendrimer binding to BC2L-A. Further analysis of the binding found that the high affinity arises from an aggregative binding mode and not a chelate complex. This is because BC2L-A is a dimer where the two sugar-binding

pockets are located on opposite sides of the protein. This prevents the ligand interacting with both sites at the same time. The flexibility of compound **PD_{24}** allows it to interact with multiple protein monomers (up to 15 simultaneously).

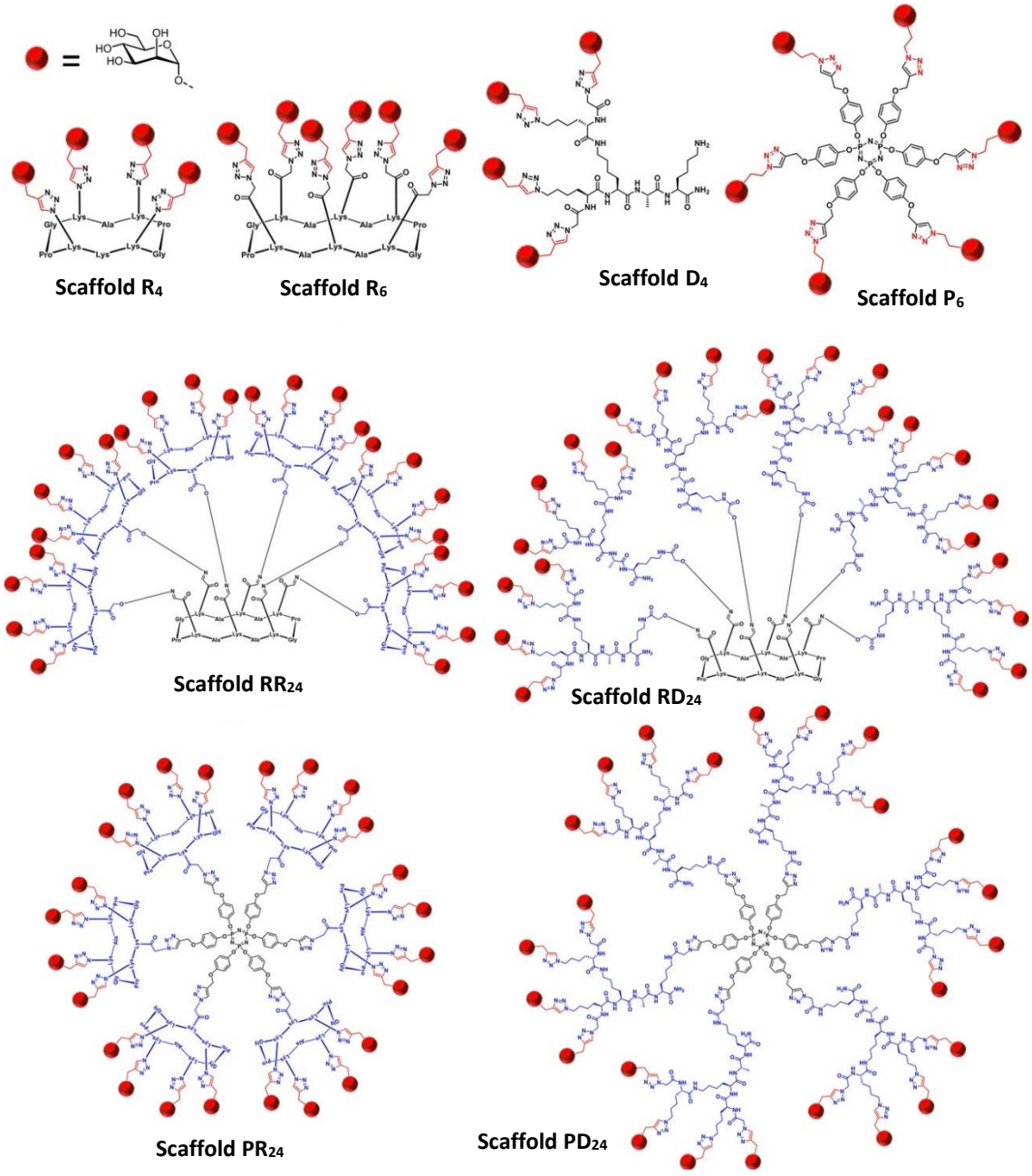

Figure 4.3: Structure of tetra-, hexa- and tetracosavalent glycoclusters used as ligands for BC2L-A lectin in *B. cenocepacia* reprinted from Renaudet *et al*.[228] Reprinted with permission.

4.1.2.3 Bacterial Adhesins: LecA and LecB in *Pseudomonas aeruginosa*

The bacterial adhesins LecA and LecB have been some of the most extensively studied lectins in relation to inhibition of adherence. Many multivalent glycoconjugates have been designed and synthesised to interact with these two lectins,[229] including those shown in Section 2.1.4.2. Vidal and coworkers[161] designed calix[4]arene-based glycoclusters functionalized with galactosides or fucosides (structure shown in Figure 2.8). Triethylene glycol was used as the linker to connect the carbohydrate moieties to the multivalent core scaffold, since they provide flexibility and water solubility. Many other multivalent ligands have been synthesised for inhibiting the binding of LecA with a huge diversity of core scaffolds, including high-valency galactosylated polymers **4.15**, fullerenes **4.8**, glyconanoparticles **4.14** and glycodendrimers **4.17**. The galactosylated helical poly(phenylacetylene) polymers **4.15** showed high affinity towards LecA of 4-5 μM per galactose with an IC_{50} of 9 μM from haemagluttination inhibition assay, however ITC measurements were hindered by aggregation processes.[230] The fullerene-based dodecavelent glycocluster **4.8** displayed inhibition in the micromolar range using the hemagglutination assay. An ELLA assay provided an IC_{50} value of 0.04 μM, representing the concentration required to reduce the binding of LecA to the galactosylated surface by 50 %. The relative potency per sugar moiety was 458, calculated as the ratio of the relative potency to the valency.[231] The gold nanoparticles **4.14** exhibits a 2800-fold increase in ligand activity compared with the galactose ligand in free solution in ITC assays. A K_d of 50 nM was also determined.[232] Chabre and coworkers[233] designed and synthesised a family of *C*-galactopyranoside clusters and dendrimers containing up to 27 terminal epitopes. In this study, the nonavalent *C*-galactoconjugate **4.17** was deemed the best overall multivalent inhibitor (K_d = 230 nM). The number of LecA monomers per molecule of this ligand (n=0.18) suggests that not all of the nine galactosyl residues are involved in binding, but rather a mixture of 5-7 lectin monomers being bound to each nonavalent ligand. A 409-fold increase in efficiency compared to β-Gal-OMe and 639-fold increase compared to the monovalent azide starting material was observed.

Excellent results were also obtained with β-peptoids **4.7** (linear) and **4.9** (cyclic),[234] calix[6]arenes **4.10**,[234] porphyrins **4.11**[234], calix[4]arenes **4.12**,[235] resorcin[4]arenes **4.6**[236] and glycopeptide dendrimers **4.16** (structures shown in Figure 4.4). The 1,3-alternate conformer of calix[4]arene resulted in the most efficient and greatest increase in affinity, due to a chelate-binding mode. Two galactose residues interacting with two neighbouring binding sites in a single LecA tetramer was confirmed in an atomic force microscopy study.[237] Also, a recent study showed that the divalent ligand **4.13**, with a rigid spacer based on the alternation of glucose moieties linked at the 1 and 4 positions by triazolyl groups, was capable of inducing a chelation effect with LecA. Numerous analogues were synthesised and tested, and it was found that the linker had great importance and only compound **4.13** had the appropriate linker-length for achieving an inhibitory potency increase of 545-fold over the reference compound.[238]

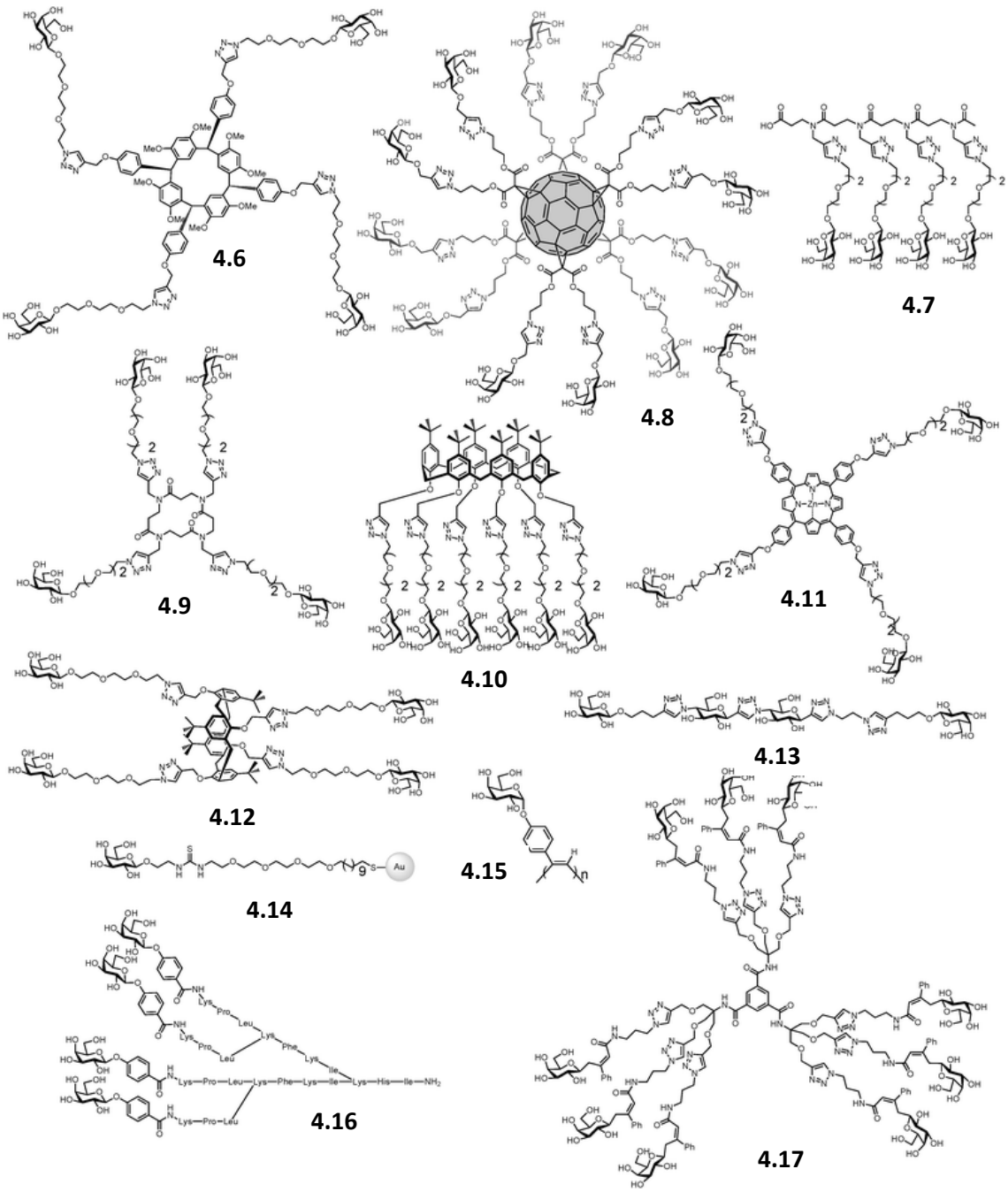

Figure 4.4: Diverse multivalent glycoconjugates as LecA high affinity ligands.[229] Reprinted with permission from The Royal Society of Chemistry.

The influence of the linker between the multivalent core and the carbohydrate moiety in multivalent ligands has also been studied. Another study by Vidal and coworkers[239] investigated the influence of linker lengths on a series of LecA-targeting glycoclusters (general structure in Figure 4.5). The influence of two linker arms (Linker 1 and Linker 2) was determined. Linker 1 was connected to the core scaffold, which in this case was a mannopyranoside, and consisted of varying lengths of

ethylene glycol, such as propyl (Pro), diethyleneglycolmethylene (EG_2M), and triethyleneglycolmethylene (EG_3M) (structures shown in Figure 4.5). Linker 2 connected to the carbohydrate moiety and these consisted of aromatic based linkers, such as phenyl, furanyl, thiophenyl, pyridinyl or tyrosinyl groups. Triazolyl groups were used to connect the two linkers. A cyanine fluorescent-dye (Cy3) was also introduced to allow for multiplexing on carbohydrate microarrays, to allow qualitative and quantitative screening of the LecA binding partners. A general trend was observed where the longer ethylene glycol linker resulted in higher affinity for the lectin, while for linker 2, phenyl and tyrosinyl groups, showed the best affinity for LecA. A low nano-molar (K_d = 19 nM) ligand with a tyrosine-based linker arm was identified after this SAR study and is now considered to be a new lead for the design of anti-infectous agents against *P. aeruginosa* lung infection.

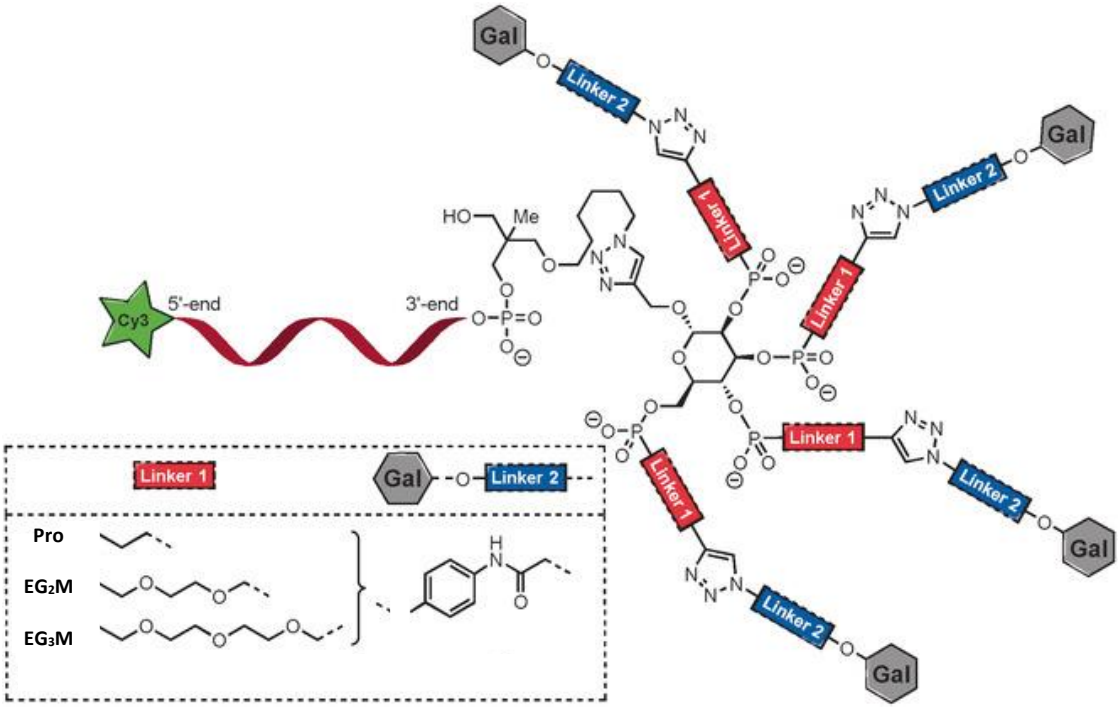

Figure 4.5: Structure of mannose-centred galactoclusters with aromatic aglycons.[239] Adapted with permission from John Wiley and Sons.

4.1.2.4 Fungal Adhesin: FleA from *Aspergillus fumigatus*

A similar phenomenom is also seen in some fungal lectins. FleA adhesin in *A. fumigatus* was discussed in Section 2.1.4.3. Multivalent structures designed by Varrot, Goudin and co-workers[166] were discussed (structures shown in Figure 2.10).

In this study, the monovalent fucoside **2.18** had low affinity for the lectin (K_d = 140 µM), whereas the octavalent fucoside **2.19** was highly potent (K_d = 0.04 µM), where these thermodynamic parameters of binding were measured using isothermal titration microcalorimetry. The linker length between the fucose residues was also important for binding to the adjacent binding site on the lectin.

4.2 Chapter Objective

The aim of this chapter is to develop multivalent displays of the initial lead compound **2.78** with the intention to increase the potency and the inhibition of the adhesion of *C. albicans* to BEC. As the structure of the target lectin in *C. albicans* is not known, ligand optimization requires the screening of diverse multivalent structures with different valencies, degree of rigidity/flexibility, linkers and architectures. A large choice of molecular scaffolds are available to do so. In this study, we have focused on (i) aromatic centred scaffolds, (ii) linear peptoid scaffolds and (iii) cyclopeptide and (iv) polylysine based scaffolds (shown in Figure 4.6). Lead compound **2.78** was modified with a suitable linker to facilitate connection with these scaffolds using CuAAC methodology. These four displays vary significantly in the orientation, the valency and the flexibility of the carbohydrate moieties, which is necessary to find the optimum display to interact efficiently with molecular targets in *C. albicans* and achieve increased anti-adhesion activities.

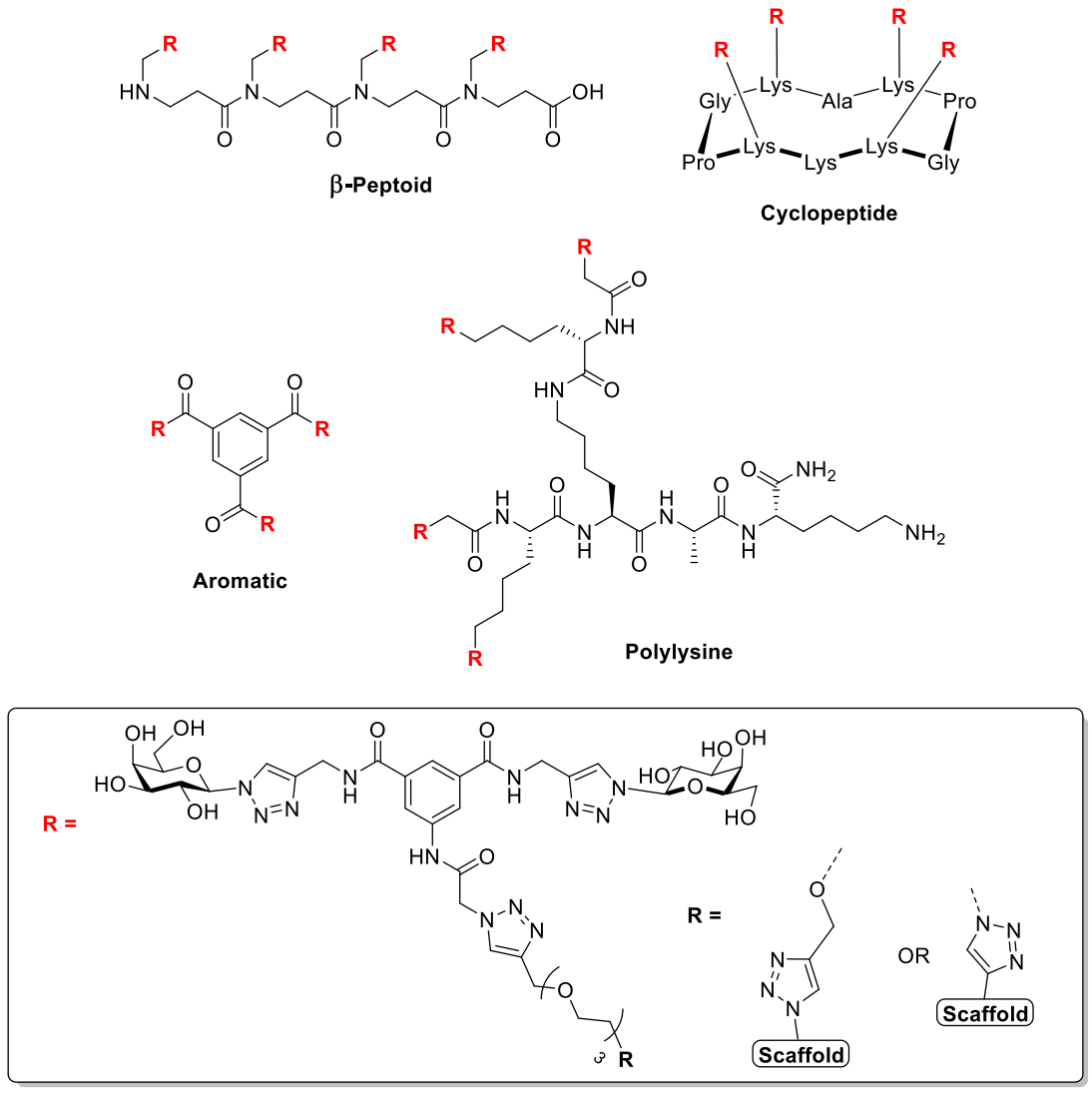

Figure 4.6: Structure of core scaffolds used in the synthesis of the next generation of multivalent anti-adhesion ligands for *C. albicans*.

4.3 Synthesis of Multivalent Glycoconjugates

4.3.1 Aromatic Scaffold

The initial approach was to develop divalent and trivalent displays of the lead compound **2.78** grafted onto an aromatic core, resulting in compounds with four and six galactose residues, respectively. Compound **2.113** is an acetylated derivative of the divalent galactoside which contains a free amine group on the aromatic centre. Direct coupling of this compound to the previously used 1,3-dicarboxylic acid **2.68**, was first attempted using the coupling reagent TBTU (Scheme 4.5). Since this reaction showed no formation of the product **4.18**, the carboxylic acid was converted to the

acyl chloride using oxalyl chloride and then reacted with compound **2.113**. Again, there was no product formed.

The reaction of compound **2.113** with the 1,4-dicarboxlic acid **3.12** was then attempted (Scheme 4.5), since this would result in a less sterically hindered product **4.19**. This was carried out using the same conditions as for the 1,3-dicarboxylic acid. No product was formed in this reaction. This is possibly due to steric factors or the fact that the aniline in compound **2.113** is quite deactivated, electron poor and weakly nucleophilic.

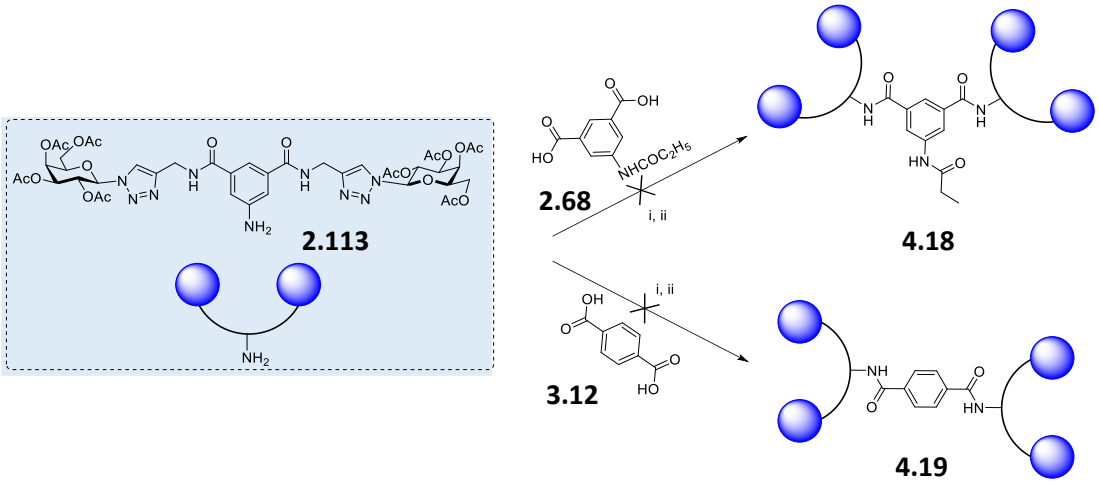

Scheme 4.5: Synthesis of divalent displays of initial lead compound. *Reagents and conditions*: i) TBTU, DMF, N_2, 16 h, No product isolated; ii) oxalyl chloride, THF:DMF (10:1), 30 mins – 16 h, No product isolated.

To overcome these problems, an azide derivative **4.21** (Scheme 4.6) was developed. Compound **2.113** was reacted with bromoacetyl bromide to give the bromo-derivative **4.20**, which was reacted with sodium azide to give the desired azide derivative **4.21**. Using the CuAAC conditions described in Chapter 2 and 3, the grafting of compound **4.21** onto the aromatic alkynyl diamides, 1,3-scaffold **2.69** and 1,4-scaffold **3.13**, was attempted. The reaction of the azide derivative **4.21** with 1,3-scaffold **2.69** did not show the formation of any product **4.22**. Interestingly, the reaction of the azide derivative **4.21** with the 1,4-scaffold **3.13** resulted in the formation of the desired product **4.23**, which was detected by MS. However, this product was extremely insoluble and did not allow proper purification or characterization. Deprotection of crude **4.23** under basic conditions did not improve

the solubility problem. Due to its insolubility, this compound could not be used in the biological assays.

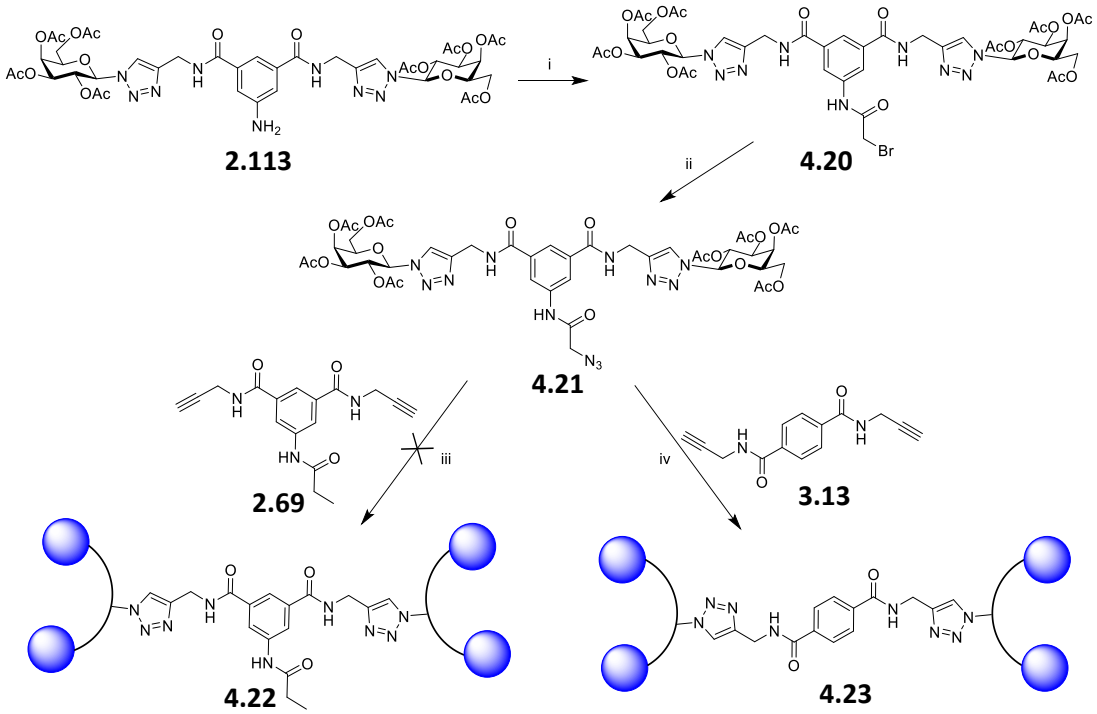

Scheme 4.6: *Reagents and conditions:* i) Bromoacetyl bromide, NEt_3, anhydrous DCM, 16 h, 83 %; ii) NaN_3, anhydrous DMF, N_2, 80 °C, 16 h, quant %; iii) $CuSO_4.5H_2O$/Na Asc, CH_3CN/H_2O, MW, 100 °C, 15 mins, No product formed; iv) $CuSO_4.5H_2O$/Na Asc, CH_3CN/H_2O, MW, 100 °C, 15 mins.

Due to the difficulty in developing multivalent scaffolds with aromatic centres directly from the aniline **2.113** or the azide **4.21**, it was decided to include a linker to join the divalent galactoside to the aromatic core (Scheme 4.7). A linker was designed starting from triethylene glycol **4.24**, which was alkynated on one end using propargyl bromide to give compound **4.25**[240]. To ensure mono-alkynation, the reaction was carried out with 3 equivalents of the triethylene glycol **4.24** and 1 equivalent of the propargyl bromide. This was then tosylated to protect the other hydroxyl group yielding compound **4.26**[241]. Using CuAAC conditions the linker was then reacted with the azide derivative **4.21** giving compound **4.27**. The tosyl group was then replaced by an azide using NaN_3 to give compound **4.28**. This key synthetic intermediate consisted of the acetylated divalent galactoside with a triethylene glycol linker functionalized with an azide available to conjugate to different alkynated scaffolds.

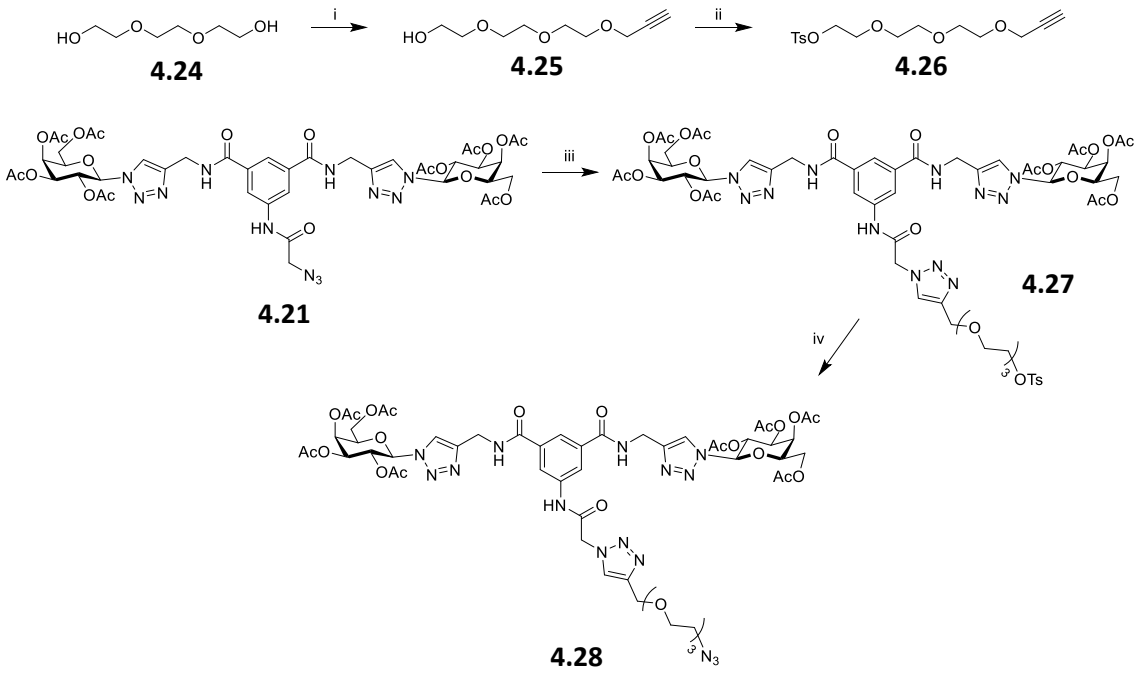

Scheme 4.7: Synthesis of azide derivative **4.16**. *Reagents and conditions*: i) propargyl bromide, NaH, anhydrous THF, N_2 16 h, 75 %; ii) TsCl, KOH, DCM, 0 °C, 2 h, 87 %; iii) **4.26**, $CuSO_4.5H_2O$/Na Asc, CH_3CN/H_2O, MW, 100 °C, 30 mins, 74 %; iv) NaN_3, CH_3CN, DMF, 80 °C, 24 h, 95 %.

Compound **4.28** was then used to generate a trivalent display of the initial lead divalent galactoside. Using CuAAC conditions, compound **4.28** was reacted with the trivalent scaffold **2.103** to give compound **4.29**, which was then deprotected under mild basic conditions to give the desired compound **4.30**, presenting a radial display of the divalent galactoside with six terminal galactose residues (Scheme 4.8). A comparison of the ^{1}H NMR spectra of compounds **4.28** and **4.29** is shown in Figure 4.7, with the major difference between the spectra being the broadness of the signals in the trivalent display of the divalent galactoside **4.29**, compared to the sharp peaks observed in the azide derivative **4.28**.

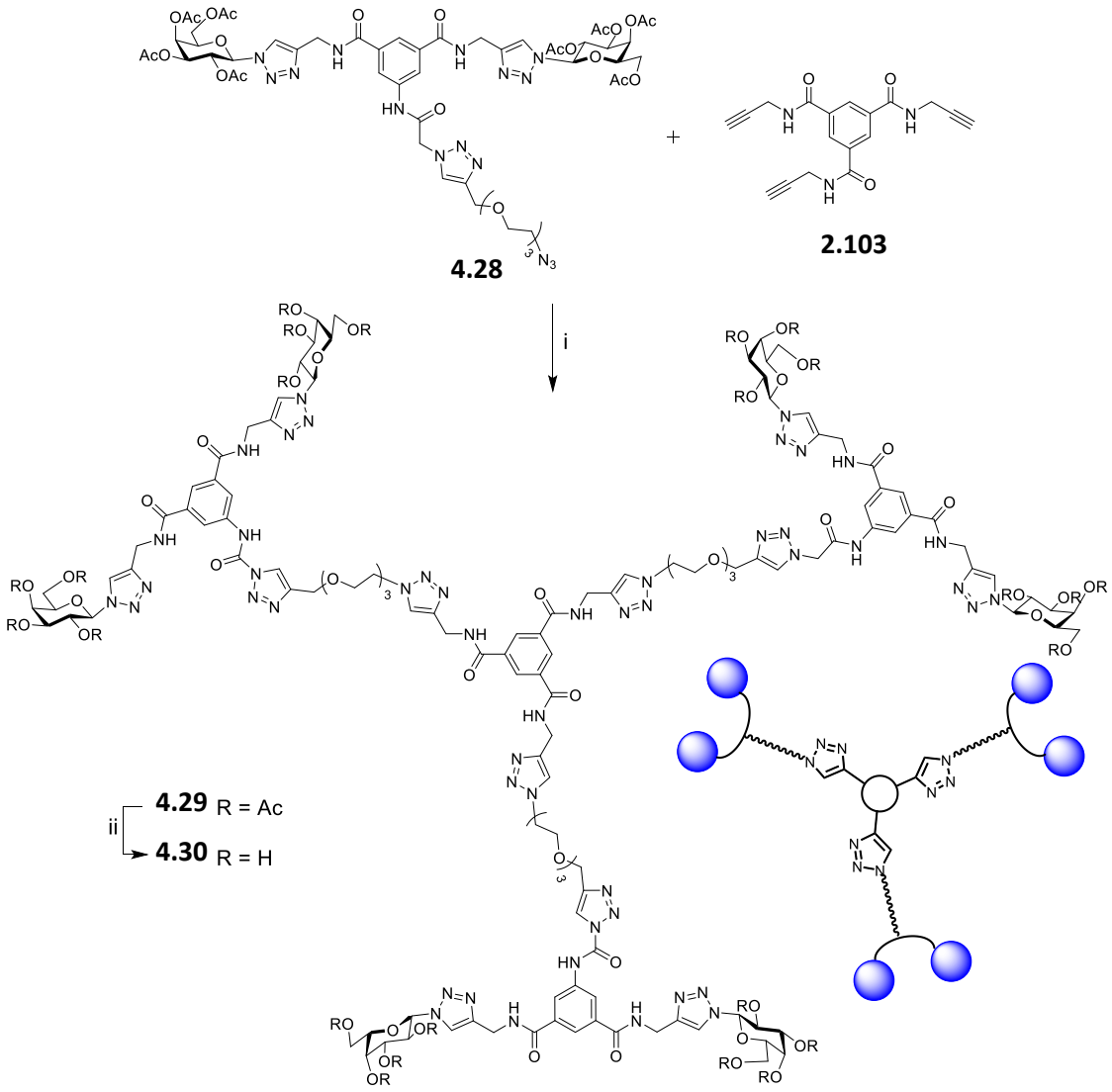

Scheme 4.8: Synthesis of trivalent display of the initial lead compound built around an aromatic-core **4.30**. *Reagents and conditions:* i) $CuSO_4.5H_2O$/Na Asc, CH_3CN/H_2O, MW, 100 °C, 30 mins, 72 %; ii) MeOH, NEt_3, H_2O, 45˚C, 6 h, 82 %.

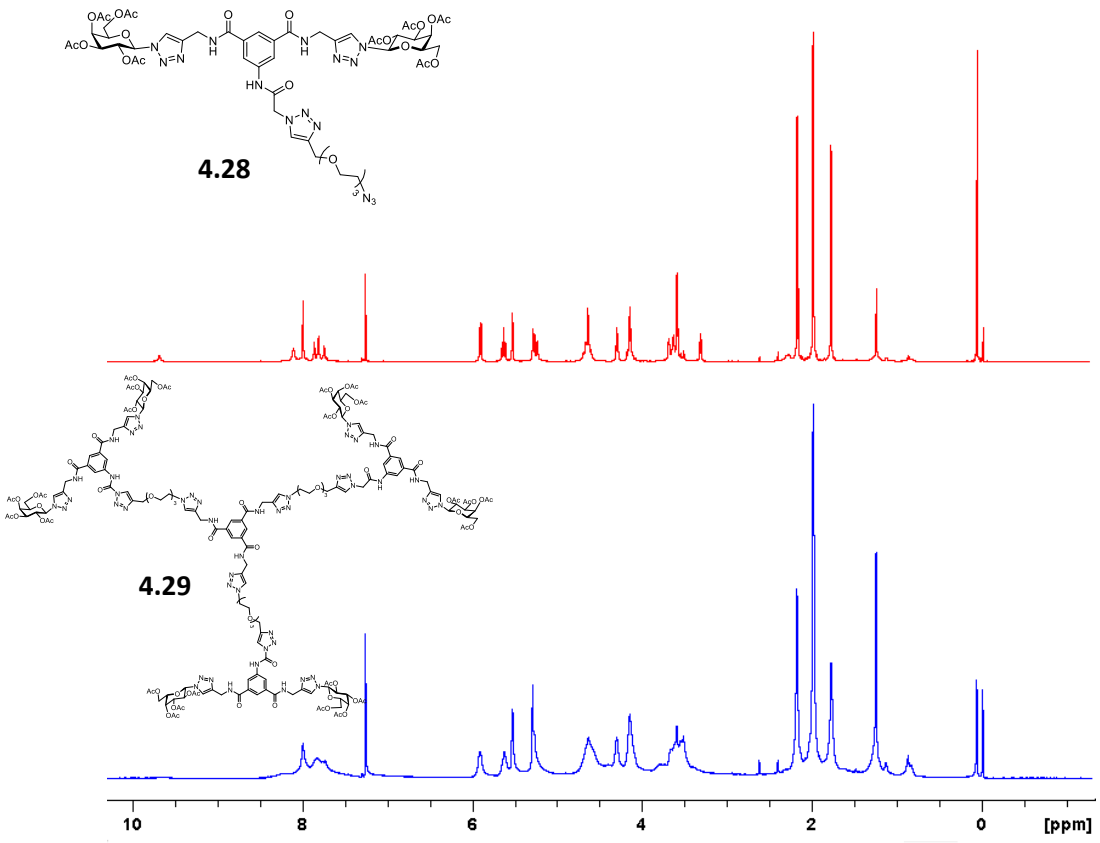

Figure 4.7: ^{1}H NMR of compounds **4.28** and **4.29** in $CDCl_3$.

4.3.2 Linear Scaffold

To display the initial lead compound in a different multivalent presentation, a linear scaffold was considered. β-Peptides have been used as artificial backbones to display diverse side chains capable of mimicking bioactive peptides,[242, 243] which do not undergo hydrolysis in the presence of peptidases and proteases.[244] β-Peptoids are a newer class of synthetic polyamides, which are structurally related to β-peptides where the amino acid side chain is switched from the β-carbon to the amide nitrogen.[245] β-peptoid scaffolds designed by Faure and coworkers have been used to create linear and cyclic displays of side chains and carbohydrates.[246] The synthesis of β-peptoids involves a two-step iterative methodology. Acryloyl chloride is reacted with an amine to give an α, β-unsaturated amide. This is then reacted with a primary amine in an aza-Michael addition to give a secondary amine (mechanisms shown in Scheme 4.10). Repeating these steps several times results in the synthesis of β-peptoid oligomers.[246]

To prepare the linear peptoid scaffold, literature procedures were followed. *Tert*-butyl acrylate **4.31** was reacted with propargylamine to give *N*-propargyl-functionalized β-alanine **4.32**[246], the key building block for the synthesis of the β-peptoid oligomer (Scheme 4.9). From this monomer, elongation according to the two-step procedure was continued until the desired length was reached. Compound **4.32** was reacted with acryloyl chloride to give the α, β-unsaturated amide **4.33**[246]. Variable temperature ^{1}H NMR experiments were carried out on this compound (Figure 4.8) to assess its conformational flexibility. Interestingly, at low temperatures, there are two sets of signals for the CH_2 (4.0 - 4.2 ppm) and the CH (2.1 – 2.4 ppm) of the propargyl group (indicated in Figure 4.8). This suggests that this compound has two main conformers due to the presence of the amide group (structures shown in Figure 4.8). Free rotation around the C-N bond of the amide group is prevented at low temperatures, locking the structure in two distinct conformations. However, when the temperature is increased the two signals begin to coalesce into one broad set of signals, as the compound has sufficient energy to rotate around the C-N bond of the amide more readily and interchange between the two conformers. Other studies have shown the presence of amide bond conformers or rotamers in β-peptoids.[247]

From this NMR data it is possible to determine activation energy parameters for the isomerisation of the amides through determination of the temperature at which the NMR resonances of two exchanging species coalesce.[248] This coalescence temperature (T_c) is used, along with the maximum peak separation in the low temperature NMR ($\Delta\nu$ in Hz). From this information the activation energy barrier ($\Delta G^{\ddagger}$) can be calculated. Gutowsky showed that the rate of rotation, k_c, at T_c is given by Eq. 1:

$$k_c = \frac{\pi(\Delta\nu)}{\sqrt{2}} \qquad \text{Eq. 1}$$

With $\Delta\nu = 40.6$ Hz (the distance between the two CH signals at 278 K), this results in k_c = 90.2 Hz. Then if the value of k_c is substituted into the following version of the Eyring equation, the value of $\Delta G^{\ddagger}$ can be determined using Eq. 2:

$$\Delta G^{\ddagger} = 19.12\, T_c\, (10.32 + \log T_c - \log k_c) \qquad \text{Eq. 2}$$

Applying the observed values in the spectra of compound **4.33** for the above equations, considering the CH signal at 2.1 – 2.4 ppm, with k_c = 90.2 Hz and T_c = 318 K, gives $\Delta G^{\ddagger}$ ≈ 66 kJ/mol or 16 kcal/mol, which is typical for amides ($\Delta G^{\ddagger}$ = 11 -21 kcal/mol)[249]. Hence, it requires 16 kcal/mol of energy for the amide to isomerize between the two conformations.

Following the NMR study of the α, β-unsaturated amide **4.33**, this compound was then reacted with propargylamine to give the dimer **4.34**[246], which was reacted with acryloyl chloride to give the α, β-unsaturated amide **4.35**[246]. This was continued until the tetramer **4.38**[246] was reached, where the secondary amine was acetylated to give **4.39**[234] to prevent further reaction. All the intermediate compounds, along with the final linear scaffold **4.39**, show the same trend in the NMR as discussed previously. Indicating that at room temperature, there are several conformations of the scaffold present.

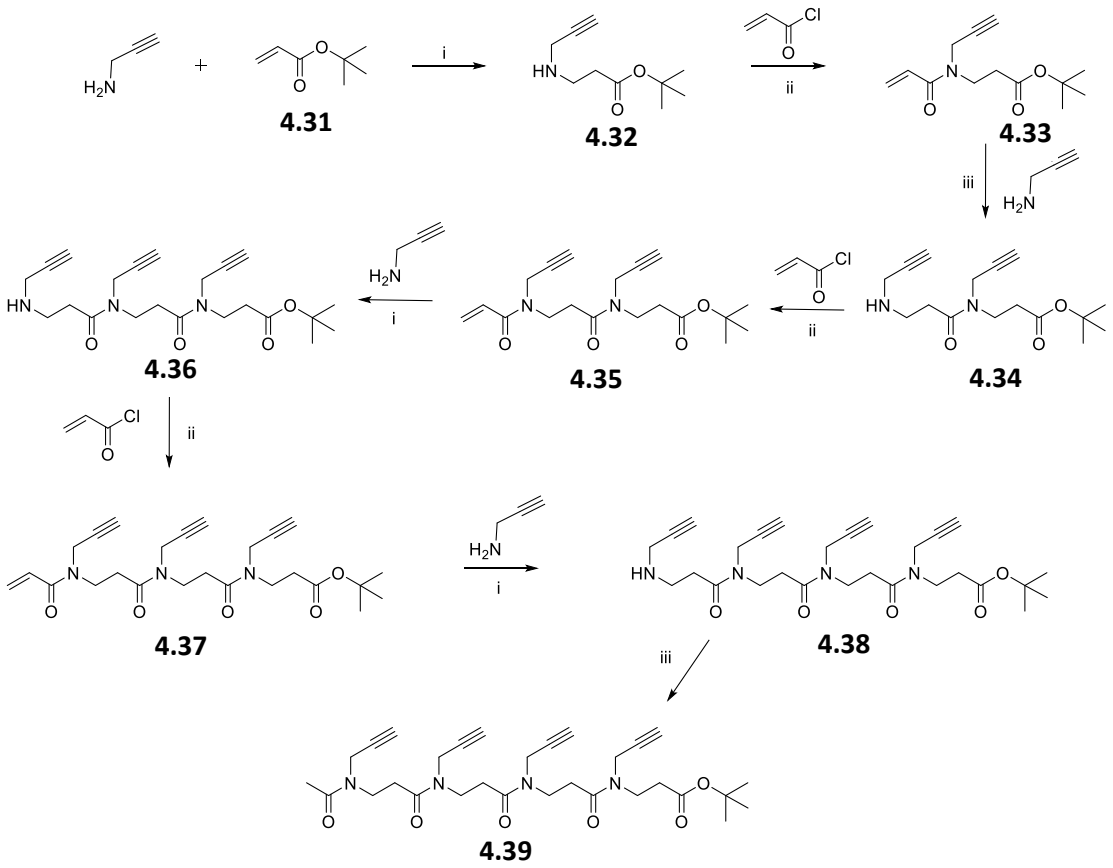

Scheme 4.9: Synthesis of the linear scaffold **4.39**. *Reagents and conditions*: i) dry methanol, N_2, 50 ˚C, 24 h, quant yield; ii) DIPEA, dry DCM, 0 ˚C, 1 h, 86–95 %; iii) Acetic anhydride, DCM, 5 h, 97 %.

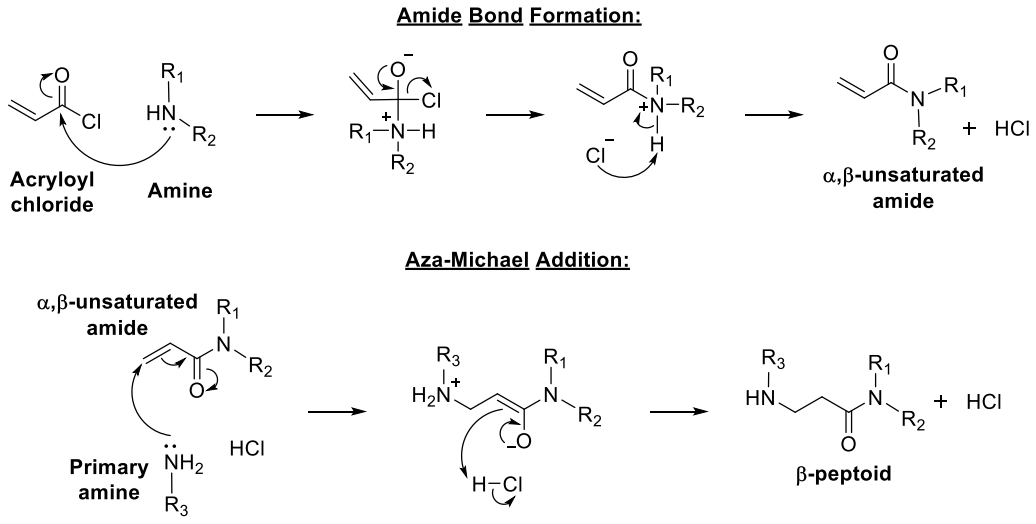

Scheme 4.10: Mechanism for the amide bond formation and the aza-Micheal addition reaction to form the β-peptoid oligomers.

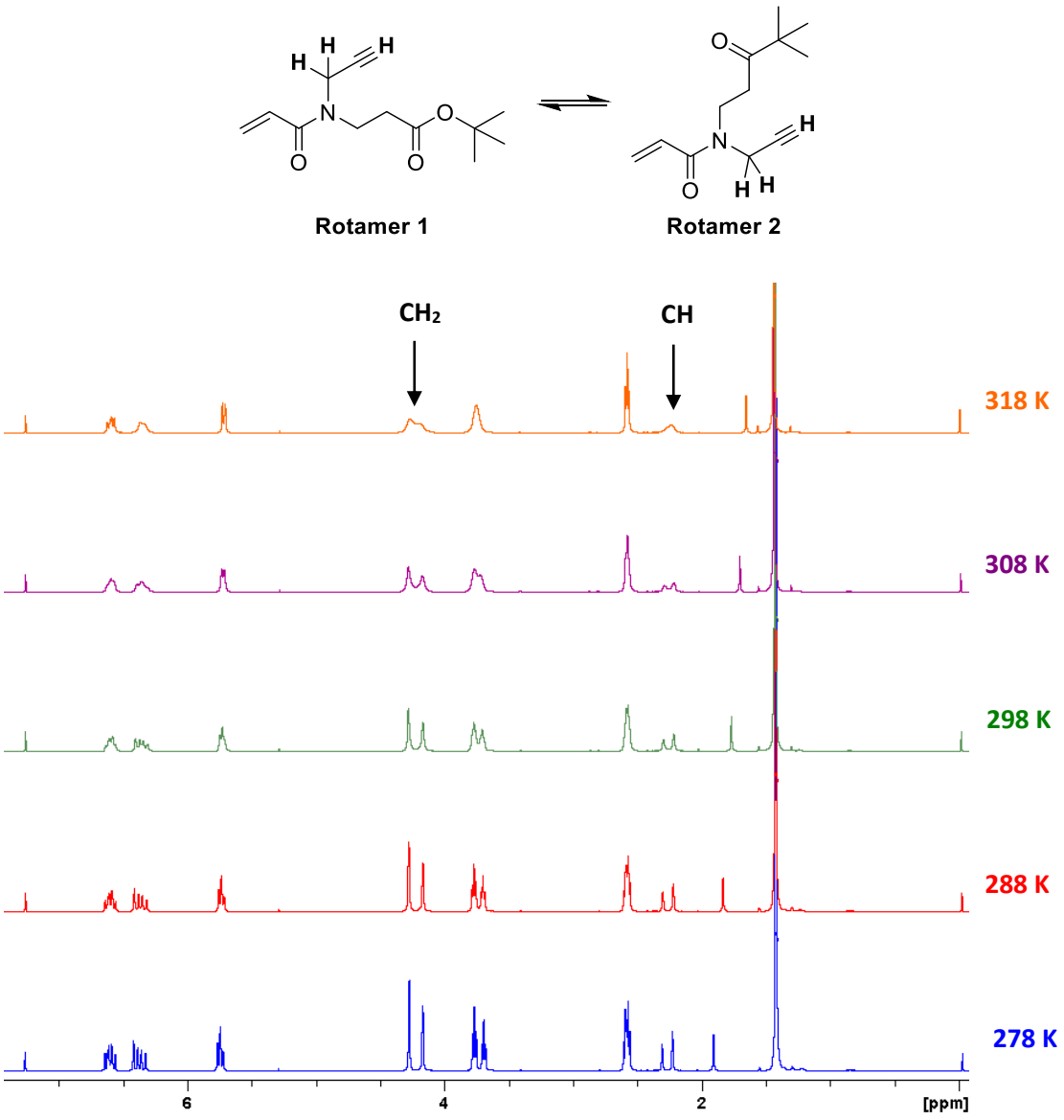

Figure 4.8: Structure of the two main rotamers of compound **4.33** and VT ^{1}H NMR spectra of α, β-unsaturated amide **4.33** in $CDCl_3$.

To assess the suitability of the linear scaffold **4.39** in CuAAC conditions, first it was reacted with galactosyl azide **2.40**, resulting in tetravalent galactoside **4.40**, which was deprotected to give tetravalent galactoside **4.41** (Scheme 4.11). Then the azide derivative **4.28** was conjugated to the linear scaffold to give compound **4.42**, which was deprotected resulting in **4.43**, a tetravalent display of the lead compound with eight galactose residues. Both compounds **4.41** and **4.43**, together with aromatic hexagalactoside **4.30**, will be tested for their anti-adhesive properties against *C. albicans*.

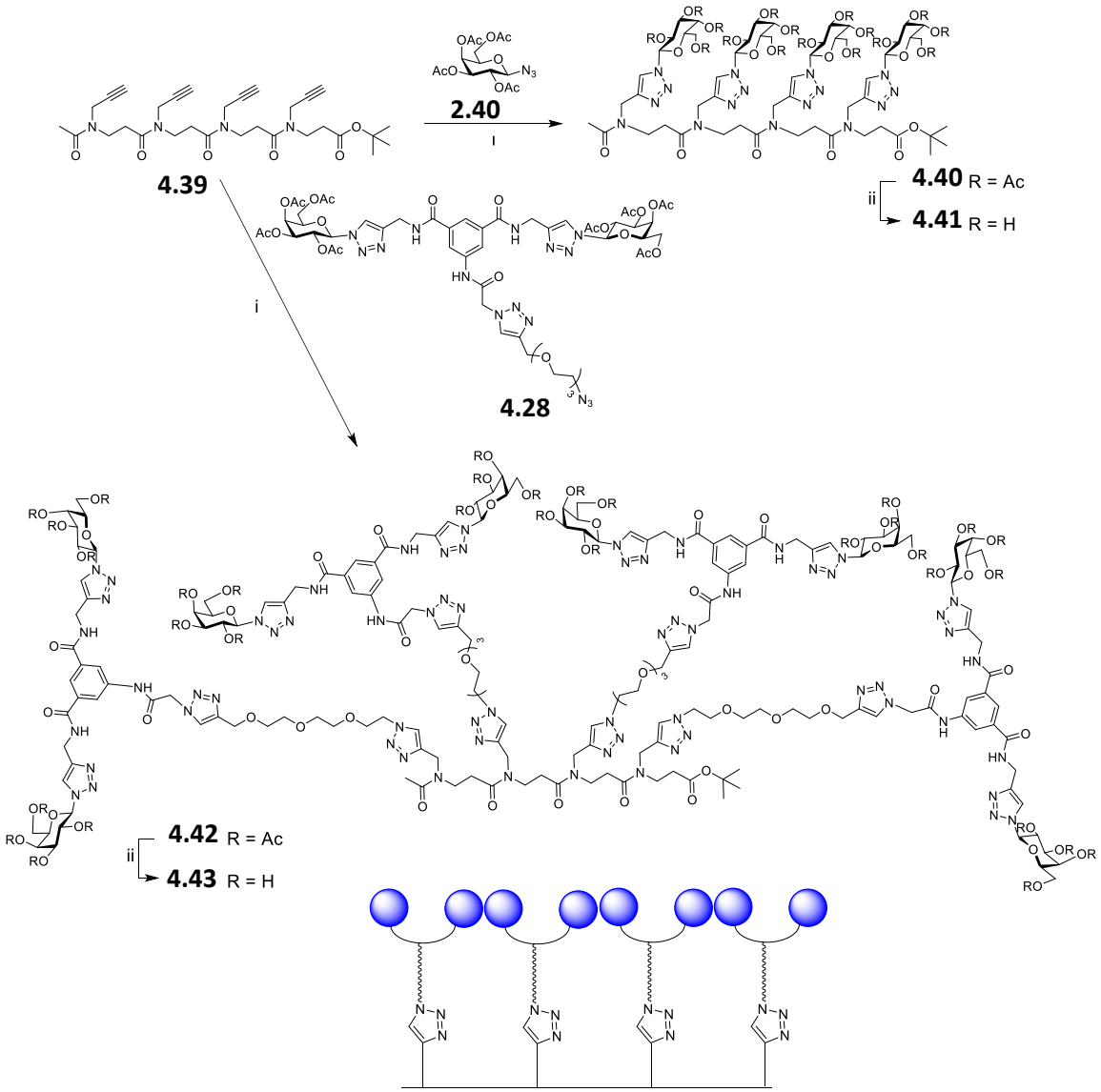

Scheme 4.11: Synthesis of a multivalent display of the initial lead compound with a linear scaffold **4.43**. *Reagents and conditions:* i) $CuSO_4.5H_2O$/Na Asc, CH_3CN/H_2O, MW, 100 °C, 30 mins, 58-68 %; ii) MeOH, NEt_3, H_2O, 45˚C, 6 h, 82-92 %.

4.3.3 Cyclopeptide Scaffold

Lysine-containing cyclodecapeptides called 'regioselectively addressable functionalized templates' (RAFT) were first described as stable scaffolds for the *de novo* design of proteins or as peptidomimics.[250] These scaffolds have a defined and constrained structure, and the presence of the amino acid lysine in the amino acid sequence allows chemical reactions. In addition, due to their planar structure, these reactions can be performed on the upper or lower face of the scaffold, depending on

the position of the functional lysine amino acids. Using these lysine side-chain addressable sites, these scaffolds have been extensively used to display carbohydrates in a multivalent manner.[251] In order to improve the recognition properties of the cyclopeptide-based glycoclusters towards lectins, newer generations with higher valency and varying levels of rigidity have been developed by Renaudet and coworkers. A modular chemoselective strategy was used to introduce either a flexible polylysine framework or a constrained cyclopeptide onto the RAFT core, providing two different hyperbranched skeletons in a controlled manner. Biologically relevant carbohydrates were then conjugated to obtain a new series of glycodendrimer-like structures.[252] These structures have been used to generate highly potent ligands for interactions with different lectins, such as described in Section 4.1.2.2.

A collaboration with the group of Prof. Renaudet involved the use of the RAFT scaffolds for the multivalent presentation of lead compound **2.67**, during a research visit to his laboratory in Université Grenoble Alpes. Since the RAFT scaffolds that their team suggested were functionalized with azides, a new derivative of the lead compound functionalised with a linker bearing an alkyne had to be developed to allow for CuAAC conjugation. Our initial approach involved the reaction of tosylated compound **4.27** with propargyl bromide to introduce the alkyne. However, the harsh basic conditions (NaH) required for this conversion resulted in side reactions, where no product could be isolated. Hence, a new strategy was required (Scheme 4.12). In this case triethylene glycol **4.24** was reacted with propargyl bromide to give the dialkynated compound **4.45**. This was then reacted with the azide derivative **4.21** using CuAAC conditions. To promote reaction with only one alkynyl group, this reaction was carried out in dilute conditions. However, some product **4.46** was formed as a result of CuAAC reaction at both ends of the linker. These compounds could be separated by column chromatography to obtain the purified compound **4.48**, which was deprotected under mild basic conditions to give the desired compound **4.49**. This compound consists of the acetylated divalent galactoside with a triethylene glycol linker appended with an alkyne available to conjugate to different

scaffolds functionalized with azides. Compound **4.46** was also deprotected to give compound **4.47**.

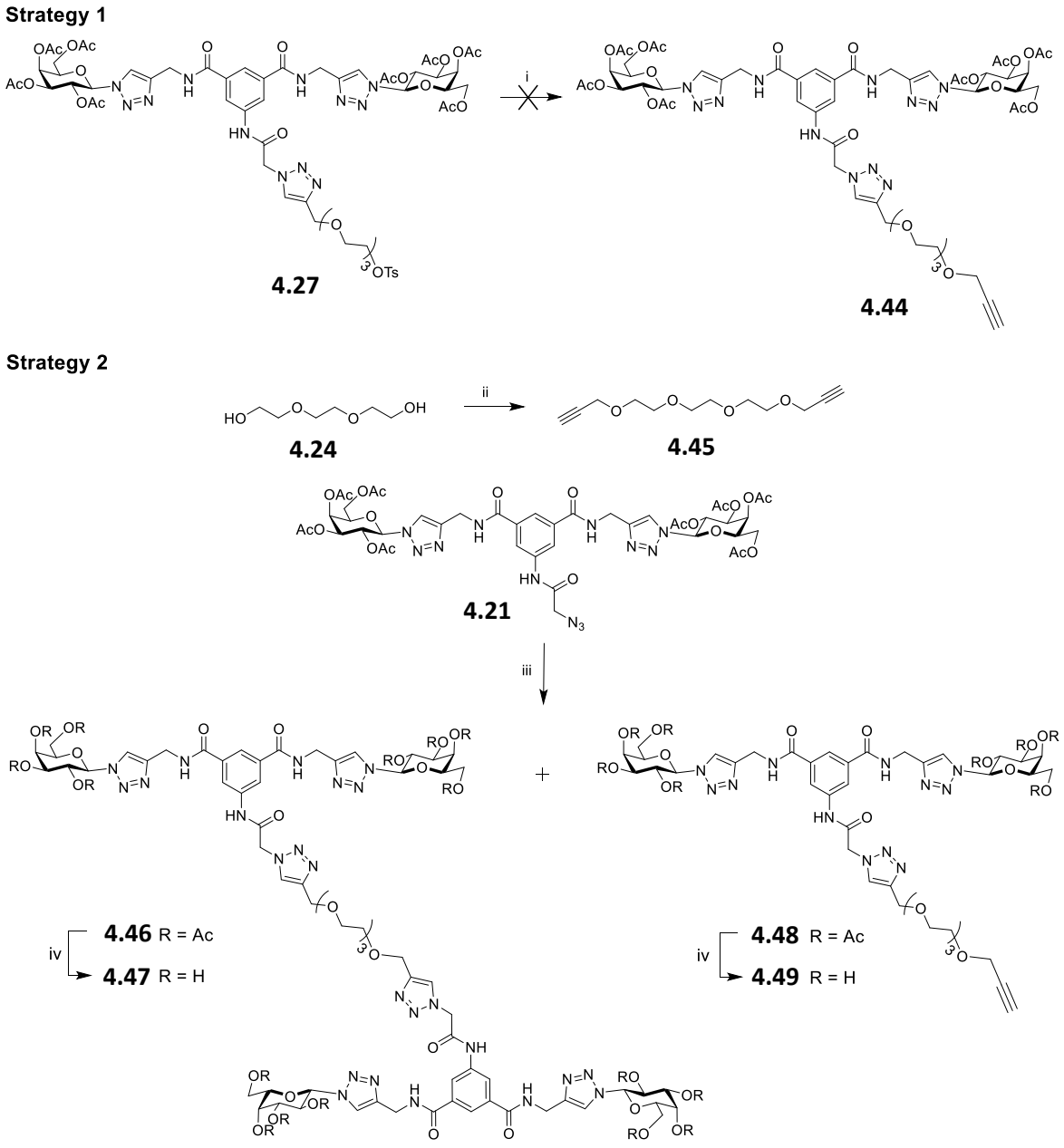

Scheme 4.12: Synthesis of the alkynated derivative of the lead compound **4.49**. *Reagents and conditions:* i) NaH, anhydrous THF, N_2, 1 h, propargyl bromide, 24 h, No product formed; ii) NaH, anhydrous THF, N_2, 1 h, propargyl bromide, 48 h, 92 %; iii) $CuSO_4.5H_2O$/Na Asc, CH_3CN/H_2O, MW, 100 °C, 10 mins, 45 %; iv) MeOH, NEt_3, H_2O, 45˚C, 6 h, 90 %.

The following reactions were carried out in the laboratory of Prof. Renaudet in the Université Grenoble Alpes. The cyclopeptide **4.50** (Scheme 4.13) used in this synthesis is a decapeptide, functionalized with four azides on the lysine residues on the scaffold. A highly efficient CuAAC protocol was used to connect compound **4.49** to the cyclopeptide scaffold, involving the use of $CuSO_4.H_2O$, THPTA (3(tris(3-hydroxypropyltriazolylmethyl)amine)) and sodium ascorbate as the catalytic system. UPLC was used to determine the endpoint of the reaction (typically 1 hour), and the product was purified using semi-preparative RP-HPLC to give compound **4.51**. This compound consists of 4-copies of the lead compound **2.78** connected to the cyclopeptide core.

This glycocluster **4.51** was then reacted with *N*-succinimidyl pentynoate under basic conditions to functionalize the underside of the RAFT scaffold with an alkyne group giving compound **4.52**. This was then coupled to another azide-functionalized RAFT **4.50** using the same CuAAC conditions to give the glycodendrimer **4.53** shown in Figure 4.9. This glycodendrimer **4.53** consists of 16 copies of the lead compound attached to rigid cyclopeptide cores, resulting in the display of 32 galactose residues.

A hexavalent glycocluster was also synthesised in a similar manner (Scheme 4.14). The cyclopeptide used in this case was a cyclic, dodecapeptide, functionalized with six azides **4.54**. CuAAc conditions were used to conjugate compound **4.49** to the hexavalent RAFT scaffold **4.54**, which was purified to give compound **4.55**. This hexavalent glycocluster **4.55** displays 6 copies of the lead compound **2.78** resulting in the presentation of 12 galactose residues.

The tetravalent cyclopeptide-based glycocluster **4.51**, the hexavalent cyclopeptide-based glycocluster **4.55** and the hexadecavalent cyclopeptide-based glycodendrimer **4.53** will be tested in the adherence assays to determine their anti-adhesive properties against *C. albicans*.

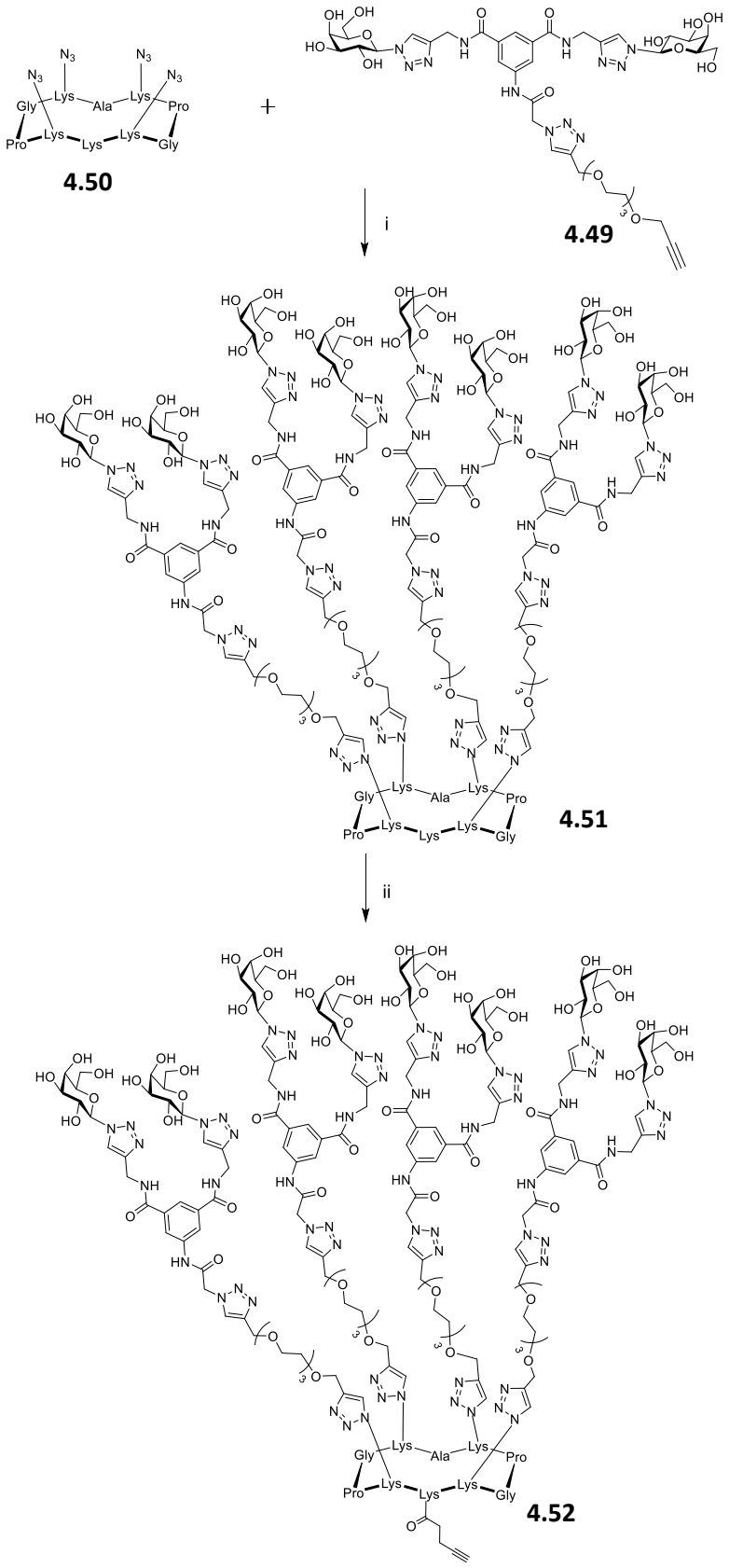

Scheme 4.13: Synthesis of tetravalent glycocluster **4.51** and the alkynated glycocluster **4.52**. *Reagents and conditions:* i) $CuSO_4$.5 H_2O/Na Asc, THPTA, DMF/PBS buffer (pH 7.5), rt, 1 h, 65 %; ii) *N*-succinimidyl pentynoate, DIPEA, DMF (pH 9), rt, 1 h, 97 %.

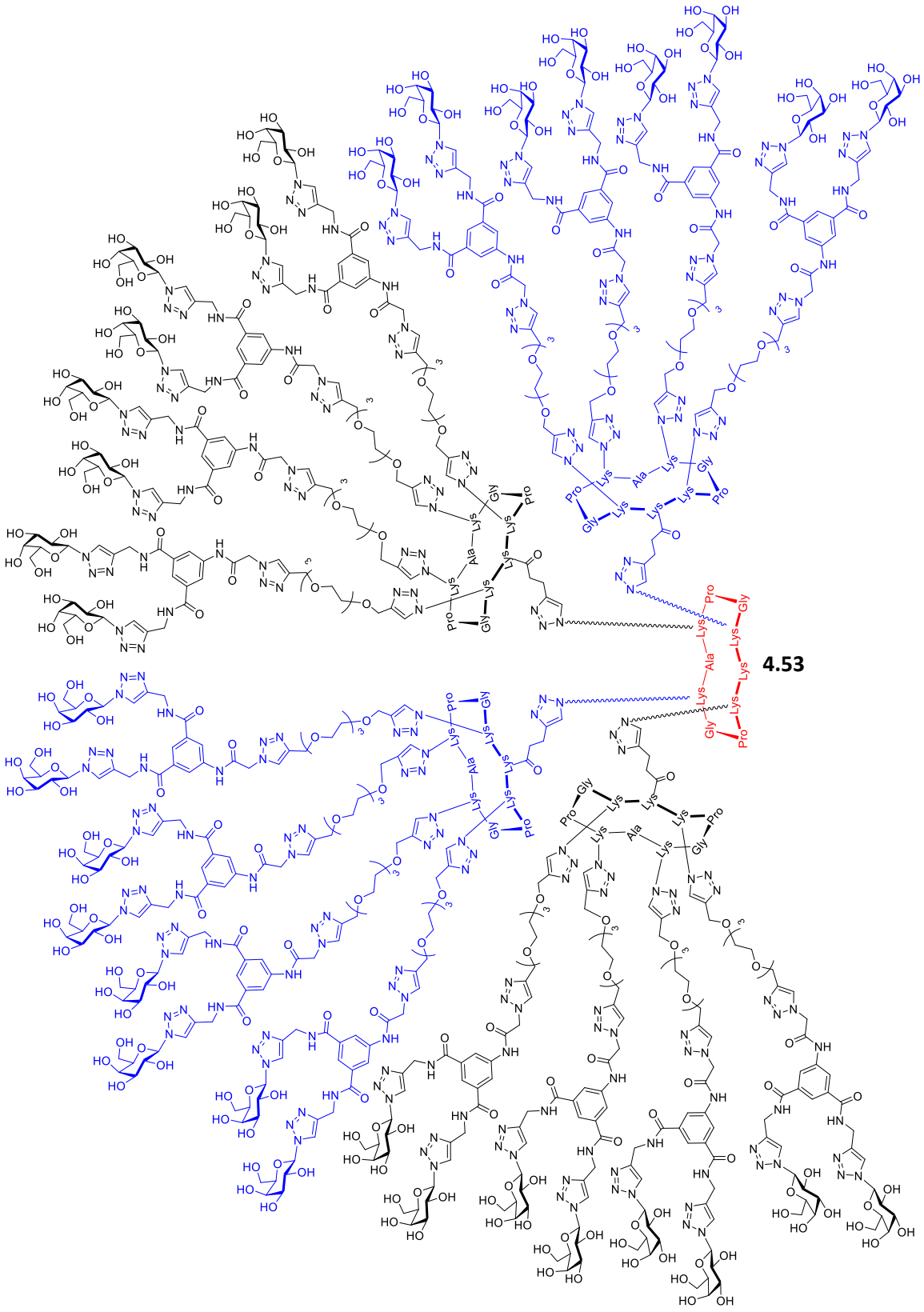

Figure 4.9: Structure of the hexadecavalent glycodendrimer **4.53** (Yield: 89 %).

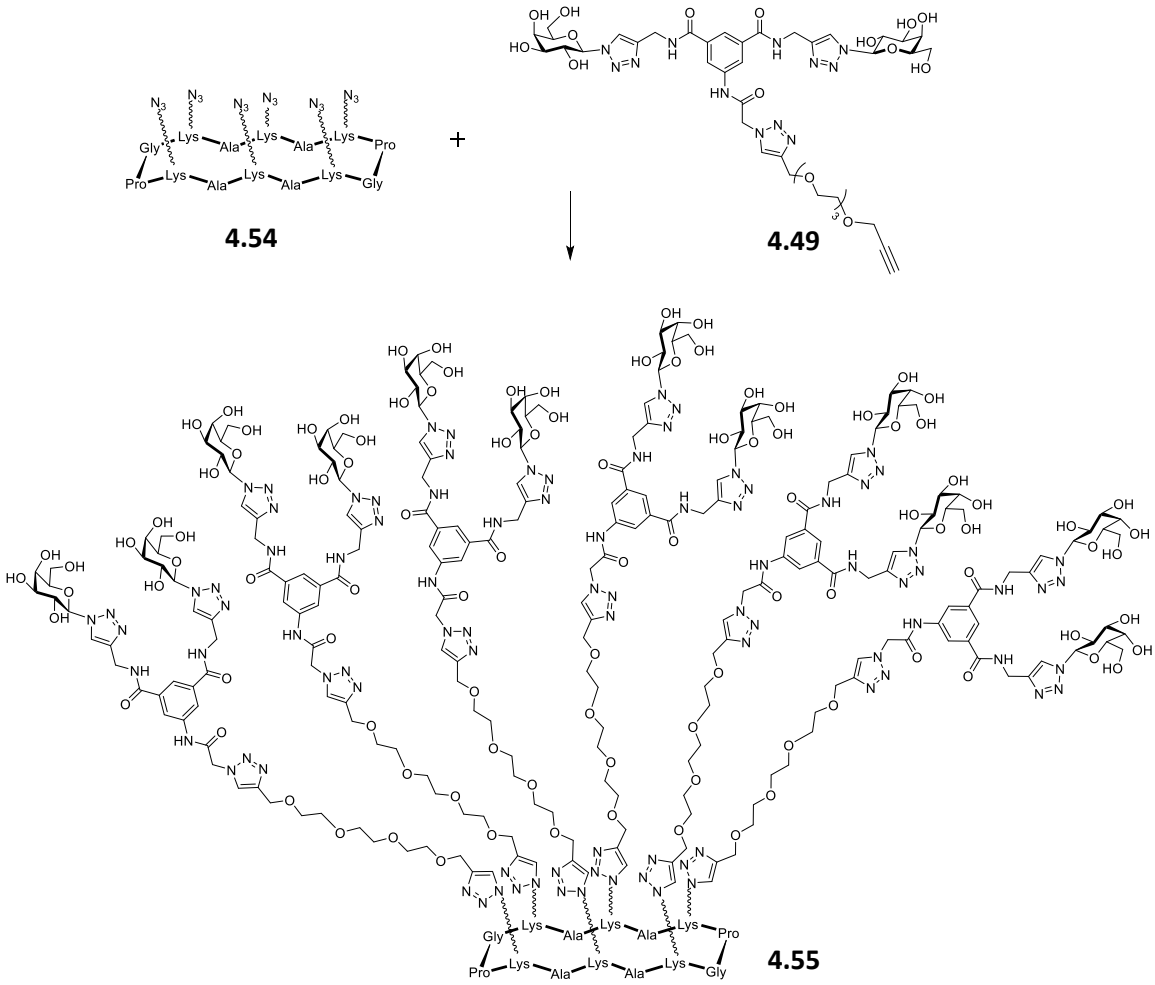

Scheme 4.14: Synthesis of hexavalent glycocluster **4.55**. *Reagents and conditions:* $CuSO_4$.5 H_2O/Na Asc, THPTA, DMF/PBS buffer (pH 7.5), rt, 1 h, 34 %.

4.3.4 Polylysine-Based Scaffold

A similar procedure as that used in the synthesis of glycodendrimer **4.53** was used to synthesis the glycodendrimer **4.59** shown in Figure 4.10. A polylysine-based scaffold **4.56** (Scheme 4.15) was used, which was also functionalized with four azide groups. The same CuAAC conditions were used to conjugate the alkynated compound **4.49** to the polylysine-based scaffold **4.56** to give the glycocluster **4.57**, consisting of 4 copies of the lead compound. This was then reacted with *N*-succinimidyl pentynoate under basic conditions to functionalize the lysine-based scaffold with an alkyne group giving compound **4.58**. This was then coupled to another azide-functionalized polylysine scaffold **4.56** using the same CuAAC conditions to give the glycodendrimer **4.59** shown in Figure 4.10, which, like glycodendrimer **4.53**, has 16 copies of the lead

compound. However, this glycocluster **4.59** provides a more flexible display of the 32 galactose residues.

The tetravalent polylysine-based glycocluster **4.57** and the hexadecavalent polylysine-based glycodendrimer **4.59** will be tested in the adherence assays to determine their anti-adhesive properties against *C. albicans*.

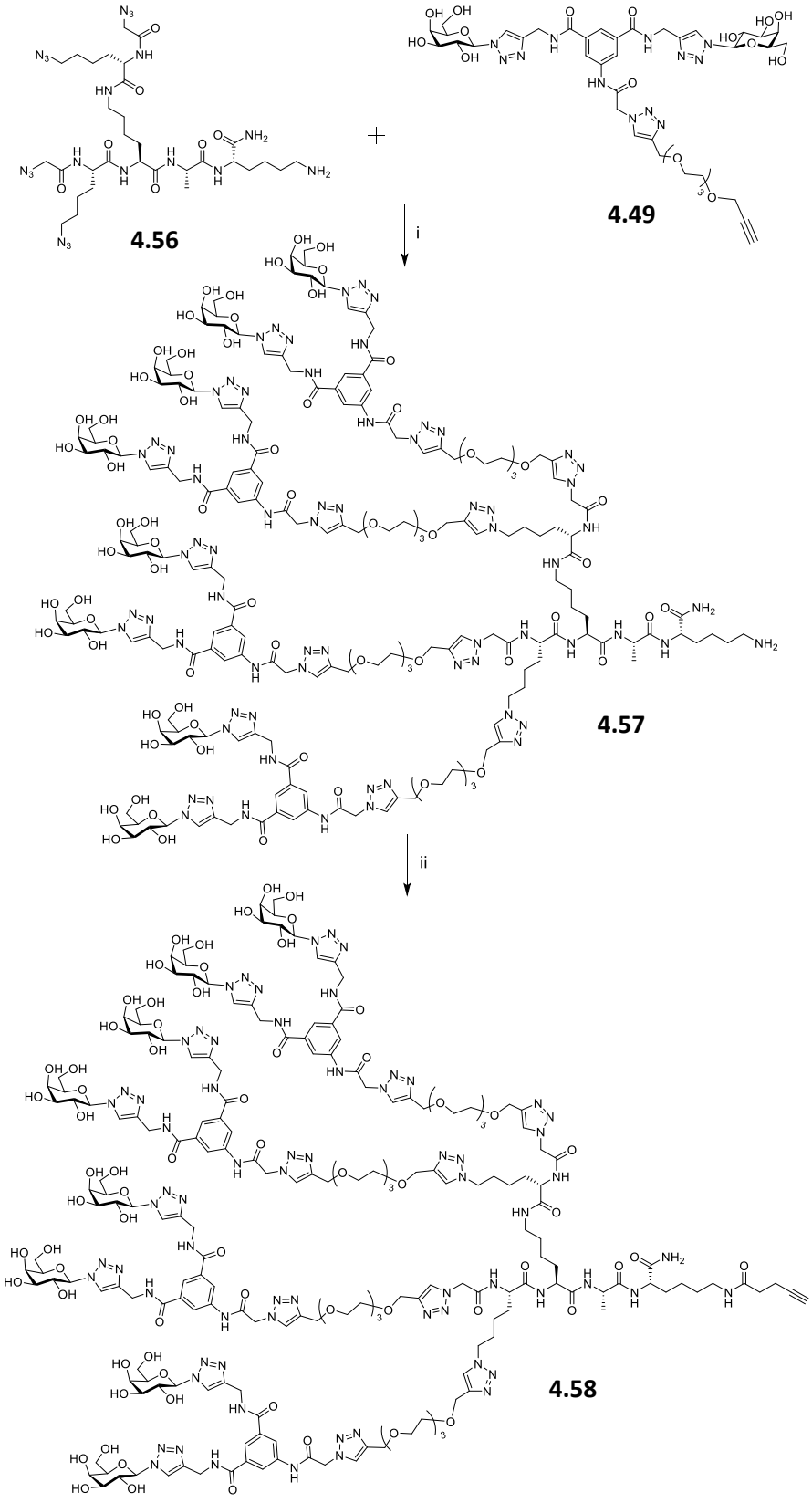

Scheme 4.15: Synthesis of tetravalent glycocluster **4.57** and the alkynated derivative **4.58**. *Reagents and conditions:* i) $CuSO_4$.5 H_2O/Na Asc, THPTA, DMF/PBS buffer (pH 7.5), rt, 1 h, 78 %; ii) *N*-succinimidyl pentynoate, DIPEA, DMF (pH 9), rt, 1 h, 82 %.

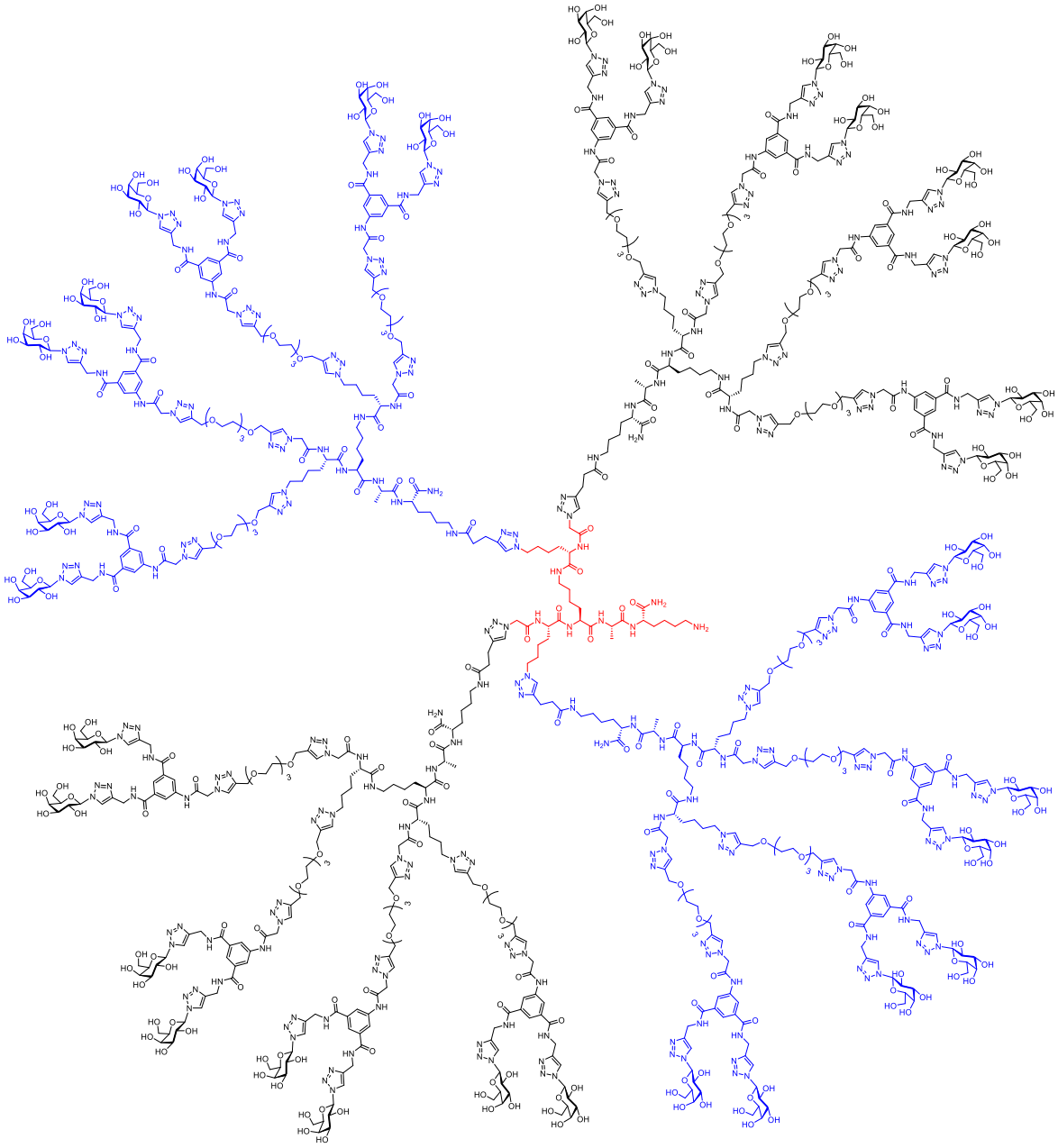

Figure 4.10: Structure of the hexadecavalent glycodendrimer **4.59** (Yield: 87 %).

4.4 Conclusion

The objective of this chapter was to design and synthesise multivalent displays of the initial lead compound **2.78**. Different scaffolds were utilized since ligand optimization requires the screening of compounds with different valencies, flexibilities and carbohydrate presentation, to find the optimum structure required to inhibit the adhesion of *C. albicans* to BEC. Since the adhesin present in the *Candida* with which

compound **2.78** is interacting is unknown, several scaffolds with different valencies and geometrical presentation of lead compound **2.78** were explored to find the optimum structure. Hence, multivalent displays of compound **2.78** built around an aromatic-core, a linear peptoid scaffold, cyclopeptide scaffold and a polylysine-based scaffold were synthesised.

Initial experiments to attach the lead compound directly to aromatic-scaffolds were unsuccessful, possibly due to steric bulk and the weak nucleophilicity of the aniline involved. The azide derivative of the lead compound **4.21** was successfully conjugated to the divalent 1,4-alkynated scaffold **3.13**, however due to the insolubilty of the acetylated product, deprotection and biological evaluation was not possible. Therefore, a linker, derived from triethylene glycol **4.24**, was developed to connect the lead compound to the aromatic scaffold. Hence compound **4.28** was synthesised, which consisted of the acetylated divalent galactoside with a linker functionalized with an azide. This was then conjugated to the aromatic scaffold, resulting in the successful synthesis of the trivalent display of the lead compound **4.30** built around an aromatic core. This also allowed the effective grafting of the lead compound onto the linear scaffold, resulting in a tetravalent display of the initial lead compound **4.43**.

On a research visit to Université Grenoble Alpes, the lead compound functionalized with an alkyne triethylene glycol linker **4.49** was successfully grafted onto cyclopeptide and polylysine-based scaffolds, resulting in the formation of tetravalent cyclopeptide **4.51**, hexadecavalent cyclopeptide **4.53**, hexavalent cyclopeptide **4.56**, tetravalent polylysine-based dendron **4.57** and hexadecavalent polylysine-based dendron **4.59**. All the compounds synthesised here utilized a highly efficient CuAAC methodology, connecting the alkynated derivative **4.49** to the different scaffolds functionalized with azides.

All the multivalent compounds synthesised and shown in this chapter will be tested for their anti-adhesive properties, with the hope that they will inhibit the adhesion of *C. albicans* to BEC more effectively than the initial lead compound **2.78**. Depending on the results from the adherence assay more multivalent displays may be synthesised to optimize the interaction between the ligands and the yeast.

Chapter 5

Photoaffinity Labelling to Identify the Target Protein in *C. albicans*

5.1 Introduction

5.1.1 Bioconjugation

Bioconjugation involves the formation of a stable covalent bond between two molecules, where at least one of them is a biomolecule. The process of creating bioconjugates is usually carried out using chemically reactive agents that can be used to couple to specific functional groups on one or more of the molecules being conjugated. Bioconjugation forms the basis for affinity cross-linking. In this application, the conjugate may contain one or more affinity molecules, which can be used to target, capture, or detect another biomolecule. The applications of affinity cross-linking can include: 1) assay and quantification of target analytes; 2) detection, tracking and imaging of biomolecules; 3) affinity-mediated purification, capture and scavenging of biomolecules; 4) catalysis and chemical modification using immobilized ligands; 5) therapeutics and *in vivo* diagnostics using targeted bioconjugates.[253]

Most bioconjugation methods utilize common organic chemical principals to form stable covalent bonds to link the bioconjugate reagents to the biomolecule of interest. For example, reactive groups able to couple with amine-containing molecules are the most common functional groups present on crosslinking or modification reagents. The primary coupling reactions for modification of amines proceed by two main routes; acylation forming stable amides or alkylation forming secondary amine bonds. Thiol, carboxylate, hydroxyl, aldehyde and ketone reactions are also used to form bioconjugates. Cycloaddition reactions, including Diels-Alder reactions and CuAAC reactions, can also be used. Photoreactive groups, induced to couple with target molecules by exposure to UV light, are becoming increasingly popular in this field. These groups are relatively non-reactive in typical thermochemical processes, until they are photolyzed. Due to these properties, molecules containing a photoreactive group can be used in highly controlled reactions, where labelling reactions can be induced by UV light at predetermined points in the experimental protocol. Covalent bonds can therefore be formed after binding of photo-labelled ligands to receptors or after some other biochemical process takes place.

5.1.2 Photoaffinity Labelling (PAL)

Photoaffinity labelling (PAL) is a method of bioconjugation that has become a commonly used technique in medicinal chemistry[254] and drug discovery for the identification of new drug targets and molecular interactions.[255] In PAL, a chemical probe is used to covalently bind to its target after being activated by light. Protein-ligand interactions may be studied using this technique, such as identifying unknown targets of ligands, assisting in the elucidation of protein structure, functions and conformational changes, in addition to identifying novel or alternative binding sites in proteins.

The technique involves incorporating a photoreactive group within an otherwise reversibly binding ligand. This photoreactive group forms an extremely reactive intermediate when exposed to a specific wavelength of light. The reactive intermediate quickly reacts with and binds to the closest molecule, which preferably will be the target protein. This method was first reported by Westheimer *et al.*[256] in 1962, where aliphatic diazo groups were incorporated into the enzyme chymotrypsin by acylation. Intramolecular crosslinks were formed by photolysis.

5.1.2.1 Photoaffinity Probes

A photoaffinity probe must include particular criteria. The probe must be stable in the dark at a range of pHs, be structurally similar to the ligand molecule with comparable affinity for the target protein and have minimum steric interference when binding. The photoaffinity probe must contain a photoreactive group that undergoes activation at wavelengths of light that do not damage biological molecules, but still form highly reactive intermediates, with the ability of cross-linking many functional groups to form stable bonds.

In general, photoaffinity probes contain three vital components:

1. The pharmacophoric or affinity group – responsible for reversible binding to the target proteins.
2. A photoreactive group – required for permanent attachment to the target after photoactivation.

3. An identification or reporter tag – involved in the detection and isolation of the target protein.

The photoaffinity probes can be designed in three distinct ways and are shown in Figure 5.1. First, the pharmacorphore, photogroup and reporter tags may all be incorporated in one molecule, isolated from each other and connected by linkers (Figure 5.1 a). Secondly, the photogroup may be directly connected within the pharmacophore, with both being isolated from the reporter tag (Figure 5.1 b). Finally, the photoaffinity probe may consist of two distinct moieties, where the pharmacophore and photogroup are in one molecule and the reporter tag is part of another molecule, which are subsequently conjugated. CuAAC methodology has been used very often for this purpose, with one molecule being designed to have an alkyne handle and the other possessing a terminal azide (Figure 5.1 c).

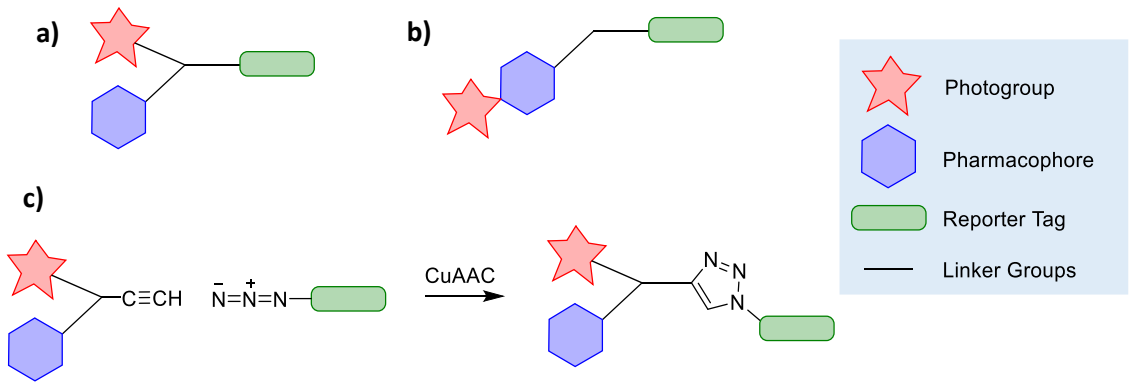

Figure 5.1: General design for photoaffinity probes. Adapted from a review by Smith and Collins.[255]

The most common photoreactive groups used in the PAL technique include phenylazides, phenyldiazirines and benzophenones, and their structures are shown in Figure 5.2. Other groups have also been used, such as enones, diazo groups, sulphur radicals, diazocarbonyls, nitrobenzenes, diazonium salts as well as alkyl derivatives of azides and diazirines. Phenylazides are frequently used in PAL since they are easily synthesised and are commercially available. However, the short wavelengths (250-350 nm) required to form the reactive nitrene intermediate can damage biological molecules such as proteins. Also, the nitrene intermediate is less reactive than other intermediates such as carbenes, may rearrange to form

undesired side products, and azides may be reduced to amines by thiols. Substituted arylazides (e.g. tetrafluorophenyazide) have been developed to improve their photoaffinity suitability.

Benzophenone derivatives are also commercially available and can be easily prepared. They form a reactive triplet diradical when irradiated with light at longer wavelengths (350-360 nm) reducing the risk of damage of biomolecules. However, they often require a longer irradiation period, which may increase nonspecific labelling. Also, since they are rather bulky, they may interfere with the interaction between the pharmacophore and the target protein. Arlydiazirines are the most common photoreactive group, in particular, the trifluoromethyl derivative. They also require a higher wavelength (350-355 nm) to form carbene species, which are extremely reactive and have a short half-life, allowing it to rapidly form covalent cross-links to biomolecules. However, due to this high reactivity, carbenes are often quenched by water, which can decrease the photoaffinity yields but can be an advantage as it may minimize nonspecific binding. Aliphatic diazirines are also used in PAL when there are spatial limitations due to their smaller size.[257]

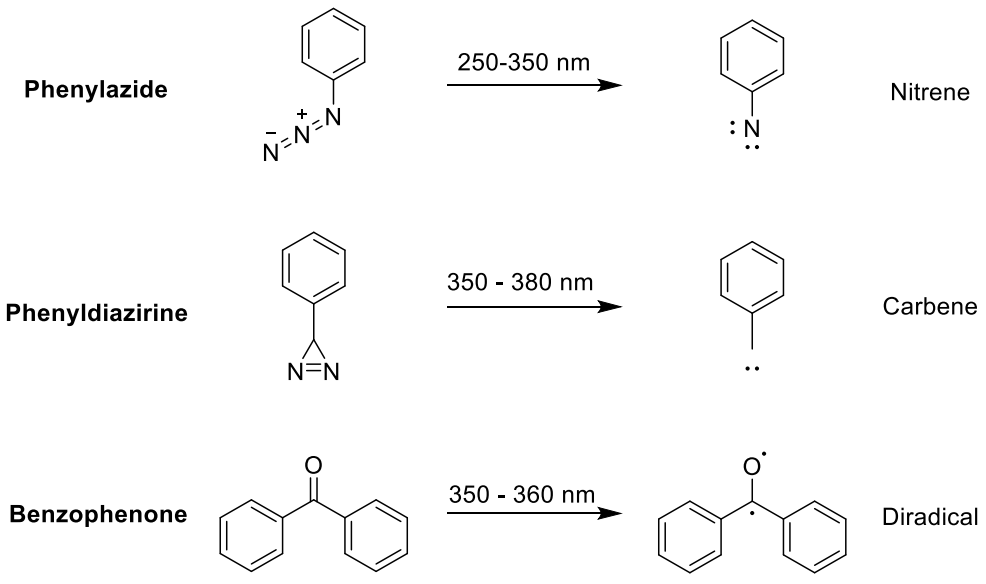

Figure 5.2: Structure of photoreactive groups commonly used in PAL and their reactive intermediate formed after exposed to the light at the wavelengths indicated.[255]

An identification or reporter tag is involved in the detection and isolation of the target protein, which can be directly or indirectly incorporated to the photoprobe. Radioactive reporter tags have been used in PAL, for example ^{125}I and ^{3}H, since they are small and cause minimal structural change to the photoprobe. However, due to short half-lives they can degrade quickly, but most importantly they do not offer a direct method to isolate the labelled proteins. Fluorescent reporter tags have also been utilised in PAL. Fluorophores, such as fluorescein, rhodamine and BODIPY (boron dipyrromethane), have been used. However, they can be easily photobleached.[255, 258]

Affinity tags are most commonly used in PAL, where biotin is most frequently employed due to its high affinity for avidin ($K_d = 10^{-15}$ mol/L). Avidin is a tetrameric biotin binding protein produced by birds, reptiles and amphibians. Streptavidin, a protein purified from *Streptomyces avidinii*, also has a very high affinity for biotin, with $K_d = 10^{-14}$ mol/L, which is one of the strongest non-covalent interactions known in nature. Avidin has only a 30 % sequence identity to streptavidin, however it has an almost identical secondary, tertiary and quaternary structure. Avidin, unlike streptavidin, is glycosylated, positively charged, has pseudo-catalytic activity and has a higher tendency to aggregate. Also, streptavidin is a better biotin-conjugate binder, avidin has a lower binding affinity than streptavidin when biotin is conjugated to another molecule. Since streptavidin is unglycosylated and has a neutral pI, it results in a lower amount of nonspecific binding.[259] Hence, streptavidin is used more frequently in PAL than avidin. Streptavidin magnetic beads are superparamagnetic particles covalently coupled to highly pure form of streptavidin. These beads can be used to capture biotin labelled substrates including antigens, antibodies and nucleic acids, and in PAL they can be used to capture the target protein.

The general protocol for PAL experiments is as follows:

1. Cells or cell lysates are treated with the photoaffinity probes.
2. An incubation period allows time for the probes to interact to their target proteins.

3. The samples are irradiated with light at a specific wavelength to active the photogroup, which forms the reactive intermediate that forms covalent bonds with the closest molecule to it (target protein ideally).
4. If the experiment is carried out using cells, they are lysed.
5. CuAAC methodology is used to conjugate the probe to the reporter tag.
6. Labelled proteins are separated from the rest of the proteome by affinity purification using the reporter tag. If biotin is used as the reporter tag, streptavidin beads are used to extract labelled proteins.
7. Analysis using SDS-PAGE and MS, allows the identification of the labelled proteins.[255]

5.1.2.2 Carbene-mediated PAL involving Carbohydrates

Carbene-mediated PAL has been used to study small molecule-protein and macromolecule-protein interactions, such as protein-protein, nucleic acid-protein, lipid-protein, steroid-protein and carbohydrate-protein interactions. It is known that carbohydrates play a crucial role in a wide range of biological processes; however, there are many carbohydrate-protein interactions that remain unknown, mostly due to the low-affinity interactions. Carbene-mediated PAL has been used to investigate the biological role of carbohydrates using diazirine-based photoactive tags.

Kohler *et al*.[260] has carried out extensive research in this area, where a series of photosugars containing diazirines have been synthesized including a sialic acid analogue **5.1** and an *N*-acetylmannosamine analogue **5.2**. These photosugars have been successfully incorporated into the cell surface. Carbene mediated PAL has been used to study the interactions between sialic acids and sialic acid recognising proteins.[260]

Sakurai, Minuzo and co-workers[261, 262] have developed a series of photoaffinity probes containing lactose moieties and different photoreactive groups, such as aryl azide, benzophenone, alkyldiazirine and trifluoromethylphenyldiazirine (TPD), which have been synthesised to determine the efficiency and selectivity of using PAL techniques to study carbohydrate binding interactions with lectins. Lactose is known to bind to the lectin peanut agglutinin (K_d = 770 μM). The diazirinyl lactose analogue **5.3** showed

low yield of cross-linking but showed high ligand-dependent reactivity. The TPD analogue **5.4** showed higher crosslinking efficiency than the alkyldiazirinyl derivative **5.5** when tested using a single binding protein. However, when tested in a cell lysate sample the alkyldiazirinyl derivative **5.5** showed significantly more selectivity than the TPD analogue **5.4.**

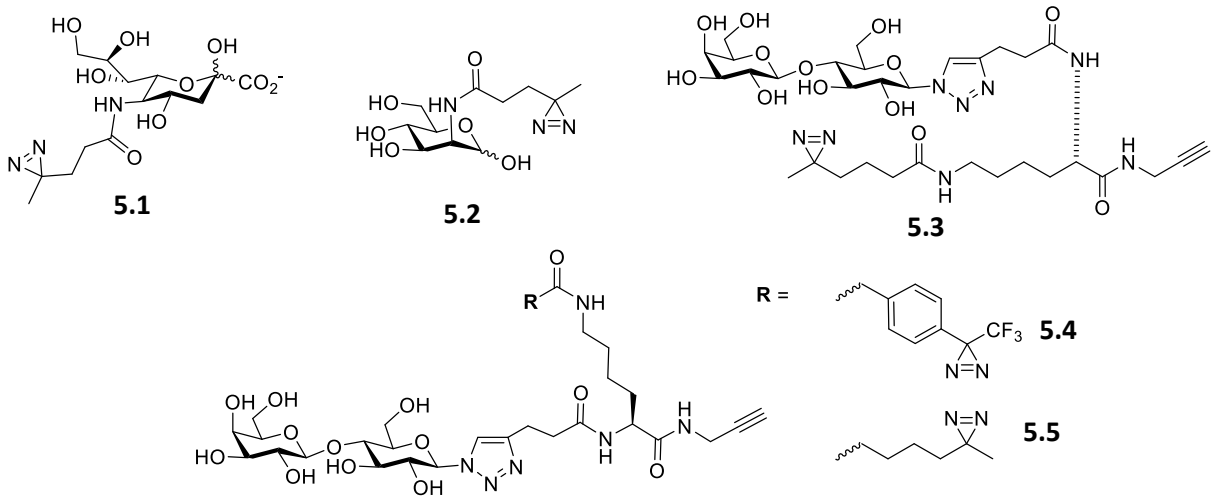

Figure 5.3: Structure of diazirine analogues of carbohydrates.

5.1.2.3 Photoaffinity Probes for the lectin FimH

For photolabelling of FimH, three mannosides **5.6**-**5.8** were designed which contain different photoactive functional groups. From crystallographic data it was found that for a mannoside to bind to the carbohydrate binding domain in FimH, the photolabels must be included into the aglycon part of the molecules. In addition, orthogonally protected mannosyl peptides were introduced as bifunctional scaffolds to combine a photoreactive functional group with an affinity label within the same mannoside **5.9** and **5.10** (similar to the design of the photoprobe in Figure 5.1 a). All of these compounds were tested as inhibitors of FimH-mediated adhesion of *E. coli* to a mannan-coated surface by ELISA. This assay found that all photoactive mannosides tested had inhibition equal to or better to that of α-D-mannoside.[263, 264]

To test the capability of the photoactive mannosides in crosslinking reactions, a model peptide angiotensin II (DRVYIHPF) was used. MS-MS experiments revealed that the two diazirines **5.7** and **5.10** gave a 1:1 photoaddition product of peptide and photolabel, resulting from the insertion of the carbene into the hydroxyl group in the

side chain of the angiotensin tyrosine (Y). These two mannosides were then tested using FimH, which resulted in the 1:1 photo-crosslinked products with the expected mass. When the biotinylated mannoside **5.10** was used for photolabelling of FimH, the photo-crosslinked product could be detected by affinity staining using a streptavidine-HRP (horseradish peroxidase) conjugate. Hence, biotin-labelled photoactive mannosides provides a feasible method for identification of carbohydrate binding sites on mannose specific lectins such as FimH using the PAL methodology.

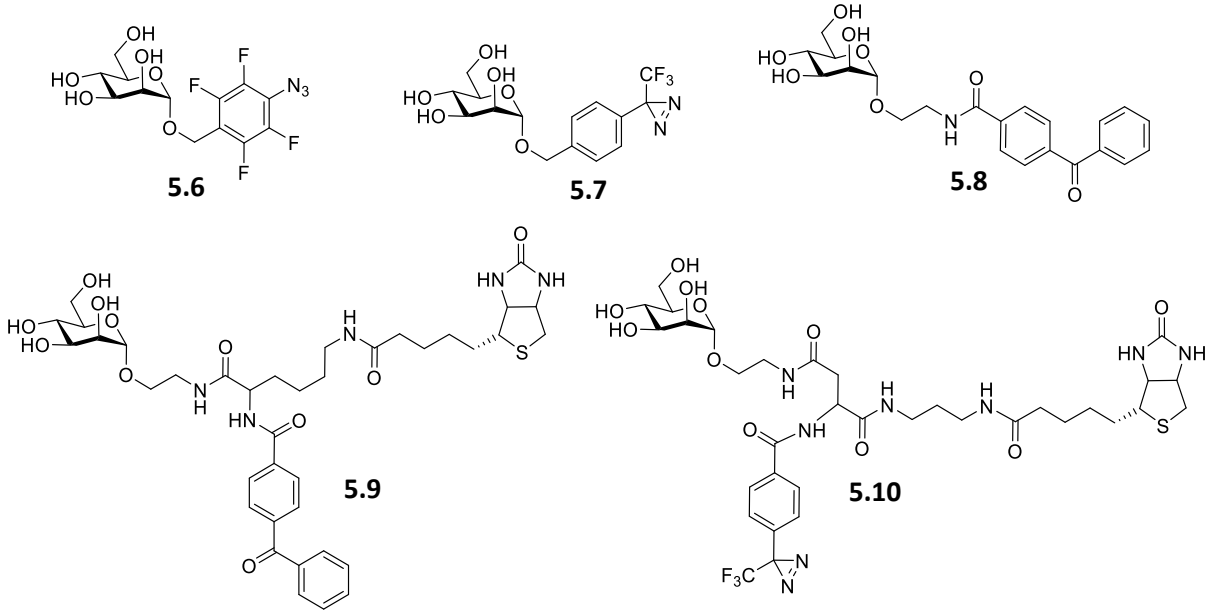

Figure 5.4: Three α-mannoside analogues with different photoactive groups **5.6**, **5.7** and **5.8**, and biotinylated mannosides **5.9** and **5.10** suitable for PAL.[265]

5.1.2.4 Photoaffinity Probes for the lectin RCA_{120}

Chang *et al*.[266] designed photoaffinity probes to study the interaction and selectivity for the probe to the castor bean lectin RCA_{120} (*Ricinus communis* Agglutinin). A monovalent and a trivalent analogue of the probe were designed to demonstrate the importance of multivalent ligand binding in lectin labelling (Figure 5.5). The monovalent photoaffinity probe **5.11** displayed a significant decrease in the band intensity in the Western blot assay compared to the trivalent photoaffinity probe **5.12**, suggesting the superior photolabelling efficiency of **5.12**. In this study it was found that the compound **5.12** selectively labelled RCA_{120} in a protein mixture and

also in *E. coli* lysates. This compound was also able to label ASGP-R (asialoglycoprotein receptor) on the surface of HepG2 cells. ASGP-R is a carbohydrate-binding protein located on hepatocytes which mediates the endocytosis of plasma glycoproteins where the terminal sialic acid residues are removed revealing terminal galactose or GalNAc. Furthermore, transient and weak protein-protein interactions between the LacNAc moiety of ovalbumin (OVA) and the carbohydrate binding chain of RCA_{120} were detected using compound **5.12**.

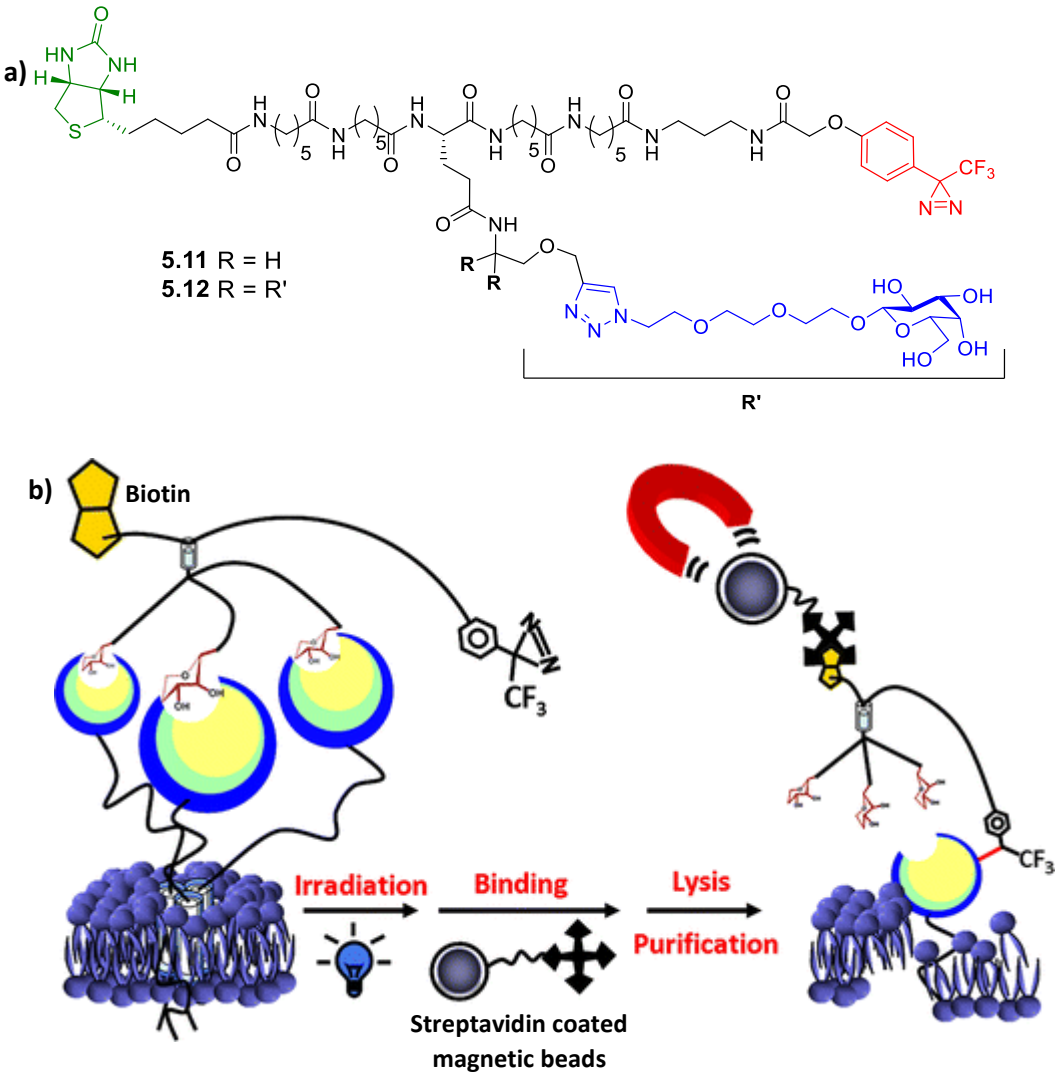

Figure 5.5: a) Structure of the monovalent **5.11** and trivalent **5.12** photoaffinity probes designed by Chang *et al.*[266]; **b)** a diagram depicting the PAL technique using the trivalent photoaffinity probe **5.12** adapted from Chang *et al*. [266] Adapted with permission from the American Chemical Society.

5.2 Chapter Objective

The objective of this chapter is to develop two photoaffinity probes based on lead compound **2.78** identified in Chapter 2. These will be used in an attempt to identify the target on the cell surface of *C. albicans* with which the glycoconjugates in previous chapters are interacting. Since the biological tests will be carried out on live cells, we chose to design the photoaffinity probe with an approach similar to that in Figure 5.1 (c), where the probe consists of two distinct units. In this model, one unit contains the photogroup connected to the pharmacophoric group with an additional alkyne handle, and the other contains the reporter tag possessing a terminal azide.

The pharmacophoric group is the divalent galactoside **2.78** identified in Chapter 2. Locating a site on the lead compound from which to build the rest of the probe and optimizing the photoreactivity of the molecule can be difficult tasks. However, from the work described in Chapter 2 and Chapter 4, we have developed synthetic routes to functionalize compound **2.78** in the 5-position of the aromatic scaffold. Hence, this is the position we chose to link the photogroup and the alkyne handle. This is also a favourable position since we know from preliminary adherence assays that having additional groups in this position does not significantly affect the anti-adherence properties of the glycoconjugates.

Since it is difficult to predict which phototag would have the best activity, two PAL probes (structure shown in Figure 5.6) were designed in an effort to optimize the photoreactivity of the photoaffinity probes. Both probes contain the divalent galactoside **2.78** and the alkyne handle but have different photogroups, one with a benzophenone and one with a diazirine moiety. The benzophenone derivatives are relatively easy to prepare and handle but can be too bulky, while the diazirine derivatives may be more difficult to prepare but are sterically smaller, which may be beneficial in the PAL technique.

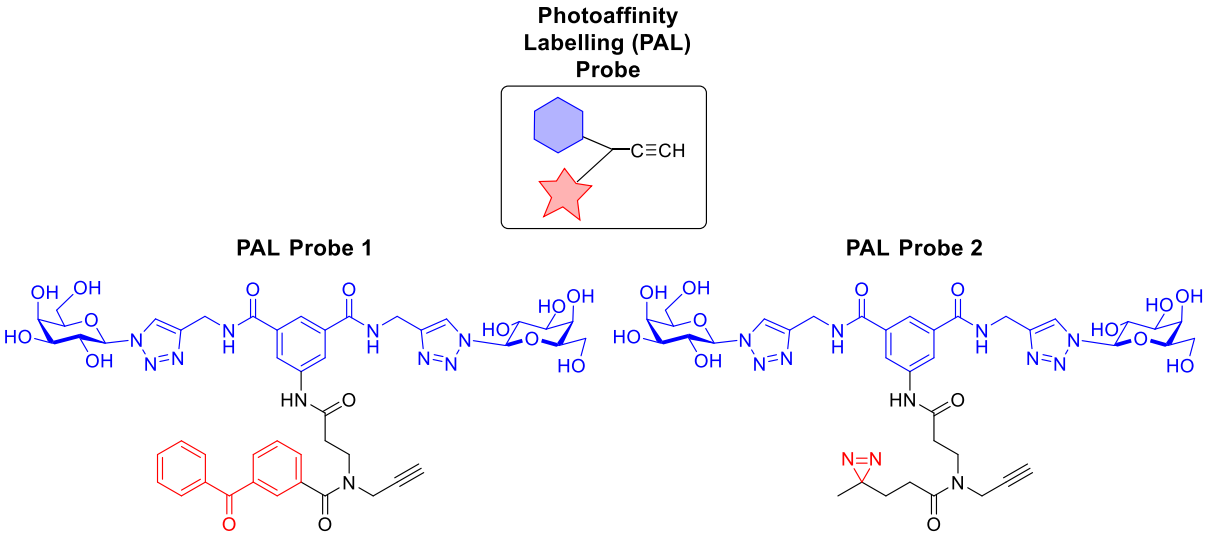

Figure 5.6: General structure of the PAL probes, where the blue hexagon represents the pharmacophoric group and the red star represents the photoactive group. Structures of PAL Probe 1 and PAL Probe 2 as also shown.

5.3 Synthesis of Photoaffinity Probes to Target *C. albicans*

5.3.1 Strategy 1

The design of the photoaffinity probes contains the divalent galactosyl anti-adherence ligand **2.78** as the pharmacophoric group that will elicit specific binding with the *C. albicans* adhesin. As discussed in previous chapters, the primary amine derivative of the acetylated divalent galactoside **2.113** was available. It was decided to utilise the chemistry involved in the synthesis of the linear peptoid scaffold **4.39** in Chapter 4, where aza-Michael conjugate addition was used to react primary amine groups with α,β-unsaturated compounds. Hence, acroylyl chloride was reacted with compound **2.113** in basic conditions to give the α,β-unsaturated derivative **5.13** with a moderate yield (Scheme 5.1). The reaction of compound **5.13** with propargylamine, using anhydrous methanol as the solvent, resulted in deacetylation and the formation of compound **5.14**. This is unfavourable, since the protected hydroxyl groups are required for following reactions. Numerous articles report the need of a protic polar solvent for aza-Michael addition reactions to occur, stating that the hydrogen-bond donor ability of the solvent significantly effects the reaction.[267, 268] However, polar aprotic solvents, such as THF and DCM, have also been used to carry out aza-Michael addition reactions, although the rate at which they occur is much

lower.[269] The reaction was attempted using anhydrous THF as the solvent, however no product was formed. Anhydrous solvent was used to minimize the deactylation of the galactose moieties. Adding equivalents of water, a polar protic solvent, also did not cause the reaction to proceed. DCM was also tested as the solvent, similarly no product was formed.

N,N'-bis[3,5-bis(trifluoromethyl)phenyl]thiourea (or Schreiner's thiourea) has been utilized as an organocatalyst in many reactions, due to its ability to activate substrates and stabilize partially developing negative charges since it possesses two hydrogen bond donors.[270] Hence, this organocatalyst was added to the reaction mixture of the aza-Michael addition reaction. Using the catalyst in DCM formed no product, even after it was heated to 50 °C. Toluene was added to allow the mixture to be heated further. The reaction mixture was heated to 90 °C for 16 h, however again no product was formed. Acetic acid has also been utilized as a co-catalyst in aza-Micheal addition reactions[271] and can also be used as a polar protic solvent. Hence the reaction of compound **5.13** with propargylamine was tried using a 1:1 DCM:acetic acid solvent system. After heating the reaction mixture to 50 °C overnight, no product was formed.

Finally, the reaction was attempted using *tert*-butanol as the solvent. This is a polar protic solvent, but due to steric bulk is not a good nucleophile to partake in deacetylating the galactose moieties. The reaction mixture was first heated to 50 °C for 16 hours, which formed no product. More equivalents of propargylamine (5 equiv) were added, however still no product formed. Phenol has been used as an additive in aza-Micheal addition reactions. The phenol acts as a proton donor and activates the Micheal acceptor by H-bonding.[267] Hence, three equivalents of phenol were added to the reaction mixture, and finally traces of the product were formed. The use of the MW further increased the yield of the reaction. After trying many conditions, the optimum conditions for the reaction to form compound **5.15** were found to involve the use of a mixture of *tert*-butanol and DCM as the solvent, 4 equivalents of propargylamine, 3 equivalents of the additive phenol and using MW irradiation at 100 °C for 1 hour. The sequential addition of propargylamine was also

found to be important. Four additions of propargylamine each followed by MW irradiation at 100 °C for 1 hour resulted in the largest yield of the product at ~70 %.

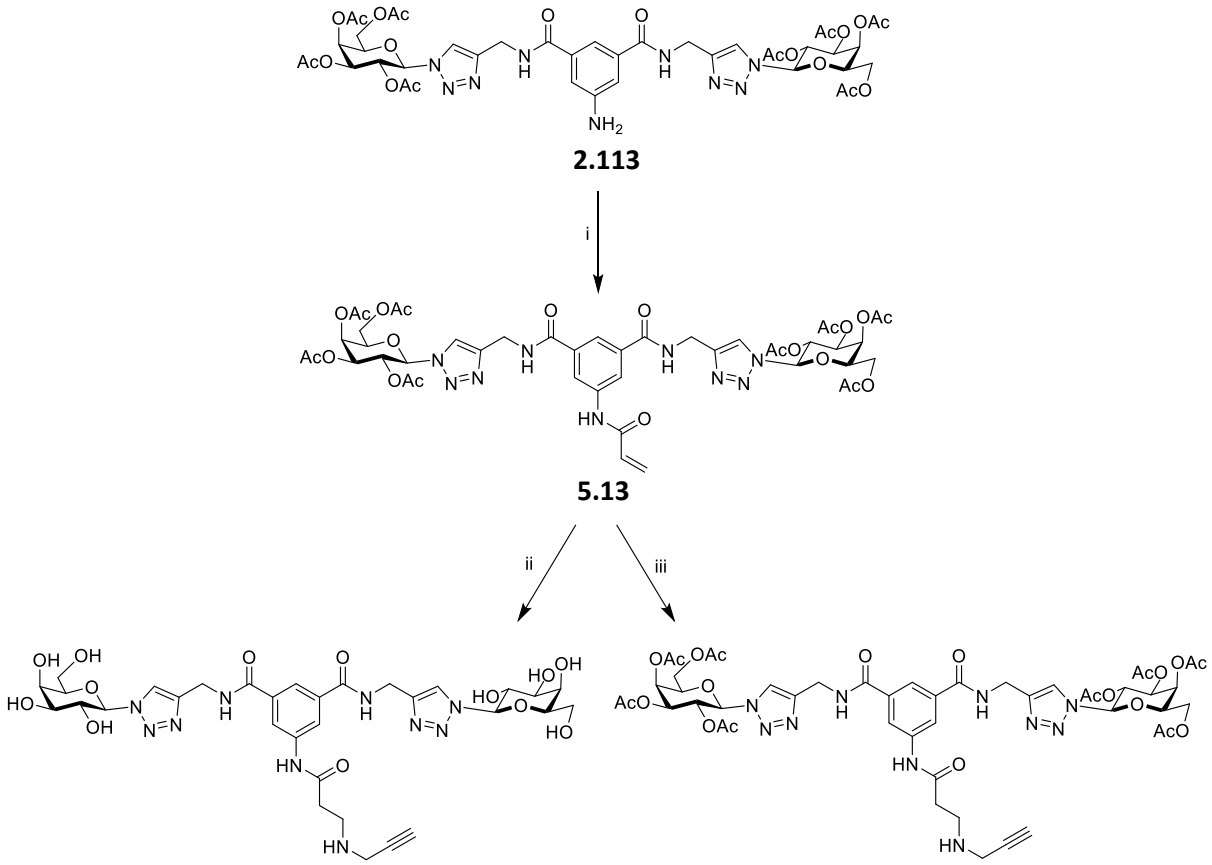

Scheme 5.1: Synthesis of compound **5.15**. *Reagents and conditions:* i) acroylyl chloride, DIPEA, N_2, DCM, 0 °C, 3 h, 57 %; ii) propargylamine, dry MeOH, 50 °C iii) propargylamine, *tert*-butanol, DCM, phenol, MW @ 100 °C, 1 h x 4, 69 %.

5.3.2 Strategy 2

Due to the difficulties of optimizing the aza-Michael reaction shown in Scheme 5.1, an alternative approach was also employed. In this approach the phototag with the alkyne handle is synthesised first (Scheme 5.2) and then coupled to the divalent galactoside compound **2.113** (Scheme 5.4). In this approach *N*-propargyl-functionalized β-alanine **4.32**[246], the key building block for the synthesis of the linear peptoid scaffold in Chapter 4, is utilized. Compound **4.32** is coupled to the benzophenone derivative, 3-benzoylbenzoic acid **5.16**, using TBTU as the coupling reagent (Scheme 5.2).

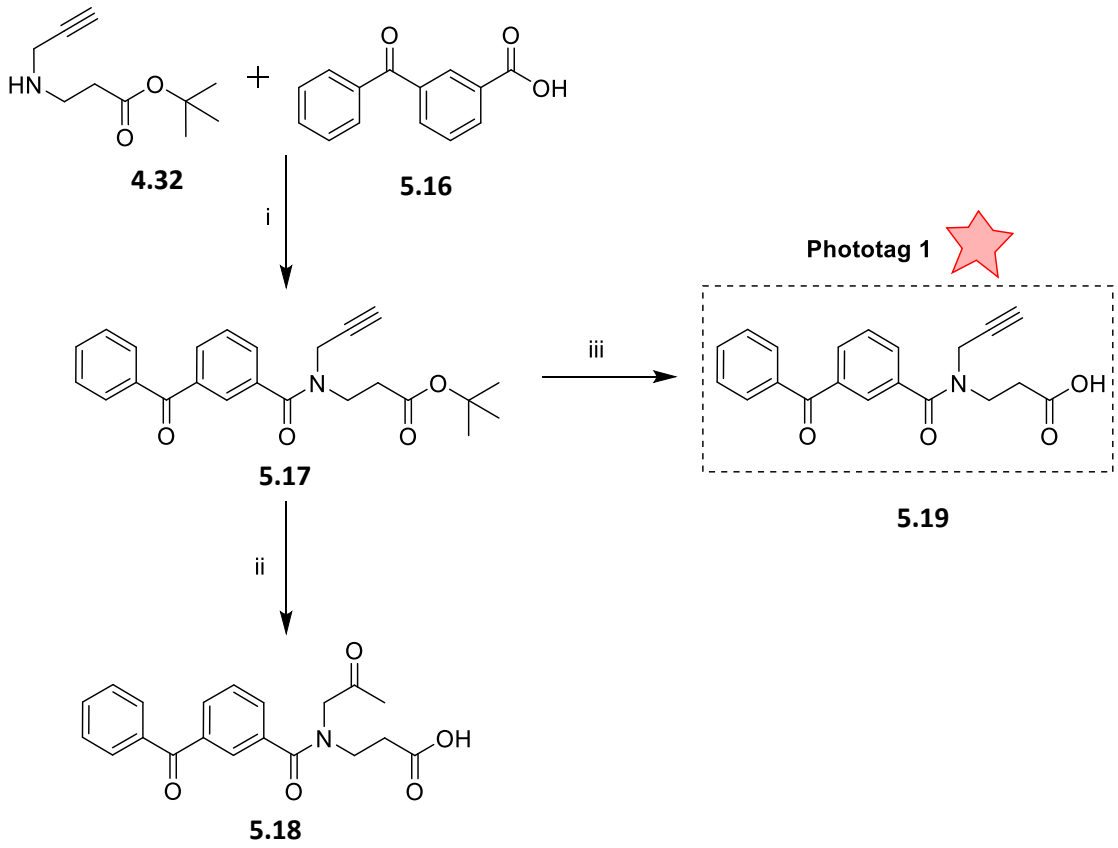

Scheme 5.2: Synthesis of the phototag **5.19**. *Reagents and conditions*: i) TBTU, NEt_3, DMF, N_2, 16 h, rt, 48 %; ii) TFA:DCM 1:2, 3 h, quant %; iii) anhydrous TFA:DCM 1:2, N_2, 3 h, quant %.

The *tert*-butyl group in compound **5.17** must then be removed to allow the coupling to compound **2.113**. The general procedure to remove a *tert*-butyl group involves the use of trifluoroacetic acid (TFA). When compound **5.17** was treated with TFA (1:2 TFA:DCM), the *tert*-butyl group was removed to reveal the carboxylic acid, however under these conditions, we found that the terminal alkyne group was also converted to a methyl ketone forming compound **5.18**. After a literature search, it was found that Chen *et al*.[272] have used TFA in the hydration of alkynes to form methyl ketones. This reaction requires the presence of H_2O (1 equivalent) and the proposed mechanism involves the formation of an alkenyl cation intermediate, which undergoes nucleophilic addition by CF_3COO^- to produce the enol trifluoroacetate, which subsequently undergoes successive hydrolysis and keto-enol tautomerism to form the methyl ketone (Scheme 5.3).

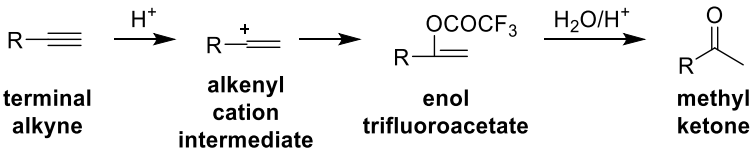

Scheme 5.3: Proposed mechanism of TFA-mediated alkyne hydration reaction.[272]

Hence, an alternative method to remove the *tert*-butyl ester group was required. The use of bases, such as NaOH and NEt_3, and acids, such as HCl, required heating, which led to the formation of side products. Therefore, the reaction using TFA was re-attempted using anhydrous conditions, since the absence of water would prevent the formation of the methyl ketone product. The TFA was subsequently pre-dried over anhydrous $NaSO_4$, anhydrous DCM was used as the solvent and the reaction was carried out under N_2. This resulted in the removal of the *tert*-butyl group to expose the carboxylic acid and did not form the methyl ketone product like observed in non-anhydrous conditions. Hence, the phototag compound **5.19** was formed, which contains the benzophenone photogroup, an alkyne handle, along with the carboxylic acid functional group to allow coupling to the aniline compound **2.113**. The coupling of compound **2.113** with the phototag **5.19** was carried out using TBTU as the coupling reagent which gave the acetylated compound **5.20** (Scheme 5.4). This was then deprotected using mild basic conditions to give the PAL probe **5.21**. This probe consists of the pharmacophoric divalent galactoside, a benzophenone photoactive group and an alkyne handle.

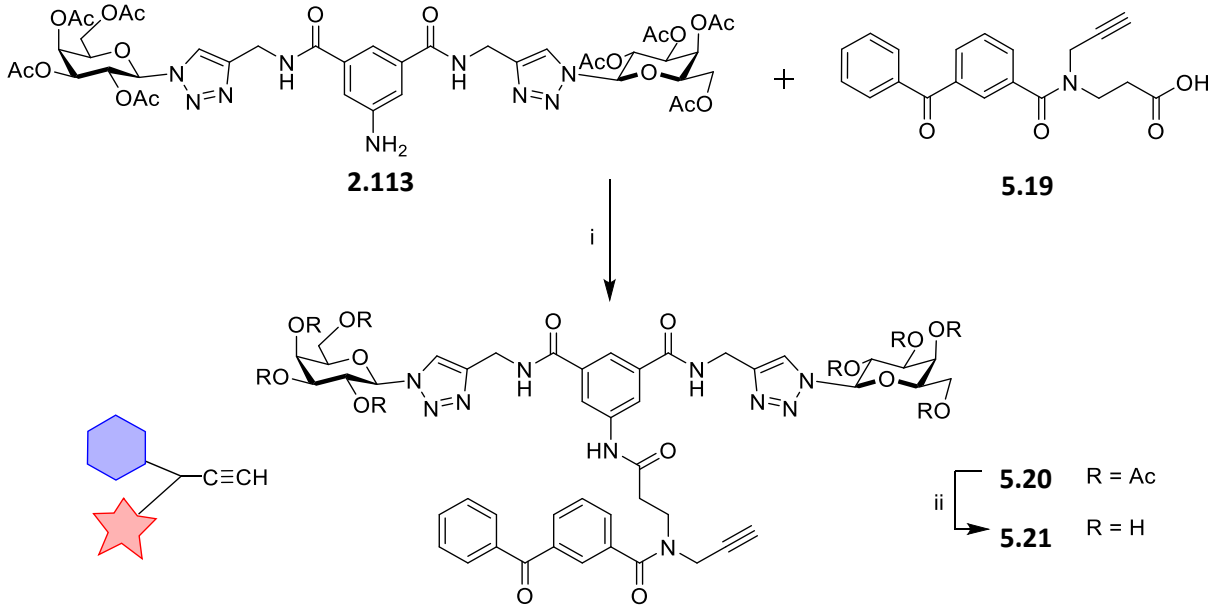

Scheme 5.4: Synthesis of photactive probe **5.21**. *Reagents and conditions*: i) TBTU, NEt_3, DMF, N_2, 16 h, rt, 49 %; ii) NEt_3, MeOH/H_2O, 45 °C, 92 %.

A photoactive probe **5.28** with a diazirine photogroup was then developed. To obtain the diazirine with a carboxylic acid functional group to allow coupling, a literature procedure was followed.[273] Levulinic acid **5.22** was reacted with ammonia in methanol to give the diaziridine acid **5.23**, which was oxidised to form the diazirine **5.24** (Scheme 5.5). The *N*-propargyl-functionalized β-alanine **4.32**[246] was utilized again, and was coupled to the diazirine **5.24** using TBTU as the coupling reagent. To remove the *tert*-butyl group, the anhydrous conditions outlined previously were employed to give the second phototag **5.26**. This phototag **5.26** was then coupled to the aniline compound **2.113** using TBTU as the coupling reagent which gave the acetylated compound **5.27**, which was deprotected using mild basic conditions to give the PAL probe **5.28** (Scheme 5.6). This probe consists of the pharmacophoric divalent galactoside, a diazirine photoactive group and an alkyne handle.

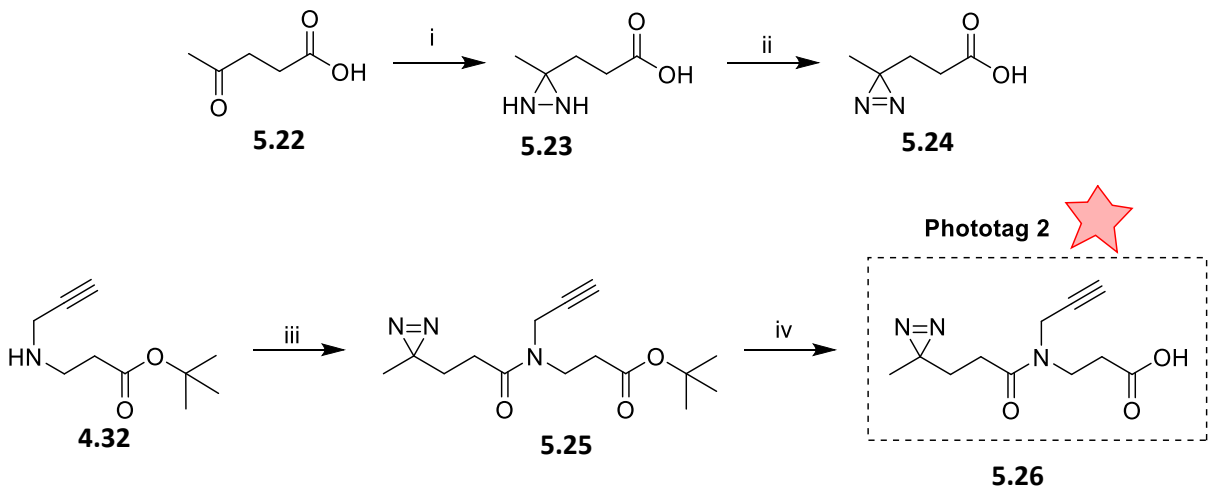

Scheme 5.5: Synthesis of Phototag **5.26**. *Reagents and conditions*: i) 7 N ammonia in MeOH, 3 h on ice, hydroxylamine-*O*-sulfonic acid, 16 h, rt; ii) MeOH, NEt_3, I_2 beads, 5 mins x 2, 0 °C, 42 %; iii) TBTU, NEt_3, DMF, N_2, 16 h, rt, 46 %; iv) anhydrous TFA:DCM 1:2, N_2, 3 h, quant %.

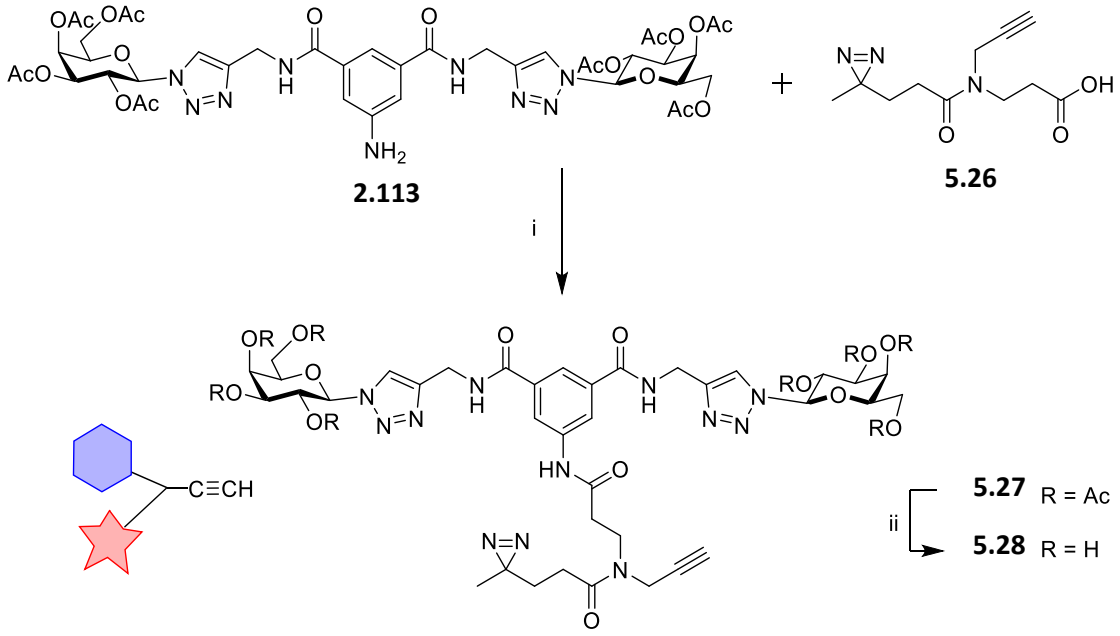

Scheme 5.6: Synthesis of photactive probe **5.28**. *Reagents and conditions*: i) TBTU, NEt_3, DMF, N_2, 16 h, rt, 47 %; ii) NEt_3, MeOH/H_2O, 45 °C, 93 %.

5.4 Conclusion

Two photoaffinity labelling (PAL) probes were successfully synthesised. These two probes were structurally similar, consisiting of the pharmacophoric group (the divalent galactoside **2.78** identified as the lead compound in Chapter 2), an alkyne handle and a photogroup. The two analogues synthesised differed only in the identity of the photogroup, where PAL probe 1 contains a benzophenone photoactive tag, and PAL probe 2 contains a diazirine photoactive tag.

Problems were encountered when using the first strategy to develop the PAL probes. During the aza-Michael reaction, which was used to introduce the propargylamine group to the α,β-unsaturated derivative **5.13**, the acetyl groups were deprotected when using methanol as the solvent. Finally, after numerous different reaction conditions, solvents, and additives, the correct combination was discovered for the synthesis compound **5.15**.

Due to the difficulties encountered in the initial strategy, a second strategy was also developed to synthesis the photoaffinity probes. In this approach, the photoactive tag with an alkyne handle was synthesised first and then coupled to the acetylated divalent galactoside **2.113**. Hence, the benzophenone functionalized with a carboxylic acid **5.16** was coupled to the *N*-propargyl-functionalized β-alanine **4.32**[246]. Removal of the *tert*-butyl ester group also presented some difficulties with the formation of the methyl ketone compound **5.18**. However, utilising anhydrous conditions eliminated this problem and allowed the formation of the Phototag 1 (**5.19**). For the synthesis of Phototag 2 (**5.26**), the diazirine tag was first synthesised using literature procedures, which was then coupled to the *N*-propargyl-functionalized β-alanine **4.32**[246]. Exposure of the carboxylic acid functional group using anhydrous conditions gave Phototag 2 (**5.26**). Both Phototags 1 & 2 could then be coupled to the aniline of the divalent galactoside **2.113**. Deprotection then gave the two PAL probes **5.21** and **5.28**.

Chapter 6

Conclusion

6.1 Conclusion

The aim of the research described in this thesis was to develop novel compounds to tackle fungal infections, in particular in the treatment of *C. albicans* infection. Since carbohydrate interactions are vitally important in the adhesion process of fungi to host cells, a series of glycoconjugates were developed to interfere with this process and block the adhesion of the yeast to BEC with the aim to prevent infection.

Chapter 2 described a SAR study to screen a small library of aromatic glycoconjugates to determine the structural features required to inhibit the adherence of pathogenic *C. albicans*. Different sugar moieties usually involved in host-pathogen recognition at the host cell surface (i.e galactose, fucose, mannose, glucosamine and galactosamine) were investigated. Different valency glycoconjugates with linkers that modified the distance and orientation of the sugar moieties were also tested. After a series of adherence assays (exclusion, competitive and displacement), the divalent galactoside **2.78** was found to be the most effective at inhibiting the adherence of the *C. albicans* to the BEC. Fluorescence studies indicate that the potential target of this compound was in the cell wall of the fungi, due to the strong localized fluorescence surrounding each yeast cell. Taking this into account, the target could be a fungal cell wall lectin, due to the high specificity observed for the type of sugar in the anti-adhesion ligand.

In an effort to increase the potency of the lead compound, a variety of analogues of this compound with alternative scaffolds were synthesised (Chapter 3). A series of divalent squaramide analogues were designed, synthesised and evaluated as anti-adhesion ligands. However, since there was no increase in the anti-adhesive properties of these compounds, a different core scaffold was tried. Two divalent galactosides and a monovalent derivative, with a norbornene core were synthesised and evaluated as anti-adhesion ligands. The *cis*-norbornene compound **3.30** consistently showed the best results in all three adherence assays, even having better activity than the initial lead compound in the exclusion and competitive assays. The norbornene scaffold provides an interesting framework that could be derivatized in different ways to incorporate different functional groups, such as fluorescent labels

and other chemically reactive groups. Also, due to the polymerizing ability of substituted norbornene compounds, polyvalent anti-adhesion ligands could be synthesised to increase the potency of these norbornene-based glycoconjugates. Future work in this project involves the polymerizing of the norbornene compounds and testing the ability of the polymers to inhibit the adhesion process.

The objective of Chapter 4 was to design and synthesise multivalent displays of the initial lead compound, to increase the potency of the ligand by utilizing the 'Multivalent Effect'. A variety of scaffolds were used to develop multivalent displays of the lead compound to investigate the optimum structure required to inhibit the adhesion of *C. albicans* to BEC. Hence, multivalent displays of compound **2.78** built around an aromatic-core, a linear peptoid scaffold, cyclopeptide scaffold and a polylysine-based scaffold were synthesised. This resulted in a wide variety of displays of the divalent galactoside, with varying valencies. These compounds vary from the trivalent aromatic scaffold exhibiting six galactose moieties to the cyclopeptide and polylysine based dendrimers, which display 32 galactose moieties (16 copies of the lead compounds). Future work will involve the biological evaluation of these compounds to determine if the multivalent effect can be utilized to increase the potency of the lead compound. If promising results are obtained, further optimization would be carried out to identify the prefered valency, flexibility and sugar-display to inhibit the adhesion process more effectively.

In Chapter 5, two photoaffinity labelling (PAL) probes were successfully synthesised. We hope to use these photoaffinity probes **5.21** and **5.28**, in conjugation with a reporter tag, to identify the target in the *C. albicans* with which the glycoconjugates discussed in this thesis are interacting. Identifying this target would provide invaluable information on the adhesins responsible for the adhesion of *C. albicans* to BEC. If the target adhesin is known, high affinity anti-adhesion ligands may be developed to tackle the emerging problem of antifungal resistance.

6.2 Future Plans

There are many future plans for this project. First, the research group of Dr. Trinidad Velasco-Torrijos will continue to search for a small molecule analogues of compound **2.78** with higher biological activity. However, this is a difficult task since *C. albicans* has numerous adhesins on it's cell surface, so blocking one adhesin may never inhibit the adhesion process fully. In an effort to overcome this, the biological assays will be carried out with combinations of the AGCs from Chapter 2. The intention is that they could inhibit numerous adhesins at the same time, increasing the potency of the ligands as individuals. We also intend on testing these AGCs on different pathogens. It has been reported that *C. albicans* and *P. aeruginosa* have some similar adhesins, hence, these AGCs could also have good anti-adhesion properties against this other pathogen.

In relation to the compounds outlined in Chapter 3 we intend on carrying out further work with the norbornene compounds. The possibility of forming polymers of these compounds would be very interesting since this would provide a multivalent display of these compounds and could significantly inhibit the adhesion process. Also, in the synthesis of compound **3.30**, the *cis*-norbornene derivate, the monovalent glycoconjugate **3.31** was inadvertently formed. When compound **3.30** was treated with Amberlite H^+, it displaced one of the galactose-triazolyl residues. We think this is an interesting avenue to pursue, since using this displacement, a smart drug-delivery system could be developed. With this in mind, we intend on testing the anti-fungal properties of the galactosyl-triazolyl residues to have dual inhibition system.

The future work relating to Chapter 4, will involve the biological evaluation of the multivalent compounds. From the results of these assays, further multivalent displays of the lead compound will be synthesised to find the optimum display of the lead compound to have the highest percentage of adhesion inhibition.

The compounds from Chapter 5 will be used try identify the adhesin in the cell wall of the *C. albicans* with which these compounds are interacting. First, they will be tested using module lectins to determine the cross-linking ability of these compounds. For example, peanut agglutin, a lectin known to bind Gal-β(1-3)-GalNAc,

will be treated with compounds **5.21** and **5.28**. The lectin will be subjected to UV light and the photo-labelled compounds will hopefully cross-link to the protein. As a negative control, the compounds will also be exposed to concanavalin A (ConA), a lectin know to bind α-D-mannosyl and α-D-glucosyl groups. Following on from successful results in these experiments, compounds **5.21** and **5.28** will be exposed to the *C. albicans* cells and the photocrosslinking experiment will be tested. From this experiment, we hope to identify the lectin involved in the adhesion process.

Chapter 7

Experimental

7.1 General Procedures and Instrumentation

All chemicals purchased were reagent grade and used without further purification, unless stated otherwise. DCM was distilled over CaH_2 and THF was distilled over Na wire and benzophenone. Anhydrous DMF was purchased from Sigma Aldrich. Molecular sieves used for glycosylation and coupling were 3 Å and were dried in the oven at 100 °C at ambient pressure prior to use. Reactions were monitored using thin layer chromatography (TLC) on Merck Silica Gel F_{254} plates. Detection was effected by visualisation in UV light and/or charring in a mixture of 5 % sulphuric acid-EtOH, in a potassium permanganate solution (3 g $KMnO_4$, 20 g K_2CO_3, 5 mL 5 % aqueous NaOH and 300 mL H_2O), or in a ninhydrin solution (0.3 g ninhydrin, 3 mL conc. H_2SO_4 and 100 mL *n*-butanol). Evaporation under reduced pressure was always effected with the bath temperature kept at or below 60 °C. NMR spectra were obtained a Bruker Ascend 500 spectrometer operated at 500 MHz for ^1H NMR analysis and 125 MHz for ^{13}C analysis at 293 K, unless otherwise stated. The residual solvent peak was used as an internal standard. Chemical shifts (δ) were reported in ppm. Proton and carbon signals were assigned with the aid of 2D NMR experiments (COSY, HSQC, HMBC, ^{15}N HSQC, ^{15}N HMBC) and DEPT experiments for novel compounds. The following abbreviations were used to explain the observed multiplicities; s (singlet), bs (broad siniglet), d (doublet), appd (apparent doublet), t (triplet), appt (apparent triplet), q (quartet), m (multiplet), bs (broad singlet). As used commonly in carbohydrate chemistry, the multiplicity of signals are reported as observed and not the expected multiplicity. Flash chromatography was performed with Merck Silica Gel 60. CEM Discover Microwave Synthesizer was used to carry out reactions requiring microwave irradiation. Optical rotations were obtained using AA-100 polarimeter. $[\alpha]_D$ values were given in 10^{-1} cm^2g^{-1}. High performance liquid chromatography (HPLC, Waters Alliance 2695) was performed in final compounds and indicated purity of ca. 95 %. High resolution mass spectrometry (HRMS) was performed on an Agilent-LC 1200 Series coupled to a 6210 Agilent Time-Of-Flight (TOF) or mass spectrometer equipped with an electrospray source in both positive and negative (ESI +/-) modes. Infrared spectra were obtained as a film on NaCl plates, as KBr disks or via ATR as a solid on a zinc selenide crystal in the region 4000-400 cm^-

[1] on a Perkin Elmer Spectrum 100 FT-IR spectrophotometer. UV-Vis spectra were recorded in a Perkin Elmer precisely Lambda 35 UV/Vis spectrometer. Compounds were lyophilized on a Labconco FreeZone 1 Freeze Dry system.

7.2 Experimental Procedures

7.2.1 Experimental Procedures for Chapter 2

2,3,4,6-Tetra-*O*-acetyl-1-β-azido-D-galactopyranoside (2.40)

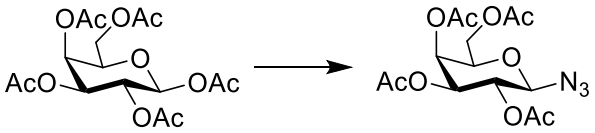

2.36 **2.40**

$TMSN_3$ (1.68 mL, 12.809 mmol, 2.5 equiv) was added to a solution of β-D-galactose pentaacetate **2.36** (2.00 g, 5.12 mmol) in anhydrous DCM (20 mL). $SnCl_4$ (0.3 mL, 2.56 mmol, 0.5 equiv) was added to this solution and the reaction mixture was stirred at rt for 18 h. Sat. $NaHCO_3$ solution (30 mL) was added and the suspension was extracted with DCM (2 x 30 mL). The combined organic layers were dried over $MgSO_4$, filtered and concentrated *in vacuo* to afford **2.40** as a white solid which was recrystallized from EtOH giving the pure product **2.41** as white crystals (1.86 g, 97 %). ^{1}H NMR (500 MHz, $CDCl_3$) δ 5.42 (d, *J* = 3.3 Hz, 1H, H-4), 5.18 – 5.13 (m, 1H, H-2), 5.03 (dd, *J* = 10.3, 3.4 Hz, 1H, H-3), 4.59 (d, *J* = 8.8 Hz, 1H, H-1), 4.20 – 4.13 (m, 2H, H-6 and H-6'), 4.01 (appt, *J* = 6.6 Hz, 1H, H-5), 2.16 (s, 3H, OAc), 2.09 (s, 3H, OAc), 2.06 (s, 3H, OAc), 1.98 (s, 3H, OAc).

The NMR data is in agreement with the data reported in the literature.[183]

2,3,4,6-Tetra-*O*-acetyl-1-β-azido-D-glucopyranoside (2.41)

2.37 **2.41**

$TMSN_3$ (1.68 mL, 12.809 mmol, 2.5 equiv) was added to a solution of β-D-glucose pentaacetate **2.37** (2.00 g, 5.12 mmol) in anhydrous DCM (20 mL). $SnCl_4$ (0.3 mL, 2.56 mmol, 0.5 equiv) was added to this solution and the reaction mixture was stirred at rt for 18 h. Sat. $NaHCO_3$ solution (30 mL) was added and the suspension was extracted

with DCM (2 x 30 mL). The combined organic layers were dried over $MgSO_4$, filtered and concentrated *in vacuo.* The crude product was obtained as a white solid, which was recrystallized from EtOH giving the pure product **2.41** as white crystals (1.79 g, 94 %). ^{1}H NMR (500 MHz, $CDCl_3$) δ 5.21 (t, *J* = 9.5, 1H, H-3), 5.09 (t, *J* = 9.7 Hz, 1H, H-4), 4.94 (t, *J* = 9.2 Hz, 1H, H-2), 4.64 (d, *J* = 8.9 Hz, 1H, H-1), 4.26 (dd, *J* = 12.5, 4.8 Hz, 1H, H-6), 4.16 (dd, *J* = 12.4, 2.1 Hz, 1H, H-6'), 3.79 (ddd, *J* = 10.1, 4.7, 2.2 Hz, 1H, H-5), 2.09 (s, 3H, OAc), 2.07 (s, 3H, OAc), 2.02 (s, 3H, OAc), 2.00 (s, 3H, OAc).

The NMR data is in agreement with the data reported in the literature.[183]

2,3,4,6-Tetra-*O*-acetyl-1-α-azido-D-mannopyranoside (2.42)

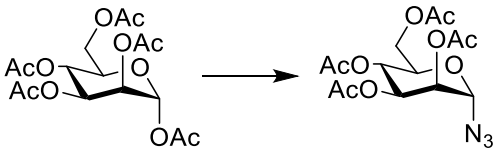

2.38 **2.42**

$TMSN_3$ (1.1 mL, 8.19 mmol, 2.5 equiv) was added to a solution of α-D-mannose pentaacetate **2.38** (1.279 g, 3.28 mmol) in anhydrous DCM (15 mL). $SnCl_4$ (0.2 mL, 1.64 mmol, 0.5 equiv) was added to this solution and the reaction mixture was stirred at rt for 18 h. Sat. $NaHCO_3$ solution (20 mL) was added and the suspension was extracted with DCM (2 x 30 mL). The combined organic layers were washed with brine (20 mL), dried over $MgSO_4$, filtered and concentrated *in vacuo* to afford **2.42** as a clear colourless oil which was used without further purification (1.18 g, 97 %). ^{1}H NMR (500 MHz, $CDCl_3$) δ 5.29 (s, 1H, H-1), 5.22 (s, 1H, H-2), 5.18 – 5.08 (m, 2H, H-3 and H-4), 4.18 (dd, *J* = 12.7, 5.8 Hz, 1H, H-6), 4.06 – 4.01 (m, 2H, H-5 and H-6'), 2.04 (s, 3H, OAc), 1.98 (s, 3H, OAc), 1.93 (s, 3H, OAc), 1.86 (s, 3H, OAc).

The NMR data is in agreement with the data reported in the literature.[185]

4-*O*-(2,3,4,6-Tetra-*O*-acetyl-β-D-galactopyranosyl)-2,3,6-tri-*O*-acetyl-1-β-azido-D-glucopyranoside (2.43)

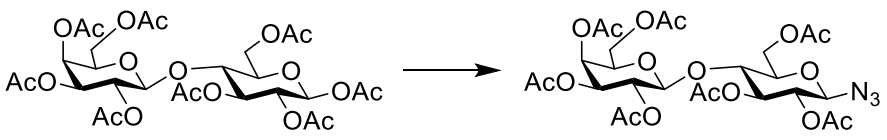

2.39 **2.43**

$TMSN_3$ (0.97 mL, 7.37 mmol, 2.5 equiv) was added to a solution of β-D-lactose octaacetate **2.39** (2.00 g, 2.95 mmol) in anhydrous DCM (20 mL). $SnCl_4$ (0.17 mL, 1.47 mmol, 0.5 equiv) was added to this solution and the reaction mixture was stirred at rt for 18 h. Sat. $NaHCO_3$ solution (30 mL) was added and the suspension was extracted with DCM (2 x 30 mL). The combined organic layers were dried over $MgSO_4$, filtered and concentrated *in vacuo* to afford the crude product, which was purified by silica gel column chromatography (EtOAc:Pet Ether 1:1) to give the pure product **2.43** as an off-white solid (1.54 g, 79 %). R_f= 0.71 (DCM:MeOH 9:1). ^{1}H NMR (500 MHz, $CDCl_3$) δ 5.23 (d, *J* = 3.3 Hz, 1H, H-4 Gal), 5.10 (dd, *J* = 11.6, 6.8 Hz, 1H, H-3 Glc), 4.98 (dd, *J* = 10.2, 8.0 Hz, 1H, H-2 Gal), 4.87 (dd, *J* = 10.4, 3.3 Hz, 1H, H-3 Gal), 4.74 (t, *J* = 9.1, 4.0 Hz, 1H, H-2 Glc), 4.56 (d, *J* = 8.8 Hz, 1H, H-1 Glc), 4.43 (d, *J* = 8.0 Hz, 1H, H-1 Gal), 4.06 – 3.95 (m, 4H, H-6 and H-6' Gal and Glc), 3.82 (t, *J* = 6.7 Hz, 1H, H-5 Gal), 3.73 (t, *J* = 9.4 Hz, 1H, H-4 Glc), 3.67 – 3.61 (m, 1H, H-5 Glc), 2.03 (s, 3H, OAc), 2.02 (s, 3H, OAc), 1.96 (s, 3H, OAc), 1.95 (s, 3H, OAc), 1.94 (s, 3H, OAc), 1.92 (s, 3H, OAc), 1.85 (s, 3H, OAc).

The NMR data is in agreement with the data reported in the literature.[184]

2,3,4-Tri-*O*-acetyl-1-β-azido-L-fucopyranoside (2.45)

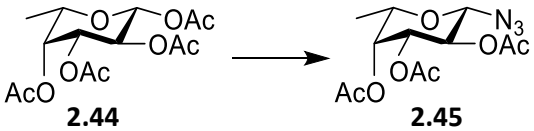

2.44 **2.45**

$TMSN_3$ (1.98 mL, 15.05 mmol, 2.5 equiv) was added to a solution of β-L-fucose tetraaacetate **2.44** (2.00 g, 6.02 mmol) in anhydrous DCM (20 mL). $SnCl_4$ (0.35 mL, 3.01 mmol, 0.5 equiv) was added to this solution and the reaction mixture was stirred at rt for 18 h. Sat. $NaHCO_3$ solution (30 mL) was added and the suspension was extracted with DCM (2 x 30 mL). The combined organic layers were dried over $MgSO_4$, filtered and concentrated *in vacuo* to afford **2.45** as an off-white solid which was used without further purification (1.59 g, 84 %). ^{1}H NMR (500 MHz, $CDCl_3$) δ 5.26 (d, *J* = 3.3 Hz, 1H, H-4), 5.14 (dd, *J* = 10.2, 8.8 Hz, 1H, H-2), 5.03 (dd, *J* = 10.3, 3.4 Hz, 1H, H-3), 4.57 (d, *J* = 8.7 Hz, 1H, H-1), 3.90 (q, *J* = 6.4 Hz, 1H, H-5), 2.19 (s, 3H, OAc), 2.08 (s, 3H, OAc), 1.98 (s, 3H, OAc), 1.25 (d, *J* = 6.4 Hz, 3H, CH_3).

The NMR data is in agreement with the data reported in the literature.[183]

2-Chloroethyl 2,3,4,6-tetra-*O*-acetyl-β-D-galactopyranoside (2.46)

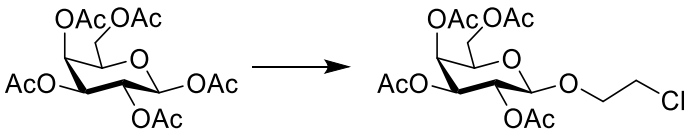

2.36 **2.46**

A solution of β-D-galactose pentaacetate **2.36** (2.00 g, 5.12 mmol) and 2-chloroethanol (0.45 mL, 6.66 mmol, 1.3 equiv) in anhydrous DCM (20 mL) with 3 Å molecular sieves (3.00 g) was stirred under N_2 in an ice bath for 15 min. A freshly prepared solution of $BF_3.OEt_2$ (1.2 mL, 9.73 mmol, 1.9 equiv) in anhydrous DCM (2 mL) was added dropwise over a period of 30 min via cannula. When addition was complete, the mixture was allowed to reach rt and stirred overnight. The molecular sieves were filtered using fluted filter paper, the solids were washed with DCM (10 mL) and the filtrate was washed with a sat. $NaHCO_3$ solution (2 x 20 mL). The combined aqueous layers were extracted with DCM (20 mL), the combined organic layers were washed with brine (20 mL) and distilled water (20 mL), dried over $MgSO_4$, filtered and concentrated *in vacuo*. The crude product was obtained as a white solid, which was recrystallized from EtOH giving the pure product **2.46** as white crystals (0.85 g, 40 %). ^{1}H NMR (500 MHz, $CDCl_3$) δ 5.39 (d, *J* = 2.7 Hz, 1H, H-4), 5.22 (dd, *J* = 10.4, 8.0 Hz, 1H, H-2), 5.02 (dd, *J* = 10.5, 3.4 Hz, 1H, H-3), 4.53 (d, *J* = 7.9 Hz, 1H, H-1), 4.20 – 4.08 (m, 3H, H-6, H-6'and OC*H*), 3.91 (t, *J* = 6.4 Hz, 1H, H-5), 3.76 (dt, *J* = 11.2, 6.6 Hz, 1H, OC*H*), 3.62 (dd, *J* = 6.3, 5.2 Hz, 2H, CH_2Cl), 2.15 (s, 3H, OAc), 2.07 (s, 3H, OAc), 2.05 (s, 3H, OAc), 1.98 (s, 3H, OAc).

The NMR data is in agreement with the data reported in the literature.[186]

2-Azidoethyl 2,3,4,6-tetra-*O*-acetyl-β-D-galactopyranoside (2.47)

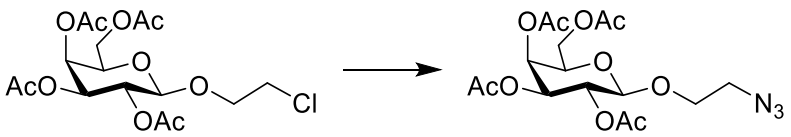

2.46 **2.47**

A solution of 2-chloroethyl 2,3,4,6-tetra-*O*-acetyl-β-D-galactopyranoside **2.46** (850 mg, 2.069 mmol) and NaN_3 (269 mg, 4.138 mmol, 2 equiv) in anhydrous DMF (30 mL) was stirred at 80 °C in a round bottomed flask equipped with a condenser and a $CaCl_2$ drying tube. After 16 h, the solvent was removed under reduced pressure. The crude product was dissolved in DCM (30 mL) and washed with brine (3 x 20 mL). The organic phases were combined, dried over $MgSO_4$ and concentrated *in vacuo* to give a clear syrup that turned into a white solid **2.47** upon exposure to high vacuum, which was reacted without further purification (518 mg, 60 %). ^{1}H NMR (500 MHz, $CDCl_3$) δ 5.33 (dd, *J* = 3.4, 1.1 Hz, 1H, H-4), 5.17 (dd, *J* = 10.5, 8.0 Hz, 1H, H-2), 4.97 (dd, *J* = 10.5, 3.4 Hz, 1H, H-3), 4.51 (d, *J* = 8.0 Hz, 1H, H-1), 4.15-4.04 (m, 2H, H-6 and H-6'), 3.98 (ddd, *J* = 10.7, 4.8, 3.5 Hz, 1H, OC*H*), 3.88 (td, *J* = 6.6, 1.1 Hz, 1H, H-5), 3.64 (ddd, *J* = 10.8, 8.4, 3.4 Hz, 1H, OC*H*), 3.44 (ddd, *J* = 13.3, 8.4, 3.5 Hz, 1H, C*H*N_3), 3.25 (ddd, *J* = 13.4, 4.8, 3.4 Hz, 1H, C*H*N_3), 2.09 (s, 3H, OAc), 2.00 (s, 3H, OAc), 1.98 (s, 3H, OAc), 1.92 (s, 3H, OAc).

The NMR data is in agreement with the data reported in the literature.[186]

2-Acetamido-2-deoxy-3,4,6-tri-*O*-acetyl-1-β-azido-D-galactopyranoside (2.52)

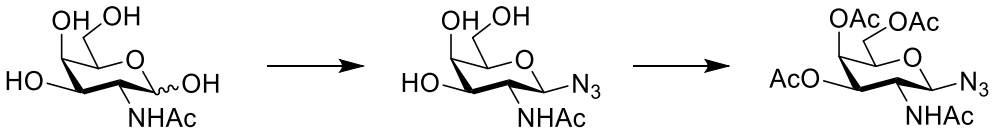

2.48 **2.50** **2.52**

2-Chloro-1,3-dimethylimidazolium chloride (DMC) (0.940 g, 5.56 mmol, 3 equiv) was added to a mixture of *N*-acetyl-D-galactosamine **2.48** (0.410 g, 1.85 mmol), 2,6-lutidine (1.3 mL, 11.10 mmol, 6 equiv) and NaN_3 (1.203 g, 18.50 mmol, 10 equiv) in D_2O (10 mL). The reaction was stirred for 3 days at 6 °C. The solvent was removed *in vacuo*, CH_3Cl:MeOH (3:1, 10 mL) was added and was sonicated for 5 mins. The solid was removed by filtration and the filtrate was concentrated *in vacuo.* The crude product was dissolved in H_2O (20 mL) and washed with DCM (2 x 20 mL). Amberlite OH^- was added to the aqueous layer, it was filtered and concentrated *in vacuo*. The crude product was purified by silica gel column chromatography ($CHCl_3$:MeOH 4:1) to give product **2.50** (0.356 g, 78 %). 2-Acetamido-2-deoxy-β-D-galactopyranosyl azide **2.50** (0.356 g, 1.45 mmol) was immediately reacted with acetic anhydride in pyridine (1:1, 10 mL) for 3 h. The solvent was removed *in vacuo* to yield a clear

colourless oil, which was dissolved in DCM (20 mL) and washed with brine (2 x 20 mL), dried over $MgSO_4$ and concentrated *in vacuo* to give the crude product which was purified by silica gel column chromatography (EtOAc:Pet Ether 1:1) to give the pure product **2.52** as a colourless oil (0.458 g, 85 %). ^{1}H NMR (500 MHz, $CDCl_3$) δ 6.09 (d, *J* = 8.9 Hz, 1H, N*H*), 5.36 (dd, *J* = 3.3, 0.8 Hz, 1H, H-4), 5.23 (dd, *J* = 11.2, 3.4 Hz, 1H, H-3), 4.79 (d, *J* = 9.2 Hz, 1H, H-1), 4.15 – 4.13 (m, 2H, H-6 and H-6'), 4.07 – 3.97 (m, 2H, H-5 and H-2), 2.14 (s, 3H, NHO*Ac*), 2.03 (s, 3H, OAc), 1.98 (s, 3H, OAc), 1.96 (s, 3H, OAc).

The NMR data is in agreement with the data reported in the literature.[274]

2-Acetamido-2-deoxy-3,4,6-tri-*O*-acetyl-1-β-azido-D-glucopyranoside (2.53)

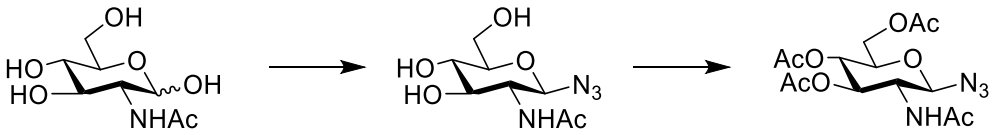

2-Chloro-1,3-dimethylimidazolium chloride (DMC) (1.076 g, 6.36 mmol, 3 equiv) was added to a mixture of *N*-acetyl-D-glucosamine **2.49** (0.469 g, 2.12 mmol), 2,6-lutidine (1.5 mL, 12.72 mmol, 6 equiv) and NaN_3 (1.378 g, 21.20 mmol, 10 equiv) in D_2O (10 mL). The reaction was stirred for 3 days at 6 °C. The solvent was removed under reduced pressure, CH_3Cl:MeOH (3:1, 10 mL) was added and was sonicated for 5 mins. The solid was removed by filtration and the filtrate was concentrated *in vacuo.* The crude product was dissolved in H_2O (20 mL) and washed with DCM (2 x 20 mL). Amberlite OH^- was added to the aqueous layer, it was filtered and concentrated under reduced pressure. The crude product was purified by silica gel column chromatography ($CHCl_3$:MeOH 4:1) to give product **2.51** (0.392 g, 75 %). 2-Acetamido-2-deoxy-β-D-glucopyranosyl azide **2.51** (0.392 g, 1.59 mmol) was immediately reacted with acetic anhydride in pyridine (1:1, 10 mL) for 3 h. The solvent was evaporated under reduced pressure to yield a clear colourless oil, which was dissolved in DCM (20 mL) and washed with brine (2 x 20 mL), dried over $MgSO_4$ and concentrated *in vacuo* to give a clear syrup (0.533 g, 90 %). ^{1}H NMR (500 MHz, $CDCl_3$) δ 6.33 (d, *J* = 9.0 Hz, 1H, N*H*), 5.26 (dd, *J* = 10.5, 9.5 Hz, 1H, H-3), 5.06 (appt, *J* = 9.7 Hz, 1H, H-4), 4.80 (d, *J* = 9.3 Hz, 1H, H-1), 4.23 (dd, *J* = 12.4, 5.0 Hz, 1H, H-6), 4.13 (dd, *J* = 12.4, 2.2 Hz, 1H, H-6'), 3.90 (appdd, *J* = 10.5, 9.2 Hz, 1H, H-2), 3.81 (ddd, *J* =

10.1, 4.9, 2.3 Hz, 1H, H-5), 2.06 (s, 3H, OAc), 2.00 (s, 3H, OAc), 1.99 (s, 3H, OAc), 1.94 (s, 3H, NH*Ac*).

The NMR data is in agreement with the data reported in the literature.[275]

***N*-(Prop-2-yn-1-yl)-3-propionamidobenzamide (2.56)**

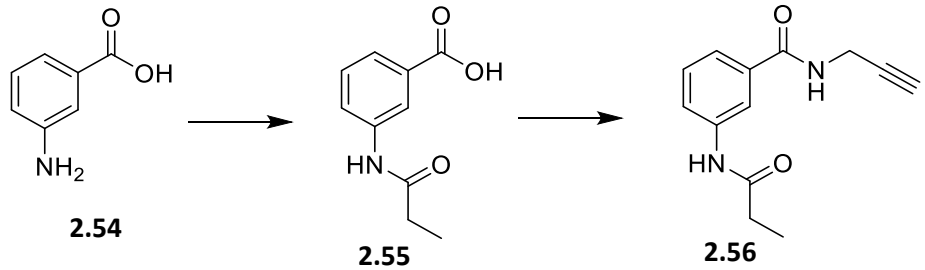

2.54 **2.55** **2.56**

3-aminobenzoic acid **2.54** (2 g, 14.6 mmol) was dissolved in anhydrous THF (15 mL) under N_2 and propionyl chloride (3.19 mL, 36.5 mmol) was added dropwise. The mixture was allowed to stir for 5 min and NEt_3 (6.1 mL, 43.8 mmol) was added slowly. The reaction was left to stir for 16 h. The solvent was removed *in vacuo*. The crude mixture was dissolved in ethyl acetate (30 mL), washed with 0.5 M HCl (30 mL), and dried ($MgSO_4$). The mixture was filtered and the solvent was removed under reduced pressure to yield the product 3-(propionylamino)benzoic acid **2.55** as an off-white solid (0.637 g, 23 %) which was used without further purification. Compound **2.55** (0.307 g, 1.59 mmol) and TBTU (0.56 g, 1.75 mmol) were dissolved in anhydrous DMF (15 mL) under N_2. NEt_3 (0.3 mL, 2.38 mmol) was added, and the reaction mixture was stirred for 10 min on ice. Propargylamine (0.15 mL, 2.38 mmol) was added, and the reaction was stirred for 16 h at rt. The solvent was removed *in vacuo*. The crude mixture was dissolved in ethyl acetate (30 mL), washed with 0.5 M HCl (30 mL), sat. $NaHCO_3$ (30 mL) and brine (30 mL), and dried ($MgSO_4$). The mixture was filtered and the solvent was removed in the rotatory evaporator to yield product **2.56** as a pale yellow solid (0.359 g, 98 %). ^{1}H NMR (500 MHz, d_6-DMSO): δ 9.99 (s, 1H, N*H*CH_2CCH), 8.86 (s, 1H, N*H*COC_2H_5), 8.04 (s, 1H, Ar-H), 7.77 (d, *J* = 8.2 Hz, 1H, Ar-H), 7.48 (d, *J* = 7.7 Hz, 1H, Ar-H), 7.37 (t, *J* = 7.9 Hz, 1H, Ar-H), 4.03 (dd, *J* = 5.5, 2.4 Hz, 2H, C*H*$_2$CCH), 3.10 (t, *J* = 2.3 Hz, 1H, CH_2CC*H*), 2.32 (q, *J* = 7.5 Hz, 2H, *CH*$_2$$CH_3$), 1.08 (t, *J* = 7.5 Hz, 3H, CH_2*CH*$_3$). ^{13}C NMR (125 MHz, d_6-DMSO): δ 172.6 (*C*OC_2H_5), 166.4 (*C*O$NHCH_2$-triaz), 139.9 (Ar-C), 135.0 (Ar-C), 129.1 (Ar-*C*H), 122.3 (Ar-*C*H), 121.8 (Ar-*C*H), 118.9 (Ar-*C*H), 81.8 (CH_2*C*CH), 73.2 (CH_2C*C*H), 30.0 (*C*H_2CH_3), 29.0 (*C*H_2CCH), 10.1 (CH_2*C*H_3). IR (KBr):

3365, 3321, 3298, 3117, 2977, 2942, 1690, 1652, 1562 cm^{-1}. HRMS (ESI+): *m/z* calcd for $C_{13}H_{15}N_2O_2 + H^+$ $[M+H]^+$ 231.1134, found 231.1135.

_N_-(2,3,4,6-Tetra-O-acetyl-β-D-galactopyranosyl-1,2,3-triazol-4-ylmethylamide)-_N'_-propyl-3-aminobenzene-1-carboxamide (2.57)

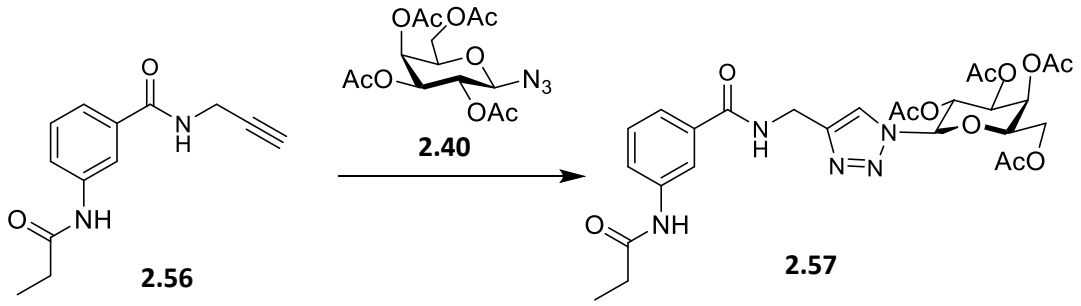

Copper sulphate pentahydrate (20 mg) and sodium ascorbate (40 mg) were added to a solution of **2.40** (266 mg, 0.476 mmol) and **2.56** (100 mg, 0.432 mmol) in acetone/H_2O (4 mL/ 2mL). The reaction was allowed to stir at room temperature for 16 h. The solvent was removed *in vacuo*. The residue was dissolved in DCM (30 mL), washed with water (20 mL x 3), and dried ($MgSO_4$). The mixture was filtered and the solvent was removed *in vacuo* to yield the crude product, which was purified by silica gel column chromatography (DCM:MeOH 98:2-93:7) to give the pure product **2.57** as an off-white solid (235 mg, 83%). R_f= 0.45 (DCM:MeOH 9:1). $[\alpha]_D^{19}$ -6.9 (c 0.9, DCM). ^{1}H NMR (500 MHz, $CDCl_3$): δ 8.62 (s, 1H, N*H*COC_2H_5), 7.95 (s, 1H, triaz-H), 7.89 – 7.78 (m, 2H, Ar-H x 2), 7.72 (s, 1H, N*H*CH_2-triaz), 7.48 (d, *J* = 7.4 Hz, 1H, Ar-H), 7.28 (t, *J* = 7.8 Hz, 1H, Ar-H), 5.91 (d, *J* = 9.2 Hz, 1H, H-1), 5.56 (m, 2H, H-2 and H-4), 5.34 – 5.24 (m, 2H, H-3), 4.68 (dd, *J* = 14.5, 3.5 Hz, 2H, C*H*$_2$-triaz), 4.31 (t, *J* = 6.1 Hz, 1H, H-5), 4.15 (dd, *J* = 11.5, 6.8 Hz, 2H, H-6 and H-6'), 2.39 (q, *J* = 7.4 Hz, 2H, C*H*$_2$$CH_3$), 2.18 (s, 3H, OAc), 2.00 (s, 6H, OAc x2), 1.82 (s, 3H, OAc), 1.18 (t, *J* = 7.5 Hz, 3H, CH_2C*H*$_3$). ^{13}C NMR (125 MHz, $CDCl_3$): δ 173.0 (NH*C*OC_2H_5), 170.4 (CO of OAc), 170.1 (CO of OAc), 169.9 (CO of OAc), 169.1 (CO of OAc), 167.5 (*C*O$NHCH_2$-triaz), 145.4 (*C*-triaz), 138.8 (Ar-C), 134.5 (Ar-C), 129.1 (Ar-*C*H), 123.1 (Ar-*C*H), 122.3 (Ar-*C*H), 121.6 (*C*H-triaz), 118.5 (Ar-*C*H), 86.1 (C-1), 73.9 (C-5), 70.8 (C-3), 68.0 (C-2), 66.9 (C-4), 61.2 (C-6), 35.3 (*C*H_2-triaz), 30.4 (CH_2*C*H_3), 20.6 (CH_3 of OAc), 20.6 (CH_3 of OAc), 20.5 (CH_3 of OAc), 20.2 (CH_3 of OAc), 9.6 (CH_2*C*H_3). IR (film on NaCl): 3311, 2980, 1753, 1652, 1591, 1553 cm^{-1}. HRMS (ESI+): *m/z* calcd for $C_{27}H_{34}N_5O_{11} + H^+$ $[M+H]^+$ 604.2255, found 604.2262.

***N*-(2,3,4-Tri-O-acetyl-β-L-fucopyranosyl-1,2,3-triazol-4-ylmethylamide)-*N*'-propyl-3-aminobenzene-1-carboxamide (2.58)**

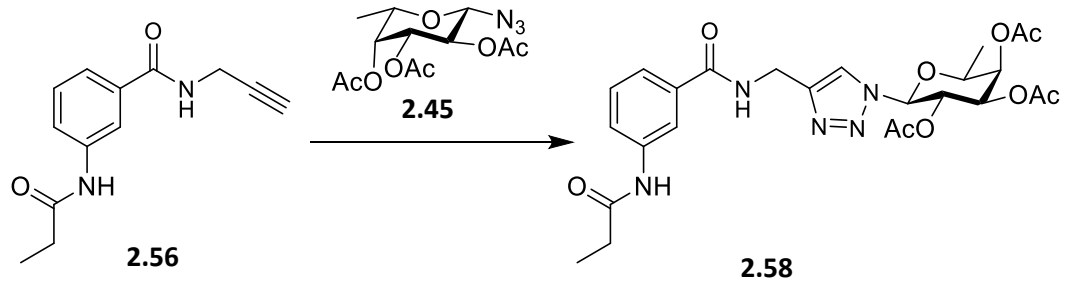

Copper sulphate pentahydrate (10 mg) and sodium ascorbate (20 mg) were added to a solution of **2.45** (75 mg, 0.239 mmol) and **2.56** (50 mg, 0.217 mmol) in acetone/H_2O (4 mL/ 2mL). The reaction was allowed to stir at room temperature for 16 h. The solvent was removed *in vacuo*. The residue was dissolved in DCM (30 mL), washed with water (20 mL x 3), and dried ($MgSO_4$). The mixture was filtered and the solvent was removed *in vacuo* to yield the crude product, which was purified by silica gel column chromatography (DCM:MeOH 98:2-93:7) to give the pure product **2.58** as an off-white solid (90 mg, 76 %). R_f=0.56 (DCM:MeOH 9:1). $[\alpha]_D^{20}$: +16.1 (c 1, DCM). ^{1}H NMR (500 MHz, $CDCl_3$): δ 8.32 (s, 1H, N*H*COC_2H_5), 7.90 (s, 1H, triaz-H), 7.87 (d, *J* = 8.0 Hz, 1H, Ar-H), 7.77 (s, 1H, Ar-H), 7.46 (m, 2H, Ar-H and N*H*CH_2-triaz), 7.28 (t, *J* = 8.0 Hz, 1H, Ar-H), 5.78 (d, *J* = 9.2 Hz, 1H, H-1), 5.52 – 5.46 (m, 1H, H-2), 5.35 (d, *J* = 2.9 Hz, 1H, H-4), 5.24 (dd, *J* = 10.3, 3.4 Hz, 1H, H-3), 4.66 (dd, *J* = 15.2, 5.6 Hz, 2H, C*H*$_2$-triaz), 4.11 (q, *J* = 6.4 Hz, 1H, H-5), 2.37 (q, *J* = 7.5 Hz, 2H, C*H*$_2$$CH_3$), 2.20 (s, 3H, OAc), 1.97 (s, 3H, OAc), 1.81 (s, 3H, OAc), 1.26 – 1.13 (m, 6H, C6-*H*$_3$ and CH_2C*H*$_3$). ^{13}C NMR (125 MHz, $CDCl_3$): δ 171.8 (*C*OC_2H_5), 169.5 (CO of OAc), 168.9 (CO of OAc), 168.2 (CO of OAc), 166.4 (*C*O$NHCH_2$-triaz), 144.3 (*C*-triaz), 137.8 (Ar-C), 133.6 (Ar-C), 128.2 (Ar-*C*H), 122.1 (Ar-*C*H), 121.4 (Ar-*C*H), 120.4 (*C*H-triaz), 117.4 (Ar-*C*H), 85.3 (C-1), 71.7 (C-5), 70.2 (C-3), 68.9 (C-4), 67.2 (C-2), 34.4 (*C*H_2-triaz), 29.5 (*C*H_2CH_3), 19.7 (CH_3 of OAc), 19.5 (CH_3 of OAc), 19.3 (CH_3 of OAc), 15.0 (C-6), 8.6 (CH_2*C*H_3). IR (film on NaCl): 3308, 3146, 3085, 2985, 2941, 2248, 1750, 1647, 1591, 1553 cm^{-1}. HRMS (ESI+): *m/z* calcd for $C_{25}H_{32}N_5O_9$ + H^+ $[M+H]^+$ 546.2200, found 546.2197.

_N_-[2-O-(2,3,4,6-Tetra-O-acetyl-β-D-galactopyranosyl)-ethyl-1,2,3-triazol-4-ylmethylamide)-_N_'-propyl-3-aminobenzene-1-carboxamide (2.59)

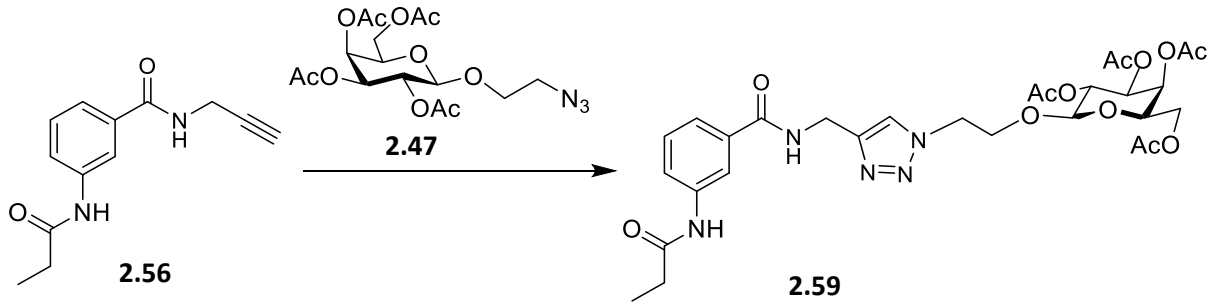

Copper sulphate pentahydrate (10 mg) and sodium ascorbate (20 mg) were added to a solution of **2.47** (71 mg, 0.694 mmol) and **2.56** (39 mg, 0.6307 mmol) in acetone/H_2O (4 mL/ 2mL). The reaction was allowed to stir at room temperature for 16 h. The solvent was removed *in vacuo*. The residue was dissolved in DCM (30 mL), washed with water (20 mL x 3), and dried ($MgSO_4$). The mixture was filtered and the solvent was removed *in vacuo* to yield the crude product, which was purified by silica gel column chromatography (DCM:MeOH 98:2-93:7) to give the pure product **2.59** as an off-white solid (97 mg, 88 %). R_f=0.36 (DCM:MeOH 9:1). $[\alpha]_D^{23}$ -3.1 (c 1, DCM). ^{1}H NMR (500 MHz, $CDCl_3$): δ 8.41 (s, 1H, N*H*COC_2H_5), 7.90 (d, *J* = 8.0 Hz, 1H, Ar-*H*), 7.80 (s, 1H, Ar-*H*), 7.63 (s, 1H, triaz-*H*), 7.56 (t, *J* = 5.1 Hz, 1H, N*H*CH_2-triaz), 7.46 (d, *J* = 7.7 Hz, 1H, Ar-*H*), 7.27 (t, *J* = 8 Hz, 1H, Ar-*H*), 5.34 (dd, *J* = 3.4, 1.0 Hz, 1H, H-4), 5.11 (dd, *J* = 12.5, 6.2 Hz, 1H, H-2), 4.96 (dd, *J* = 10.5, 3.4 Hz, 1H, H-3), 4.69 –4.59 (m, 2H, C*H*$_2$-triaz), 4.56 – 4.44 (m, 2H, C*H*$_2$$CH_2O$), 4.42 (d, J=7.9, 1H, H-1), 4.18 (dt, *J* = 10.5, 4.1 Hz, 1H, C*H*O-Gal), 4.08 (dd, *J* = 11.3, 6.6 Hz, 2H, H-6 and H-6'), 3.95 – 3.85 (m, 2H, C*H*O-Gal and H-5), 2.36 (q, *J* = 7.5 Hz, 2H, C*H*$_2$$CH_3$), 2.09 (s, 3H, OAc), 1.99 (s, 3H, OAc), 1.93 (s, 3H, OAc), 1.90 (s, 3H, OAc), 1.16 (t, *J* = 7.6 Hz, 3H, CH_2C*H*$_3$). ^{13}C NMR (125 MHz, $CDCl_3$): δ 172.8 (*C*OC_2H_5), 170.4 (CO of OAc), 170.2 (CO of OAc), 170.0 (CO of OAc), 169.7 (CO of OAc), 167.3 (*C*O$NHCH_2$-triaz), 144.5 (*C*-triaz), 138.9 (Ar-C), 134.6 (Ar-C), 129.1 (Ar-*C*H), 123.8 (*C*H-triaz), 123.0 (Ar-*C*H), 122.2 (Ar-*C*H), 118.5 (Ar-*C*H), 100.9 (C-1), 70.9 (C-5), 70.6 (C-3), 68.6 (C-2), 67.5 (CH_2*C*H_2O-Gal), 66.9 (C-4), 61.2 (C-6), 50.1 (*C*H_2CH_2O-Gal), 35.5 (*C*H_2-triaz), 30.5 (*C*H_2CH_3), 20.6 (CH_3 of OAc), 20.6 (CH_3 of OAc), 20.6 (CH_3 of OAc), 20.5 (CH_3 of OAc), 9.6 (CH_2*C*H_3). IR (film on NaCl): 3312, 3146, 2980,

2941, 2250, 2111, 1750, 1649, 1591, 1552 cm^{-1}. HRMS (ESI+): *m/z* calcd for $C_{29}H_{37}N_5O_{12}$ + H^+ $[M+H]^+$ 648.2517, found 648.2581.

_N_-(β-D-Galactopyranosyl-1,2,3-triazol-4-ylmethylamide)-_N'_-propyl-3-aminobenzene-1-carboxamide (2.60)

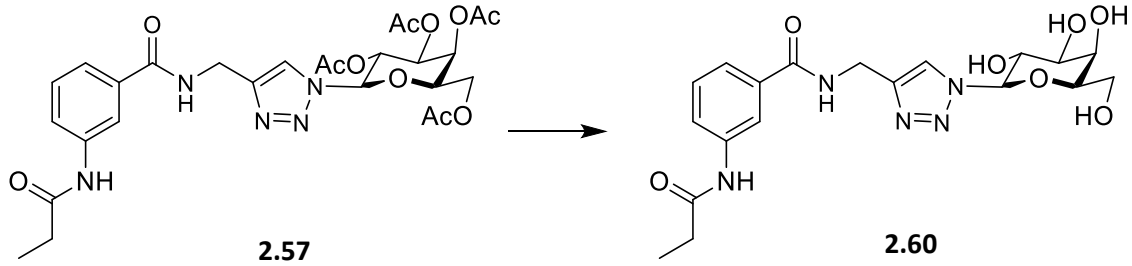

2.57 **2.60**

2.57 (110 mg) was dissolved in methanol/H_2O (4 mL, 2 mL). NEt_3 (0.1 mL) was added, and the reaction mixture was allowed to stir at 45 °C for 6 h. The solution was cooled, Amberlite H^+ was added and the mixture was allowed to stir for 30 mins. The solution was filtered and the solvent was removed *in vacuo*. The residue was dried under high vacuum and lyophilized to give the pure product **2.60** as a fluffy white solid (73 mg, 92 %). $[\alpha]_D^{19}$ +11.6 (c 0.7, H_2O). ^{1}H NMR (500 MHz, D_2O): δ 8.09 (s, 1H, triaz-H), 7.55 (t, *J* = 1.8 Hz, 1H, Ar-H), 7.34 (ddd, *J* = 8.0, 2.1, 1.0 Hz, 1H, Ar-H), 7.32 – 7.29 (m, 1H, Ar-H), 7.21 (t, *J* = 7.9 Hz, 1H, Ar-H), 5.53 (d, *J* = 9.2 Hz, 1H, H-1), 4.48 (s, 2H, C*H*$_2$-triaz), 4.07 (t, *J* = 9.5 Hz, 1H, H-2), 3.93 (dd, *J* = 3.3, 0.6 Hz, 1H, H-4), 3.83 (td, *J* = 6.0, 0.8 Hz, 1H, H-5), 3.72 (dd, *J* = 9.8, 3.3 Hz, 1H, H-3), 3.62 (d, *J* = 6.1 Hz, 2H, H-6 and H-6'), 2.24 – 2.18 (q, *J* = 7.7 Hz, 2H, C*H*$_2$CH$_3$), 0.99 (t, *J* = 7.6 Hz, 3H, CH$_2$C*H*$_3$). ^{13}C NMR (125 MHz, D_2O): δ 176.5 (NH*C*OC$_2$H$_5$), 169.7 (*C*ONHCH$_2$-triaz), 145.0 (*C*-triaz), 137.5 (Ar-C), 133.7 (Ar-C), 129.4 (Ar-*C*H), 124.8 (Ar-*C*H), dos sant5 (Ar-*C*H), 123.1 (*C*H-triaz), 119.8 (Ar-*C*H), 88.2 (C-1), 78.3 (C-5), 72.9 (C-3), 69.8 (C-2), 68.6 (C-4), 60.9 (C-6), 34.9 (*C*H$_2$-triaz), 29.8 (*C*H$_2$CH$_3$), 9.2 (CH$_2$*C*H$_3$). IR (ATR): 3268, 1643, 1588, 1542 cm^{-1}. HRMS (ESI+): *m/z* calcd for $C_{19}H_{26}N_5O_7$ +H^+ $[M+H]^+$ 436.1882, found 436.1826.

***N*-(β-L-Fucopyranosyl-1,2,3-triazol-4-ylmethylamide)-*N*'-propyl-3-aminobenzene-1-carboxamide (2.61)**

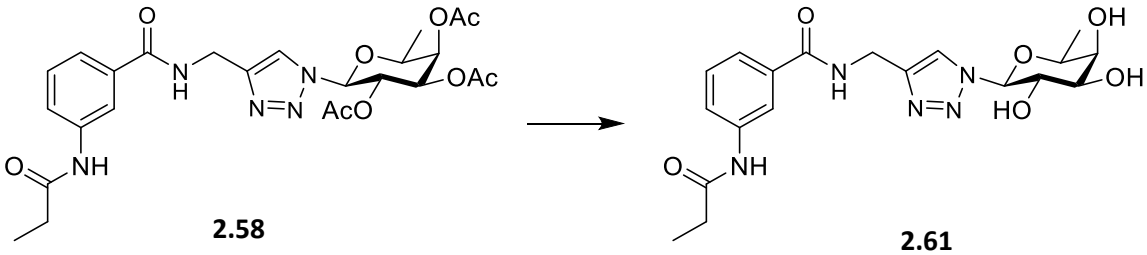

2.58 **2.61**

2.58 (87 mg) was dissolved in methanol/H_2O (4 mL, 2 mL). NEt_3 (0.1 mL) was added, and the reaction mixture was allowed to stir at 45 °C for 6 h. The solution was cooled, Amberlite H^+ was added and the mixture was allowed to stir for 30 mins. The solution was filtered and the solvent was removed *in vacuo*. The residue was dried under high vacuum and lyophilized to give the pure product **2.61** as a yellow solid (63 mg, 94 %). $[\alpha]_D^{23}$ -6.3 (c 0.6, H_2O). ^{1}H NMR (500 MHz, d_6-DMSO): δ 10.02 (s, 1H, N*H*COC_2H_5), 9.01 (t, *J* = 5.6 Hz, 1H, N*H*CH_2-triaz), 8.07 (m, 2H, triaz-H and Ar-H), 7.82 (d, *J* = 8.2 Hz, 1H, Ar-H), 7.56 (d, *J* = 7.7 Hz, 1H, Ar-H), 7.40 (t, *J* = 7.9 Hz, 1H, Ar-H), 5.47 (d, *J* = 9.2 Hz, 1H, H-1), 5.20 (d, *J* = 5.9 Hz, 1H, OH), 4.96 (d, *J* = 5.4 Hz, 1H, OH), 4.67 (d, *J* = 5.7 Hz, 1H, OH), 4.61 – 4.49 (m, 2H, C*H*$_2$-triaz), 3.99 (dd, *J* = 15.0, 9.1 Hz, 1H, H-2), 3.89 (q, *J* = 6.4 Hz, 1H, H-5), 3.56 (m, 2H, H-3 and H-4), 2.36 (q, *J* = 7.6 Hz, 2H, C*H*$_2$$CH_3$), 1.16 (d, *J* = 6.4 Hz, 3H, C6-*H*$_3$), 1.12 (t, *J* = 7.5 Hz, 3H, CH_2C*H*$_3$). ^{13}C NMR (125 MHz, d_6-DMSO): δ 172.6 (*C*OC_2H_5), 166.7 (*C*O$NHCH_2$-triaz), 145.6 (*C*-triaz), 139.9 (Ar-C), 135.3 (Ar-C), 129.1 (Ar-*C*H), 122.3 (Ar-*C*H), 122.0 (Ar-*C*H), 122.0 (*C*H-triaz), 119.0 (Ar-*C*H), 88.5 (C-1), 74.4 (C-3), 73.7 (C-5), 71.6 (C-4), 69.5 (C-2), 35.4 (*C*H_2-triaz), 30.0 (*C*H_2CH_3), 16.9 (C-6), 10.1 (CH_2*C*H_3). IR (KBr): 3401, 2925, 1645, 1589, 1542 cm^{-1}. HRMS (ESI+): *m/z* calcd for $C_{19}H_{25}N_7O_7$ + H^+ $[M+H]^+$ 436.1832, found 436.1849.

***N*-[2-O-(β-D-Galactopyranosyl)-ethyl-1,2,3-triazol-4-ylmethylamide)-*N*'-propyl-3-aminobenzene-1-carboxamide (2.62)**

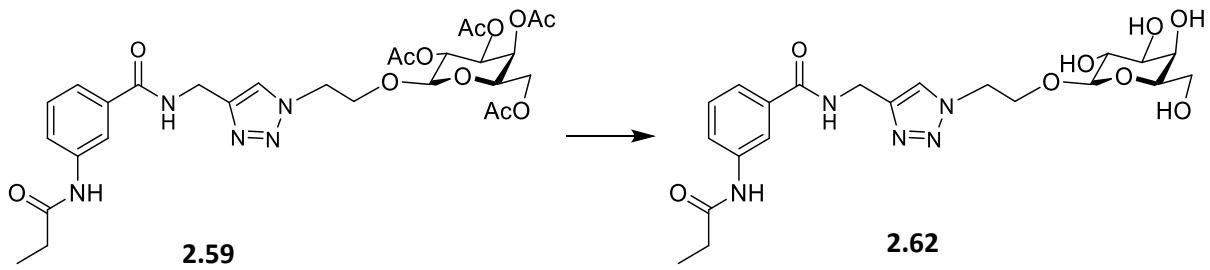

2.59 **2.62**

2.62 (122 mg) was dissolved in methanol/H_2O (4 mL, 2 mL). NEt_3 (0.1 mL) was added, and the reaction mixture was allowed to stir at 45 °C for 6 h. The solution was cooled, Amberlite H^+ was added and the mixture was allowed to stir for 30 mins. The solution was filtered and the solvent was removed *in vacuo*. The residue was dried under high vacuum and lyophilized to give the pure product **2.56** as an off-white solid (104 mg, 87 %). $[\alpha]_D^{24}$ +3.8 (c 1, MeOH). ^{1}H NMR (500 MHz, D_2O): δ 8.00 (s, 1H, triaz-H), 7.75 (s, 1H, Ar-H), 7.56-7.53 (m, 2H, Ar-H), 7.40 (t, *J* = 7.8 Hz, 1H, Ar-H), 4.50-4.46 (m, 4H, C*H*$_2$-triaz and C*H*$_2$CH$_2$), 4.29-4.20 (m, 2H, H-1 and C*H*CH$_2$), 4.15-4.10 (m, 1H, C*H*CH$_2$), 3.89 (s, 1H, H-4), 3.80-3.40 (m, 5H, H-6, H-6', H-2, H-3 and H-5), 2.33 (s, 2H, C*H*$_2$CH$_3$), 1.08 (s, 3H, CH$_2$C*H*$_3$). ^{13}C NMR (125 MHz, D_2O) δ 176.9 (*C*OC$_2$H$_5$), 168.8 (*C*ONHCH$_2$-triaz), 144.4 (*C*-triaz), 137.3 (Ar-C), 134.0 (Ar-C), 130.7 (Ar-*C*H), 127.8 (Ar-*C*H), 126.6 (Ar-*C*H), 125.2 (*C*H-triaz), 122.1 (Ar-*C*H), 103.0 (C-1), 75.1 (C-5), 72.6 (C-3), 70.6 (C-2), 68.5 (C-4), 67.8 (*C*H$_2$CH$_2$), 60.9 (C-6), 50.8 (*C*H$_2$CH$_2$), 34.8 (*C*H$_2$-triaz), 29.8 (*C*H$_2$CH$_3$), 9.3 (CH$_2$*C*H$_3$). IR (KBr): 3400, 2934, 2615, 1648, 1590, 1549 cm^{-1}. HRMS (ESI+): *m/z* calcd for $C_{21}H_{29}N_5O_8$ + H^+ $[M+H]^+$ 480.2094, found 480.2107.

***N,N'*-Di(prop-2-yn-1-yl)-5-propionamidoisophthalamide** (**2.69**)

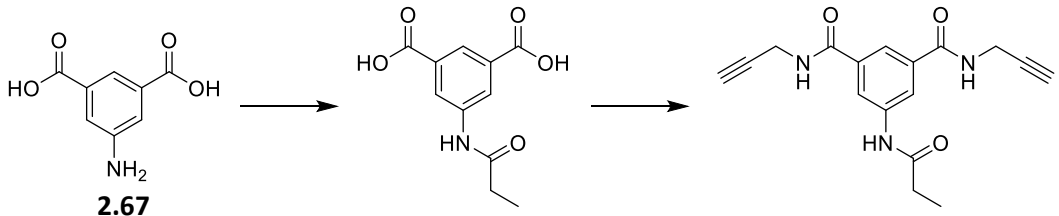

2.67 **2.68** **2.69**

5-aminoisophathalic acid **2.67** (5.00 g, 27.6 mmol) was dissolved in anhydrous THF (60 mL) under N_2 and propionyl chloride (2.7 mL, 30.4 mmol) was added dropwise. The mixture was allowed to stir for 5 min and NEt_3 (5 mL, 35.8 mmol) was added slowly. The reaction was left to stir for 22 h. The solvent was removed under reduced pressure, and the residue was dissolved in hot methanol. The insoluble material was filtered off and the filtrate was concentrated *in vacuo* to give 5-propionoamidoisophthalic acid **2.68**, which was used without further purification (5.03 g, 77 %). 5-propionoamidoisophthalic acid **2.68** (0.78 g, 3.27 mmol) and DMTMM (1.99 g, 7.20 mmol) were suspended in anhydrous DMF (25 mL) under N_2. After 10 min, propargylamine (0.46 mL, 7.2 mmol) was added and the reaction mixture went clear. It was left to stir at rt for 16 h. The reaction mixture was poured

into ice/water (30 mL) and the precipitate formed, which was then filtered and dried in the fume cupboard to give **2.69** as a white amorphous solid (0.79 g, 78%). ^{1}H NMR (500 MHz, d_6-DMSO): δ 10.15 (s, 1H, N*H*COC$_2$H$_5$), 8.94 (t, *J* = 5.3 Hz, 2H, N*H*CH$_2$CCH), 8.18 (s, 2H, Ar-H), 7.93 (s, 1H, Ar-H), 4.11-4.00 (m, 4H, NHC*H*$_2$CCH), 3.13 (s, 2H, NHCH$_2$CC*H*), 2.35 (q, *J* = 7.5 Hz, 2H, *CH*$_2$CH$_3$), 1.10 (t, *J* = 7.5 Hz, 3H, CH$_2$*CH*$_3$). ^{13}C NMR (125 MHz, d_6-DMSO): δ 172.8 (*C*OC$_2$H$_5$), 166.2 (*C*ONHCH$_2$CCH), 140.0 (Ar-*C*), 135.3 (Ar-*C*), 121.4 (Ar-*C*H), 120.7 (Ar-*C*H), 81.6 (CH$_2$*C*CH), 73.4 (CH$_2$C*C*H), 29.1 (*C*H$_2$CH$_3$), 10.0 (CH$_2$*C*H$_3$). IR (KBr): 3289.16, 3241.00, 3093.06, 2977.14, 2116.87, 1682.50, 1570.58 cm^{-1}. HRMS (ESI+): *m/z* calcd for $C_{17}H_{17}N_3O_3$ +H$^+$ [M+H]$^+$ 312.1343, found 312.1361.

_N,N'_-Di-(2,3,4,6-tetra-_O_-acetyl-β-D-galactopyranosyl-1,2,3-triazol-4-ylmethylamide)-_N''_-propyl-5-aminobenzene-1,3-dicarboxamide (2.78)

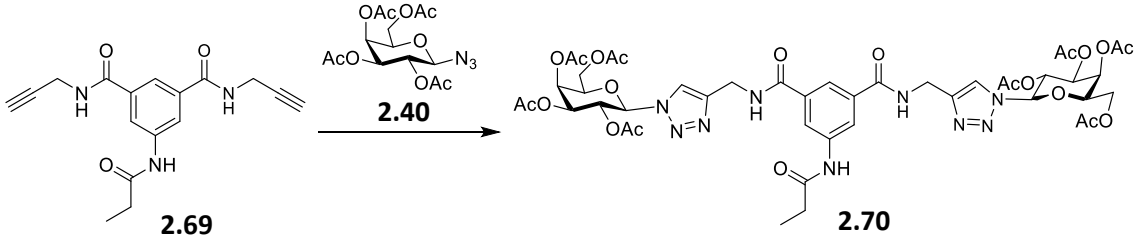

Copper sulphate pentahydrate (40 mg) and sodium ascorbate (80 mg) were added to a solution of **2.40** (534 mg, 1.43 mmol) and **2.69** (212 mg, 0.68 mmol) in CH$_3$CN/H$_2$O (4 mL/ 2mL). The reaction was allowed to stir in the MW at 100 ^{o}C until deemed complete by TLC analysis (10 mins). The solvent was removed *in vacuo*. The residue was dissolved in DCM (30 mL), washed with water (20 mL x 3), and dried (MgSO$_4$). The mixture was filtered and the solvent was removed *in vacuo* to yield the crude product, which was purified by silica gel column chromatography (DCM:MeOH 98:2-93:7) to give the pure product **2.70** as a sticky, yellow solid (608 mg, 84%). R$_f$ = 0.29 (DCM: methanol 9:1). $[\alpha]_D^{21}$ -4.3 (c 0.7, DCM). ^{1}H NMR (500 MHz, CDCl$_3$): δ 9.09 (s, 1H, N*H*COC$_2$H$_5$), 8.21 (s, 2H, N*H*CH$_2$-triaz), 7.97-7.95 (overlapping of 2 s, 4H, Ar-H and triaz-*H*), 7.78 (s, 1H, Ar-H), 5.89 (d, *J* = 9.2 Hz, 2H, H-1), 5.54 (t, *J* = 9.7 Hz, 2H, H-2), 5.49 (d, *J* = 3.2 Hz, 2H, H-4), 5.27 (dd, *J* = 10.3, 3.2 Hz, 2H, H-3), 4.68-4.50 (m, 4H, C*H*$_2$-triaz), 4.29 (t, *J* = 6.5 Hz, 2H, H-5), 4.16 – 4.05 (m, 4H, H-6 and H-6'), 2.30 (q, *J* = 7.5 Hz, 2H, C*H*$_2$CH$_3$), 2.14 (s, 3H, OAc), 1.93 (s, 6H, OAc x 2), 1.76 (s, 3H, OAc), 1.06 (t, *J* =

7.5 Hz, 3H, CH_2CH_3). ^{13}C NMR (125 MHz, $CDCl_3$): δ 173.4 (COC_2H_5), 170.4 (CO of OAc), 170.2 (CO of OAc), 169.9 (CO of OAc), 169.3 (CO of OAc), 166.9 ($CONHCH_2$-triaz), 145.4 (*C*-triaz), 139.1 (Ar-*C*), 134.7 (Ar-*C*), 121.7 (*C*H-triaz), 121.4 (Ar-*C*H), 120.9 (Ar-*C*H), 86.0 (C-1), 73.8 (C-5), 70.8 (C-3), 68.1 (C-2), 67.0 (C-4), 61.2 (C-6), 35.3 (CH_2-triaz), 30.2 (CH_2CH_3), 20.6 (CH_3 of OAc), 20.6 (CH_3 of OAc), 20.5 (CH_3 of OAc), 20.2 (CH_3 of OAc), 9.4 (CH_2CH_3). IR (film on NaCl): 3290, 2979, 2940, 2120, 1753, 1655, 1599, 1536 cm^{-1}. HRMS (ESI+): *m/z* calcd. for $C_{45}H_{56}N_9O_{21}$ $+H^+$ $[M+H]^+$ 1058.3591, found 1058.3602.

_N,N'_-Di-(2,3,4-tri-_O_-acetyl-β-L-fucopyranosyl-1,2,3-triazol-4-ylmethylamide)-_N''_-propyl-5-aminobenzene-1,3-dicarboxamide (2.71)

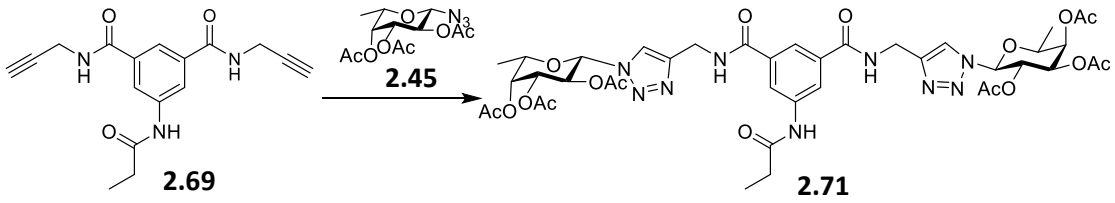

Copper sulphate pentahydrate (20 mg) and sodium ascorbate (40 mg) were added to a solution of **2.45** (106 mg, 0.34 mmol) and **2.69** (50 mg, 0.16 mmol) in CH_3CN/H_2O (4 mL/ 2mL). The reaction was allowed to stir in the MW at 100 ^oC until deemed complete by TLC analysis (10 mins). The solvent was removed *in vacuo*. The residue was dissolved in DCM (30 mL), washed with water (20 mL x 3), and dried ($MgSO_4$). The mixture was filtered and the solvent was removed *in vacuo* to yield the crude product, which was purified by silica gel column chromatography (DCM:MeOH 98:2-93:7) to give the pure product **2.71** as a yellow solid (93 mg, 62 %). R_f=0.44 (DCM:MeOH 9:1). $[\alpha]_D^{19}$ +1.6 (c 0.9, DCM). ^1H NMR (500 MHz, $CDCl_3$): δ 8.37 (s, 1H, N*H*COC_2H_5), 7.97 (s, 2H, triaz-H), 7.94 (s, 2H, Ar-H), 7.83 (t, *J* = 5.1 Hz, 2H, CON*H*CH_2-triaz), 7.70 (s, 1H, Ar-H), 5.84 (d, *J* = 9.2 Hz, 2H, H-1), 5.58 – 5.51 (m, 2H, H-2), 5.38 (d, *J* = 3.3 Hz, 2H, H-4), 5.27 – 5.23 (m, 2H, H-3), 4.74-4.58 (m, 4H, C*H*$_2$-triaz), 4.15 (q, *J* = 6.4 Hz, 2H, H-5), 2.38 (qd, *J* = 7.7, 3.7 Hz, 2H, C*H*$_2$$CH_3$), 2.22 (s, 6H, OAc), 1.99 (s, 6H, OAc), 1.83 (s, 6H, OAc), 1.24 (d, *J* = 6.4 Hz, 6H, C6-*H*$_3$), 1.17 (t, *J* = 7.5 Hz, 3H, CH_2CH_3). ^{13}C NMR (125 MHz, $CDCl_3$): δ 172.8 (NH*C*OC_2H_5), 170.5 (CO of OAc), 169.9 (CO of OAc), 169.4 (CO of OAc), 166.7 (*C*O$NHCH_2$-triaz), 145.5 (*C*-triaz), 139.1 (Ar-C), 135.0 (Ar-C), 121.4 (*C*H-triaz), 121.2 (Ar-*C*H), 120.5 (Ar-*C*H), 86.3 (C-1), 72.8 (C-5), 71.3 (C-

3), 69.9 (C-4), 68.2 (C-2), 35.5 (*C*H_2-triaz), 30.4 (*C*H_2CH_3), 20.7 (CH_3 of OAc), 20.5 (CH_3 of OAc), 20.3 (CH_3 of OAc), 16.1 (C-6), 9.5 (CH_2*C*H_3). IR (film on NaCl): 3318, 2924, 1749, 1656, 1535 cm^{-1}. HRMS (ESI+): *m/z* calcd for $C_{41}H_{51}N_9O_{17}$ + H^+ $[M+H]^+$ 942.9130, found 942.9142.

***N, N'*-Di-[2-O-(2,3,4,6-tetra-*O*-acetyl-β-D-galactopyranosyl)-ethyl-1,2,3-triazol-4-ylmethylamide)-*N''*-propyl-5-aminobenzene-1,3-dicarboxamide (2.72)**

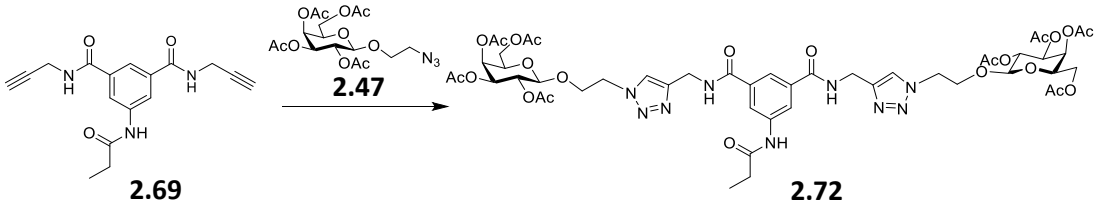

2.69 **2.72**

Copper sulphate pentahydrate (40 mg) and sodium ascorbate (80 mg) were added to a solution of **2.47** (604 mg, 1.45 mmol) and **2.69** (180 mg, 0.58 mmol) in CH_3CN/H_2O (4 mL/ 2mL). The reaction was allowed to stir in the MW at 100 ^oC until deemed complete by TLC analysis (10 mins). The solvent was removed *in vacuo*. The residue was dissolved in DCM (30 mL), washed with water (20 mL x 3), and dried ($MgSO_4$). The mixture was filtered and the solvent was removed *in vacuo* to yield the crude product, which was purified by silica gel column chromatography (DCM:MeOH 98:2-93:7) to give the pure product **2.72** as a sticky, yellow solid (545 mg, 82 %). R_f = 0.38 (DCM:MeOH 9:1). $[\alpha]_D^{25}$ -9.1 (c 1.1, DCM). ^{1}H NMR (500 MHz, $CDCl_3$): δ 9.11 (s, 1H, N*H*COC_2H_5), 8.14 (s, 2H, CON*H*CH_2-triaz), 7.96 (s, 2H, Ar-H), 7.64 (appd, *J* = 16.6 Hz, 3H, Ar-H and triaz-H), 5.30 (d, *J* = 3.2 Hz, 2H, H-4), 5.07 (dd, *J* = 10.3, 8.1 Hz, 2H, H-2), 4.94 (dd, *J* = 10.5, 3.2 Hz, 2H, H-3), 4.66 – 4.36 (m, 10H, C*H*$_2$-triaz and C*H*$_2CH_2O$ and H-1), 4.15 (dd, *J* = 13.6, 6.4 Hz, 2H, C*H*O-Gal), 4.09-4.01 (m, 4H, H-6 and H-6'), 3.88 (ap t, *J* = 6.4 Hz, 4H, C*H*O-Gal and H-5), 2.27 (d, *J* = 7.0 Hz, 2H, C*H*$_2CH_3$), 2.06 (s, 6H, OAc), 1.95 (s, 6H, OAc), 1.89 (appd, *J* = 2.1 Hz, 12H, OAc x 2), 1.03 (t, *J* = 7.3 Hz, 3H, CH_2C*H*$_3$). ^{13}C NMR (125 MHz, $CDCl_3$): δ 173.2 (NH*C*OC_2H_5), 170.4 (CO of OAc), 170.2 (CO of OAc), 170.0 (CO of OAc), 169.7 (CO of OAc), 166.8 (*C*O$NHCH_2$-triaz), 144.7 (*C*-triaz), 139.3 (Ar-*C*), 134.7 (Ar-*C*), 123.6 (*C*H-triaz), 121.1 (Ar-*C*H), 120.2 (Ar-*C*H), 100.8 (C-1), 70.7 (C-5), 70.6 (C-3), 68.5 (C-2), 67.5 (CH_2*C*H_2O), 66.9 (C-4), 61.1 (C-6), 50.00 (*C*H_2CH_2O), 35.5 (*C*H_2-triaz), 30.2 (*C*H_2CH_3), 20.7 (CH_3 of OAc), 20.6 (CH_3 of OAc), 20.6 (CH_3 of OAc), 20.5 (CH_3 of OAc), 9.5 (CH_2*C*H_3). IR (film on NaCl): 3311, 3148, 3071,

2980, 1750, 1656, 1599, 1543 cm^{-1}. HRMS (ESI+): *m/z* calcd for $C_{49}H_{64}N_9O_{23}$ + H^+ $[M+H]^+$ 1146.4115, found 1146.4208.

_N,N'_-Di-(2,3,4,6-tetra-_O_-acetyl-α-D-mannopyranosyl-1,2,3-triazol-4-ylmethylamide)-_N''_-propyl-5-aminobenzene-1,3-dicarboxamide (2.73)

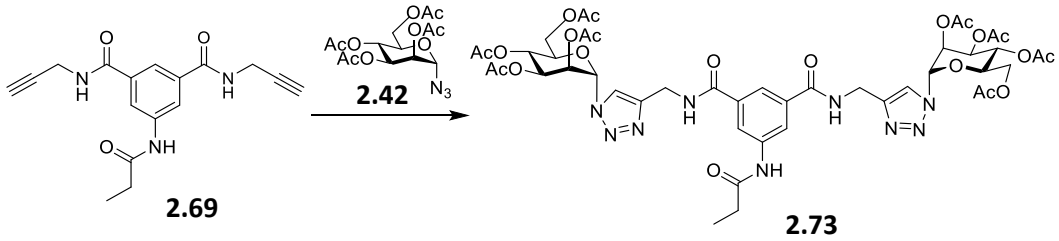

Copper sulphate pentahydrate (20 mg) and sodium ascorbate (40 mg) were added to a solution of **2.42** (67 mg, 0.18 mmol) and **2.69** (27 mg, 0.09 mmol) in CH_3CN/H_2O (4 mL/ 2mL). The reaction was allowed to stir in the MW at 100 ^oC until deemed complete by TLC analysis (10 mins). The solvent was removed *in vacuo*. The residue was dissolved in DCM (30 mL), washed with water (20 mL x 3), and dried ($MgSO_4$). The mixture was filtered and the solvent was removed *in vacuo* to yield the crude product, which was purified by silica gel column chromatography (DCM:MeOH 98:2-93:7) to give the pure product **2.73** as a sticky, yellow solid (110 mg, 82 %).R_f = 0.42 (DCM:MeOH 9:1). $[\alpha]_D^{22}$ +3 (c 1, DCM). ^{1}H NMR (500 MHz, $CDCl_3$): δ 8.93 (s, 1H, N*H*COC_2H_5), 8.23 (s, 2H, N*H*CH_2-triaz), 7.94 (s, 2H, triaz-H), 7.78 (s, 2H, Ar-H), 7.55 (s, 1H, Ar-H), 6.11 (s, 2H, H-1), 5.99 (s, 2H, H-2), 5.90 (d, *J* = 9.8 Hz, 2H, H-3), 5.41 (t, *J* = 9.6 Hz, 2H, H-4), 4.65 –4.54 (m, 4H, C*H*$_2$-triaz), 4.27 (dd, *J* = 12.5, 2.9 Hz, 2H, H-6), 4.05 (dd, *J* = 12.4, 3 Hz, 2H, H-6'), 3.97 (dd, *J* = 6.0, 3.5 Hz, 2H, H-5), 2.48 – 2.33 (m, 4H, C*H*$_2$$CH_3$), 2.17 (d, *J* = 1.2 Hz, 6H, OAc), 2.06 (d, *J* = 1.6 Hz, 6H, OAc), 2.02 – 1.96 (m, 12H, OAc x2), 1.14 (dd, *J* = 9.4, 5.5 Hz, 6H, CH_2C*H*$_3$). ^{13}C NMR (125 MHz, $CDCl_3$): δ 173.5 (*C*OC_2H_5), 170.7 (*C*O of OAc), 170.0 (*C*O of OAc), 169.9 (*C*O of OAc), 169.7 (*C*O of OAc), 166.6 (*C*O$NHCH_2$-triaz), 145.6 (*C*-triaz), 138.9 (Ar-C), 134.4 (Ar-*C*), 123.5 (*C*H-triaz), 121.4 (Ar-*C*H), 120.2 (Ar-*C*H), 84.2 (C-1), 71.8 (C-5), 69.3 (C-3), 68.3 (C-2), 65.6 (C-4), 61.7 (C-6), 35.1 (C*H*$_2$-triaz), 30.3 (*C*H_2CH_3), 20.8 (CH_3 of OAc), 20.7 (CH_3 of OAc), 20.7 (CH_3 of OAc), 20.6 (CH_3 of OAc), 20.4 (CH_3 of OAc), 9.5 (CH_2*C*H_3). IR (film on NaCl): 3429, 2115, 1748, 1646 cm^{-1}. HRMS (ESI+): *m/z* calcd for $C_{45}H_{56}N_9O_{21}$ + H^+ $[M+H]^+$ 1058.3591, found 1058.3593.

_N,N'_-Di-[{4-O-(2,3,4,6-tetra-_O_-acetyl-β-D-galactopyranosyl)-2,3,6-tri-O-acetyl-β-D-glucopyranosyl}-1,2,3-triazol-4-ylmethylamide]-_N''_-propyl-5-aminobenzene-1,3-dicarboxamide (2.74)

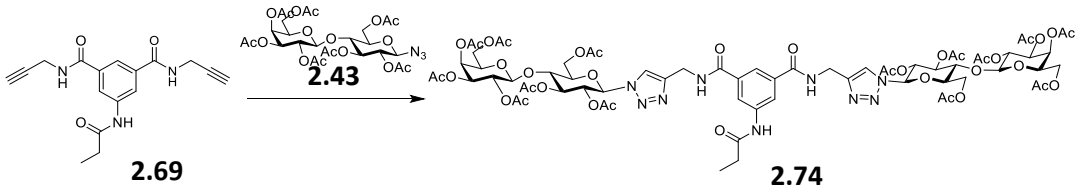

Copper sulphate pentahydrate (20 mg) and sodium ascorbate (40 mg) were added to a solution of **2.43** (62 mg, 0.09 mmol) and **2.69** (14 mg, 0.05 mmol) in CH_3CN/H_2O (4 mL/ 2mL). The reaction was allowed to stir in the MW at 100 ^oC until deemed complete by TLC analysis (10 mins). The solvent was removed *in vacuo*. The residue was dissolved in DCM (30 mL), washed with water (20 mL x 3), and dried ($MgSO_4$). The mixture was filtered and the solvent was removed *in vacuo* to yield the crude product, which was purified by silica gel column chromatography (DCM:MeOH 98:2-93:7) to give the pure product **2.74** as a sticky, yellow solid (102 mg, 72 %). R_f = 0.62 (DCM:MeOH 9:1). $[\alpha]_D^{22}$ +11 (c 1, DCM). ^{1}H NMR (500 MHz, $CDCl_3$): δ 8.55 (s, 1H, N*H*COC_2H_5), 7.93 – 7.84 (m, 6H, N*H*CH_2-triaz, triaz-H and Ar-H), 7.68 (s, 1H, Ar-H), 5.84 (d, *J* = 9.2 Hz, 2H, H-1 Gal), 5.53 – 5.45 (m, 2H, H-2 Gal), 5.40 (dd, *J* = 11.2, 7.2 Hz, 2H, H-3 Gal), 5.35 (dd, *J* = 7.0, 3.5 Hz, 2H, H-4 Glc), 5.11 (dd, *J* = 10.3, 7.9 Hz, 2H, H-2 Glc), 5.02 – 4.96 (m, 2H, H-3 Glc), 4.66-4.60 (m, 4H, C*H*$_2$-triaz), 4.57 (d, *J* = 7.9 Hz, 2H, H-1 Glc), 4.47 (dd, *J* = 11.1, 7.8 Hz, 2H, H-6 Glc), 4.18 – 4.05 (m, 6H, H-6' Glc and H-6 and H-6' Gal), 4.04 – 3.99 (m, 2H, H-4 Gal), 3.93 (dd, *J* = 14.4, 8.4 Hz, 4H, H-5 Gal and H-5 Glc), 2.40 (q, *J* = 7.2 Hz, 2H, C*H*$_2$$CH_3$), 2.19 – 1.92 (m, 42H, OAc x 14), 1.19 (t, *J* = 7.5 Hz, 2H, CH_2C*H*$_3$). ^{13}C NMR (125 MHz, $CDCl_3$): δ 173.1 (*C*OC_2H_5), 170.4 (*C*O of OAc), 170.1 (*C*O of OAc), 170.1 (*C*O of OAc), 169.6 (*C*O of OAc), 169.5 (*C*O of OAc), 169.1 (*C*O of OAc), 166.6 (*C*O$NHCH_2$-triaz), 145.6 (*C*-triaz), 138.9 (Ar-*C*), 134.7 (Ar-*C*), 121.5 (*C*H-triaz), 121.2 (Ar-*C*H), 120.7 (Ar-*C*H), 101.1 (C-1 Glc), 85.5 (C-1 Gal), 76.0 (C-5 Gal), 75.6 (C-4 Gal), 72.6 (C-3 Gal), 70.9 (C-3 Glc), 70.8 (C-2 Gal), 70.7 (C-5 Glc) , 69.1 (C-2 Glc), 66.7 (C-4 Glc), 61.9 (C-6 Glc), 60.8 (C-6 Gal), 35.5 (C*H*$_2$-triaz), 30.4 (*C*H_2CH_3), 20.7 (CH_3 of OAc), 20.6 (CH_3 of OAc), 20.6 (CH_3 of OAc), 20.5 (CH_3 of OAc), 20.4 (CH_3 of OAc), 9.5 (CH_2*C*H_3). IR (film on NaCl): 3293, 2942, 1749, 1656, 1599, 1537 cm^{-1}. HRMS (ESI+): *m/z* calcd for $C_{69}H_{88}N_9O_{37}$ + H^+ $[M+H]^+$ 1634.5281, found 1634.5287.

***N,N'*-Di-(2,3,4,6-tetra-*O*-acetyl-β-D-glucopyranosyl-1,2,3-triazol-4-ylmethylamide)-*N''*-propyl-5-aminobenzene-1,3-dicarboxamide (2.75)**

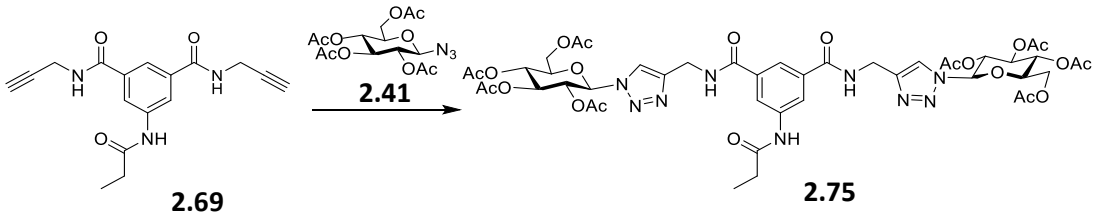

2.69 **2.75**

Copper sulphate pentahydrate (20 mg) and sodium ascorbate (40 mg) were added to a solution of **2.41** (105 mg, 0.28 mmol) and **2.69** (42 mg, 0.13 mmol) in CH_3CN/H_2O (4 mL/ 2mL). The reaction was allowed to stir in the MW at 100 ^oC until deemed complete by TLC analysis (10 mins). The solvent was removed *in vacuo*. The residue was dissolved in DCM (30 mL), washed with water (20 mL x 3), and dried ($MgSO_4$). The mixture was filtered and the solvent was removed *in vacuo* to yield the crude product, which was purified by silica gel column chromatography (DCM:MeOH 98:2-93:7) to give the pure product **2.75** as a sticky, white solid (110 mg, 77 %). R_f = 0.44 (DCM:MeOH 9:1). $[\alpha]_D^{25}$: +17.27˚ (c 1.1, DCM). ^{1}H NMR (500 MHz, $CDCl_3$) δ 8.68 (s, 1H, N*H*COC_2H_5), 8.06 (s, 2H, triaz-H), 7.94 (s, 2H, N*H*CH_2CCH), 7.86 (s, 2H, Ar-H), 7.61 (s, 1H, Ar-H), 5.94 (d, *J* = 9.3 Hz, 2H, H-1), 5.63 (t, *J* = 9.4 Hz, 2H, H-2), 5.42 (t, *J* = 9.5 Hz, 2H, H-3), 5.30 (t, *J* = 9.8 Hz, 2H, H-4), 4.75-4.58 (m, 4H, C*H*$_2$-triaz), 4.33-4.20 (m, 2H, H-6), 4.20-4.05 (m, 4H, H-6' and H-5), 2.37 (d, *J* = 6.6 Hz, 2H, C*H*$_2CH_3$), 2.05 (s, 6H, OAc), 2.00 (s, 6H, OAc), 1.96 (s, 6H, OAc), 1.79 (s, 6H, OAc), 1.16 (t, *J* = 7.2 Hz, 3H, CH_2CH_3). ^{13}C NMR (125 MHz, $CDCl_3$) δ 173.4 (*C*OC_2H_5), 170.5 (*C*O of OAc), 170.0 (*C*O of OAc), 169.4 (*C*O of OAc), 169.2 (*C*O of OAc), 166.9 (*C*O$NHCH_2CCH$), 145.7 (*C*-triaz), 139.1 (Ar-*C*), 134.6 (Ar-*C*), 121.9 (*C*H-triaz), 121.3 (Ar-*C*H), 120.6 (Ar-*C*H), 85.7 (C-1), 75.0 (C-5), 72.8 (C-3), 70.5 (C-2), 67.8 (C-4), 61.7 (C-6), 35.4 (C*H*$_2$-triaz), 30.2 (*C*H_2CH_3), 20.6 (CH_3 of OAc), 20.5 (CH_3 of OAc), 20.1 (CH_3 of OAc), 9.4 (CH_2*C*H_3). ATR: 3595, 3312, 3070, 2943, 1754, 1649, 1543, 1451, 1370, 1231, 1042, 925 cm^{-1}. HRMS (ESI+): m/z calculated for $C_{45}H_{55}N_9O_{21}$ + H^+ [M+H$^+$]: 1058.3531, found 1058.3599.

_N,N'_-Di-(2-Acetamido-2-deoxy-3,4,6-tri-O-acetyl-β-D-galactopyranosyl-1,2,3-triazol-4-ylmethylamide)-_N''_-propyl-5-aminobenzene-1,3-dicarboxamide (2.76)

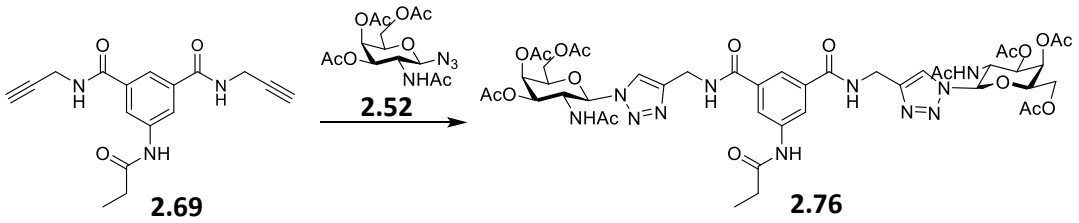

Copper sulphate pentahydrate (20 mg) and sodium ascorbate (40 mg) were added to a solution of **2.52** (286 mg, 0.768 mmol) and **2.69** (140 mg, 0.366 mmol) in CH_3CN/H_2O (4 mL/ 2mL). The reaction was allowed to stir in the MW at 100 ^oC until deemed complete by TLC analysis (10 mins). The solvent was removed *in vacuo*. The residue was dissolved in DCM (30 mL), washed with water (20 mL x 3). A precipitate formed in the aqueous layer, which was filtered to give the pure product **2.76** as an off-white solid (219 mg, 57 %). R_f = 0.24 (DCM:MeOH 9:1). $[\alpha]_D^{25}$ -20.9 (c 1.1, DCM:MeOH 1:1). ^1H NMR (500 MHz, DMSO) δ 10.15 (s, 1H, N*H*COC_2H_5), 9.04 (t, *J* = 5.8 Hz, 2H, N*H*CH_2-triaz), 8.21 (s, 2H, Ar-H), 8.08 – 7.97 (m, 5H, triaz-H, Ar-H and N*H*Ac), 6.02 (d, *J* = 9.9 Hz, 2H, H-1), 5.38 (d, *J* = 3.3 Hz, 2H, H-4), 5.27 (dd, *J* = 10.9, 3.4 Hz, 2H, H-3), 4.62 – 4.44 (m, 8H, H-2, H-5 and C*H*$_2$-triaz), 4.11 (dd, *J* = 11.6, 5.2 Hz, 1H, H-6), 3.98 (dd, *J* = 11.5, 7.1 Hz, 1H, H-6'), 2.35 (q, *J* = 7.5 Hz, 2H, C*H*$_2$$CH_3$), 2.17 (s, 3H, CH_3 of OAc), 1.98 (s, 3H, CH_3 of OAc), 1.93 (s, 3H, CH_3 of OAc), 1.61 (s, 3H, CH_3 of NHAc), 1.10 (t, *J* = 7.5 Hz, 3H, CH_2C*H*$_3$). ^{13}C NMR (125 MHz, DMSO) δ 172.4 (*C*OC_2H_5), 170.0 (CO of OAc), 169.9 (CO of OAc), 169.6 (CO of NHAc), 169.5 (CO of OAc), 166.0 (*C*O$NHCH_2$-triaz), 144.9 (*C*-triaz), 135.0 (Ar-*C*), 134.9 (Ar-*C*), 121.8 (*C*H-triaz), 120.9 (Ar-*C*H), 120.3 (Ar-*C*H), 85.4 (C-1), 72.9 (C-5), 70.3 (C-3), 66.7 (C-4), 61.6 (C-6), 48.3 (C-2), 34.7 (*C*H_2-triaz), 30.0 (*C*H_2CH_3), 22.4 (CH_3 of NHAc), 20.5 (CH_3 of OAc), 20.4 (CH_3 of OAc), 20.3 (CH_3 of OAc), 9.5 (CH_2*C*H_3). ATR: 3315, 1749, 1669, 1548, 1449, 1373, 1237, 1101, 1048, 923, 602 cm^{-1}. HRMS (ESI+): m/z calculated for $C_{45}H_{57}N_{11}O_{19}$ + H^+ [M+H^+]: 1056.3910, found 1056.3906.

_N,N'_-Di-(2-Acetamido-2-deoxy-3,4,6-tri-O-acetyl-β-D-glucopyranosyl-1,2,3-triazol-4-ylmethylamide)-_N''_-propyl-5-aminobenzene-1,3-dicarboxamide (2.77)

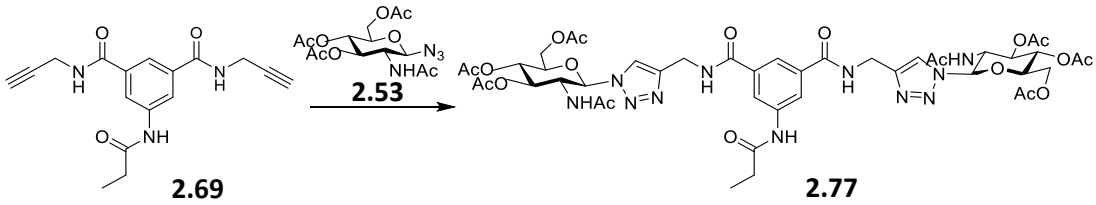

2.69 **2.77**

Copper sulphate pentahydrate (20 mg) and sodium ascorbate (40 mg) were added to a solution of **2.53** (89 mg, 0.23 mmol) and **2.69** (35 mg, 0.11 mmol) in CH_3CN/H_2O (4 mL/ 2mL). The reaction was allowed to stir in the MW at 100 ^oC until deemed complete by TLC analysis (10 mins). The solvent was removed *in vacuo*. The residue was dissolved in DCM (30 mL), washed with water (20 mL x 3), and dried ($MgSO_4$). The mixture was filtered and the solvent was removed *in vacuo* to yield the crude product, which was purified by silica gel column chromatography (DCM:MeOH 98:2-93:7) to give the pure product **2.77** as a yellow solid (60 mg, 42 %). R_f = 0.36 (DCM:MeOH 9:1). $[\alpha]_D^{26}$ -30 (c 0.4, DCM). ^{1}H NMR (500 MHz, d_5-Pyr): δ 10.87 (s, 1H, NH), 9.88 (t, *J* = 5.6 Hz, 2H, NH), 9.74 (d, *J* = 9.0 Hz, 2H, NH), 8.90 (s, 2H, triaz-H), 8.62 (s, 2H, Ar-H), 8.57 (s, 1H, Ar-H), 6.77 (d, *J* = 9.9 Hz, 2H, H-1), 6.06 (t, *J* = 9.6 Hz, 2H, H-3 or 4), 5.61 (t, *J* = 9.7 Hz, 2H, H-2), 5.23 – 5.14 (m, 2H, H-3 or 4), 4.48 (dd, *J* = 12.3, 5.0 Hz, 2H, H-6), 4.38 (d, *J* = 8.2 Hz, 2H, H-5), 4.32 (d, *J* = 12.3 Hz, 2H, H-6'), 2.43 (q, *J* = 7.5 Hz, 2H, CH_2CH_3), 2.10 (s, 3H, OAc), 2.01 (s, 3H, OAc), 1.89 (s, 3H, OAc), 1.72 (s, 3H, OAc), 1.19 (t, *J* = 7.6 Hz, 3H, CH_2CH_3). IR (ATR): 3305, 3078, 2924, 2850, 1743, 1667, 1651, 1529 cm^{-1}. HRMS (ESI+): *m/z* calcd for $C_{45}H_{57}N_{11}O_{19}$ + H^+ $[M+H]^+$ 1056.3910, found 1056.3942.

_N,N'_-Di-(β-D-galactopyranosyl-1,2,3-triazol-4-ylmethylamide)-_N''_-propyl-5-aminobenzene-1,3-dicarboxamide (2.78)

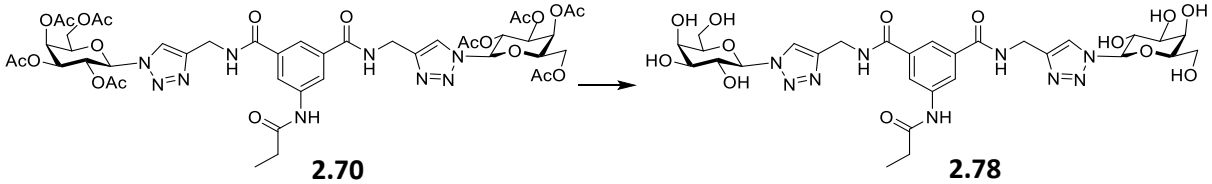

2.70 **2.78**

2.70 (83 mg) was dissolved in methanol/H_2O (4 mL, 2 mL). NEt_3 (0.1 mL) was added, and the reaction mixture was allowed to stir at 45 °C for 6 h. The solution was cooled,

Amberlite H^+ was added and the mixture was allowed to stir for 30 mins. The solution was filtered and the solvent was removed *in vacuo*. The residue was dried under high vacuum and lyophilized to give the pure product **2.78** as a white amorphous solid (60 mg, 94 %). $[\alpha]_D^{25}$ +12.7 (c 0.5, H_2O). ^{1}H NMR (500 MHz, D_2O): δ 8.24 (s, 2H, triaz-H), 7.85 (s, 2H, Ar-H), 7.79 (s, 1H, Ar-H), 5.66 (d, *J* = 8.8 Hz, 2H, H-1), 4.64 (s, 4H, C*H*$_2$-triaz), 4.20 (t, *J* = 9.2 Hz, 2H, H-2), 4.08 (d, *J* = 8.6 Hz, 2H, H-4), 3.97 (s, 2H, H-5), 3.86 (d, *J* = 9.7 Hz, 2H, H-3), 3.75 (d, *J* = 4.7 Hz, 2H, H-6 and H-6'), 2.37 (d, *J* = 7.4 Hz, 2H, C*H*$_2$CH$_3$), 1.12 (t, *J* = 7.3 Hz, 3H, CH$_2$C*H*$_3$). ^{13}C NMR (125 MHz, D_2O): δ 176.8 (*C*OC$_2$H$_5$), 169.0 (*C*ONHCH$_2$-triaz), 145.2 (*C*-triaz), 138.2 (Ar-*C*), 134.6 (Ar-*C*), 123.0 (*C*H-triaz), 122.9 (Ar-*C*H), 122.1 (Ar-*C*H), 88.1 (C-1), 78.3 (C-5), 72.9 (C-3), 69.8 (C-2), 68.6 (C-4), 60.9 (C-6), 35.1 (C*H*$_2$-triaz), 29.9 (*C*H$_2$CH$_3$), 9.2 (CH$_2$*C*H$_3$). IR (KBr): 3368, 2940, 2121, 1649, 1598, 1546 cm^{-1}. HRMS (ESI+): *m/z* calcd. for $C_{29}H_{40}N_9O_{13}$ +H$^+$ [M+H]$^+$ 722.2746, found 722.2730.

_N,N'_-Di-(β-L-fucopyranosyl-1,2,3-triazol-4-ylmethylamide)-_N''_-propyl-5-aminobenzene-1,3-dicarboxamide (2.79)

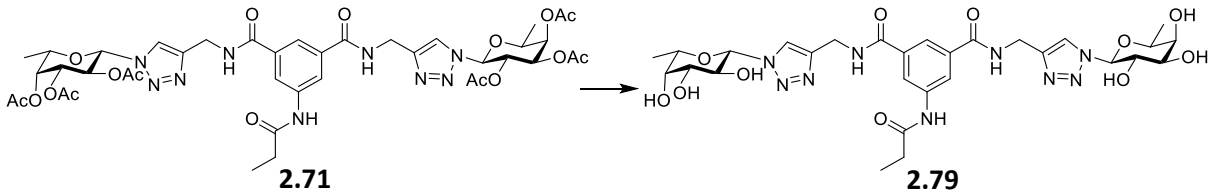

2.71 **2.79**

2.71 (113 mg) was dissolved in methanol/H_2O (4 mL, 2 mL). NEt_3 (0.1 mL) was added, and the reaction mixture was allowed to stir at 45 °C for 6 h. The solution was cooled, Amberlite H^+ was added and the mixture was allowed to stir for 30 mins. The solution was filtered and the solvent was removed *in vacuo*. The residue was dried under high vacuum to give the pure product **2.79** as a pale yellow, sticky solid (76 mg, 92 %). $[\alpha]_D^{23}$ +4.3 (c 0.4, H_2O). ^{1}H NMR (500 MHz, D_2O): δ 8.22 (d, *J* = 4.1 Hz, 2H, triaz-H), 7.88 (d, *J* = 1.5 Hz, 2H, Ar-H), 7.81 (s, 1H, Ar-H), 5.65 – 5.61 (d, *J* = 9.2 Hz, 2H, H-1), 4.65 (s, 4H, C*H*$_2$-triaz), 4.15 (t, *J* = 9.5 Hz, 2H, H-2), 4.08 – 4.02 (m, 2H, H-5), 3.90 – 3.82 (m, 4H, H-3 and H-4), 2.37 (q, *J* = 7.6 Hz, 2H, C*H*$_2$CH$_3$), 1.25 – 1.22 (m, 6H, C6-*H*$_3$), 1.12 (t, *J* = 7.6 Hz, 3H, CH$_2$C*H*$_3$). ^{13}C NMR (125 MHz, D_2O): δ 176.6 (*C*OC$_2$H$_5$), 168.7 (*C*ONHCH$_2$-triaz), 144.8 (*C*-triaz), 138.2 (Ar-C), 134.4 (Ar-C), 123.0 (*C*H-triaz), 122.7 (Ar-*C*H), 121.9 (Ar-*C*H), 88.1 (C-1), 74.4 (C-5), 73.1 (C-3), 71.2 (C-4), 69.5 (C-2), 35.0 (C*H*$_2$-triaz), 29.9

(*C*$H_2$$CH_3$), 15.5 (C-6), 9.1 ($CH_2$*C*$H_3$). IR (ATR): 3261, 2917, 2851, 1646, 1601, 1536 cm^{-1}. HRMS (ESI+): *m/z* calcd for $C_{29}H_{39}N_9O_{11}$ + H^+ $[M+H]^+$ 690.6910, found 690.6923.

_N,N'_-Di-[2-O-(β-D-galactopyranosyl)-ethyl-1,2,3-triazol-4-ylmethylamide)-_N''_-propyl-5-aminobenzene-1,3-dicarboxamide (2.80)

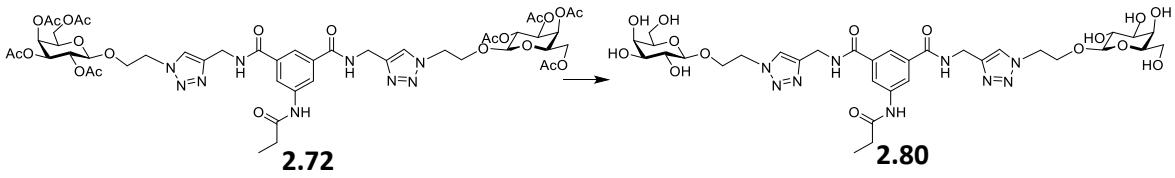

2.72 **2.80**

2.72 (71 mg) was dissolved in methanol/H_2O (4 mL, 2 mL). NEt_3 (0.1 mL) was added, and the reaction mixture was allowed to stir at 45 °C for 6 h. The solution was cooled, Amberlite H^+ was added and the mixture was allowed to stir for 30 mins. The solution was filtered and the solvent was removed *in vacuo*. The residue was dried under high vacuum to give the pure product **2.80** as a pale brown sticky solid (55 mg, 91 %). $[\alpha]_D^{20}$ +2.9 (c 0.3, H_2O). ^{1}H NMR (500 MHz, D_2O): δ 8.10 (s, 2H, triaz-H), 8.00 (d, *J* = 1.5 Hz, 2H, Ar-H), 7.93 (s, 1H, Ar-H), 4.73 – 4.67 (m, 8H, C*H*$_2$-triaz and C*H*$_2$$CH_2$), 4.39 – 4.27 (m, 4H, H-1 and C*H*CH_2), 4.18 – 4.10 (m, 2H, C*H*CH_2), 3.90 (dd, *J* = 3.4, 0.8 Hz, 2H, H-4), 3.77 – 3.68 (m, 4H, H-6 and H-6'), 3.68 – 3.61 (m, 2H, H-5), 3.59 (dd, *J* = 9.9, 3.4 Hz, 2H, H-3), 3.48 (dd, *J* = 10.0, 7.8 Hz, 2H, H-2), 2.47 (q, *J* = 7.6 Hz, 2H, C*H*$_2$$CH_3$), 1.20 (td, *J* = 7.6, 1.6 Hz, 3H, CH_2C*H*$_3$). ^{13}C NMR (125 MHz, D_2O): δ 176.8 (*C*OC_2H_5), 168.8 (*C*ONHCH_2-triaz), 144.3 (*C*-triaz), 138.1 (Ar-C), 134.6 (Ar-C), 124.8 (*C*H-triaz), 123.0 (Ar-*C*H), 122.1 (Ar-*C*H), 103.0 (C-1), 75.1 (C-5), 72.6 (C-3), 70.6 (C-2), 68.5 (C-4), 60.9 (C-6), 35.0 (*C*H_2-triaz), 29.9 (*C*$H_2$$CH_3$), 9.2 ($CH_2$*C*$H_3$). IR (KBr): 3365, 3323, 3117, 3053, 2977, 2942, 2882, 1691, 1651, 1614, 1564 cm^{-1}. HRMS (ESI+): *m/z* calcd for $C_{33}H_{48}N_9O_{15}$ + H^+ $[M+H]^+$ 810.3270, found 810.3322.

_N,N'_-Di-(α-D-mannopyranosyl-1,2,3-triazol-4-ylmethylamide)-_N''_-propyl-5-aminobenzene-1,3-dicarboxamide (2.81)

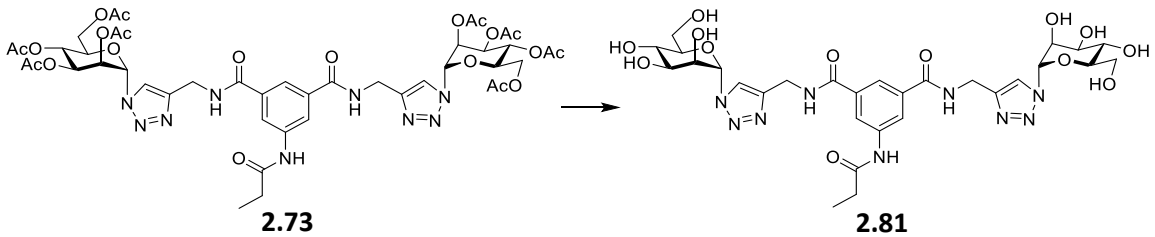

2.73 **2.81**

2.73 (70 mg) was dissolved in methanol/H_2O (4 mL, 2 mL). NEt_3 (0.1 mL) was added, and the reaction mixture was allowed to stir at 45 °C for 6 h. The solution was cooled, Amberlite H^+ was added and the mixture was allowed to stir for 30 mins. The solution was filtered and the solvent was removed *in vacuo*. The residue was dried under high vacuum to give the pure product **2.81** as a pale yellow, sticky solid (42 mg, 88 %). $[\alpha]_D^{22}$ +19.1 (c 0.4, H_2O). ^{1}H NMR (500 MHz, D_2O): δ 8.14 (s, 2H, triaz-H), 7.85 (s, 2H, Ar-H), 7.78 (s, 1H, Ar-H), 6.08 (s, 2H, H-1), 4.75 (s, 2H, H-2), 4.64 (s, 4H, C*H*$_2$-triaz), 4.14 (dd, *J* = 9.0, 3.2 Hz, 2H, H-3), 3.86 – 3.74 (m, 6H, H-4 and H-6 and H-6'), 3.38 – 3.29 (m, 2H, H-5), 2.37 (q, *J* = 7.6 Hz, 2H, C*H*$_2$CH$_3$), 1.12 (t, *J* = 7.6 Hz, 3H, CH$_2$C*H*$_3$). ^{13}C NMR (125 MHz, D_2O): δ 176.4 (*C*OC$_2$H$_5$), 168.5 (*C*ONHCH$_2$-triaz), 145.0 (*C*-triaz), 138.2 (Ar-*C*), 134.4 (Ar-*C*), 123.7 (*C*H-triaz), 122.4 (Ar-*C*H), 121.7 (Ar-*C*H), 86.7 (C-1), 76.2 (C-5), 70.6 (C-3), 68.3 (C-2), 66.6 (C-4), 60.5 (C-6), 35.0 (*C*H$_2$-triaz), 29.9 (*C*H$_2$CH$_3$), 9.1 (CH$_2$*C*H$_3$). IR (KBr): 3375, 2941, 1649, 1555 cm^{-1}. HRMS (ESI+): *m/z* calcd for $C_{29}H_{40}N_9O_{13}$ + H^+ $[M+H]^+$ 722.2746, found 722.2740.

N,N'-Di-[{4-O-(β-D-galactopyranosyl)-β-D-glucopyranosyl}-1,2,3-triazol-4-ylmethylamide]-*N''*-propyl-5-aminobenzene-1,3-dicarboxamide (2.82)

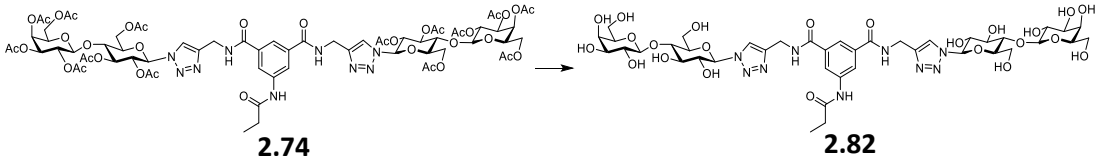

2.74 **2.82**

2.74 (91 mg) was dissolved in methanol/H_2O (4 mL, 2 mL). NEt_3 (0.1 mL) was added, and the reaction mixture was allowed to stir at 45 °C for 6 h. The solution was cooled, Amberlite H^+ was added and the mixture was allowed to stir for 30 mins. The solution was filtered and the solvent was removed *in vacuo*. The residue was dried under high vacuum to give the pure product **2.82** as a white solid (65 mg, 90 %). $[\alpha]_D^{17}$ +1.5 (c 0.6, H_2O). ^{1}H NMR (500 MHz, D_2O): δ 8.16 (s, 2H, triaz-H), 7.91 (s, 2H, Ar-H), 7.84 (s, 1H, Ar-H), 5.72 (d, *J* = 9.2 Hz, 2H, H-1 Glc), 4.64 (s, 4H, C*H*$_2$-triaz), 4.45 (d, *J* = 7.8 Hz, 2H, H-1 Gal), 4.00 (t, *J* = 9.0 Hz, 2H, H-2 Glc), 3.93 – 3.87 (m, 3H, H-6 Glc and H-4 Gal), 3.85 – 3.79 (m, 4H, H-3 Glc, H-4 Glc, H-5 Glc and H-6' Glc), 3.78 – 3.65 (m, 4H, H-6 Gal, H-6' Gal and H-5 Gal), 3.65 – 3.57 (m, 2H, H-3 Gal), 3.56 – 3.49 (m, 2H, H-2 Gal), 2.38 (q, *J* = 7.6 Hz, 1H, C*H*$_2$CH$_3$), 1.12 (dd, *J* = 9.4, 5.8 Hz, 3H, CH$_2$C*H*$_3$). ^{13}C NMR (125 MHz, D_2O): δ 168.8 (*C*ONHCH$_2$-triaz), 145.0 (*C*-triaz), 138.2 (Ar-*C*), 134.4 (Ar-*C*), 123.1

(*C*H-triaz), 122.8 (Ar-*C*H), 102.8 (C-1 Gal), 87.2 (C-1 Glc), 77.6 (C-4/5 Glc), 77.2 (C-4/5 Glc), 75.3 (C-5 Gal), 74.4 (C-3 Glc), 72.4 (C-3 Gal), 71.9 (C-2 Glc), 70.9 (C-2 Gal), 68.5 (C-4 Gal), 61.0 (C-6 Gal), 59.7 (C-6 Glc), 35.0 (C*H*$_2$-triaz), 29.8 (*C*H$_2$CH$_3$), 9.1 (CH$_2$*C*H$_3$). IR (KBr): 3412, 2923, 2125, 1644, 1548 cm^{-1}. HRMS (ESI+): *m/z* calcd for $C_{41}H_{60}N_9O_{23}$ + H$^+$ [M+H]$^+$ 1046.3802, found 1046.2788.

_N,N'_-Di-(β-D-glucopyranosyl-1,2,3-triazol-4-ylmethylamide)-_N''_-propyl-5-aminobenzene-1,3-dicarboxamide (2.83)

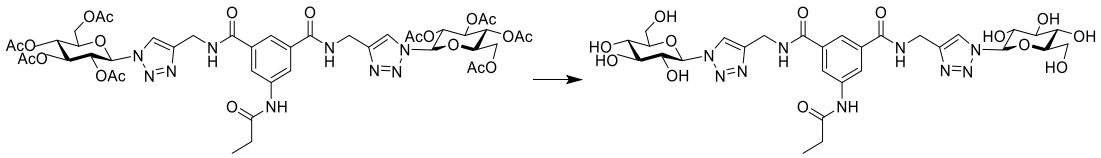

2.75 **2.83**

2.75 (145 mg) was dissolved in methanol/H_2O (4 mL, 2 mL). NEt_3 (0.1 mL) was added, and the reaction mixture was allowed to stir at 45 °C for 6 h. The solution was cooled, Amberlite H$^+$ was added and the mixture was allowed to stir for 30 mins. The solution was filtered and the solvent was removed *in vacuo*. The residue was dried under high vacuum to give the pure product **2.83** as a white solid (95 mg, 96 %). $[\alpha]_D^{20}$ 0.0 (c 0.95, H_2O). ^{1}H NMR (500 MHz, D_2O) δ 8.19 (s, 2H, triaz-H), 7.83 (d, *J* = 1.5 Hz, 2H, Ar-H), 7.76 (d, *J* = 1.4 Hz, 1H, Ar-H), 5.71 (d, *J* = 9.2 Hz, 2H, H-1), 4.62 (s, 4H, C*H*$_2$-triaz), 3.98 (t, *J* = 9.2 Hz, 2H, H-2), 3.87 (d, *J* = 10.7 Hz, 2H, H-6), 3.77 – 3.66 (m, 6H, H-6' and H-4 and H-3), 3.60 (t, *J* = 9.3 Hz, 2H, H-5), 2.38 – 2.32 (m, 2H, C*H*$_2$CH$_3$), 1.12 (t, *J* = 7.6 Hz, 3H, CH$_2$C*H*$_3$). ^{13}C NMR (125 MHz, D_2O) δ 176.4 (*C*OC$_2$H$_5$), 168.5 (*C*ONHCH$_2$CCH), 144.8 (CH$_2$*C*CH), 138.2 (Ar-*C*), 134.3 (Ar-*C*), 123.3 (CH$_2$C*C*H), 122.4 (Ar-*C*H), 121.7 (Ar-*C*H), 87.5 (C-1), 78.9 (C-3/4), 75.9 (C-3/4), 72.3 (C-2), 69.0 (C-5), 60.5 (C-6), 35.0 (C*H*$_2$CCH), 29.9 (*C*H$_2$CH$_3$), 20.4, 9.1 (CH$_2$*C*H$_3$). ATR: 3261, 2922, 1648, 1598, 1542, 1447, 1421, 1335, 1287, 1211, 1098, 1044, 896 cm^{-1}. HRMS (ESI+): m/z calculated for $C_{29}H_{39}N_9O_{13}$ + H$^+$ [M+H$^+$]: 722.2746, found 722.2763.

_N,N'_-Di-(2-Acetamido-2-deoxy-β-D-galactopyranosyl-1,2,3-triazol-4-ylmethylamide)-_N''_-propyl-5-aminobenzene-1,3-dicarboxamide (2.84)

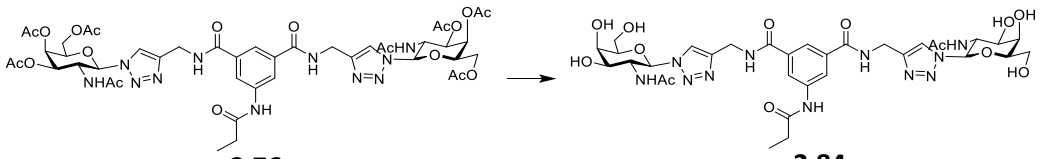

2.76 **2.84**

2.76 (245 mg) was dissolved in methanol/H_2O (4 mL, 2 mL). NEt_3 (0.1 mL) was added, and the reaction mixture was allowed to stir at 45 °C for 6 h. The solution was cooled, Amberlite H^+ was added and the mixture was allowed to stir for 30 mins. The solution was filtered and the solvent was removed *in vacuo*. The residue was dried under high vacuum to give the pure product **2.84** as a white solid (172 mg, 92 %). ^{1}H NMR (500 MHz, D_2O) δ 8.29 (s, 2H, triaz-H), 7.97 (s, 2H, Ar-H), 7.91 (s, 1H, Ar-H), 5.79 (d, *J* = 9.7 Hz, 2H, H-1), 4.68 (s, 4H, C*H*$_2$-triaz), 4.46 (t, *J* = 10.2 Hz, 2H, H-2), 4.13 (d, *J* = 3.1 Hz, 2H, H-4), 4.05 – 3.98 (m, 2H, H-3 and H-5), 3.90 – 3.79 (m, 2H, H-6 and H-6'), 2.44 (q, *J* = 7.6 Hz, 2H, C*H*$_2$CH$_3$), 1.80 (s, 3H, CH_3 of NHAc), 1.18 (t, *J* = 7.6 Hz, 3H, CH_2C*H*$_3$). ^{13}C NMR (125 MHz, D_2O) δ 176.5 (*C*OC_2H_5), 174.3 (*C*O of NHAc), 168.6 (*C*ONHCH_2-triaz), 144.6 (*C*-triaz) 138.2 (Ar-*C*), 134.5 (Ar-*C*), 122.9 (*C*H-triaz), 122.7 (Ar-*C*H), 121.9 (Ar-*C*H), 87.0 (C-1), 78.4 (C-5), 70.6 (C-3), 67.7 (C-4), 61.0 (C-6), 52.0 (C-2), 34.8 (*C*H_2-triaz), 29.8 (*C*H_2CH_3), 21.9 (CH_3 of NHAc), 9.1 (CH_2*C*H_3). HRMS (ESI+): m/z calculated for $C_{33}H_{45}N_{11}O_{13}$ + H^+ [M+H^+]: 804.3277, found 804.3268.

_N,N'_-Di-(2-Acetamido-2-deoxy-β-D-glucopyranosyl-1,2,3-triazol-4-ylmethylamide)-_N''_-propyl-5-aminobenzene-1,3-dicarboxamide (2.85)

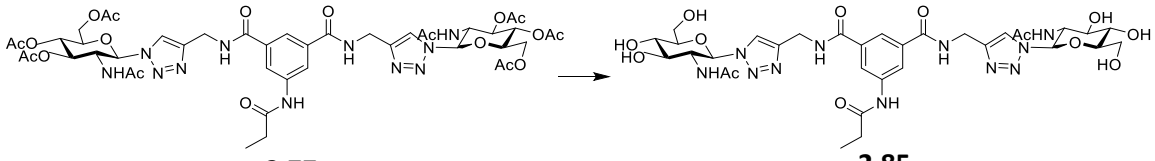

2.77 **2.85**

2.77 (145 mg) was dissolved in methanol/H_2O (4 mL, 2 mL). NEt_3 (0.1 mL) was added, and the reaction mixture was allowed to stir at 45 °C for 6 h. The solution was cooled, Amberlite H^+ was added and the mixture was allowed to stir for 30 mins. The solution was filtered and the solvent was removed *in vacuo*. The residue was dried under high vacuum to give the pure product **2.85** as a pale yellow, sticky solid (34 mg, 75 %).

$[\alpha]_D^{22}$ -5.2 (c 0.3, H_2O). ^{1}H NMR (500 MHz, D_2O): δ 8.20 (s, 2H, triaz-H), 8.01 (t, *J* = 3.9 Hz, 2H, Ar-H), 7.96 – 7.89 (m, 1H, Ar-H), 5.86 (d, *J* = 9.7 Hz, 2H, H-1), 4.72 – 4.66 (m, 4H, C*H*$_2$-triaz), 4.27 (t, *J* = 10.0 Hz, 2H, H-2), 4.01 – 3.64 (m, 10H, H-3, H-4, H-5, H-6 and H-6'), 2.48 (q, *J* = 7.6 Hz, 2H, C*H*$_2$CH$_3$), 1.79 (s, 3H, NHAc), 1.21 (t, *J* = 7.6 Hz, 3H, CH$_2$C*H*$_3$). ^{13}C NMR (126 MHz, D_2O) δ 172.3 (*C*OC$_2$H$_5$), 169.3 (*C*O of NHAc), 165.9 (*C*ONHCH$_2$-triaz), 144.7 (*C*-triaz), 139.5 (Ar-*C*), 134.9 (Ar-*C*), 121.5 (*C*-triaz), 121.0 (Ar-*C*H), 120.2 (Ar-*C*H), 85.9 (C-1), 80.1 (C-5), 74.0 (C-3), 70.0 (C-4), 60.6 (C-6), 54.4 (C-2), 34.8 (*C*H$_2$-triaz), 29.5 (*C*H$_2$CH$_3$), 22.7 (CH$_3$ of NHAc), 9.6 (CH$_2$*C*H$_3$). HRMS (ESI+): *m/z* calcd for $C_{33}H_{45}N_{11}O_{13}$ + Na^+ $[M+Na]^+$ 826.3096, found 826.3102.

2,3,4,6-Tetra-*O*-acetyl-β-D-galactopyranosylamine (2.96)

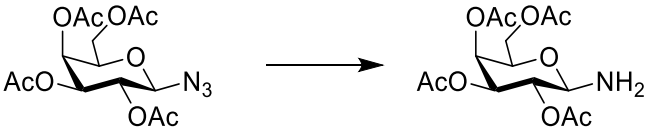

2.40 **2.96**

H_2 gas was bubbled through a suspension of **2.40** (500 mg, 1.339 mmol) and Pd/C (50 mg, 10 % w/w) in EtOAc (20 mL). It was left to stir for 18 h at rt. The mixture was then filtered through celite, which was washed with EtOAc (20 mL). The filtrate was concentrated *in vacuo* to afford product **2.96** as a white, foamy solid which was used without further purification (437 mg, 98 %). ^{1}H NMR (500 MHz, $CDCl_3$) δ 5.21 (d, *J* = 3.5 Hz, 1H, H-4), 4.92 – 4.79 (m, 2H, H-2 and H-3), 4.01 (d, *J* = 8.7 Hz, 1H, H-1), 3.97-3.85 (m, 2H, H-6 and H-6'), 3.77 (t, *J* = 6.7 Hz, 1H, H-5), 2.08 (s, 1H, N*H*$_2$), 1.98 (s, 3H, OAc), 1.90 (s, 3H, OAc), 1.87 (s, 3H, OAc), 1.80 (s, 3H, OAc).

The NMR data is in agreement with the data reported in the literature.[194]

***N,N'*-Di-(2,3,4,6-tetra-*O*-acetyl-β-D-galactopyranosyl)-*N''*-propyl-5-aminobenzene-1,3-dicarboxamide (2.97)**

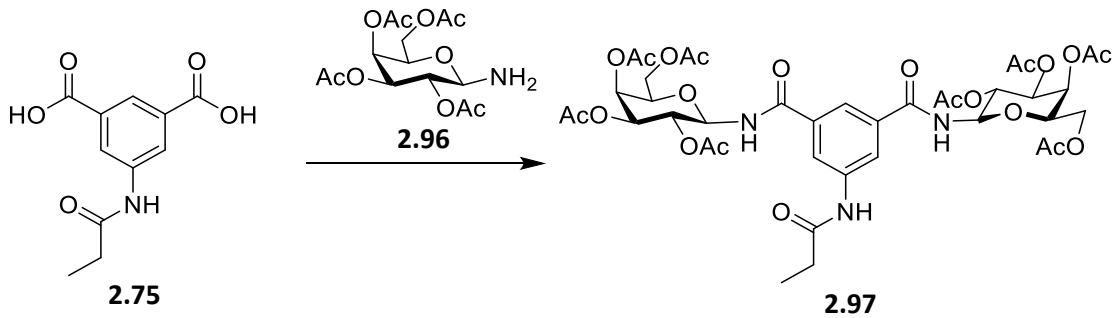

2.75 **2.97**

5-propionamidoisophthalic acid **2.75** (0.133 g, 5.61 mmol) and TBTU (0.396 g, 1.23 mmol) were dissolved in DMF (10 mL) under N_2. NEt_3 (0.312 mL, 2.24 mmol) was added and the mixture was allowed to stir for 15 mins. 2,3,4,6-tetra-*O*-acetyl-β-D-galactopyranosylamine **2.96** (0.487 g, 1.40 mmol) was dissolved in DMF (5 mL) and was added to the reaction mixture. The solution was stirred for 24 h. The crude mixture was dissolved in DCM (30 mL), washed with 0.5 M HCl (30 mL), sat. $NaHCO_3$ (30 mL) and brine (30 mL), and dried ($MgSO_4$). The mixture was filtered and the solvent was removed *in vacuo* to yield the crude product, which was purified by silica gel column chromatography (EtOAc) to give the pure product: sticky yellow solid (343 mg, 68 %). R_f = 0.64 (DCM:MeOH 9:1). $[\alpha]_D^{25}$ -18.1 (c 1.1, DCM).^{1}H NMR (500 MHz, CDCl3): δ 8.41 (s, 1H, NH), 8.23 (s, 2H, Ar-H), 7.86 (s, 1H, Ar-H), 7.54 (d, *J* = 9.1 Hz, 2H, NH), 5.59 (t, *J* = 8.9 Hz, 2H, H-1), 5.47 (d, *J* = 1.5 Hz, 2H, H-4), 5.31–5.29 (m, 4H, H-2 and H-3), 4.20 (t, *J* = 6.6 Hz, 2H, H-5), 4.16–4.05 (m, 4H, H-6 and H6‘), 2.42 (q, *J* = 7.5 Hz, 2H, C*H*$_2$CH$_3$), 2.17 (s, 6 H, CH_3 of OAc), 2.01 (s, 6H, CH_3 of OAc), 1.99 (s, 6H, CH_3 of OAc), 1.97 (s, 6H, CH_3 of OAc), 1.22 (t, *J* = 7.5 Hz, 3H, CH$_2$C*H*$_3$). ^{13}C NMR (125 MHz, $CDCl_3$) δ 172.8 (*C*OC$_2$H$_5$), 171.3 (CO of OAc), 170.5 (CO of OAc), 170.2 (CO of OAc), 170.1 (CO of OAc), 166.2 (*C*ONH-Gal), 139.7 (Ar-*C*), 134.3 (Ar-*C*), 121.9 (Ar-*C*H), 120.7 (Ar-*C*H), 79.0 (C-1), 72.4 (C-5), 71.1 (C-2/C-3), 68.6 (C-2/C-3), 67.4 (C-4), 61.3 (C-6), 30.5 (*C*H$_2$CH$_3$), 20.8 (CH_3 of OAc), 20.7 (CH_3 of OAc), 20.7 (CH_3 of OAc), 20.6 (CH_3 of OAc), 9.4 (CH$_2$*C*H$_3$). IR (film on NaCl): 3338.9, 1750.6, 1602.2, 1535.2, 1370.1, 1228.3, 1083.4, 1052.1, 956.25, 909.15, 802.3 cm^{-1}. HRMS (ESI+): m/z calculated for $C_{39}H_{50}N_3O_{21}$ + H^+ [M+H$^+$]: 896.2931, found 896.2956.

N,N’-Di-(β-D-galactopyranosyl)-*N’’*-propyl-5-aminobenzene-1,3-dicarboxamide (2.98)

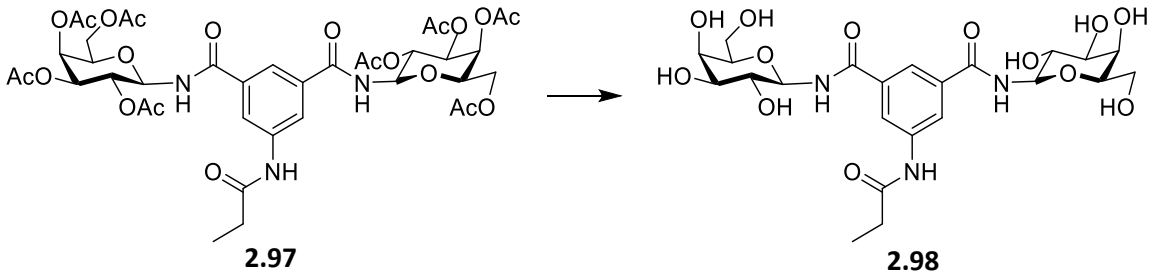

2.97 **2.98**

2.97 (44 mg) was dissolved in methanol/H_2O (4 mL, 2 mL). NEt_3 (0.1 mL) was added, and the reaction mixture was allowed to stir at 45 °C for 6 h. The solution was cooled,

Amberlite H^+ was added and the mixture was allowed to stir for 30 mins. The solution was filtered and the solvent was removed *in vacuo*. The residue was dried under high vacuum to give the pure product **2.98** as a white solid (26 mg, 96 %). $[\alpha]_D^{20}$ +10.0 (c 1, MeOH). ^{1}H NMR (500 MHz, D_2O): δ 8.04 (d, *J* = 1.4 Hz, 2H, Ar-H), 8.03 (d, *J* = 1.5 Hz, 1H, Ar-H), 5.10 (d, *J* = 8.4 Hz, 2H, H-1), 3.97 (d, *J* = 3.0 Hz, 2H, H-4), 3.82 (t, *J* = 6.2 Hz, 2H, H-5), 3.79 – 3.67 (m, 8H, H-2, H-3, H-6, H-6'), 2.47 – 2.37 (m, 2H, C*H*$_2$CH$_3$), 1.19 – 1.11 (m, 3H, CH$_2$C*H*$_3$). ^{13}C NMR (125 MHz, D_2O) δ 176.9 (*C*OC$_2$H$_5$), 170.2 (*C*ONH-Gal), 137.6 (Ar-*C*), 134.4 (Ar-*C*), 124.1 (Ar-*C*H), 123.0 (Ar-*C*H), 80.5 (C-1), 77.0 (C-5), 73.5 (C-3), 69.3 (C-2), 68.7 (C-4), 61.0 (C-6), 29.9 (*C*H$_2$CH$_3$) 9.2 (CH$_2$*C*H$_3$). HRMS (ESI+): *m/z* calcd for $C_{23}H_{34}N_3O_{13}$ + H^+ $[M+H]^+$ 560.2086, found 560.2072.

_N_-2,3,4,6-Tetra-O-acetyl-β-D-mannopyranosyl-1,2,3-triazol-4-ylmethylamide-_N'_-prop-2-yn-1-yl-_N''_-propyl-5-aminobenzene-1,3-dicarboxamide (2.99)

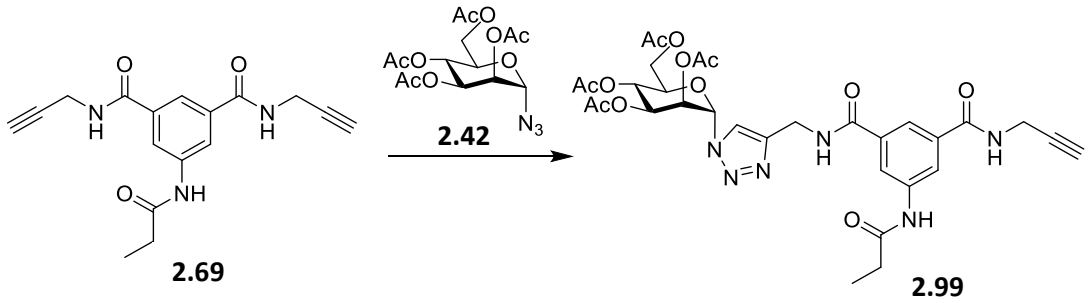

Copper sulphate pentahydrate (20 mg) and sodium ascorbate (40 mg) were added to a solution of **2.42** (131 mg, 0.349 mmol) and **2.69** (435 mg, 1.40 mmol) in acetonitrile/H_2O (7 mL/ 3.5mL). The reaction was allowed to stir in the MW at 100 °C until deemed complete by TLC analysis (10 mins). The solvent was removed *in vacuo*. The crude mixture was purified by silica gel column chromatography (EtOAc:Pet Ether 1:1 2%-5% MeOH) and triturated with hot water to give the pure product **2.99** as a yellow, sticky solid (91 mg, 34 %). R_f = 0.45 (DCM:MeOH 9:1). $[\alpha]_D^{23}$+12.1 (c 0.9, MeOH). ^{1}H NMR (500 MHz, $CDCl_3$): δ 9.15 (s, 1H, N*H*COC$_2$H$_5$), 8.13 (s, 1H, N*H*CH$_2$-triaz), 8.07 (s, 1H, Ar-H), 8.02 (s, 1H, Ar-H), 7.87 (s, 1H, triaz-H), 7.78 (s, 1H, Ar-H), 7.68 (s, 1H, N*H*CH$_2$-triaz), 6.04 (s, 1H, H-1), 5.91 – 5.84 (m, 2H, H-2 and H-3), 5.40 (t, *J* = 9.5 Hz, 1H, H-4), 4.73 – 4.58 (m, 2H, C*H*$_2$-triaz), 4.27 (dd, *J* = 12.5, 4.7 Hz, 1H, H-6), 4.13 (s, 2H, C*H*$_2$CCH), 4.03 (d, *J* = 10.6 Hz, 1H, H-6'), 3.96 – 3.87 (m, 1H, H-5), 2.36 (q, *J* = 7.4 Hz, 2H, C*H*$_2$CH$_3$), 2.19 (d, *J* = 7.6 Hz, 1H, CH$_2$CC*H*), 2.17 (s, 3H, OAc), 2.05 (s, 3H,

OAc), 2.02 (s, 3H, OAc), 2.00 (s, 3H, OAc), 1.11 (t, *J* = 7.5 Hz, 3H, CH_2CH_3). ^{13}C NMR (125 MHz, $CDCl_3$): δ 173.5 (COC_2H_5), 170.6 (*C*O of OAc), 170.0 (*C*O of OAc), 169.7 (*C*O of OAc), 169.6 (*C*O of OAc), 166.8 (*C*ONHCH$_2$-triaz), 166.7 (*C*ONHCH$_2$CCH), 145.4 (*C*-triaz), 139.3 (Ar-*C*), 134.6 (Ar-*C*), 123.4 (*C*H-triaz), 121.4 (Ar-*C*H x 2), 120.7 (Ar-*C*H), 84.0 (C-1), 79.7 (CH_2CCH), 71.9 (C-5), 69.3 (C-2/C-3), 68.3 (C-2/C-3), 65.6 (C-4), 61.7 (C-6), 35.3 (*C*H$_2$-triaz), 30.3 (CH_2CCH), 29.7 (CH_2CH_3), 29.3 (CH_2CCH), 20.8 (CH_3 of OAc), 20.7 (CH_3 of OAc), 20.7 (CH_3 of OAc), 20.6 (CH_3 of OAc), 9.4 (CH_2CH_3). IR (film on NaCl): 3289, 3082, 2981, 1751, 1653, 1598, 1535 cm^{-1}. HRMS (ESI+): *m/z* calcd for $C_{29}H_{39}N_9O_{13}$ + Na^+ $[M+Na]^+$ 744.2565, found 744.2575.

_N_-2,3,4,6-Tetra-_O_-acetyl-β-D-galactopyranosyl-1,2,3-triazol-4-ylmethylamide-_N'_-2,3,4,6-tetra-_O_-acetyl-α-D-mannopyranosyl-1,2,3-triazol-4-ylmethylamide- _N''_-propyl-5-aminobenzene-1,3-dicarboxamide (2.100)

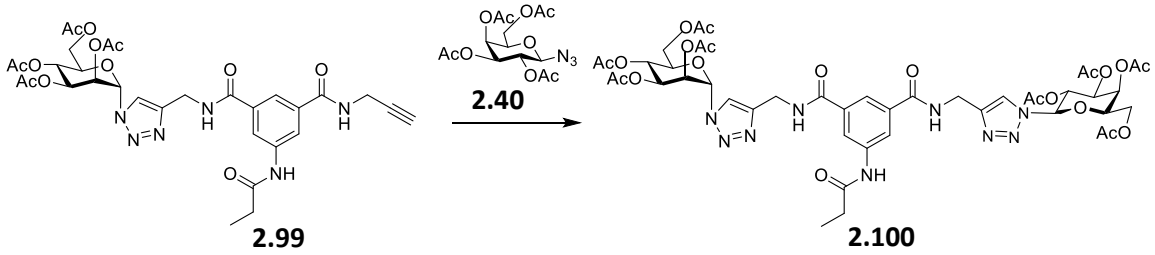

Copper sulphate pentahydrate (20 mg) and sodium ascorbate (40 mg) were added to a solution of **2.40** (50 mg, 0.134 mmol) and **2.99** (77 mg, 0.112 mmol) in acetone/H_2O (4 mL/ 2mL). The reaction was allowed to stir in the MW at 100 ^oC until deemed complete by TLC analysis (10 mins). The solvent was removed *in vacuo*. The residue was dissolve in DCM (30 mL), washed with water (20 mL x 3), and dried ($MgSO_4$). The mixture was filtered and the solvent was removed *in vacuo* to yield the crude product, which was purified by silica gel column chromatography (DCM:MeOH 98:2-93:7) to give the pure product **2.100** as a yellow, sticky solid (100 mg, 84 %). R_f = 0.48 (DCM:MeOH 9:1). $[\alpha]_D^{21}$ +9.0 (c 1, DCM). ^1H NMR (500 MHz, $CDCl_3$): δ 8.89 (s, 1H, NH), 8.20 (s, 1H, NH), 8.14 (s, 2H, triaz-H), 8.02 (m, 3H, Ar-H x 2 and NH), 7.81 (s, 1H, Ar-H), 6.22 (d, *J* = 1.8 Hz, 1H, H-1 Man), 6.12 (dd, *J* = 3.6, 2.0 Hz, 1H, H-2 Man), 6.09 – 6.02 (m, 2H, H-3 Man and H-1 Gal), 5.75 (t, *J* = 9.7 Hz, 1H, H-2 Gal), 5.67 (dd, *J* = 3.3, 0.7 Hz, 1H, H-4 Gal), 5.55 (dd, *J* = 12.5, 6.8 Hz, 1H, H-2 Gal), 5.44 – 5.39 (m, 1H, H-3 Gal), 4.87 – 4.71 (m, 4H, C*H$_2$*-triaz x 2), 4.47 – 4.39 (m, 2H, H-6 Man and H-5 Gal), 4.29

(dd, *J* = 11.5, 6.5 Hz, 2H, H-6 and H-6' Gal), 4.22 – 4.15 (m, 1H, H-6' Man), 4.09 (ddd, *J* = 9.6, 4.4, 2.5 Hz, 1H, H-5 Man), 2.52 (q, *J* = 7.4 Hz, 2H, C*H*$_2$CH$_3$), 2.32 (d, *J* = 4.0 Hz, 6H, OAc x 2), 2.20 (s, 3H, OAc), 2.16 (s, 3H, OAc), 2.14 (s, 3H, OAc), 2.12 (s, 6H, OAc x 2), 1.96 (s, 3H, OAc), 1.28 (t, *J* = 7.5 Hz, 3H, CH$_2$C*H*$_3$). ^{13}C NMR (125 MHz, CDCl$_3$): δ 173.4 (*C*OC$_2$H$_5$), 170.8 (*C*O of OAc), 170.5 (*C*O of OAc), 170.3 (*C*O of OAc), 170.0 (*C*O of OAc), 170.0 (*C*O of OAc), 169.8 (*C*O of OAc), 169.4 (*C*O of OAc), 166.9 (*C*ONHCH$_2$-triaz), 166.8 (*C'*ONHCH$_2$-triaz), 145.8 (*C*-triaz), 145.7 (*C'*-triaz), 139.2 (Ar-C), 134.9 (Ar-*C*), 134.8 (Ar-*C*), 123.6 (Ar-*C*H), 121.6 (*C*H-triaz), 120.7 (Ar-CH), 86.3 (C-1 Gal), 84.2 (C-1 Man), 74.1 (C-5 Gal), 72.0 (C-5 Man), 71.0 (C-3 Gal), 69.4 (C-3 Man), 68.5 (C-2 Man), 68.2 (C-2 Gal), 67.1 (C-4 Gal), 65.8 (C-4 Man), 61.9 (C-6 Man), 61.3 (C-6 Gal), 35.6 (*C*H$_2$-triaz), 35.4 (*C*H$_2$-triaz), 30.5 (*C*H$_2$CH$_3$), 20.9 (CH$_3$ of OAc), 20.8 (CH$_3$ of OAc), 20.8 (CH$_3$ of OAc), 20.8 (CH$_3$ of OAc), 20.7 (CH$_3$ of OAc), 20.4 (CH$_3$ of OAc), 9.6 (CH$_2$*C*H$_3$). IR (film on NaCl): 3311, 3147, 3082, 2981, 1750, 1657, 1599, 1548 cm^{-1}. HRMS (ESI+): *m/z* calcd for $C_{45}H_{56}N_9O_{21}$ + H$^+$ [M+H$^+$]: 1058.3591, found 1058.3607.

_N_-β-D-Galactopyranosyl-1,2,3-triazol-4-ylmethylamide-_N'_-α-D-mannopyranosyl-1,2,3-triazol-4-ylmethylamide)-_N''_-propyl-5-aminobenzene-1,3-dicarboxamide (2.101)

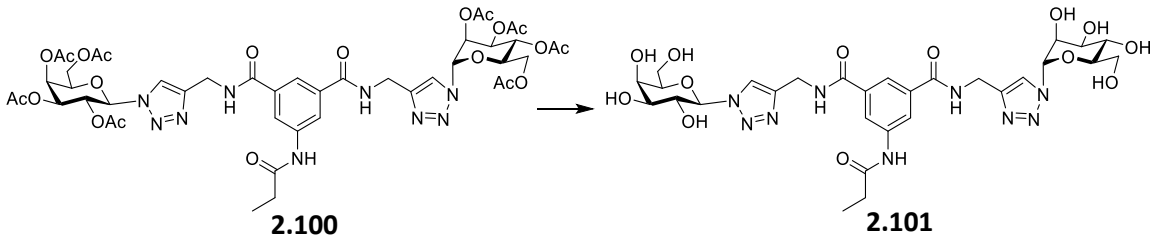

2.100 **2.101**

2.100 (138 mg) was dissolved in methanol/H$_2$O (4 mL, 2 mL). NEt$_3$ (0.1 mL) was added, and the reaction mixture was allowed to stir at 45 °C for 6 h. The solution was cooled, Amberlite H$^+$ was added and the mixture was allowed to stir for 30 mins. The solution was filtered and the solvent was removed *in vacuo*. The residue was dried under high vacuum to give the pure product **2.101** as a pale yellow solid (84 mg, 89 %). $[\alpha]_D^{26}$ +13.1 (c 0.8, H$_2$O). ^{1}H NMR (500 MHz, D$_2$O): δ 8.23 (s, 1H, triaz-H), 8.14 (s, 1H, triaz-H'), 7.85 (s, 1H, Ar-H), 7.83 (s, 1H, Ar-H), 7.77 (s, 1H, Ar-H), 6.07 (d, *J* = 2.2 Hz, 1H, H-1 Man), 5.65 (d, *J* = 9.2 Hz, 1H, H-1 Gal), 4.72 (dd, *J* = 6.4, 3.6 Hz, 1H, H-2 Man), 4.62 (s, 4H, C*H*$_2$-triaz x 2), 4.18 (t, *J* = 9.5 Hz, 1H, H-2 Gal), 4.10 (dd, *J* = 9.0, 3.4 Hz, 1H, H-3 Man), 4.06 (d, *J* = 3.2 Hz, 1H, H-4 Gal), 3.96 (t, *J* = 6.0 Hz, 1H, H-5 Gal), 3.85 (dd, *J* =

9.8, 3.2 Hz, 1H, H-3 Gal), 3.81 – 3.70 (m, 5H, H-4 Man, H-6, H-6' Gal, H-6, H-6' Man), 3.30 (ddd, *J* = 8.9, 5.1, 1.7 Hz, 1H, H-5 Man), 2.35 (q, *J* = 7.6 Hz, 2H, C*H*$_2$CH$_3$), 1.10 (t, *J* = 7.6 Hz, 3H, CH$_2$C*H*$_3$). ^{13}C NMR (125 MHz, D$_2$O): δ 176.3 (*C*OC$_2$H$_5$), 168.4 (*C*ONHCH$_2$-triaz), 144.7 (*C*-triaz x 2), 138.2 (Ar-*C*), 134.2 (Ar-*C*), 123.8 (*C*H-triaz), 123.1 (*C'*H-triaz), 122.3 (Ar-*C*H), 121.7 (Ar-*C*H), 88.2 (C-1 Gal), 86.8 (C-1 Man), 78.3 (C-5 Gal), 76.2 (C-2 Man), 72.9 (C-3 Gal), 70.5 (C-3 Man), 69.8 (C-2 Gal), 68.6 (C-4 Gal), 68.3 (C-2 Man), 66.6 (C-4 Man), 60.9 (C-6 Gal), 60.5 (C-6 Man), 35.0 (*C*H$_2$-triaz), 34.9 (*C*H$_2$-triaz), 29.8 (*C*H$_2$CH$_3$), 9.1 (CH$_2$*C*H$_3$). IR (ATR): 3259, 2922, 2597, 1648, 1600, 1536 cm^{-1}. HRMS (ESI+): *m/z* calcd for C$_{29}$H$_{39}$N$_9$O$_{13}$ + Na$^+$ [M+Na]$^+$ 744.2565, found 744.2575.

***N, N', N''*-Tri(prop-2-yn-1-yl)benzene-1, 3, 5-tricarboxamide (2.103)**

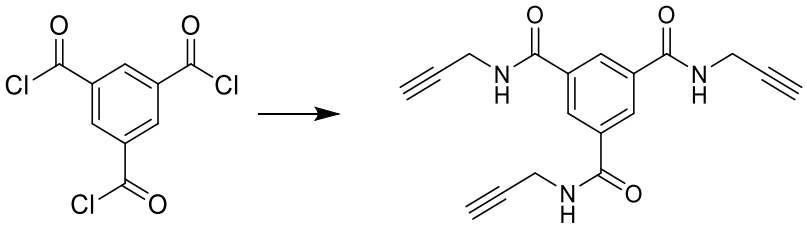

2.102 **2.103**

Benzene-1,3,5-tricarbonyl trichloride **2.102** (1.00 g, 3.76 mmol) was dissolved in anhydrous DCM (10 mL) under N$_2$. A solution of propargylamine (0.84 mL, 13.18 mmol) and NEt$_3$ (1.84 mL, 18.18 mmol) in anhydrous DCM (5 mL) was added to the acid chloride solution. The reaction was cooled on ice. After the addition was complete, the reaction mixture was allowed to stir for 3 h. The product precipitated from the solution. The solvent was removed *in vacuo* and the product was recrystallized from hot ethanol (the crystalline material contained propargyl amine salts). H$_2$O (20 mL) was added and the mixture was stirred for 10 min, it was then filtered to give the pure product **2.103** as a pale yellow solid (532 mg, 44 %). ^{1}H NMR (500 MHz, DMSO) δ 9.23 – 9.15 (m, 3H, NH), 8.46 (s, 3H, Ar-H), 4.11-4.05 (m, 6H, C*H*$_2$CCH), 3.14 (t, *J* = 2.5 Hz, 3H, CH$_2$CC*H*).

The NMR data is in agreement with the data reported in the literature.[233]

***N,N',N''*-Tri-[2-O-(2,3,4,6-tetra-*O*-acetyl-β-D-galactopyranosyl)-ethyl-1,2,3-triazol-4-ylmethylamide)-benzene-1,3,5-tricarboxamide (2.104)**

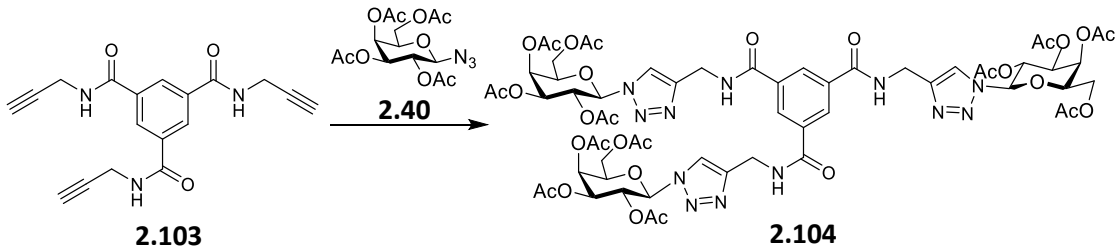

2.103 **2.104**

Copper sulphate pentahydrate (20 mg) and sodium ascorbate (40 mg) were added to a solution of **2.40** (180 mg, 0.482 mmol) and **2.103** (50 mg, 0.156 mmol) in acetone/H_2O (4 mL/ 2mL). The reaction was allowed to stir at room temperature for 16 h. The solvent was removed *in vacuo*. The residue was dissolved in DCM (30 mL), washed with water (20 mL x 3), and dried ($MgSO_4$). The mixture was filtered and the solvent was removed *in vacuo* to yield the crude product, which was purified by silica gel column chromatography (DCM:MeOH 98:2-93:7) to give the pure product **2.104** as an off-white solid (158 mg, 71 %). R_f = 0.42 (DCM:MeOH 9:1). $[\alpha]_D^{18}$ -11.7 (c 1, DCM). ^{1}H NMR (500 MHz, $CDCl_3$): δ 8.20 (s, 3H, Ar-H), 8.05 (t, *J* = 5.3 Hz, 3H, N*H*CH_2-triaz), 8.00 (s, 3H, triaz-H), 5.94 (d, *J* = 9.3 Hz, 3H, H-1), 5.63 (t, *J* = 9.8 Hz, 3H, H-2), 5.54 (d, *J* = 2.7 Hz, 3H, H-4), 5.28 (dd, *J* = 10.3, 3.4 Hz, 3H, H-3), 4.80-4.63 (m, 6H, C*H*$_2$-triaz), 4.31 (t, *J* = 6.8 Hz, 3H, H-5), 4.16 (d, *J* = 7.0 Hz, 4H, H-6 and H-6'), 2.20 (s, 9H, OAc), 2.00 (overlapping of 2 s, 18H, OAc x 2), 1.78 (s, 9H, OAc). ^{13}C NMR (125 MHz, $CDCl_3$): δ 169.3 (CO of OAc), 169.1 (CO of OAc), 168.8 (CO of OAc), 168.2 (CO of OAc), 165.0 (*C*O$NHCH_2$-triaz), 144.4 (*C*-triaz), 133.8 (Ar-*C*), 127.6 (Ar-*C*H), 120.6 (CH-triaz), 85.2 (C-1), 72.9 (C-5), 69.9 (C-3), 67.1 (C-2), 65.9 (C-4), 60.0 (C-6), 34.5 (*C*H_2-triaz), 19.6 (CH_3 of OAc), 19.6 (CH_3 of OAc), 19.5 (CH_3 of OAc), 19.2 (CH_3 of OAc). IR (KBr): 3396, 3147, 2976, 2252, 2113, 1748, 1649, 1548 cm^{-1}. HRMS (ESI+): *m/z* calcd for $C_{60}H_{73}N_{12}O_{30}$ + H^+ $[M+H]^+$ 1441.4556, found 1442.4567.

***N,N',N''*-Tri-(2,3,4,6-tetra-*O*-acetyl-β-D-galactopyranosyl-1,2,3-triazol-4-ylmethylamide)-benzene-1,3,5-tricarboxamide (2.108)**

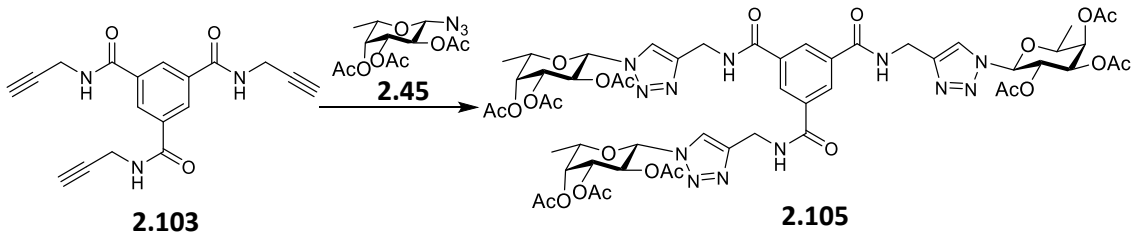

2.103 **2.105**

Copper sulphate pentahydrate (20 mg) and sodium ascorbate (40 mg) were added to a solution **2.45** (52 mg, 0.1638 mmol) and **2.103** (17 mg, 0.0528 mmol) in acetone/H_2O (4 mL/ 2mL). The reaction was allowed to stir at room temperature for 16 h. The solvent was removed *in vacuo*. The residue was dissolved in DCM (30 mL), washed with water (20 mL x 3), and dried ($MgSO_4$). The mixture was filtered and the solvent was removed *in vacuo* to yield the crude product, which was purified by silica gel column chromatography (DCM:MeOH 98:2-93:7) to give the pure product **2.105** as a yellow sticky solid (93 mg, 72 %). $[\alpha]_D^{20}$ +24.7 (c 0.9, DCM). ^{1}H NMR (500 MHz, $CDCl_3$): δ 8.22 (s, 3H, Ar-H), 8.06 (s, 3H, N*H*CH_2-triaz), 8.00 (s, 3H, triaz-H), 5.89 (d, *J* = 9.2 Hz, 3H, H-1), 5.55 (t, *J* = 9.7 Hz, 3H, H-2), 5.36 (d, *J* = 3.0 Hz, 3H, H-4), 5.25 (dd, *J* = 10.2, 3.3 Hz, 3H, H-3), 4.78-4.58 (m, 6H, C*H*$_2$-triaz), 4.17 (q, *J* = 6.2 Hz, 3H, H-5), 2.21 (s, 9H, OAc), 1.98 (s, 9H, OAc), 1.77 (s, 9H, OAc), 1.21 (d, *J* = 6.3 Hz, 9H, C6-H_3). ^{13}C NMR (125 MHz, $CDCl_3$): δ 169.5 (CO of OAc), 168.9 (CO of OAc), 168.2 (CO of OAc), 165.1 (*C*ONHCH_2-triaz), 144.4 (*C*-triaz), 135.4 (Ar-C), 127.7 (Ar-CH), 120.6 (*C*H-triaz), 85.3 (C-1), 71.7 (C-5), 70.2 (C-3), 68.9 (C-4), 67.2 (C-2), 34.4 (*C*H_2-triaz), 19.7 (CH_3 of OAc), 19.6 (CH_3 of OAc), 19.3 (CH_3 of OAc), 15.0 (C-6). IR (KBr): 3411, 2989, 2942, 2115, 1751, 1659, 1537 cm^{-1}. HRMS (ESI+): *m/z* calcd for $C_{52}H_{67}N_{12}O_{20}$ + H^+ $[M+H]^+$ 1179.4595, found 1179.4610.

***N,N',N''*-Tri-(2,3,4,-tri-*O*-acetyl-β-D-fucopyranosyl-1,2,3-triazol-4-ylmethylamide)-benzene-1,3,5-tricarboxamide (2.106)**

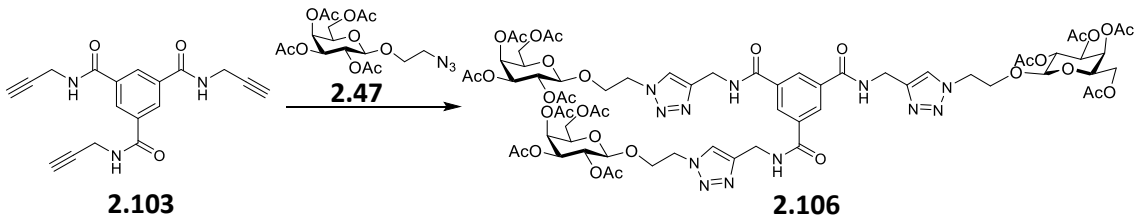

2.103 **2.106**

Copper sulphate pentahydrate (20 mg) and sodium ascorbate (40 mg) were added to a solution of **2.47** (113 mg, 0.27 mmol) and **2.103** (28 mg, 0.087 mmol) in acetone/H_2O (4 mL/ 2mL). The reaction was allowed to stir at room temperature for 16 h. The solvent was removed *in vacuo*. The residue was dissolved in DCM (30 mL), washed with water (20 mL x 3), and dried ($MgSO_4$). The mixture was filtered and the solvent was removed *in vacuo* to yield the crude product, which was purified by silica gel column chromatography (DCM:MeOH 98:2-50:50) to give the pure product **2.106** as an off-white solid (69 mg, 50 %). $[\alpha]_D^{23}$ -5.8 (c 0.7, DCM). ^{1}H NMR (500 MHz, $CDCl_3$): δ 8.22 (s, 3H, N*H*CH_2-triaz), 8.16 (s, 3H, triaz-*H*), 7.67 (s, 3H, Ar-*H*), 5.34 (d, *J* = 3.2 Hz, 3H, H-4), 5.12 (dd, *J* = 10.4, 8.0 Hz, 3H, H-2), 4.98 (dd, *J* = 10.5, 3.4 Hz, 3H, H-3), 4.79 – 4.50 (m, 12H, C*H*$_2$-triaz and C*H*$_2$$CH_2O$), 4.47 (d, *J* = 7.9 Hz, 3H, H-1), 4.28 – 4.18 (m, 3H, C*H*O-Gal), 4.15-4.03 (m, 6H, H-6 and H-6'), 4.00-3.86 (m, 6H, C*H*O-Gal and H-5), 2.11 (s, 9H, OAc), 2.00 (s, 9H, OAc), 1.93 (s, 18H, OAc x 2). ^{13}C NMR (125 MHz, $CDCl_3$): δ 170.4 (CO of OAc), 170.1 (CO of OAc), 170.0 (CO of OAc), 169.7 (CO of OAc), 165.9 (*C*O$NHCH_2$-triaz), 144.7 (*C*-triaz), 134.6 (Ar-C), 128.5 (*C*H-triaz), 123.6 (Ar-*C*H), 100.9 (C-1), 70.6 (C-5), 68.6 (C-3), 67.5 (C-2), 67.0 (CH_2*C*H_2O-Gal), 61.2 (C-4), 50.1 (C-6), 35.5 (*C*H_2-triaz), 20.7 (CH_3 of OAc), 20.6 (CH_3 of OAc), 20.6 (CH_3 of OAc), 20.5 (CH_3 of OAc). IR (film on NaCl): 3391, 2939, 1748, 1661, 1537 cm^{-1}. HRMS (ESI+): *m/z* calcd for $C_{66}H_{84}N_{12}O_{33}$ + H^+ $[M+H]^+$ 1573.5342, found 1574.5422.

***N, N', N''*-Tri-(β-D-galactopyranosyl-1,2,3-triazol-4-ylmethylamide)-benzene-1,3,5-tricarboxamide (2.107)**

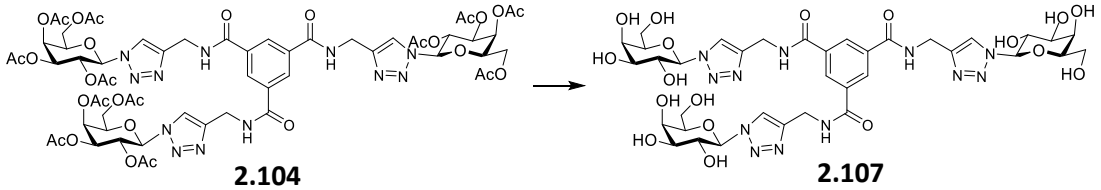

2.104 **2.107**

2.104 (110 mg) was dissolved in methanol/H_2O (4 mL, 2 mL). NEt_3 (0.1 mL) was added, and the reaction mixture was allowed to stir at 45 °C for 6 h. The solution was cooled, Amberlite H^+ was added and the mixture was allowed to stir for 30 mins. The solution was filtered and the solvent was removed *in vacuo*. The residue was dried under high vacuum to give the pure product **2.107** as a sticky yellow solid (63 mg, 89 %). $[\alpha]_D^{23}$ +11.1 (c 0.6, H_2O). ^{1}H NMR (500 MHz, D_2O): δ 8.24 (s, 3H, triaz-*H*), 8.19 (s, 3H, Ar-*H*),

5.65 (d, *J* = 9.2 Hz, 3H, H-1), 4.64 (s, 6H, C*H*$_2$-triaz), 4.19 (t, *J* = 9.5 Hz, 3H, H-2), 4.06 (d, *J* = 3.2 Hz, 3H, H-4), 3.96 (t, *J* = 6.1 Hz, 3H, H-5), 3.85 (dd, *J* = 9.8, 3.3 Hz, 3H, H-3), 3.76-3.72 (m, 6H, H-6 and H-6'). ^{13}C NMR (125 MHz, D_2O): δ 168.1 (*C*ONHCH$_2$-triaz), 144.8 (C-triaz), 134.3 (Ar-*C*), 129.2 (Ar-*C*H), 123.2 (CH-triaz), 88.2 (C-1), 78.3 (C-5), 73.0 (C-3), 69.8 (C-2), 68.6 (C-4), 60.9 (C-6), 35.1 (*C*H$_2$-triaz). IR (KBr): 3402, 1658, 1539, cm^{-1}. HRMS (ESI+): *m/z* calcd for $C_{36}H_{48}N_{12}O_{18}$ + H$^+$ [M+H]$^+$ 937.3288, found 937.3201.

N,N',N''-Tri-(β-L-fucopyranosyl-1,2,3-triazol-4-ylmethylamide)-benzene-1,3,5-tricarboxamide (2.108)

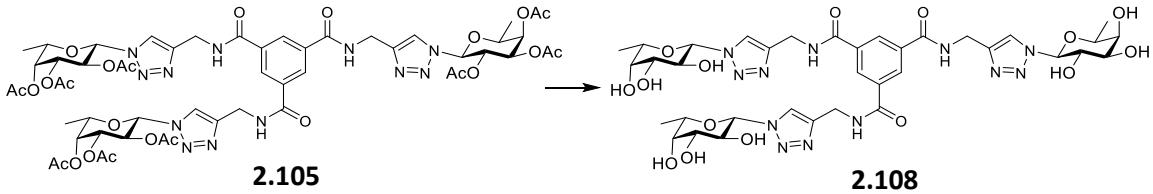

2.105 **2.108**

2.105 (85 mg) was dissolved in methanol/H_2O (4 mL, 2 mL). NEt_3 (0.1 mL) was added, and the reaction mixture was allowed to stir at 45 °C for 6 h. The solution was cooled, Amberlite H$^+$ was added and the mixture was allowed to stir for 30 mins. The solution was filtered and the solvent was removed *in vacuo*. The residue was dried under high vacuum to give the pure product **2.108** as a sticky, yellow solid (53 mg, 88 %). $[\alpha]_D^{21.5}$ -5.6 (c 0.5, H_2O). ^{1}H NMR (500 MHz, D_2O): δ 8.26 (s, 3H, Ar-*H*), 8.25 (s, 3H, triaz-*H*), 5.66 (d, *J* = 9.2 Hz, 3H, H-1), 4.70 (s, 6H, C*H*$_2$-triaz), 4.19 (t, *J* = 9.4 Hz, 3H, H-2), 4.10 – 4.06 (m, 3H, H-5), 3.91 (dd, *J* = 3.4, 0.8 Hz, 3H, H-4), 3.88 (dd, *J* = 9.7, 3.4 Hz, 3H, H-3), 1.28 – 1.26 (m, 9H, C6-*H*$_3$). ^{13}C NMR (125 MHz, D_2O): δ 168.3 (*C*ONHCH$_2$-triaz), 144.9 (*C*-triaz), 134.3 (Ar-*C*), 129.2 (Ar-*C*H), 123.0 (*C*H-triaz), 88.1 (C-1), 74.4 (C-5), 73.1 (C-3), 71.2 (C-4), 69.5 (C-2), 35.1 (*C*H$_2$-triaz), 15.6 (C-6). IR (KBr): 3381, 1659, 1536 cm^{-1}. HRMS (ESI+): *m/z* calcd for $C_{38}H_{54}N_{12}O_{15}$ + Na$^+$ [M+Na]$^+$ 941.3729, found 941.3709.

N, N', N''-Tri-[2-O-(β-D-galactopyranosyl)-ethyl-1,2,3-triazol-4-ylmethylamide)-benzene-1,3,5-tricarboxamide (2.109)

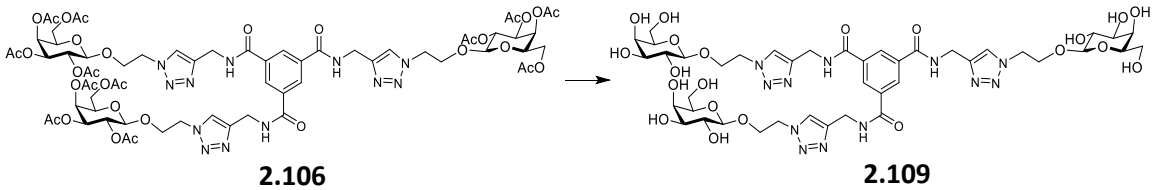

2.106 **2.109**

2.106 (60 mg) was dissolved in methanol/H_2O (4 mL, 2 mL). NEt_3 (0.1 mL) was added, and the reaction mixture was allowed to stir at 45 °C for 6 h. The solution was cooled, Amberlite H^+ was added and the mixture was allowed to stir for 30 mins. The solution was filtered and the solvent was removed *in vacuo*. The residue was dried under high vacuum to give the pure product **2.109** as a pale yellow solid (34 mg, 83 %). $[\alpha]_D^{20}$ +5.9 (c 0.7, H_2O). ^{1}H NMR (500 MHz, D_2O): δ 8.31 (bs, 3H, triaz-H), 8.18 (s, 2H, Ar-H), 8.12 (s, 1H, Ar-H), 4.71 (bs, 6H, C*H*$_2$-triaz), 4.58-4.56 (m, 3H, C*H*CH_2), 4.37 – 4.26 (m, 6H, H-1 and C*H*CH_2), 4.12 (m, 3H, C*H*CH_2), 3.96 – 3.90 (m, 3H, C*H*CH_2), 3.87 (d, *J* = 3.3 Hz, 3H, H-4), 3.76 – 3.68 (m, 6H, H-6 and H-6'), 3.65 – 3.60 (m, 3H, H-5), 3.59-3.56 (m, 3H, H-3), 3.49–3.42 (m, 3H, H-2). ^{13}C NMR (125 MHz, D_2O): δ 167.8 (*C*ONHCH_2-triaz), 143.8 (*C*-triaz), 134.4 (Ar-*C*), 129.3 (*C*H-triaz), 125.3 (Ar-*C*H), 103.0 (C-1), 75.1 (C-5), 72.8 (H-3), 70.6 (C-2), 68.6 (C-4), 67.8 (*C*H_2CH_2), 60.9 (C-6), 51.0 (*C*H_2CH_2), 34.8 (C*H*$_2$-triaz). IR (ATR): 3267, 2931, 1655, 1537 cm^{-1}. HRMS (ESI+): *m/z* calcd for $C_{42}H_{60}N_{12}O_{21}$ + H^+ $[M+H]^+$ 1069.4074, found 1069.4091.

5-[[(1,1-Dimethylethoxy)carbonyl]amino]-1,3-benzenedicarboxylic acid (2.110)

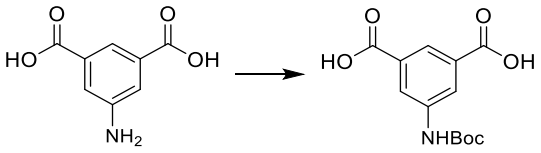

2.67 **2.110**

5-Aminoisophthalic acid **2.67** (1.0 g, 5.5 mmol) was dissolved in aqueous NaOH (1N, 10 mL) at 0 °C. Di-*tert*-butyl dicarbonate (1.32 g, 6.05 mmol) was dissolved in 1,4-dioxane (12 mL), which was added dropwise to the other solution over 2 h. The reaction mixture was stirred at 0-5 °C for 3 h, and then left to stir overnight at room temperature. The reaction mixture was evaporated to half it's original volume *in vacuo* and then cooled in an ice-bath. The solution was acidified to pH 5 with a 20 % aqueous $KHSO_4$ (w/v, 20 g in 100 mL) solution. The precipitated was filtered and washed with water. The product was allowed to dry in the fumehood overnight to give the pure product **2.110** as an off-white solid (1.338 g, 86 %). ^{1}H NMR (500 MHz, DMSO) δ 9.79 (s, 1H, NH), 8.30 (appd, *J* = 1.5 Hz, 2H, Ar-H), 8.08 (appt, *J* = 1.6 Hz, 1H, Ar-H), 1.48 (s, 9H, C(C*H*$_3$)$_3$).

The NMR data is in agreement with the data reported in the literature.[276]

***N,N'*-Di(prop-2-yn-1-yl)-5-[[(1,1-Dimethylethoxy)carbonyl]amino]isophthalamide (2.111)**

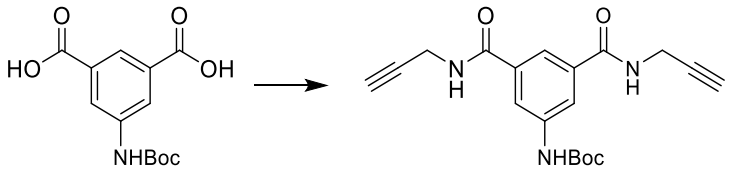

2.110 **2.111**

2.110 (0.5 g, 1.77 mmol) and DMTMM (1.082 g, 3.91 mmol) were suspended in anhydrous THF (20 mL) under N_2. After 10 mins, propargylamine (0.25 mL) was added leaving a cloudy solution. The reaction mixture was allowed to stir for 48 h. Water was added until the solution went clear. The solution was then washed with EtOAc (30 mL x2). The organic layer was concentrated *in vacuo* and the product was purified using column chromatography (Pet Ether:EtOAc 2:1) to give **2.111** as a white solid (0.595 g, 95 %). ^{1}H NMR (500 MHz, DMSO) δ 9.65 (s, 1H, N*H*Boc), 8.90 (t, *J* = 5.6 Hz, 2H, N*H*CH_2CCH), 8.02 (s, 2H, Ar-H), 7.83 (s, 1H, Ar-H), 4.04 (dd, *J* = 5.6, 2.5 Hz, 4H, C*H*$_2$CCH), 3.11 (t, *J* = 2.5 Hz, 2H, CH_2CC*H*), 1.48 (s, 9H, C(C*H*$_3$)$_3$).

The NMR data is in agreement with the data reported in the literature.[277]

***N,N'*-Di-(2,3,4,6-tetra-O-acetyl-β-D-galactopyranosyl-1,2,3-triazol-4-ylmethylamide)-*N''*-tert-tbutoxycarbonyl-5-aminobenzene-1,3-dicarboxamide**

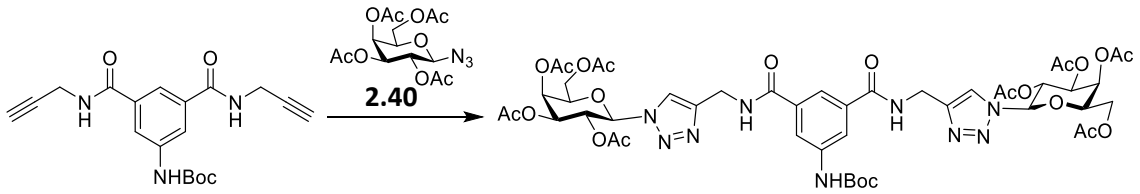

2.111 **2.40** **2.112**

Copper sulphate pentahydrate (60 mg) and sodium ascorbate (120 mg) were added to a solution of **2.40** (1.267 g, 3.39 mmol) and **2.111** (0.574 g, 1.62 mmol) in acetone/H_2O (4 mL/ 2mL). The reaction was allowed to stir at room temperature for 16 h. The solvent was removed *in vacuo*. The residue was dissolved in DCM (30 mL), washed with water (20 mL x 3), and dried ($MgSO_4$). The mixture was filtered and the solvent was removed *in vacuo* to yield the crude product, which was purified by silica gel column chromatography (DCM:MeOH 98:2-93:7) to give the pure product **2.112** white solid (1.255 g, 71 %). R_f = 0.38 (DCM:MeOH 9:1). $[\alpha]_D^{20}$ -6.5 (c 1.1, H_2O). ^{1}H NMR (500 MHz, $CDCl_3$): δ 8.08 (s, 2H, Ar-H), 7.98 – 7.84 (m, 4H, triaz-H and N*H*CH_2-triaz),

7.81 (bs, 2H, Ar-H and N*H*Boc), 5.95 (d, *J* = 9.2 Hz, 2H, H-1), 5.48 (t, *J* = 9.7 Hz, 4H, H-2 and H-4), 5.27 (dd, *J* = 10.3, 3.1 Hz, 2H, H-3), 4.74-4.52 (m, 4H, C*H*$_2$-triaz), 4.31 (t, *J* = 6.4 Hz, 2H, H-5), 4.09 (dd, *J* = 11.5, 6.4 Hz, 4H, H-6 and H-6'), 2.14 (s, 6H, OAc), 1.92 (overlapping of 2 s, 12H, OAc x 2), 1.72 (s, 6H, OAc), 1.41 (s, 9H, Boc). ^{13}C NMR (125 MHz, $CDCl_3$): δ 170.3 (CO of OAc), 170.1 (CO of OAc), 169.8 (CO of OAc), 169.0 (CO of OAc), 166.7 (*C*ONHCH$_2$-triaz), 152.8 (CO of Boc), 145.5 (*C*-triaz), 139.9 (Ar-C), 134.9 (Ar-C), 121.8 (CH$_2$-triaz), 120.5 (Ar-CH), 119.3 (Ar-CH), 86.0 (C-1), 73.8 (C-5), 70.8 (C-3), 68.1 (C-2), 67.0 (C-4), 61.2 (C-6), 35.3 (*C*H$_2$-triaz), 28.2 (CH_3 of Boc), 20.6 (CH_3 of OAc), 20.8 (CH_3 of OAc), 20.5 (CH_3 of OAc), 20.1 (CH_3 of OAc). IR (film on NaCl): 3434, 2106, 1752, 1648, 1558 cm^{-1}. HRMS (ESI+): *m/z* calcd for $C_{47}H_{59}N_9O_{22}$ + H^+ $[M+H]^+$ 1102.3853, found 1102.3847.

N, N'-Di-(2,3,4,6-tetra-O-acetyl-β-D-galactopyranosyl-1,2,3-triazol-4-ylmethylamide)-5-aminobenzene-1,3-dicarboxamide (2.113)

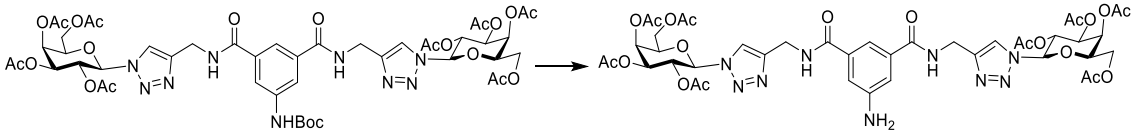

2.112 **2.113**

Compound **2.12** (0.725 g, 0.658 mmol) was dissolved in DCM (5 mL) and was cooled to 0 ^{o}C in an ice-bath. TFA (1.5 mL) was added and the reaction mixture was stirred at rt for 2 h. DCM (40 mL) was added to the reaction mixture, it was washed with sat. $NaHCO_3$ (40 mL) and brine (40 mL), and dried ($MgSO_4$). The mixture was filtered, and the solvent was removed *in vacuo* to yield the product **2.113** which was used without further purification: pale yellow solid (0.689 g, 99 %). R$_f$ = 0.53 (DCM:MeOH 9:1). $[\alpha]_D^{24}$ -4.3 (c 0.9, DCM). ^{1}H NMR (500 MHz, $CDCl_3$): δ 7.95 (s, 4H, triaz-H, N*H*CH$_2$-triaz), 7.43 (s, 1H, Ar-H), 7.17 (s, 2H, Ar-H), 5.96 (d, *J* = 9.2 Hz, 2H, H-1), 5.50 (m, 4H, H-2 and H-4), 5.29 (dd, *J* = 10.3, 3.3 Hz, 2H, H-3), 4.75-4.53 (m, 4H, C*H*$_2$-triaz), 4.32 (t, *J* = 6.5 Hz, 2H, H-5), 4.23 – 4.00 (m, 4H, H-6 and H-6'), 2.16 (s, 6H, OAc), 1.94 (s, 12H, OAc), 1.73 (s, 6H, OAc). ^{13}C NMR (125 MHz, d_6-DMSO) δ 170.5 (CO of OAc), 170.4 (CO of OAc), 169.9 (CO of OAc), 169.0 (CO of OAc), 167.1 (*C*ONHCH$_2$-triaz), 146.1 (C-triaz), 135.6 (Ar-C), 122.8 (CH-triaz), 115.7 (Ar-CH) 113.8 (Ar-CH) 84.7 (C-1), 73.4 (C-5), 71.0 (C-3), 68.1 (C-2), 67.8 (C-4), 62.0 (C-6), 35.1 (*C*H$_2$NH), 21.0 (CH_3 of OAc), 20.9 (CH_3 of OAc), 20.8 (CH_3 of OAc), 20.5 (CH_3 of OAc). IR (film on NaCl): 3434, 2103, 1751, 1642,

1534 cm^{-1}. HRMS (ESI+): *m/z* calcd for $C_{42}H_{51}N_9O_{20}$ + H^+ $[M+H]^+$ 1002.3329, found 1002.3323.

***N, N'*-Di-(β-D-galactopyranosyl-1,2,3-triazol-4-ylmethylamide)-5-(fluorescein-thiourea)-benzene-1,3-dicarboxamide (2.115)**

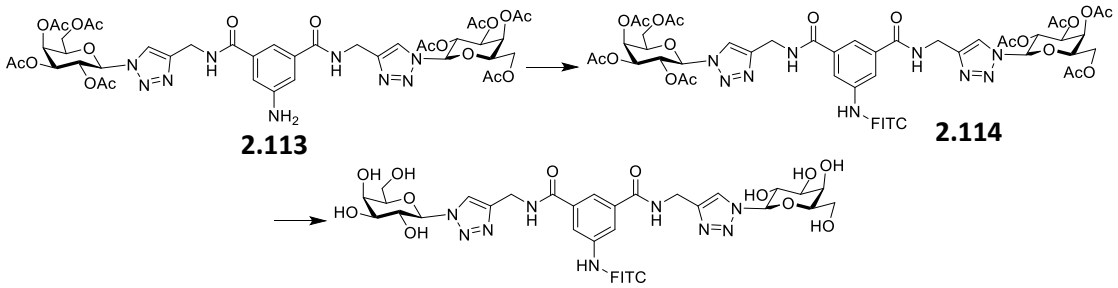

2.113 **2.114** **2.115**

Compound **2.113** (0.087 g, 0.087 mmol) was dissolved in acetone (10 mL). FITC (0.034 g, 0.087 mmol) was added and the reaction mixture was allowed to stir overnight in the dark. Further FITC (0.034 g, 0.087 mmol) was added and the reaction mixture was allowed to stir in the MW at 50 ^oC for 1 h. The solvent was removed *in vacuo* to leave the crude product **2.114**. R_f = 0.47 (DCM:MeOH 8.5:1.5). The crude product was then deprotected. It was dissolved in methanol/H_2O (4 mL, 2 mL). NEt_3 (0.1 mL) was added, and the reaction mixture was allowed to stir at 45 ^oC for 6 h. The solvent was removed *in vacuo*. Crude product was then triturated with chloroform to give product **2.115**. ^1H NMR analysis (Figure 2.32) showed that ~40 % of the product was fluorescently labelled with FITC. HRMS (ESI+): *m/z* calcd for $C_{47}H_{46}N_{10}O_{17}S$ + H^+ $[M+H]^+$ 1055.2841, found 1055.2863.

7.2.2 Experimental Procedures for Chapter 3

***N*'-Di(prop-2-yn-1-yl)terephthalamide (3.13)**

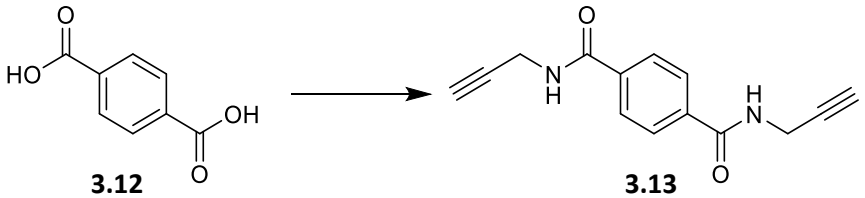

3.12 **3.13**

Terephthalic acid **3.12** (200 mg, 1.204 mmol) and DMTMM (733 mg, 2.649 mmol) were suspended in anhydrous DMF (15 mL) under N_2. Propargylamine (0.169 mL, 2.649 mmol) was added to the reaction mixture, which went clear upon addition. The

reaction was allowed to stir for 16 h. The reaction mixture was poured into ice/water (20 mL). The resulting precipitate was filtered and washed with cold water. The pure product was allowed to dry overnight in the fume cupboard to give the pure product **3.13** as a white solid (234 mg, 81 %). ^{1}H NMR (500 MHz, DMSO) δ 9.05 (t, *J* = 5.5 Hz, 2H, N*H*), 7.93 (s, 4H, Ar-H), 4.07 (dd, *J* = 5.5, 2.5 Hz, 4H, C*H*$_2$CCH), 3.13 (t, *J* = 2.5 Hz, 2H, CH$_2$CC*H*). ^{13}C NMR (125 MHz, DMSO) δ 165.8 (CO), 136.7 (Ar-*C*), 127.8 (Ar-*C*H), 81.6 (CH$_2$*C*CH), 73.5 (CH$_2$C*C*H), 29.0 (*C*H$_2$CCH). IR (ATR): 3278, 3237, 1619, 1534, 1493, 1439, 1352, 1309, 1279, 1224, 1160, 1063, 991, 710 cm^{-1}. HRMS (ESI+): m/z calculated for $C_{14}H_{12}N_2O_2$ + Na^+ [M+Na^+]: 263.0796, found 263.0795.

N, N'-Di-(2,3,4,6-tetra-*O*-acetyl-β-D-galactopyranosyl-1,2,3-triazol-4-ylmethylamide)-terephthalamide (3.14)

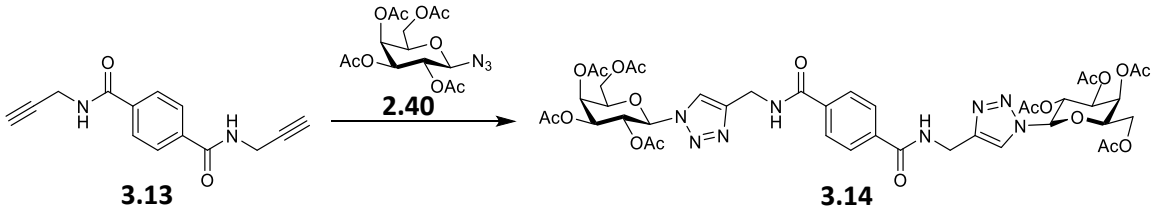

Copper sulphate pentahydrate (20 mg) and sodium ascorbate (40 mg) were added to a solution of **2.40** (187 mg, 0.501 mmol) and **3.13** (55 mg, 0.229 mmol) in CH$_3$CN/H$_2$O (4 mL/ 2 mL). The reaction was allowed to stir in the MW at 100 ^{o}C until deemed complete by TLC analysis (10 min). The solvent was removed *in vacuo*. The residue was dissolved in DCM (30 mL), washed with water (20 mL x 3), and dried (MgSO$_4$). The mixture was filtered and the solvent was removed *in vacuo* to yield the crude product, which was purified by silica gel column chromatography (DCM:MeOH 98:2-95:5) to give the pure product **3.14** as an off-white solid (164 mg, 73 %). R$_f$= 0.36 (DCM:MeOH 9:1). $[\alpha]_D^{24}$ -10.9 (c 1.1, DCM). ^{1}H NMR (500 MHz, CDCl$_3$) δ 7.95 (s, 2H, triaz-H), 7.83 (s, 4H, Ar-H), 7.34 – 7.27 (m, 2H, N*H*CH$_2$-triaz), 5.85 (d, *J* = 9.3 Hz, 2H, H-1), 5.58 – 5.51 (m, 4H, H-2 and H-4), 5.27 (dd, *J* = 10.3, 3.4 Hz, 2H, H-3), 4.82 – 4.64 (m, 4H, C*H*$_2$-triaz), 4.28 – 4.23 (m, 2H, H-5), 4.20-4.10 (m, 4H, H-6 and H-6'), 2.22 (s, 6H, OAc), 2.03 (s, 6H, OAc), 2.01 (s, 6H, OAc), 1.86 (s, 6H, OAc). ^{13}C NMR (125 MHz, CDCl$_3$) δ 170.3 (CO of OAc), 170.0 (CO of OAc), 169.8 (CO of OAc), 169.0 (CO of OAc), 166.6 (*C*ONH), 145.1 (*C*-triaz), 136.7 (Ar-C), 127.4 (Ar-*C*H), 121.3 (*C*H-triaz), 86.3 (C-1), 74.1 (C-5), 70.7 (C-3), 68.1 (C-2/C-4), 66.8 (C-2/C-4), 61.2 (C-6), 35.4 (*C*H$_2$-triaz),

20.7 (CH_3 of OAc), 20.6 (CH_3 of OAc), 20.5 (CH_3 of OAc), 20.2 (CH_3 of OAc). IR (ATR): 3380, 1743, 1644, 1533, 1495, 1431, 1368, 1212, 1046, 923 cm^{-1}. HRMS (ESI+): m/z calculated for $C_{42}H_{50}N_8O_{20}$ + Na^+ [M+Na^+]: 1009.3039, found 1009.3032.

***N, N'*-Di-(β-D-galactopyranosyl-1,2,3-triazol-4-ylmethylamide)-terephthalamide (3.15)**

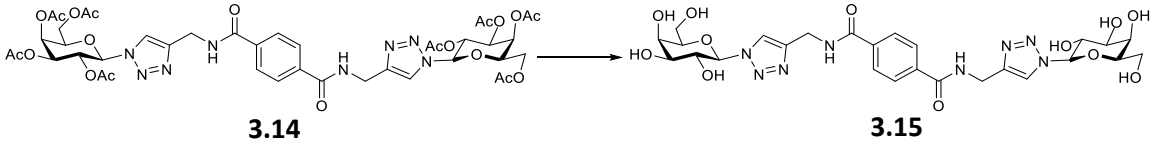

3.14 **3.15**

3.14 (100 mg, 0.101 mmol) was dissolved in methanol/H_2O (4 mL, 2 mL). NEt_3 (0.1 mL) was added, and the reaction mixture was allowed to stir at 45 ^oC for 6 h. The solution was cooled, Amberlite H^+ was added and the mixture was allowed to stir for 30 mins. The solution was filtered, and the solvent was removed *in vacuo*. Excess NEt_3 was removed using the Schlenk line. The product was freeze-dried over night to yield the pure product **3.15** as a white solid (59 mg, 90 %). $[\alpha]_D^{23}$ +13.8 (c 0.8, H_2O). ^1H NMR (500 MHz, D_2O) δ 8.15 (s, 2H, triaz-H), 7.54 (s, 4H, Ar-H), 5.56 (d, *J* = 9.2 Hz, 2H, H-1), 4.47 (s, 4H, C*H*$_2$-triaz), 4.11 (t, *J* = 9.5 Hz, 2H, H-2), 3.96 (d, *J* = 3.2 Hz, 2H, H-4), 3.85 (t, *J* = 6.1 Hz, 2H, H-5), 3.76 (dd, *J* = 9.8, 3.3 Hz, 2H, H-3), 3.64 (d, *J* = 6.2 Hz, 4H, H-6 and H-6'). ^{13}C NMR (125 MHz, D_2O) δ 168.9 (CO), 144.6 (*C*-triaz), 135.9 (Ar-C), 127.4 (Ar-*C*H), 123.2 (*C*H-triaz), 88.2 (C-1), 78.3 (C-5), 72.9 (C-3), 69.8 (C-2), 68.6 (C-4), 60.9 (C-6), 34.8 (*C*H_2-triaz). IR (film on NaCl): 3290, 1636, 1542, 1498, 1293, 1091, 1053, 890 cm^{-1}. HRMS (ESI+): m/z calculated for $C_{26}H_{34}N_8O_{12}$ + Na^+ [M+Na^+]: 673.2194, found 673.2206.

3,4-Di-(prop-2-yn-1-ylamino)cyclobut-3-ene-1,2-dione (3.16)

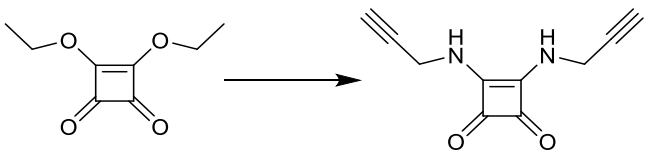

3.2 **3.16**

Ethyl squarate **3.2** (0.2 mL, 1.35 mmol), propargylamine (0.18 mL, 2.8 mmol) and triethylamine (0.75 mL, 5.4 mmol) were allowed to stir in ethanol (2 mL) for 16 h at room temperature. A precipitate formed, which was filtered using a sintered glass funnel, washed with ethanol and allowed to dry to give the pure product **3.16** in

quantitative yield as a pale yellow solid (254 mg). ^{1}H NMR (500 MHz, DMSO) δ 7.79 (s, 2H, N*H*), 4.34 (d, *J* = 3.8 Hz, 4H, C*H*$_2$CCH), 3.36 (t, *J* = 2.5 Hz, 2H, CH$_2$CC*H*). ^{13}C NMR (125 MHz, DMSO) δ 183.26 (CO), 167.84 (C=C), 81.03 (CH$_2$*C*CH), 75.71 (CH$_2$C*C*H), 33.23 (*C*H$_2$CCH). IR (ATR): 3280, 3149, 2922, 1801, 1648, 1551, 1472, 1415, 1343, 1298, 1272, 1132, 972, 915, 827, 747, 670 cm^{-1}. HRMS (ESI+): m/z calculated for $C_{10}H_8N_2O_2$ + Na$^+$ [M+Na$^+$]: 211.0483, found 211.0479.

3,4-Di-(2,3,4,6-tetra-*O*-acetyl-β-D-galactopyranosyl-1,2,3-triazol-4-ylmethylamino)cyclobut-3-ene-1,2-dione (3.17)

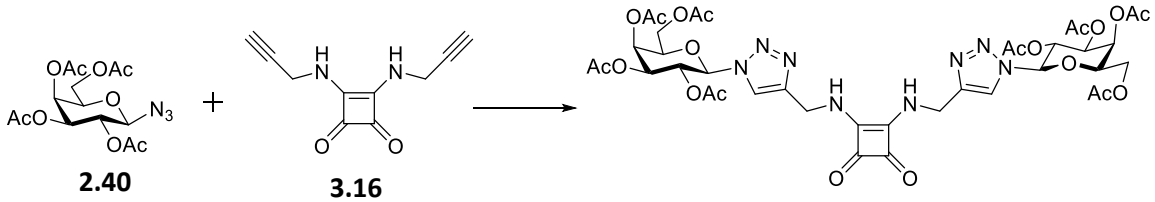

Copper sulphate pentahydrate (20 mg) and sodium ascorbate (40 mg) were added to a solution of **2.40** (375 mg, 1.004 mmol) and **3.16** (90 mg, 0.478 mmol) in CH$_3$CN/H$_2$O (4 mL/ 2mL). The reaction was allowed to stir in the MW at 100 ^{o}C until deemed complete by TLC analysis (typically 10 min). The solvent was removed *in vacuo*. The residue was dissolved in DCM (30 mL), washed with water (3 x 20 mL), and dried (MgSO$_4$). The mixture was filtered and the solvent was removed *in vacuo* to yield the crude product, which was purified by silica gel column chromatography (DCM:MeOH 98:2-93:7) to give the pure product **3.17** as an off-white solid (362 mg, 81 %). R$_f$=0.5 (DCM:MeOH 9:1). $[\alpha]_D^{27}$ -8.0 (c 1, DCM). ^{1}H NMR (500 MHz, DMSO) δ 8.27 (s, 2H, triaz-H), 7.84 (s, 2H, N*H*CH$_2$-triaz), 6.25 (d, *J* = 9.3 Hz, 2H, H-1), 5.59 (t, *J* = 9.6 Hz, 2H, H-2), 5.46 – 5.40 (m, 2H, H-3 and H-4), 4.85-4.75 (m, 4H, C*H*$_2$-triaz), 4.59 – 4.54 (m, 2H, H-5), 4.15-4.10 (m, 2H, H-6), 4.05-4.00 (m, 2H, H-6'), , 2.18 (s, 6H, OAc), 1.99 (s, 6H, OAc), 1.94 (s, 6H, OAc), 1.80 (s, 6H, OAc). ^{13}C NMR (125 MHz, DMSO) δ 183.3 (CO), 170.4 (CO of OAc), 170.4 (CO of OAc), 169.9 (CO of OAc), 169.0 (CO of OAc), 145.1 (*C*-triaz), 123.0 (*C*H-triaz), 84.7 (C-1), 73.4 (C-5), 70.9 (C-3/4), 68.2 (C-2), 67.8 (C-3/4), 62.0 (C-6), 38.9 (*C*H$_2$-triaz), 21.0 (CH$_3$ of OAc), 20.9 (CH$_3$ of OAc), 20.8 (CH$_3$ of OAc), 20.4 (CH$_3$ of OAc). IR (film on NaCl): 3155, 2938, 2121, 1754, 1653, 1581, 1431, 1371, 1220, 1052, 923, 598 cm^{-1}. HRMS (ESI+): m/z calculated for $C_{38}H_{46}N_8O_{20}$ + Na$^+$ [M+Na$^+$]: 957.2726, found 957.2741.

3,4-Di-(2-O-(2,3,4,6-tetra-*O*-acetyl-β-D-galactopyranosyl)-ethyl-1,2,3-triazol-4-ylmethylamino)cyclobut-3-ene-1,2-dione (3.18)

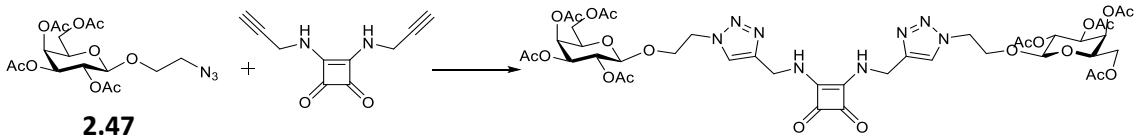

2.47 **3.16** **3.18**

Copper sulphate pentahydrate (20 mg) and sodium ascorbate (40 mg) were added to a solution of **2.40** (227 mg, 0.540 mmol) and **3.16** (49 mg, 0.259 mmol) in CH_3CN/H_2O (4 mL/ 2mL). The reaction was allowed to stir in the MW at 100 ^oC until deemed complete by TLC analysis (10 min). The solvent was removed *in vacuo*. The residue was dissolved in DCM (30 mL), washed with water (20 mL x 3), and dried ($MgSO_4$). The mixture was filtered and the solvent was removed *in vacuo* to yield the crude product, which was purified by silica gel column chromatography (DCM:MeOH 98:2-93:7) to give the pure product **3.18** as a yellow solid (197 mg, 80 %). R_f= 0.5 (DCM:MeOH 9:1). $[\alpha]_D^{22}$ -3.8 (c 1.05, DCM). ^{1}H NMR (500 MHz, $CDCl_3$) δ 8.06 (s, 2H, N*H*CH_2-triaz), 7.78 (s, 2H, triaz-H), 5.38 (d, *J* = 3.4 Hz, 2H, H-4), 5.15 (dd, *J* = 10.4, 8.0 Hz, 2H, H-2), 5.04 – 4.86 (m, 6H, H-3 and C*H*$_2$-triaz), 4.68 – 4.53 (m, 4H, C*H*$_2$$CH_2O$), 4.51 (d, *J* = 7.9 Hz, 2H, H-1), 4.25 – 4.18 (m, 2H, C*H*O-Gal), 4.15-4.07 (m, 4H, H-6 and H-6'), 4.02 – 3.94 (m, 2H, C*H*O-Gal), 3.92 (t, *J* = 6.6 Hz, 2H, H-5), 2.17 (s, 6H, OAc), 2.04 (s, 6H, OAc), 1.98 (s, 6H, OAc), 1.96 (s, 6H, OAc). ^{13}C NMR (125 MHz, $CDCl_3$) δ 183.6 (CO), 170.4 (CO of OAc), 170.2 (CO of OAc), 170.1 (CO of OAc), 169.4 (CO of OAc), 167.7 (NH*C*CO), 144.7 (*C*-triaz), 124.4 (*C*H-triaz), 100.9 (C-1), 70.9 (C-5), 70.6 (C-3), 68.5 (C-2), 67.3 (CH_2*C*H_2O), 66.9 (C-4), 61.1 (C-6), 50.3 (*C*H_2CH_2O), 38.6 (*C*H_2-triaz), 20.7 (CH_3 of OAc), 20.7 (CH_3 of OAc), 20.5 (CH_3 of OAc). IR (film on NaCl): 3261, 2964, 1750, 1677, 1602, 1535, 1432, 1370, 1227, 1175, 1139, 1059 cm^{-1}. HRMS (ESI+): m/z calculated for $C_{42}H_{54}N_8O_{22}$ + Na^+ [M+Na^+]: 1045.3250, found 1045.3249.

3,4-Di-[{4-O-(2,3,4,6-tetra-*O*-acetyl-β-D-galactopyranosyl)-2,3,6-tri-O-acetyl-β-D-glucopyranosyl}-1,2,3-triazol-4-ylmethylamino]cyclobut-3-ene-1,2-dione (3.19)

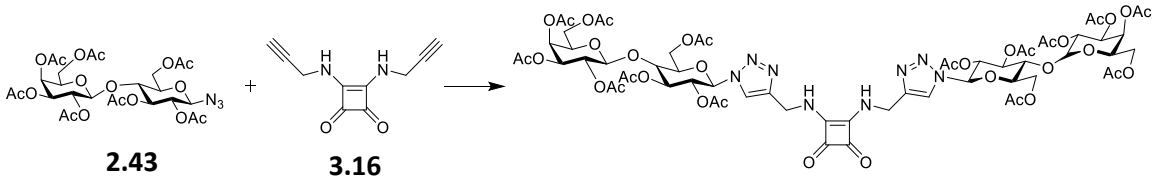

2.43 **3.16** **3.19**

Copper sulphate pentahydrate (30 mg) and sodium ascorbate (60 mg) were added to a solution of **2.43** (664 mg, 0.478 mmol) and **3.16** (90 mg, 1.004 mmol) in CH_3CN/H_2O (4 mL/ 2mL). The reaction was allowed to stir in the MW at 100 ^oC until deemed complete by TLC analysis (typically 10 min). The solvent was removed *in vacuo*. The residue was dissolved in DCM (30 mL), washed with water (20 mL x 3), and dried ($MgSO_4$). The mixture was filtered and the solvent was removed *in vacuo* to yield the crude product, which was purified by silica gel column chromatography (DCM:MeOH 98:2-93:7) to give the pure product **3.19** as a white solid (529 mg, 75 %). R_f= 0.27 (DCM:MeOH 9:1). $[\alpha]_D^{24}$ +7.0 (c 1.0, DCM). ^{1}H NMR (500 MHz, $CDCl_3$) δ 8.23 (s, 2H, N*H*CH_2-triaz), 8.09 (s, 2H, triaz-H), 6.07 (d, *J* = 6.4 Hz, 2H, H-1 Gal), 5.49 – 5.38 (m, 4H, H-2 Gal and H-3 Gal), 5.36 (d, *J* = 3.3 Hz, 2H, H-4 Glc), 5.11 (dd, *J* = 10.2, 8.0 Hz, 2H, H-2 Glc), 4.99 (dd, *J* = 10.4, 3.3 Hz, 2H, H-3 Glc), 4.94 (apps, 4H, C*H*$_2$-triaz), 4.58 (d, *J* = 7.9 Hz, 2H, H-1 Glc), 4.51 (d, *J* = 11.6 Hz, 2H, H-6 Glc), 4.28 – 4.05 (m, 10H, H-6' Glc, H-5 Gal, H-4 Gal, H-6 and H-6' Gal), 4.03 – 3.92 (m, 2H, H-5 Glc), 2.14 (s, 6H, OAc), 2.06 (s, 6H, OAc), 2.04 (appd, 18H, 3 x OAc), 1.95 (s, 6H, OAc), 1.76 (s, 6H, OAc). ^{13}C NMR (125 MHz, $CDCl_3$) δ 183.6 (CO), 170.4 (CO of OAc), 170.2 (CO of OAc), 170.0 (CO of OAc), 169.9 (CO of OAc), 169.7 (CO of OAc), 169.2 (CO of OAc), 168.9 (CO of OAc), 167.6 (NH*C*CO), 145.1 (*C*-triaz), 123.5 (*C*H-triaz), 101.2 (C-1 Glc), 85.4 (C-1 Gal), 75.9 (C-4/5 Gal), 75.6 (C-4/5 Gal), 72.6 (C-3 Gal), 71.0 (C-3 Glc), 70.8 (C-2 Gal), 70.7 (C-5 Glc), 69.1 (C-2 Glc), 66.8 (C-4 Glc), 61.9 (C-6 Glc), 60.8 (C-6 Gal), 38.4 (*C*H_2-triaz), 20.9 (CH_3 of OAc), 20.8 (CH_3 of OAc), 20.7 (CH_3 of OAc), 20.6 (CH_3 of OAc), 20.5 (CH_3 of OAc), 20.3 (CH_3 of OAc), 20.1 (CH_3 of OAc). IR (film on NaCl): 3478, 3263, 2964, 1753, 1597, 1536, 1370, 1227, 1048 cm^{-1}. HRMS (ESI+): m/z calculated for $C_{62}H_{78}N_8O_{36}$ + Na^+ [M+Na^+]: 1533.4416, found 1533.3743.

3,4-Di-(β-D-galactopyranosyl-1,2,3-triazol-4-ylmethylamino)cyclobut-3-ene-1,2-dione (3.20)

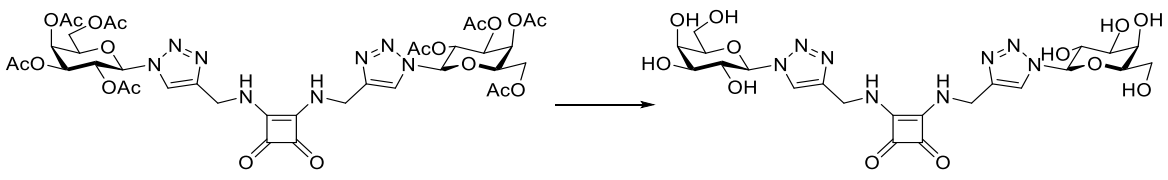

3.17 **3.20**

3.17 (167 mg, 0.179 mmol) was dissolved in methanol/H_2O (4 mL, 2 mL). NEt_3 (0.1 mL) was added, and the reaction mixture was allowed to stir at 45 ^oC for 6 h. The solution was cooled, Amberlite H^+ was added and the mixture was allowed to stir for 30 mins. The solution was filtered, and the solvent was removed *in vacuo*. Excess NEt_3 was removed using the Schlenk line. The product was freeze-dried over night to yield the pure product **3.20** as a white solid (82 mg, 77 %). $[\alpha]_D^{22}$ +3.0 (c 1, DMSO). ^1H NMR (500 MHz, DMSO) δ 8.24 (s, 2H, triaz-H), 7.88 (bs, 2H, N*H*CH_2-triaz), 5.54 (d, *J* = 9.2 Hz, 2H, H-1), 5.28 (d, *J* = 6.0 Hz, 2H, OH), 5.05 (d, *J* = 5.7 Hz, 2H, OH), 4.87 (s, 4H, C*H*$_2$-triaz), 4.74 (t, *J* = 5.7 Hz, 2H, OH), 4.69 (d, *J* = 5.6 Hz, 2H, OH), 4.07 (td, *J* = 9.3, 6.3 Hz, 2H, H-2), 3.83 – 3.79 (m, 2H, H-4), 3.76 (t, *J* = 6.1 Hz, 2H, H-5), 3.63 – 3.49 (m, 6H, H-3, H-6 and H-6'). ^{13}C NMR (125 MHz, DMSO) δ 183.2 (CO), 167.9 (NH*C*CO), 144.8 (*C*-triaz), 122.3 (*C*H-triaz), 88.6 (C-1), 78.9 (C-5), 74.2 (C-3), 69.8 (C-2), 68.9 (C-4), 60.9 (C-6), 39.1 (*C*H_2-triaz). IR (ATR): 3370, 2940, 2502, 1794, 1652, 1551, 1432, 1368, 1287, 1095, 1053, 1024, 892, 700 cm^{-1}. HRMS (ESI+): m/z calculated for $C_{22}H_{30}N_8O_{12}$ + Na^+ [M+Na^+]: 621.1881, found 621.1896.

3,4-Di-(2-O-(β-D-galactopyranosyl)-ethyl-1,2,3-triazol-4-ylmethylamino)cyclobut-3-ene-1,2-dione (3.21)

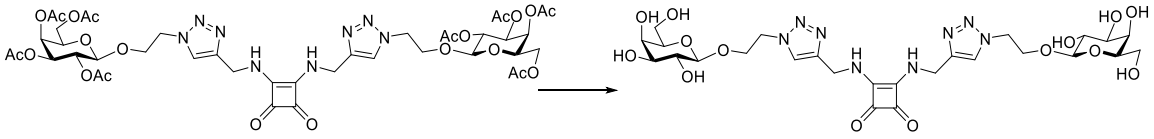

3.18 **3.21**

3.18 (150 mg, 0.147 mmol) was dissolved in methanol/H_2O (4 mL, 2 mL). NEt_3 (0.1 mL) was added, and the reaction mixture was allowed to stir at 45 ^oC for 6 h. The solution was cooled, Amberlite H^+ was added and the mixture was allowed to stir for 30 mins. The solution was filtered, and the solvent was removed *in vacuo*. Excess NEt_3 was removed using the Schlenk line. The product was freeze-dried over night to yield the pure product as a white solid (95 mg, 94 %). $[\alpha]_D^{22}$ +12.0 (c 1, H_2O). ^1H NMR (500 MHz, D_2O) δ 8.01 (s, 2H, triaz-H), 4.85 (s, 4H, C*H*$_2$-triaz), 4.62 (t, *J* = 5.0 Hz, 4H, O-CH_2C*H*$_2$), 4.27 (d, *J* = 7.9 Hz, 2H, H-1), 4.25 – 4.20 (m, 2H, O-C*H*-CH_2), 4.09 – 4.02 (m, 2H, O-C*H*-CH_2), 3.84 (d, *J* = 3.4 Hz, 2H, H-4), 3.70 – 3.63 (m, 4H, H-6 and H-6'), 3.59 (dd, *J* = 7.4, 4.8 Hz, 2H, H-5), 3.54 (dd, *J* = 9.9, 3.5 Hz, 2H, H-3), 3.41 (dd, *J* = 9.9, 7.9 Hz, 2H, H-2). ^{13}C NMR (125 MHz, D_2O) δ 182.22 (CO), 168.0 (*C*CO), 144.5 (*C*-triaz),

124.70 (*C*H-triaz), 102.95 (C-1), 75.07 (C-5), 72.54 (C-3), 70.51 (C-2), 68.48 (C-4), 67.95 (O-*C*H_2CH$_2$), 60.85 (C-6), 50.38 (O-CH$_2$*C*H_2), 38.82 (*C*H_2-triaz). IR (ATR): 3269, 2924, 1800, 1662, 1591, 1531, 1427, 1338, 1224, 1140, 1042, 889, 826, 775 cm^{-1}. HRMS (ESI+): m/z calculated for $C_{26}H_{38}N_8O_{14}$ + H^+ [M+H$^+$]: 686.2586, found 687.2576.

3,4-Di-[{4-O-(β-D-galactopyranosyl)-β-D-glucopyranosyl}-1,2,3-triazol-4-ylmethylamino]cyclobut-3-ene-1,2-dione (3.22)

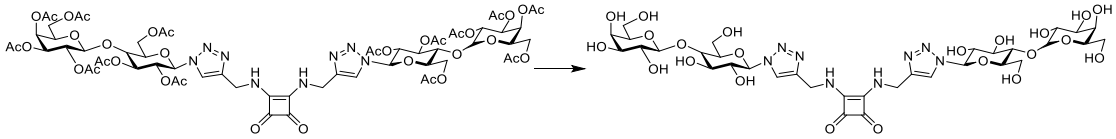

3.19 **3.22**

3.19 (276 mg, 0.188 mmol) was dissolved in methanol/H_2O (4 mL, 2 mL). NEt_3 (0.1 mL) was added, and the reaction mixture was allowed to stir at 45 ^{o}C for 6 h. The solution was cooled, Amberlite H$^+$ was added and the mixture was allowed to stir for 30 mins. The solution was filtered, and the solvent was removed *in vacuo*. Excess NEt_3 was removed using the Schlenk line. The product was freeze-dried over night to yield the pure product as a white solid (172 mg, 99 %). $[\alpha]_D^{22}$ +10 (c 1, H_2O). ^{1}H NMR (500 MHz, D_2O) δ 8.11 (s, 2H, triaz-H), 5.70 – 5.59 (m, 2H, H-1), 4.81 (s, 4H, C*H*$_2$-triaz), 4.47 (d, *J* = 7.9 Hz, 1H, H-1 Glc), 4.40 (d, *J* = 7.8 Hz, 1H, H-1 Glc), 3.99 – 3.42 (m, 24H). ^{13}C NMR (125 MHz, D_2O) δ 182.3 (CO), 168.2 (*C*CO), 144.9 (*C*-triaz), 123.3 (*C*H-triaz), 102.9 (C-1 Glc), 96.4 (C-1 Glc), 87.5 (C-1 Gal), 78.9, 77.7, 77.4, 75.9, 75.4, 75.1, 74.5, 72.8, 72.5, 72.2, 71.9, 71.9, 70.9, 70.5, 69.2, 68.9, 68.7, 68.6, 68.3, 61.2, 61.1, 61.0, 60.4, 59.7, 38.8 (*C*H_2-triaz). IR (ATR): 3300, 2939, 2452, 1803, 1670, 1585, 1516, 1379, 1015 cm^{-1}. HRMS (ESI+): m/z calculated for $C_{34}H_{50}N_8O_{22}$ + Na^+ [M+Na$^+$]: 945.2937, found 945.2967.

Bicyclo[2.2.1]hept-5-ene-2-*endo*,3-*exo*-2,3-dicarboxamide, *N*-(prop-2-yn-1-yl) (3.25)

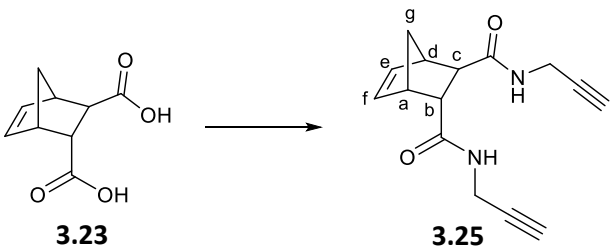

3.23 **3.25**

5-Norbornene-2-*endo*,3-*exo*-dicarboxylic acid **3.23** (200 mg, 1.098 mmol) and TBTU (881 mg, 2.7 mmol) were dissolved in anhydrous DMF (15 mL) under N_2. NEt_3 (0.38 mL, 2.7 mmol) and propargylamine (0.15 mL, 2.3 mmol) were added after 10 mins. The reaction was allowed to stir for 48 h. The DMF was removed *in vacuo*, the resulting residue was dissolved in DCM (20 mL) and washed with brine (3 x 20 mL), dried over $MgSO_4$, filtered and concentrated *in vacuo* to yield the crude product. This was then purified by silica gel column chromatography (1:1-1.5:1 EtOAc:Pet Ether) to give the pure product **3.25** as a white solid (260 mg, 93 %). R_f=0.25 (1:1 EtOAc:Pet. Ether). ^{1}H NMR (500 MHz, MeOD) δ 6.29 (dd, *J* = 5.6, 3.1 Hz, 1H, $H_{e/f}$), 6.05 (dd, *J* = 5.6, 2.8 Hz, 1H, $H_{e/f}$), 4.04 – 3.87 (m, 4H, C*H*$_2$CCH), 3.26 (dd, *J* = 4.6, 3.7 Hz, 1H, $H_{b/c}$), 3.21 (d, *J* = 0.6 Hz, 1H, $H_{a/d}$), 2.95 (dd, *J* = 1.9, 1.1 Hz, 1H, $H_{a/d}$), 2.59 – 2.55 (m, 3H, CH_2CCH and $H_{b/c}$), 1.82 (d, *J* = 8.4 Hz, 1H, H_g), 1.41 (dq, *J* = 8.4, 1.7 Hz, 1H, $H_{g'}$). ^{13}C NMR (125 MHz, MeOD) δ 174.8 (CO), 173.7 (CO), 137.4 ($C_{e/f}$), 134.1 ($C_{e/f}$), 70.6 (CH_2CCH), 70.4 (CH_2CCH), 48.5 ($C_{a/d}$), 48.1 ($C_{b/c}$), 47.1 ($C_{b/c}$), 47.0 (C_g), 46.1 ($C_{a/d}$), 28.3 (CH_2CCH), 28.1 (CH_2CCH), 13.1. IR (ATR): 3284, 1635, 1531, 1447, 1333, 1276, 1215, 1031, 862 cm^{-1}. HRMS (ESI+): m/z calculated for $C_{15}H_{16}N_2O_2$ + Na^+ [M+Na^+]: 279.1109, found 279.1119.

Bicyclo[2.2.1]hept-5-ene-2,3-*endo*-2,3-dicarboxamide, *N*-(prop-2-yn-1-yl) (3.26)

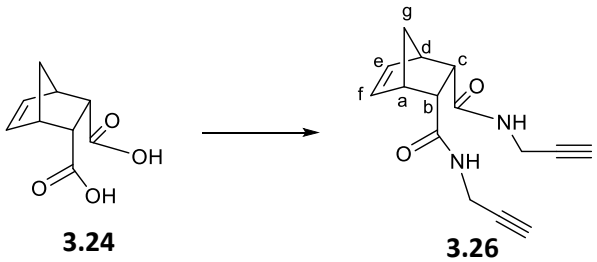

3.24 **3.26**

Cis-5-Norbornene-2-*endo*,3-*exo*-dicarboxylic acid **3.24** (300 mg, 1.65 mmol) and TBTU (1.323 g, 4.12 mmol) were dissolved in anhydrous DMF (15 mL) under N_2. Triethylamine (0.57 mL, 4.12 mmol) and propargylamine (0.22 mL, 3.46 mmol) were added after 10 mins. The reaction was allowed to stir for 48 h. The DMF was removed *in vacuo*, the resulting residue was dissolved in DCM (20 mL) and washed with brine (3 x 20 mL) and sat. $NaHCO_3$ (2 x 20 mL), dried of $MgSO_4$, filtered and concentrated *in vacuo* to yield the crude product. This was then purified by silica gel column chromatography (1:1-1.5:1 EtOAc:Pet Ether) to give the pure product **3.26** as a white

solid (334 mg, 79 %). R_f=0.08 (1:1 EtOAc:Pet. Ether). ^{1}H NMR (500 MHz, DMSO) δ 7.70 (t, *J* = 5.3 Hz, 2H, N*H*), 6.09 (d, *J* = 1.8 Hz, 2H, H_e and H_f), 3.82 – 3.64 (m, 4H, CH_2CCH), 3.12 – 3.09 (m, 2H, H_b and H_C), 3.04 (t, *J* = 2.5 Hz, 2H, CH_2CC*H*), 2.96 – 2.94 (m, 2H, H_a and H_d), 2.08 (s, 1H), 1.25 – 1.19 (m, 1H). ^{13}C NMR (125 MHz, DMSO) δ 171.5 (CO), 134.9 (C_e and C_f), 81.9 (CH_2*C*CH), 73.2 (CH_2C*C*H), 50.1 (C_b and C_c), 48.9 (C_g), 46.7 (C_a and C_d), 28.4 (*C*H_2CCH). IR (ATR): 3286, 1654, 1525, 1415, 1333, 1278, 1256, 1226, 1098, 1029, 908, 846 cm^{-1}. HRMS (ESI+): m/z calculated for $C_{15}H_{16}N_2O_2$ + Na^+ [M+Na^+]: 279.1109, found 279.1105.

Bicyclo[2.2.1]hept-5-ene-2-*endo*,3-*exo*-2,3-dicarboxamide, *N*-(2,3,4,6-tetra-*O*-acetyl-β-D-galactopyranosyl-1,2,3-triazol-4-ylmethylamino) (3.27)

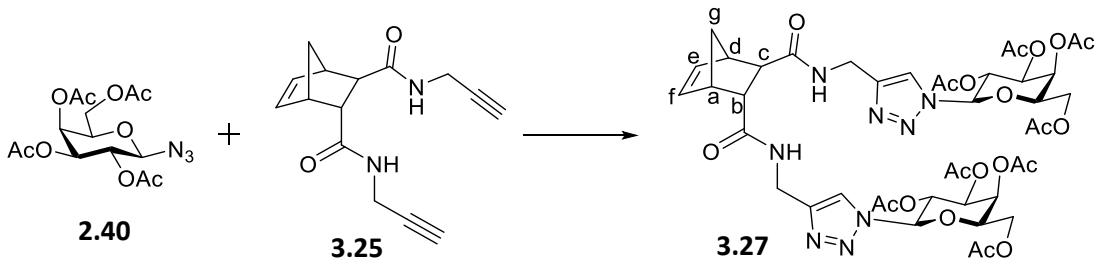

Copper sulphate pentahydrate (30 mg) and sodium ascorbate (60 mg) were added to a solution of **2.40** (700 mg, 1.87 mmol) and **3.25** (229 mg, 0.893 mmol) in CH_3CN/H_2O (4 mL/ 2mL). The reaction was allowed to stir in the MW at 100 ^{o}C until deemed complete by TLC analysis (20 min). The solvent was removed *in vacuo*. The residue was dissolved in DCM (30 mL), washed with water (20 mL x 3), and dried ($MgSO_4$). The mixture was filtered and the solvent was removed *in vacuo* to yield the crude product, which was purified by silica gel column chromatography (DCM:MeOH 98:2-93:7) to give the pure product **3.27** as an off-white solid (488 mg, 54 %). R_f=0.58 (DCM:MeOH 9:1). $[\alpha]_D^{23}$ -6.0 (c 1, DCM). ^{1}H NMR (500 MHz, $CDCl_3$) δ 7.82-7.74 (m, 2H, triaz-H and triaz-H'), 7.17 (dt, *J* = 9.0, 5.8 Hz, 1H, N*H*CH_2-triaz), 6.93 (dt, *J* = 24.9, 5.7 Hz, 1H, N*H'*CH_2-triaz), 6.16 (td, *J* = 5.7, 3.2 Hz, 1H, $H_{e/f}$), 6.08 – 6.02 (m, 1H, $H_{e/f}$), 5.82 (d, *J* = 9.2, 2H, H-1), 5.52 – 5.42 (m, 4H, H-2 and H-4), 5.24 (dd, *J* = 10.3, 3.2 Hz, 2H, H-3), 4.49 – 4.37 (m, 4H, CH_2-triaz x 2), 4.29 – 4.18 (m, 2H, H-5), 4.18 – 4.04 (m, 4H, H-6 and H-6'), 3.11 – 3.00 (m, 2H, $H_{a/d}$ and $H_{b/c}$), 2.97 (s, 1H, $H_{a/d}$), 2.40 (dd, *J* = 12.7, 3.7 Hz, 1H, $H_{b/c}$), 2.18 – 2.13 (m, 6H, OAc), 1.98 – 1.92 (m, 12H, OAc), 1.86 – 1.75 (m, 6H, OAc), 1.75 – 1.70 (m, 1H, H_g), 1.41 (d, *J* = 8.5 Hz, 1H, $H_{g'}$). ^{13}C NMR (125 MHz, $CDCl_3$)

δ 173.7 and 173.6 (*C*O-NHCH$_2$), 172.6 and 172.5 (*C'*O-NHCH$_2$), 169.3 (CO of OAc), 169.1 (CO of OAc), 169.0 (CO of OAc), 168.8 (CO of OAc), 168.1 (CO of OAc), 168.0 (CO of OAc), 144.7 and 144.6 (*C*-triaz), 136.6 and 136.5(C$_{e/f}$), 134.0 and 133.9 (C$_{e/f}$), 119.9 and 119.7 (*C*H-triaz), 85.2 (C-1), 73.0 (C-5), 69.8 and 69.7 (C-3), 67.1 and 67.0 (C-2/4), 66.0 (C-2/4), 60.3 and 60.2 (C-6), 49.4 and 49.2 (C$_{b/c}$), 47.6 (C$_{b/c}$), 47.2 (C$_g$), 45.5 and 45.3 (C$_{a/d}$), 44.1 and 44.0 (C$_{a/d}$), 34.0 and 33.9 (*C*H$_2$-triaz), 19.7 (CH$_3$ of OAc), 19.6 (CH$_3$ of OAc), 19.5 (CH$_3$ of OAc), 19.3 (CH$_3$ of OAc), 19.2 (CH$_3$ of OAc). IR (ATR): 3387, 2972, 1745, 1651, 1526, 1368, 1210, 1044, 923, 733 cm^{-1}. HRMS (ESI+): m/z calculated for $C_{43}H_{54}N_8O_{20}$ + H$^+$ [M+H$^+$]: 1003.3533, found 1003.3555.

Bicyclo[2.2.1]cis-hept-5-ene-2,3-*endo*-2,3-dicarboxamide, *N*-(2,3,4,6-tetra-*O*-acetyl-β-D-galactopyranosyl-1,2,3-triazol-4-ylmethylamino) (3.28)

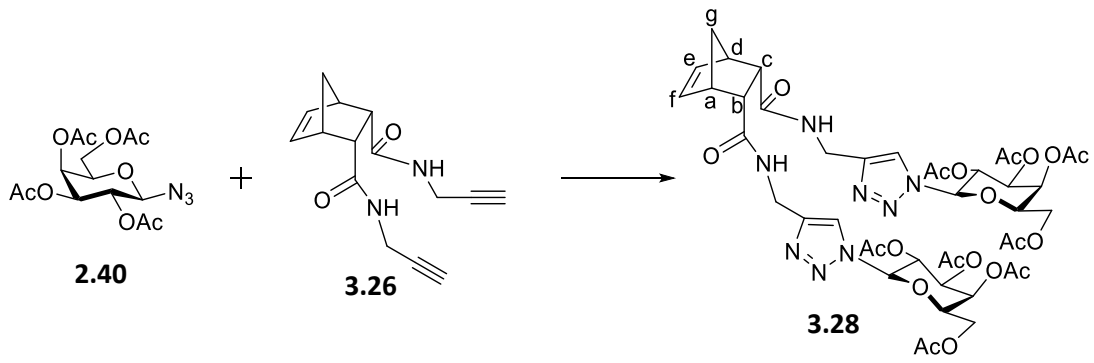

Copper sulphate pentahydrate (20 mg) and sodium ascorbate (40 mg) were added to a solution of 2,3,4,6-tetra-O-acetyl-β-D-galactopyranosyl azide **2.40** (211 mg, 1.87 mmol) and *cis*-5-Norbornene-*endo*-2,3-dicarboxylic acid **3.26** (69 mg, 0.893 mmol) in CH$_3$CN/H$_2$O (4 mL/ 2mL). The reaction was allowed to stir in the MW at 100 ^{o}C until deemed complete by TLC analysis (20 min). The solvent was removed *in vacuo*. The residue was dissolved in DCM (30 mL), washed with water (20 mL x 3), and dried (MgSO$_4$). The mixture was filtered and the solvent was removed *in vacuo* to yield the crude product, which was purified by silica gel column chromatography (DCM:MeOH 98:2-93:7) to give the pure product **3.28** as an off-white solid (200 mg, 74 %). R$_f$=0.41 (DCM:MeOH 9:1). $[\alpha]_D^{22}$ -6.4 (c 1.1, DCM). ^{1}H NMR (500 MHz, CDCl$_3$) δ 7.83 (s, 1H, triaz-H), 7.79 (s, 1H, triaz-H'), 6.97 (t, *J* = 5.5 Hz, 1H, N*H*CH$_2$-triaz), 6.83 (t, *J* = 5.6 Hz, 1H, N*H*CH$_2$-triaz), 6.35-6.22 (m, 2H, H$_e$ and H$_f$), 5.83 – 5.77 (m, 2H, H-1 and H-1'), 5.52 – 5.46 (m, 4H, H-2, H-2', H-4 and H-4'), 5.24 – 5.18 (m, 2H, H-3 and H-3'), 4.42 – 4.01

(m, 10H, C*H*$_2$-triaz x2, H-5, H-5', H-6, H-6', H-6'' and H-6'''), 3.25 – 3.17 (m, 2H, H_b and H_c), 3.06 (app s, 2H, H_a and H_d), 2.16 (s, 6H, OAc), 2.01 – 1.88 (m, 12H, OAc x 4), 1.80 (m, 6H, OAc), 1.43 – 1.23 (m, 2H, H_g and $H_{g'}$). ^{13}C NMR (125 MHz, $CDCl_3$) δ 171.7 (CO), 171.7 (CO), 169.3 (CO of OAc), 169.3 (CO of OAc), 169.1 (CO of OAc), 168.9 (CO of OAc), 168.8 (CO of OAc), 167.9 (CO of OAc), 167.9 (CO of OAc), 144.6 (*C*-triaz), 144.5 (*C'*-triaz), 134.6 ($C_{e/f}$), 134.2 ($C_{e/f}$), 120.4 (*C*H-triaz), 120.2 (*C*H-triaz), 85.1 (C-1), 72.9 (C-5), 69.9 (C-3), 67.0 (C-2/4), 65.9 (C-2/4), 60.2 (C-6), 60.1 (C-6'), 50.5 ($C_{b/c}$), 50.3 ($C_{b/c}$), 48.7 (C_g), 46.1 (C_a and C_d), 33.7 (*C*H$_2$-triaz), 19.7 (CH_3 of OAc), 19.6 (CH_3 of OAc), 19.6 (CH_3 of OAc), 19.5 (CH_3 of OAc), 19.2 (CH_3 of OAc). IR (ATR): 3392, 2967, 1746, 1663, 1527, 1368, 1211, 1045, 922 cm^{-1}. HRMS (ESI+): m/z calculated for $C_{43}H_{54}N_8O_{20}$ + Na^+ [M+Na^+]: 1025.3352, found 1025.3387.

Bicyclo[2.2.1]hept-5-ene-2-endo,3-exo-2,3-dicarboxamide, *N*-(β-D-galactopyranosyl-1,2,3-triazol-4-ylmethylamino) (3.29)

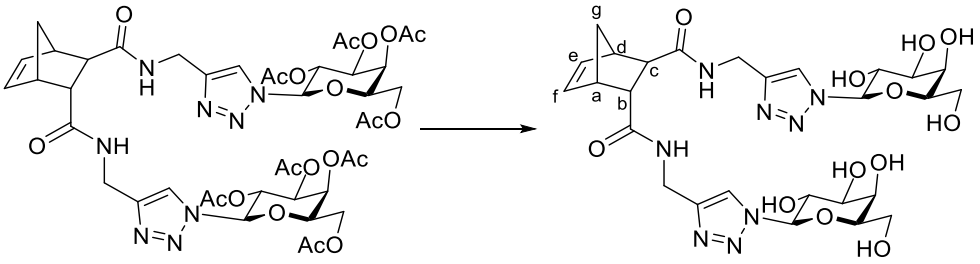

3.27 **3.29**

3.27 (375 mg, 0.374 mmol) was dissolved in methanol/H_2O (4 mL, 2 mL). NEt_3 (0.1 mL) was added, and the reaction mixture was allowed to stir at 45 ^{o}C for 6 h. The solution was cooled, and the solvent was removed *in vacuo*. The product was dried under high vacuum and lyophilized for 3 nights to yield the pure product **3.29** (242 mg, 97 %). $[\alpha]_D^{19}$: 11.0˚ (c 1, H_2O). ^{1}H NMR (500 MHz, D_2O) δ 8.18 (s, 1H, triaz-H), 8.15 8.18 (s, 1H, triaz-H'), 6.33 – 6.28 (m, 1H, H_e/H_f), 6.05 – 5.99 (m, 1H, H_e/H_f), 5.71-5.67 (m, 2H, H-1), 4.53 – 4.43 (m, 4H, C*H*$_2$-triaz), 4.19 (appt, *J* = 9.5 Hz, 2H, H-2), 4.08 (appd, *J* = 3.3 Hz, 2H, H-4), 3.99 (appt, *J* = 6.1 Hz, 2H, H-5), 3.87 (dd, *J* = 9.8, 3.3 Hz, 2H, H-3), 3.78 (appd, *J* = 6.0 Hz, 4H, H-6 and H-6'), 3.25 – 3.19 (m, 2H, H_a/H_d and H_b/H_c), 3.01 (s, 1H, H_a/H_d), 2.53 (d, *J* = 4.1 Hz, 1H, H_b/H_c), 1.66 (d, *J* = 8.6 Hz, 1H, H_g), 1.42 (d, *J* = 7.6 Hz, 1H, $H_{g'}$). ^{13}C NMR (125 MHz, D_2O) δ 176.8 (CO), 175.8 (C'O), 145.2 (*C*-triaz), 138.2 ($C_{e/f}$), 134.6 ($C_{e/f}$), 123.1 (*C*H-triaz), 88.2 (C-1), 78.4 (C-5), 73.0 (C-3), 69.8 (C-2), 68.7 (C-4), 60.9 (C-6), 48.6 (C_b/C_c), 48.2 (C_a/C_d), 47.8 (C_b/C_c), 47.5 (C_g), 46.4 (C_a/C_d),

34.6 (*C*H_2-triaz), 34.5 (*C'*H_2CCH). IR (ATR): 3282, 2929, 1760, 1642, 1535, 1355, 1300, 1243, 1089, 1052, 986, 889 cm^{-1}. HRMS (ESI+): m/z calculated for $C_{27}H_{38}N_8O_{12}$ + Na^+ [M+Na^+]: 689.2507, found 689.2490.

Bicyclo[2.2.1]cis-hept-5-ene-2,3-*endo*-2,3-dicarboxamide, *N*-(β-D-galactopyranosyl-1,2,3-triazol-4-ylmethylamino) (3.30)

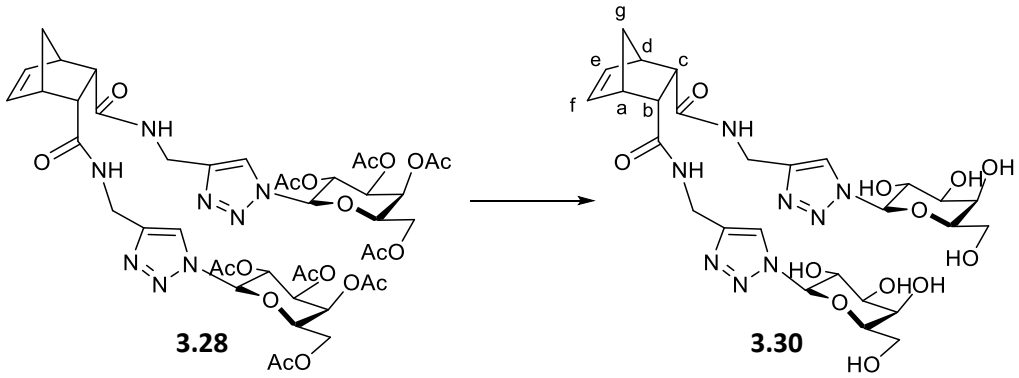

3.28 (265 mg, 0.264 mmol) was dissolved in methanol/H_2O (4 mL, 2 mL). NEt_3 (0.1 mL) was added, and the reaction mixture was allowed to stir at 45 °C for 6 h. The solution was cooled, and the solvent was removed *in vacuo*. The product was dried under high vacuum and lyophilized for 3 nights to yield the pure product **3.30** (169 mg, 96 %). $[\alpha]_D^{18}$ +14.0 (c 1, H_2O). ^{1}H NMR (500 MHz, D_2O) δ 8.32 (s, 1H, triaz-H), 8.18 (s, 1H, triaz-H'), 5.92-5.86 (m, 2H, H_e and H_f), , 5.74 (d, *J* = 9.2 Hz, 1H, H-1), 5.68 (d, *J* = 9.2 Hz, 1H, H-1'), 4.68 (s, 4H, C*H*$_2$-triaz), 4.29 – 4.18 (m, 4H, H-2 and H-2'), 4.13 (dd, *J* = 3.3, 0.6 Hz, 1H, H-4), 4.11 (dd, *J* = 3.3, 0.6 Hz, 1H, H-4'), 4.06 – 3.99 (m, 2H, H-5 and H-5'), 3.92 (dd, *J* = 9.8, 3.3 Hz, 1H, H-3), 3.89 (dd, *J* = 9.8, 3.3 Hz, 1H, H-3'), 3.81 (appdd, *J* = 7.4, 6.2 Hz, 4H, H-6, H-6', H-6'' and H-6'''), 3.50 (dd, *J* = 3.0, 1.5 Hz, 2H, H_b and H_c), 3.35 (dd, *J* = 2.5, 1.2 Hz, 2H, H_a and H_d), 1.67 (dt, *J* = 8.9, 1.6 Hz, 1H, H_g), 1.60 (d, *J* = 8.9 Hz, 1H, $H_{g'}$). ^{13}C NMR (125 MHz, D_2O) δ 180.8 (CO), 143.4 (*C*-triaz), 142.3 (*C'*-triaz), 134.3 (C_e and C_f), 124.0 (*C*H-triaz), 123.6 ($CH_2CC'H$), 88.0 (C-1), 87.9 (C'-1), 78.4 (C-5), 78.3 (C'-5), 73.1 (C-3), 73.0 (C'-3), 69.7 (C-2), 69.7 (C'-2), 68.6 (C-4), 68.6 (C'-4), 60.9 (C-6), 60.8 (C'-6), 51.9 (C_g), 45.7 (C_b and C_c), 44.9 (C_a and C_d), 32.8 (*C*H_2-triaz). IR (ATR): 3293, 2932, 1764, 1688, 1560, 1401, 1336, 1232, 1091, 1051, 886, 815, 728 cm^{-1}. HRMS (ESI+): m/z calculated for $C_{27}H_{38}N_8O_{12}$ + Na^+ [M+Na^+]: 689.2507, found 689.2501.

_N_-(β-D-Galactopyranosyl-1,2,3-triazol-4-ylmethyl)bicylco[2.2.1]*cis*-hept-5-ene-2,3-*endo*-dicarboximide (3.31)

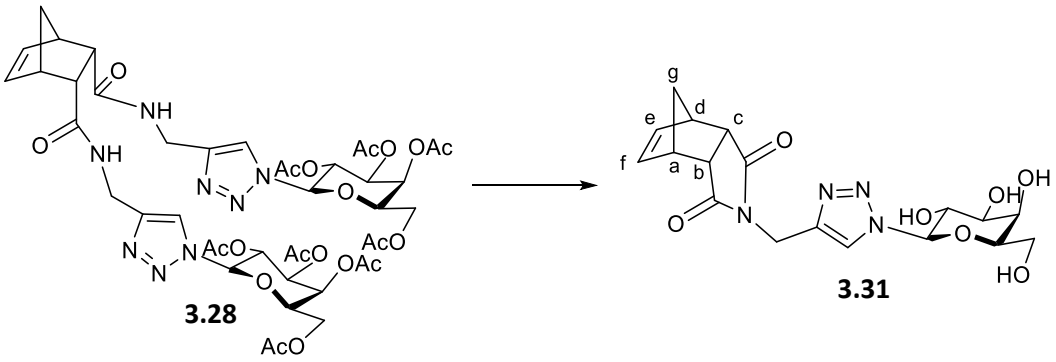

3.28 (155 mg, 0.155 mmol) was dissolved in methanol/H_2O (4 mL, 2 mL). NEt_3 (0.1 mL) was added, and the reaction mixture was allowed to stir at 45 ^oC for 6 h. The solution was cooled, Amberlite H^+ was added and the mixture was allowed to stir for 30 mins. The solution was filtered, and the solvent was removed *in vacuo*. Monovalent-imide analogue **3.31** was formed (63 mg, 100 %). $[\alpha]_D^{26}$ +5 (c 1.2, MeOH). ^1H NMR (500 MHz, D_2O) δ 8.10 (s, 1H, triaz-H), 5.85-5.79 (m, 2H, H_e and H_f), 5.60 (d, *J* = 9.2 Hz, 1H, H-1), 4.61 (s, 2H, C*H*$_2$-triaz), 4.13 (t, *J* = 9.5 Hz, 1H, H-2), 4.03 (dd, *J* = 3.3, 0.7 Hz, 1H, H-4), 3.93 (td, *J* = 6.0, 0.8 Hz, 1H, H-5), 3.81 (dd, *J* = 9.8, 3.3 Hz, 1H, H-3), 3.72 (d, *J* = 6.1 Hz, 2H, H-6 and H-6'), 3.44 – 3.41 (m, 2H, H_b and H_c), 3.28 – 3.26 (m, 2H, H_a and H_d), 1.62 – 1.49 (m, 2H, H_g and $H_{g'}$). ^{13}C NMR (125 MHz, D_2O) δ 180.8 (CO), 142.4 (*C*-triaz), 134.3 (C_e and C_f), 124.1 (*C*H-triaz), 88.0 (C-1), 78.4 (C-5), 73.1 (C-3), 69.8 (C-2), 68.7 (C-4), 60.9 (C-6), 52.0 (C_g), 45.8 (C_b and C_c), 45.0 (C_a and C_d), 32.9 (*C*H_2-triaz). IR (ATR): 3346, 2943, 1765, 1686, 1399, 1336, 1168, 1091, 1050, 883, 727 cm^{-1}. HRMS (ESI+): m/z calculated for $C_{18}H_{22}N_4O_7$ + Na^+ [M+Na^+]: 429.1386, found 429.1362.

Bicyclo[2.2.1]hept-5-ene-2,3-*endo*-2,3-dicarboxamide, *N*-(propyl) (3.32)

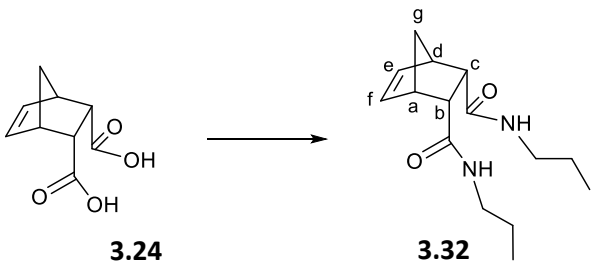

Cis-5-Norbornene-2-*endo*,3-*exo*-dicarboxylic acid **3.24** (75 mg, 0.412 mmol) and TBTU (0.330 g, 1.029 mmol) were dissolved in anhydrous DMF (5 mL) under N_2. NEt_3 (0.14 mL, 1.029 mmol) and propylamine (0.07 mL, 0.865 mmol) were added after 10 mins. The reaction was allowed to stir for 16 h. A further equivalent of TBTU (0.132 g), NEt_3 (0.06 mL) and propylamine (0.03 mL) were added to the reaction mixture and the solution was heated to 50 °C for 5 h. The DMF was removed *in vacuo*, the resulting residue was dissolved in DCM (20 mL) and washed with brine (20 mL x 3) and sat $NaHCO_3$ (20 mL x 2), dried ($MgSO_4$), filtered and concentrated *in vacuo* to yield the crude product. This was then purified by silica gel column chromatography (2:1 EtOAc:Pet Ether to 100 % EtOAc) to give the pure product **3.32** as an off-white solid (89 mg, 82 %). R_f= 0.24 (2:1 EtOAc:Pet Ether). ^{1}H NMR (500 MHz, $CDCl_3$) δ 6.76 (t, *J* = 5.0 Hz, 2H, NH), 6.30 (t, *J* = 1.9 Hz, 2H, H_e and H_f), 3.16 – 3.13 (m, 2H, H_b and H_c), 3.08 – 2.96 (m, 6H, H_a, H_d and C*H*$_2$-NHCO), 1.43 – 1.34 (m, 5H, C*H*$_2$CH$_3$ and H_g), 1.23 – 1.17 (m, 1H, $H_{g'}$), 0.82 (t, *J* = 7.4 Hz, 6H, CH_2CH_3). ^{13}C NMR (125 MHz, $CDCl_3$) δ 172.1 (CO), 134.6 (C_e and C_f), 51.1 (C_b and C_c), 48.8 (C_g), 46.5 (C_a and C_d), 40.3 (*C*H_2-NHCO), 21.6 (*C*H_2CH$_3$), 10.5 (CH_2*C*H$_3$). IR (ATR): 3300, 2966, 2933, 1650, 1546, 1464, 1369, 1336, 1258, 1226, 903 cm^{-1}. HRMS (ESI+): m/z calculated for $C_{15}H_{24}N_2O_2$ + H^+ [M+$^+$]: 265.1916, found 265.1929.

Bicyclo[2.2.1]hept-5-ene-2,3-*endo*-2,3-dicarboxamide, *N*-(benzyl) (3.33)

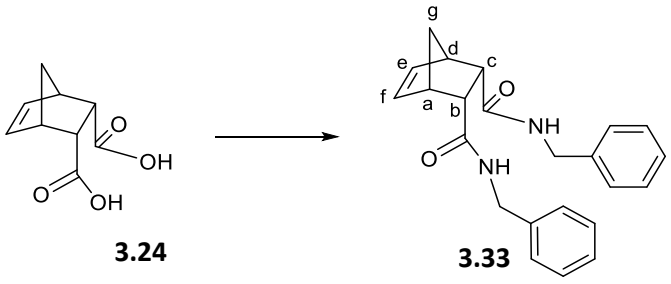

3.24 **3.33**

Cis-5-Norbornene-2-*endo*,3-*exo*-dicarboxylic acid **3.24** (75 mg, 0.412 mmol) and TBTU (0.330 g, 1.029 mmol) were dissolved in anhydrous DMF (5 mL) under N_2. NEt_3 (0.14 mL, 1.029 mmol) and benzylamine (0.1 mL, 0.865 mmol) were added after 10 mins. The reaction was allowed to stir for 16 h. A further equivalent of TBTU (0.132 g), NEt_3 (0.06 mL) and propargylamine (0.04 mL) were added to the reaction mixture and the solution was heated to 50 °C for 5 h. The DMF was removed *in vacuo*, the

resulting residue was dissolved in DCM (20 mL) and washed with brine (20 mL x 3) and $NaHCO_3$ (20 mL x 2), dried ($MgSO_4$), filtered and concentrated *in vacuo* to yield the crude product. This was then purified by silica gel column chromatography (2:1 EtOAc:Pet Ether to 100 % EtOAc) to give the pure product **3.33** as an off-white solid (144 mg, 97 %). R_f= 0.26 (2:1 EtOAc:Pet Ether). ^{1}H NMR (500 MHz, $CDCl_3$) δ 7.35 – 7.16 (m, 10H, Ar-H x 10), 6.96 (bs, 2H, NH), 6.31 (s, 2H, H_e and H_f), 4.27-4.13 (m, 4H, CH_2-NHCO), 3.19 (s, 2H, H_b and H_c), 3.04 (s, 2H, H_a and H_d), 1.41 (d, *J* = 8.3 Hz, 1H, H_g), 1.17 (d, *J* = 7.8 Hz, 1H, $H_{g'}$). ^{13}C NMR (125 MHz, $CDCl_3$) δ 173.0 (CO), 138.3 (Ar-C), 135.7 (C_e and C_f), 128.6 (Ar-*C*H), 127.7 (Ar-*C*H), 127.3 (Ar-*C*H), 52.0 (C_b and C_c), 49.9 (C_g), 47.4 (C_a and C_d), 43.5 (*C*H_2-NHCO). IR (ATR): 3269, 3068, 2966, 1646, 1547, 1455, 1335, 1229, 1062, 1028, 907 cm^{-1}. HRMS (ESI+): m/z calculated for $C_{23}H_{24}N_2O_2$ + H^+ [M+H^+]: 361.1916, found 361.1938.

7.2.3 Experimental for Chapter 4

_N, N'_-Di-(2,3,4,6-tetra-O-acetyl-β-D-galactopyranosyl-1,2,3-triazol-4-ylmethylamide)-_N''_-(2-bromoacetamido)-5-aminobenzene-1,3-dicarboxamide (4.20)

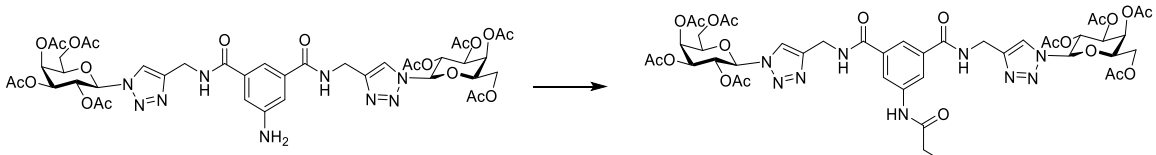

2.113 **4.20**

2.113 (1.128 g, 1.13 mmol) was dissolved in dry DCM (20 mL). NEt_3 (0.19 mL, 1.35mmol) was added to this solution. Bromoacetyl bromide (0.12 mL, 1.35 mmol) was dissolved in dry DCM (5 mL) in a separate round-bottom flask. The first solution was added to the second dropwise via a cannula and the resulting reaction mixture was allowed to stir for 16 h. The reaction mixture was washed with water (20 mL), HCl (1 N, 20 mL), sat. $NaHCO_3$ solution (20 mL), followed by brine (20 mL). The organic phase was dried ($MgSO_4$) and the solvent was removed *in vacuo* to obtain the pure product **4.20** without further purification as a brown, sticky solid (1.056 g, 83 %). R_f= 0.65 (DCM, 5% MeOH). $[\alpha]_D^{24}$ -4.0 (c 1.0, DCM). ^{1}H NMR (500 MHz, $CDCl_3$) δ 9.10 (s, 1H, N*H*COCH$_2$Br), 8.09 – 7.90 (m, 6H, triaz-H, CON*H*CH$_2$-triaz and Ar-H), 7.75 (s, 1H, Ar-H), 5.93 (d, *J* = 9.2 Hz, 2H, H-1), 5.60 (t, *J* = 9.7 Hz, 2H, H-2), 5.54 (d, *J* = 2.9 Hz, 2H,

H-4), 5.32 – 5.26 (m, 2H, H-3), 4.75-4.59 (m, 4H, C*H*$_2$-triaz), 4.31 (t, *J* = 6.4 Hz, 2H, H-5), 4.22 – 4.11 (m, 4H, H-6 and H-6'), 3.98 (s, 2H, C*H*$_2$-Br), 2.21 (s, 6H, OAc), 2.00 (m, 12H, OAc x 2), 1.82 (s, 6H, OAc). ^{13}C NMR (125 MHz, $CDCl_3$) δ 170.4 (CO of OAc), 170.1 (CO of OAc), 169.8 (CO of OAc), 169.4 (CO of OAc), 166.5 (*C*ONHCH$_2$-triaz), 165.0 (*C*OCH$_2$Br), 145.6 (*C*-triaz), 138.3 (Ar-*C*), 135.0 (Ar-*C*), 121.6 (*C*H-triaz), 121.4 (Ar-*C*H), 121.2 (Ar-*C*H), 86.2 (C-1), 74.0 (C-5), 70.8 (C-3), 68.1 (C-2), 66.8 (C-4), 61.2 (C-6), 35.5 (*C*H$_2$-triaz), 29.6 (NHCO*C*H$_2$Br), 20.7 (CH_3 of OAc), 20.6 (CH_3 of OAc), 20.5 (CH_3 of OAc), 20.3 (CH_3 of OAc). IR (film on NaCl): 3345, 3087, 2975, 1752, 1651, 1536, 1446, 1371, 1227, 1063, 924 732 cm^{-1}. HRMS (ESI+): m/z calculated for $C_{44}H_{52}BrN_{12}O_{21}$ + H^+ [M+H$^+$]: 1122.2539, found 1122.2545.

N, N'-Di-(2,3,4,6-tetra-O-acetyl-β-D-galactopyranosyl-1,2,3-triazol-4-ylmethylamide)-*N"*-(2-azidoacetamido)-5-aminobenzene-1,3-dicarboxamide (4.21)

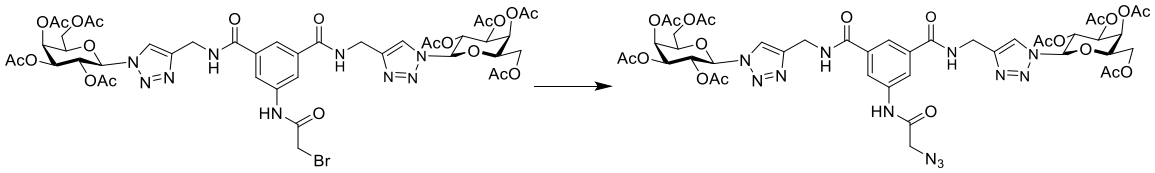

4.20 **4.21**

4.20 (231 mg, 0.206 mmol) and NaN_3 (30 mg, 0.412 mmol) were dissolved in anhydrous DMF (10 mL) and heated to 80 °C. The reaction mixture was allowed to stir for 16 h. The solvent was removed *in vacuo*, and the resulting residue was re-dissolved in DCM (20 mL) and was washed with brine (20 mL x 3). The organic phase was dried over $MgSO_4$ and the solvent was removed *in vacuo* to obtain the pure product **4.21** without further purification as a yellow solid (1.056 g, 83 %). R$_f$= 0.41 (DCM:MeOH 9:1). $[\alpha]_D^{22}$ -5.6 (c 0.9, DCM). ^{1}H NMR (500 MHz, $CDCl_3$) δ 9.10 (s, 1H, N*H*COCH$_2$N$_3$), 8.18 (s, 2H, N*H*CH$_2$CCH), 8.02 (s, 2H, Ar-H), 7.97 (s, 2H, C*H*-triaz), 7.82 (s, 1H, Ar-H), 5.95 (d, *J* = 9.2 Hz, 2H, H-1), 5.61 (t, *J* = 9.7 Hz, 2H, H-2), 5.56 (d, *J* = 3.1 Hz, 2H, H-4), 5.32 (dd, *J* = 10.1, 3.5 Hz, 2H, H-3), 4.73-4.60 (m, 4H, C*H*$_2$-triaz), 4.67 (ddd, *J* = 20.4, 15.4, 5.5 Hz, 4H, C*H*$_2$-triaz), 4.34 (t, *J* = 6.6 Hz, 2H, H-5), 4.23 – 4.13 (m, 4H, H-6 and H-6'), 4.06 (s, 2H, C*H*$_2$-N$_3$), 2.21 (s, 6H, OAc), 2.01 (s, 12H, OAc x 2), 1.82 (s, 6H, OAc). ^{13}C NMR (125 MHz, $CDCl_3$) δ 170.4 (CO of OAc), 170.1 (CO of OAc), 169.9 (CO of OAc), 169.3 (CO of OAc), 166.5 (*C*ONHCH$_2$CCH), 166.3 (*C*OCH$_2$N$_3$), 145.5 (*C*-

triaz), 138.0 (Ar-*C*), 134.9 (Ar-*C*), 121.6 (Ar-*C*H and *C*H-triaz), 121.4 (Ar-*C*H), 86.1 (C-1), 73.9 (C-5), 70.8 (C-3), 68.1 (C-2), 66.9 (C-4), 61.2 (C-6), 52.5 (CH_2N_3), 35.4 (CH_2-triaz), 20.7 (CH_3 of OAc), 20.6 (CH_3 of OAc), 20.5 (CH_3 of OAc), 20.2 (CH_3 of OAc). IR (film on NaCl): 3342, 2942, 2110, 1747, 1655, 1528, 1427, 1368, 1211, 1046, 923, 733 cm^{-1}. HRMS (ESI+): m/z calculated for $C_{44}H_{52}N_{12}O_{21}$ + Na^+ [M+Na^+]: 1107.3268, found 1107.3303.

2-[2-(2-Propargyloxyethoxy)ethoxy]ethanol (4.25)

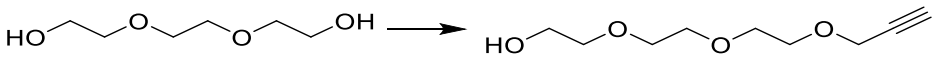

4.24 **4.25**

Triethylene glycol **4.24** (1 mL, 7.48 mmol, 3 equiv) was diluted with dry THF (10 mL) under N_2. The solution was cooled to 0°C and NaH (60% oil dispersion) (0.1 g, 2.49 mmol) was added portion-wise. The reaction was allowed to warm up to rt and was stirred for 20 mins. Propargyl bromide (0.27 mL, 2.49 mmol) was added dropwise. The reaction mixture was allowed to stir overnight. Column chromatography (100% EtOAc) eluted the pure product **4.25** as a clear oil (0.292 g, 75 %). (R_f=0.42: EtOAc) ^{1}H NMR (500 MHz, $CDCl_3$) δ 4.09 – 4.08 (m, 2H, CH_2CCH), 3.63 – 3.53 (m, 10H, CH_2 x 5), 3.50 – 3.46 (m, 2H, CH_2-OH), 3.11 (s, 1H, OH), 2.39 (t, *J* = 2.8 Hz, 1H, CH_2CC*H*).

The NMR data is in agreement with the data reported in the literature.[240]

2-(2-(2-Propargyloxyethoxy)ethoxy)ethyl-4-methylbenzenesulfonate (4.26)

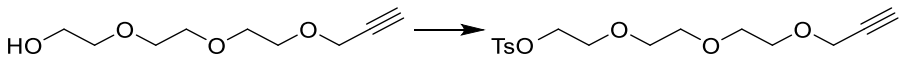

4.25 **4.26**

4.25 (0.288 g, 1.53 mmol) was dissolved in DCM (5 mL). TsCl (0.321 g, 1.68 mmol, 1.1 equiv) was added and the mixture was cooled to 0 °C on ice. KOH (0.343 g, 6.12 mmol, 4 equiv) was added slowly after grinding. The mixture was vigorously stirred for 2 h. The mixture was poured onto ice-water and extracted with DCM (3 x20 mL). The combined organic layers were dries over $MgSO_4$, filtered and concentrated *in vacuo* to give the pure product **4.26** as a clear oil (0.457 g, 87 %). ^{1}H NMR (500 MHz, $CDCl_3$) δ 7.79 (d, *J* = 8.3 Hz, 2H, Ar-H), 7.33 (d, *J* = 8.2 Hz, 2H, Ar-H), 4.18 (d, *J* = 2.4 Hz, 2H,

C*H*$_2$CCH), 4.16 – 4.13 (m, 2H, C*H*$_2$OTs), 3.69 – 3.65 (m, 4H, CH$_2$ x 2), 3.65 – 3.61 (m, 2H, CH$_2$), 3.58 (s, 4H, CH$_2$ x 2), 2.43 (s, 3H, CH$_3$-Ar), 2.42 (t, *J* = 2.4 Hz, 1H, CH$_2$CC*H*).

The NMR data is in agreement with the data reported in the literature.[241]

_N, N'_-Di-(2,3,4,6-tetra-O-acetyl-β-D-galactopyranosyl-1,2,3-triazol-4-ylmethyl amide)-_N"_-(2-4-((2-(2-(2-(4-methylbenzenesulfonate)ethoxy)ethoxy)ethoxy) methyl)-1H-1,2,3-triazol-1-yl)acetamido)-5-aminobenzene-1,3-dicarboxamide (4.27)

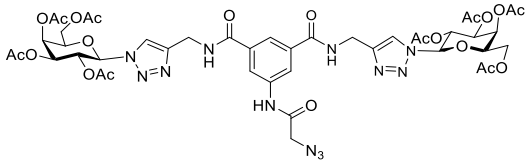

4.21

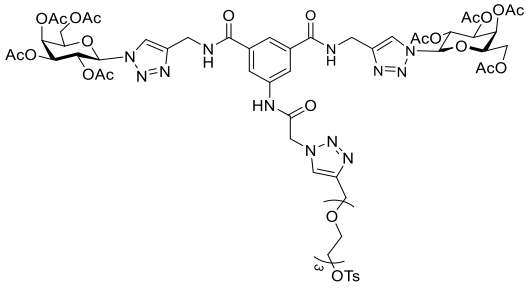

4.27

Copper sulphate pentahydrate (20 mg) and sodium ascorbate (40 mg) were added to a solution **4.21** (0.516 g, 0.476 mmol) and **4.26** (0.163 g, 0.476 mmol) in CH$_3$CN/H$_2$O (4 mL/ 2 mL). The reaction was allowed to stir in the MW at 100 ^{o}C until deemed complete by TLC analysis (15 min). The solvent was removed *in vacuo*. The residue was dissolved in DCM (30 mL), washed with brine (20 mL x 3), and dried (MgSO$_4$). The mixture was filtered and the solvent was removed *in vacuo* to yield the crude product, which was purified by silica gel column chromatography (DCM:MeOH 98:2-95:5) to give the pure product as a yellow solid (0.307 g, 74 %). R$_f$= 0.45 (DCM:MeOH 9:1). $[\alpha]_D^{22}$ -5 (c 1, DCM). ^{1}H NMR (500 MHz, CDCl$_3$) δ 9.82 (s, 1H, N*H*COCH$_2$-triaz), 8.16 (s, 2H, CON*H*CH$_2$-triaz), 7.97 (s, 2H, C*H*-triaz), 7.84 (appd, *J* = 2.8 Hz, 3H, Ar-H x 2 and C*H*-triaz), 7.76 (s, 1H, Ar-H), 7.69 (d, *J* = 8.3 Hz, 2H, Ar-H of OTs), 7.26 (d, *J* = 8.1 Hz, 2H, Ar-H of OTs), 5.89 (d, *J* = 9.2 Hz, 2H, H-1), 5.60 (t, *J* = 9.7 Hz, 2H, H-2) 5.50 (d, *J* = 2.9 Hz, 2H, H-4), 5.26 (dd, *J* = 10.3, 3.3 Hz, 2H, H-3), 5.21 (s, 2H, CH$_2$), 4.67 – 4.55 (m, 6H, CONHC*H*$_2$-triaz and NHCOC*H*$_2$-triaz), 4.28 (t, *J* = 6.6 Hz, 2H, H-5), 4.20-4.10 (m, 4H, H-6 and H-6'), 4.11 (qd, *J* = 11.5, 6.6 Hz, 2H, H-6 and H-6'), 4.06 – 4.04 (m, 2H, CH$_2$), 3.65 – 3.59 (m, 2H, CH$_2$), 3.58 – 3.54 (m, 4H, CH$_2$ x 2), 3.48 (s, 2H, CH$_2$), 2.37 (s, 3H, CH$_3$ of OTs), 2.14 (s, 6H, CH$_3$ of OAc), 1.96 (s, 6H, CH$_3$ of OAc), 1.95 (s, 6H, CH$_3$ of OAc), 1.75 (s, 6H, CH$_3$ of OAc). ^{13}C NMR (125 MHz, CDCl$_3$) δ 170.4 (CO of OAc), 170.1

(CO of OAc), 169.9 (CO of OAc), 169.3 (CO of OAc), 166.6 (*C*ONHCH$_2$CCH), 164.5 (*C*OCH$_2$N$_3$), 145.4 (*C*-triaz), 144.9 (Ar-C of OTs), 144.8 (CH*C*N$_3$), 138.1 (Ar-*C*), 134.8 (Ar-*C*), 132.7 (Ar-*C* of OTs), 129.9 (Ar-*C*H of OTs), 127.9 (Ar-*C*H of OTs), 125.3 (*C*HCN$_3$), 121.9 (*C*H-triaz), 121.6 (Ar-*C*H), 121.3 (Ar-*C*H), 86.0 (C-1), 73.8 (C-5), 70.9 (C-3), 70.5 (CH$_2$), 70.4 (CH$_2$), 70.3 (CH$_2$), 69.7 (CH$_2$), 69.4 (CH$_2$), 68.6 (CH$_2$), 68.0 (C-2), 66.9 (C-4), 64.3 (NHCO*C*H$_2$N$_3$), 61.1 (C-6), 52.8 (CH$_2$), 35.4 (*C*H$_2$-triaz), 21.6 (CH$_3$ of OAc), 20.6 (CH$_3$ of OAc), 20.5 (CH$_3$ of OAc), 20.2 (CH$_3$ of OAc). IR (film on NaCl): 3344, 3091, 2939, 1754, 1657, 1599, 1535, 1448, 1370, 1223, 1176, 1095, 1054, 924 cm^{-1}. HRMS (ESI+): m/z calculated for $C_{60}H_{74}N_{12}O_{27}S + Na^+$ [M+Na$^+$]: 1449.4405, found 1449.4332.

N, N'-Di-(2,3,4,6-tetra-O-acetyl-β-D-galactopyranosyl-1,2,3-triazol-4-ylmethylamide)-*N"*-(2-4-((2-(2-(2-azidoethoxy)ethoxy)ethoxy)methyl)-1H-1,2,3-triazol-1-yl)acetamido)-5-aminobenzene-1,3-dicarboxamide (4.28)

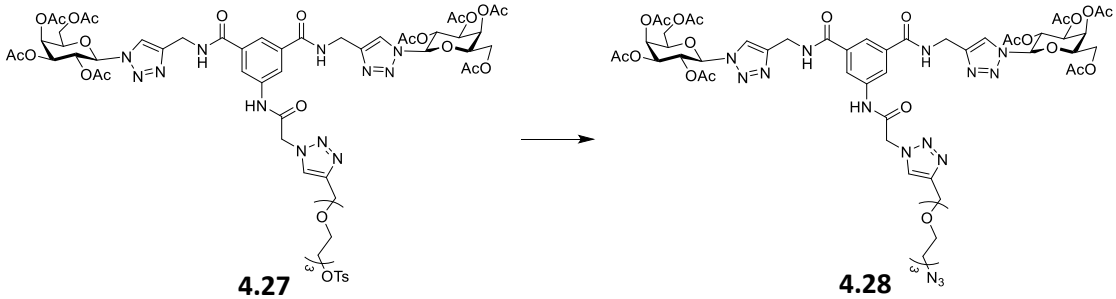

4.27 **4.28**

Compound **4.27** (183 mg, 0.128 mmol) and NaN$_3$ (17 mg, 0.256 mmol) were dissolved in anhydrous DMF (10 mL) and heated to 80 °C. The reaction mixture was allowed to stir for 16 h. The solvent was removed *in vacuo*, and the resulting residue was dissolved in DCM (20 mL) and was washed with brine (20 mL x 3). The organic phase was dried (MgSO$_4$) and the solvent was removed *in vacuo* to obtain the pure product without further purification as a yellow solid (167 g, 100 %). R$_f$= 0.42 (DCM:MeOH 9:1). $[\alpha]_D^{22}$ -3 (c 1, DCM). ^{1}H NMR (500 MHz, CDCl$_3$) δ 9.79 (s, 1H, N*H*CH$_2$N$_3$), 8.13 (s, 2H, N*H*CH$_2$-triaz), 7.94 (s, 2H, C*H*-triaz), 7.82 (s, 1H, C*H*-triaz), 7.77 (s, 2H, Ar-H), 7.70 (s, 1H, Ar-H), 5.85 (d, *J* = 9.2 Hz, 2H, H-1), 5.57 (t, *J* = 9.8 Hz, 2H, H-2), 5.47 (d, *J* = 2.7 Hz, 2H, H-4), 5.25 – 5.15 (m, 4H, H-3 and CH$_2$), 4.66 – 4.48 (m, 6H, C*H$_2$*-triaz x 3), 4.24 (t, *J* = 6.3 Hz, 2H, H-5), 4.13 – 4.04 (m, 4H, H-6 and H-6'), 3.67 – 3.47 (m, 8H, CH$_2$ x 4), 3.27 – 3.24 (m, 2H, CH$_2$), 2.12 (s, 6H, CH$_3$ of OAc), 1.94 (s, 6H, CH$_3$ of OAc), 1.93 (s, 6H, CH$_3$ of OAc), 1.73 (s, 6H, CH$_3$ of OAc). ^{13}C NMR (125 MHz, CDCl$_3$) δ 170.5 (CO of

OAc), 170.2 (CO of OAc), 170.0 (CO of OAc), 169.4 (CO of OAc), 166.7 (*C*ONHCH$_2$-triaz), 164.5 (*C*OCH$_2$N$_3$), 145.6 (*C*-triaz), 145.0 (CH*C*N$_3$), 134.9 (Ar-C), 125.4 (*C*HCN$_3$), 121.9 (*C*H-triaz), 121.7 (Ar-*C*H), 121.3 (Ar-*C*H), 86.2 (C-1), 74.0 (C-5), 71.0 (C-3), 70.6 (CH$_2$ x 2), 70.0 (CH$_2$), 69.9 (CH$_2$), 68.1 (C-2), 67.0 (C-4), 64.5 (NHCO*C*H$_2$N$_3$), 61.2 (C-6), 50.7 (CH$_2$), 35.5 (*C*H$_2$-triaz), 20.7 (CH$_3$ of OAc x 2), 20.6 (CH$_3$ of OAc), 20.4 (CH$_3$ of OAc). IR (film on NaCl): 3335, 3088, 2924, 2109, 1754, 1658, 1600, 1534, 1447, 1370, 1222, 1054, 924 cm^{-1}. HRMS (ESI+): m/z calculated for $C_{53}H_{67}N_{15}O_{24}$ + Na^+ [M+Na^+]: 1320.4381, found 1320.4375.

Acetylated Aromatic-Centred Trivalent Glycoconjugate (4.29)

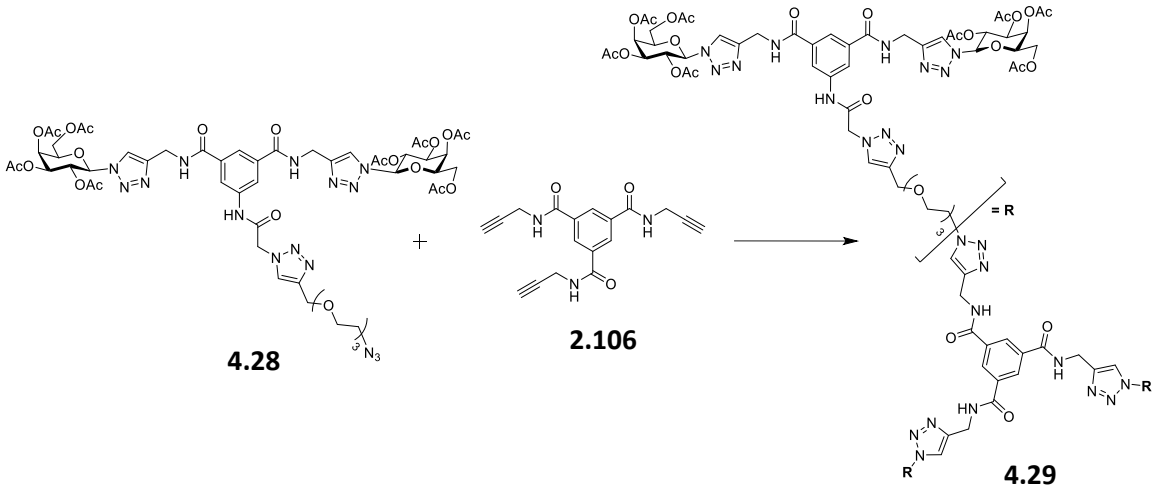

Copper sulphate pentahydrate (20 mg) and sodium ascorbate (40 mg) were added to a solution of compound **4.28** (40 mg, 0.0311 mmol) and *N, N', N''*-tri(prop-2-yn-1-yl)benzene-1, 3, 5-tricarboxamide **2.106** (10 mg, 0.0311 mmol) in CH$_3$CN/H$_2$O (4 mL/ 2 mL). The reaction was allowed to stir in the MW at 100 ^{o}C until deemed complete by TLC analysis (20 min). The solvent was removed *in vacuo*. The residue was dissolved in DCM (30 mL), washed with brine (20 mL x 3), and dried (MgSO$_4$). The mixture was filtered and the solvent was removed *in vacuo* to yield the crude product, which was purified by silica gel column chromatography (DCM:MeOH 98:2-95:5) to give the pure product as a yellow solid (94 mg, 72 %). R$_f$= 0.48 (DCM:MeOH 9:1). $[\alpha]_D^{23}$ -5.0˚ (c= 0.5, DCM). ^{1}H NMR (500 MHz, CDCl$_3$) δ 10.22 – 9.50 (m, 3H, NH), 8.52 – 7.62 (m, 28H, Ar-H's, C*H*-triaz's, NH's), 5.94 – 5.84 (m, 6H, H-1), 5.65 – 5.58 (m, 6H, H-2), 5.51 (bs, 6H, H-4), 5.30 – 5.25 (m, 12H, H-3), 4.74 – 4.48 (m, 20H, CH$_2$-triaz), 4.30 (bs, 10H, H-5 and CH$_2$'s), 4.22 – 4.02 (m, 16H, H-6 and H-6'), 3.90-3.30 (m, 30H,

CH_2's), 2.16 (s, 18H, OAc), 1.97 (s, 36H, OAc), 1.76 (s, 18H, OAc). ^{13}C NMR (125 MHz, $CDCl_3$) δ 170.4, 170.2, 170.0, 168.8, 145.7, 138.3, 135.2, 130.1, 128.0, 122.2, 121.3, 86.2, 77.4, 77.2, 76.9, 73.9, 71.0, 70.5, 68.1, 67.0, 61.2, 54.0, 53.9, 43.1, 41.1, 35.5, 29.8, 29.4, 22.8, 20.7, 20.6, 20.3, 14.2. HRMS (ESI+): m/z calculated for $C_{177}H_{216}N_{48}O_{75}$ + $3H^+$ $[M+3H]^{3+}$: 1405.4855, found 1405.4834.

***Tert*-butyl 3-(prop-2-yn-1-ylamino)propanoate (4.32)**

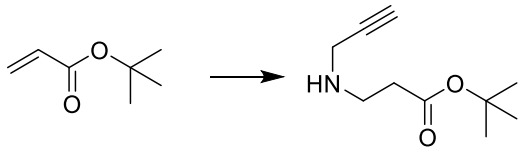

4.31 **4.32**

Tert-butyl acrylate **4.31** (0.64 mL, 4.38 mmol) was dissolved in methanol previously dried over 4 Å molecular sieves (10 mL) under N_2. Propargylamine (0.6 mL, 8.76 mmol) was added to the solution, and the mixture was warmed to 50 °C and was allowed to stir for 24 h. The methanol and propargylamine were removed *in vacuo* to yield the pure product **4.32** in quantitative yield as an orange/brown liquid (0.821 g). ^{1}H NMR (500 MHz, $CDCl_3$) δ 3.38 (d, *J* = 2.4 Hz, 2H, C*H*$_2$CCH), 2.87 (t, *J* = 6.5 Hz, 2H, C*H*$_2$CH$_2$), 2.40 (t, *J* = 6.5 Hz, 2H, C*H*$_2$CH$_2$), 2.18 (t, *J* = 2.4 Hz, 1H, CH$_2$CC*H*), 1.59 (bs, 1H, N*H*), 1.41 (s, 9H, C(C*H*$_3$)$_3$). ^{13}C NMR (125 MHz, $CDCl_3$) δ 171.9 (CO), 82.0 (C), 80.6 (C), 71.4 (*C*H), 44.1 (*C*H$_2$), 38.1 (*C*H$_2$), 35.7 (*C*H$_2$), 28.1 (C(*C*H$_3$)$_3$).

^{1}H NMR and ^{13}C NMR spectroscopic data corresponded to that found in the literature.[246]

***Tert*-butyl 3-(*N*-(prop-2-yn-1-yl)acrylamido)propanoate (4.33)**

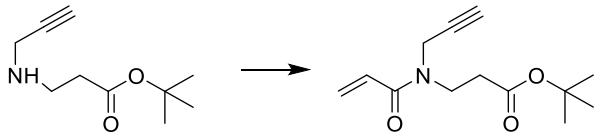

4.32 **4.33**

4.32 (0.821 g, 4.48 mmol) was dissolved in dry DCM (20 mL) under N_2 at 0 °C. Acryloyl chloride (0.44 mL, 5.38 mmol) and *N*,*N*-diisopropylethylamine (1.56 mL, 8.96 mmol) were added to the solution. The reaction mixture was allowed to stir for 1 hour, and the solution was washed with water (20 mL x 2). The organic phase was dried over

$MgSO_4$ and concentrated under reduced pressure to give the crude product, which was purified by silica gel column chromatography (cyclohexane:ethyl acetate 3:2) to give the pure product **4.33** as a yellow liquid (0.758 g, 72 %). ^{1}H NMR (500 MHz, $CDCl_3$) δ 6.65-6.52 (m, 1H, CH_2=C*H*CO), 6.42-6.25 (m, 1H, C*H*=CHCO), 5.76-5.65 (m, 1H, C*H'*=CHCO), 4.28 (s, 1H, C*H*$_2$CCH rotamer 1), 4.17 (s, 1H, C*H*$_2$CCH rotamer 2), 3.81 – 3.65 (m, 2H, C*H*$_2$CH$_2$), 2.58 (d, *J* = 6.4 Hz, 2H, CH$_2$C*H*$_2$), 2.30 (s, 1H, CH$_2$CC*H* rotamer 1), 2.22 (s, 1H, CH$_2$CC*H* rotamer 2), 1.43 (s, 9H, C(C*H*$_3$)$_3$).

^{1}H NMR spectroscopic data corresponded to that found in the literature.[278]

Tert-butyl 3-(*N*-(prop-2-yn-1-yl)-3-(prop-2-yn-1-ylamino)propanamido)propanoate (4.34)

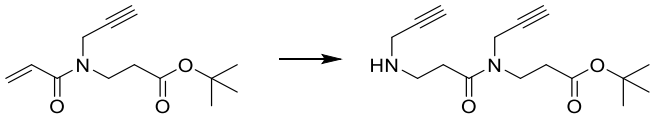

4.33 **4.34**

4.33 (0.758, 3.19 mmol) was dissolved in methanol previously dried over 4 Å molecular sieves (20 mL) under N_2. Propargylamine (0.31 mL, 4.79 mmol) was added to the solution, and the mixture was warmed to 50 °C and was allowed to stir for 24 h. The methanol and propargylamine was removed *in vacuo* to yield the pure product **4.34** in quantitative yield as a dark yellow liquid (0.934 g). ^{1}H NMR (500 MHz, $CDCl_3$) δ 4.19 (d, *J* = 2.4 Hz, 2H, C*H*$_2$CCH rotamer 2), 4.09 (d, *J* = 2.4 Hz, 2H, C*H*$_2$CCH rotamer 1), 3.68 (t, *J* = 7.3 Hz, 2H, CH_2), 3.63 (t, *J* = 6.9 Hz, 2H, CH_2), 3.41 – 3.39 (m, 4H, CH_2), 2.95 (t, *J* = 6.1 Hz, 4H, CH_2), 2.60 (td, *J* = 6.1, 2.7 Hz, 4H, CH_2), 2.54 (dt, *J* = 14.1, 7.2 Hz, 4H, CH_2), 2.27 (t, *J* = 2.4 Hz, 1H, C*H* rotamer 1), 2.20 – 2.18 (m, 1H, C*H* rotamer 2 and), 1.92 (bs, 1H, NH), 1.42 (s, 9H, C(C*H*$_3$)$_3$), 1.41 (s, 9H, C(C*H*$_3$)$_3$). ^{13}C NMR (125 MHz, $CDCl_3$) δ 171.8 (CH$_2$*C*CH), 171.5 (CH$_2$*C*CH), 171.3 (CO), 170.2 (CO), 82.0, 81.4 (*C*(CH$_3$)$_3$), 80.8 (*C*(CH$_3$)$_3$), 78.9, 78.6, 72.7 (CH rotamer 1), 71.9 (CH rotamer 2), 71.4 (CH), 44.3 (CH_2), 44.2 (CH_2), 43.0 (CH_2 rotamer 1), 42.8 (CH_2 rotamer 2), 38.4 (*C*H$_2$CCH rotamer 1), 38.3 (CH_2), 34.5 (CH_2), 34.1 (*C*H$_2$CCH rotamer 2), 33.3 (CH_2), 33.1 (CH_2), 28.1 (C(*C*H$_3$)$_3$), 28.0 (C(*C*H$_3$)$_3$).

^{1}H NMR and ^{13}C NMR spectroscopic data corresponded to that found in the literature.[246]

***Tert*-butyl 3-(N-(prop-2-yn-1-yl)-3-(N-(prop-2-yn-1-yl)acrylamido)propanamido) propanoate (4.35)**

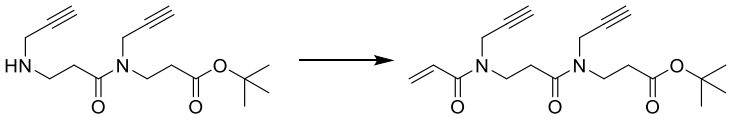

4.34 **4.35**

4.34 (0.905 g, 3.09 mmol) was dissolved in dry DCM (20 mL) under N_2 at 0 °C. Acryloyl chloride (0.30 mL, 3.71 mmol) and *N*,*N*-diisopropylethylamine (1.07 mL, 6.18 mmol) were added to the solution. The reaction mixture was allowed to stir for 1 hour, and the solution was washed with water (20 mL x 2). The organic phase was dried over $MgSO_4$ and concentrated under reduced pressure to give the crude product, which was purified by silica gel column chromatography (cyclohexane:ethyl acetate 3:2) to give the pure product **4.35** as a yellow liquid (0.729 g, 68 %). ^{1}H NMR (500 MHz, $CDCl_3$) δ 6.77-6.53 (m, 1H, *H*C=C), 6.44 – 6.27 (m, 1H, *H*C=C), 5.73 (t, *J* = 9.1 Hz, 1H, *H*C=C), 4.34 – 4.17 (m, 1H), 4.15 – 4.07 (m, 2H), 3.87 (t, *J* = 7.4 Hz, 1H), 3.77 (q, *J* = 5.8 Hz, 1H), 3.73 – 3.58 (m, 2H), 2.88-2.74 (m, 2H), 2.54 (t, *J* = 6.9 Hz, 2H), 2.32 – 2.17 (m, 2H), 2.03 (d, *J* = 1.2 Hz, 1H), 1.43 (bs, 9H, C(C*H*$_3$)$_3$).

^{1}H NMR spectroscopic data corresponded to that found in the literature.[278]

***Tert*-butyl 3-(*N*-(prop-2-yn-1-yl)-3-(*N*-(prop-2-yn-1-yl)-3-(prop-2-yn-1-ylamino)propanamido) propanamido)propanoate (4.36)**

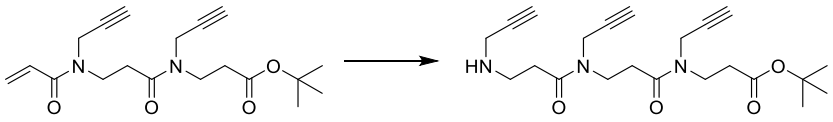

4.35 **4.36**

4.35 (0.710 g, 2.05 mmol) was dissolved in methanol previously dried over 4 Å molecular sieves (20 mL) under N_2. Propargylamine (0.26 mL, 4.10 mmol) was added to the solution, and the mixture was warmed to 50 °C and was allowed to stir for 24 h. The methanol and propargylamine was removed *in vacuo* to yield the pure product as a dark yellow liquid (0.782 g, 95 %). ^{1}H NMR (500 MHz, $CDCl_3$) δ 4.25 – 4.17 (m, 3H), 4.10 (dd, *J* = 4.6, 2.5 Hz, 1H), 3.83 – 3.77 (m, 1H), 3.74 – 3.61 (m, 3H), 3.42 (dd, *J* = 4.5, 2.5 Hz, 2H), 2.97 (t, *J* = 6.1 Hz, 2H), 2.83 – 2.71 (m, 2H), 2.66 – 2.60 (m, 2H), 2.59 – 2.49 (m, 2H), 2.35 – 2.24 (m, 1H), 2.21 (ddt, *J* = 9.4, 4.5, 2.4 Hz, 2H), 1.44 (bs, 9H, C(C*H*$_3$)$_3$).

^{1}H NMR spectroscopic data corresponded to that found in the literature.[246]

***Tert*-butyl 3-(*N*-(prop-2-yn-1-yl)-3-(*N*-(prop-2-yn-1-yl)-3-(*N*-(prop-2-yn-1-yl)acrylamido) propanamido)propanamido)propanoate (4.37)**

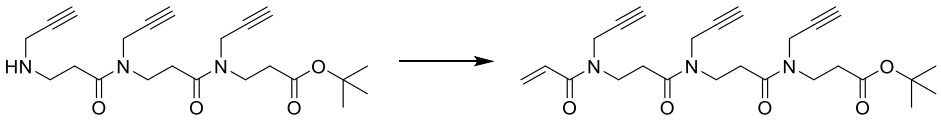

4.36 **4.37**

4.36 (0.754 g, 1.88 mmol) was dissolved in dry DCM (20 mL) under N_2 at 0 °C. Acryloyl chloride (0.18 mL, 2.25 mmol) and *N*,*N*-diisopropylethylamine (0.24 mL, 3.76 mmol) were added to the solution. The reaction mixture was allowed to stir for 1 hour, and the solution was washed with water (20 mL x 2). The organic phase was dried over $MgSO_4$ and concentrated under reduced pressure to give the crude product, which was purified by silica gel column chromatography (cyclohexane:ethyl acetate 3:2) to give the pure product **4.37** as a yellow liquid (0.557 g, 65 %). ^{1}H NMR (500 MHz, $CDCl_3$) δ 6.70-6.56 (m, 1H, *H*C=C), 6.44 – 6.29 (m, 1H, *H*C=C), 5.73 (s, 1H, *H*C=C), 4.31 (s, 1H), 4.26 – 4.22 (m, 2H), 4.22 – 4.18 (m, 2H), 3.89 (s, 1H), 3.79 (t, *J* = 6.6 Hz, 2H), 3.73 – 3.62 (m, 4H), 2.87-2.72 (m, 4H), 2.58-2.52 (m, 2H), 2.35 – 2.19 (m, 3H), 1.46 – 1.41 (m, 9H, C(C*H*$_3$)$_3$).

^{1}H NMR spectroscopic data corresponded to that found in the literature.[278]

***Tert*-butyl 5,9,13-trioxo-4,8,12-tri(prop-2-yn-1-yl)-4,8,12,16-tetraazanonadec-18-ynoate (4.38)**

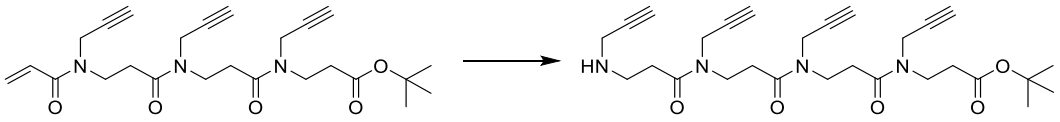

4.37 **4.38**

4.37 (0.542 g, 1.19 mmol) was dissolved in methanol previously dried over 4 Å molecular sieves (20 mL) under N_2. Propargylamine (0.15 mL, 2.38 mmol) was added to the solution, and the mixture was warmed to 50 °C and was allowed to stir for 24 h. The methanol and propagylamine was removed *in vacuo* to yield the pure product **4.38** as a dark yellow liquid (0.498 g, 82 %). ^{1}H NMR (500 MHz, $CDCl_3$) δ 4.25 – 4.17 (m, 5H), 4.15 – 4.09 (m, 1H), 3.79 (dt, *J* = 14.7, 6.4 Hz, 2H), 3.75 – 3.59 (m, 5H), 3.46 – 3.41 (m, 2H), 3.01 – 2.95 (m, 2H), 2.76 (q, *J* = 7.0, 5.8 Hz, 3H), 2.68 – 2.60 (m, 2H),

2.56 (dt, *J* = 14.0, 6.9 Hz, 2H), 2.33 – 2.17 (m, 4H), 1.58 (bs, 1H, N*H*), 1.47 – 1.42 (m, 9H, C(C*H*$_3$)$_3$).

^{1}H NMR spectroscopic data corresponded to that found in the literature.[246, 278]

Tert-butyl 16-acetyl-5,9,13-trioxo-4,8,12-tri(prop-2-yn-1-yl)-4,8,12,16-tetraazanonadec-18-ynoate (4.39)

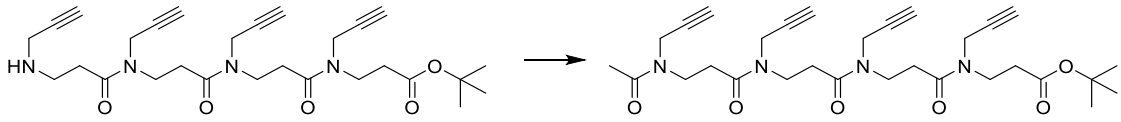

4.38 **4.39**

4.38 (0.490 g, 0.96 mmol) was dissolved in DCM (20 mL). Acetic anhydride (0.91 mL, 9.6 mmol) was added to the solution. The reaction mixture was allowed to stir for 6 h at rt and was concentrated under reduced pressure. The crude mixture was dissolved in ethyl acetate (20 mL) and was washed with sat $NaHCO_3$ (20 mL x 2) and brine (20 mL x 2). The organic layer was dried ($MgSO_4$), filtered and then concentrated *in vacuo*. The crude product was purified by silica gel column chromatography (DCM:MeOH 9:1) to give the pure product as a pale-yellow oil (515 mg, 97 %). ^{1}H NMR (500 MHz, $CDCl_3$) δ 4.24 – 4.06 (m, 8H), 3.83 – 3.70 (m, 3H), 3.72 – 3.60 (m, 5H), 2.91 – 2.68 (m, 6H), 2.55 (dt, *J* = 14.4, 6.9 Hz, 2H), 2.37 – 2.23 (m, 2H), 2.24 – 2.10 (m, 4H), 1.43 (m, 9H, C(C*H*$_3$)$_3$). ^{13}C NMR (125 MHz, $CDCl_3$) δ 171.5, 171.2, 170.9, 170.1, 81.7, 81.6, 81.4, 80.9, 78.9, 78.9, 78.6, 72.9, 72.8, 72.6, 72.5, 72.5, 72.1, 71.9, 71.7, 44.4, 44.2, 43.9, 43.7, 43.6, 43.5, 43.0, 42.8, 39.8, 39.1, 39.0, 38.9, 38.6, 38.4, 34.8, 34.5, 34.4, 34.3, 34.1, 32.2, 31.8, 29.7, 28.1, 21.8, 21.5. HRMS (ESI+): m/z calculated for $C_{30}H_{40}N_4O_6$ + H^+ [M+H^+]:553.3026, found 553.3015.

^{1}H NMR and ^{13}C NMR spectroscopic data corresponded to that found in the literature.[234]

2,6,10,14-Tetraoxo-3,7,11,15-tetrakis((1-(2,3,4,6-tetra-O-acetyl-β-D-galactopyranosyl -1H-1,2,3-triazol-4-yl)methyl)-3,7,11,15-tetraazaoctadecan-18-oic acid (4.40)

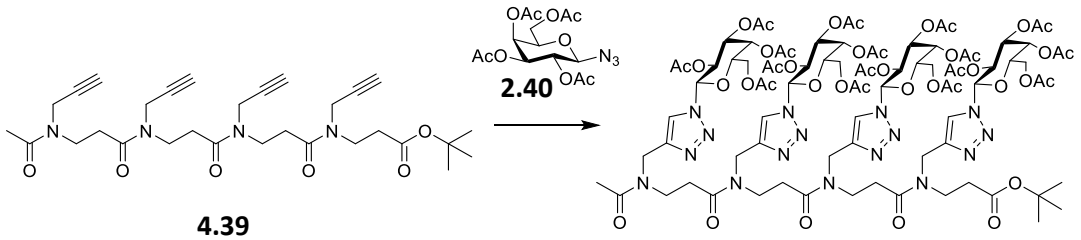

4.39 **2.40** **4.40**

Copper sulphate pentahydrate (40 mg) and sodium ascorbate (80 mg) were added to a solution of galactose azide **2.40** (567 mg, 1.520 mmol) and **4.39** (200 mg, 0.362 mmol) in CH_3CN/H_2O (4 mL/ 2 mL). The reaction was allowed to stir in the MW at 100 ^oC for 20 mins (10 mins x 2). The solvent was removed *in vacuo*. The residue was dissolved in DCM (30 mL), washed with brine (20 mL x 3), and dried ($MgSO_4$). The mixture was filtered and the solvent was removed *in vacuo* to yield the crude product, which was purified by silica gel column chromatography (DCM:MeOH 98:2-95:5) to give the pure product **4.40** as a yellow sticky solid (503 mg, 68 %). R_f= 0.47 (DCM:MeOH 9:1). $[\alpha]_D^{27}$ -4.71 (c 0.85, DCM). ^{1}H NMR (500 MHz, $CDCl_3$) δ 7.98 – 7.77 (m, 4H, triaz-H), 5.98 – 5.74 (m, 4H, H-1), 5.59 – 5.42 (m, 8H, H-2 and H-4), 5.37 – 5.18 (m, 4H, H-3), 4.81 – 4.49 (m, 8H, CH_2 x4), 4.35 – 4.08 (m, 12H, H-5, H-6 and H-6'), 3.83 – 3.53 (m, 8H, CH_2 x4), 3.02 – 2.68 (m, 6H, CH_2 x3), 2.65 – 2.47 (m, 2H, CH_2), 2.27 – 2.21 (m, 12H, OAc), 2.20 – 2.15 (m, 3H, NAc), 2.06 – 1.98 (m, 24H, OAc), 1.92 – 1.80 (m, 12H, OAc), 1.47 – 1.40 (m, 9H, C(CH_3)$_3$). ^{13}C NMR (125 MHz, $CDCl_3$) δ 171.3, 170.3, 170.1, 169.8, 168.8, 144.8, 144.6, 122.3, 122.2, 86.3, 77.3, 77.0, 76.8, 74.0, 70.8, 68.0, 66.8, 61.1, 45.2, 44.2, 40.8, 34.6, 31.9, 31.8, 28.1, 22.0, 21.5, 20.7, 20.6, 20.5, 20.2. IR (ATR): 2938, 1746, 1638, 1423, 1368, 1211, 1157, 1091, 1044, 952, 922, 841, 733 cm^{-1}. HRMS (ESI+): m/z calculated for $C_{86}H_{116}N_{16}O_{42}$ + Na^+ [M+Na^+]: 2067.7331, found 2067.7223.

2,6,10,14-Tetraoxo-3,7,11,15-tetrakis((1-(β-D-galactopyranosyl -1H-1,2,3-triazol-4-yl)methyl)-3,7,11,15-tetraazaoctadecan-18-oic acid (4.41)

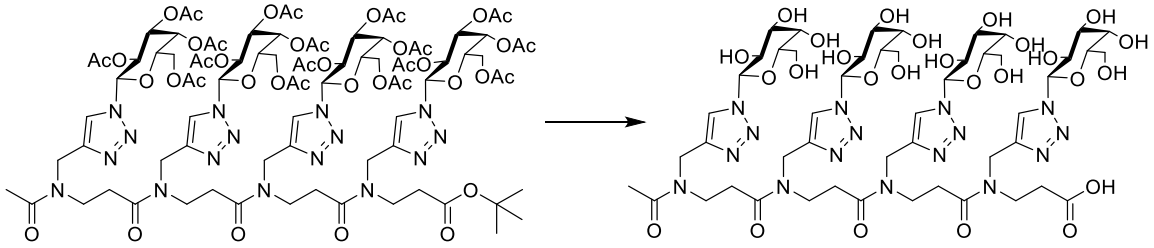

4.40 **4.41**

Compound **4.40** (452 mg, 0.221 mmol) was dissolved in methanol/H_2O (4 mL, 2 mL). NEt_3 (0.1 mL) was added, and the reaction mixture was allowed to stir at 45 ^oC for 6 h. The solution was cooled, Amberlite H^+ was added and the mixture was allowed to stir for 30 mins. The solution was filtered, and the solvent was removed *in vacuo*. Excess NEt_3 was removed using the Schlenk line. The product was freeze-dried over night to yield the pure product **4.41** as a white fluffy solid (267 mg, 92 %). $[\alpha]_D^{24}$ 14.0 (c 0.5, H_2O). ^1H NMR (500 MHz, D_2O) δ 8.23 – 8.16 (m, 2H), 8.08 (s, 2H), 5.64 – 5.54 (m, 4H, H-1), 4.65 – 4.42 (m, 8H, CH_2-triaz and CH_2), 4.19 – 4.06 (m, 4H, H-2), 4.01 (appdd, *J* = 5.2, 3.2 Hz, 4H, H-4), 3.97 – 3.86 (m, 4H, H-5), 3.85 – 3.76 (m, 4H, H-3), 3.75 – 3.61 (m, 12H, H-6, H-6' and CH_2 x 2), 3.58 – 3.51 (m, 4H), 2.80 – 2.46 (m, 8H, CH_2 x 4), 2.13 – 2.04 (m, 1H), 1.16 (s, 3H, CH_3). ^{13}C NMR (126 MHz, DMSO) δ 173.1, 170.5, 170.3, 144.6, 122.5, 122.3, 88.6, 88.5, 78.9, 75.6, 74.2, 69.9, 68.9, 60.9, 58.6, 45.7, 44.7, 43.8, 43.0, 42.9, 39.9, 22.1, 21.7, 9.0. IR (film on NaCl): 3299, 2916, 1719, 1620, 1451, 1421, 1365, 1224, 1087, 1053, 885 cm^{-1}. HRMS (ESI+): m/z calculated for $C_{50}H_{76}N_{16}O_{26}$ + Na^+ [M+Na^+]: 1339.5014, found 1339.5032.

Acetylated Tetravalent β-Peptoid Glycocluster (4.42)

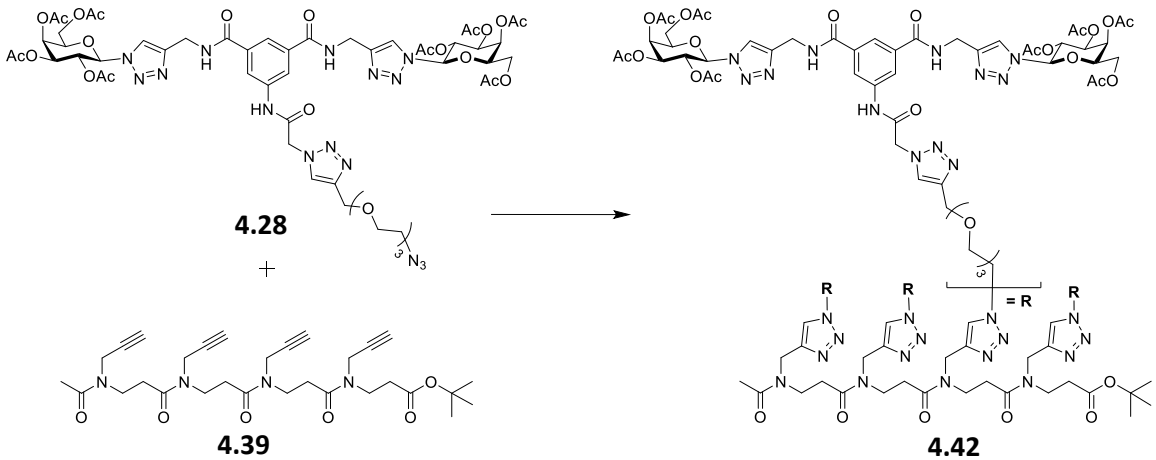

4.28 **4.39** **4.42**

Copper sulphate pentahydrate (40 mg) and sodium ascorbate (80 mg) were added to a solution of **4.28** (30 mg, 0.0231 mmol) and **4.39** (13 mg, 0.0231 mmol) in CH_3CN/H_2O (4 mL/ 2 mL). The reaction was allowed to stir in the MW at 100 ^oC for 10 mins x 2. The solvent was removed *in vacuo*. The residue was dissolved in DCM (30 mL), washed with brine (20 mL x 3), and dried ($MgSO_4$). The mixture was filtered and the solvent was removed *in vacuo* to yield the crude product, which was purified by silica gel column chromatography (DCM:MeOH 98:2-95:5) to give the pure product as a yellow sticky solid (77 mg, 58 %). R_f= 0.48 (DCM:MeOH 9:1). $[\alpha]_D^{24}$ -7 (c 1, DCM). ^{1}H NMR (500 MHz, $CDCl_3$) δ 10.08 (s, 4H, N*H*COCH$_2$-triaz), 8.56 – 7.59 (m, 36H, N*H*CH$_2$CCH x 8, CH$_2$CC*H* x 16 and Ar-H x 12), 5.91 (s, 8H, H-1), 5.63 (t, *J* = 10.2 Hz, 8H, H-2), 5.53 (s, 8H, H-4), 5.28 (appd, *J* = 10.2 Hz, 16H, H-3 and CH$_2$ x 4), 4.80 – 4.39 (m, 6H, C*H$_2$*-triaz, CH$_2$'s), 4.38-4.05 (m, H, H-5 and H-6, CH$_2$'s), 3.86 – 3.31 (m, 13H, CH$_2$'s), 3.11 – 2.31 (m, 4H, CH$_2$'s), 2.18 (s, 7H, OAc and NAc), 1.99 (s, 15H, OAc), 1.79 (s, 6H, OAc), 1.43 (s, 9H, C(C*H$_3$*)$_3$). ^{13}C NMR (125 MHz, $CDCl_3$) δ 170.59, 170.35, 170.09, 122.1, 121.6, 120.7, 86.3 (C-1), 74.1 (C-5), 71.1 (C-3), 71.0 (CH$_2$), 70.7 (CH$_2$), 70.6 (CH$_2$), 70.5 (CH$_2$), 69.8 (CH$_2$), 69.3 (CH$_2$), 68.2 (C-2), 67.1 (C-4), 64.7 (CH$_2$), 61.3 (C-6), 52.9 (CH$_2$), 50.3 (CH$_2$), 44.2 (CH$_2$), 43.5 (CH$_2$), 43.2 (CH$_2$), 42.8 (CH$_2$), 40.0 (CH$_2$), 39.8 (CH$_2$), 38.7 (CH$_2$), 35.5 (CH$_2$-triaz), 34.3 (CH$_2$), 33.8 (CH$_2$), 32.1 (CH$_2$), 29.89, 28.3 (C(*C*H$_3$)), 21.7 (CH$_3$ of NHAc), 20.84 (CH$_3$ of OAc), 20.72 (CH$_3$ of OAc), 20.45 (CH$_3$ of OAc), 1.21. IR (film on NaCl): 3392, 2927, 1753, 1647, 1536, 1448, 1370, 1223, 1092, 1060, 923, 732 cm^{-1}. MALDI-TOF-MS [M+H]$^+$: m/z calculated for $C_{242}H_{309}N_{64}O_{102}$ +H$^+$: 5744.104, found 5744.346.

Tetravalent β-Peptoid Glycocluster (4.43)

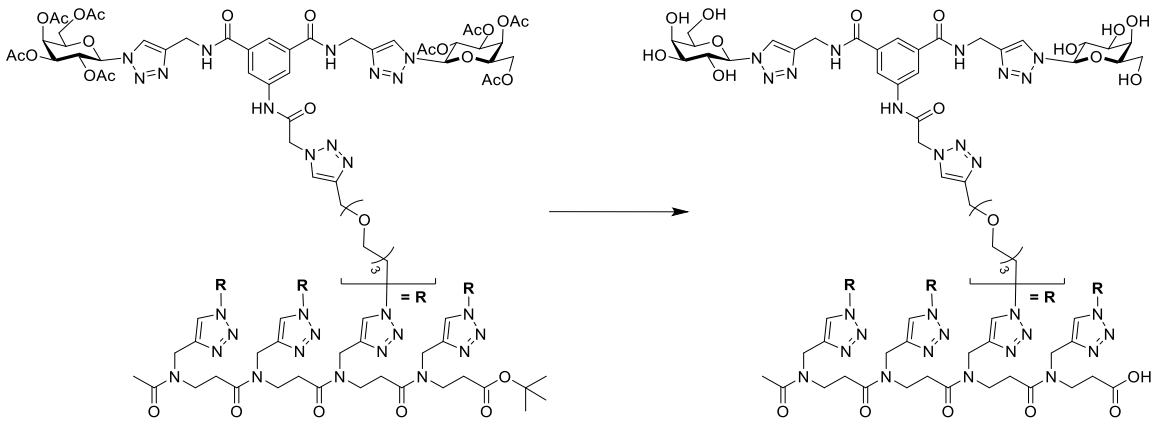

4.42 **4.43**

Compound **4.42** (70 mg, 0.0122 mmol) was dissolved in methanol/H_2O (4 mL, 2 mL). NEt_3 (0.1 mL) was added, and the reaction mixture was allowed to stir at 45 ^oC for 6 h. The solution was cooled, Amberlite H^+ was added and the mixture was allowed to stir for 30 mins. The solution was filtered, and the solvent was removed *in vacuo*. Excess NEt_3 was removed using the Schlenk line. The product was freeze-dried over night to yield the pure product **4.43** as a white fluffy solid (44 mg, 82 %). ^1H NMR (500 MHz, D_2O) δ 8.62 – 7.72 (m, 28H, Ar-H and triaz-H), 5.69 (s, 10H, H-1 and CH_2s), 5.47 (s, 6H, CH_2s), 4.74 – 4.44 (m, 24H, CH_2-triaz and CH_2s), 4.22 (s, 14H, H-2 and CH_2s), 4.11 (appd, *J* = 20.3 Hz, 14H, H-4 and CH_2s), 3.99 (s, 8H, H-5), 3.88 (appd, *J* = 9.8 Hz, 14H, H-3 and CH_2s), 3.84 – 3.36 (m, 60H, H-6, H-6' and CH_2s), 2.99 – 2.31 (m, 24H, CH_2s), 1.99 – 1.86 (m, 3H CH_3). ^{13}C NMR (125 MHz, DMSO) δ 171.1, 170.9, 166.1, 166.0, 165.1, 162.8, 145.5, 144.3, 139.1, 135.6, 126.2, 124.0, 122.3, 121.7, 88.5, 78.9, 74.2, 70.2, 70.1, 70.0, 69.8, 69.5, 69.4, 69.1, 68.9, 63.9, 60.9, 60.7, 52.6, 49.9, 49.8, 45.9, 40.5, 40.4, 40.2, 40.0, 39.9, 39.7, 39.5, 36.3, 35.4, 31.3, 28.2, 9.1. IR (ATR): 3301, 2925, 1650, 1540, 1443, 1388, 1253, 1092, 1055, 891 cm^{-1}. MALDI-TOF-MS $[M+H]^+$: m/z calculated for $C_{242}H_{309}N_{64}O_{102}$ $+Na^+$: 4422.7465, found 4422.807.

Triethylene glycol dipropargyl ether (4.45)

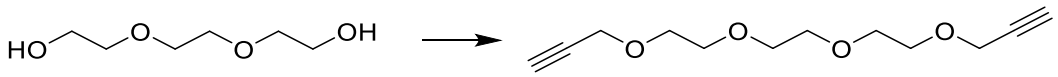

4.24 **4.45**

Triethylene glycol (1 mL, 7.33 mmol) was dissolved in dry THF under N_2. NaH (60 % dispersion in oil, 1.172 g, 29.3 mmol) was added and the reaction mixture was allowed to stir for 1 h. Propargyl bromide (mL, mmol) was added and the reaction mixture was allowed to stir for at rt for 48 h. The solvent was removed *in vacuo* and the resulting residue was dissolved in DCM (20 mL) and washed with water (10 mL x 2), dried ($MgSO_4$), filtered and concemtrated *in vacuo*. The crude product was purified by silica gel column chromatography (EtOAc:Pet Ether 2:1) to give the pure product as a yellow oil (1.526 g, 92 %). ^1H NMR (500 MHz, $CDCl_3$) δ 4.20 (d, *J* = 2.4 Hz, 4H, C*H*$_2$CCH), 3.72 – 3.51 (m, 12H, OC*H*$_2$ x 6), 2.42 (t, *J* = 2.4 Hz, 2H, CH_2CC*H*).

^1H NMR and ^{13}C NMR spectroscopic data corresponded to that found in the literature.[279]

_N,N'_-Di-(2,3,4,6-tetra-O-acetyl-β-D-galactopyranosyl-1,2,3-triazol-4-ylmethyl amide)-_N"_-(2-4-((2-(2-(2-(prop-2-yn-1-yloxy)ethoxy)ethoxy)ethoxy)methyl)-1H-1,2,3-triazol-1-yl)acetamido)-5-aminobenzene-1,3-dicarboxamide (4.28)

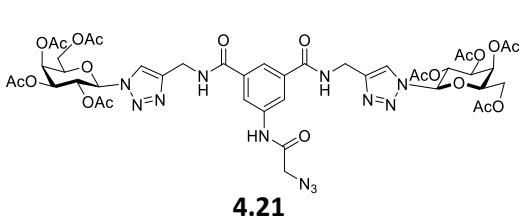

4.21

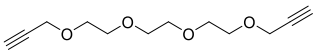

4.45

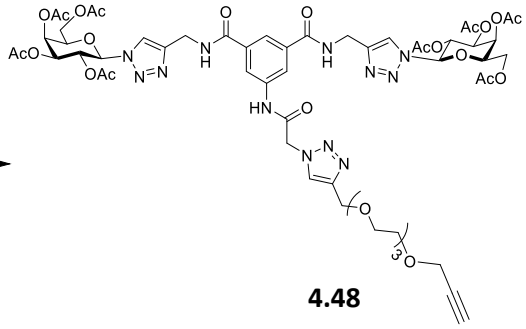

4.48

5 mL of a solution of compound **4.21** (prepared by dissolving 293 mg in 22 mL CH_3CN and 5 mL of water, [1 mM]) was combined with 5 mL of a solution of compound **4.45** (prepared by dissolving 223 mg in 22 mL CH_3CN and 5 mL of water, [36 mM]) in a microwave flask. To this solution, 0.5 mL of a solution of sodium ascorbate (prepared by dissolving 180 mg in 2 mL of water) were added, followed by 0.5 mL of a solution of copper sulfate pentahydrate (prepared by dissolving 70 mg in 2 mL of water). The mixture was allowed to react in the MW at 100 ^{o}C for 10 mins. TLC was used to monitor the reaction; staining the TLC using potassium permanganate solution displayed the product as a bright yellow spot, whereas the starting compound **4.21** was a white spot and the di-click product was a brown spot on the TLC plate after staining. This procedure was repeated until all the stock solutions was used to give a pale yellow solid (160 mg, 45 %). R_f= 0.65 (DCM:MeOH 9:1). $[\alpha]_D^{23}$ -1 (c 1, DCM). ^{1}H NMR (500 MHz, $CDCl_3$) δ 9.63 (s, 1H, N*H*COCH$_2$-triaz), 8.10 (bs, 2H, CON*H*CH$_2$-triaz), 7.91 (s, 2H, C*H*-triaz), 7.80 (s, 1H, C*H'*-triaz), 7.78 (s, 2H, Ar-H), 7.73 (s, 1H, Ar-H), 5.85 (d, *J* = 9.2 Hz, 2H, H-1), 5.57 (t, *J* = 9.8 Hz, 2H, H-2), 5.47 (d, *J* = 2.7 Hz, 2H, H-4), 5.23 – 5.19 (m, 4H, H-3 and C*H*$_2$), 4.65 – 4.56 (m, 6H, C*H*$_2$-triaz), 4.24 (t, *J* = 6.3 Hz, 2H, H-5), 4.13 – 4.04 (m, 6H, H-6, H-6' and OC*H*$_2$CCH), 3.61 – 3.53 (m, 12H, 3 x OC*H*$_2$C*H*$_2$O), 2.32 (s, 1H, CC*H*), 2.12 (s, 6H, CH_3 of OAc), 1.94 (s, 12H, CH_3 of OAc), 1.73 (s, 6H, CH_3 of OAc). ^{13}C NMR (125 MHz, $CDCl_3$) δ 169.3 (CO of OAc), 169.1 (CO of OAc), 168.9 (CO of OAc), 168.4 (CO of OAc), 165.6 (*C*ONHCH$_2$-triaz), 163.3 (*C*OCH$_2$-triaz), 144.5 (*C*-triaz), 143.9 (*C*-triaz), 137.1 (Ar-*C*), 133.9 (Ar-*C*), 124.2 (*CH*-triaz), 120.7 (*C*H-triaz and Ar-*C*H), 120.4 (Ar-*C*H), 85.1 (C-1), 78.5 (*C*CH), 73.9 (C-5), 72.8 (*C*CH), 69.7 (C-3), 69.4

(CH_2 x 2), 69.2 (CH_2), 68.8 (CH_2), 68.0 (C-2), 67.0 (C-4), 65.9 (NHCO*C*H_2N_3), 60.1 (C-6), 57.3 (O*C*H_2CCH), 52.4 (CH_2), 34.5 (*C*H_2-triaz), 19.6 (CH_3 of OAc x 2), 19.5 (CH_3 of OAc), 19.2 (CH_3 of OAc). IR (film on NaCl): 3290, 3145, 2917, 2115, 1752, 1657, 1535, 1447, 1370, 1225, 1093, 1054, 924 cm^{-1}. HRMS (ESI+): m/z calculated for $C_{56}H_{70}N_{12}O_{25}$ + Na^+ [M+Na^+]: 1333.4473, found 1333.4456.

_N, N'_-Di-(β-D-galactopyranosyl-1,2,3-triazol-4-ylmethylamide)-_N"_-(2-4-((2-(2-(2-(prop-2-yn-1-yloxy)ethoxy)ethoxy)methyl)-1H-1,2,3-triazol-1-yl) acetamido)-5-aminobenzene-1,3-dicarboxamide (4.29)

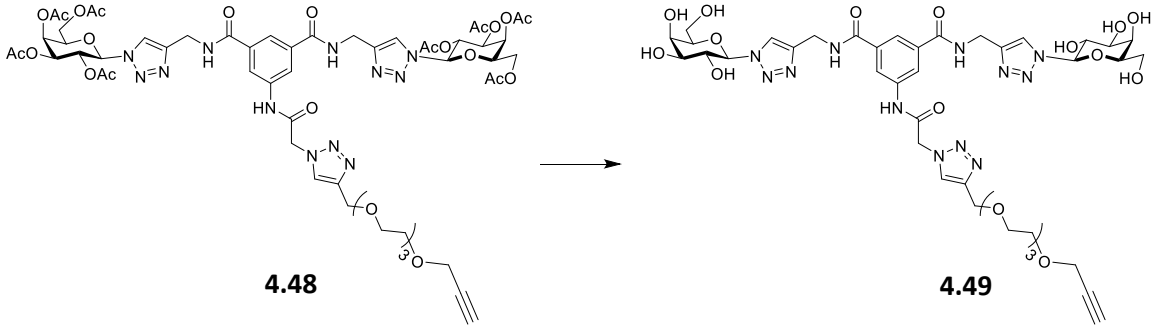

4.48 **4.49**

Compound **4.48** (150 mg, 0.114 mmol) was dissolved in methanol/H_2O (4 mL, 2 mL). NEt_3 (0.1 mL) was added, and the reaction mixture was allowed to stir at 45 ^oC for 6 h. The solution was cooled, Amberlite H^+ was added and the mixture was allowed to stir for 30 mins. The solution was filtered, and the solvent was removed *in vacuo*. Excess NEt_3 was removed using the Schlenk line. The product was freeze-dried over night to yield the pure product **4.43** as a white solid (100 mg, 90 %). $[\alpha]_D^{23}$ +7 (c 1, MeOH:H_2O 1:1). ^{1}H NMR (500 MHz, D2O) δ 8.19 (s, 2H, C*H*-triaz), 8.02 (s, 1H, C*H*-triaz), 7.86 (s, 2H, Ar-H), 7.78 (s, 1H, Ar-H), 5.58 (d, *J* = 9.3 Hz, 2H, H-1), 5.34 (s, 2H, CH_2), 4.58 (s, 2H, CH_2-triaz), 4.55 (s, 4H, CH_2-triaz), 4.13 (t, *J* = 9.8 Hz, 2H, H-2), 4.02 (s, 2H, OCH_2CCH), 3.99 (s, 2H, H-4), 3.89 (m, 2H, H-5), 3.79-3.77 (m, 2H, H-3), 3.68-3.63 (m. 4H, H-6 and H-6'), 3.61 (bs, 2H, OCH_2), 3.57-3.53 (m, 10H, 3 x CH_2), 2.67 (s, 1H, CC*H)*. ^{13}C NMR (125 MHz, $CDCl_3$) δ 168.4 (*C*ONHCH_2-triaz), 166.1 (*C*OCH_2-triaz), 144.9 (*C*-triaz), 144.2 (*C*-triaz), 137.6 (Ar-*C*), 134.6 (Ar-*C*), 126.6 (*CH*-triaz), 123.1 (*C*H-triaz), 123.4 (Ar-*C*H x2), 88.1 (C-1), 78.3 (*C*-5), 73.1 (C-3), 69.8 (C-2), 69.5 (CH_2), 69.3 (CH_2), 68.6 (C-4), 68.6, 68.5 (2 x CH_2), 63.1 (NHCO*C*H_2N_3), 60.1 (C-6), 57.8 (O*C*H_2CCH), 52.5 (CH_2), 34.1 (*C*H_2-triaz). IR (ATR): 3269, 2927, 2491, 1704, 1645, 1598, 1538, 1447,

1347, 1227, 1090, 1052, 890 cm^{-1}. HRMS (ESI+): m/z calculated for $C_{40}H_{54}N_{12}O_{17}$ + Na^+ [M+Na^+]: 997.3628, found 997.3615.

Tetravalent RAFT Glycocluster (4.51)

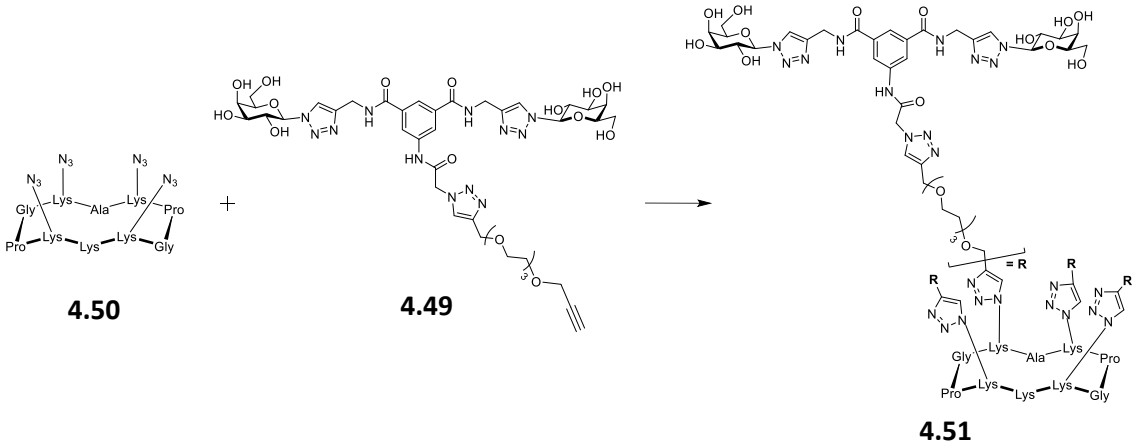

4.50 **4.49** **4.51**

A solution of $CuSO_4.5H_2O$ (0.79 mg, 0.0032 mmol), THPTA (2.8 mg, 0.0064 mmol), and sodium ascorbate (3.8 mg, 0.0192 mmol) in PBS buffer (400 µL, pH 7.5) was added to a solution of the **4.50** (7.2 mg, 0.0064 mmol) and **4.49** (2.74 mL of 10 mg/mL solution in PBS, 0.0282 mmol) in 500 µL of DMF. The mixture was degassed under argon and stirred at room temperature for 1 hour. UPLC analysis showed the reaction was not complete. A further 2 equivalents of **4.49** was added (1.24 mL of 10 mg/mL solution in PBS, 0.013 mmol). The mixture was degassed under argon and stirred at room temperature for 1 hour. UPLC analysis showed complete coupling. Chelex resin was added to the reaction mixture, which was stirred for an additional 30 min and purified by semipreparative RP-HPLC (5-40 % CH_3CN in 15 mins) to afford the desired compound **4.51** as a white fluffy solid after lyophilization (21 mg, 65 %). ^{1}H NMR (500 MHz, D_2O) δ 8.47 (s, 1H), 8.22 (s, 8H), 8.05 (s, 4H), 7.95 – 7.85 (m, 8H), 7.87 – 7.71 (m, 8H), 5.64 (d, *J* = 9.2 Hz, 8H), 5.37 (s, 8H), 4.59 (s, 26H), 4.50 (s, 9H), 4.44 – 4.31 (m, 5H), 4.31 – 4.18 (m, 19H), 4.08 (d, *J* = 3.3 Hz, 8H), 4.07-4.00 (m, 2H), 3.97 (t, *J* = 6.1 Hz, 8H), 3.86 (dd, *J* = 9.8, 3.3 Hz, 10H), 3.75 (d, *J* = 6.0 Hz, 21H), 3.67 – 3.48 (m, 53H), 2.96 (t, *J* = 7.6 Hz, 2H), 2.25 (s, 3H), 2.09 – 1.47 (m, 29H), 1.43 – 1.11 (m, 15H). HRMS (ESI+): m/z calculated for $C_{207}H_{297}N_{71}O_{78}$ + $4H^+$ $[M+4H]^{4+}$: 1256.28586, found 1256.28652.

Alkynated Tetravalent RAFT Glycocluster (4.52)

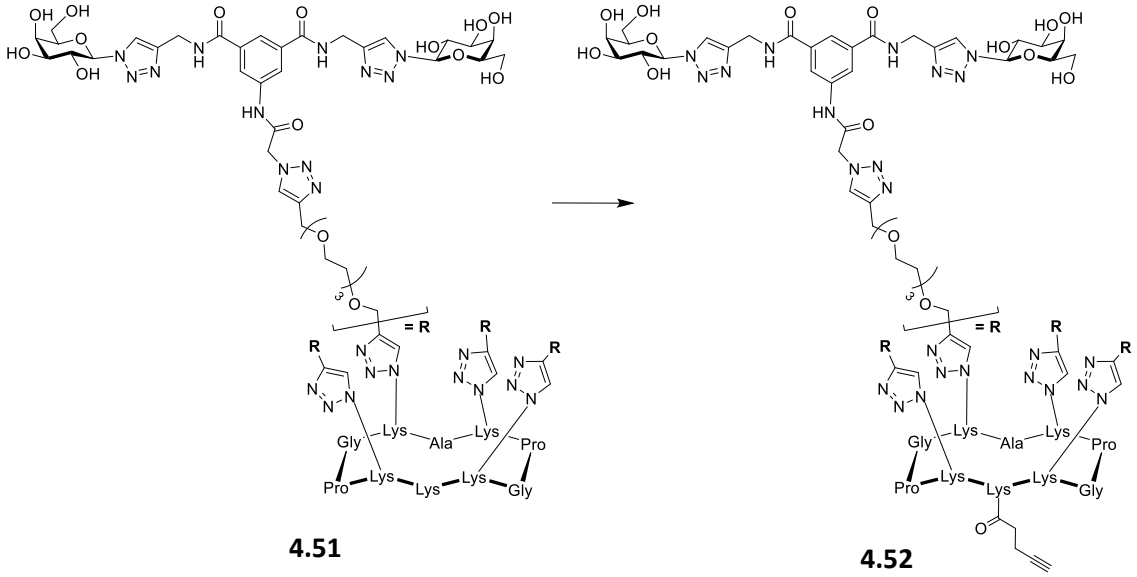

4.51 **4.52**

Compound **4.51** (15.8 mg, 0.00315 mmol) and *N*-succinimidyl pentynoate (0.9 mg, 0.0046 mmol) were dissolved in dry DMF (1 mL). Diisopropylethylamine (2 µL x3, mmol) were added until the solution was at pH 9. The mixture was stirred at room temperature for 1 hour after which UPLC analysis showed complete conversion. H_2O (3 mL) was added to the mixture, which was then purified by semipreparative RP-HPLC (5-40 % CH_3CN in 15 mins) to afford the desired compound **4.52** as a white fluffy solid after lyophilization (15.5 mg, 97 %).

Hexadecavalent RAFT Glycodendrimer (4.53)

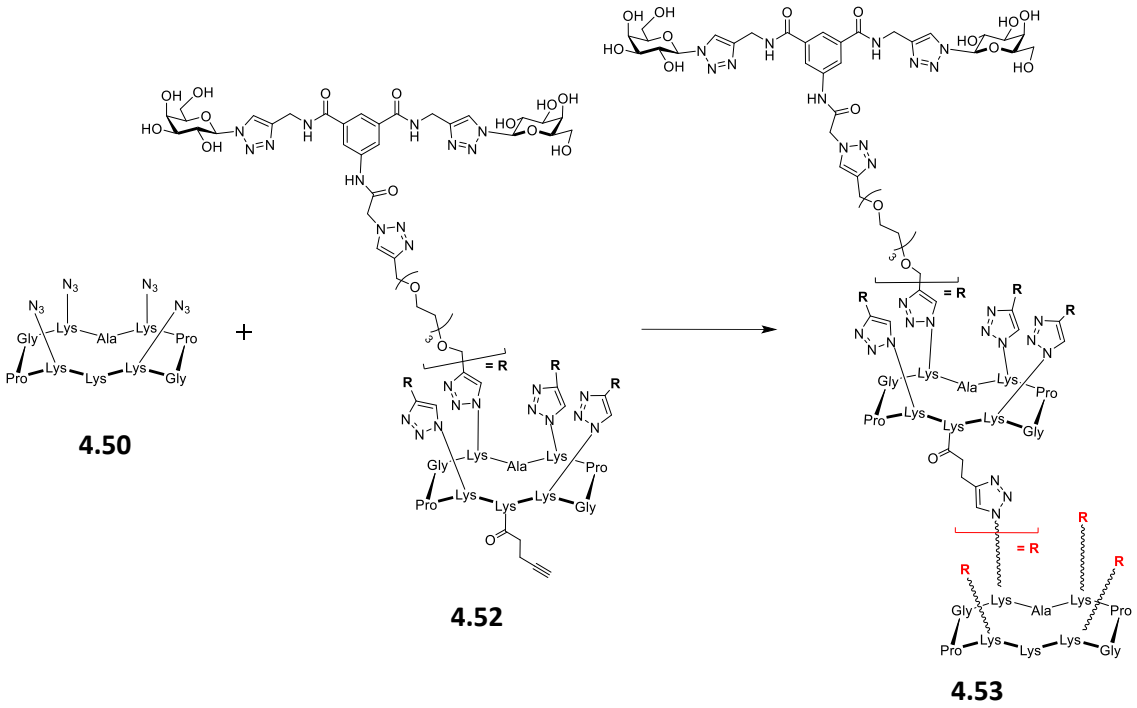

4.50 **4.52** **4.53**

A solution of $CuSO_4.5H_2O$ (0.08 mg, 0.00032 mmol), THPTA (0.27 mg, 0.00062 mmol), and sodium ascorbate (0.37 mg, 0.0019 mmol) in PBS buffer (400 µL, pH 7.5) was added to a solution of the **4.50** (0.7 mg, 0.00062 mmol) and **4.52** (14 mg, 0.00274 mmol) in 500 µL of DMF. The mixture was degassed under argon and stirred at room temperature for 1 hour. UPLC analysis showed complete coupling. Chelex resin was added to the reaction mixture, which was stirred for an additional 30 min and purified by semipreparative RP-HPLC (5-40 % CH_3CN in 15 mins) to afford the desired compound **4.53** as a white fluffy solid after lyophilization (12 mg, 89 %).^{1}H NMR (500 MHz, DMSO) δ = 10.81 (s, 31H), 9.11 (s, 42H), 8.43 (s, 36H), 8.22 (s, 39H), 8.08 (m, 84H), 7.82 (m, 32H), 7.39 (s, 40H), 6.86 (s, 12H), 6.66 (m, 12H), 5.46 (d, *J*=9.1, 32H, H-1), 5.36 (s, 34H), 5.23 (s, 34H), 5.02 (s, 36H), 4.67 (m, 70H), 4.53 (m, 123H), 4.27 (s, 64H), 4.11 (s, 27H), 4.00 (d, *J* = 4.2, 40H), 3.75 (s, 42H), 3.69 (t, *J* = 5.9, 40H), 3.52 (m, 266H), 3.00 (s, 29H), 2.80 (s, 24H), 2.64 (s, 17H), 2.40 (m, 31H), 2.07 (m, 66H), 1.73 (m, 125H), 1.50 (m, 40H), 1.23 (m, 156H), 0.86 (m, 17H). MALDI-TOF-MS $[M+H]^+$: m/z calculated for $C_{895}H_{1263}N_{307}O_{326} + H^+$: 21539.474, found 21539.616.

Hexavalent RAFT glycocluster (4.55)

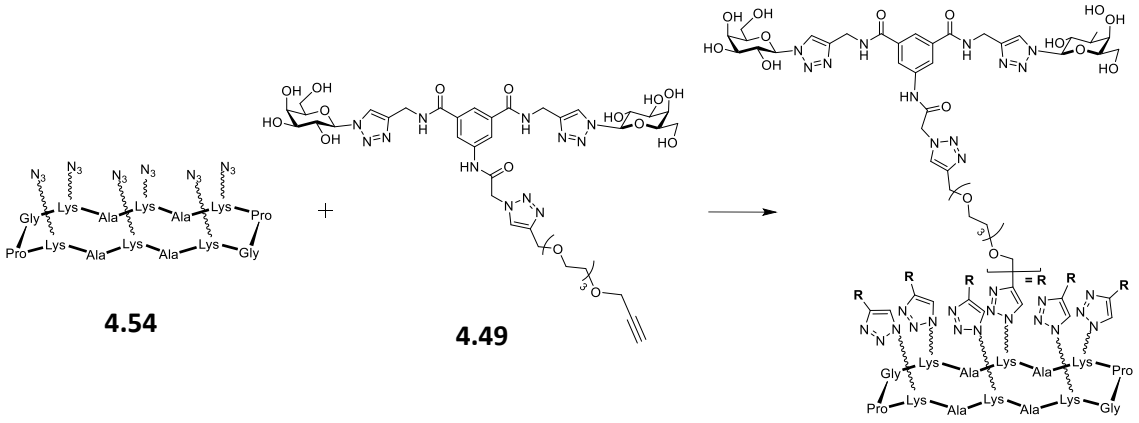

4.54 **4.49** **4.55**

A solution of $CuSO_4.5H_2O$ (0.6 mg, 0.0024 mmol), THPTA (2.1 mg, 0.0048 mmol), and sodium ascorbate (2.9 mg, 0.0288 mmol) in PBS buffer (400 µL, pH 7.5) was added to a solution of the **4.54** (4 mg, 0.0024 mmol) and **4.49** (21 mg, 0.0216 mmol) in 500 µL of DMF. The mixture was degassed under argon and stirred at room temperature for 1 hour. UPLC analysis showed complete coupling. Chelex resin was added to the

reaction mixture, which was stirred for an additional 30 min and purified by semipreparative RP-HPLC (5-40 % CH_3CN in 15 mins) to afford the desired compound **4.55** as a white fluffy solid after lyophilization (6.2 mg, 34 %). ^{1}H NMR (500 MHz, DMSO) δ = 10.71 (s, 9H), 9.02 (m, 14H), 8.31-8.11 (m, 17H), 8.01 (m, 17H), 7.95-7.65 (m, 26H), 5.37 (d, *J*=9.2, 12H, H-1), 5.26 (d, *J*=8.1, 14H), 5.13 (d, *J*=5.8, 16H), 4.94 (m, 20H), 4.60 (t, *J*=5.6, 13H), 4.55 (d, *J*=5.5, 9H), 4.45 (dd, *J*=12.0, 7.6, 29H), 4.16 (bs, 26H), 3.91 (dd, *J*=15.1, 9.2, 18H), 3.65 (m, 11H), 3.60 (m, 12H), 3.41 (m, 55H), 2.97 (bs, 20H), 2.58-2.53 (m, 7H), 2.37-2.25 (m, 6H), 2.1-1.5 (m, 54H), 1.5-1.0 (m, 65H), 0.81-0.73 (m, 9H). MALDI-TOF-MS $[M+H]^+$: m/z calculated for $C_{314}H_{442}N_{110}O_{122}$ + H^+: 7706.184, found 7706.360.

Tetravalent Polylysine-Centred Glycocluster (4.57)

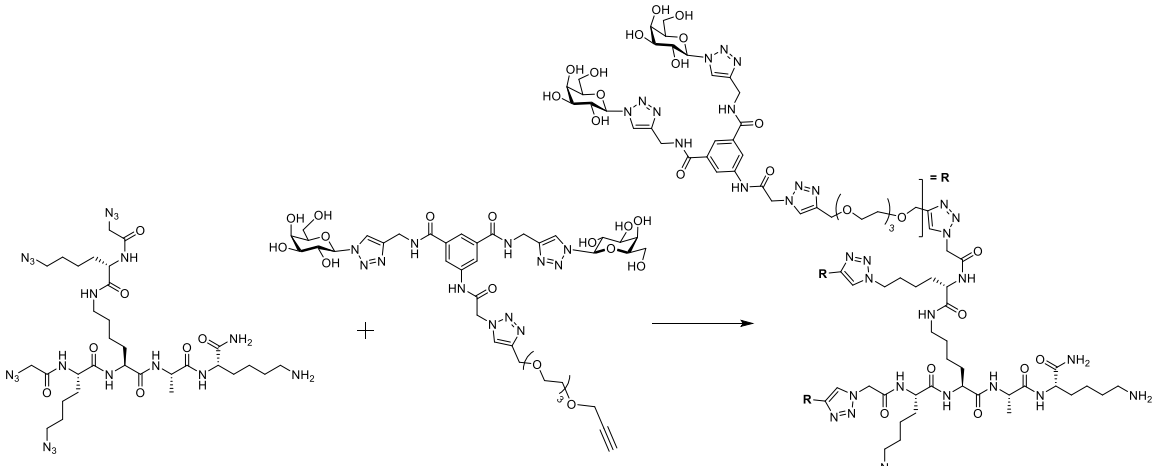

4.56 **4.49** **4.57**

A solution of $CuSO_4.5H_2O$ (0.79 mg, 0.0032 mmol), THPTA (2.8 mg, 0.0064 mmol), and sodium ascorbate (3.8 mg, 0.0192 mmol) in PBS buffer (400 µL, pH 7.5) was added to a solution of the **4.56** (7 mg, 0.0068 mmol) and **4.49** (3.9 mL of 10 mg/mL solution in PBS, 0.0407 mmol) in 500 µL of DMF. The mixture was degassed under argon and stirred at room temperature for 1 hour. UPLC analysis showed complete coupling. Chelex resin was added to the reaction mixture, which was stirred for an additional 30 min and purified by semipreparative RP-HPLC (5-40 % CH_3CN in 15 mins) to afford the desired compound **4.57** as a white fluffy solid after lyophilization (25 mg, 78 %). ^{1}H NMR (500 MHz, D_2O) δ 8.47 (s, 1H), 8.21 (s, 8H), 8.05 (d, *J* = 2.4 Hz, 4H), 7.97-7.88 (m, 10H), 7.85 – 7.78 (m, 6H), 5.65 (d, *J* = 9.1 Hz, 8H), 5.38 (s, 8H), 5.22 (d, *J* = 8.2 Hz, 4H), 4.68 – 4.55 (m, 24H), 4.52 (d, *J* = 5.2 Hz, 9H), 4.30-4.14 (m, 17H),

4.08 (d, *J* = 3.3 Hz, 8H), 3.97 (t, *J* = 6.1 Hz, 8H), 3.86 (dd, *J* = 9.8, 3.3 Hz, 9H), 3.75 (d, *J* = 6.0 Hz, 17H), 3.67 – 3.47 (m, 51H), 3.00 (s, 2H), 2.94 (t, *J* = 7.6 Hz, 2H), 1.88 – 1.52 (m, 15H), 1.48 – 1.06 (m, 14H). HRMS (ESI+): m/z calculated for $C_{191}H_{274}N_{68}O_{75}$ + $4H^+$ $[M+4H]^{4+}$: 1179.99237, found 1179.99202.

Alkynated Tetravalent Polylysine-Centred Glycocluster (4.58)

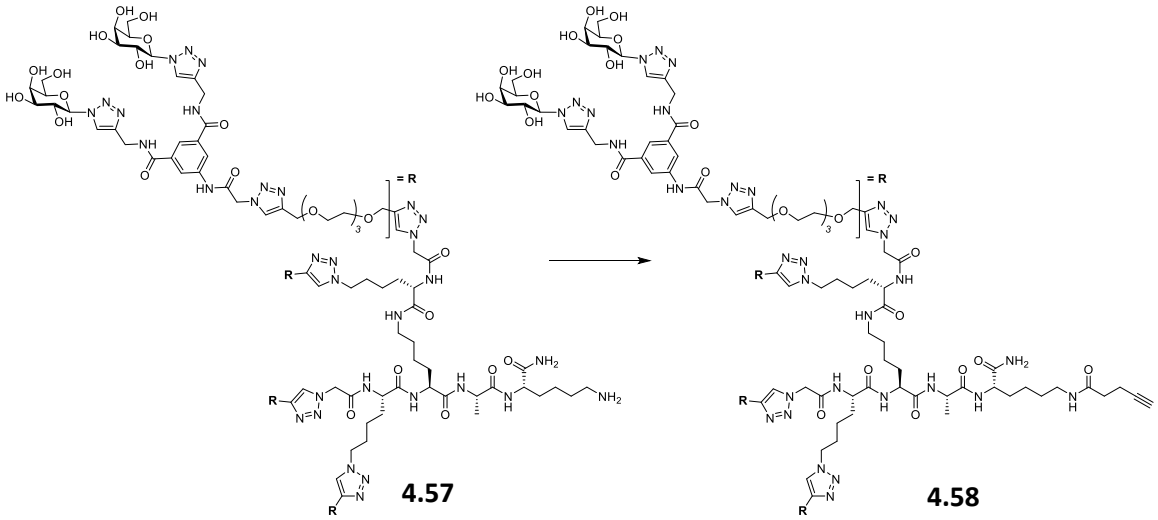

Compound **4.57** (23.6 mg, 0.0050 mmol) and *N*-succinimidyl pentynoate (1.46 mg, 0.0075 mmol) were dissolved in dry DMF (1 mL). Diisopropylethylamine (2 µL x3, mmol) were added until the solution was pH 9. The mixture was stirred at room temperature for 1 hour after which UPLC analysis showed complete conversion. H_2O (3 mL) was added to the mixture, which was then purified by semipreparative RP-HPLC (5-40 % CH_3CN in 15 mins) to afford the desired compound as a white fluffy solid after lyophilization (19.7 mg, 82 %).

Hexadecavalent Polylysine-Centred Glycodendrimer (4.59)

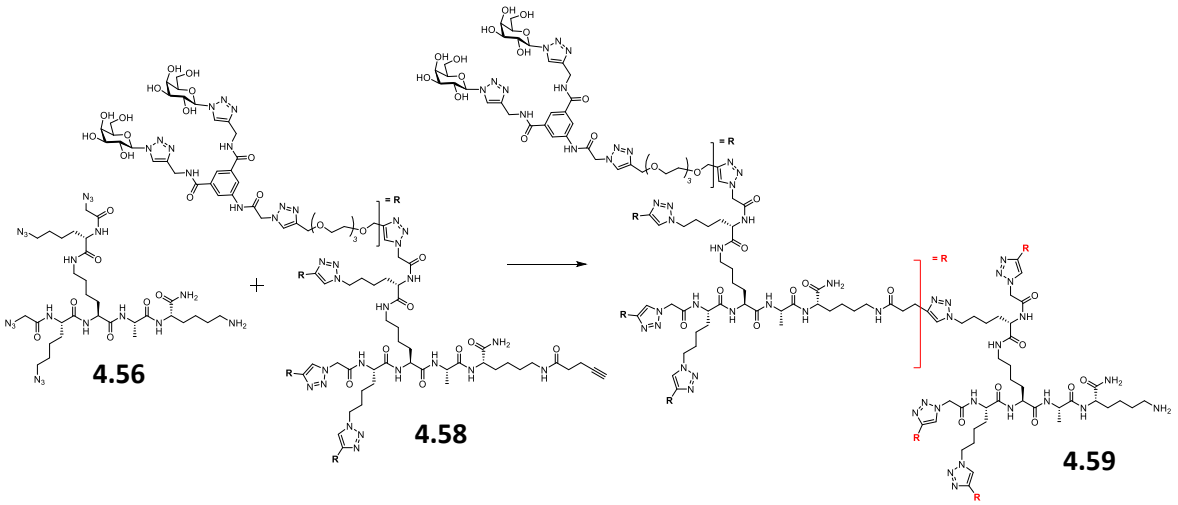

A solution of $CuSO_4.5H_2O$ (0.1 mg, 0.00046 mmol), THPTA (0.41 mg, 0.00093 mmol), and sodium ascorbate (0.56 mg, 0.00279 mmol) in PBS buffer (400 µL, pH 7.5) was added to a solution of the **4.56** (0.76 mg, 0.00093 mmol) and **4.58** (19.7 mg, 0.00411 mmol) in 500 µL of DMF. The mixture was degassed under argon and stirred at room temperature for 1 hour. UPLC analysis showed complete coupling. Chelex resin was added to the reaction mixture, which was stirred for an additional 30 min and purified by semipreparative RP-HPLC (5-40 % CH_3CN in 15 mins) to afford the desired compound **4.59** as a white fluffy solid after lyophilization (16.2 mg, 87 %). ^{1}H NMR (500 MHz, DMSO) δ = 10.86 (s, 24H), 9.17 (s, 32H), 8.59 (m, 26H), 8.28 (s, 34H), 8.13 (m, 80H), 7.87 (m, 28H), 7.34 (s, 10H), 7.07 (s, 10H), 5.52 (d, *J*=9.1, 32H, H-1), 5.42 (s, 32H), 5.29 (s, 30H), 5.20 (s, 22H), 5.07 (s, 30H), 4.73 (m, 60H), 4.57 (m, 110H), 4.25 (m, 96H), 3.80 (s, 32H), 3.75 (t, *J*=5.9, 30H), 3.57 (m, 260H), 3.23 (s, 16H), 3.06 (s, 24H), 2.92 (m, 18H), 2.71 (m, 15H), 2.43 (m, 18H), 1.79 (m, 80H), 1.30 (m, 82H), 0.91 (m, 6H). MALDI-TOF-MS $[M+H]^+$: m/z calculated for $C_{815}H_{1151}N_{292}O_{311}$ + H^+: 20015.637, found 20015.456.

7.2.4 Experimental for Chapter 5

_N, N'_-Di-(2,3,4,6-tetra-_O_-acetyl-β-D-galactopyranosyl-1,2,3-triazol-4-ylmethylamide)-_N''_-(1-oxo-2-propen-1-yl)-5-aminobenzene-1,3-dicarboxamide (5.13)

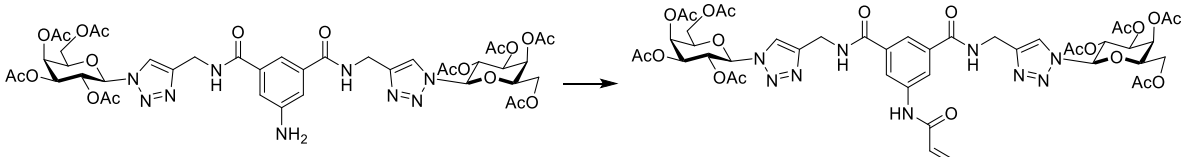

2.113 **5.13**

2.113 (371 mg, 0.369 mmol) was dissolved in anhydrous DCM (20 mL) under N_2 and cooled on ice. DIPEA (0.13 mL, 0.739 mmol) and acryloyl chloride (0.036 mL, 0.443 mmol) were added to the solution. The reaction was allowed to stir for 3 h, washed with water (20 mL x 2), dried over $MgSO_4$ and concentrated *in vacuo* to give the crude product, which was purified by silica gel column chromatography (DCM:MeOH 98:2-93:5) to give the pure product **5.13** as a sticky, yellow solid (224 mg, 57 %). R_f = 0.43 (DCM:MeOH 9:1). $[\alpha]_D^{22}$ -6.4 (c 1.4, DCM). ^{1}H NMR (500 MHz, $CDCl_3$) δ 9.27 (s, 1H,

N*H*COCH=CH_2), 8.08 (bs, 4H, Ar-H and N*H*CH_2-triaz), 7.98 (s, 2H, triaz-H), 7.74 (s, 1H, Ar-H), 6.34 – 6.21 (m, 2H, *H*C=CHCO and HC=C*H*CO), 5.93 (d, *J* = 9.2 Hz, 2H, H-1), 5.66-5.56 (m, 3H, H-2 and *H*C=CHCO), 5.51 (d, *J* = 3.3 Hz, 2H, H-4), 5.28 (dd, *J* = 10.3, 3.3 Hz, 2H, H-3), 4.62 (dd, *J* = 47.1, 10.3 Hz, 4H, CH_2CCH), 4.31 (t, *J* = 6.5 Hz, 2H, H-5), 4.20-4.09 (m, 4H, H-6 and H-6'), 2.16 (s, 6H, OAc), 1.96 (s, 6H, OAc), 1.95 (s, 6H, OAc), 1.76 (s, 6H, OAc). ^{13}C NMR (125 MHz, $CDCl_3$) δ 169.4 (CO of OAc), 169.2 (CO of OAc), 168.9 (CO of OAc), 168.2 (CO of OAc), 165.8 (*C*ONHCH_2-triaz), 163.2 (*C*OCH=CH_2), 144.5 (*C*-triaz), 138.1 (Ar-C), 133.8 (Ar-C), 130.0 (H_2C=*C*HCO), 127.1 (H_2*C*=CHCO), 120.7 (*C*H-triaz), 120.4 (Ar-*C*H), 119.9 (Ar-*C*H), 85.0 (C-1), 72.9 (C-5), 69.8 (C-3), 67.0 (C-2), 65.9 (C-4), 60.2 (C-6), 34.5 (*C*H_2-triaz), 19.7 (CH_3 of OAc), 19.6 (CH_3 of OAc), 19.5 (CH_3 of OAc), 19.2 (CH_3 of OAc). IR (film on NaCl) = 3351, 3099, 2967, 1754, 1658, 1599, 1536, 1445, 1371, 1224, 1092, 1063, 924 cm^{-1}. HRMS (ESI+): *m/z* calcd for $C_{45}H_{53}N_9O_{21}$ +Na^+ $[M+Na]^+$ 1078.3254, found 1078.3253.

_N,N'_-Di-(2,3,4,6-tetra-_O_-acetyl-β-D-galactopyranosyl-1,2,3-triazol-4-ylmethylamide)-_N''_-(3-(prop-2-yn-1-ylamino)propanamido)-5-aminobenzene-1,3-dicarboxamide (5.15)

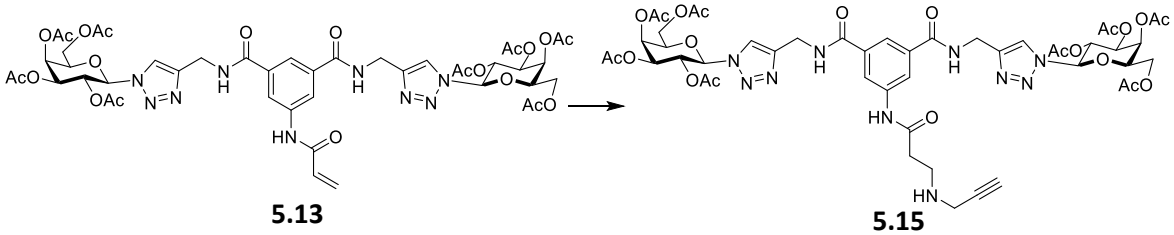

5.13 **5.15**

5.13 (82 mg, 0.078 mmol) was dissolved in a mixture of *tert*-butanol and DCM (5:1, 5 mL). Phenol (22 mg, 0.233 mmol) and propargylamine (10 µL, 0.156 mmol) were added and the reaction mixture was allowed to stir in the MW at 100 ^{o}C for 1 h. A further amount of propargylamine (10 µL, 0.156 mmol) was added. The reaction mixture was allowed to stir in the MW at 100 °C for 1 h. This was repeated again, where propargylamine (10 µL, 0.156 mmol) was added and the reaction mixture was allowed to stir in the MW at 100 ^{o}C for 1 h. The sequential addition of propargylamine was required for completion of reaction. The solvent was removed *in* vacuo and resulting residue was redissolved in DCM (20 mL), which was washed with water (20 mL x 2), dried over $MgSO_4$ and concentrated *in vacuo* to give the crude product, which was purified by silica gel column chromatography (DCM:MeOH 98:2-93:7) to

give the pure product **5.15** as a sticky, yellow solid (60 mg, 69 %). R_f = 0.39 (DCM:MeOH 9:1). $[\alpha]_D^{25}$ +13 (c 1, DCM). ^{1}H NMR (500 MHz, $CDCl_3$) δ 10.07 (s, 1H, N*H*COC_2H_4), 7.99 (s, 2H, triaz-H), 7.94 – 7.85 (m, 2H, Ar-H and N*H*CH_2-triaz), 7.78 (s, 1H, Ar-H), 5.91 (d, *J* = 9.3 Hz, 2H, H-1), 5.62 – 5.57 (m, 2H, H-2), 5.53 (dd, *J* = 3.3, 0.8 Hz, 2H, H-4), 5.27 (dd, *J* = 10.3, 3.4 Hz, 2H, H-3), 4.78-4.57 (m, 4H, C*H*$_2$-triaz), 4.28 (t, *J* = 6.5 Hz, 2H, H-5), 4.21-4.09 (m, 4H, H-6 and H-6'), 3.53 (d, *J* = 1.8 Hz, 2H, C*H*$_2$CCH), 3.11 – 3.05 (m, 2H, CH_2, $COCH_2CH_2$NH), 2.57 – 2.51 (m, 2H, CH_2, $COCH_2CH_2$NH), 2.30 (t, *J* = 2.3 Hz, 1H, CH_2CCH), 2.20 (s, 3H, OAc), 2.00 (s, 3H, OAc), 1.99 (s, 3H, OAc), 1.81 (s, 3H, OAc), 1.29 – 1.21 (m, 1H). ^{13}C NMR (125 MHz, $CDCl_3$) δ 171.4 ($COCH_2CH_2$NH), 170.5 (CO of OAc), 170.3 (CO of OAc), 170.0 (CO of OAc), 169.4 (CO of OAc), 166.8 ($CONHCH_2$-triaz), 145.7 (*C*-triaz), 139.3 (Ar-*C*), 135.0 (Ar-*C*), 121.7 (*C*H-triaz), 121.2 (Ar-*C*H), 120.8 (Ar-*C*H), 86.4 (C-1), 74.2 (C-5), 72.8 (CH_2CCH), 71.1 (C-3), 68.2 (C-2), 67.1 (C-4), 61.4 (C-6), 44.2 ($COCH_2CH_2$NH), 37.8 (CH_2CCH), 36.2 ($COCH_2CH_2$NH), 35.6 (CH_2-triaz), 20.9 (CH_3 of OAc), 20.8 (CH_3 of OAc), 20.7 (CH_3 of OAc), 20.4 (CH_3 of OAc). IR (film on NaCl): 3287, 2923, 1744, 1651, 1598, 1540, 1447, 1368, 1214, 1046, 921 cm^{-1}. HRMS (ESI+): *m/z* calcd for $C_{48}H_{58}N_{10}O_{21}$ +H$^+$ $[M+H]^+$ 1111.3856, found 1111.3813.

***Tert*-butyl 3-(3-benzoyl-*N*-(prop-2-yn-1-yl)benzamido)propanoate (5.17)**

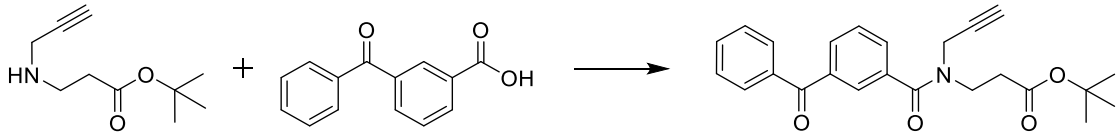

4.32 **5.16** **5.17**

4-benzoylbenzoic acid **5.16** (151 mg, 0.669 mmol) and TBTU (258 mg, 0.802 mmol) were dissolved in anhydrous DMF (10 mL) under N_2. NEt_3 (0.112 mL, 0.802 mmol) was added followed by compound **4.32** (147 mg, 0.802 mmol). The reaction mixture was allowed to stir overnight at rt. The solvent was removed *in* vacuo and resulting residue was re-dissolved in DCM (20 mL), which was washed with water (20 mL x 3), dried ($MgSO_4$) and concentrated *in vacuo* to give the crude product, which was purified by silica gel column chromatography (EtOAc:Pet Ether 1:2) to give the pure product **5.17** as a yellow solid (125 mg, 48 %). R_f = 0.78 (EtOAc:Pet Ether 1:1). ^{1}H NMR (500 MHz, $CDCl_3$) δ 7.85 – 7.81 (m, 2H, Ar-H x 2), 7.79 (ddd, *J* = 9.1, 5.0, 3.1 Hz, 2H,

Ar-H x 2), 7.66 – 7.51 (m, 3H, Ar-H x 3), 7.50 – 7.45 (m, 2H, Ar-H x 2), 4.49 – 3.97 (m, 2H, C*H*$_2$CCH), 3.97 – 3.59 (m, 2H, C*H*$_2$CH$_2$), 2.80 – 2.41 (m, 2H, CH$_2$C*H*$_2$), 2.34 (s, 1H, CH$_2$CC*H*), 1.44 (s, 9H, C(CH$_3$)$_3$). ^{13}C NMR (125 MHz, CDCl$_3$) δ 195.9 (Ar-*C*O-Ar), 171.0 (*C*OC(CH$_3$)$_3$), 170.4 (Ar-*C*O-N), 139.2 (Ar-*C*), 138.8 (Ar-*C*), 137.1 (Ar-*C*), 132.8 (Ar-*C*H), 130.2 (Ar-*C*H), 130.1 (Ar-*C*H), 128.4 (Ar-*C*H), 126.8 (Ar-*C*H), 81.0 (*C*(CH$_3$)$_3$), 78.5 (CH$_2$*C*CH), 73.5 (CH$_2$C*C*H rotamer 1), 72.7 (CH$_2$C*C*H rotamer 2), 44.4 (CH$_2$ rotamer 2), 41.9 (CH$_2$ rotamer 1), 40.1 (*C*H$_2$CCH rotamer 1), 34.4 (CH$_2$ rotamer 2), 34.1 (*C*H$_2$CCH rotamer 2), 33.7 (CH$_2$ rotamer 1), 28.1 (C(*C*H$_3$)$_3$). IR (film on NaCl): 3262, 2978, 2119, 1725, 1646, 1504, 1447, 1419, 1368, 1276, 1153, 1044, 939, 926, 846, 702 cm^{-1}. HRMS (ESI+): *m/z* calcd for C$_{24}$H$_{25}$NO$_4$ +Na$^+$ [M+Na]$^+$ 414.1681, found 414.1674.

3-(3-Benzoyl-*N*-(prop-2-yn-1-yl)benzamido)propanoic acid (5.18)

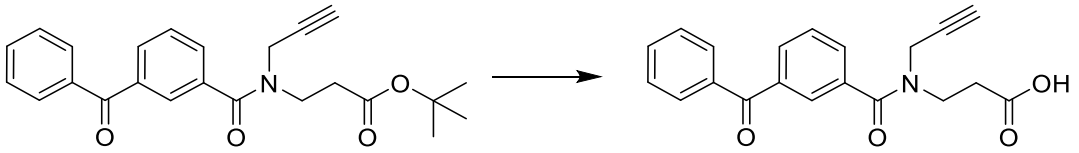

5.17 **5.18**

5.17 (50 mg, 0.128 mmol) was placed into an oven-dried round-bottom flask and was flushed with N$_2$. Anhydrous DCM (4 mL) and pre-dried TFA over anhydrous Na$_2$SO$_4$ (2 mL) was added to the flask on ice. Reaction was allowed to stir for 3 h, until TLC showed full conversion to the product. Reaction mixture was washed with brine (20 mL x 2) to give the pure product **5.18** as an off-white solid (43 mg, 100 %). R$_f$ = 0 (EtOAc:Pet Ether 1:1). ^{1}H NMR (500 MHz, CDCl$_3$) δ 10.01 (s, 1H, COO*H*), 7.75 (d, *J* = 8.3 Hz, 2H, Ar-H x 2), 7.73 – 7.68 (m, 2H, Ar-H x 2), 7.58 – 7.47 (m, 3H, Ar-H x 3), 7.47 – 7.35 (m, 2H, Ar-H x 2), 4.42 – 3.91 (m, 2H, C*H*$_2$CCH), 3.90 – 3.55 (m, 2H, CH$_2$CH$_2$), 2.89 – 2.48 (m, 2H, CH$_2$CH$_2$), 2.33 – 2.18 (m, 1H, CH$_2$CC*H*). ^{13}C NMR (125 MHz, CDCl$_3$) δ 195.7 (Ar-*C*O-Ar), 177.1 (*C*OOH), 171.2 (Ar-*C*O-N), 138.9 (Ar-*C*), 138.7 (Ar-*C*), 136.9 (Ar-*C*), 132.8 (Ar-*C*H), 130.3 (Ar-*C*H), 130.0 (Ar-*C*H), 128.4 (Ar-*C*H), 126.9 (Ar-*C*H), 78.9 (CH$_2$*C*CH), 73.8 (CH$_2$C*C*H), 60.4, 50.8, 42.8 (*C*H$_2$CH$_2$) 39.4 (*C*H$_2$CCH), 35.2 (CH$_2$*C*H$_2$). IR (Film on NaCl): 3262, 3060, 2919, 2849, 2121, 1731, 1657, 1598, 1506, 1447, 1277, 1179, 1044, 940, 926, 859, 800, 702 cm^{-1}. HRMS (ESI+): *m/z* calcd for C$_{20}$H$_{17}$NO$_4$ +Na$^+$ [M+Na]$^+$ 358.1055, found 358.1055.

***N,N'*-Di-(2,3,4,6-tetra-*O*-acetyl-β-D-galactopyranosyl-1,2,3-triazol-4-ylmethylamide)-*N''*-(3-(3-benzoyl-*N*-(prop-2-yn-1-yl)benzamido)propanamido)-5-aminobenzene-1,3-dicarboxamide (5.20)**

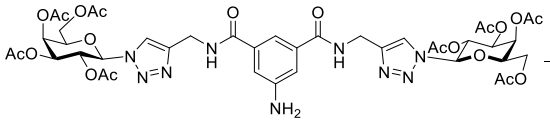

2.113

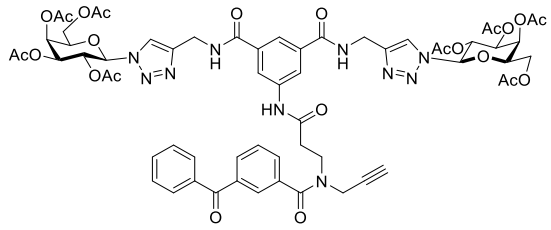

5.20

5.18 (44 mg, 0.131 mmol) and TBTU (51 mg, 0.157 mmol) were dissolved in anhydrous DMF (2 mL) in a round bottom flask covered in tinfoil. **2.113** (158 mg, 0.157 mmol) was also dissolved in anhydrous DMF (2 mL) in a separate round-bottom flask, which was added to the previous mixture via cannula. This reaction mixture was allowed to stir for 16 h at rt. The solvent was removed *in* vacuo and resulting residue was re-dissolved in DCM (20 mL), which was washed with brine (20 mL x 3), dried ($MgSO_4$) and concentrated *in vacuo* to give the crude product, which was purified by silica gel column chromatography (DCM:MeOH 95:5) to give the pure product **5.20** as a sticky, yellow solid (85 mg, 49 %). R_f = 0.64 (DCM:MeOH 9:1). $[\alpha]_D^{22}$ -8 (c 1, DCM). ^{1}H NMR (500 MHz, $CDCl_3$) δ 9.19 (s, 1H, N*H*COC_2H_4), 8.05 – 7.70 (m, 5H, triaz-H x 2, Ar-H x 2, Ar-H, N*H*CH_2-triaz x 2, Ar-H of benzophenone x 2), 7.66 – 7.56 (m, 1H, Ar-H of benzophenone x 3), 7.49 (t, *J* = 7.6 Hz, 1H, Ar-H of benzophenone x 2), 5.93 (d, *J* = 9.3 Hz, 2H, H-1), 5.62 (t, *J* = 9.7 Hz, 2H, H-2), 5.54 (dd, *J* = 3.4, 1.1 Hz, 2H, H-4), 5.29 (dd, *J* = 10.3, 3.4 Hz, 2H, H-3), 4.78 – 4.57 (m, 4H, C*H*$_2$-triaz), 4.34 – 4.23 (m, 2H, H-5), 4.20 – 4.09 (m, 6H, H-6 and H-6' and C*H*$_2$CCH), 4.02 – 3.77 (m, 2H, C*H*$_2$$CH_2$), 2.96 – 2.68 (m, 1H, CH_2C*H*$_2$), 2.41 (s, 1H, CH_2CC*H*), 2.19 (s, 6H, OAc), 2.00 (appd, *J* = 1.5 Hz, 12H, OAc x 2), 1.80 (s, 6H, OAc). ^{13}C NMR (125 MHz, $CDCl_3$) δ 171.0 (*C*OC_2H_4N) 170.3 (CO of OAc), 170.1 (CO of OAc), 169.8 (CO of OAc), 169.2 (CO of OAc), 166.6 (*C*O$NHCH_2$-triaz), 145.5 (*C*-triaz), 139.2 (Ar-*C*) 138.7 (Ar-*C* of benzophenone), 136.9 (Ar-*C* of benzophenone), 134.9 (Ar-*C*), 132.9 (Ar-*C*H of benzophenone), 130.2 (Ar-*C*H of benzophenone), 130.1 (Ar-*C*H of benzophenone), 128.5 (Ar-*C*H of benzophenone), 126.9 (Ar-*C*H of benzophenone), 121.6 (*C*H-triaz), 121.2 (Ar-*C*H), 120.7 (Ar-*C*H) 86.1 (C-1), 78.1 (CH_2*C*CH) 74.1 (CH_2C*C*H) 73.9 (C-5), 70.9

(C-3), 68.0 (C-2), 66.9 (C-4), 61.1 (C-6), 42.4 (*C*H_2CH_2) 40.4 (*C*H_2CCH) 35.5 (*C*H_2-triaz and *C*H_2CH_2), 20.6 (CH_3 of OAc), 20.6 (CH_3 of OAc), 20.5 (CH_3 of OAc), 20.3 (CH_3 of OAc). IR (film on NaCl): 3287, 2967, 1753, 1656, 1536, 1446, 1370, 1224, 1092, 1052, 925 cm^{-1}. HRMS (ESI+): *m/z* calcd for $C_{62}H_{66}N_{10}O_{23}$ +Na^+ $[M+Na]^+$ 1341.4200, found 1341.4185.

_N, N'_-Di-(β-D-galactopyranosyl-1,2,3-triazol-4-ylmethylamide)-_N''_-(3-(3-benzoyl-_N_-(prop-2-yn-1-yl)benzamido)propanamido)-5-aminobenzene-1,3-dicarboxamide (5.21)

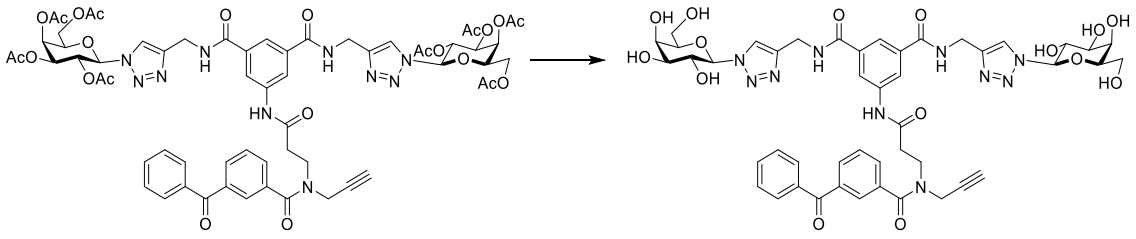

5.20 **5.21**

5.20 (80 mg) was dissolved in methanol/H_2O (4 mL, 2 mL) in a round bottom flask covered in tinfoil. NEt_3 (0.1 mL) was added, and the reaction mixture was allowed to stir for 45 °C for 6 h. The solution was cooled, Amberlite H^+ was added and the mixture was allowed to stir for 30 mins. The solution was filtered, and the solvent was removed *in vacuo*. The residue was dried under high vacuum and lyophilized to give the pure product **5.21** as an off-white solid (55 mg, 92 %). $[\alpha]_D^{24}$ +6 (c 0.5, MeOH:H_2O 1:1). ^{1}H NMR (500 MHz, D_2O) δ 8.22 (s, 2H, triaz-H), 8.13 – 7.98 (m, 2H, Ar-H), 7.91 (s, 1H, Ar-H), 7.83 – 7.66 (m, 4H, Ar-Hs of benzophenone), 7.63 – 7.41 (m, 6H, Ar-Hs of benzophenone), 5.52 (d, *J* = 9.1 Hz, 2H, H-1), 4.61 (s, 4H, *CH*$_2$-triaz), 4.39 (s, 1H, C*H*CCH), 4.15 – 4.01 (m, 3H, H-2 and C*H*CCH), 3.99 – 3.87 (m, 4H, H-4 and C*H*$_2$CH$_2$), 3.77 (t, *J* = 5.9 Hz, 2H, H-5), 3.70 – 3.59 (m, 6H, H-3, H-6 and H-6'), 2.88 – 2.65 (m, 2H, C*H*$_2$CH$_2$ and CH$_2$CC*H*). ^{13}C NMR (125 MHz, DMSO) δ 195.7 (CO), 170.0 (CO), 166.3 (*C*ONHCH$_2$-triaz), 145.3 (C-triaz), 137.1 (Ar-C of benzophenone), 135.5 (Ar-C), 133.4 (Ar-CH of benzophenone), 130.3 (Ar-CH of benzophenone), 130.2 (Ar-CH of benzophenone), 129.1 (Ar-CH of benzophenone), 127.2 (Ar-CH of benzophenone), 122.2 (CH-triaz), 121.6 (Ar-CH), 121.1 (Ar-CH), 88.5 (C-1), 79.9 (CH$_2$*C*CH), 78.9 (C-5), 74.2 (C-3), 72.9 (CH$_2$C*C*H), 69.8 (C-2), 68.9 (C-4), 60.9 (C-6), 55.4,

49.1, 45.0 (CH_2), 42.3 (CH_2), 40.1 (CH_2), 35.4 (CH_2-triaz), 35.3 (CH_2), 34.1 (CH_2). IR (ATR): 3283, 3221, 2851, 1642, 1696, 1542, 1446, 1276, 1257, 1090, 1051, 890 cm^{-1}. HRMS (ESI+): *m/z* calcd for $C_{46}H_{50}N_{10}O_{15}$ + Na^+ $[M+ Na]^+$ 1005.3355, found 1341.4185.

3-(3-Methyl-3*H*-diazirin-3-yl)propanoic acid (5.24)

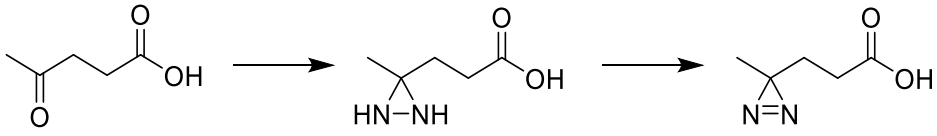

5.22 **5.23** **5.24**

Liquid levulinic acid **5.22** (0.88 mL, 8.59 mmol) was placed in round-bottom flask and was cooled on ice. 7N ammonia in methanol (9 mL) was added. A rubber septum and an empty balloon on a needle was placed on the flask. The reaction mixture was allowed to stir for 3 h. Hydroxylamine-*O*-sulfonic acid (1.459 g, 12.89 mmol) was dissolved in MeOH (10 mL) and using a dropping funnel was added to the reaction mixture dropwise (rate of 1 per sec). The reaction mixture was allowed to stir overnight at rt. Ammonia was removed by gently blowing air into the suspension using a glass pipette for 1 h. The white precipitate was removed by filtration, and the filtrate was concentrated *in vacuo* leaving a yellow residue **5.23**. The flask was covered in tinfoil and MeOH (8 mL) was added. The mixture was allowed to stir on an ice-bath for 5 mins. NEt_3 (1.8 mL, 12.89 mmol) was added and the reaction was allowed to stir for a further 5 mins. I_2 beads (1.278 g, 5.035 mmol) (calculated based on yield of diaziridine) were slowly added until the solution remained persistently red-brown. EtOAc (8 mL) was added and organic layer was washed with HCl (1 M, 20 mL), Na_2S_2O (10 %, 20 mL) and brine (20 mL), dried ($NaSO_4$), filtered and concentrated *in vacuo* to give the diazirine product **5.24** as a yellow/orange liquid (1.100 g, 42 %). ^{1}H NMR (500 MHz, $CDCl_3$) δ 11.13 (s, 1H, O*H*), 2.21 (t, *J* =7.7 Hz, 2H, CH_2), 1.70 (t, *J* =7.7 Hz, 2H, CH_2), 1.02 (s, 3H, CH_3).

The NMR data is in agreement with the data reported in the literature.[273]

***Tert*-butyl 3-(3-(3-methyl-3*H*-diazirin-3-yl)-*N*-(prop-2-yn-1-yl)propanamido) propanoate (5.25)**

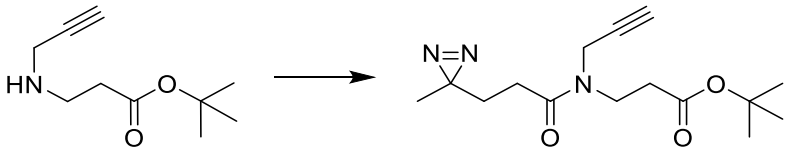

4.32 **5.25**

5.24 (108 mg, 0.843 mmol) and TBTU (325 mg, 1.011 mmol) were dissolved in anhydrous DMF (10 mL) under N_2 in a round bottom flask covered in tinfoil. NEt_3 (0.14 mL, 1.011 mmol) was added followed by **4.32** (185 mg, 1.011 mmol). The reaction mixture was allowed to stir overnight at rt. The solvent was removed *in* vacuo and resulting residue was re-dissolved in DCM (20 mL), which was washed with water (20 mL x 3), dried ($MgSO_4$) and concentrated under reduced pressure to give the crude product, which was purified by silica gel column chromatography (EtOAc:Pet Ether 1:2) to give the pure product **5.25** as a yellow sticky solid (114 mg, 46 %). R_f = 0.81 (EtOAc:Pet Ether 1:1). ^{1}H NMR (500 MHz, $CDCl_3$) δ 4.16 (d, *J* = 2.6 Hz, 2H, C*H*$_2$CCH rotamer 1), 4.04 (d, *J* = 2.5 Hz, 2H, C*H*$_2$CCH rotamer 2), 3.66-3.56 (m, 4H, NC*H*$_2$CH$_2$CO rotamer 1 & 2), 2.50 (td, *J* = 7.0, 3.4 Hz, 4H, NCH$_2$C*H*$_2$CO rotamer 1 & 2), 2.27 (t, *J* = 2.5 Hz, 1H, CH$_2$CC*H* rotamer 2), 2.20 – 2.14 (m, 5H, CH$_2$CC*H* rotamer 2 and CH$_3$C(N=N)CH$_2$C*H*$_2$CO rotamer 1 & 2), 1.75 – 1.67 (m, 4H, CH$_3$C(N=N)C*H*$_2$CH$_2$CO rotamer 1 & 2), 1.40 and 1.38 (s x 2, C(C*H*$_3$)$_3$ of rotamer 1 & 2), 0.99 (s, 3H, CH$_3$). ^{13}C NMR (126 MHz, $CDCl_3$) δ 171.2 (*C*OOC(CH$_3$)$_3$ rotamer 1), 171.2 (CH$_3$C(N=N)CH$_2$CH$_2$*C*O rotamer 1), 170.9 (CH$_3$C(N=N)CH$_2$CH$_2$*C*O rotamer 2), 170.1 (*C*OOC(CH$_3$)$_3$ rotamer 2), 124.7, 120.4, 81.4 (*C*(CH$_3$)$_3$ rotamer 1), 80.7 (*C*(CH$_3$)$_3$ rotamer 2), 78.9 (CH$_2$*C*CH rotamer 1), 78.6 (CH$_2$*C*CH rotamer 2), 72.8 (CH$_2$C*C*H rotamer 1), 71.9 (CH$_2$C*C*H rotamer 2), 43.2 (N*C*H$_2$CH$_2$CO rotamer 1), 42.7 (N*C*H$_2$CH$_2$CO rotamer 2), 38.4 (*C*H$_2$CCH rotamer 2), 34.5 (NCH$_2$*C*H$_2$CO rotamer 2), 34.2 (*C*H$_2$CCH rotamer 1), 34.0 (NCH$_2$*C*H$_2$CO rotamer 2), 29.6 (CH$_3$C(N=N)*C*H$_2$CH$_2$CO rotamer 1), 29.5 (CH$_3$C(N=N)*C*H$_2$CH$_2$CO rotamer 2), 28.0 (C(*C*H$_3$)$_3$ rotamer 1 & 2), 27.4 (CH$_3$C(N=N)CH$_2$*C*H$_2$CO rotamer 1), 27.1 (CH$_3$C(N=N)CH$_2$*C*H$_2$CO rotamer 2), 25.4, 20.0 (CH$_3$ rotamer 1), 19.9 (CH$_3$ rotamer 1). IR (film on NaCl): 3294, 2979, 2931, 2115, 1726, 1655, 1446, 1368, 1252, 1218, 1154,

846 cm^{-1}. HRMS (ESI+): *m/z* calcd for $C_{15}H_{23}N_3O_3$ $+H^+$ $[M+H]^+$ 294.1818, found 295.1825.

3-(3-(3-Methyl-3*H*-diazirin-3-yl)-*N*-(prop-2-yn-1-yl)propanamido)propanoate (5.26)

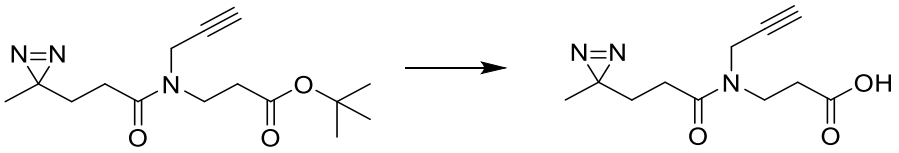

5.25 **5.26**

5.25 (50 mg, 0.170 mmol) was placed into an oven-dried round-bottom flask covered in tinfoil and was flushed with N_2. Anhydrous DCM (4 mL) and pre-dried TFA over anhydrous Na_2SO_4 (2 mL) was added to the flask on ice. The reaction was allowed to stir for 3 h, until TLC showed full conversion to the product. Reaction mixture was washed with brine (20 mL x 2) to give the pure product **5.26** as a sticky solid (40 mg, 100 %). R_f = 0 (EtOAc:Pet Ether 1:1). ^{1}H NMR (500 MHz, $CDCl_3$) δ 9.42 (s, 1H, OH), 4.22 (d, *J* = 2.6 Hz, 2H, C*H*$_2$CCH rotamer 1), 4.09 (d, *J* = 2.5 Hz, 2H, C*H*$_2$CCH rotamer 2), 3.74 (t, *J* = 7.1 Hz, 2H, NC*H*$_2$CH$_2$CO rotamer 1), 3.67 (t, *J* = 6.7 Hz, 2H, NC*H*$_2$CH$_2$CO rotamer 2), 2.71 (td, *J* = 6.9, 4.3 Hz, 4H, NCH$_2$C*H*$_2$CO rotamer 1 & 2), 2.33 (t, *J* = 2.4 Hz, 1H, CH$_2$CC*H* rotamer 2), 2.25-2.19 (m, CH$_2$CC*H* rotamer 2 and CH$_3$C(N=N)CH$_2$C*H*$_2$CO rotamer 1 & 2), 1.80 – 1.72 (m, 4H, CH$_3$C(N=N)C*H*$_2$CH$_2$CO rotamer 1 & 2), 1.04 (s, 6H, CH$_3$ of rotamer 1 & 2).

***N,N'*-Di-(2,3,4,6-tetra-*O*-acetyl-β-D-galactopyranosyl-1,2,3-triazol-4-ylmethyl amide)-*N''*-(3-(3-(3-(3-methyl-3H-diazirin-3-yl)-N-(prop-2-yn-1-yl)propanamido) propanamido)-5-aminobenzene-1,3-dicarboxamide (5.27)**

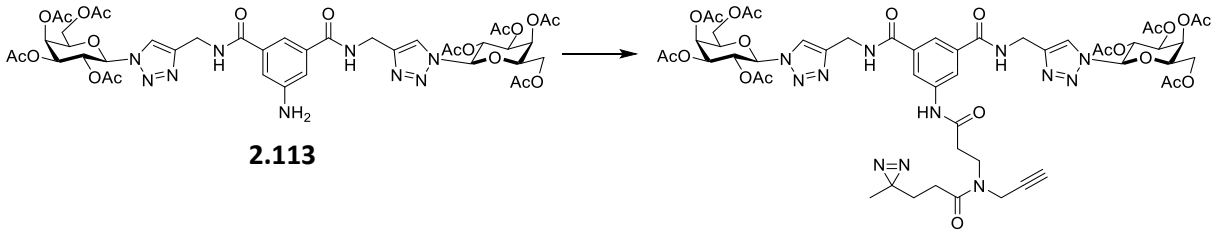

2.113 **5.27**

5.26 (20 mg, 0.085 mmol) and TBTU (33 mg, 0.102 mmol) were dissolved in anhydrous DMF (2 mL). **2.113** (102 mg, 0.102 mmol) was also dissolved in anhydrous

DMF (2 mL) in a separate round-bottom flask, which was added to the previous mixture via cannula. This reaction mixture was allowed to stir for 16 h at rt. The solvent was removed *in* vacuo and resulting residue was redissolved in DCM (20 mL), which was washed with brine (20 mL x 3), dried over $MgSO_4$ and concentrated under reduced pressure to give the crude product, which was purified by silica gel column chromatography (DCM:MeOH 95:5) to give the pure product **5.27** as a pale yellow syrup. (49 mg, 47 %). R_f = 0.59 (DCM:MeOH 9:1). $[\alpha]_D^{26}$ -4 (c 0.5, DCM). ^{1}H NMR (500 MHz, $CDCl_3$) δ 9.01 (bs, 1H, N*H*COC_2H_4), 7.99 (s, 2H, triaz-H), 7.96-7.88 (m, 2H, Ar-H), 7.84-7.73 (m, 3H, N*H*CH_2-triaz and Ar-H), 5.91 (d, *J* = 9.0 Hz, 2H, H-1), 5.60 (td, J = 9.7, 5.2 Hz, 2H, H-2), 5.54 (d, J = 3.4 Hz, 2H, H-4), 5.31 – 5.25 (m, 2H, H-3), 4.76 – 4.59 (m, 4H, CH_2-triaz), 4.33-4.22 (m, 3H, H-5 and C*H*$_2$CCH rotamer 1), 4.21 – 4.10 (m, 5H, H-6, H-6' and C*H*$_2$CCH rotamer 2), 3.88 – 3.74 (m, 2H, NC*H*$_2$$CH_2$CO), 2.84 (dt, J = 5.0, 0.8 Hz, 1H), 2.81-2.71 (m, 2H, NCH_2C*H*$_2$CO), 2.34 (dt, J = 2.7, 1.2 Hz, 1H, CH_2CC*H*), 2.32 – 2.21 (m, 2H, CH_3C(N=N)CH_2C*H*$_2$CO), 2.20 (s, 6H, OAc), 2.01 (s, 6H, OAc), 2.00 (s, 6H, OAc), 1.82 (s, 6H, OAc), 1.75 (t, J = 7.5 Hz, 2H, CH_3C(N=N)C*H*$_2$$CH_2$CO), 1.00 (s, 3H, CH_3). ^{13}C NMR (126 MHz, $CDCl_3$) δ 172.3 (CH_3C(N=N)$CH_2$$CH_2$*C*O), 170.3 (CO of OAc), 170.1 (CO of OAc), 169.9 ($NCH_2$$CH_2$*C*O), 169.8 (CO of OAc), 169.2 (CO of OAc), 166.5 (*C*ONHCH_2-triaz), 145.5 (*C*-triaz), 138.9 (Ar-*C*), 134.9 (Ar-*C*), 121.5 (triaz-*C*H), 121.2 (Ar-*C*H), 120.9 (Ar-*C*H), 86.2 (C-1), 78.4 (CH_2*C*CH), 74.0 (C-5), 73.4 (CH_2C*C*H), 70.8 (C-3), 68.0 (C-2), 66.8 (C-4), 61.2 (C-6), 53.8, 53.2, 43.6 (N*C*$H_2$$CH_2$CO), 38.6 (*C*$H_2$CCH rotamer 1), 36.0 ($NCH_2$*C*$H_2$CO), 35.4 (*C*$H_2$-triaz), 34.8 (*C*$H_2$CCH rotamer 2), 30.9, 29.4 (CH_3C(N=N)*C*$H_2$$CH_2$CO), 27.5 ($CH_3$C(N=N)$CH_2$C*H*$_2$CO), 25.4 ($CH_3$*C*(N=N)), 20.7 ($CH_3$ of OAc), 20.6 (CH_3 of OAc), 20.5 (CH_3 of OAc), 20.3 (CH_3 of OAc), 19.9 (CH_3). IR (film on NaCl): 3286, 3149, 2918, 2849, 2118, 1753, 1649, 1536, 1445, 1370, 1222, 1092, 1053, 924 cm^{-1}. HRMS (ESI+): *m/z* calcd for $C_{53}H_{64}N_{12}O_{22}$ +H$^+$ $[M+H]^+$ 1221.4336, found 1221.4298.

***N,N'*-Di-(β-D-galactopyranosyl-1,2,3-triazol-4-ylmethylamide)-*N''*-(3-(3-(3-(3-methyl-3H-diazirin-3-yl)-N-(prop-2-yn-1-yl)propanamido)propanamido)-5-aminobenzene-1,3-dicarboxamide (5.28)**

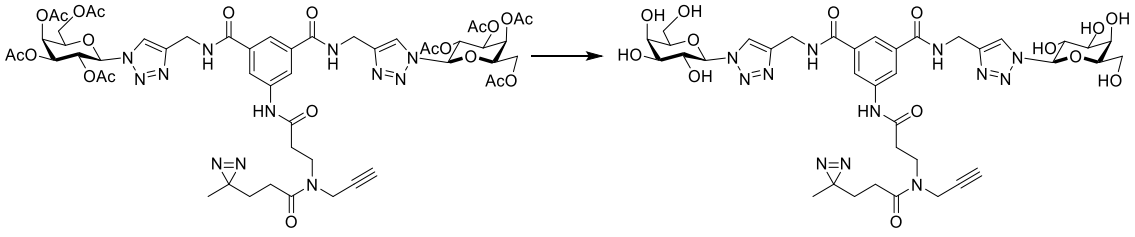

5.27 **5.28**

5.27 (45 mg) was dissolved in methanol/H_2O (4 mL, 2 mL). NEt_3 (0.1 mL) was added, and the reaction mixture was allowed to stir for 45 °C for 6 h. The solution was cooled, Amberlite H^+ was added and the mixture was allowed to stir for 30 mins. The solution was filtered, and the solvent was removed *in vacuo*. The residue was dried under high vacuum and lyophilized to give the pure product **5.28** as an off-white solid (30 mg, 93 %). $[\alpha]_D^{23}$ +16 (c 0.5, MeOH:H_2O 1:1). ^{1}H NMR (500 MHz, D_2O) δ 8.25 (s, 2H, triaz-H), 8.09 – 7.97 (m, 2H, Ar-H), 7.97 – 7.83 (m, 1H, Ar-H), 5.69 (d, *J* = 9.3 Hz, 2H, H-1), 4.70 (s, 4H, CH_2-triaz), 4.27 – 4.19 (m, 3H, H-2 and C*H*CCH), 4.15 (s, 1H, C*H*CCH), 4.09 (d, *J* = 2.5 Hz, 2H, H-4), 4.04 – 3.97 (m, 2H, H-5), 3.93 – 3.83 (m, 3H, H-3 and NC*H*CH_2CO), 3.84-3.75 (m, 5H, H-6 and H-6' and NC*H*CH_2CO), 2.80 (s, 1H, NCH_2C*H*CO), 2.77 – 2.69 (m, 1H, NCH_2C*H*CO), 2.61 (d, *J* = 2.4 Hz, 1H, CH_2CC*H*), 2.35 (dt, *J* = 15.0, 7.2 Hz, 2H, CH_3C(N=N)CH_2C*H*$_2$CO), 1.66-1.59 (m, 2H, CH_3C(N=N)C*H*$_2CH_2$CO), 0.91 and 0.89 (s x 2, 3H, C*H*$_3$), 0.90 (appd, *J* = 10.7 Hz, 3H, C*H*$_3$). ^{13}C NMR (126 MHz, D_2O) δ 174.8 (CH_3C(N=N)CH_2CH_2C'O), 174.4 (CH_3C(N=N)CH_2CH_2C'O), 171.9 (NCH_2CH_2CO), 168.9 (*C*O$NHCH_2$-triaz), 144.9 (*C*-triaz), 138.1 (Ar-*C*), 134.7 (Ar-*C*), 123.0, 122.8 (*C*H-triaz), 122.3 (Ar-*C*H), 122.2 (Ar-*C*H), 97.0, 88.1 (C-1), 78.8 (CH_2*C*CH), 78.3 (C-5), 73.9 (CH_2C*C*H), 72.9 (C-3), 69.8 (C-2), 68.6 (C-4), 60.8 (C-6), 44.7 (N*C*H_2CH_2CO), 43.8 (N*C'*H_2CH_2CO), 38.5 (*C*H_2CCH), 35.7 (*C'*H_2CCH), 35.5 (NCH_2*C*H_2CO), 35.2 (NCH_2*C'*H_2CO), 35.1 (*C*H_2-triaz), 29.0 (CH_3C(N=N)*C*H_2CH_2CO), 28.9 (CH_3C(N=N)*C'*H_2CH_2CO), 27.3 (CH_3C(N=N)CH_2*C*H_2CO), 26.9 (CH_3C(N=N)CH_2*C'*H_2CO), 26.2 (CH_3*C*(N=N)), 18.8 (*C*H_3), 18.7 (*C'*H_3). IR (ATR): 3280, 2924, 1640, 1546, 1445, 1421, 1340, 1287, 1092, 1053, 890 cm^{-1}. HRMS (ESI+): *m/z* calcd for $C_{37}H_{48}N_{12}O_{14}$ +H^+ $[M+H]^+$ 885.3491, found 885.3487.

7.3 Biological Evaluation

7.3.1 Sample Preparation

Compounds were dissolved in distilled water at the required concentration (e.g. 10 mg/mL) and dilutions from these stock solutions were preformed as appropriate (e.g. to 1 or 0.1 mg/mL). Compounds not soluble in water (e.g. monovalent fucoside **2.61**) were dissolved in the minimum amount of DMSO and diluted with water to the required concentration, ensuring that the final DMSO content was below 10 %. Dilutions from this stock solution were performed as appropriate.

7.3.2 Fungal Strains

C. albicans was maintained on sabouraud dextrose agar (SDA) and cultures were grown to the stationary phase (1-2x10^8/mL) overnight in YEPD broth (1 % w/v yeast extract, 2 % w/v bacteriological peptone, 2 % w/v glucose) at 30 ^oC and 200 rpm. Stationary phase yeast cells were harvested, washed with PBS and resuspended at a density of 1x10^8/mL in PBS.

7.3.3 Buccal Epithelial Cells

Buccal epithelial cells (BECs) were harvested from healthy volunteers by gently scraping the inside of the cheek with a sterile tongue depressor. Cells were washed in PBS and resuspended at a density of 5x10^5/mL.

7.3.4 Adherence Assays

Yeast cells were mixed with BECs in a ratioi of 50:1 in a final volumn of 2 mL and incubated at 30 ^oC and 200 rpm for 90 mins. The BEC/yeast cell mixture was harvested by passing through a polycarbonate membrane containing 30 µm pores which trapped the BECs but allowed unattached yeast cells to pass through. This was washed x 2 with 10 mL PBS and cells remaining on the membrane were collected and placed on glass slides which were left to air dry overnight. The cells were heat fixed and stained using 0.5 % (w/v) crystal violet, rinsed using cold water to remove any surplus stain and left to air dry for 30 min. The number of *C. albicans* cells adhering to a sample of 200 BECs per treatment was assessed microscopically.

7.3.4.1 Exclusion Assay

In the exclusion assay, the yeast cells were incubated for 90 mins in the presence of each compound. After this time the cells were harvested and washed twice with PBS before being resuspended in 1 mL PBS before being mixed with BECs (as described above).

7.3.4.2 Competitive Assay

In the competitive assay, yeast cells, BECs and compound were co-incubated for 90 mins prior to harvesting.

7.3.4.3 Displacement Assay

In the displacement assay, adherence was allowed to occur by mixing the yeast cells and BECs together first. BECs and adherent yeast cells were harvested and re-incubated with the compound for a further 90 mins after which time the level of adherence was measured.

7.3.4.4 Statistics

All adherence assays were performed on three indepent occasions. In each assay the number of yeast cells adhering to 200 randomly chosen BECs was determined. Results are mean ± SEM (standard error of the mean).

Bibliography

1. Havlickova, B.; Czaika, V. A.; Friedrich, M., Epidemiological trends in skin mycoses worldwide. *Mycoses* **2008,** *51* (s4), 2-15.
2. Brown, G. D.; Denning, D. W.; Gow, N. A. R.; Levitz, S. M.; Netea, M. G.; White, T. C., Hidden Killers: Human Fungal Infections. *Science Translational Medicine* **2012,** *4* (165), 165rv13.
3. World Health Organization Tuberculosis. https://www.who.int/en/news-room/fact-sheets/detail/tuberculosis (accessed June 14, 2019).
4. World Health Organization Malaria. https://www.who.int/en/news-room/fact-sheets/detail/malaria (accessed June 14, 2019).
5. Bongomin, F.; Gago, S.; Oladele, O. R.; Denning, W. D., Global and Multi-National Prevalence of Fungal Diseases—Estimate Precision. *Journal of Fungi* **2017,** *3* (4).
6. Spampinato, C.; Leonardi, D., Candida infections, causes, targets, and resistance mechanisms: traditional and alternative antifungal agents. *BioMed research international* **2013,** *2013*, 204237-204237.
7. López-Martínez, R., Candidosis, a new challenge. *Clinics in Dermatology* **2010,** *28* (2), 178-184.
8. Chahoud, J.; Kanafani, Z. A.; Kanj, S. S., Management of candidaemia and invasive candidiasis in critically ill patients. *International Journal of Antimicrobial Agents* **2013,** *42*, S29-S35.
9. Kontoyiannis, D. P.; Mantadakis, E.; Samonis, G., Systemic mycoses in the immunocompromised host: an update in antifungal therapy. *Journal of Hospital Infection* **2003,** *53* (4), 243-258.
10. Kontoyiannis, D. P., Antifungal Resistance: An Emerging Reality and A Global Challenge. *The Journal of Infectious Diseases* **2017,** *216* (suppl_3), S431-S435.
11. Cowen, L. E.; Sanglard, D.; Howard, S. J.; Rogers, P. D.; Perlin, D. S., Mechanisms of Antifungal Drug Resistance. *Cold Spring Harbor Perspectives in Medicine* **2015,** *5* (7).
12. Akins, R. A., An update on antifungal targets and mechanisms of resistance in Candida albicans. *Medical Mycology* **2005,** *43* (4), 285-318.
13. D. Katsambas, A.; M. Lotti, T., *European Handbook of Dermatological Treatments*. 2000.
14. Pappas, P. G.; Rex, J. H.; Sobel, J. D.; Filler, S. G.; Dismukes, W. E.; Walsh, T. J.; Edwards, J. E., Guidelines for Treatment of Candidiasis. *Clinical Infectious Diseases* **2004,** *38* (2), 161-189.
15. Noël, T., The cellular and molecular defense mechanisms of the Candida yeasts against azole antifungal drugs. *Journal de Mycologie Médicale* **2012,** *22* (2), 173-178.
16. Perlin, D. S., Echinocandin Resistance in Candida. *Clinical infectious diseases : an official publication of the Infectious Diseases Society of America* **2015,** *61 Suppl 6* (Suppl 6), S612-S617.
17. Canuto, M. M.; Rodero, F. G., Antifungal drug resistance to azoles and polyenes. *The Lancet Infectious Diseases* **2002,** *2* (9), 550-563.
18. Whaley, S. G.; Berkow, E. L.; Rybak, J. M.; Nishimoto, A. T.; Barker, K. S.; Rogers, P. D., Azole Antifungal Resistance in Candida albicans and Emerging Non-albicans Candida Species. *Frontiers in Microbiology* **2017,** *7*, 2173-2173.
19. Cotter, G.; Kavanagh, K., Adherence mechanisms of Candida albicans. *British Journal of Biomedical Science* **2000,** *57*, 241-9.
20. Rupp, S., Interactions of the fungal pathogen Candida albicans with the host. *Future Microbiology* **2007,** *2* (2), 141-151.
21. Latgé, J.-P., The pathobiology of Aspergillus fumigatus. *Trends in Microbiology* **2001,** *9* (8), 382-389.
22. Tronchin, G.; Pihet, M.; Lopes-Bezerra, L. M.; Bouchara, J.-P., Adherence mechanisms in human pathogenic fungi. *Medical Mycology* **2008,** *46* (8), 749-772.

23. Stajich, J. E., Fungal Genomes and Insights into the Evolution of the Kingdom. *Microbiology spectrum* **2017,** *5* (4), 10.1128/microbiolspec.FUNK-0055-2016.
24. Lipke, P. N., What We Do Not Know about Fungal Cell Adhesion Molecules. *Journal of fungi (Basel, Switzerland)* **2018,** *4* (2), 59.
25. de Groot, P. W. J.; Bader, O.; de Boer, A. D.; Weig, M.; Chauhan, N., Adhesins in human fungal pathogens: glue with plenty of stick. *Eukaryotic Cell* **2013,** *12* (4), 470-481.
26. Linder, M.; Szilvay, G. R.; Nakari-Setälä, T.; Söderlund, H.; Penttilä, M., Surface adhesion of fusion proteins containing the hydrophobins HFBI and HFBII from Trichoderma reesei. *Protein science : a publication of the Protein Society* **2002,** *11* (9), 2257-2266.
27. Reuter, L.; Ritala, A.; Linder, M.; Joensuu, J., Novel Hydrophobin Fusion Tags for Plant-Produced Fusion Proteins. *PLOS ONE* **2016,** *11* (10), e0164032.
28. Inoue, K.; Kitaoka, H.; Park, P.; Ikeda, K., Novel aspects of hydrophobins in wheat isolate of Magnaporthe oryzae: Mpg1, but not Mhp1, is essential for adhesion and pathogenicity. *Journal of General Plant Pathology* **2016,** *82* (1), 18-28.
29. Linder, T.; Gustafsson, C. M., Molecular phylogenetics of ascomycotal adhesins—A novel family of putative cell-surface adhesive proteins in fission yeasts. *Fungal Genetics and Biology* **2008,** *45* (4), 485-497.
30. Kottom, T. J.; Kennedy, C. C.; Limper, A. H., Pneumocystis PCINT1, a molecule with integrin-like features that mediates organism adhesion to fibronectin. *Molecular Microbiology* **2008,** *67* (4), 747-761.
31. Teixeira, P. A. C.; Penha, L. L.; Mendonça-Previato, L.; Previato, J. O., Mannoprotein MP84 mediates the adhesion of *Cryptococcus neoformans* to epithelial lung cells. *Frontiers in Cellular and Infection Microbiology* **2014,** *4*, 106-106.
32. Soares, R. M. A.; de A. Soares, R. M.; Alviano, D. S.; Angluster, J.; Alviano, C. S.; Travassos, L. R., Identification of sialic acids on the cell surface of Candida albicans. *Biochimica et Biophysica Acta (BBA) - General Subjects* **2000,** *1474* (2), 262-268.
33. Bowman, S. M.; Free, S. J., The structure and synthesis of the fungal cell wall. *BioEssays* **2006,** *28* (8), 799-808.
34. Masuoka, J., Surface Glycans of *Candida albicans*; and Other Pathogenic Fungi: Physiological Roles, Clinical Uses, and Experimental Challenges. *Clinical Microbiology Reviews* **2004,** *17* (2), 281.
35. Gow, N. A. R.; van de Veerdonk, F. L.; Brown, A. J. P.; Netea, M. G., Candida albicans morphogenesis and host defence: discriminating invasion from colonization. *Nature reviews. Microbiology* **2011,** *10* (2), 112-122.
36. Kanbe, T.; Han, Y.; Redgrave, B.; Riesselman, M. H.; Cutler, J. E., Evidence that mannans of Candida albicans are responsible for adherence of yeast forms to spleen and lymph node tissue. *Infection and Immunity* **1993,** *61* (6), 2578-2584.
37. Kanbe, T.; Cutler, J. E., Minimum chemical requirements for adhesin activity of the acid-stable part of Candida albicans cell wall phosphomannoprotein complex. *Infection and Immunity* **1998,** *66* (12), 5812-5818.
38. Dalle, F.; Jouault, T.; Trinel, P. A.; Esnault, J.; Mallet, J. M.; d'Athis, P.; Poulain, D.; Bonnin, A., Beta-1,2- and alpha-1,2-linked oligomannosides mediate adherence of Candida albicans blastospores to human enterocytes in vitro. *Infection and Immunity* **2003,** *71* (12), 7061-7068.
39. Dromer, F.; Chevalier, R.; Sendid, B.; Improvisi, L.; Jouault, T.; Robert, R.; Mallet, J. M.; Poulain, D., Synthetic analogues of beta-1,2 oligomannosides prevent intestinal colonization by the pathogenic yeast Candida albicans. *Antimicrobial Agents and Chemotherapy* **2002,** *46* (12), 3869-3876.
40. Timpel, C.; Zink, S.; Strahl-Bolsinger, S.; Schröppel, K.; Ernst, J., Morphogenesis, adhesive properties, and antifungal resistance depend on the Pmt6 protein

mannosyltransferase in the fungal pathogen Candida albicans. *Journal of Bacteriology* **2000,** *182* (11), 3063-3071.
41. Munro, C. A.; Bates, S.; Buurman, E. T.; Hughes, H. B.; Maccallum, D. M.; Bertram, G.; Atrih, A.; Ferguson, M. A. J.; Bain, J. M.; Brand, A.; Hamilton, S.; Westwater, C.; Thomson, L. M.; Brown, A. J. P.; Odds, F. C.; Gow, N. A. R., Mnt1p and Mnt2p of Candida albicans are partially redundant alpha-1,2-mannosyltransferases that participate in O-linked mannosylation and are required for adhesion and virulence. *The Journal of Biological Chemistry* **2005,** *280* (2), 1051-1060.
42. Timpel, C.; Strahl-Bolsinger, S.; Ziegelbauer, K.; Ernst, J. F., Multiple Functions of Pmt1p-mediated ProteinO-Mannosylation in the Fungal Pathogen Candida albicans. *Journal of Biological Chemistry* **1998,** *273* (33), 20837-20846.
43. Filler, S. G., Candida–host cell receptor–ligand interactions. *Current Opinion in Microbiology* **2006,** *9* (4), 333-339.
44. Braun, B. R.; van het Hoog, M.; d'Enfert, C.; Martchenko, M.; Dungan, J.; Kuo, A.; Inglis, D. O.; Uhl, M. A.; Hogues, H.; Berriman, M.; Lorenz, M.; Levitin, A.; Oberholzer, U.; Bachewich, C.; Harcus, D.; Marcil, A.; Dignard, D.; Iouk, T.; Zito, R.; Frangeul, L.; Tekaia, F.; Rutherford, K.; Wang, E.; Munro, C. A.; Bates, S.; Gow, N. A.; Hoyer, L. L.; Köhler, G.; Morschhäuser, J.; Newport, G.; Znaidi, S.; Raymond, M.; Turcotte, B.; Sherlock, G.; Costanzo, M.; Ihmels, J.; Berman, J.; Sanglard, D.; Agabian, N.; Mitchell, A. P.; Johnson, A. D.; Whiteway, M.; Nantel, A., A Human-Curated Annotation of the Candida albicans Genome. *PLOS Genetics* **2005,** *1* (1), e1.
45. Gaur, N. K.; Klotz, S. A., Expression, cloning, and characterization of a Candida albicans gene, ALA1, that confers adherence properties upon Saccharomyces cerevisiae for extracellular matrix proteins. *Infection and I mmunity* **1997,** *65* (12), 5289-5294.
46. Sheppard, D. C.; Yeaman, M. R.; Welch, W. H.; Phan, Q. T.; Fu, Y.; Ibrahim, A. S.; Filler, S. G.; Zhang, M.; Waring, A. J.; Edwards, J. E., Functional and Structural Diversity in the Als Protein Family of Candida albicans. *Journal of Biological Chemistry* **2004,** *279* (29), 30480-30489.
47. Loza, L.; Fu, Y.; Ibrahim, A. S.; Sheppard, D. C.; Filler, S. G.; Edwards Jr, J. E., Functional analysis of the Candida albicans ALS1 gene product. *Yeast* **2004,** *21* (6), 473-482.
48. Zhao, X.; Oh, S.-H.; Cheng, G.; Green, C. B.; Nuessen, J. A.; Yeater, K.; Leng, R. P.; Brown, A. J. P.; Hoyer , L. L., ALS3 and ALS8 represent a single locus that encodes a Candida albicans adhesin; functional comparisons between Als3p and Als1p. *Microbiology* **2004,** *150* (7), 2415-2428.
49. Kamai, Y.; Kubota, M.; Kamai, Y.; Hosokawa, T.; Fukuoka, T.; Filler, S. G., Contribution of Candida albicans ALS1 to the pathogenesis of experimental oropharyngeal candidiasis. *Infection and Immunity* **2002,** *70* (9), 5256-5258.
50. Gaur, N. K.; Smith, R. L.; Klotz, S. A., Candida albicans and Saccharomyces cerevisiae Expressing ALA1/ALS5 Adhere to Accessible Threonine, Serine, or Alanine Patches. *Cell Communication & Adhesion* **2002,** *9* (1), 45-57.
51. Klotz, S. A.; Gaur, N. K.; Lake, D. F.; Chan, V.; Rauceo, J.; Lipke, P. N., Degenerate peptide recognition by Candida albicans adhesins Als5p and Als1p. *Infection and Immunity* **2004,** *72* (4), 2029-2034.
52. Nobile, C. J.; Nett, J. E.; Andes, D. R.; Mitchell, A. P., Function of Candida albicans adhesin Hwp1 in biofilm formation. *Eukaryotic Cell* **2006,** *5* (10), 1604-1610.
53. Sundstrom, P.; Balish, E.; Allen, C. M., Essential Role of the Candida albicans Transglutaminase Substrate, Hyphal Wall Protein 1, in Lethal Oroesophageal Candidiasis in Immunodeficient Mice. *The Journal of Infectious Diseases* **2002,** *185* (4), 521-530.
54. Santoni , G.; Gismondi , A.; Liu , J. H.; Punturieri , A.; Santoni , A.; Frati , L.; Piccoli , M.; Djeu, J. Y., Candida albicans expresses a fibronectin receptor antigenically related to α5β1 integrin. *Microbiology* **1994,** *140* (11), 2971-2979.

55. Gale, C. A.; Bendel, C. M.; McClellan, M.; Hauser, M.; Becker, J. M.; Berman, J.; Hostetter, M. K., Linkage of Adhesion, Filamentous Growth, and Virulence in Candida albicans to a Single Gene, INT1. *Science* **1998,** *279* (5355), 1355.
56. Klotz, S. A.; Pendrak, M. L.; Hein , R. C., Antibodies to α5β1 and αvβ3 integrins react with *Candida albicans* alcohol dehydrogenase. *Microbiology* **2001,** *147* (11), 3159-3164
57. Ambrosi, M.; Cameron, N. R.; Davis, B. G., Lectins: tools for the molecular understanding of the glycocode. *Organic & Biomolecular Chemistry* **2005,** *3* (9), 1593-1608.
58. De Las Peñas, A.; Pan, S.-J.; Castaño, I.; Alder, J.; Cregg, R.; Cormack, B., Virulence-related surface glycoproteins in the yeast pathogen Candida glabrata are encoded in subtelomeric clusters and subject to RAP1- and SIR-dependent transcriptional silencing. *Genes & Development* **2003,** *17*, 2245-58.
59. Cormack, B. P.; Ghori, N.; Falkow, S., An Adhesin of the Yeast Pathogen Candida glabrata Mediating Adherence to Human Epithelial Cells. *Science* **1999,** *285* (5427), 578.
60. Sandin, R. L.; Rogers, A. L.; Patterson, R. J.; Beneke, E. S., Evidence for mannose-mediated adherence of Candida albicans to human buccal cells in vitro. *Infection and Immunity* **1982,** *35* (1), 79-85.
61. Critchley, I.; J Douglas, L., Role of Glycosides as Epithelial Cell Receptors for Candida albicans. *Journal of General Microbiology* **1987,** *133*, 637-43.
62. Brassart, D.; Woltz, A.; Golliard, M.; Neeser, J. R., In vitro inhibition of adhesion of Candida albicans clinical isolates to human buccal epithelial cells by Fuc alpha 1 → 2Gal beta-bearing complex carbohydrates. *Infection and Immunity* **1991,** *59* (5), 1605.
63. Alonso, R.; Llopis, I.; Flores, C.; Murgui, A.; Timoneda, J. n., Different adhesins for type IV collagen on Candida albicans : identification of a lectin-like adhesin recognizing the 7S(IV) domain. *Microbiology* **2001,** *147* (7), 1971-1981.
64. Krachler, A. M.; Orth, K., Targeting the bacteria–host interface. *Virulence* **2013,** *4* (4), 284-294.
65. Ofek, I.; Hasty, D. L.; Sharon, N., Anti-adhesion therapy of bacterial diseases: prospects and problems. *FEMS Immunology & Medical Microbiology* **2003,** *38* (3), 181-191.
66. Breines, D. M.; Burnham, J. C., Modulation of Escherichia coli type 1 fimbrial expression and adherence to uroepithelial cells following exposure of logarithmic phase cells to quinolones at subinhibitory concentrations. *Journal of Antimicrobial Chemotherapy* **1994,** *34* (2), 205-221.
67. Wojnicz, D.; Jankowski, S., Effects of subinhibitory concentrations of amikacin and ciprofloxacin on the hydrophobicity and adherence to epithelial cells of uropathogenic Escherichia coli strains. *International Journal of Antimicrobial Agents* **2007,** *29* (6), 700-704.
68. Dal, S. M.; Bovio, C.; Culici, M.; Braga, P. C., The combination of the SH metabolite of erdosteine (a mucoactive drug) and ciprofloxacin increases the inhibition of bacterial adhesiveness achieved by ciprofloxacin alone. *Drugs Under Experimental and Clinical Research* **2002,** *28* (2-3), 75-82.
69. Svensson, A.; Larsson, A.; Emtenäs, H.; Hedenström, M.; Fex, T.; Hultgren, S. J.; Pinkner, J. S.; Almqvist, F.; Kihlberg, J., Design and Evaluation of Pilicides: Potential Novel Antibacterial Agents Directed Against Uropathogenic Escherichia coli. *ChemBioChem* **2001,** *2* (12), 915-918.
70. Pinkner, J. S.; Remaut, H.; Buelens, F.; Miller, E.; Aberg, V.; Pemberton, N.; Hedenström, M.; Larsson, A.; Seed, P.; Waksman, G.; Hultgren, S. J.; Almqvist, F., Rationally designed small compounds inhibit pilus biogenesis in uropathogenic bacteria. *Proceedings of the National Academy of Sciences of the United States of America* **2006,** *103* (47), 17897-17902.
71. Chorell, E.; Pinkner, J. S.; Phan, G.; Edvinsson, S.; Buelens, F.; Remaut, H.; Waksman, G.; Hultgren, S. J.; Almqvist, F., Design and synthesis of C-2 substituted thiazolo

and dihydrothiazolo ring-fused 2-pyridones: pilicides with increased antivirulence activity. *Journal of Medicinal Chemistry* **2010,** *53* (15), 5690-5695.
72. Cho, J. A.; Chinnapen, D. J. F.; Aamar, E.; te Welscher, Y. M.; Lencer, W. I.; Massol, R., Insights on the trafficking and retro-translocation of glycosphingolipid-binding bacterial toxins. *Frontiers in Cellular and Infection Microbiology* **2012,** *2*, 51-51.
73. Radin, N. S., Preventing the binding of pathogens to the host by controlling sphingolipid metabolism. *Microbes and Infection* **2006,** *8* (3), 938-945.
74. Svensson, M.; Frendeus, B.; Butters, T.; Platt, F.; Dwek, R.; Svanborg, C., Glycolipid depletion in antimicrobial therapy. *Molecular Microbiology* **2003,** *47* (2), 453-461.
75. Ofek, I.; Doyle, R. J., Principles of Bacterial Adhesion. In *Bacterial Adhesion to Cells and Tissues*, Ofek, I.; Doyle, R. J., Eds. Springer US: Boston, MA, 1994; pp 1-15.
76. Ofek, I.; Doyle, R. J., Relationship Between Bacterial Cell Surfaces and Adhesins. In *Bacterial Adhesion to Cells and Tissues*, Ofek, I.; Doyle, R. J., Eds. Springer US: Boston, MA, 1994; pp 54-93.
77. Shoaf-Sweeney, K. D.; Hutkins, R. W., Chapter 2 Adherence, Anti-Adherence, and Oligosaccharides: Preventing Pathogens from Sticking to the Host. In *Advances in Food and Nutrition Research*, Academic Press: 2008; Vol. 55, pp 101-161.
78. Abraham, S. N.; Sharon, N.; Ofek, I.; Schwartzman, J. D., Chapter 24 - Adhesion and Colonization. In *Molecular Medical Microbiology (Second Edition)*, Tang, Y.-W.; Sussman, M.; Liu, D.; Poxton, I.; Schwartzman, J., Eds. Academic Press: Boston, 2015; pp 409-421.
79. Firon, N.; Ashkenazi, S.; Mirelman, D.; Ofek, I.; Sharon, N., Aromatic alpha-glycosides of mannose are powerful inhibitors of the adherence of type 1 fimbriated Escherichia coli to yeast and intestinal epithelial cells. *Infection and Immunity* **1987,** *55* (2), 472-476.
80. Lindhorst, T. K.; Kieburg, C.; Krallmann-Wenzel, U., Inhibition of the type 1 fimbriae-mediated adhesion of Escherichia coli to erythrocytes by multiantennary α-mannosyl clusters: The effect of multivalency. *Glycoconjugate Journal* **1998,** *15* (6), 605-613.
81. Simon, P. M.; Goode, P. L.; Mobasseri, A.; Zopf, D., Inhibition of Helicobacter pylori binding to gastrointestinal epithelial cells by sialic acid-containing oligosaccharides. *Infection and Immunity* **1997,** *65* (2), 750-757.
82. Haataja, S.; Tikkanen, K.; Nilsson, U.; Magnusson, G.; Karlsson, K. A.; Finne, J., Oligosaccharide-receptor interaction of the Gal alpha 1-4Gal binding adhesin of Streptococcus suis. Combining site architecture and characterization of two variant adhesin specificities. *Journal of Biological Chemistry* **1994,** *269* (44), 27466-27472.
83. Kouki, A.; Haataja, S.; Loimaranta, V.; Pulliainen, A. T.; Nilsson, U. J.; Finne, J., Identification of a novel streptococcal adhesin P (SadP) protein recognizing galactosyl-α1-4-galactose-containing glycoconjugates: convergent evolution of bacterial pathogens to binding of the same host receptor. *Journal of Biological Chemistry* **2011,** *286* (45), 38854-38864.
84. Ohlsson, J.; Larsson, A.; Haataja, S.; Alajaaski, J.; Stenlund, P.; Pinkner, J. S.; Hultgren, S. J.; Finne, J.; Kihlberg, J.; Nilsson, U. J., Structure-activity relationships of galabioside derivatives as inhibitors of E. coli and S. suis adhesins: nanomolar inhibitors of S. suis adhesins. *Organic & Biomolecular Chemistry* **2005,** *3* (5), 886-900.
85. Hansen, H. C.; Haataja, S.; Finne, J.; Magnusson, G., Di-, Tri-, and Tetravalent Dendritic Galabiosides That Inhibit Hemagglutination by Streptococcus suis at Nanomolar Concentration. *Journal of the American Chemical Society* **1997,** *119* (30), 6974-6979.
86. Kitamura, A.; Higuchi, S.; Hata, M.; Kawakami, K.; Yoshida, K.; Namba, K.; Nakajima, R., Effect of β -1,6-glucan inhibitors on the invasion process of *Candida albicans*:

potential mechanism of their in vivo efficacy. *Antimicrobial Agents and Chemotherapy* **2009,** *53* (9), 3963-3971.
87. Darwazeh, A. M. G.; Lamey, P. J.; Lewis, M. A. O.; Samaranayake, L. P., Systemic fluconazole therapy and in vitro adhesion of Candida albicans to human buccal epithelial cells. *Journal of Oral Pathology & Medicine* **1991,** *20* (1), 17-19.
88. Ellepola, A. N. B.; Samaranayake, L. P., Adhesion of oral Candida albicans isolates to denture acrylic following limited exposure to antifungal agents. *Archives of Oral Biology* **1998,** *43* (12), 999-1007.
89. Lyon, J. P.; de Resende, M. A., Correlation between adhesion, enzyme production, and susceptibility to fluconazole in Candida albicans obtained from denture wearers. *Oral Surgery, Oral Medicine, Oral Pathology, Oral Radiology, and Endodontology* **2006,** *102* (5), 632-638.
90. Willis, A. M.; Coulter, W. A.; Fulton, C. R.; Hayes, J. R.; Bell, P. M.; Lamey, P.-J., The influence of antifungal drugs on virulence properties of Candida albicans in patients with diabetes mellitus. *Oral Surgery, Oral Medicine, Oral Pathology, Oral Radiology, and Endodontology* **2001,** *91* (3), 317-321.
91. Bondaryk, M.; Łukowska-Chojnacka, E.; Staniszewska, M., Tetrazole activity against Candida albicans. The role of KEX2 mutations in the sensitivity to (±)-1-[5-(2-chlorophenyl)-2H-tetrazol-2-yl]propan-2-yl acetate. *Bioorganic & Medicinal Chemistry Letters* **2015,** *25* (13), 2657-2663.
92. Staniszewska, M.; Gizińska, M.; Mikulak, E.; Adamus, K.; Koronkiewicz, M.; Łukowska-Chojnacka, E., New 1,5 and 2,5-disubstituted tetrazoles-dependent activity towards surface barrier of Candida albicans. *European Journal of Medicinal Chemistry* **2018,** *145*, 124-139.
93. Łukowska-Chojnacka, E.; Kowalkowska, A.; Gizińska, M.; Koronkiewicz, M.; Staniszewska, M., Synthesis of tetrazole derivatives bearing pyrrolidine scaffold and evaluation of their antifungal activity against Candida albicans. *European Journal of Medicinal Chemistry* **2019,** *164*, 106-120.
94. Tsukahara, K.; Hata, K.; Nakamoto, K.; Sagane, K.; Watanabe, N.-a.; Kuromitsu, J.; Kai, J.; Tsuchiya, M.; Ohba, F.; Jigami, Y.; Yoshimatsu, K.; Nagasu, T., Medicinal genetics approach towards identifying the molecular target of a novel inhibitor of fungal cell wall assembly. *Molecular Microbiology* **2003,** *48* (4), 1029-1042.
95. Bondaryk, M.; Ochal, Z.; Staniszewska, M., Sulfone derivatives reduce growth, adhesion and aspartic protease SAP2 gene expression. *World Journal of Microbiology and Biotechnology* **2014,** *30* (9), 2511-2521.
96. Staniszewska, M.; Bondaryk, M.; Ochal, Z., New synthetic sulfone derivatives inhibit growth, adhesion and the leucine arylamidase APE2 gene expression of Candida albicans in vitro. *Bioorganic & Medicinal Chemistry* **2015,** *23* (2), 314-321.
97. Bondaryk, M.; Grabowska-Jadach, I.; Ochal, Z.; Sygitowicz, G.; Staniszewska, M., Possible role of hydrolytic enzymes (Sap, Kex2) in Candida albicans response to aromatic compounds bearing a sulfone moiety. *Chemical Papers* **2016,** *70* (10), 1336-1350.
98. Martins, C. V. B.; da Silva, D. L.; Neres, A. T. M.; Magalhães, T. F. F.; Watanabe, G. A.; Modolo, L. V.; Sabino, A. A.; de Fátima, Â.; de Resende, M. A., Curcumin as a promising antifungal of clinical interest. *Journal of Antimicrobial Chemotherapy* **2009,** *63* (2), 337-339.
99. Shahzad, M.; Sherry, L.; Rajendran, R.; Edwards, C. A.; Combet, E.; Ramage, G., Utilising polyphenols for the clinical management of Candida albicans biofilms. *International Journal of Antimicrobial Agents* **2014,** *44* (3), 269-273.
100. Sun, L.; Liao, K.; Wang, D., Effects of Magnolol and Honokiol on Adhesion, Yeast-Hyphal Transition, and Formation of Biofilm by Candida albicans. *PLOS ONE* **2015,** *10* (2), e0117695.

101. Zhang, H.; Li, J.; Zhang, J.; Shi, H.; Lin, X.; Sun, H., Purpurin inhibits the adhesion of Candida albicans biofilms. *International Journal of Clinical and Experimental Medicine* **2016,** *9* (6), 10070-10076.
102. Manoharan, R. K.; Lee, J.-H.; Kim, Y.-G.; Lee, J., Alizarin and Chrysazin Inhibit Biofilm and Hyphal Formation by Candida albicans. *Frontiers in Cellular and Infection Microbiology* **2017,** *7*, 447-447.
103. Janeczko, M.; Masłyk, M.; Kubiński, K.; Golczyk, H., Emodin, a natural inhibitor of protein kinase CK2, suppresses growth, hyphal development, and biofilm formation of Candida albicans. *Yeast* **2017,** *34* (6), 253-265.
104. Fowler, S.; Jones, D. S., Modified adherence of Candida albicans to human buccal epithelial cells in vitro following treatment with cationic, non-antibiotic antimicrobial agents. *International Journal of Pharmaceutics* **1992,** *84* (1), 77-83.
105. Lyon, J. P.; dos Santos, F. V.; de Moraes, P. C. G.; Moreira, L. M., Inhibition of Virulence Factors of Candida spp. by Different Surfactants. *Mycopathologia* **2011,** *171* (2), 93-101.
106. Obłąk, E.; Piecuch, A.; Dworniczek, E.; Olejniczak, T., The Influence of Biodegradable Gemini Surfactants, N,N'-bis(1-Decyloxy-1-Oxopronan-2-yl)-N,N,N',N' Tetramethylpropane-1,3-Diammonium Dibromide and N,N'-bis(1-Dodecyloxy-1-Oxopronan-2-yl) N,N,N',N'-Tetramethylethane-1,2-Diammonium Dibromide, on Fungal Biofilm and Adhesion. *Journal of Oleo Science* **2015,** *64* (5), 527-537.
107. Jain, T.; Muktapuram, P. R.; Pochampalli, S.; Sharma, K.; Pant, G.; Mitra, K.; Bathula, S. R.; Banerjee, D., Chain-length-specific anti-Candida activity of cationic lipo-oxazoles: a new class of quaternary ammonium compounds. *Journal of Medical Microbiology* **2017,** *66* (12), 1706-1714.
108. Jain, T.; Muktapuram, P. R.; Sharma, K.; Ravi, O.; Pant, G.; Mitra, K.; Bathula, S. R.; Banerjee, D., Biofilm inhibition and anti-Candida activity of a cationic lipo-benzamide molecule with twin-nonyl chain. *Bioorganic & Medicinal Chemistry Letters* **2018,** *28* (10), 1776-1780.
109. Paluch, E.; Piecuch, A.; Obłąk, E.; Lamch, Ł.; Wilk, K. A., Antifungal activity of newly synthesized chemodegradable dicephalic-type cationic surfactants. *Colloids and Surfaces B: Biointerfaces* **2018,** *164*, 34-41.
110. McCourtie, J.; W MacFarlane, T.; Samaranayake, L., Effect of chorhexidine gluconate on the adherence of Candida species to denture acrylic. *Journal of Medical Microbiology* **1985,** *20* (1), 97-104.
111. Gorman, S. P.; McCafferty, D. F.; Woolfson, A. D.; Jones, D. S., A Comparative Study of the Microbial Anti-Adherence Capacities of Three Antimicrobial Agents. *Journal of Clinical Pharmacy and Therapeutics* **1987,** *12* (6), 393-399.
112. Tobgi, R. S.; Samaranayake, L. P.; Macfarlane, T. W., Adhesion of Candida albicans to buccal epithelial cells exposed to chlorhexidine gluconate. *Journal of Medical and Veterinary Mycology* **1987,** *25* (5), 335-338.
113. Matsuura, E.; Godoy, J. S. R.; Bonfim-Mendonça, P. d. S.; de Mello, J. C. P.; Svidzinski, T. I. E.; Gasparetto, A.; Maciel, S. M., In vitro effect of Paullinia cupana (guaraná) on hydrophobicity, biofilm formation, and adhesion of Candida albicans' to polystyrene, composites, and buccal epithelial cells. *Archives of Oral Biology* **2015,** *60* (3), 471-478.
114. Mafojane, T.; Shangase, S. L.; Patel, M., The effect of subinhibitory concentrations of gentian violet on the germ tube formation by Candida albicans and its adherence to oral epithelial cells. *Archives of Oral Biology* **2017,** *82*, 1-5.
115. Polaquini, S. R. B.; Svidzinski, T. I. E.; Kemmelmeier, C.; Gasparetto, A., Effect of aqueous extract from Neem (Azadirachta indica A. Juss) on hydrophobicity, biofilm formation and adhesion in composite resin by Candida albicans. *Archives of Oral Biology* **2006,** *51* (6), 482-490.

116. Bucci, A. R.; Marcelino, L.; Mendes, R. K.; Etchegaray, A., The antimicrobial and antiadhesion activities of micellar solutions of surfactin, CTAB and CPCl with terpinen-4-ol: applications to control oral pathogens. *World Journal of Microbiology and Biotechnology* **2018,** *34* (6), 86.
117. Jones, D. S.; Gorman, S. P.; McCafferty, D. F.; Woolfson, A. D., Microbial Anti-Adherence of Taurolidine. *Journal of Pharmacy and Pharmacology* **1986,** *38* (S12), 39P-39P.
118. Jones, D. S.; Fowler, S., A preliminary report concerning the effects of Brolene® on the adherence of Candida albicans to human buccal epithelial cells and on hyphal development in vitro. *International Journal of Pharmaceutics* **1994,** *105* (1), 71-75.
119. Johann, S.; Soldi, C.; Lyon, J. P.; Pizzolatti, M. G.; Resende, M. A., Antifungal activity of the amyrin derivatives and in vitro inhibition of Candida albicans adhesion to human epithelial cells. *Letters in Applied Microbiology* **2007,** *45* (2), 148-153.
120. Sadowska, B.; Kuźma, Ł.; Micota, B.; Budzyńska, A.; Wysokińska, H.; Kłys, A.; Więckowska-Szakiel, M.; Różalska, B., New biological potential of abietane diterpenoids isolated from Salvia austriaca against microbial virulence factors. *Microbial Pathogenesis* **2016,** *98*, 132-139.
121. Segal, E., Inhibitors of Candida Albicans Adhesion to Prevent Candidiasis. In *Toward Anti-Adhesion Therapy for Microbial Diseases*, Kahane, I.; Ofek, I., Eds. Springer US: Boston, MA, 1996; pp 197-206.
122. Marc, G.; Araniciu, C.; Oniga, D. S.; Vlase, L.; Pîrnău, A.; Duma, M.; Măruțescu, L.; Chifiriuc, C. M.; Oniga, O., New N-(oxazolylmethyl)-thiazolidinedione Active against Candida albicans Biofilm: Potential Als Proteins Inhibitors. *Molecules* **2018,** *23* (10).
123. Sá, N. P.; Lima, C. M.; A Dos Santos, J. R.; Costa, M. C.; de Barros, P. P.; Junqueira, J. C.; Vaz, J. A.; Oliveira, R. B.; Fuchs, B. B.; Mylonakis, E.; Rosa, C. A.; Santos, D. A.; Johann, S., A phenylthiazole derivative demonstrates efficacy on treatment of the cryptococcosis & candidiasis in animal models. *Future Science OA* **2018,** *4* (6), FSO305-FSO305.
124. Masłyk, M.; Janeczko, M.; Martyna, A.; Kubiński, K., CX-4945: the protein kinase CK2 inhibitor and anti-cancer drug shows anti-fungal activity. *Molecular and Cellular Biochemistry* **2017,** *435* (1-2), 193-196.
125. Fazly, A.; Jain, C.; Dehner, A. C.; Issi, L.; Lilly, E. A.; Ali, A.; Cao, H.; Fidel, P. L.; P. Rao, R.; Kaufman, P. D., Chemical screening identifies filastatin, a small molecule inhibitor of Candida albicans adhesion, morphogenesis, and pathogenesis. *Proceedings of the National Academy of Sciences* **2013,** *110* (33), 13594.
126. Abdelmegeed, E.; Shaaban, M. I., Cyclooxygenase inhibitors reduce biofilm formation and yeast-hypha conversion of fluconazole resistant Candida albicans. *Journal of Microbiology* **2013,** *51* (5), 598-604.
127. Privett, B. J.; Nutz, S. T.; Schoenfisch, M. H., Efficacy of surface-generated nitric oxide against Candida albicans adhesion and biofilm formation. *Biofouling* **2010,** *26* (8), 973-983.
128. Madariaga-Venegas, F.; Fernández-Soto, R.; Duarte, L.; Suarez, N.; Delgadillo, D.; A. Jara, J.; Fernández-Ramires, R.; urzúa, B.; Molina-Berríos, A., Characterization of a novel antibiofilm effect of nitric oxide-releasing aspirin (NCX-4040) on Candida albicans isolates from denture stomatitis patients. *PLOS One* **2017,** *12* (5), e0176755.
129. Wong, S. S. W.; Kao, R. Y. T.; Yuen, K. Y.; Wang, Y.; Yang, D.; Samaranayake, L. P.; Seneviratne, C. J., In Vitro and In Vivo Activity of a Novel Antifungal Small Molecule against Candida Infections. *PLOS ONE* **2014,** *9* (1), e85836.
130. Nazzaro, F.; Fratianni, F.; Coppola, R.; Feo, V. D., Essential Oils and Antifungal Activity. *Pharmaceuticals (Basel, Switzerland)* **2017,** *10* (4), 86.
131. Rane, H. S.; Bernardo, S. M.; Howell, A. B.; Lee, S. A., Cranberry-derived proanthocyanidins prevent formation of Candida albicans biofilms in artificial urine through

biofilm- and adherence-specific mechanisms. *The Journal of Antimicrobial Chemotherapy* **2014,** *69* (2), 428-436.
132. Cannas, S.; Molicotti, P.; Usai, D.; Maxia, A.; Zanetti, S., Antifungal, anti-biofilm and adhesion activity of the essential oil of Myrtus communis L. against Candida species. *Natural Product Research* **2014,** *28* (23), 2173-2177.
133. Souza, L. B. F. C.; Silva-Rocha, W. P.; Ferreira, M. R. A.; Soares, L. A. L.; Svidzinski, T. I. E.; Milan, E. P.; Pires, R. H.; Fusco Almeida, A. M.; Mendes-Giannini, M. J. S.; Maranhão Chaves, G., Influence of Eugenia uniflora Extract on Adhesion to Human Buccal Epithelial Cells, Biofilm Formation, and Cell Surface Hydrophobicity of Candida spp. from the Oral Cavity of Kidney Transplant Recipients. *Molecules (Basel, Switzerland)* **2018,** *23* (10), 2418.
134. Chabre, Y. M.; Roy, R., Multivalent glycoconjugate syntheses and applications using aromatic scaffolds. *Chemical Society Reviews* **2013,** *42* (11), 4657-4708.
135. Yariv, J.; Rapport, M. M.; Graf, L., The interaction of glycosides and saccharides with antibody to the corresponding phenylazo glycosides. *The Biochemical Journal* **1962,** *85* (2), 383-388.
136. Patch, R. J.; Chen, H.; Pandit, C. R., Multivalent Templated Saccharides: Convenient Syntheses of Spacer-Linked 1,1‘-Bis -and 1,1‘,1‘‘-Tris-β-glycosides by the Glycal Epoxide Glycosidation Method. *The Journal of Organic Chemistry* **1997,** *62* (5), 1543-1546.
137. Pagé, D.; Roy, R., Synthesis of divalent α-D-mannopyranosylated clusters having enhanced binding affinities towards concanavalin A and pea lectins. *Bioorganic & Medicinal Chemistry Letters* **1996,** *6* (15), 1765-1770.
138. Roy, R.; Pagé, D.; Figueroa Perez, S.; Verez, V., Effect of shape, size, and valency of multivalent mannosides on their binding properties to phytohemagglutinins. *Glycoconjugate Journal* **1998,** *15* (3), 251-263.
139. Pérez-Balderas, F.; Ortega-Muñoz, M.; Morales-Sanfrutos, J.; Hernández-Mateo, F.; Calvo-Flores, F. G.; Calvo-Asín, J. A.; Isac-García, J.; Santoyo-González, F., Multivalent Neoglycoconjugates by Regiospecific Cycloaddition of Alkynes and Azides Using Organic-Soluble Copper Catalysts. *Organic Letters* **2003,** *5* (11), 1951-1954.
140. Wang, G.-N.; André, S.; Gabius, H.-J.; Murphy, P. V., Bi- to tetravalent glycoclusters: synthesis, structure–activity profiles as lectin inhibitors and impact of combining both valency and headgroup tailoring on selectivity. *Organic & Biomolecular Chemistry* **2012,** *10* (34), 6893-6907.
141. Roy, R.; Das, S. K.; Santoyo-González, F.; Hernández-Mateo, F.; Dam, T. K.; Brewer, C. F., Synthesis of “Sugar-Rods” with Phytohemagglutinin Cross-Linking Properties by Using the Palladium-Catalyzed Sonogashira Reaction. *Chemistry – A European Journal* **2000,** *6* (10), 1757-1762.
142. Sengupta, S.; Sadhukhan, S. K., Synthetic studies on dendritic glycoclusters: a convergent palladium-catalyzed strategy. *Carbohydrate Research* **2001,** *332* (2), 215-219.
143. Bergeron-Brlek, M.; Shiao, T. C.; Trono, M. C.; Roy, R., Synthesis of a small library of bivalent α-d-mannopyranosides for lectin cross-linking. *Carbohydrate Research* **2011,** *346* (12), 1479-1489.
144. Perez-Balderas, F.; Morales-Sanfrutos, J.; Hernandez-Mateo, F.; Isac-García, J.; Santoyo-Gonzalez, F., Click Multivalent Homogeneous Neoglycoconjugates – Synthesis and Evaluation of Their Binding Affinities. *European Journal of Organic Chemistry* **2009,** *2009* (15), 2441-2453.
145. Dominique, R.; Das, S. K.; Liu, B.; Nahra, J.; Schmor, B.; Gan, Z.; Roy, R., Ruthenium Carbenoids as Catalysts for Olefin Metathesis of ω-Alkenyl Glycosides. In *Methods in Enzymology*, Academic Press: 2003; Vol. 362, pp 17-28.

146. Martinez, J. J.; Mulvey, M. A.; Schilling, J. D.; Pinkner, J. S.; Hultgren, S. J., Type 1 pilus-mediated bacterial invasion of bladder epithelial cells. *The EMBO Journal* **2000,** *19* (12), 2803-2812.
147. Hung, C.-S.; Bouckaert, J.; Hung, D.; Pinkner, J.; Widberg, C.; DeFusco, A.; Auguste, C. G.; Strouse, R.; Langermann, S.; Waksman, G.; Hultgren, S. J., Structural basis of tropism of Escherichia coli to the bladder during urinary tract infection. *Molecular Microbiology* **2002,** *44* (4), 903-915.
148. Bouckaert, J.; Berglund, J.; Schembri, M.; De Genst, E.; Cools, L.; Wuhrer, M.; Hung, C.-S.; Pinkner, J.; Slättegård, R.; Zavialov, A.; Choudhury, D.; Langermann, S.; Hultgren, S. J.; Wyns, L.; Klemm, P.; Oscarson, S.; Knight, S. D.; De Greve, H., Receptor binding studies disclose a novel class of high-affinity inhibitors of the Escherichia coli FimH adhesin. *Molecular Microbiology* **2005,** *55* (2), 441-455.
149. Wellens, A.; Garofalo, C.; Nguyen, H.; Van Gerven, N.; Slättegård, R.; Hernalsteens, J.-P.; Wyns, L.; Oscarson, S.; De Greve, H.; Hultgren, S.; Bouckaert, J., Intervening with Urinary Tract Infections Using Anti-Adhesives Based on the Crystal Structure of the FimH–Oligomannose-3 Complex. *PLOS ONE* **2008,** *3* (4), e2040.
150. Han, Z.; Pinkner, J. S.; Ford, B.; Obermann, R.; Nolan, W.; Wildman, S. A.; Hobbs, D.; Ellenberger, T.; Cusumano, C. K.; Hultgren, S. J.; Janetka, J. W., Structure-Based Drug Design and Optimization of Mannoside Bacterial FimH Antagonists. *Journal of Medicinal Chemistry* **2010,** *53* (12), 4779-4792.
151. Bucior, I.; Pielage, J. F.; Engel, J. N., Pseudomonas aeruginosa Pili and Flagella Mediate Distinct Binding and Signaling Events at the Apical and Basolateral Surface of Airway Epithelium. *PLOS Pathogens* **2012,** *8* (4), e1002616.
152. Gilboa-Garber, N., Pseudomonas aeruginosa lectins. In *Methods in Enzymology*, Academic Press: 1982; Vol. 83, pp 378-385.
153. Imberty, A.; Wimmerová, M.; Mitchell, E. P.; Gilboa-Garber, N., Structures of the lectins from Pseudomonas aeruginosa: insights into the molecular basis for host glycan recognition. *Microbes and Infection* **2004,** *6* (2), 221-228.
154. Blanchard, B.; Nurisso, A.; Hollville, E.; Tétaud, C.; Wiels, J.; Pokorná, M.; Wimmerová, M.; Varrot, A.; Imberty, A., Structural Basis of the Preferential Binding for Globo-Series Glycosphingolipids Displayed by Pseudomonas aeruginosa Lectin I. *Journal of Molecular Biology* **2008,** *383* (4), 837-853.
155. Lanne, B.; Cîopraga, J.; Bergström, J.; Motas, C.; Karlsson, K.-A., Binding of the galactose-specificPseudomonas aeruginosa lectin, PA-I, to glycosphingolipids and other glycoconjugates. *Glycoconjugate Journal* **1994,** *11* (4), 292-298.
156. Perret, S.; Sabin, C.; Dumon, C.; Pokorná, M.; Gautier, C.; Galanina, O.; Ilia, S.; Bovin, N.; Nicaise, M.; Desmadril, M.; Gilboa-Garber, N.; Wimmerová, M.; Mitchell, E. P.; Imberty, A., Structural basis for the interaction between human milk oligosaccharides and the bacterial lectin PA-IIL of Pseudomonas aeruginosa. *The Biochemical Journal* **2005,** *389* (Pt 2), 325-332.
157. Mitchell, E.; Houles, C.; Sudakevitz, D.; Wimmerova, M.; Gautier, C.; Pérez, S.; Wu, A. M.; Gilboa-Garber, N.; Imberty, A., Structural basis for oligosaccharide-mediated adhesion of Pseudomonas aeruginosa in the lungs of cystic fibrosis patients. *Nature Structural Biology* **2002,** *9* (12), 918-921.
158. Chemani, C.; Imberty, A.; de Bentzmann, S.; Pierre, M.; Wimmerová, M.; Guery, B. P.; Faure, K., Role of LecA and LecB lectins in Pseudomonas aeruginosa-induced lung injury and effect of carbohydrate ligands. *Infection and Immunity* **2009,** *77* (5), 2065-2075.
159. Weichert, S.; Jennewein, S.; Hüfner, E.; Weiss, C.; Borkowski, J.; Putze, J.; Schroten, H., Bioengineered 2'-fucosyllactose and 3-fucosyllactose inhibit the adhesion of Pseudomonas aeruginosa and enteric pathogens to human intestinal and respiratory cell lines. *Nutrition Research* **2013,** *33* (10), 831-838.

160. Novoa, A.; Eierhoff, T.; Topin, J.; Varrot, A.; Barluenga, S.; Imberty, A.; Römer, W.; Winssinger, N., A LecA Ligand Identified from a Galactoside-Conjugate Array Inhibits Host Cell Invasion by Pseudomonas aeruginosa. *Angewandte Chemie International Edition* **2014,** *53* (34), 8885-8889.
161. Boukerb, A. M.; Rousset, A.; Galanos, N.; Méar, J.-B.; Thépaut, M.; Grandjean, T.; Gillon, E.; Cecioni, S.; Abderrahmen, C.; Faure, K.; Redelberger, D.; Kipnis, E.; Dessein, R.; Havet, S.; Darblade, B.; Matthews, S. E.; de Bentzmann, S.; Guéry, B.; Cournoyer, B.; Imberty, A.; Vidal, S., Antiadhesive Properties of Glycoclusters against Pseudomonas aeruginosa Lung Infection. *Journal of Medicinal Chemistry* **2014,** *57* (24), 10275-10289.
162. Kuboi, S.; Ishimaru, T.; Tamada, S.; Bernard, E. M.; Perlin, D. S.; Armstrong, D., Molecular characterization of AfuFleA, an l-fucose-specific lectin from Aspergillus fumigatus. *Journal of Infection and Chemotherapy* **2013,** *19* (6), 1021-1028.
163. Houser, J.; Komarek, J.; Kostlanova, N.; Cioci, G.; Varrot, A.; Kerr, S. C.; Lahmann, M.; Balloy, V.; Fahy, J. V.; Chignard, M.; Imberty, A.; Wimmerova, M., A Soluble Fucose-Specific Lectin from Aspergillus fumigatus Conidia - Structure, Specificity and Possible Role in Fungal Pathogenicity. *PLOS ONE* **2013,** *8* (12), e83077.
164. Houser, J.; Komárek, J.; Cioci, G.; Varrot, A.; Imberty, A.; Wimmerová, M., Structural insights into Aspergillus fumigatus lectin specificity: AFL binding sites are functionally non-equivalent. *Acta Crystallographica Section D* **2015,** *71*, 442-53.
165. Kerr, S. C.; Fischer, G. J.; Sinha, M.; McCabe, O.; Palmer, J. M.; Choera, T.; Yun Lim, F.; Wimmerova, M.; Carrington, S. D.; Yuan, S.; Lowell, C. A.; Oscarson, S.; Keller, N. P.; Fahy, J. V., FleA Expression in Aspergillus fumigatus Is Recognized by Fucosylated Structures on Mucins and Macrophages to Prevent Lung Infection. *PLOS Pathogens* **2016,** *12* (4), e1005555.
166. Lehot, V.; Brissonnet, Y.; Dussouy, C.; Brument, S.; Cabanettes, A.; Gillon, E.; Deniaud, D.; Varrot, A.; Pape, P. L.; Gouin, S. G., Multivalent Fucosides with Nanomolar Affinity for the Aspergillus fumigatus Lectin FleA Prevent Spore Adhesion to Pneumocytes. *Chemistry – A European Journal* **2018,** *24* (72), 19243-19249.
167. Wright, C.; Leyden, R.; Murphy, P. V.; Callaghan, M.; Velasco-Torrijos, T.; McClean, S., Inhibition of Burkholderia multivorans Adhesion to Lung Epithelial Cells by Bivalent Lactosides. *Molecules* **2012,** *17* (9).
168. Krivan, H. C.; Roberts, D. D.; Ginsburg, V., Many pulmonary pathogenic bacteria bind specifically to the carbohydrate sequence GalNAc beta 1-4Gal found in some glycolipids. *Proceedings of the National Academy of Sciences of the United States of America* **1988,** *85* (16), 6157-6161.
169. Wright, C.; Herbert, G.; Pilkington, R.; Callaghan, M.; McClean, S., Real-time PCR method for the quantification of Burkholderia cepacia complex attached to lung epithelial cells and inhibition of that attachment. *Letters in Applied Microbiology* **2010,** *50* (5), 500-506.
170. Jimenez-Lucho, V.; Ginsburg, V.; Krivan, H. C., Cryptococcus neoformans, Candida albicans, and other fungi bind specifically to the glycosphingolipid lactosylceramide (Gal beta 1-4Glc beta 1-1Cer), a possible adhesion receptor for yeasts. *Infection and Immunity* **1990,** *58* (7), 2085-2090.
171. Yu, L.; Lee, K. K.; Sheth, H. B.; Lane-Bell, P.; Srivastava, G.; Hindsgaul, O.; Paranchych, W.; Hodges, R. S.; Irvin, R. T., Fimbria-mediated adherence of Candida albicans to glycosphingolipid receptors on human buccal epithelial cells. *Infection and Immunity* **1994,** *62* (7), 2843-2848.
172. Foldvari, M.; Jaafari, M. R.; Radhi, J.; Segal, D., Efficacy of the antiadhesin octyl O-(2-acetamido-2-deoxy-beta-D-galactopyranosyl)-(1-4)-2-O-propyl-beta-D-galactopyranoside (Fimbrigal-P) in a rat oral candidiasis model. *Antimicrobial Agents and Chemotherapy* **2005,** *49* (7), 2887-2894.

173. Hein, J. E.; Fokin, V. V., Copper-catalyzed azide-alkyne cycloaddition (CuAAC) and beyond: new reactivity of copper(I) acetylides. *Chemical Society Reviews* **2010,** *39* (4), 1302-1315.
174. Bock, V. D.; Hiemstra, H.; van Maarseveen, J. H., CuI-Catalyzed Alkyne–Azide "Click" Cycloadditions from a Mechanistic and Synthetic Perspective. *European Journal of Organic Chemistry* **2006,** *2006* (1), 51-68.
175. He, X.-P.; Zeng, Y.-L.; Zang, Y.; Li, J.; Field, R. A.; Chen, G.-R., Carbohydrate CuAAC click chemistry for therapy and diagnosis. *Carbohydrate Research* **2016,** *429*, 1-22.
176. Tornøe, C. W.; Christensen, C.; Meldal, M., Peptidotriazoles on Solid Phase: [1,2,3]-Triazoles by Regiospecific Copper(I)-Catalyzed 1,3-Dipolar Cycloadditions of Terminal Alkynes to Azides. *The Journal of Organic Chemistry* **2002,** *67* (9), 3057-3064.
177. Rostovtsev, V. V.; Green, L. G.; Fokin, V. V.; Sharpless, K. B., A Stepwise Huisgen Cycloaddition Process: Copper(I)-Catalyzed Regioselective "Ligation" of Azides and Terminal Alkynes. *Angewandte Chemie International Edition* **2002,** *41* (14), 2596-2599.
178. Jin, L.; Tolentino, D. R.; Melaimi, M.; Bertrand, G., Isolation of bis(copper) key intermediates in Cu-catalyzed azide-alkyne "click reaction". *Science Advances* **2015,** *1* (5).
179. Nolte, C.; Mayer, P.; Straub, B. F., Isolation of a Copper(I) Triazolide: A "Click" Intermediate. *Angewandte Chemie International Edition* **2007,** *46* (12), 2101-2103.
180. Iacobucci, C.; Reale, S.; Gal, J.-F.; De Angelis, F., Dinuclear Copper Intermediates in Copper(I)-Catalyzed Azide–Alkyne Cycloaddition Directly Observed by Electrospray Ionization Mass Spectrometry. *Angewandte Chemie International Edition* **2015,** *54* (10), 3065-3068.
181. Worrell, B. T.; Malik, J. A.; Fokin, V. V., Direct Evidence of a Dinuclear Copper Intermediate in Cu(I)-Catalyzed Azide-Alkyne Cycloadditions. *Science* **2013,** *340* (6131), 457.
182. Zhu, L.; Brassard, C. J.; Zhang, X.; Guha, P. M.; Clark, R. J., On the Mechanism of Copper(I)-Catalyzed Azide–Alkyne Cycloaddition. *The Chemical Record* **2016,** *16* (3), 1501-1517.
183. Badía, C.; Souard, F.; Vicent, C., Sugar–Oligoamides: Synthesis of DNA Minor Groove Binders. *The Journal of Organic Chemistry* **2012,** *77* (23), 10870-10881.
184. D'Onofrio, J.; de Champdoré, M.; De Napoli, L.; Montesarchio, D.; Di Fabio, G., Glycomimetics as Decorating Motifs for Oligonucleotides: Solid-Phase Synthesis, Stability, and Hybridization Properties of Carbopeptoid−Oligonucleotide Conjugates. *Bioconjugate Chemistry* **2005,** *16* (5), 1299-1309.
185. Kang, B.; Okwieka, P.; Schöttler, S.; Winzen, S.; Langhanki, J.; Mohr, K.; Opatz, T.; Mailänder, V.; Landfester, K.; Wurm, F. R., Carbohydrate-Based Nanocarriers Exhibiting Specific Cell Targeting with Minimum Influence from the Protein Corona. *Angewandte Chemie International Edition* **2015,** *54* (25), 7436-7440.
186. Reddy, A.; Ramos-Ondono, J.; Abbey, L.; Velasco-Torrijos, T.; Ziegler, T., 2-Chloroethyl and 2-Azidoethyl 2,3,4,6-tetra-O-acetyl-β-D-gluco-and β-D-galactopyranosides. In *Carbohydrate Chemistry, Proven Synthetic Methods*, Taylor & Francis: 2017; Vol. 37, pp 201-208.
187. Tanaka, T.; Nagai, H.; Noguchi, M.; Kobayashi, A.; Shoda, S.-i., One-step conversion of unprotected sugars to β-glycosyl azides using 2-chloroimidazolinium salt in aqueous solution. *Chemical Communications* **2009,** (23), 3378-3379.
188. Knorr, R.; Trzeciak, A.; Bannwarth, W.; Gillessen, D., New coupling reagents in peptide chemistry. *Tetrahedron Letters* **1989,** *30* (15), 1927-1930.
189. Abdelmoty, I.; Albericio, F.; A. Carpino, L.; M. Foxman, B.; A. Kates, S., Structural studies of reagents for peptide bond formation: Crystal and molecular structures of HBTU and HATU. *Letters in Peptide Science* **1994,** *1*, 57-67.

190. Falchi, A.; Giacomelli, G.; Porcheddu, A.; Taddei, M., 4-(4,6-Dimethoxy[1,3,5]triazin-2-yl)-4-methyl-morpholinium Chloride (DMTMM): A Valuable Alternative to PyBOP for Solid Phase Peptide Synthesis. *Synlett* **2000,** *2000* (02), 275-277.
191. Kamiński, Z. J.; Paneth, P.; Rudziński, J., A Study on the Activation of Carboxylic Acids by Means of 2-Chloro-4,6-dimethoxy-1,3,5-triazine and 2-Chloro-4,6-diphenoxy-1,3,5-triazine. *The Journal of Organic Chemistry* **1998,** *63* (13), 4248-4255.
192. Kunishima, M.; Kawachi, C.; Monta, J.; Terao, K.; Iwasaki, F.; Tani, S., 4-(4,6-dimethoxy-1,3,5-triazin-2-yl)-4-methyl-morpholinium chloride: an efficient condensing agent leading to the formation of amides and esters. *Tetrahedron* **1999,** *55* (46), 13159-13170.
193. Kunishima, M.; Kawachi, C.; Iwasaki, F.; Terao, K.; Tani, S., Synthesis and characterization of 4-(4,6-dimethoxy-1,3,5-triazin-2-yl)-4-methylmorpholinium chloride. *Tetrahedron Letters* **1999,** *40* (29), 5327-5330.
194. Maier, M. A.; Yannopoulos, C. G.; Mohamed, N.; Roland, A.; Fritz, H.; Mohan, V.; Just, G.; Manoharan, M., Synthesis of Antisense Oligonucleotides Conjugated to a Multivalent Carbohydrate Cluster for Cellular Targeting. *Bioconjugate Chemistry* **2003,** *14* (1), 18-29.
195. Datry, A.; Bart-Delabesse, E., La caspofungine : du mécanisme d'action aux applications thérapeutiques. *La Revue de Médecine Interne* **2006,** *27* (1), 32-39.
196. Lee, H. M.; Kim, M. H.; Yoon, Y. I.; Park, W. H., Fluorescent Property of Chitosan Oligomer and Its Application as a Metal Ion Sensor. *Marine Drugs* **2017,** *15* (4), 105.
197. Gonil, P.; Sajomsang, W.; Ruktanonchai, U. R.; Na Ubol, P.; Treetong, A.; Opanasopit, P.; Puttipipatkhachorn, S., Synthesis and Fluorescence Properties of N-Substituted 1-Cyanobenz[f]isoindole Chitosan Polymers and Nanoparticles for Live Cell Imaging. *Biomacromolecules* **2014,** *15* (8), 2879-2888.
198. Chabre, Y. M.; Roy, R., Chapter 6 - Design and Creativity in Synthesis of Multivalent Neoglycoconjugates. In *Advances in Carbohydrate Chemistry and Biochemistry*, Horton, D., Ed. Academic Press: 2010; Vol. 63, pp 165-393.
199. Talaga, M. L.; Fan, N.; Fueri, A. L.; Brown, R. K.; Chabre, Y. M.; Bandyopadhyay, P.; Roy, R.; Dam, T. K., Significant Other Half of a Glycoconjugate: Contributions of Scaffolds to Lectin–Glycoconjugate Interactions. *Biochemistry* **2014,** *53* (27), 4445-4454.
200. Ian Storer, R.; Aciro, C.; Jones, L. H., Squaramides: physical properties, synthesis and applications. *Chemical Society Reviews* **2011,** *40* (5), 2330-2346.
201. Tietze, L. F.; Arlt, M.; Beller, M.; Gl üsenkamp, K.-H.; Jähde, E.; Rajewsky, M. F., Anticancer Agents, 15. Squaric Acid Diethyl Ester: A New Coupling Reagent for the Formation of Drug Biopolymer Conjugates. Synthesis of Squaric Acid Ester Amides and Diamides. *Chemische Berichte* **1991,** *124* (5), 1215-1221.
202. Wurm, F. R.; Klok, H.-A., Be squared: expanding the horizon of squaric acid-mediated conjugations. *Chemical Society Reviews* **2013,** *42* (21), 8220-8236.
203. Marchetti, L. A.; Kumawat, L. K.; Mao, N.; Stephens, J. C.; Elmes, R. B. P., The Versatility of Squaramides: From Supramolecular Chemistry to Chemical Biology. *Chem* **2019,** *5* (6), 1398-1485.
204. Karelin, A. A.; Tsvetkov, Y. E.; Paulovičová, L.; Bystrický, S.; Paulovičová, E.; Nifantiev, N. E., Synthesis of a heptasaccharide fragment of the mannan from Candida guilliermondii cell wall and its conjugate with BSA. *Carbohydrate Research* **2009,** *344* (1), 29-35.
205. Paulovičová, L.; Paulovičová, E.; Karelin, A. A.; Tsvetkov, Y. E.; Nifantiev, N. E.; Bystrický, S., Humoral and cell-mediated immunity following vaccination with synthetic Candida cell wall mannan derived heptamannoside–protein conjugate: Immunomodulatory properties of heptamannoside–BSA conjugate. *International Immunopharmacology* **2012,** *14* (2), 179-187.

206. Lindhorst, T. K.; Bruegge, K.; Fuchs, A.; Sperling, O., A bivalent glycopeptide to target two putative carbohydrate binding sites on FimH. *Beilstein Journal of Organic Chemistry* **2010,** *6*, 801-809.
207. Sperling, O.; Fuchs, A.; Lindhorst, T. K., Evaluation of the carbohydrate recognition domain of the bacterial adhesin FimH: design, synthesis and binding properties of mannoside ligands. *Organic & Biomolecular Chemistry* **2006,** *4* (21), 3913-3922.
208. Grabosch, C.; Hartmann, M.; Schmidt-Lassen, J.; Lindhorst, T. K., Squaric Acid Monoamide Mannosides as Ligands for the Bacterial Lectin FimH: Covalent Inhibition or Not? *ChemBioChem* **2011,** *12* (7), 1066-1074.
209. Janiak, C.; Lassahn, P. G., The Vinyl Homopolymerization of Norbornene. *Macromolecular Rapid Communications* **2001,** *22* (7), 479-493.
210. Mortell, K. H.; Weatherman, R. V.; Kiessling, L. L., Recognition Specificity of Neoglycopolymers Prepared by Ring-Opening Metathesis Polymerization. *Journal of the American Chemical Society* **1996,** *118* (9), 2297-2298.
211. Lang, K.; Davis, L.; Torres-Kolbus, J.; Chou, C.; Deiters, A.; Chin, J. W., Genetically encoded norbornene directs site-specific cellular protein labelling via a rapid bioorthogonal reaction. *Nature Chemistry* **2012,** *4*, 298.
212. Späte, A.-K.; Dold, J. E. G. A.; Batroff, E.; Schart, V. F.; Wieland, D. E.; Baudendistel, O. R.; Wittmann, V., Exploring the Potential of Norbornene-Modified Mannosamine Derivatives for Metabolic Glycoengineering. *ChemBioChem* **2016,** *17* (14), 1374-1383.
213. Ramos Ondono, J. The Synthesis and Characterization of Novel Low Molecular Weight Gelators and their Application in Electrospinning to Develop Biocompatible Materials and Tissue Scaffolds. PhD Thesis, Maynooth Univeristy, Ireland., 2017.
214. Dimick, S. M.; Powell, S. C.; McMahon, S. A.; Moothoo, D. N.; Naismith, J. H.; Toone, E. J., On the Meaning of Affinity: Cluster Glycoside Effects and Concanavalin A. *Journal of the American Chemical Society* **1999,** *121* (44), 10286-10296.
215. Lee, Y. C.; Lee, R. T., Carbohydrate-Protein Interactions: Basis of Glycobiology. *Accounts of Chemical Research* **1995,** *28* (8), 321-327.
216. Matassini, C.; Parmeggiani, C.; Cardona, F.; Goti, A., Are enzymes sensitive to the multivalent effect? Emerging evidence with glycosidases. *Tetrahedron Letters* **2016,** *57* (49), 5407-5415.
217. Lundquist, J. J.; Toone, E. J., The Cluster Glycoside Effect. *Chemical Reviews* **2002,** *102* (2), 555-578.
218. Osawa, T.; Matsumoto, I., [36] Gorse (Ulex europeus) phytohemagglutinins. In *Methods in Enzymology*, Academic Press: 1972; Vol. 28, pp 323-327.
219. McCoy, J. P.; Varani, J.; Goldstein, I. J., Enzyme-linked lectin assay (ELLA): II. Detection of carbohydrate groups on the surface of unfixed cells. *Experimental Cell Research* **1984,** *151* (1), 96-103.
220. Dam, T. K.; Brewer, C. F., Multivalent Protein–Carbohydrate Interactions: Isothermal Titration Microcalorimetry Studies. In *Methods in Enzymology*, Academic Press: 2004; Vol. 379, pp 107-128.
221. Smith, E. A.; Thomas, W. D.; Kiessling, L. L.; Corn, R. M., Surface Plasmon Resonance Imaging Studies of Protein-Carbohydrate Interactions. *Journal of the American Chemical Society* **2003,** *125* (20), 6140-6148.
222. Cecioni, S.; Praly, J.-P.; Matthews, S. E.; Wimmerová, M.; Imberty, A.; Vidal, S., Rational Design and Synthesis of Optimized Glycoclusters for Multivalent Lectin–Carbohydrate Interactions: Influence of the Linker Arm. *Chemistry – A European Journal* **2012,** *18* (20), 6250-6263.

223. Hasegawa, T.; Yonemura, T.; Matsuura, K.; Kobayashi, K., Artificial Metalloglycoclusters: Compact Saccharide Shell to Induce High Lectin Affinity as Well as Strong Luminescence. *Bioconjugate Chemistry* **2003,** *14* (4), 728-737.
224. Kanai, M.; Mortell, K. H.; Kiessling, L. L., Varying the Size of Multivalent Ligands: The Dependence of Concanavalin A Binding on Neoglycopolymer Length. *Journal of the American Chemical Society* **1997,** *119* (41), 9931-9932.
225. Lin, C.-C.; Yeh, Y.-C.; Yang, C.-Y.; Chen, G.-F.; Chen, Y.-C.; Wu, Y.-C.; Chen, C.-C., Quantitative analysis of multivalent interactions of carbohydrate-encapsulated gold nanoparticles with concanavalin A. *Chemical Communications* **2003,** (23), 2920-2921.
226. Kim, B.-S.; Hong, D.-J.; Bae, J.; Lee, M., Controlled Self-Assembly of Carbohydrate Conjugate Rod−Coil Amphiphiles for Supramolecular Multivalent Ligands. *Journal of the American Chemical Society* **2005,** *127* (46), 16333-16337.
227. Pieters, R. J., Maximising multivalency effects in protein–carbohydrate interactions. *Organic & Biomolecular Chemistry* **2009,** *7* (10), 2013-2025.
228. Pifferi, C.; Goyard, D.; Gillon, E.; Imberty, A.; Renaudet, O., Synthesis of Mannosylated Glycodendrimers and Evaluation against BC2L-A Lectin from Burkholderia Cenocepacia. *ChemPlusChem* **2017,** *82* (3), 390-398.
229. Bernardi, A.; Jimenez-Barbero, J.; Casnati, A.; De Castro, C.; Darbre, T.; Fieschi, F.; Finne, J.; Funken, H.; Jaeger, K.-E.; Lahmann, M.; Lindhorst, T. K.; Marradi, M.; Messner, P.; Molinaro, A.; Murphy, P. V.; Nativi, C.; Oscarson, S.; Penades, S.; Peri, F.; Pieters, R. J.; Renaudet, O.; Reymond, J.-L.; Richichi, B.; Rojo, J.; Sansone, F.; Schaffer, C.; Turnbull, W. B.; Velasco-Torrijos, T.; Vidal, S.; Vincent, S.; Wennekes, T.; Zuilhof, H.; Imberty, A., Multivalent glycoconjugates as anti-pathogenic agents. *Chemical Society Reviews* **2013,** *42* (11), 4709-4727.
230. Otsuka , I.; Blanchard, B.; Borsali, R.; Imberty, A.; Kakuchi, T., Enhancement of Plant and Bacterial Lectin Binding Affinities by Three-Dimensional Organized Cluster Glycosides Constructed on Helical Poly(phenylacetylene) Backbones. *ChemBioChem* **2010,** *11* (17), 2399-2408.
231. Cecioni, S.; Oerthel, V.; Iehl, J.; Holler, M.; Goyard, D.; Praly, J.-P.; Imberty, A.; Nierengarten, J.-F.; Vidal, S., Synthesis of Dodecavalent Fullerene-Based Glycoclusters and Evaluation of Their Binding Properties towards a Bacterial Lectin. *Chemistry – A European Journal* **2011,** *17* (11), 3252-3261.
232. Reynolds, M.; Marradi, M.; Imberty, A.; Penadés, S.; Pérez, S., Multivalent Gold Glycoclusters: High Affinity Molecular Recognition by Bacterial Lectin PA-IL. *Chemistry – A European Journal* **2012,** *18* (14), 4264-4273.
233. Chabre, Y. M.; Giguère, D.; Blanchard, B.; Rodrigue, J.; Rocheleau, S.; Neault, M.; Rauthu, S.; Papadopoulos, A.; Arnold Alexandre, A.; Imberty, A.; Roy, R., Combining Glycomimetic and Multivalent Strategies toward Designing Potent Bacterial Lectin Inhibitors. *Chemistry – A European Journal* **2011,** *17* (23), 6545-6562.
234. Cecioni, S.; Faure, S.; Darbost, U.; Bonnamour, I.; Parrot-Lopez, H.; Roy, O.; Taillefumier, C.; Wimmerová, M.; Praly, J.-P.; Imberty, A.; Vidal, S., Selectivity among Two Lectins: Probing the Effect of Topology, Multivalency and Flexibility of "Clicked" Multivalent Glycoclusters. *Chemistry – A European Journal* **2011,** *17* (7), 2146-2159.
235. Cecioni, S.; Lalor, R.; Blanchard, B.; Praly, J.-P.; Imberty, A.; Matthews, S. E.; Vidal, S., Achieving High Affinity towards a Bacterial Lectin through Multivalent Topological Isomers of Calix[4]arene Glycoconjugates. *Chemistry – A European Journal* **2009,** *15* (47), 13232-13240.
236. Soomro, Z. H.; Cecioni, S.; Blanchard, H.; Praly, J.-P.; Imberty, A.; Vidal, S.; Matthews, S. E., CuAAC synthesis of resorcin[4]arene-based glycoclusters as multivalent ligands of lectins. *Organic & Biomolecular Chemistry* **2011,** *9* (19), 6587-6597.

237. Sicard, D.; Cecioni, S.; Iazykov, M.; Chevolot, Y.; Matthews, S. E.; Praly, J.-P.; Souteyrand, E.; Imberty, A.; Vidal, S.; Phaner-Goutorbe, M., AFM investigation of Pseudomonas aeruginosa lectin LecA (PA-IL) filaments induced by multivalent glycoclusters. *Chemical Communications* **2011,** *47* (33), 9483-9485.
238. Pertici, F.; Pieters, R. J., Potent divalent inhibitors with rigid glucose click spacers for Pseudomonas aeruginosa lectin LecA. *Chemical Communications* **2012,** *48* (33), 4008-4010.
239. Wang, S.; Dupin, L.; Noël, M.; Carroux, C. J.; Renaud, L.; Géhin, T.; Meyer, A.; Souteyrand, E.; Vasseur, J.-J.; Vergoten, G.; Chevolot, Y.; Morvan, F.; Vidal, S., Toward the Rational Design of Galactosylated Glycoclusters That Target Pseudomonas aeruginosa Lectin A (LecA): Influence of Linker Arms That Lead to Low-Nanomolar Multivalent Ligands. *Chemistry – A European Journal* **2016,** *22* (33), 11785-11794.
240. Michel, O.; Ravoo, B. J., Carbohydrate Microarrays by Microcontact "Click" Chemistry. *Langmuir* **2008,** *24* (21), 12116-12118.
241. Norberg, O.; Deng, L.; Yan, M.; Ramström, O., Photo-Click Immobilization of Carbohydrates on Polymeric Surfaces—A Quick Method to Functionalize Surfaces for Biomolecular Recognition Studies. *Bioconjugate Chemistry* **2009,** *20* (12), 2364-2370.
242. Seebach, D.; Beck, A. K.; Bierbaum, D. J., The World of β- and γ-Peptides Comprised of Homologated Proteinogenic Amino Acids and Other Components. *Chemistry & Biodiversity* **2004,** *1* (8), 1111-1239.
243. Seebach, D.; Gardiner, J., β-Peptidic Peptidomimetics. *Accounts of Chemical Research* **2008,** *41* (10), 1366-1375.
244. Frackenpohl, J.; Arvidsson, P. I.; Schreiber, J. V.; Seebach, D., The Outstanding Biological Stability of β- and γ-Peptides toward Proteolytic Enzymes: An In Vitro Investigation with Fifteen Peptidases. *ChemBioChem* **2001,** *2* (6), 445-455.
245. Fowler, S. A.; Blackwell, H. E., Structure-function relationships in peptoids: recent advances toward deciphering the structural requirements for biological function. *Organic & Biomolecular Chemistry* **2009,** *7* (8), 1508-1524.
246. Roy, O.; Faure, S.; Thery, V.; Didierjean, C.; Taillefumier, C., Cyclic β-Peptoids. *Organic Letters* **2008,** *10* (5), 921-924.
247. Laursen, J. S.; Engel-Andreasen, J.; Fristrup, P.; Harris, P.; Olsen, C. A., Cis–Trans Amide Bond Rotamers in β-Peptoids and Peptoids: Evaluation of Stereoelectronic Effects in Backbone and Side Chains. *Journal of the American Chemical Society* **2013,** *135* (7), 2835-2844.
248. Kemp, W., *NMR in Chemistry: A Multinuclear Introduction*. MacMillan: 1988.
249. Drakenberg, T.; Dahlqvist, K. I.; Forsen, S., Barrier to internal rotation in amides. IV. N,N-Dimethylamides. Substituent and solvent effects. *The Journal of Physical Chemistry* **1972,** *76* (15), 2178-2183.
250. Dumy, P.; Eggleston, I. M.; Cervigni, S.; Sila, U.; Sun, X.; Mutter, M., A convenient synthesis of cyclic peptides as regioselectively addressable functionalized templates (RAFT). *Tetrahedron Letters* **1995,** *36* (8), 1255-1258.
251. Renaudet, O.; Dumy, P., Chemoselectively Template-Assembled Glycoconjugates as Mimics for Multivalent Presentation of Carbohydrates. *Organic Letters* **2003,** *5* (3), 243-246.
252. Bossu, I.; Šulc, M.; Křenek, K.; Dufour, E.; Garcia, J.; Berthet, N.; Dumy, P.; Křen, V.; Renaudet, O., Dendri-RAFTs: a second generation of cyclopeptide-based glycoclusters. *Organic & Biomolecular Chemistry* **2011,** *9* (6), 1948-1959.
253. Hermanson, G. T., *Bioconjugate Techniques*. Elsevier Science & Technology: San Diego, UNITED STATES, 2013.
254. Ge, S.-S.; Chen, B.; Wu, Y.-Y.; Long, Q.-S.; Zhao, Y.-L.; Wang, P.-Y.; Yang, S., Current advances of carbene-mediated photoaffinity labeling in medicinal chemistry. *RSC Advances* **2018,** *8* (51), 29428-29454.

255. Smith, E.; Collins, I., Photoaffinity labeling in target- and binding-site identification. *Future Medicinal Chemistry* **2015,** *7* (2), 159-183.
256. Singh, A.; Thornton, E. R.; Westheimer, F. H., The Photolysis of Diazoacetylchymotrypsin. *Journal of Biological Chemistry* **1962,** *237* (9), PC3006-PC3008.
257. Das, J., Aliphatic Diazirines as Photoaffinity Probes for Proteins: Recent Developments. *Chemical Reviews* **2011,** *111* (8), 4405-4417.
258. Sadaghiani, A. M.; Verhelst, S. H. L.; Bogyo, M., Tagging and detection strategies for activity-based proteomics. *Current Opinion in Chemical Biology* **2007,** *11* (1), 20-28.
259. Green, N. M., Avidin. In *Advances in Protein Chemistry*, Anfinsen, C. B.; Edsall, J. T.; Richards, F. M., Eds. Academic Press: 1975; Vol. 29, pp 85-133.
260. McCombs, J. E.; Zou, C.; Parker, R. B.; Cairo, C. W.; Kohler, J. J., Enhanced Cross-Linking of Diazirine-Modified Sialylated Glycoproteins Enabled through Profiling of Sialidase Specificities. *ACS Chemical Biology* **2016,** *11* (1), 185-192.
261. Sakurai, K.; Ozawa, S.; Yamada, R.; Yasui, T.; Mizuno, S., Comparison of the Reactivity of Carbohydrate Photoaffinity Probes with Different Photoreactive Groups. *ChemBioChem* **2014,** *15* (10), 1399-1403.
262. Sakurai, K.; Yasui, T.; Mizuno, S., Comparative Analysis of the Reactivity of Diazirine-Based Photoaffinity Probes toward a Carbohydrate-Binding Protein. *Asian Journal of Organic Chemistry* **2015,** *4* (8), 724-728.
263. Wiegand, M.; Lindhorst, T. K., Synthesis of Photoactive α-Mannosides and Mannosyl Peptides and Their Evaluation for Lectin Labeling. *European Journal of Organic Chemistry* **2006,** *2006* (21), 4841-4851.
264. Lindhorst, T. K.; Märten, M.; Fuchs, A.; Knight, S. D., En route to photoaffinity labeling of the bacterial lectin FimH. *Beilstein journal of organic chemistry* **2010,** *6*, 810-822.
265. Renaudet, O.; Spinelli, N., *Synthesis and Biological Applications of Glycoconjugates*. Bentham Science Publishers: 2011.
266. Chang, T.-C.; Lai, C.-H.; Chien, C.-W.; Liang, C.-F.; Adak, A. K.; Chuang, Y.-J.; Chen, Y.-J.; Lin, C.-C., Synthesis and Evaluation of a Photoactive Probe with a Multivalent Carbohydrate for Capturing Carbohydrate–Lectin Interactions. *Bioconjugate Chemistry* **2013,** *24* (11), 1895-1906.
267. Fedotova, A.; Kondrashov, E.; Legros, J.; Maddaluno, J.; Rulev, A. Y., Solvent effects in the aza-Michael addition of anilines. *Comptes Rendus Chimie* **2018,** *21* (7), 639-643.
268. De, K.; Legros, J.; Crousse, B.; Bonnet-Delpon, D., Solvent-Promoted and -Controlled Aza-Michael Reaction with Aromatic Amines. *The Journal of Organic Chemistry* **2009,** *74* (16), 6260-6265.
269. Genest, A.; Portinha, D.; Fleury, E.; Ganachaud, F., The aza-Michael reaction as an alternative strategy to generate advanced silicon-based (macro)molecules and materials. *Progress in Polymer Science* **2017,** *72*, 61-110.
270. Zhang, Z.; Bao, Z.; Xing, H., N,N'-Bis[3,5-bis(trifluoromethyl)phenyl]thiourea: a privileged motif for catalyst development. *Organic & Biomolecular Chemistry* **2014,** *12* (20), 3151-3162.
271. Amara, Z.; Caron, J.; Joseph, D., Recent contributions from the asymmetric aza-Michael reaction to alkaloids total synthesis. *Natural Product Reports* **2013,** *30* (9), 1211-1225.
272. Chen, Z. W.; Luo, M. T.; Ye, D. N., TFA-Mediated Alkyne Hydration Reaction to Synthesize Methyl Ketones. *Asian Journal of Chemistry* **2014,** *26* (19), 6528-6530.
273. Bond, M. R.; Zhang, H.; Vu, P. D.; Kohler, J. J., Photocrosslinking of glycoconjugates using metabolically incorporated diazirine-containing sugars. *Nature Protocols* **2009,** *4*, 1044.

274. Farrell, M.; Zhou, J.; Murphy, P. V., Regiospecific Anomerisation of Acylated Glycosyl Azides and Benzoylated Disaccharides by Using TiCl4. *Chemistry – A European Journal* **2013,** *19* (44), 14836-14851.
275. Meinjohanns, E.; Meldal, M.; Paulsen, H.; Bock, K., Dithiasuccinoyl (Dts) amino-protecting group used in syntheses of 1,2-trans-amino sugar glycosides. *Journal of the Chemical Society, Perkin Transactions 1* **1995,** (4), 405-415.
276. Hwang, I. H.; Lee, S. J.; Chang, J. Y., Supramolecular discotic liquid crystals from wedge-shaped diacetylenes and their polymerization. *Journal of Polymer Science Part A: Polymer Chemistry* **2003,** *41* (13), 1881-1891.
277. Kale, R. R.; Clancy, C. M.; Vermillion, R. M.; Johnson, E. A.; Iyer, S. S., Synthesis of soluble multivalent glycoconjugates that target the Hc region of botulinum neurotoxin A. *Bioorganic & Medicinal Chemistry Letters* **2007,** *17* (9), 2459-2464.
278. Caumes, C.; Hjelmgaard, T.; Remuson, R.; Faure, S.; Taillefumier, C., Highly Convenient Gram-Scale Solution-Phase Peptoid Synthesis and Orthogonal Side-Chain Post-Modification. *Synthesis* **2011,** *2011* (02), 257-264.
279. Feng, Y.; Li, J.; Jiang, L.; Gao, Z.; Huang, W.; Jiang, F.; Luo, N.; Han, S.; Zeng, R.; Yang, D., Efficient Syntheses and Complexation Studies of Diacetylene-Containing Macrocyclic Polyethers. *European Journal of Organic Chemistry* **2011,** *2011* (3), 562-568.

Appendix

Publications

Martin, H.; Govern, M. M.; Abbey, L.; Gilroy, A.; Mullins, S.; Howell, S.; Kavanagh, K.; Velasco-Torrijos, T., Inhibition of Adherence of the Yeast *Candida albicans* to Buccal Epithelial Cells by Synthetic Aromatic Glycoconjugates. *European Journal of Medicinal Chemistry* **2018**, *160*, 82-93.

Martin, H.; Kavanagh, K.; Velasco-Torrijos, T., Targeting Adhesion in Fungal Pathogen *Candida albicans. Future Medicinal Chemistry.* Accepted.

Martin, H.; Pfeiffer, P.; Kramer, T.; Kavanagh, K.; Velasco-Torrijos, T., Scaffold Diversity for Enhanced Activity of Glycosylated Inhibitors of Fungal Adhesion. Submitted

Oral Presentation

Martin, H.; *Exploiting the Sweet Tooth of Candida albicans using Synthetic Glycoconjugates*, 71st Irish Universities Chemistry Research Colloquium, Royal College of Surgeons, Dublin, 2019.

Martin, H.; *Exploiting the Sweet Tooth of Candida albicans using Synthetic Glycoconjugates*, BOC Award Presentation, Maynooth University, 2019.

Poster Presentations

Martin, H.; Kavanagh K.; Velasco-Torrijos, T.; *Glycoconjugates to Prevent Candida albicans Adhesion,* 1st Medicinal Chemistry Ireland Conference, Trinity Biomedical Sciences Institute, 2016.

Martin, H.; Kavanagh K.; Velasco-Torrijos, T.; *Glycoconjugates to Prevent Candida albicans Adhesion,* Organic Division Regional Meeting (RSC), Royal College of Surgeons, 2016.

Martin, H.; Kavanagh K.; Velasco-Torrijos, T.; *Glycoconjugates to Prevent Candida albicans Adhesion,* 68th Irish Universities Chemistry Research Colloquium, University College Cork, 2016.

Martin, H.; Kavanagh K.; Velasco-Torrijos, T.; *Glycoconjugates to Prevent Candida albicans Adhesion,* 69th Irish Universities Chemistry Research Colloquium, Dublin City University, 2017.

Martin, H.; Kavanagh K.; Velasco-Torrijos, T.; *Glycoconjugates to Prevent Candida albicans Adhesion,* 19th European Carbohydrate Symposium EUROCARB, Barcelona, 2017.

Martin, H.; Kavanagh K.; Velasco-Torrijos, T.; *Glycoconjugates to Prevent Candida albicans Adhesion,* 2nd Medicinal Chemistry Ireland Conference, Dublin City University, 2018 - Best Poster Prize.

Graduate Modules

Chemistry Specific Modules:

CH801 – Core Skills and Research Techniques in Chemistry

CH308 – Teaching Skills in Chemistry

CH806 – Research Training Workshops in Chemistry

CH808 – Research Supervision Training

Generic/Transferable Modules:

GST1 – Personal Development and Employability Module

GST2 – Finding Information for Your Thesis

GST5 – Creative Thinking and Problem Solving

NMR Data:

HSQC for compound 2.85 (d_5-Pyr)

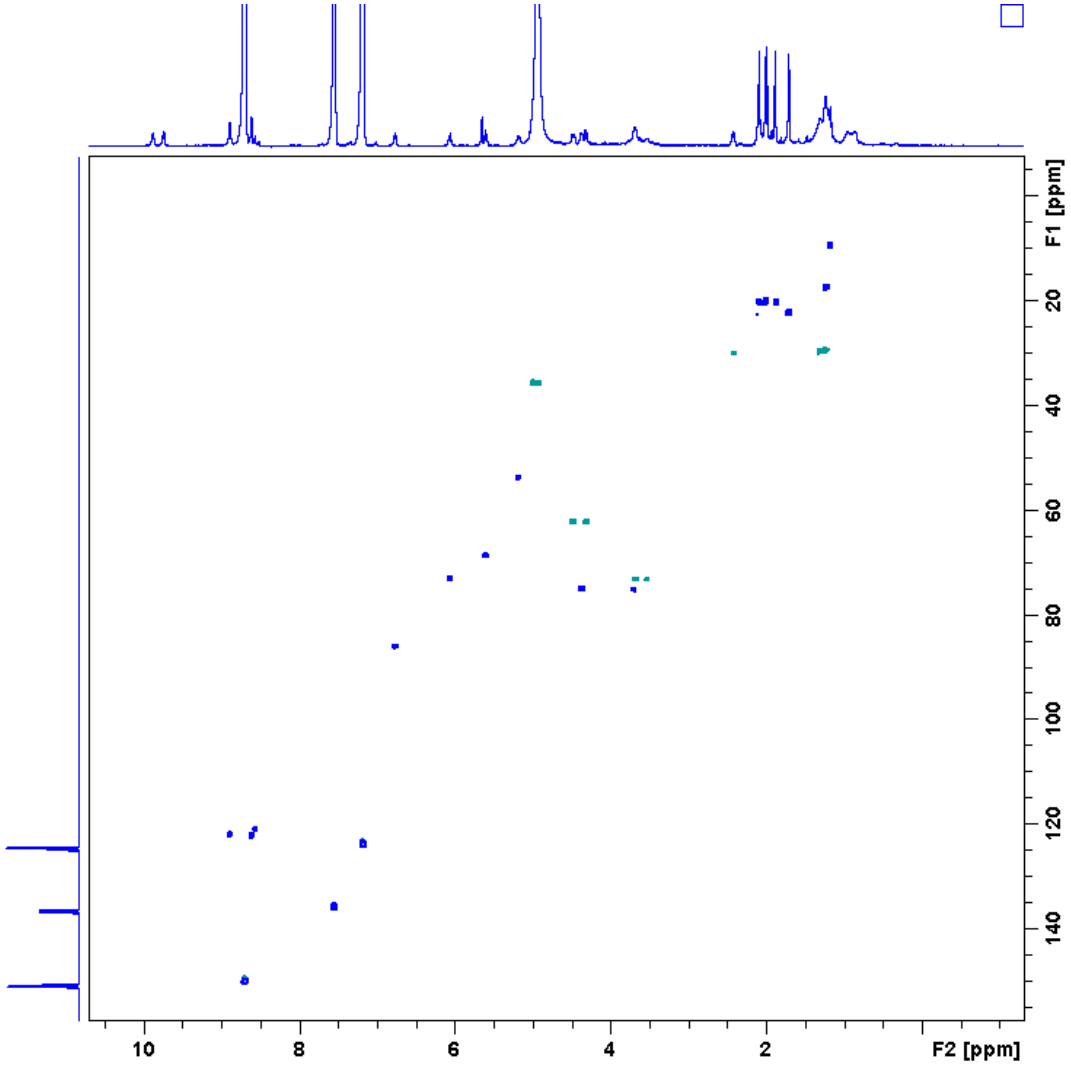

^{1}H NMR of Compound 4.53

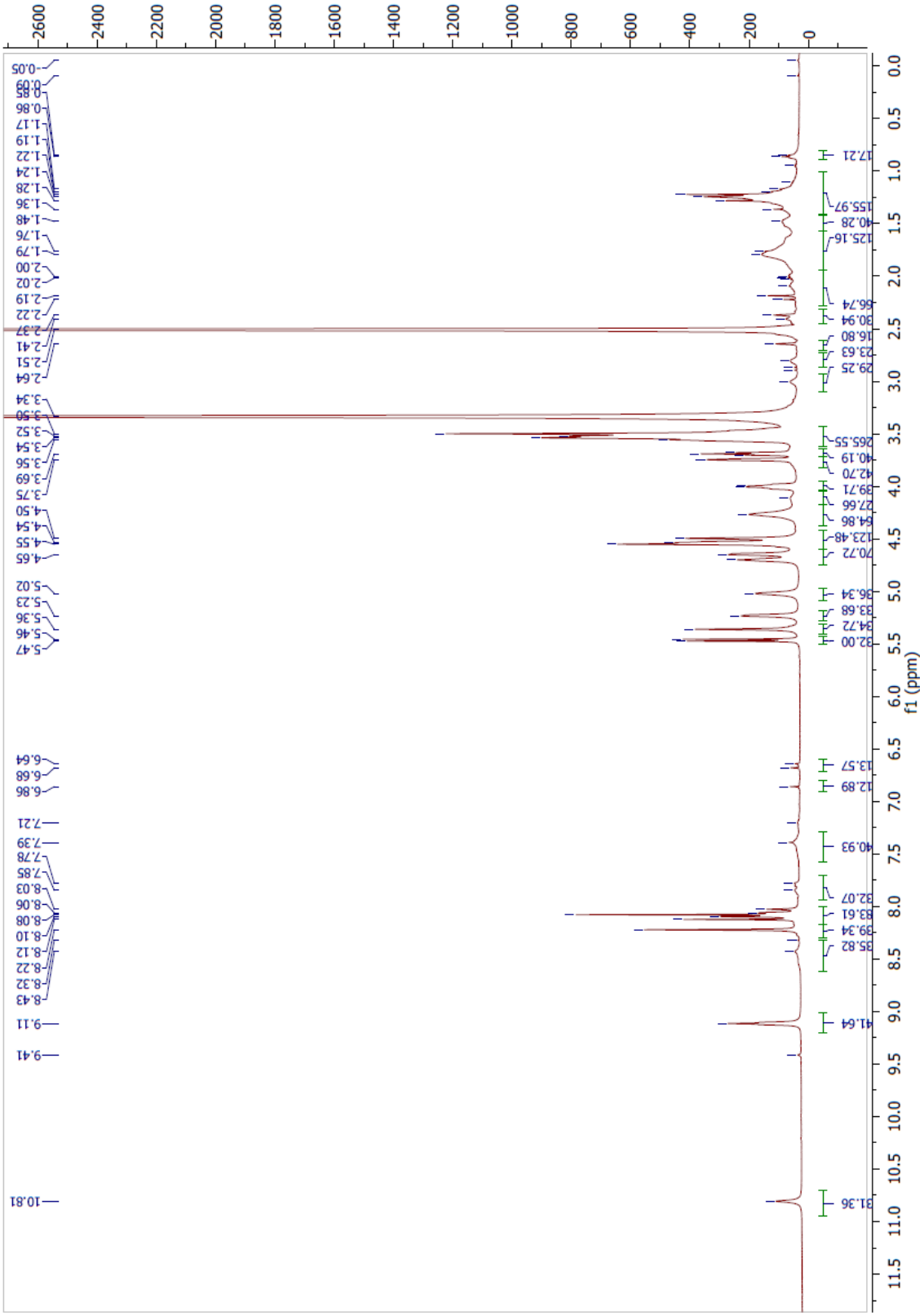

^{1}H NMR of Compound 4.59

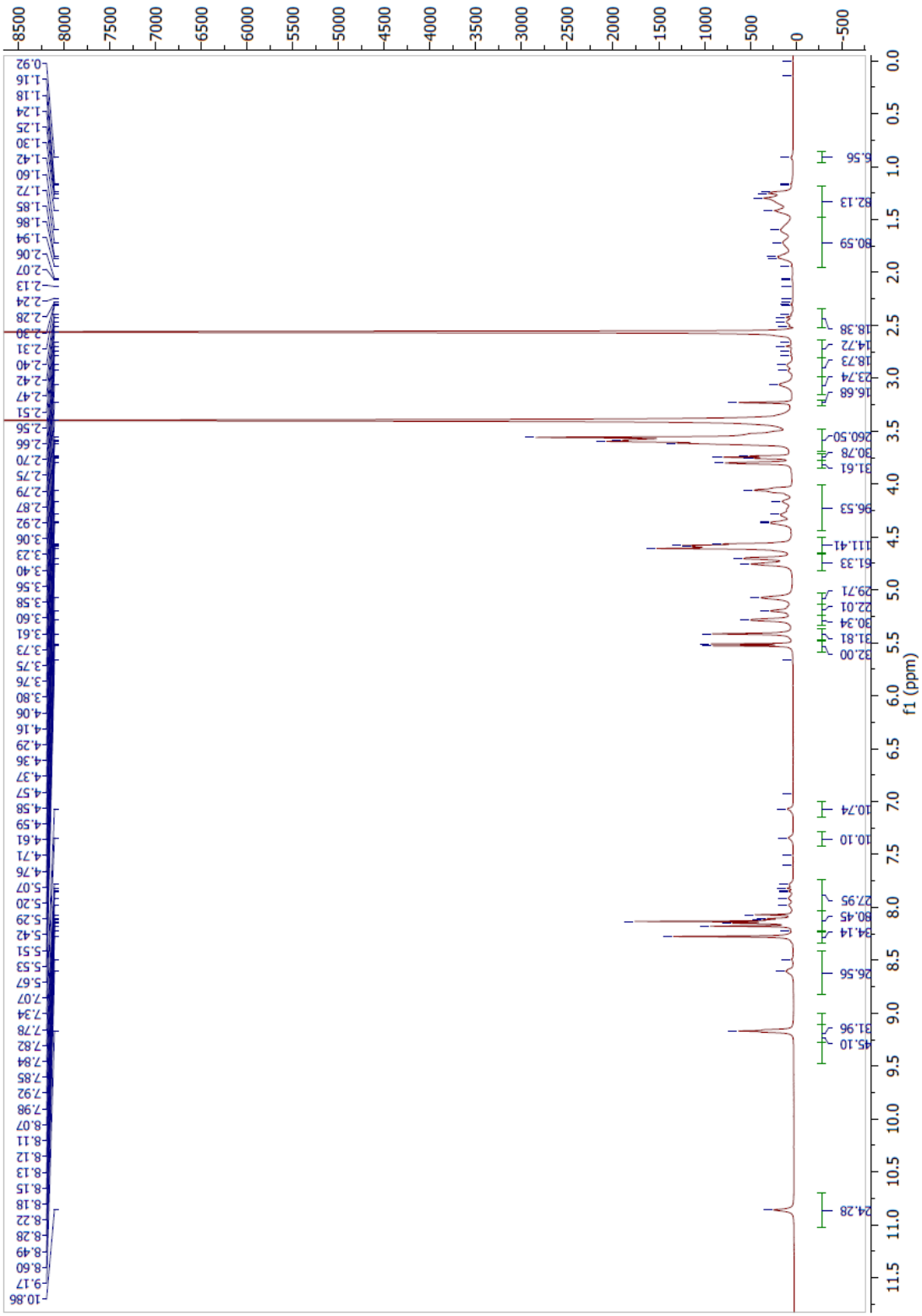

Analytical HPLC Traces:

Compound 2.67

RP-HPLC (C_{18}, 254 nm, 10 % B in 15 mins)

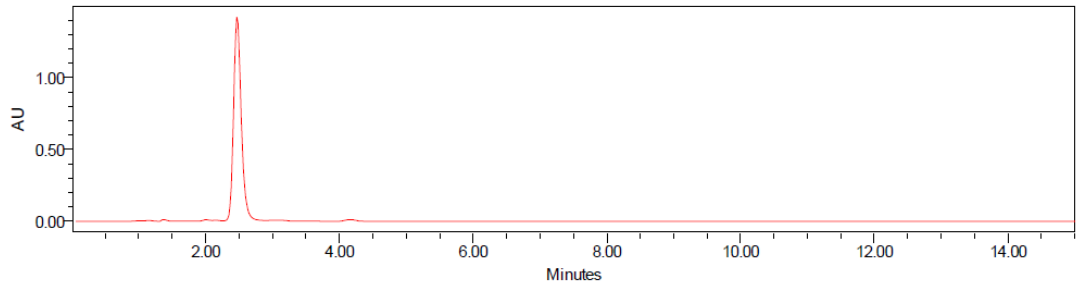

Compound 4.51

RP-HPLC (C_{18}, 214 nm, 5-40 % B in 25 mins)

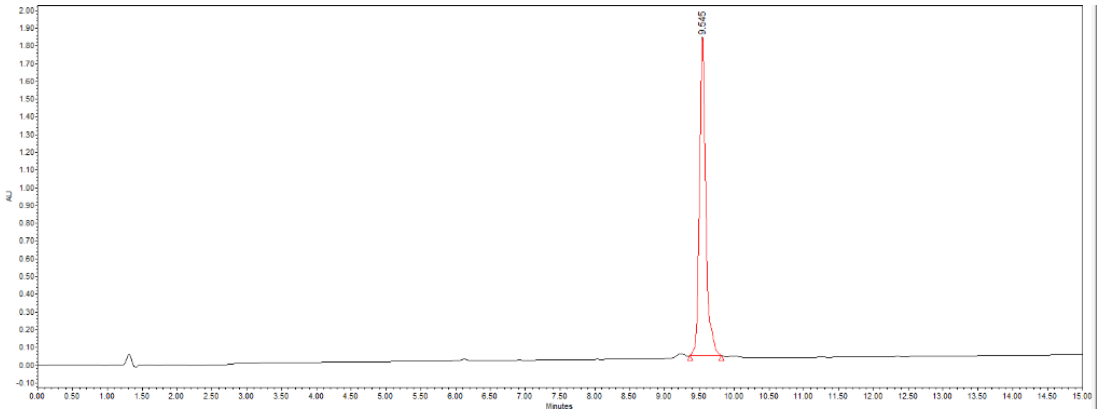

Compound 4.53

RP-HPLC (C_{18}, 214 nm, 5-40 % B in 25 mins)

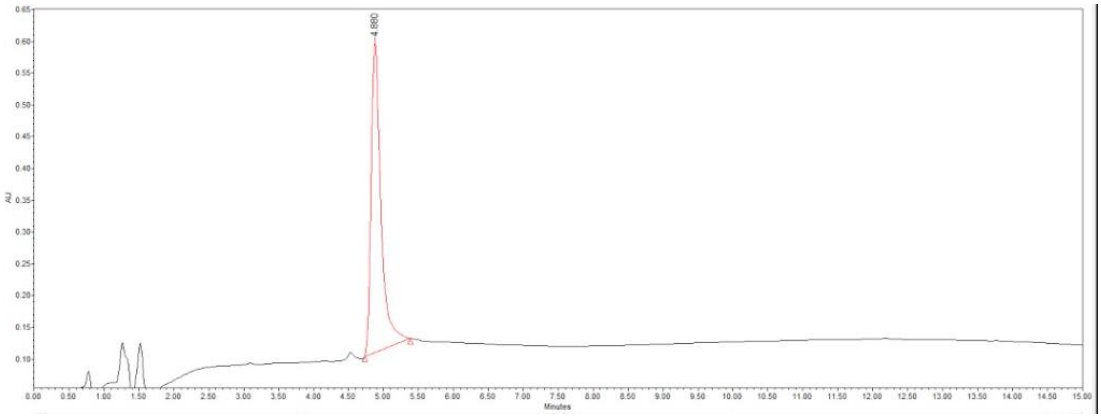

Compound 4.55

RP-HPLC (C_{18}, 214 nm, 5-40 % B in 25 mins)

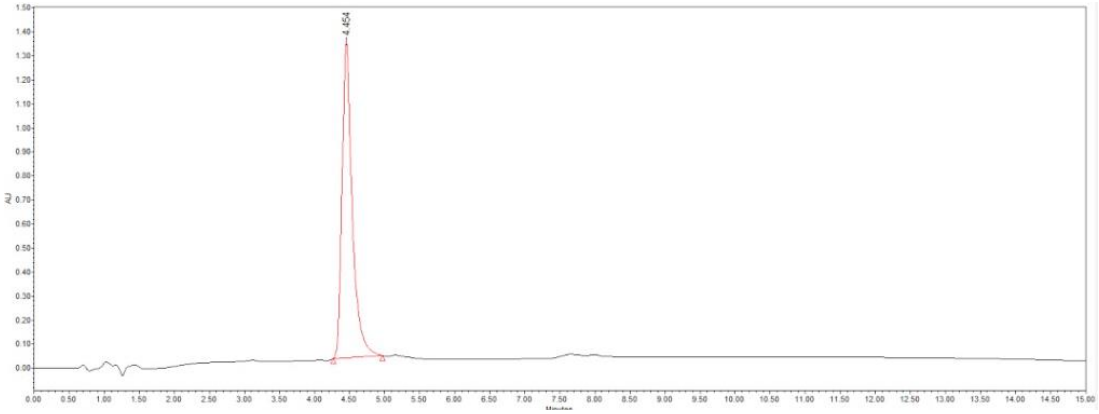

Compound 4.57

RP-HPLC (C_{18}, 214 nm, 5-40 % B in 25 mins)

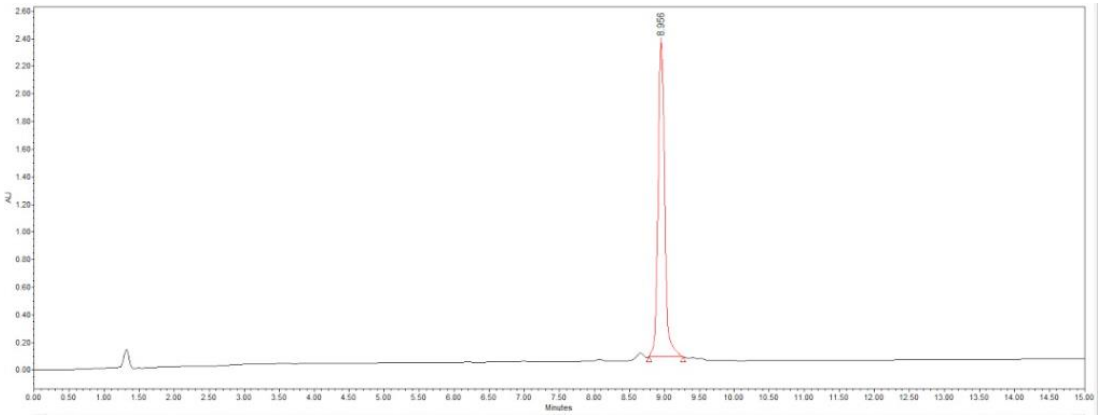

Compound 4.59

RP-HPLC (C_{18}, 214 nm, 5-40 % B in 25 mins)

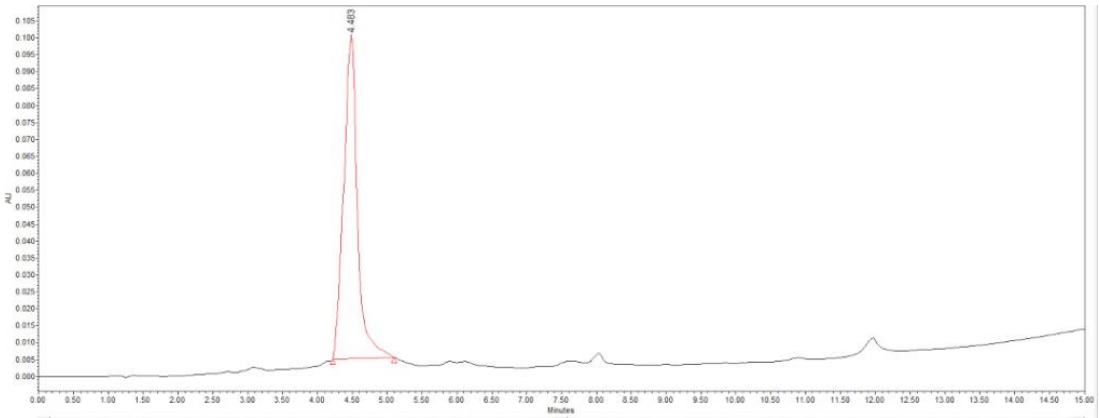

MALDI-TOF MS Spectra

Compound 4.42

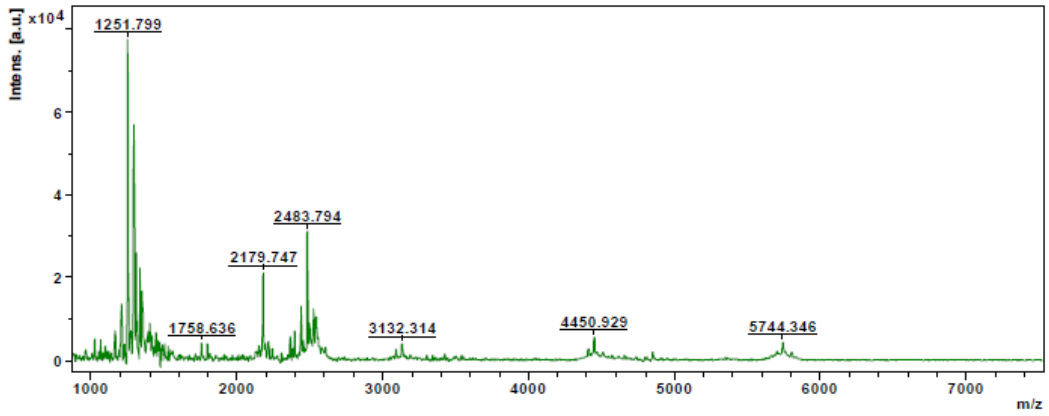

Compound 4.43